Nitrate attenuation in a restored river floodplain system: River Cole (Oxfordshire - UK)

Sgouridis, Fotis

Nitrate attenuation in a restored river floodplain system: River Cole (Oxfordshire - UK)

by

Fotis Sgouridis

A thesis submitted for the degree of Doctor of Philosophy

Department of Geography and School of Biological and Chemical Sciences

Queen Mary, University of London

2010

SIGNED DECLARATION

I hereby declare that the work presented in this thesis is entirely my own

Signed:……

Fotis Sgouridis

Abstract

Restoring river-floodplain connectivity has been proposed as an alternative management measure for natural flood defence through the temporary storage of floodwaters and the attenuation of flood peaks downstream. Whilst several studies have documented the associated ecological and landscape amenity values of such hydrological measures, the water quality benefits to the adjacent water bodies have been inadequately studied. To date, the focus of scientific research and natural resource management has been on the role of riparian buffer zones for the alleviation of agricultural diffuse nitrate pollution. This research investigated the potential for nitrate attenuation in a restored river-floodplain system, the River Cole (Coleshill, England), with the aim of informing future restoration schemes of the best management practices for enhanced nitrate removal.

Following restoration, the increased river-floodplain connectivity has encouraged overbank flooding of the different land use zones throughout the year. The flood pulse supplies the floodplain soil with river water nitrate and creates the necessary anaerobic conditions for the effective removal of nitrate via heterotrophic denitrification, while organic carbon is supplied mainly through the traditional land use management practices of grazing and mowing. The conservation of nitrogen via DNRA is of minimal importance in this lowland agricultural catchment setting, mainly due to the non-limiting nitrate supply from the surrounding agricultural land but also the intermittent saturation regime that restricts the low redox conditions to the low elevation riparian areas. This presents the added benefit of restricting methane emission to the more frequently waterlogged riparian soils, while denitrification is effective across the whole floodplain area. Additionally, more than 90% of nitrate removal occurs in the top 30 cm of the soil during the flood, while the role of subsurface denitrification is restricted by the limited availability of organic carbon and nitrate. Based on these findings, this study demonstrates that, for similar catchments, the nitrate removal capacity of a floodplain can be assessed by the denitrification capacity of the surface soil. The assessment of the denitrification capacity can be undertaken inexpensively using a simple empirical model that requires a single microbial denitrification potential measurement, and a seasonal or monthly record of soil nitrate content, soil moisture, and temperature. Assessments can be undertaken as part of the design process to optimise nitrate removal or post restoration to appraise the functioning of the scheme.

Acknowledgements

I would like to thank the University of London for providing me with a college studentship and the Alexander S. Onassis Public Benefit Foundation for the financial support, especially during the writing up stage of this PhD. I am also grateful to the University of London, Central Research Fund for a grant towards fieldwork expenses, and the British Hydrological Society for three conference attendance grants. Without access to the River Cole floodplain this research would not have been possible and I am indebted to Mr Martin Janes from the RRC, Mr Keith Blaxhall from the National Trust at Coleshill and Mrs Vicky Mace, the tenant farmer, who kindly allowed the installation of the monitoring equipment on her land.

A special thanks goes to my research supervisors: Dr Geraldene Wharton, Dr Kate Heppell and Dr Mark Trimmer for their support and guidance throughout the PhD process and for challenging my thinking. I would also like to thank Prof. Gilles Pinay for his advice on the biogeochemical aspect of my research. Having to cope with a very fieldwork demanding PhD, I am grateful to my numerous fieldwork assistants: Simon Dobinson, Laura Shotbolt, Kalmond Ma, Margaret Kadiri, Kate Heppell, Stuart Glenday, Mark Trimmer, Andrew Voak, Christine Rooks, Danni Pearce, Grieg Davies, Bob Grabowski and Lorna Linch. I would also like to thank Dr Laura Shotbolt, Dr Ian Sanders and Dr Joanna Nichols for their patience while teaching me the laboratory techniques. Thanks also to all the other postgrad students who have made working at Queen Mary a great experience.

Finally, I would like to thank my friends and housemates: Daniel, Margarita, Konstantina, Jan, Ebony and Hugo, who with the ‘occasional’ barbeques and parties made my PhD years a lot easier and enjoyable.

This thesis is dedicated to my parents, Kostas and Anna, because without their emotional support, I would never have completed this PhD.

Table of Contents

Chapter 7: Predicting denitrification rates at the field scale for the design and appraisal of river restoration schemes

Chapter 8: Summary and Conclusions

List of Figures

List of Tables

Chapter 1: Introduction

1.1 ***River-floodplain ecosystems***

Floodplains are defined as 'areas of low lying land that are subject to inundation by lateral overflow water from rivers with which they are associated' (Junk and Welcomme, 1990). They are usually created by the deposition of sediment as the channel migrates laterally, while their characteristics and functions are intimately linked to the river type (e.g. braided, anastomosed, meandering) that flows upon them (Marriot, 1998). Floodplain landform assemblage has a potentially complex sedimentological background with three-dimensional flow dynamics (lateral flow between the river and/or the upland, groundwater and direct precipitation) that lead to high temporal and spatial heterogeneity (Anderson *et al.,* 1996). The spatial and temporal heterogeneity is maintained due to a 'disturbance' regime related to hydrogeomorphic processes such as flooding, erosion, accumulation and reworking of sediment along the fluvial corridor (Steiger *et al.*, 2005). These processes generate for example various channel patterns, channel migration, avulsion, bar and island formation, and floodplain deposition, whilst they also interact with vegetation dynamics and create the geomorphic template for floodplain habitat according to different physiographic contexts, valley forms and river styles (Steiger *et al.,* 2005). The larger alluvial floodplains may also contain riparian zones (Figure 1.1) primarily reflecting species-specific responses to soil moisture/oxygenation, sediment deposition, the frequency and duration of inundation, and the erosive action of flooding along a lateral gradient (Ward *et al.,* 2002).

Large floodplains, like the narrower riparian zones of headwater streams, can also be defined as ecotones between terrestrial and aquatic ecosystems (Gregory *et al.,* 1991; Malanson, 1993) that extend from the low-water mark to the high-water line and also include the terrestrial vegetation influenced by elevated groundwater tables or extreme floods (Naiman *et al.,* 2000). Due to their position in the landscape, floodplains, in their natural state, perform a number of functions that are important from both an environmental and a human perspective (Tockner and Stanford, 2002).

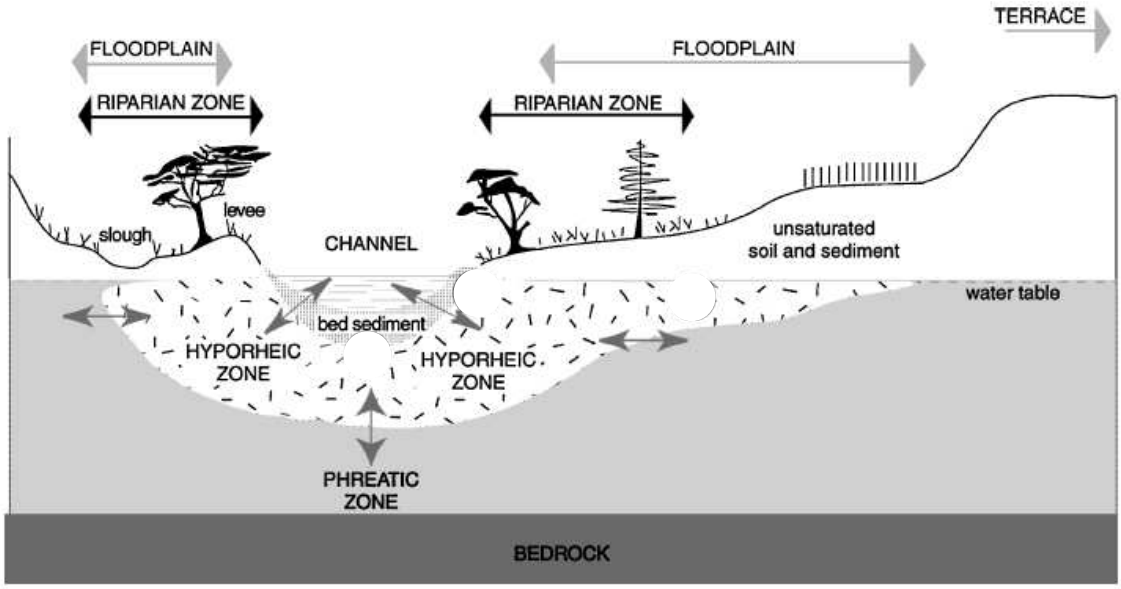

Figure 1.1: Schematic diagram of the vertical and lateral structure of a river-floodplain-aquifer system indicating also the relative positions of the riparian zone and the floodplain (modified from Steiger *et al.*, 2005).

1.2 *River - floodplain functions*

The hydrological connectivity between the river and the floodplain is the single most important factor defining the natural state of a river-floodplain system while also affecting its functioning (Tockner and Stanford, 2002). It is widely recognised that the storage of floodwater on floodplains can reduce flood magnitude downstream (Acreman *et al.*, 2003, 2007), while it has also been shown to recharge groundwater bodies (Bullock and Acreman, 2003). The hydrological variability of a connected river-floodplain system, together with the vegetation cover type, determine the erosion and sedimentation rates on the floodplain (Steiger and Gurnell, 2003). In turn, the stream function is influenced by the contributing particulate organic matter and woody debris (Gurnell *et al.*, 2002) that support microorganism, invertebrate and fish populations through the provision of food and shelter (Gregory *et al.*, 1991, Vervier *et al.*, 1993). Floodplains are among the most productive landscapes on Earth, owing to the continual enrichment by import and retention of nutrient-rich sediments from the headwaters and from lateral sources (Tockner and Stanford, 2002). Floodplains are also considered as centres of bio-complexity and bio-production (Amoros and Bornette, 2002). More species of plants and animals by far occur on floodplains than in any other landscape unit in most regions of the world (Tockner and Stanford, 2002). The hydrology of

floodplains provides the natural controls for floodplain ecology as the patchwork of soils with different water regimes, stabilities and nutrient contents allows plants with different adaptive strategies to co-exist on floodplains (Brown, 1996). In these environments, biotic communities relate to the dynamic interaction of fluvial and terrestrial processes, and comprise a continuum of dependencies on flooding frequency from terrestrial species requiring regular inundation, to aquatic species requiring occasional desiccation, as well as, often opportunistic aquatic and terrestrial taxa (Petts, 1996). Finally, an important function of floodplains, and their associated riparian zones, is the improvement and maintenance of water quality by filtering sediment, nutrients, organic matter, and pesticides from surface and groundwater flow, through the processes of deposition, adsorption, plant uptake and denitrification (Peterjohn and Correll, 1984; Décamps, 1993; Pinay *et al.*, 1999). The estimated worldwide value of the services provided by floodplains is US$ 3,920 x 10^9 yr^{-1} (Constanza *et al.*, 1997). In total, floodplains contribute >25 % of all terrestrial ecosystem services, although they cover only 1.4 % of the land surface area (Mitsch and Gosselink, 2000).

1.3 *Floodplain degradation and function loss*

Despite the recent appreciation of the ecosystem services provided by floodplains, many rivers and streams in Northern Europe and in most developed parts of the world have been, and still are, markedly modified. Floodplain 'reclamation' (i.e. elimination) is much higher than for most other landscape types (Vitousek *et al.*, 1997). The impacts on rivers and floodplains by humans can be of either a proximal or distal nature (WWF, 2000). Proximal impacts include those that result directly in the modification of channel form or hydrology, such as channelisation, embankment, dam construction and river water abstraction. Distal impacts originate mainly from catchment land use and other activities that affect runoff and pollution.

Floodplain biodiversity decline has been attributed to habitat alteration, pollution, competition for water, invasive species and overharvest (Abramovitz, 1996). Due to restricted hydrological connectivity between the river and its floodplain, the migration of permanent aquatic organisms such as fish or aquatic molluscs is seriously restricted (Buijse *et al.*, 2002). The isolation of large rivers from their floodplains has been a major factor in habitat degradation. Thus channelisation, embankment, and lowering of the channel bed for navigation, flood control and land drainage have contributed

significantly to biological impoverishment not only locally but also at the landscape scale (Naiman and Décamps, 1990; Petts, 1996).

Over the past few hundred years, urban and agricultural development had priority on many floodplains in Europe leading to their protection from flooding either by building embankments along the river or enlarging the channel's flow capacity so that it is exceeded less often (Boon *et al.,* 2000). River channelisation, although highly effective as a means of improving land drainage and controlling flooding, is equally acknowledged to bring with it a wide range of adverse environmental impacts (Biggs *et al.,* 1998). One of them is the significant reduction of the capacity of floodplains to attenuate floods and retain water, thereby reducing water transit time and changing hydrographs by inducing higher peak discharges (Kronvang *et al.,* 1998). Moreover, the reduction in hydrological contact between streams and their adjacent floodplains reduces their nutrient retention capacity significantly (Iversen *et al.,* 1993; Holmes and Nielsen, 1998). The drainage of floodplains can cause hillslope water to move rapidly across the floodplain, minimising the potential impact of any buffering processes. Furthermore, the riparian zone itself also becomes a source of pollution, the more so given the proximity to the channel (Burt *et al.,* 2002a).

Nutrient pollution, and specifically nitrogen (N) pollution, is degrading surface water (Cherry *et al.,* 2008) and groundwater (Rivett *et al.,* 2008) quality throughout Europe. Human activities such as excessive fertiliser application and the combustion of fossil fuel has increased the availability of reactive N into the biosphere, which now exceeds the rate of biological nitrogen fixation in native terrestrial ecosystems (Davidson and Seitzinger, 2006; Galloway *et al.,* 2008). Nitrate specifically, being a highly water soluble anion, persists in water bodies where it can cause eutrophication (Jacobs and Gilliam, 1985) and a range of associated effects, including damage to fisheries in coastal systems (Rabalais, 2002). Eighty percent of European surface waters exceed the European Commission's drinking water standard of 50 mg NO_3^- L^{-1} (Molenat and Gascuel-Odoux, 2002). In England and Wales, 28 % of rivers exceed N concentration of 30 mg NO_3^- L^{-1} (Environment Agency, 2007a). In addition, nitrate has been found to be toxic to both human and animal health. When consumed in drinking water it can cause a condition known as methemoglobinemia linked to brain damage and death by suffocation in infants and asphyxiation in livestock (Prasad and Power, 1995). Nitrite

produced from the reduction of nitrate may also react in the stomach to form carcinogenic nitrosamines (Starr and Gillham, 1993; Prasad and Power, 1995). The above suggest that the control of nitrate in freshwater systems is important from both an environmental and human health perspective (Martin *et al.,* 1999).

Within the next decades, the sharp increase in human population combined with economic expansion will lead to greater pressures on freshwater resources (Tockner and Stanford, 2002). The effects of growing water consumption will also be accentuated by land-use changes and by changes in the flow and flood regime driven by climate change (IPCC, 2007). Because rivers and floodplains are among the most threatened ecosystems worldwide (Vitousek *et al.,* 1997), one of the major challenges will be to meet increasing resource demands while conserving aquatic ecosystems and the ecosystem services they provide for future decades (Tockner and Stanford, 2002).

1.4 *River - floodplain restoration*

Over the last few decades, in several countries in Northern Europe there has been a desire to re-instate the natural functioning of river-floodplain systems. The objectives of such river restoration have been diverse, including increased nutrient retention, improved summer low flows, increased floodwater storage and therefore reduced flood risk downstream, minimised maintenance costs and improved fishery, recreation, landscape and ecological value (Holmes and Nielsen, 1998).

However, Buijse *et al.,* (2002) in a review of the state of floodplain rehabilitation in Europe and North America concluded that relatively few cases of river-floodplain restoration, that include the riparian zone and the floodplain, have been documented and that most of the projects focus narrowly on permanent aquatic habitats.

However, due to the influences of the EU Common Agricultural Policy in intensifying food production, and then its set-aside policies for agricultural land, there has been an increasing awareness of the value of river and watershed restoration for integrated catchment management (Holmes and Nielsen, 1998). More recently, the Water Framework Directive (WFD) and the 11 water related Directives associated with it provide a mechanism for the support of floodplain restoration (Blackwell and Maltby, 2005). The WFD by taking a river basin approach acknowledges that what happens in

waters depends substantially on what happens on land in the catchments (Wharton and Gilvear, 2007). It is impossible to manage a waterway without sympathetic management of the land, though almost all previous legislation had ignored this and was directed largely within the bounds of the wetted perimeter (Moss, 2008). The importance of managing water and land together is being increasingly recognised and articulated, for the purpose of flood and coastal erosion risk management (Defra, 2004), but also by integrating the different aspects of water policy (water quality, water resources and flood management) (Defra, 2002). For example, combined river-floodplain management can benefit flood storage, aquifer recharge, water quality, low flow water demand and biodiversity (Wharton and Gilvear, 2007).

The majority of floodplain restoration projects so far, have had as main target to increase the flood storage capacity of the floodplain, providing in this way sustainable, inexpensive flood defence and as a side effect ecological benefits for the floodplain, in terms of increased biodiversity. This is documented in the 14 case studies of floodplain restoration presented as part of the EcoFlood Guidelines by Blackwell and Maltby (2005) and in a recent compilation of wetland restoration studies by Acreman *et al.* (2007).

There are numerous studies documenting the ecological effects of river restoration for macrophytes (Biggs *et al.,* 1998; Claassen, 2000; Clarke and Wharton, 2000), macroinvertebrates (Biggs *et al.,* 1998; Friberg *et al.,* 1998; Harrison *et al.*, 2004) and fisheries (Kelly *et al.,* 1998; Pretty *et al.,* 2003). Fewer studies refer to ecological restoration of the actual restored floodplain (Bissels *et al.*, 2004). Most studies on the conditions needed for sustainable ecological development of floodplains have focused on hydrological and geomorphological rather than biogeochemical issues (including nutrient availability and limitation). Lamers *et al.* (2006) review the biogeochemical constraints on the successful ecological restoration of floodplains and conclude that N, P and toxic contaminants from heavily fertilised floodplains can impose serious problems in achieving high ecological targets in restored floodplain wetlands. Therefore, biogeochemical knowledge is a prerequisite for successful ecological rehabilitation, ensuring that space for the river also implies space for ecologically sound floodplains.

Very few floodplain restoration projects have had as a main target the increase of nutrient retention capacity of the floodplain. Only three out of the 14 case studies presented in Blackwell and Maltby (2005) had as a key target the enhancement of water quality through nutrient retention on the floodplain. Two of the three projects were in Denmark (Hoffmann *et al.*, 1998a and 1998b; Hansen, 2003), where in 1998 a national programme for the restoration of freshwater wetlands was initiated with the purpose of reducing N-load to downstream recipients (Hoffmann and Baattrup-Pedersen, 2007). Other countries in Europe have recently added as an objective the improvement of water quality in flood retention areas (e.g. polders in the Upper Rhine), but these projects are still at the planning or the construction stage (Brettar *et al.*, 2002).

It should be acknowledged that river-floodplain restoration and rehabilitation are long-term undertakings. The inherent complexity of floodplain ecosystems and our limited scientific understanding of their spatio-temporal dynamics significantly constrain planning (Buijse *et al.*, 2002). Of all the political, economic and technical constraints on floodplain restoration, perhaps the most significant is the lack of scientific knowledge (Brookes, 1996). A handful of studies in large floodplains of European rivers (Tockner *et al.*, 1999; Olde Venterink *et al.*, 2003; Van der Lee *et al.*, 2004) have provided evidence that nutrient in general and specifically nitrogen removal is possible via a number of pathways, while very few studies have actually evaluated those pathways in restored floodplains (Hoffmann *et al.*, 1998a; Sheibley *et al.*, 2006; Orr *et al.*, 2007).

There is therefore a need for further scientific evidence to elucidate the effect of the increased hydrological connectivity in restored river-floodplain systems on the spatial and temporal efficiency of the biogeochemical cycling of nutrients with the aim of informing the design of floodplain restoration projects for maximising N, P and sediment retention.

Chapter 2: Literature Review

2.1 *Introduction*

Hydrologic connectivity, a key process in riverine floodplains, refers to water-mediated transfer of energy, matter and organisms within or among elements of riverine corridors (Tockner and Stanford, 2002). Inundation of floodplains is a complex phenomenon caused by different water sources via multiple pathways (Tockner and Stanford, 2002). These pathways together with the flood hydroperiod (i.e. flood duration, frequency and magnitude) largely control the transfer of nutrients, and specifically nitrogen, on the floodplain (Pinay *et al.*, 2002). Subsequently, several mechanisms can affect the transformation of N-species (Cirmo and McDonnell, 1997), while the relative importance of each mechanism will determine the final fate of N, that is whether it will be permanently removed or re-cycled in the floodplain, and thus the effectiveness of the restored floodplain as a N sink contributing to the improvement of water quality.

This literature review describes the various hydrological mechanisms likely to influence the supply and transformation of nitrate in a re-connected temperate floodplain. Moreover, it gives an overview of the possible processes of nitrate attenuation, their controlling factors and the reasons for their spatial and temporal variability, while discriminating between those processes that result in the permanent removal of nitrate from the system and those that re-cycle nitrate through its different forms. Finally, it provides the rationale for the development of a decision support tool aimed at the evaluation of candidate areas for floodplain restoration, at the landscape scale, with respect to their nitrate removal capacity and/or the assessment of the ability of re-connected floodplains to effectively remove nitrate. This chapter concludes with the presentation of the aim and objectives of the study.

2.2 *Hydrological connectivity between the river and the floodplain*

Several researchers have emphasised the importance of hydrological controls over the biogeochemical functions of floodplains and riparian zones (Hill, 1996; Cirmo and McDonnell 1997; Burt, 2005). The ability of a floodplain to attenuate nitrate depends fundamentally on the hydrological properties of the floodplain sediments. Permeable alluvium favours subsurface flow, providing the opportunity for interaction between water and sediment. Impermeable alluvium tends to deflect influent groundwater through aquifers below the floodplain or across the floodplain surface; in either case, the attenuation capacity of the floodplain is greatly reduced (Burt, 1997). There is the need, therefore, to establish the hydrological conditions under which particular nitrate attenuation processes can operate effectively. The precise pathway taken by water draining from farmland or inundating the banks of the river will determine whether that water is resident within the floodplain system for a sufficiently long period of time to allow internal processes to operate effectively. The hydrological pathways govern not only the flux of sediment and nutrients into and across the floodplain but may also be responsible for the concurrent transport of substrates required for their effective removal or transformation (Burt and Haycock, 1996).

The majority of floodplain hydrology studies have concentrated on hillslope runoff processes in steep headwater catchments (Burt *et al.*, 2002b) without considerable attention being paid to wide, low-angle floodplains, of higher stream order, where drainage from surrounding slopes, and also overbank flows, may be expected to particularly favour the development of extensive areas of surface saturation (Burt and Haycock, 1996) and thus affect the biogeochemical transformations of nitrate.

Large parts of agricultural land in southern England, and also in other North and Central European countries, are found on medium to low permeability clay-silt alluvia bordering streams through gently sloping floodplains. There is therefore the need to research the specific hydrological mechanisms operating under these topographical and lithological conditions that can in turn directly affect their nitrate attenuation capacity. Therefore, this literature review focuses on the specific conditions that are expected to influence the groundwater (GW) - surface water (SW) interactions in the landscape setting of a temperate lowland medium-permeability floodplain.

2.2.1 *Topographical and lithological controls on surface water - groundwater interactions*

The hydrological exchange between the GW and the SW at the landscape scale is a function of: 1) the distribution and magnitudes of hydraulic conductivities associated with the alluvial-plain sediments; 2) the relation of stream stage to the adjacent groundwater level; and 3) the geometry and position of the stream channel within the alluvial plain (Woessner, 2000). The direction of the exchange processes varies with hydraulic head, whereas flow (volume/unit time) depends on sediment hydraulic conductivity (Sophocleous, 2002).

Recent attention has focused on the important role that subsurface lithology and stratigraphy play in controlling nutrient cycling and transport in riparian zones (Devito *et al.* 2000; Hill *et al.* 2004; Schilling and Jacobson, 2008). Because groundwater flowpaths in valleys are often complex with highly conductive sand and gravel lenses interspersed with less permeable silts, clays and peats (Haycock and Burt 1993; Simpkins *et al.* 2002; Hill *et al.* 2004), groundwater residence times are strongly affected by the stratigraphy of floodplains and riparian zones (Cirmo and McDonell, 1997).

Alluvia that are too permeable may not be able to sustain high water tables for long periods, while too impermeable alluvia allow little or no flow through and thus minimise the opportunity for nitrate removal (Burt and Pinay, 2005). A confining layer at a shallow depth increases the interaction of subsurface flow with vegetation root systems and surface soils and enhances the potential of the riparian zone for nitrate removal (Hill, 1996). In contrast, gravel layers in the soil profile beneath less permeable sediments can be zones of preferential subsurface flow across the riparian zone (Burt *et al.*, 1999) and thus hillslope runoff may be directed straight to the stream with little chance of interacting with the sediments of the riparian zone (Burt, 2005). Moreover, gravel lenses underlying less permeable layers enhance the drainage of these layers by stronger downward gradients of GW recharge, providing they are connected to higher permeability zones (Burt and Haycock, 1996).

Vidon and Hill (2004b) studied the effect of landscape position and subsurface lithology on the water table dynamics in eight riparian zones across Ontario in Canada. They

concluded that a minimum depth of two meters for permeable sediments above a confining layer was adequate to retain the hydrological connection with an upland aquifer throughout the year. Moreover, in gently sloping riparian zones (slope <5 %) the GW table was primarily controlled by the stream stage, and under baseflow conditions flow reversal from the stream towards the riparian zone was observed. On the other hand, in riparian zones with steep topography (slope >15 %) a continuous hillslope discharge through the riparian zone towards the river was predominant throughout the year.

Schilling and Jacobson (2008) related the water table fluctuations in the riparian zone of an incised stream to subsurface lithology and land management. They showed that the nitrate-rich sediments of the recent Holocene alluvium were a potential nitrate source to the stream, due to the low GW table level in the near stream zone affected by the low stage of the incised stream (Schilling *et al.,* 2006) and the prevalence of aerobic soils promoting ammonium nitrification. In contrast, in a tributary of the River Seine, where stage is regulated and kept level throughout the year, a shallow water table is maintained at the near stream zone promoting nitrate removal mainly via denitrification (Curie *et al.,* 2009). Sabater *et al.* (2003) showed that nitrate reduction is possible in riparian zones in a wide European climatic range and the influence of vegetation cover is minimal compared to the effect of the water table level creating the necessary conditions for denitrification to occur.

Therefore, soils of medium hydraulic conductivity in combination with the appropriate geomorphology (i.e. low surface gradient encouraging high water tables) can increase the residence time of water in the floodplain creating more favourable conditions for nitrate removal.

2.2.2 *Hydrological mechanisms of surface water - groundwater interactions*

Catchment hydrologic dynamics have traditionally been described by combinations of Hortonian infiltration excess overland flow (Horton, 1933), saturation excess overland flow (Dunne and Black, 1970), near-stream groundwater ridging (Sklash and Farvolden, 1979), shallow near-surface flow through more transmissive soil layers (Hewlett and Hibbert, 1967), and macropore flow (McDonnell, 1990). For N transport, it is important to distinguish between these possible flowpaths and their link to the near-stream zone,

as the different mechanisms may result in significant differences in the water residence time and loading of N that can in turn affect the efficiency of nitrate attenuation processes (Cirmo and McDonnell, 1997). Additionally, hydrologic functions of near-stream unsaturated zones include flood storage and peak flow moderation (Daniel, 1981), discharge or exfiltration (and occasionally recharge) to local surface waters, and maintenance/moderation of baseflow (Novitzki, 1979). The response of any particular catchment may be dominated by a single mechanism or by a combination of mechanisms, depending on the magnitude of the rainfall event, the topography of the catchment, the antecedent soil-moisture conditions, and/or the heterogeneity in soil hydraulic properties (Sophocleous, 2002).

2.2.2.1 *Infiltration Excess Overland Flow (IEOF)*

Regarding the surface runoff generation mechanisms during a storm event, the concept that dominated for many years was the Infiltration Excess Overland Flow (IEOF) by Horton (1933). When rainfall intensity exceeds the infiltration capacity of the soil, the excess begins to fill up surface depressions; once these are full, the excess overflows downslope and surface runoff begins (Figure 2.1A). The infiltration capacity of the soil decreases asymptotically with time as the upper part of the soil becomes progressively saturated from the surface down. Changes in the soil surface (e.g. swelling of clay particles, in-washing of fine particles into pores, compaction by rainbeat) may also reduce infiltration capacity during the course of a storm (Burt and Haycock, 1996). IEOF can generate large flood peaks and is often associated with soil erosion. However, since its residence time is short and there is little interaction with the soil, the solute content of IEOF is usually low and it resembles the rainfall characteristics (Burt and Pinay, 2005).

Ideal conditions for the generation of IEOF are found where bare soil is exposed to raindrop impact, as in arid and semi-arid areas, since in most cases, vegetation cover increases the soil infiltration capacity and restricts IEOF only in very intense storms (Ward and Robinson, 2000). Few riparian buffer zone studies have related surface runoff generation by IEOF to the nutrient transport to near-stream zones and the streamflow. The frequency of IEOF occurrence increased as a result of deforestation and pasture establishment with the subsequent effect of surface soil compaction by cattle in a hillslope pasture of the south-western Brazilian Amazon. Although

subsurface stormflow dominated annually, storms with rainfall intensity >5 mm h^{-1} produced IEOF, which was responsible for increased export of phosphorus from upslope (Biggs *et al.*, 2006). A eucalyptus riparian buffer in Western Australia produced IEOF during storm events throughout the year due to crusting of surface soils, while an adjacent grass buffer zone displayed only subsurface runoff and saturation excess overland flow during the winter months, when the water table was near the surface. Therefore, these two types of buffer zones in the same catchment were at the same time sinks and sources of runoff, while the high hydraulic conductivity of the subsurface sediments did not allow adequate residence time for nutrient transformations (McKergow *et al.*, 2006). Land use zones in a temperate floodplain setting where grazing activity occurs may potentially become sources of IEOF. However, due to the existence of permanent pasture throughout the year, the infiltration capacity of the soil would be expected to be high and therefore minimise the relative role of IEOF.

2.2.2.2 *Saturation Excess Overland Flow (SEOF)*

When the rainfall intensity is less than the infiltration capacity, falling precipitation infiltrates the subsurface causing the water table to rise to the ground surface, first in the shallow water table areas immediately adjacent to stream channels, and subsequently in the lower valley slopes (Ward and Robinson, 2000). In these surface-saturated areas infiltration capacity is zero, so that the additional precipitation causes the generation of saturation excess overland flow (Dunne and Black, 1970). SEOF usually is a mixture of 'return flow', exfiltrating 'old' soil water, and 'direct runoff', 'new' rainfall unable to infiltrate the saturated surface (Burt and Pinay, 2005), as shown in Figure 2.1B.

The rapid water table rise in near stream zones has also been attributed to the conversion of a tension-saturated zone, or capillary fringe, overlying the pre-storm water table to a zone of positive potentials. When even a small amount of water percolates to the top of this zone, the menisci that maintain the tension saturation are obliterated and the pressure state of the water is immediately changed from negative to positive (Gillham, 1984). If the water table and capillary fringe are close to the soil surface, then only small amounts of rainfall are necessary to saturate the soil profile completely (Sophocleous, 2002). The thickness of the capillary fringe zone is inversely proportional to median particle size, and can be affected by porosity, permeability and particle size distribution (Cirmo and McDonnell, 1997).

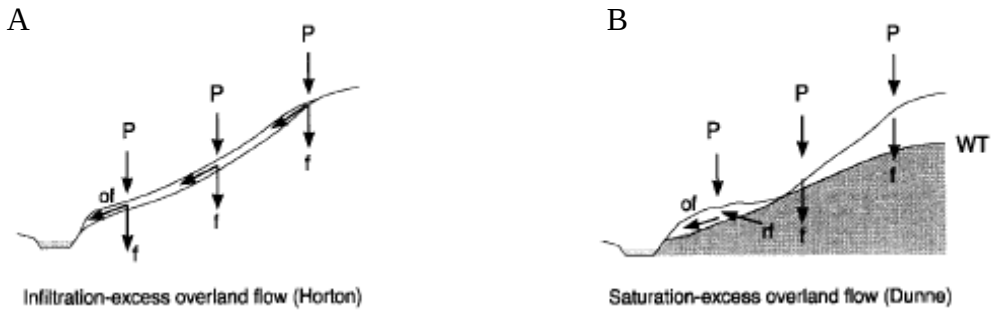

Figure 2.1: Mechanisms of surface runoff production. P; Precipitation, f; Infiltration, of; Overland flow, rf; Return flow, WT; Water table (adapted from Sophocleous, 2002).

SEOF generation has been rarely studied in temperate floodplains, while most SEOF studies refer to tropical or semi-arid climatic conditions. SEOF occurred at roughly equal proportions to IEOF in a pasture hillslope of the southwestern Brazilian Amazon during storm events and it was related to the export of N and K in the near stream zone (Biggs *et al.,* 2006). SEOF was observed together with subsurface runoff during winter storms, when the water table was near the surface, in a deciduous forest and eucalyptus riparian buffer zones in western Australia (McKergow *et al.,* 2006). In a semi-arid, cultivated, Mediterranean environment, SEOF was observed to occur at the near-stream edge of the valley and in surface depressions (Ribolzi *et al.,* 2000). Finally, the contribution of GW to the flood peak hydrograph through the generation of SEOF at the near stream zone in a steep headwater riparian zone in Germany was shown to be >80 % (Wenninger *et al.,* 2004). The above studies indicate that SEOF can be of importance in a variety of climatic gradients but it is mostly localised in near stream and depression zones with high water table. This mechanism may be of importance in a temperate floodplain for creating surface saturation conditions especially in surface micro-depressions in areas of low angle relief. This in turn can affect nitrate attenuation processes by creating spatial activity ‘hotspots’ in those surface depressions away from the stream margin.

2.2.2.3 *Subsurface stormflow*

It is difficult to discriminate between SEOF and subsurface stormflow since both depend to a large extent on the generation of flow through the soil profile. Subsurface stormflow will be most important where steep slopes with permeable soils are contiguous with the channel (Anderson and Burt, 1990). Although subsurface flow through porous media is usually sluggish, Beven (1989) identifies three mechanisms to account for fast subsurface contributions to the storm hydrograph: 1) translatory flow; 2) macropore flow; and 3) groundwater ridging. Translatory flow (Hewlett and Hibbert, 1967) or piston flow develops when, according to the kinematic theory, pressure waves, caused by infiltrating precipitation, push stored water in hillslope hollows downslope. Rapid subsurface responses to storm inputs may also be the result of fast flow through larger non-capillary soil pores, or macropores (McDonnell, 1990). Macropore flow is particularly important in cracked clay soils (Heppell *et al.,* 2000) and in forest soils (McGlynn *et al.,* 2002). Macropore flow can occur either when the soil matrix is saturated or after surface ponding (Anderson and Burt, 1990). The formation of a saturated groundwater wedge (Sklash and Farvolden, 1979) in low slopes at the near stream zone has been observed to contribute to stormflow at the initial rising limb of an event. As the event proceeds, the saturated wedge advances upslope on the hillslope forming a groundwater ridge, which upon recession discharges to the near stream zone maintaining a higher water table at the low slope areas (Burt and Pinay, 2005). Although subsurface stormflow is not expected to be of great significance in the low angled floodplains of mid-catchment locations (as opposed to steep hillslope landscapes) its importance may vary depending on the subsurface lithology. Lateral subsurface flow will be one control on the residence time of the storm water in the subsurface, thus increasing or decreasing the potential for further nitrate transformations below the soil surface.

2.2.2.4 *Bank storage and reversed groundwater ridge*

In gently sloping, wide floodplains, surface inundation is likely to remain for longer periods (Bates *et al.,* 2000); in these areas, channel-floodplain interactions are perhaps more important than the hillslope-floodplain linkages (Pinay *et al.,* 1998). Under low precipitation conditions, baseflow in many streams is maintained via groundwater discharge from the adjacent floodplain. However, during high precipitation, the stream stage with the contribution of falling rainfall, surface and subsurface runoff, increases

and the river loses water to bank infiltration, which reduces the flood level and recharges the aquifer. The volume of this bank storage depends on duration, height, and shape of the flood hydrograph, as well as on the transmissivity and storage capacity of the aquifer (Sophocleous, 2002). Figure 2.2 illustrates the bank storage process as described by Dingman (1994). In (a) baseflow conditions are maintained through groundwater discharge from the floodplain. In (b) a flood peak occurs and the river stage rises above the GW table reversing the hydraulic gradient from the river to the floodplain. In (c) the flood peak passes and while the river stage declines, SW-GW interaction is maintained for a short time in both directions but ultimately a streamward gradient is re-established.

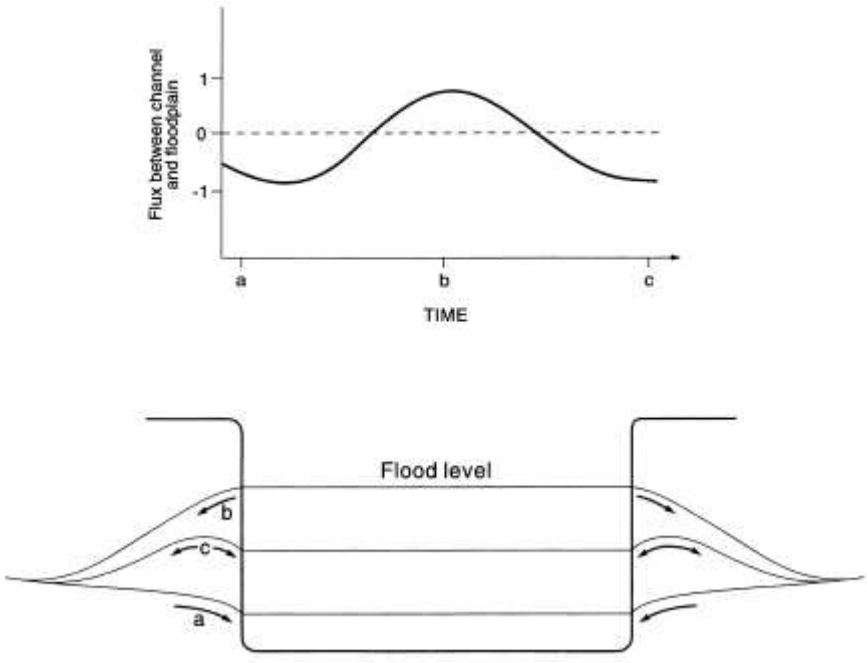

Figure 2.2: The bank storage process. For details see text. (after Burt *et al.*, 2002b based in part on Dingman, 1994).

A number of studies (e.g. Pinder and Sauer, 1971; Hunt, 1990) have shown that the infiltration of river water during bank storage can result in attenuation of the downstream flood peak. However, until recently very few studies were concerned with the detailed groundwater table fluctuation in relation to river stage during flood events and its effect on the conditions for nutrient biogeochemical transformations. Near stream bank storage has been observed during high flow conditions in an incised stream

in Iowa (Schilling *et al.,* 2004, 2006) contributing to the shallow water table near the break in slope. However, during low flow, channel incision lowered the water table in the near stream zone creating a potential nitrate source area to the stream. In contrast, bank storage and shallow water table conditions were maintained throughout the year between a stage regulated tributary of the River Seine and a ditch running parallel to the tributary which also collected hillslope runoff, thus creating an effective nitrate sink (Curie *et al.,* 2009).

Detailed modelling and field studies in a lowland floodplain of the River Severn, UK, (Stewart *et al.,* 1999; Bates *et al.,* 2000; Burt *et al.,* 2002b and Jung *et al.,* 2004) have produced evidence that a reversed groundwater ridge with direction from the river across the floodplain towards the base of the hillslope is produced during in-bank and out-of-bank events effectively 'damming' hillslope contributions of subsurface stormflow to the near-stream zone. The flow velocities observed from hydrometric data could not have been explained by Darcian one-dimensional GW flow due to the low saturated hydraulic conductivities of the floodplain sediments. Instead Jung *et al.* (2004) suggested that the almost simultaneous increase of the water table with the rising river, at about the same rate, could only be explained by a kinematic wave similar to translatory or 'piston' flow (Anderson and Burt, 1982) that pushes 'old' floodplain water at a perpendicular direction away from the river towards the floodplain. During the recession limb of the flood, the hydraulic gradient reverses from the floodplain to the river and therefore the hillslope-floodplain connection is re-established contributing further to the maintenance of a high water table in the near-stream zone during the discharge period. Furthermore, the work by Jung *et al.* (2004) showed that the accumulation of storm runoff at a hillslope hollow during the reverse GW ridge induced down-valley flow, parallel to the stream, highlighting the need for more complex three-dimensional modelling of floodplain-hydrology dynamics rather than the traditional 2D approach (Bates *et al.,* 2000).

Over the last decade, the occurrence of a reversed groundwater ridge has been shown in: lowland semi-arid riparian zones during high flow conditions (Martí *et al.,* 2000; Butturini, *et al.,* 2003; Lamontagne *et al.,* 2005; Rassam *et al.,* 2006; Schilling *et al.,* 2006); in temperate riparian zones throughout the year at baseflow conditions (Duval and Hill, 2006; Hill and Duval, 2009); or during low flow conditions when the water

table on the floodplain drops below the river stage (Burt *et al.*, 2002a; Vidon and Hill, 2004b). The relatively widespread occurrence of the reversed GW ridge mechanism seems to support the proposition that the limits of the hyporheic zone, defined as a continuum containing water from both the groundwater table and the river channel (Jones and Holmes, 1986), may extend up to the hillslope break during flood events (Burt *et al.*, 2002b).

The above studies suggest that the bank storage and/or the reversed groundwater ridge mechanisms can occur at various lithological and landscape settings depending mainly on the relative position of river stage and groundwater table heights. Furthermore, this mechanism can further influence subsurface nitrate attenuation by the provision of nitrate loading at the near stream zone and through the promotion of a higher water table closer to the soil surface.

2.2.2.5 *Overbank flooding*

River flood events, under climatic conditions conducive to flooding, are a product of the complex interactions between catchment character, network routing dynamics, and both local channel and valley hydraulics. In general, flood frequency (number of events per unit time) increases with reduced upstream storage attenuation of high flows and locally inefficient transport, whereas flood duration (length of inundation per event) increases when both local and catchment transport hydraulics are less efficient and result in longer total periods of event-flow transport (Bedient and Huber, 2002).

Lewin and Hughes (1980) summarise the hydrological processes involved in the movement of water between a river and its floodplain and also show that these processes operate in a specific order as a flood rises (inundation sequence) and recedes (recession sequence). Rising GW and infiltration of precipitation are the first inundation steps, while stage rise, although sometimes delayed by bank storage, eventually creates overbank spilling and filling of surface depressions. As individual depressions fill up they amalgamate and lead to a transient (i.e. observed only during the flood) current occupying the whole floodplain. Recession processes operate at the same time as inundating ones, with the floodplain acting as part of an equilibrating throughput system. However, once the overbank spilling ceases, movement within the inundated zone declines through overbank return and discharge by ebb channels, and discrete

ponds remain in topographic lows to gradually shrink with the combined effect of infiltration and evaporation. The relative importance of the different inundation and recession sequence steps depends on the conductivity of the surface, defined in turn by the flood hydrograph characteristics and the hydraulic characteristics of the surface (floodplain relief and roughness). Moreover, Mertes (1997) considered the effect of multiple 'local water' sources such as, direct rainfall, tributary water, overland runoff and rising groundwater levels that may create flooded surfaces before bankfull discharge is reached. When eventually overbank flooding occurs, the river water will mix with the 'local' water according to the composition and the pressure distributions between the different water bodies creating a 'perirheic' zone.

The importance of overbank flooding as the main mechanism responsible for the hydrological connectivity between river-floodplain that in turn influences the exchange processes of matter and organisms across river-floodplain gradients, was emphasized by the introduction of the Flood Pulse Concept (FPC) by Junk *et al.* (1989), for large tropical river-floodplain systems with predictable flood pulse of long duration under dry antecedent floodplain conditions, and it was recently expanded by Tockner *et al.* (2000) to include temperate floodplains.

Even though different combinations of flood frequency and duration can result in highly distinct floodplain conditions (Baker and Wiley, 2009), most floodplain hydrology studies lack explicit distinction between flood frequency and flood duration, while floods are typically defined with respect to bank-full discharge and not necessarily individual floodplain surfaces (Dunne and Leopold 1978). The specific flow paths between SW-GW that affect the surface inundation pattern have been described in detail mainly for wetlands (Waddington *et al.*, 1993; Bradley, 2002; Andersen, 2004) rather than lowland floodplains with intermittent surface saturation, while other studies have focused on the surface water recharge of alluvial aquifers (Winter, 1995).

Despite the importance of overbank flooding for energy, matter and organisms exchange between the river and the floodplain, the detailed sequence of events during surface inundation has not been adequately studied in lowland temperate floodplains. Following river-floodplain restoration, increased frequency of overbank flooding is usually observed. There is therefore scope for a detailed investigation of this mechanism

which is expected to significantly affect the transport of nitrate and the conditions for its transformation in restored lowland floodplains.

2.2.3 *Effect of hydrological flow paths on nitrate cycling in re-connected floodplains and riparian zones*

The various hydrological mechanisms operating during and between flood events and leading to variable degrees of SW-GW interaction between hillslope, floodplain, the near-stream zone and the stream itself have a marked effect on the transport and transformation of nitrate along these flowpaths. Cirmo and McDonnell (1997) compiled a comprehensive review of the hydrological and biogeochemical controls on nitrate transport in temperate forested catchments while more recently, Burt and Pinay (2005) extended this approach to lowland agricultural catchments.

Figure 2.3 summarises the main possible routes of event and pre-event water interaction, in a model lowland hillslope-floodplain setting, with respect to their likely effect on nitrate concentration in SW and GW. 'New' event water, low in nitrate concentration, may reach the stream quickly via direct precipitation, IEOF, SEOF or rapid macropore flow discharging straight to the stream (not shown in Fig. 2.3). The water table is rising from its 'pre-event' position through soil matrix, macropore flow and possibly the capillary fringe effect, and lateral subsurface flow begins towards the stream while nitrate concentration is increasing through mixing of 'event' and 'pre-event' water and flushing of previously unsaturated soil. As the mixed source subsurface flow passes through the saturated near-stream zone, nitrate concentration can be reduced before reaching the stream, or if the near stream zone is bypassed by return flow it could become a source of nitrate to the stream. Additionally, the near stream zone could be responsible for flushing accumulated nitrate directly to the stream, especially during re-wetting after a dry period (Cirmo and McDonnell, 1997). Moreover, the near stream zone could be bypassed by rapid groundwater flow of mixed nitrate concentration where permeable strata are found below the floodplain alluvium (Burt *et al.*, 1999). However, the conceptual model of Figure 2.3 does not include the effect of overbank flooding on nitrate transport and transformation, as the focus is on a hillslope-floodplain setting, and therefore this potentially important mechanism for lowland floodplains should be further investigated and subsequently added to the existing model.

Both reviews (Cirmo and McDonnell, 1997; Burt and Pinay, 2005) have emphasised the critical role of the near stream zone in decoupling hillslope hydrology from biogeochemical transformations of nitrate. The possibility and effectiveness of this decoupling will depend on the opportunity for mixing of different water sources at the zone and the residence time of the flow paths. Therefore, it is important to identify where within a catchment saturated near-stream zones are located (Burt and Pinay, 2005).

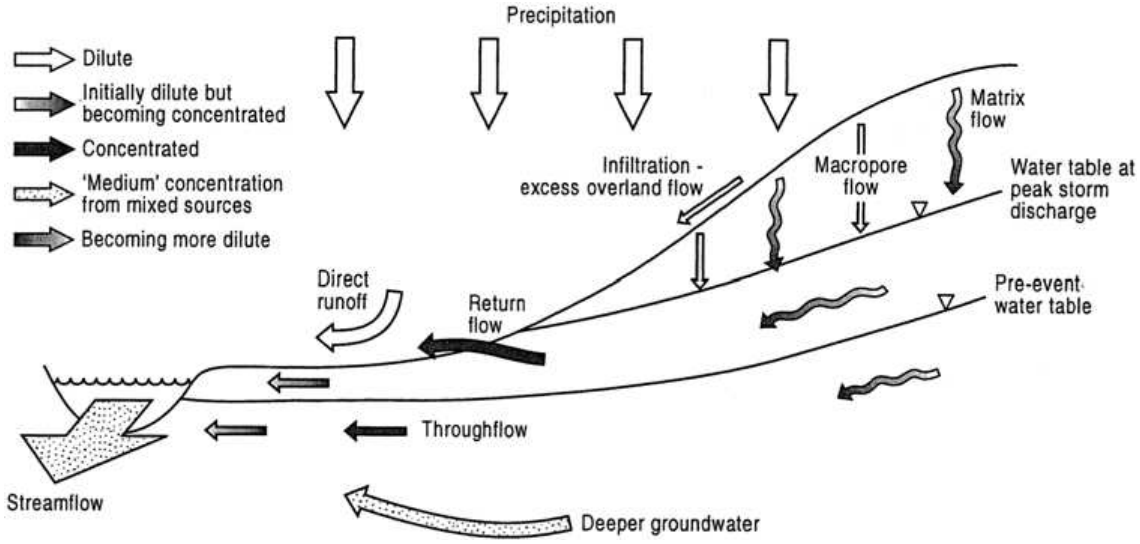

Figure 2.3: A schematic diagram of nitrate transport within a lowland hillslope-floodplain setting (after Burt and Pinay, 2005 and references therein). Direct runoff means SEOF.

Several studies have provided evidence of nitrate transformation along subsurface flowpaths in floodplains and riparian zones. Some floodplain hydrology studies have used Cl^- as a conservative tracer in order to discriminate between nitrate dilution along subsurface flowpaths and biological removal, mainly via denitrification and plant uptake (Pinay *et al.,* 1998; Sanchez-Perez *et al.,* 1999; Devito *et al.,* 2000; Clement *et al.,* 2003; Butturini *et al.,* 2003; Baker and Vervier, 2004; Hefting *et al.,* 2006a; Schilling *et al.,* 2006; Curie *et al.,* 2009). This is because Cl^- is considered biologically inactive with regards to processes occurring in water bodies (Hill *et al.,* 1998). When there is lack of variability in Cl^- concentrations along a groundwater flow path, but the ratio NO_3^-:Cl^- displays similar variability as the NO_3^- concentration, then processes

other than physical mixing or dilution are likely to be responsible for nitrate reduction (Schilling *et al.*, 2006).

Nitrate removal rates have been very variable across different riparian floodplain settings and various hydrological flow paths. In some cases physical mixing was found to be more important than biological removal, as for example in Pinay *et al.* (1998), where extensive mixing between river water and groundwater, in a large floodplain of the Garonne River, was found responsible for most of the nitrate reduction while denitrification accounted only for 10 - 25 % of the reduction. Moreover, in the Ill floodplain (eastern France), 95 % of nitrate was reduced by dilution along the groundwater flowpath, while very little reduction was observed in the streambed (Sanchez-Perez *et al.*, 1999).

On the other hand, several floodplain studies have documented effective nitrate removal along SW-GW flowpaths that could not have been explained only by mixing and dilution of different nitrate sources, and therefore the importance of different biological removal mechanisms was highlighted. The relative importance between the different mechanisms was variable and depended on the specific conditions of each landscape. For example, in the Rhine floodplain (eastern France) nitrate inputs by river floods were reduced by 73 % in the shallow groundwater of the forested ecosystem, and only by 37 % in the meadow, highlighting the higher uptake efficiency of woody species compared to herbaceous vegetation (Takatert *et al.*, 1999). Exactly the opposite was observed by Hefting *et al.* (2006a) in the Netherlands, where the grassland buffer zone removed 63 % of the incoming nitrate load, while the forested buffer, showing symptoms of nitrate saturation, removed only 38 % of the nitrate load. However, it should be noted that floodplain type, vegetation species and differences in nitrate loading, can also affect the uptake efficiency in both grassland and forested type buffer zones. In the study of Clément *et al.* (2003) nitrate reduction ranged between 76 and 99 % and concentrated within the first 10 m from the hillslope boundary, limiting nitrate supply to the near-stream zone. Nitrate reduction was more efficient in winter when the vegetation was dormant and the mixing was minimum, indicating high denitrification rates.

To summarise, the ability of a floodplain to attenuate nitrate depends fundamentally on the hydrological properties of the floodplain sediments and the hydrological pathways

that govern not only the flux of nitrate and organic carbon into and across the floodplain but also the necessary conditions for effective nitrate attenuation. Medium permeability alluvia, where saturated hydraulic conductivity ranges between 10^{-5} - 10^{-2} cm s^{-1} (Bear, 1972), in gently sloping floodplains, allow adequate water residence times for nitrate attenuation processes to occur, while the occurrence of high permeability subsurface layers (saturated hydraulic conductivity >1 cm s^{-1}) may constitute conduits of fast subsurface flow limiting the interaction of GW nitrate with subsurface sediments. Hydrological mechanisms of surface runoff generation such as the IEOF and the SEOF, generally have little influence in nitrate transport, but can create localised surface saturation conditions, thus promoting nitrate attenuation processes, before the onset of more widespread inundation by overbank flooding. Subsurface flows in the form of stormflow and groundwater ridge, although they may be limited in their extent by low hydraulic conductivities, can contribute to nitrate loading especially in near-stream sediments. They can also maintain higher water tables in the floodplain, hence giving the opportunity for subsurface nitrate attenuation to occur especially between overbank flood events. Finally, overbank flooding, especially in intermittently saturated lowland floodplains, is expected to constitute the main mechanism of nitrate transport into and across the floodplain, while it also influences the conditions (i.e. redox potential, supply of necessary substrates) for the occurrence of nitrate attenuation processes.

Detailed studies of the hydrological event sequence during flooding in lowland floodplains are generally lacking. The objective of the present study is to identify the main hydrological mechanisms operating during and between the surface inundation of a re-connected floodplain and evaluate their relative importance with respect to their contribution to nitrate transport into and across the floodplain and to the creation of the necessary conditions for effective nitrate attenuation. Moreover, the spatial and temporal pattern of occurrence of the different mechanisms is expected to significantly influence the partitioning of nitrate attenuation between different processes as well as their relative efficiency.

2.3 *Nitrate attenuation in re-connected floodplains*

In the previous section, the role of hydrological flowpaths between river-floodplain for the transport of nitrate (Pinay *et al.*, 2002) and its subsequent transformation (Hill, 1996) was presented. Moreover, several studies where nitrate removal along SW-GW flowpaths could not be explained only by mixing and dilution of different nitrate sources have highlighted the importance of biological nitrate attenuation along these flowpaths. The focus, therefore, of the present section is to describe the different biological mechanisms involved in nitrate attenuation and identify the main controlling factors for their spatial and temporal variability in the context of temperate agricultural re-connected floodplains and riparian zones.

Nitrate attenuation mechanisms

Three possible mechanisms have been cited to explain the biological attenuation of nitrate in floodplains and riparian zones: 1) vegetation uptake; 2) microbial immobilisation; and 3) microbial heterotrophic denitrification (Martin *et al.*, 1999). Moreover, the chemoautotrophic reduction of nitrate to N_2, the dissimilatory reduction of nitrate to ammonium (DNRA) and the anaerobic oxidation of ammonium with nitrite to N_2 (Anammox) have also been shown to occur in a variety of ecosystems, but their role in floodplain nitrate attenuation has not yet been established (Burgin and Hamilton, 2007). The relative position of the three main biological attenuation mechanisms and also that of DNRA in the nitrogen cycle of floodplain soils is shown in Figure 2.4.

2.3.1 *Vegetation uptake*

Many studies have shown significant N uptake by plants in riparian floodplains (Peterjohn and Correll, 1984; Groffman *et al.*, 1992; Osborne and Kovacic, 1993; Haycock and Pinay, 1993; Zhu and Ehrenfeld, 2000; Hefting *et al.*, 2005). The morphological and physiological adaptations of the flood-tolerant species found in riparian floodplains frequently facilitate N uptake under low-oxygen conditions. However, the importance of plants as N filters may be reduced by restricted accessibility to water, when the water table is below the root zone or during storms, when concentrated surface flow and macropore-dominated percolation to deeper strata may restrict water availability to plants (Naiman and Décamps, 1997).

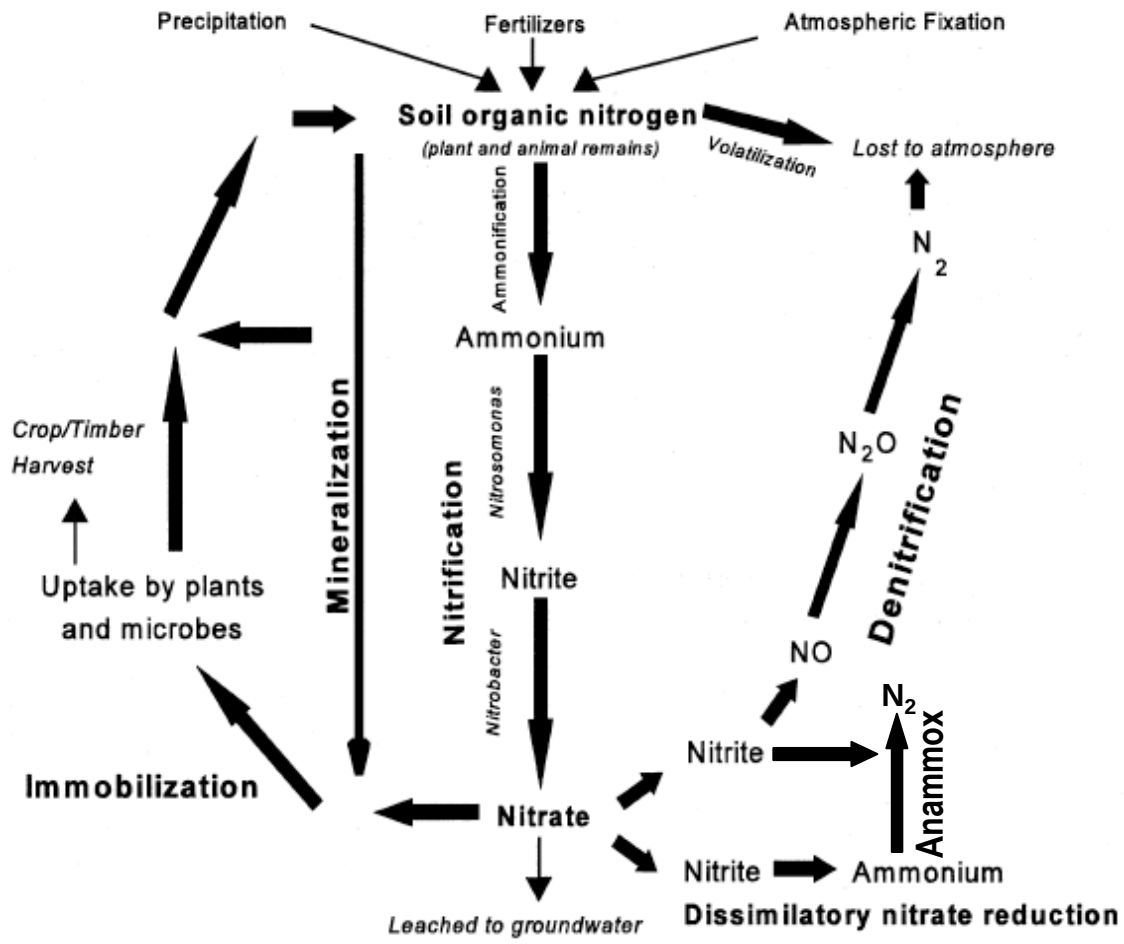

Figure 2.4: Nitrogen transformations in the nitrogen cycle in soils (adapted from Martin *et al.*, 1999).

The contribution of different vegetation types (forest versus herbaceous) to N retention has also been extensively studied, but the results have not been consistent. A number of studies have shown that forest cover is more effective in nitrate removal due to higher total biomass, (semi-) permanent storage of nutrients in wood and a deeper root system (Cooper, 1990; Osborne and Kovacic, 1993; Haycock and Pinay, 1993; Hefting *et al.*, 2005). Opposite results, i.e. higher nitrate removal efficiencies in grassland, were found by Groffman *et al.* (1991), Schnabel *et al.* (1996), Kuusemets *et al.*, (2001) and Mankin *et al.* (2007). Finally some studies have indicated no significant difference in N removal between vegetation types (Vought *et al.*, 1994; Lyons *et al.*, 2000; Syversen, 2002; Sabater *et al.*, 2003). Moreover, nitrate uptake by vegetation varies seasonally in its importance. Haycock and Pinay (1993) have inferred that vegetation uptake is the major retention mechanism during summer, because this is the season of maximum plant

growth and denitrification may be less important because soils become more aerated as the water table declines. However, this may not be necessarily true in regions where winters are mild (Hill, 1996) or during summer floods that can cause increased denitrification in conjunction with the higher temperature (Banach *et al.,* 2009).

Although there is no general consensus (Hefting *et al.,* 2005), most studies in riparian floodplains have indicated that denitrification is probably more important than plant uptake for nitrate removal (Verchot *et al.,* 1997; Schade *et al.,* 2001). This is because plants only temporarily retain nitrate, which returns to the available pool once mineralised, whereas denitrification permanently removes nitrate from the soil to the atmosphere. However, the relative importance of vegetation in N mitigation in floodplains may increase with biomass harvesting, e.g. mowing or logging (Hefting *et al.,* 2005). Furthermore, the presence of plants in riparian zones and floodplains has several indirect benefits for denitrification; plant litter provides habitat for microbe colonisation (Fennessy and Cronk, 1997), while root exudates together with dead leaves and roots are sources of organic carbon used in denitrification (Bastviken *et al.,* 2007; Frank and Groffman, 2009). The presence of vegetation in areas of saturated soils significantly increases oxygen in the soil through the formation of oxidised rhizospheres (Frank and Groffman, 2009), where nitrification can take place and be directly coupled to denitrification (Seitzinger *et al.,* 2006). Finally, vegetation tends to improve soil structure and leads to higher soil infiltration capacity (Vought *et al.,* 1994). Nitrate retention via plant uptake is not considered *per se* in the present study; however the indirect effect of vegetation through land use management on affecting the spatial variability of denitrification is taken into account.

2.3.2 *Microbial immobilisation*

Although many heterotrophic microbes can assimilate nitrate for growth, it appears that in the presence of ammonium, the latter compound is taken up preferentially (Hill, 1996). However, studies using the ^{15}N-isotope dilution method suggest that considerable microbial assimilation of NO_3^- occurs in agricultural and forest soils (Davidson *et al.,* 1992). Microbial assimilation of NO_3^- probably occurs at microsites where NH_4^+ is absent within the heterogeneous soil environment (Rice and Tiedje, 1989). Ambus *et al.* (1992) showed that in intact soil cores from a riparian fen soil that were low in ammonium, microbial assimilation of nitrate probably accounted for up to

20 % of the removed nitrate, while where NH_4^+ was present, the assimilation of nitrate was negligible. However, in an N-limited forest soil in Norway, nitrate immobilisation accounted for more than 85 % of nitrate removal as the microbial reduction of nitrate was limited probably by the availability of N (Bengtsson and Bergwall, 2000). As litter decomposition predominantly begins with plant senescence in autumn, the immobilization and retention of N in the litter fraction (decomposers) is most important during the dormant (winter) period. Moreover, low temperatures in this period limit N removal by denitrification activity (Maag *et al.,* 1997) and hence, in winter, immobilization may have a more significant role in N retention in floodplains (Hefting *et al.,* 2005). However, in temperate agricultural floodplains with N-rich soils, even if microbial assimilation of nitrate occurs, it will constitute a small fraction of the organic N pool that due to the short life cycle of the bacteria is rapidly re-mineralised and becomes available for further nitrification-denitrification cycles (Rivett *et al.,* 2008).

2.3.3 *Heterotrophic denitrification*

Heterotrophic denitrification, as classically defined, is the microbial oxidation of organic matter coupled to the reduction of ionic nitrogen oxides (nitrate, NO_3^- and nitrite, NO_2^-) to the gaseous oxides (nitric oxide, NO and nitrous oxide, N_2O), which may themselves be further reduced to dinitrogen (N_2) (Knowles, 1982). The general equation (2.1) if glucose acts as electron donor is (Wetzel, 2001):

$$C_6H_{12}O_6 + 4NO_3^- \rightarrow 6CO_2 + 6H_2O + 2N_2\uparrow \qquad (2.1)$$

It is a heterotrophic process of anaerobic respiration that occurs when respiratory denitrifiers use ionic nitrogen oxides to gain energy by coupling their reduction to electron transport phosphoryliation (Knowles, 1982). The electron-accepting capacity of denitrification is shown by equation (2.2) according to Tiedje *et al.* (1982):

$$2NO_3^- + 10e^- + 12H^+ \rightarrow N_2 + 6H_2O \qquad (2.2)$$

Denitrification can accept five electrons (e^-) per mole of nitrate reduced. Nearly all respiratory denitrifiers are facultative anaerobs that prefer to use oxygen (O_2) as a terminal electron acceptor, and in the presence of O_2, synthesis and activity of denitrifying enzymes is repressed (Tiedje, 1988). Denitrification has an endpoint at

nitrogen gas, in which the triple bond between the two N atoms makes it extremely stable and unreactive (Davidson and Seitzinger, 2006). Therefore, denitrification is considered as the most desirable nitrate reduction mechanism, since it represents a permanent removal of N to the atmosphere and completes the nitrogen cycle (Martin *et al.*, 1999).

However, denitrification can be arrested at any of its intermediate stages (Figure 2.4) with important consequences for health and the environment. For example nitrite is significantly more toxic than nitrate (WHO, 2004). However, nitrite is more reactive than nitrate and is stable only within a limited range of redox conditions. A build-up of nitrite may occur due to the time lag between the onset of nitrate reduction and the subsequent onset of nitrite reduction, as nitrite reductase is more sensitive to high O_2 concentrations (Betlach and Tiedje, 1981; Gale *et al.*, 1994). Nitric oxide (NO) and nitrous oxide (N_2O) are formed during denitrification but, in favourable conditions, transform rapidly to benign nitrogen gas. Both NO and N_2O contribute to acid rain, promote the formation of ground-level ozone and contribute to global warming; N_2O also destroys ozone in the upper atmosphere (Rivett *et al.*, 2008). Free NO is rarely observed because it transforms to N_2O rapidly under typical environmental conditions. It is usually observed only in small-scale laboratory studies as an intracellular intermediate (Scheible, 1993). When oxygen levels are very low, nitrogen gas (N_2) is the end product of the denitrification process; but, where oxygen levels are more intermediate or variable, the reactions may stop with the formation of NO_x (Brady and Weil, 2002). Very high nitrate concentrations or low pH values may also arrest denitrification at the N_2O stage (Hefting *et al.*, 2003, 2006b). Finally, the production of bicarbonate ions and carbon dioxide when organic carbon is used as electron donor buffers the porewater pH around the neutral conditions that are more favourable for denitrification and also lowers the ratio of N_2O/N_2 (Groffman *et al.*, 2000).

2.3.3.1 *Factors controlling denitrification*

Bacteria capable of denitrification are ubiquitous, and thus denitrification occurs widely throughout terrestrial, freshwater and marine environments, where the combined conditions of nitrate availability, low oxygen concentrations and sufficient organic matter occur (Seitzinger *et al.*, 2006).

Oxygen

It is generally assumed that the nitrogen oxide reductases are repressed by O_2, and that, when O_2 is removed, even in the absence of nitrogen oxides, the reductase enzymes are de-repressed within a period of 40 min to 3 hours (Knowles, 1982). In groundwater, given all other prerequisites, denitrification usually occurs at dissolved oxygen concentrations below 1-2 mg L^{-1} (Duval and Hill, 2007; Schilling and Jacobson, 2008; Hill and Duval, 2009; Curie *et al.*, 2009), while completely anoxic conditions are not required (Seitzinger *et al.*, 2006). In floodplain soils, the O_2 concentration depends on: 1) the O_2 consumption rate, 2) the O_2 diffusion rate, 3) the geometry of the diffusion path (Knowles, 1982), and when inundation occurs, on the percentage of the water filled pore space (WFPS) (Groffman and Tiedje, 1988). Pinay *et al.* (2007a) have observed maximum denitrification at around 70 % WFPS and not 100 % WFPS. This was explained by the fact that partial waterlogging conditions favour the co-existence of aerobic and anaerobic sites at the soil micro-scale. This, in turn, allows the close coupling of nitrification and denitrification between adjacent aerobic and anaerobic sites in the soil matrix (Seitzinger *et al.*, 2006), thus maximising the denitrification activity. Similarly, alternate aerobic and anaerobic conditions triggered by the short-term periodic flooding of the soil are also expected to enhance denitrification in floodplains by promoting more frequent nitrification-denitrification cycles (Fennessy and Cronk, 1997; Pinay *et al.*, 2007a).

Nitrate concentration

In some denitrifying bacteria, the presence of nitrate is required for, or very much stimulates the de-repression of the nitrate reductase (Knowles, 1982). The half saturation constant (Km) of denitrification in *in vivo* and in cell-free systems ranges between 0.3 and 18 mg N L^{-1} (Knowles, 1982), while the kinetics of denitrification at nitrate concentrations >1 mg N L^{-1} are usually zero order (i.e. independent of concentration) (Rivett *et al.*, 2008) in groundwater, and therefore denitrification is usually limited by the electron donor supply. However, in waterlogged soils, the diffusion of NO_3^- in the denitrifying sites within the soil matrix may be a limitation (Olde-Venterink *et al.*, 2003). Generally, increased nitrate supply leads to increased denitrification rates in agricultural grasslands and floodplains (De Klein and Van Logtestijn, 1994; van Beek *et al.*, 2004; Ullah and Zinati, 2006), while even when N saturation of the soil has been observed, from chronic nitrate loading, denitrification

still occurs (Hanson *et al.*, 1994; Ullah and Zinati, 2006), but its efficiency may be significantly decreased (Hefting *et al.*, 2006a; Seitzinger, 2008). In a typical lowland agricultural catchment, such as the River Cole at Coleshill, nitrate supply is not expected to be limiting for denitrification. However, the relative availability of nitrate and electron donors will likely influence the partitioning of nitrate between denitrification and other dissimilatory reduction processes (Rivett *et al.*, 2008).

Organic carbon

The availability of electrons in organic carbon compounds is one of the most important factors controlling the activity of the heterotrophs, which comprise the bulk of denitrifiers (Knowles, 1982). Several studies have found significant positive relationships between denitrification rates and groundwater and porewater dissolved organic carbon (DOC) in riparian zones and floodplains (Devito *et al.*, 2000; Baker and Vervier, 2004; Hill and Duval, 2009; Curie *et al.*, 2009). The stoichiometry of the denitrification reaction shown in equation 2.1 indicates that 1 mg C L^{-1} is required for the reduction of 0.93 mg NO_3^--N L^{-1} to nitrogen gas. Although aquifers may be limited in their DOC availability (typically <5 mg C L^{-1}) (Rivett *et al.*, 2007), the shallow groundwater of riparian zones and floodplains usually contains higher concentrations of DOC (Rivett *et al.*, 2008) that can support high denitrification rates (Haycock *et al.*, 1993; Burt *et al.*, 1999; van Beek *et al.*, 2004) especially where buried deposits of organic matter are found in the subsurface (Hill *et al.*, 2000; Hill *et al.*, 2004; Gurwick *et al.*, 2008).

Not only the quantity but also the quality of organic carbon affects the denitrification rate. Postma *et al.* (1991) noted that denitrification was minimal in groundwater when organic carbon was present as lignite or coal fragments. In floodplain soils, the availability of labile organic carbon increases by plant root exudates (Frank and Groffman, 2009) such as polysaccharides (Bastviken *et al.*, 2007) that are readily available to denitrifiers. Moreover, Beauchamp *et al.* (1989) indicated that denitrification in the presence of more complex organic molecules (e.g. proteins, lipids and lignin) may be facilitated by fermenters that break down those complex molecules to simpler organic compounds. However, fermentation requires low redox potential and therefore this mechanism will be more important in flooded soils or within anaerobic microsites. Dahl *et al.* (2007) reported that an organic carbon fraction of 3 % in riparian

zone soils was an effective indicator of increased potential denitrification. The available labile organic carbon has also an indirect effect on denitrification, enhancing oxygen consumption by aerobic bacteria which leads to anaerobiosis (Tiedje, 1988). Finally, the land use management of floodplains in agricultural catchments can significantly affect both the quantity and the quality of the available organic carbon for denitrification (see below).

Temperature

The optimum temperature for denitrification is between 25 and 35^{o}C, but denitrification processes will normally occur in the range 2 - 50^{o}C (Brady and Weil, 2002) and possibly beyond, where bacteria have evolved to cope with specific environmental conditions (Knowles, 1982). Groundwater temperatures are typically around 10^{o}C (in northern Europe), and therefore denitrification occurs at sub-optimal temperature, while the relatively small range of temperature fluctuations results in low temperature dependency of denitrification in groundwater (Rivett *et al.,* 2008). In surface soils the effect of temperature is more pronounced and reaction rates are typically assumed to double for every 10^{o}C increase in temperature (Q_{10} range 1.5 - 3) (Knowles, 1982). Stanford *et al.* (1975), based on experimental soil data, suggested a linear relationship between temperature and the denitrification rate until 11^{o}C, above which the relationship becomes exponential increase with Q_{10} = 2.1. Finally, denitrification occurring at the lowest or highest temperature range usually results in a higher ratio of N_2O/N_2 (Knowles, 1982).

pH

The pH range preferred by heterotrophic denitrifiers is generally between 5.5 and 8, while denitrification almost ceases for pH <4 or pH> 10 (Paul and Clark, 1989). The optimal pH is site-specific because of the effects of acclimation and adaptation on the microbial ecosystem (Rivett *et al.,* 2008). In agricultural catchments, where clay soils are dominant, the soil pH is usually around neutral or slightly alkaline (Rowell, 1994) and therefore denitrification is not expected to be adversely affected by pH. Denitrification itself can increase pH within the anaerobic microsites of the soil by releasing CO_2 and hydroxide (OH^-), and hence create locally favourable pH conditions for denitrification (Rivett *et al.,* 2008).

2.3.3.2 *Denitrification in restored floodplains*

Numerous studies have documented significant potential for nitrate removal via denitrification in hydric surface soils of riparian buffer zones across various climatic gradients (Peterjohn and Correll, 1984; Ambus and Lowrance, 1991; Groffman *et al.*, 1992; Pinay *et al.*, 1993; Hefting *et al.*, 2003; Pinay *et al.*, 2007a) and in subsurface soils of riparian zones where nitrate is supplied from the upland via groundwater flow (Hill *et al.*, 2000, 2004). More recently, the potential of restored urban riparian zones to remove nitrate via denitrification has also been established (Groffman and Crawford, 2003; Kaushal *et al.*, 2008; Gift *et al.*, 2008). However, surprisingly few studies have investigated the potential for denitrification in restored floodplains (Hoffmann *et al.*, 1998a; Sheibley *et al.*, 2006; Orr *et al.*, 2007).

One reason for this is that floodplain restoration has been advocated as a means of natural flood control and groundwater recharge, while also delivering ecological services such as fish rearing habitat and wildlife biodiversity, but not explicitly for water quality improvement (Sheibley *et al.*, 2006). Moreover, the limited attention given to floodplains likely reflects the fact that many rivers have been disconnected from their historic floodplain by levees and flow modification (Gergel *et al.*, 2002), while the inherent physical and ecological complexity of floodplains makes these systems difficult to study (Orr *et al.*, 2007). Finally, the urgent need to tackle diffuse nitrate pollution from surface and sub-surface agricultural runoff has focused the scientific and natural resource management interest to the restoration of restricted width riparian buffer zones adjacent to agricultural land (Fennessy and Cronk, 1997), instead of wider floodplains. However, more recently, flood retention areas in northern Europe (e.g. polders in the Upper Rhine) have also as an objective the improvement of water quality. The management of the flooding regime in a way to optimise nitrogen elimination by denitrification is an important task for restoration managers (Brettar *et al.*, 2002).

There are studies that provide evidence for potentially significant nitrate retention in large flooded floodplains. In Tockner *et al.* (1999) the increased hydrological connectivity between the river and the floodplain, following the Danube Restoration Project, enhanced suspended sediment and particulate organic carbon retention, while the floodplain also became a sink for nitrate. However, the authors did not discriminate

between sedimentation, plant and algal nitrate uptake and denitrification. Olde Venterink *et al.* (2003) and Van der Lee *et al.* (2004) attempted to discriminate between the above retention processes in floodplains of the Rhine in The Netherlands. Their results indicated that nitrate denitrification during flooding is possible mainly in the waterlogged soil, rather than the water column, while it is regulated by the extent of discharge on the floodplain, the floodwater velocity and the diffusion rate of nitrate from the floodwater into the soil. Other studies have focused on the denitrification potential of the soil in large floodplains, where experimental NO_3^- additions showed significant denitrification in the topsoil which depended on the regular flood pulse for the supply of nitrate (Forshay and Stanley, 2005). Pinay *et al.* (2000) found that flood duration can indirectly influence denitrification by the deposition of fine sediments that in turn positively affect denitrification rates, whilst the deposition of organic matter and the creation of low redox conditions, as a consequence of flooding, can also increase denitrification rates (Brettar and Höfle, 2002; Brettar *et al.*, 2002).

The results from the few studies conducted in restored floodplains with respect to their potential for denitrification have not been consistent. Sheibley *et al.* (2006) have found significant denitrification potential in the topsoil of a restored floodplain in the Lower Cosumnes River in California, four years after the restoration was completed. Denitrification was limited by the amount of the bio-available carbon on the floodplain, while the annual N-removal contribution of denitrification ranged between 1 and 24 % depending on the differing supply of NO_3^- during flooding on a wet or dry year. In contrast, in a study that was conducted one year after the restoration of the River Brede floodplain in Denmark (Hoffmann *et al.*, 1998a) no significant effect of the restoration was observed in the hydrology and the nitrate retention capacity of the floodplain, which was explained by the unusually dry weather conditions during the study and the short duration of the monitoring period. Similarly, two years after the restoration of the River Baraboo floodplain in Wisconsin (Orr *et al.*, 2007), although the floodplain soil showed potential to denitrify, this was not well-correlated with any of the denitrification controlling factors, while no difference was observed between pre- and post- restoration rates. They suggested that the short time after the completion of the restoration may not have been enough for the physical soil properties to change and/or the microbial communities to adapt to the new conditions.

It becomes apparent that further studies are needed in order to assess the potential of restored floodplains for nitrate removal, if this is going to be a key management measure for river water quality improvement, especially with respect to the effect of the hydrological regime in the supply of nitrate and the temporal and spatial patterns of nitrate removal. Additionally, further insight is needed in the combined effect of the hydrological regime and the land use management on the floodplain soil properties that in turn control the partitioning of nitrate between different retention processes.

2.3.3.3 *Temporal variability of denitrification*

The temporal variability of denitrification is an important consideration as it has been suggested that, in temperate climates, the most concentrated nitrate discharges occur in the winter months, when the bioassimilation of nitrogen by plants is not possible (Groffman *et al*., 1992; Haycock and Pinay, 1993). Attenuation of nitrate discharges occurring in the winter months is generally assumed to be the result of denitrification (Groffman *et al*., 1992; Haycock and Pinay, 1993; Pinay *et al.,* 1993; Burt *et al.,* 1999), which predominantly occurs below the ground surface where temperatures are more moderate throughout the cold season (Fennessy and Cronk, 1997). Therefore, the combination of plant uptake during the growing season and denitrification throughout the year, but especially during the cold season, provides all-year round nitrate attenuation in a temperate floodplain (Fennessy and Cronk, 1997).

However, denitrification may be more important during flood pulses in spring and autumn (Groffman and Tiedje, 1989; Hanson *et al.,* 1994) or even in summer (Hefting *et al.,* 2003, 2006b), when nitrate supply by floodwater is combined with higher temperature, thus greatly enhancing denitrification rates. Therefore, the occurrence of a summer flood pulse may constitute a 'hot-moment' (*sensu* McClain *et al.,* 2003) of biogeochemical activity in general (Banach *et al.,* 2009) and of denitrification specifically, that needs to be taken into account in the annual N-removal budget (Groffman *et al.,* 2009) of the floodplain, especially in the light of the predicted increase of air temperature and summer flooding frequency in north-western Europe due to climate change (Bronstert, 2003). The temporal variability induced by the perturbation of wetting-drying cycles in the hydrological regime of floodplains is particularly considered below.

Drying-wetting cycles

Lowland-river floodplain systems are characterised by a high degree of variability in both the frequency and period of inundation of the various morphological elements of the system due to topographical gradients and the timing of the flood pulses (Baldwin and Mitchell, 2000). The timing of flooding, and subsequently the dry-wet cycle sequence, will be further affected by global warming (Miller and Russell, 1992), as more frequent extreme events such as floods and droughts are forecasted (Mirza *et al.* 2003), as well as an increase in the annual average runoff in Northern Europe (Arnell, 1999). Consequently, forecast hydrologic variations will have profound effects on the processes responsible for nutrient cycling in wetland and river-floodplain systems (Baldwin and Mitchell, 2000). Soil and sediment drying promotes the aerobic mineralisation of organic matter and the release of cell-bound C from sediment bacteria killed during drying (Scholz *et al.*, 2002). Moreover, several studies have shown a flush of mineralised-N and subsequent increase in nitrate and ammonium concentrations in soils and sediments upon re-wetting by flooding, due to flushing of accumulated ammonium and enhanced nitrification (Baldwin and Mitchell, 2000; Olde-Venterink *et al.*, 2002; Heffernan and Sponseller, 2004; McIntyre *et al.*, 2009). Additionally, several studies suggest that the frequency of drying-rewetting events alters the response of microbial processes more than expected when only soil nutrient availability is taken into account (Schimel *et al.* 1999; Baldwin and Mitchell 2000; Fay *et al.* 2000; Fierer and Schimel 2002; Pinay *et al.*, 2007b).

Cavigelli and Robertson (2000) have shown that variability in denitrification activity may not only be due to differences in environmental conditions but also due to changes in the microbial community composition. Drying-rewetting cycles apart from representing a significant physiological stress for soil biota, that can undergo an osmotic shock with possible cell lyses and release of intracellular solutes (Fierer *et al.*, 2003), they can also directly alter the denitrifier community composition (Fierer *et al.*, 2003; Fromin *et al.*, in press). More diverse microbial groups such as decomposers may be more resistant and resilient to the effect of drying-wetting cycles compared to more specialist groups such as nitrate respirers (Pinay *et al.*, 2007b). In addition, the spatial variability in denitrification potential due to possible changes in the denitrifier community composition has not been previously studied in restored floodplains that experience frequent dry-wet cycles due to an intermittent flooding regime.

2.3.3.4 *Spatial variability of denitrification*

Denitrification is spatially highly variable from both a soil matrix perspective (Parkin, 1987), due to the existence of aerobic and anaerobic microsites and the presence of organic carbon patches, and at the landscape scale due to land use management practices, surficial hydrogeomorphic features and subsurface lithology.

Land use management

The different land use types within a watershed have been shown to vary significantly in their soil properties and consequently in their denitrification potential (Ullah and Faulkner, 2006). Traditional land use management of lowland agricultural grasslands includes bi-annual or annual mowing and grazing by ungulates (Robson *et al.,* 2007). Higher denitrification potential in areas affected by grazing cattle has been reported in numerous studies (Frank and Groffman, 1998b; Meneer *et al.,* 2005; Patra *et al.,* 2005; Philippot *et al.,* 2009). The stimulation of denitrification by grazing associated with animal activities has been attributed to changes in hydraulic soil properties through soil compaction and in nutrient availability through the deposition of urine and faeces and limited plant N uptake after defoliation (Luo *et al.,* 1999; Meneer *et al.,* 2005). Moreover, grazing has been shown to increase the availability of labile organic carbon and decrease the ratio of C/N, both contributing to enhanced denitrification rates (Frank and Groffman, 1998a). Mowing has been shown to increase species richness in managed grasslands by increasing the competition between plants and although root mass is reduced, the availability of C and N as well as the microbial activity is not negatively affected (Patra *et al.,* 2006; Ilmarinen *et al.,* 2009). Moreover, increased release of easily extractable carbon via rhizo-deposition processes due to mowing has been reported in mown pastures of the Mediterranean (Gavrichkova *et al.,* 2008). The availability of easily extractable carbon and the accelerated N cycling due to the short life-cycle of plants in mown grassland has been positively related to enhanced denitrification (Robson *et al.,* 2007). Finally, cultivation has been shown to negatively affect the availability of labile organic carbon in soils (Bowman *et al.,* 1990; Groffman *et al.,* 1993b; Boyer and Groffman, 1996; Ullah and Faulkner, 2006) and consequently significantly decrease their denitrification potential (Groffman *et al.,* 1993b; Cavigelli and Robertson, 2000; Ullah and Faulkner, 2006). It is anticipated that the above land use management practices, found also in the River Cole re-connected floodplain, may significantly affect the denitrification potential across the floodplain land use zones.

Hydrogeomorphic variability

Spatial variability of denitrification has also been attributed to differences in the hydrogeomorphic template of floodplains (Harms *et al.*, 2009). The hydrogeomorphic template consists of both temporal and spatial variation in hydrology (i.e. the hydrologic regime), and spatial variation conferred by landform (Hauer and Smith, 1998) and topography (Florinsky *et al.*, 2004). The convergence of hydrologic flowpaths carrying the necessary substrates (C and N) or the hydrologic transport of a missing reactant in a pool of substrate have been described as the main hydrological mechanisms for the occurrence of biogeochemical 'hotspots' (McClain *et al.*, 2003).

Soil texture may determine the capacity of soils to retain C and N (Pinay *et al.*, 2000), and spatial variation in texture of floodplain soils often occurs along topographic gradients (Bruland and Richardson 2004; Bechtold and Naiman 2006), which would then produce gradual spatial variation in denitrification. Moreover, topographic gradients also affect soil moisture distribution as well as the transport of C and N with floodwaters, while the residence time of the floodwaters controls the redox potential of the soil. Therefore, many studies have found increased denitrification potential in low-lying areas of floodplains, where the above conditions concur (Florinsky *et al.*, 2004; Ullah and Faulkner, 2006; Harms and Grimm, 2008). Finally, the timing and spatial pattern of the hydrologic regime can influence directly the spatial variability of denitrification. Homogenisation in soil characteristics and microbial activity occurs when the hydrologic driver (i.e. flooding) is frequent and spreads across the floodplain, whereas infrequent hydrologic regimes or unevenly distributed in space contribute to spatial heterogeneity (Harms *et al.*, 2009).

Vertical variability

Martin *et al.* (1999) suggest that apart from the horizontal spatial variability, the heterogeneity of denitrification in the vertical dimension should also be considered, where groundwater flow is a significant component of the hydrological regime and couples the transport of nitrate from arable land to the floodplain riparian zone. The vertical variability in denitrification is a function of hydrology, sediment characteristics (lithology) and availability of electron donors and acceptors (biogeochemistry) (Hill, 1996). None of the studies in restored floodplains (Hoffmann *et al.*, 1998a; Sheibley *et al.*, 2006; Orr *et al.*, 2007) have considered the potential for denitrification in the

vertical dimension, while most studies conducted in flooded floodplains have focused on nitrate processing in the water column or at the interface between water and sediment (Olde Venterink *et al.*, 2003; Van der Lee *et al.*, 2004; Andersen, 2004). Exceptions are the studies of Brettar *et al.* (2002) and Brettar and Höfle (2002), in candidate restoration floodplains of the Upper Rhine, where they investigated the relationship between denitrification potential and redox conditions and organic matter availability respectively, between the ground surface and 1 m depth.

However, several studies in riparian buffer zones have indicated that subsurface lithology may significantly affect nitrate processing in shallow groundwater, especially where localised distinct gravel layers are found (Burt *et al.*, 1999; Hill *et al.*, 2004). Reineck and Singh (1980) indicate that gravel layers are often the former bed sediments of laterally migrating stream channels and are common features of floodplain lithology. These highly conductive coarse sediments can increase groundwater flow rates (as discussed in section 2.2) and limit nitrate removal in some riparian areas (Correll *et al.*, 1997; Burt *et al.*, 1999).

A possible explanation for the lack of research on denitrification in subsurface soils of floodplains may stem from past assumptions that conditions favourable for denitrification, such as the availability of labile organic carbon and microbial activity (Parkin and Meisinger, 1989), do not exist at depth (Martin *et al.*, 1999). However, recent studies in a variety of riparian zones in North Europe and Canada (Burt *et al.*, 1999; Clément *et al.*, 2002; van Beek *et al.*, 2004; Hill *et al.*, 2004) have documented significant denitrification potential with depth, which decayed exponentially with depth following closely the availability of organic carbon (Boyer and Groffman, 1996; Brettar *et al.*, 2002; Brettar and Höfle, 2002; Gift *et al.*, 2008) and/or the availability of nitrate (Dick *et al.*, 2000; Clément *et al.*, 2002; Brettar *et al.*, 2002; van Beek *et al.*, 2004; Schilling *et al.*, 2009). There are some exceptions though where denitrification may not decrease with depth, or in fact may be more important in deeper layers, where buried patches of organic matter are combined with the transport of nitrate via groundwater (Hill *et al.*, 2000; Vidon and Hill, 2004b; Hill *et al.*, 2004).

2.3.4 *Dissimilatory Nitrate Reduction to Ammonium (DNRA)*

Another dissimilatory reduction pathway for NO_3^-, as opposed to the assimilatory pathways of microbial and plant uptake, is the reduction of NO_3^- to NO_2^- and then to NH_4^+ (equation 2.3 after Tiedje *et al.,* 1982):

$$NO_3^- + 8e^- + 10H^+ \rightarrow NH_4^+ + 3H_2O \qquad (2.3)$$

DNRA is carried out primarily by obligate anaerobic fermentative bacteria (e.g. *Clostridia*, *Bacillus*, and most Enterobacteriaceae) that do not perform oxidative metabolism, which is the opposite from denitrification (Tiedje, 1988). The reduction of NO_3^- to NH_4^+, although less favourable energetically than the reduction to N_2, it is a more efficient electron sink, since eight electrons (e^-) are transferred per mole of nitrate reduced (2.3), which is three more electrons than in the denitrification reduction reaction (2.2) (Tiedje *et al.,* 1982). Therefore, DNRA is thought to be more favourable where electron acceptors (i.e. nitrate) are limiting, while denitrification is more favourable where electron donors (i.e. organic carbon) are limiting (Tiedje *et al.,* 1982).

Whereas the conditions promoting DNRA and heterotrophic denitrification are similar (i.e. low O_2 availability, available nitrate and organic substrates), denitrification represents a permanent nitrate removal pathway, while DNRA is a N-conserving mechanism that transforms nitrate to another more bio-available inorganic-N form (NH_4^+). The produced ammonium can be subsequently nitrified under oxic conditions, taken up by plants and microbes and be temporarily retained in biomass, or abiotically adsorbed to negatively charged particles in the soil or sediment matrix (Burgin and Hamilton, 2007). Therefore, the determination of the nitrate partitioning between denitrification and DNRA can have important consequences for N management, especially where diffuse nitrate pollution is an important issue, such as in temperate lowland agricultural catchments. Moreover, the fact that the fermentative bacteria that carry out DNRA are obligate anaerobes, and thus cannot occupy all the niches that denitrifiers can (Rivett *et al.,* 2008) and the relative availability of electron donors and acceptors in a given environment (Tiedje *et al.,* 1982), are expected to be the main determinants of the relative importance between DNRA and denitrification as nitrate attenuation mechanisms.

2.3.4.1 *Evidence for the occurrence of DNRA*

Several studies in marine and estuarine sediments have documented significant DNRA rates that can be comparable to denitrification. This could occur when for example NO_3^- supply via nitrification is limited and the presence of macrophytes increases the competition for nitrate (Rysgaard *et al.*, 1996), while DNRA can be significantly higher than denitrification in organically enriched anaerobic sediments under fish farms (Christensen *et al.*, 2000) and in anaerobic estuarine sediments rich in sulphide (see also section 2.3.5) that can inhibit nitrification and denitrification (An and Gardner, 2002). DNRA may be relatively more important in marine than freshwater ecosystems due to the co-occurrence of permanently reduced conditions, high organic carbon availability (especially in near coastal areas) and limited nitrate supply (Revsbech *et al.*, 2006), but this is a tenuous conclusion because of the small number of studies of DNRA in freshwater environments (Burgin and Hamilton, 2007).

Difficulties in directly measuring DNRA (Silver *et al.*, 2001), and the common assumption that due to its strict anoxic nature DNRA either plays no role or only a negligible role in aerobic topsoils (Tiedje, 1988), has resulted in this process being overlooked by terrestrial biogeochemists (Silver *et al.*, 2001). However, recently, the role of DNRA as an N-conserving mechanism has been established in N-limited tropical forest soils (Silver *et al.*, 2001, 2005; Pett-Ridge and Firestone, 2005; Pett-Ridge *et al.*, 2006; Huygens *et al.*, 2007; Rütting *et al.*, 2008; Templer *et al.*, 2008). DNRA was shown to be at least three times higher than denitrification, or in some cases account for nearly 99 % of nitrate reduction (Huygens *et al.*, 2007), in these humid tropical forest topsoils, characterised by a small NO_3^- pool and rapid NH_4^+ turnover rates and as a result limiting the availability of NO_3^- for denitrification, leaching or immobilisation (Silver *et al.*, 2001). The main controlling factor of DNRA in these systems appears to be the relative availability of electron donors and acceptors (high ratio of C/N), while the DNRA bacteria seem to be adapted to fluctuating redox regimes and be able to withstand unfavourable redox periods of higher O_2 concentration (Pett-Ridge and Firestone, 2005; Silver *et al.*, 2005; Pett-Ridge *et al.*, 2006), therefore increasing their competitive advantage against the more tolerant to oxic conditions, denitrifiers.

The occurrence of DNRA has also been documented in other freshwater environments, such as a riparian fen in Denmark (Ambus *et al.*, 1992), in two Chinese and Australian

paddy soils (Yin *et al.,* 2002), in a riparian wetland in the UK (Matheson *et al.,* 2003) and in a created freshwater wetland in Texas (Scott *et al.,* 2008). In all cases, denitrification was responsible for most of nitrate removal, while DNRA accounted for between 5 and 15 % of nitrate removal, being controlled mainly by the low redox potential and the increased organic carbon availability of the wetland sediments.

The above studies in both the N-limited tropical forest soils and in wetland sediments, on one hand show that DNRA can occur in freshwater environments and aerobic soils, and on the other hand seem to verify the assumption that the partitioning of nitrate between denitrification and DNRA depends on the relative availability of electron donors and acceptors (Tiedje, 1988). However, this assumption has not yet been thoroughly tested in temperate agricultural floodplain soils. In a recent study of an herbaceous riparian zone in Oregon (Davis *et al.,* 2008), DNRA was shown to occur in the top 15 cm of the soil and at 1 m depth, but its relative importance compared to denitrification was not consistent. Moreover, DNRA probably accounted for 3 % of *in situ* nitrate removal in the riparian zone of an ephemeral stream in Australia (Woodward *et al.,* 2009), where denitrification was also low, accounting for another 3 % of nitrate removal, mainly due to the high concentration of dissolved oxygen in the groundwater.

It becomes apparent that further studies are needed in temperate agricultural settings in order to give more insight into the role of DNRA as a nitrate attenuation process. This in turn will have important management implications for these human impacted environments, suggesting for example a more efficient use of fertilisers, in the case that DNRA is a significant N-conservation mechanism, or influencing the design of river-floodplain restoration projects with the aim of maximising the N-removal capacity of denitrification while keeping N-conservation by DNRA to a minimum. Furthermore, the effect of the hydrological regime and that of the land use management of restored floodplains and riparian zones on the relative importance of DNRA as well as on its horizontal and vertical spatial distribution have not yet been investigated.

2.3.5 *Chemoautotrophic Denitrification and DNRA*

Denitrifiers are mostly facultative anaerobic heterotrophs and therefore they obtain both their energy and carbon from the oxidation of organic compounds. However, some denitrifying bacteria are autotrophs, so obtain their energy from the oxidation of inorganic species, and their carbon from carbon dioxide (CO_2). Inorganic e^- donors found mostly in groundwater include reduced manganese (Mn^{2+}), ferrous iron (Fe^{2+}) and sulphides (Korom, 1992). If these 'chemolithoautotrophic' bacteria are present in groundwater, they can reduce NO_3^- with simultaneous oxidation of manganese, iron or sulphide, and this is called chemoautotrophic denitrification.

The nitrate reduction by Fe^{2+} is due to the bacterium *Gallionella ferruginea,* and can be described by the equation 2.4 (Korom, 1992):

$$5Fe^{+2} + NO_3^- + 12H_2O \rightarrow 5Fe(OH)_3 + 1/2N_2 + 9H^+ \qquad (2.4)$$

G. ferruginea does require a small amount of oxygen for growth, so a likely ecological niche is at an aerobic/anaerobic interface where Fe^{2+} and dissolved oxygen meet in opposing diffusion gradients (Korom, 1992). This biotic reduction occurs at relatively low temperatures and circumneutral pH (between 5.5 - 7.2; Weber *et al.*, 2001), and its occurrence has been documented in freshwater sediments (Weber *et al.*, 2006). The controls on this process remain poorly understood, although it may be important in areas of high reduced iron and a limited supply of organic carbon (Weber *et al.*, 2001). The presence of this process has not yet been reported in floodplain soils, where the high availability of organic carbon and the presence of Fe in oxidised form probably promote the dominance of heterotrophic denitrification. However, in groundwater, where organic carbon is usually restricted with depth, and if Fe^{2+} is present, chemoautotrophic denitrification could be possible (Postma *et al.*, 1991).

Electrons needed for chemoautotrophic denitrification can also originate from the microbial oxidation of reduced sulphur to the S (+VI) state as sulphate. The reduced sulphur may be present as the S (-II) state in H_2S, S (-I) in FeS_2, S (0) in elemental sulphur, S (+II) in thiosulphate $S_2O_3^{2-}$, or S (+IV) in sulphide SO_3^{2-}. In groundwater, iron (and sometimes manganese) sulphide can be utilised as the electron donor (Korom, 1992):

$$5FeS_2 + 14NO_3^- + 4H^+ \rightarrow 7N_2 + 10SO_4^{-2} + 5Fe^{+2} + 2H_2O \quad (2.5)$$

The oxidation of pyrite (equation 2.5) has been shown to provide an alternative electron donor in carbon-limited aquifer systems (Robertson *et al.*, 1996; Pauwels *et al.*, 1998; Tesoriero *et al.*, 2000; Schwientek *et al.*, 2008), but its importance in floodplain soils has not yet been established.

Recently, the role of sulphur oxidisers in the reduction of nitrate in freshwater sediments and floodplain pools (Whitmire and Hamilton, 2005; Burgin and Hamilton, 2008; Payne *et al.*, 2009) has received more attention, despite the notion that this biogeochemical pathway has been considered unimportant in freshwater sediments due to the low sulphide concentrations. Bacteria genera such as *Thiobacillus*, *Thiomicrospira* and *Thioploca* have now been isolated from such freshwater systems (Burgin and Hamilton, 2008). These microbes are capable of oxidising H_2S to S^0 and/or SO_4^{2-} coupled to the reduction of NO_3^- to N_2 (denitrification) or NH_4^+ (DNRA) according to the following reactions (Fossing *et al.*, 1995; Sayama *et al.*, 2005):

$$5HS^- + 8NO_3^- + 3H^+ \rightarrow 5SO_4^{2-} + 4N_2 + 4H_2O \quad (2.6)$$

$$4H_2S + 4NO_3^- + 4H_2O \rightarrow 4NH_4^+ + 4SO_4^{2-} \quad (2.7)$$

Burgin and Hamilton (2008) reported a range between 25 and 40 % of nitrate removal attributed to the simultaneous oxidation of H_2S in stream, lake and wetland sediments in Southern Michigan. Apart from the presence of the responsible bacteria, this process requires anoxic conditions, although some species may be able to survive in micro-aerophilic environments (Burgin and Hamilton, 2008), but most importantly reduced sulphur is needed to serve as an energy source for the sulphur oxidisers. Brunet and Garcia-Gil (1996) have also hypothesized that H_2S, that inhibits the last reduction steps in heterotrophic denitrification, may effectively favour the DNRA pathway. It is not known whether fermentative and chemoautotrophic DNRA can occur together or are mutually exclusive (Burgin and Hamilton, 2007). Due to the anaerobic nature of this process and its dependence on available reduced sulphur, its occurrence would be more

likely to be of significance in frequently saturated riparian zones or depression wetlands than in intermittently saturated floodplain soils.

2.3.6 *Anaerobic Ammonium Oxidation (Anammox)*

Anaerobic ammonium oxidation (Anammox) is a chemoautotrophic process by which ammonium is combined with nitrite under anaerobic conditions, producing N_2 (2.8; Trimmer *et al.*, 2003):

$$NO_2^- + NH_4^+ \rightarrow N_2 + 2H_2O \quad (2.8)$$

The nitrite can derive from the reduction of nitrate via denitrification or possibly DNRA (Trimmer *et al.*, 2003) and therefore Anammox constitutes another mechanism for the permanent removal of nitrate as N_2 gas. It was first discovered in wastewater treatment systems (van de Graaf *et al*., 1995; Mulder *et al*., 1995) and subsequently documented in oxygen depleted zones of the ocean, temperate shelf sediments, where it can account for as much as 24 and 60 % of N_2 formation (Dalsgaard *et al.*, 2005), and estuarine sediments, representing between 1 and 11 % of N_2 potential production (Nicholls and Trimmer, 2009). Anammox was shown to be favoured, compared to denitrification, by lower temperatures and organic carbon in deep marine sediments (Dalsgaard and Thamdrup, 2002), while in estuaries it is mostly regulated by the supply of NO_3^- and NO_2^- from the water column (Trimmer *et al.*, 2003, 2005). While little is known about Anammox in freshwaters, one might expect that it would be more important in very deep, large oligotrophic lakes (Burgin and Hamilton, 2007). The only study to date on Anammox in freshwaters was in Lake Tanganyika (Schubert *et al.*, 2006). Although the occurrence of Anammox in floodplain soils and shallow groundwater sediments is rather unlikely due to the fluctuating oxic-suboxic conditions and the high availability in organic carbon, it is worth assaying the soils and sediments for its detection.

To summarise, the reduction of nitrate in floodplains and riparian zones can be due to mixing and dilution between different water sources but also due to biological processes such as uptake by vegetation and microbes and heterotrophic denitrification. Of these three possible biological mechanisms, plant and microbial uptake although relevant in a restored floodplain context, constitute only a temporary retention mechanism through biomass storage that eventually leads to the release of N back to the system in a different form. However, heterotrophic denitrification that reduces nitrate to dinitrogen gas leads to the permanent removal of nitrate from the system and thus completes the N cycle. It is therefore the preferred nitrate attenuation pathway in restored agricultural floodplains targeting water quality improvement. However, denitrification is subject to a complex control by the availability of O_2 and the relative availability of electron donors and acceptors, while as a microbial process it is also regulated by temperature and pH. These factors are in turn affected by the hydrological regime, the land use management and the geomorphological and topographical characteristics of the re-connected floodplain both in the temporal and spatial dimensions.

In order to understand how to restore river-floodplain systems for maximising nitrate removal, the above controlling factors need to be identified, and their interactions assessed in both space and time. Furthermore, the relative importance of alternative nitrate reduction pathways, such as DNRA, chemoautotrophic denitrification and Anammox, which can affect the final fate of nitrate, can have important implications for the management of restored floodplains and therefore their role needs to be established in temperate agricultural restored floodplains. The knowledge gained from the above research could be used in the design of future river-floodplain restoration projects aimed at water quality improvement through nitrate attenuation. One way of contributing to the design of future floodplain restoration projects could be the construction of a decision support tool for the selection of appropriate areas for restoration where effective nitrate removal can be achieved and/or for assessing the nitrate removal ability of restored floodplains as part of post-project monitoring.

2.4 *Decision support tools for River-Floodplain restoration*

Despite the new policy drivers for river-floodplain restoration, restoration sites are still often selected opportunistically and on an *ad hoc* basis rather than according to a strategic planning process (Clarke *et al.*, 2003, Rohde *et al.*, 2006). Natural resource managers now face the challenge of restoring or recreating riparian zones and floodplains in many different settings, and this is a rather recent challenge with relatively little experience upon which managers can rely for guidance (Correll, 2005). Moreover, any proposed restoration strategy, regardless of its ecological merits, needs to be economically feasible and socially acceptable, and since the economic costs of such programs can be high, it is imperative that decision be based on sound scientific information (Osborne and Kovacic, 1993). Furthermore, Correll (2005) in his recent review acknowledges the fact that much more is known generally about the water quality functions of buffer zones, than about how quickly and effectively these functions were regained after restoration, highlighting the need for more effective post-restoration assessment (Orr *et al.*, 2007). Therefore, the need for a comprehensive yet rapid assessment tool to assist resource managers in evaluating restored floodplain functions and conditions pre- or post-project is more timely than ever before (Ducros and Joyce, 2003, Trepel and Kluge, 2004, Vidon and Dosskey, 2008).

The existing decision support tools are mainly targeting buffer zone establishment or rehabilitation and can be grouped into two broad categories. Those that use spatial information, frequently incorporating it into a Geographic Information System (GIS), for specific landscape attributes that indicate potential effective buffer zone functionality and those that are based on models simulating hydrological and/or biogeochemical functioning at the field scale or catchment scale and are more detailed in estimating the potential water quality function of a restored floodplain or buffer zone.

Pinay *et al.* (1995) suggested that geomorphic features can provide insight into riparian zone denitrification capacity. Gold *et al.* (2001) and Rosenblatt *et al.* (2001) used site-specific reconnaissance studies in combination with spatial data such as the SSURGO (1:15840 Soil Survey Geographic database) map classification (slope class, geomorphology, and hydric soil designation) to identify riparian sites with high capacity for groundwater nitrate removal for the purpose of watershed modelling, protection and restoration efforts. By combining the site soil surveys and map database they classified

riparian soils into two functionally distinct classes: i) Soils where groundwater flows through a functionally significant width of hydric soils (> 10 m) and there is absence of groundwater surface seeps and are therefore characterised by high groundwater nitrate removal capacity; ii) Soils where groundwater nitrate removal may be constrained by either minimal hydric soil width or by surface seepage and rapid flow across the riparian zone. The observed agreement between SSURGO drainage class and the field-observed drainage class of hydric soils suggested that SSURGO could be a useful database for the parameterisation of more site-specific riparian biogeochemical models such as the Riparian Ecosystem Management Model (REMM) (Lowrance *et al.,* 2000), although the use of the database is restricted to the U.S. only.

A similar landscape based approach was presented more recently by Tomer *et al.* (2009). In this, soil survey data (slope, soil texture and soil erodibility) can be used to identify locations where buffers can function better to trap sediment and associated pollutants from surface runoff. In general, better locations for buffers are those where slope and soil conditions lead to greater runoff and sediment generation. In conjunction with soil survey maps, or in their own right, digital terrain analyses can be applied to determine a range of landform parameters such as slope, aspect and upslope contributing area. Mapping these parameters provides images that reveal pathways of water movement and areas of water accumulation on the landscape, indicating where buffers will intercept more runoff. In general, better opportunities to intercept runoff and/or baseflow occur along first order streams than along larger streams. Although both techniques can provide detailed spatial resolution and can be incorporated in a GIS system, their dependence on detailed databases restricts their use in the U.S. Moreover, the authors suggest that due to the simplifying assumptions involved in both methods and the lack of uniform quality across the various databases, these techniques should be used only as a general guide for locating buffers. Another GIS-based catchment mapping tool to identify riparian areas where rehabilitation would most likely yield optimal reduction in stream nitrogen loads was developed by Rassam and Pagendam (2006).

Cosandey *et al.* (2003b) followed a more detailed two step approach for relating riparian zone denitrification functionality with 3D soil cartography. Specifically they measured potential denitrification activity, which then related to soil physicochemical

parameters, of which organic carbon and soil texture were the main determinants of variability. Subsequently they grouped the soil horizons with similar denitrification activity to delimit functional horizons. At a second step they related thickness maps of soil horizons to the denitrification functional horizons permitting the 3D pattern of denitrification to be estimated in a GIS environment. Although this approach allowed the prediction of the variation of denitrification based on field criteria, the high spatial variability of organic carbon in different soil types renders this method rather costly and unsuitable for wide application for management purposes.

Another simplified field method to assess riparian zone nitrate removal at the field scale was recently proposed by Vidon and Dosskey (2008). The method is based on assessing nitrate depletion in riparian zone groundwater along a 3-well transect between the edge of a field and an adjacent stream. This approach was accurate in estimating nitrate concentration depletion but failed in assessing water and nitrate fluxes, as well as the necessary buffer zone width for 90% reduction of nitrate in the groundwater. Moreover, the method provided better estimates where groundwater flow was parallel to the water table through homogeneous aquifer material, and was therefore characterised as unsuitable for general use in sites where site-scale hydrogeomorphic patterns are not well established.

A number of tools that do not involve detailed field studies but rather rely on literature information and sometimes simple field observations have been developed to assist management decisions for floodplain/buffer zone restoration aiming at ecological and/or water quality objectives. The appropriate buffer width for the purpose of atlantic salmon habitat protection can be estimated through the selection of a number of buffer attributes such as slope, soil hydrologic group and percent canopy closure, which then are evaluated through a buffer width key and further weighted with adjustment factors to finally determine a suggested riparian buffer width (Haberstock *et al.,* 2000). The Buffer Zone Inventory and Evaluation Form (BZIEF) (Ducros and Joyce, 2003), built from a matrix of vegetation-related attributes as indicators of habitat quality and hydrological attributes that facilitate water quality improvements, is another score assessment based tool aimed at the rapid field reconnaissance of buffer zone potential for water quality and wildlife habitat improvement. A more strategic tool aimed at landscape and catchment scale planning integrates ecological key factors that drive

floodplain restoration (e.g. hydrology, bed load, connectivity, biodiversity, water quality), as well as crucial socio-economic aspects (e.g. flood protection, public attitude) with GIS and multi criteria decision analysis (MCDA) to derive a single Ecological Restoration Suitability Index (ERSI) (Rohde *et al.,* 2006). A conceptual model that identifies riparian hydrologic types based on topography and depth of permeable sediments in the riparian zone and then links that information to soil texture to estimate effectiveness of nitrate removal and optimum width of riparian zones was developed as a management tool by Vidon and Hill (2006) in Ontario, Canada. The identification of Operational Landscape Units (OLU), defined as combinations of landscape patches with their hydrogeological and biotic connections, is another tool to analyse best options for restoration of wetland ecosystem functioning and plant biodiversity in fragmented landscapes (Verhoeven *et al.,* 2008). These tools, although likely to be popular among natural resource managers and consultants due to their desktop based approach and/or use of field reconnaissance forms, are too general for site specific applications. Moreover, the water quality function is evaluated through hydrogeomorphic characteristics that assume effective nitrate removal via the main pathway of denitrification, ignoring other nitrate attenuation processes, and more importantly not accounting for the high spatial and temporal variability of denitrification.

Detailed numerical models that enable a more accurate prediction of the nitrate removal function in riparian zones also exist. According to Correll (2005), the best developed and tested overall model for multi-zone riparian buffer water quality functions is the Riparian Ecosystem Management Model (REMM; Inamdar *et al.,* 1999a,b). REMM predicts reductions in nonpoint source pollutants within riparian vegetative buffer zones by simulating subsurface and surface hydraulic movement, nutrient dynamics, sediment transport and vegetation growth at a daily time step by incorporating a large number of variables including topographic properties, vegetation types and local weather (Lowrance *et al.,* 2000). To date, REMM has been tested and validated only with field-scale data from the South-eastern Coastal Plain region of the U.S. (Kim *et al.,* 2007).

Rassam *et al.* (2008) developed conceptual models for SW-GW interactions in riparian zones of ephemeral and perennial streams of Australia and then formulated analytical solutions that describe nitrate removal via denitrification in these riparian zones. These

conceptualisations were included in a GIS-based model called Riparian Nitrogen Model (RNM). According to the authors the RNM should be used in identifying catchments that have more potential for nitrate attenuation than others and not to produce absolute numbers of nitrate removal. This is due to issues of scale in terms of the land use and soil data availability, the mathematical formulation of the denitrification function and the estimation of the groundwater depth that dictates the extent of the anoxic saturated zone.

The dynamical process-based eco-hydrological model SWIM (Krysanova *et al.,* 1998), which simulates water and nutrient fluxes in soil and vegetation, as well as transport of water and nutrients to and within the river network, was used for identifying point and diffuse sources of nutrient pollution, assess possible influences of climate and land use change scenarios and finally evaluate potential measures to achieve the "good ecological status" target of the WFD in the meso-scale Rhin catchment (Hesse, *et al.,* 2008). Models such as SWIM that are process-oriented and of average complexity, can have several advantages when used at a strategic planning stage, but are rather complicated for a rapid assessment of a re-connected floodplain water quality function for the needs of natural resource managers.

The Soil Water Assessment Tool (SWAT) is a continuous spatially explicit hydrologic and water quality model that requires specific information about weather, soil properties, topography, vegetation, and land management practices occurring in the watershed in order to quantify effects of land use and management change on water quality within agricultural basins (Arnold *et al.,* 1995). Cerucci and Conrad (2003) used a combination of the SWAT and REMM models to predict nitrate loads from different source areas with and without riparian buffers in order to select the most cost efficient land parcels to form a riparian buffer. Barlund *et al.* (2007) tested SWAT's applicability to assess the effectiveness of potential management options such as buffer strips as measures for achieving lake water quality targets set under the requirements of the WFD. Although SWAT showed some promise in evaluating impacts of different management options, it also demonstrated the effort needed to parameterise, calibrate and validate the model appropriately. Liu *et al.* (2008) improved further the SWAT model by embedding an additional module for assessing the effects of riparian wetlands

on runoff and sediment yields at the watershed scale with the aim to more effectively assess various wetland restoration scenarios.

A more hydrodynamic-based model, including detailed inflow and outflow hydrological processes, is WETTRANS (Trepel and Kluge, 2004), a matrix model, which uses a quasi-stationary mass balance to approximate flow paths and nitrogen transformation and to evaluate the effects of various water management options on nitrogen retention in a riparian peatland in northern Germany. A process based hydrological model (TNT) and a generic crop model (STICS), for simulating crop growth and nitrogen biotransformations, were combined to study the effect of the spatial distribution of agricultural practices on nitrogen fluxes in streams. The results suggested that placing crops that act as nitrogen sinks downslope from potentially nitrogen polluting crops could reduce significantly the streamwater contamination by nitrate. Moreover, in this study, nitrogen uptake by sink crops was found to be quantitatively more important than denitrification in reducing nitrogen output (Beaujouan *et al.,* 2001).

Those conceptual models and assessment tools that are GIS-based, or depend on geomorphological databases or field observations and scoring criteria usually provide a qualitative assessment of the suitability of sites for water quality improvement. While they could constitute a first approach in selecting appropriate areas within a wider catchment, their use is restricted in pre-project management decisions. On the other hand, existing process-based models for quantitative predictions of hydrological interactions and nitrogen transformations are usually data intensive, which restricts their use to scientific applications, since these data are not usually available during the first stages of restoration planning or for the evaluation of the restoration success intensive monitoring programmes are required. However, there is need for a rapid, cost-effective and yet reliable assessment tool to support the management decisions for river-floodplain restoration aimed at effective nitrate removal. This tool should be based on a scientifically sound assessment of the nitrate removal capacity based on data that can be fairly inexpensively obtained at a pre- or post- restoration stage. In this way uncertainties associated with the indirect estimation of nitrate removal through for example geomorphological characteristics can be avoided, while spatial and temporal variability can be accounted for without the need for extensive datasets that in most cases are not available.

2.5 *Research Aim and Objectives*

The overarching aim of the present study is to investigate the hydrological and biological processes by which the floodplain of a temperate restored river reach can reduce nitrate concentration in surrounding surface and groundwaters with the aim of informing future river-floodplain restoration projects about best management practices with respect to water quality improvement via nitrate removal.

The research will address the following research objectives:

1. Identify the main hydrological mechanisms responsible for the inundation regime in a temperate re-connected floodplain. Assess the relative importance of each hydrological mechanism for (i) the transport of nitrate and (ii) the creation of the necessary conditions for denitrification and DNRA in the soil.

2A. Quantify the relative importance of potential heterotrophic denitrification and DNRA in the reconnected floodplain.

2B. Investigate the main controlling factors influencing the two processes in a temperate agricultural re-connected floodplain. This research will focus in particular on:

(i) The role of land use management in influencing the magnitude and relative importance of heterotrophic denitrification and DNRA.

(ii) The role of vertical changes in soil stratigraphy and electron donor and acceptor availability in influencing the magnitude and relative importance of denitrification and DNRA.

(iii) The role of wetting-drying cycles in controlling the spatial and temporal variability of heterotrophic denitrification and DNRA.

3. Develop, validate and apply a management tool aimed at evaluating the nitrate removal capacity of candidate sites for river-floodplain restoration and/or assessing the nitrate removal capacity of restored floodplains as part of a post-project appraisal.

Chapter 3: Study Site

3.1 *Introduction*

The River Cole catchment at Coleshill, Oxfordshire UK, was selected as the study site, since it is a temperate rural floodplain where diffuse nitrate pollution from urban and agricultural sources is a current issue. Moreover, the river-floodplain connectivity was restored 14 years ago, for the purpose of increased flood storage and habitat creation, and the frequency of overbank inundation was markedly increased. Therefore it was a suitable site for studying the research objectives of the study.

3.2 *The River Cole catchment*

The study reach is a section of the River Cole located on the National Trust Buscot and Coleshill Estate, on the Oxfordshire/Wiltshire border (NGR: SU 234935), covering a catchment area of approximately 130 km^2 that consists of 2 km reach of river with approximately 50 ha of floodplain. The River Cole is a tributary of the River Thames located in the upper part of the catchment. Its headwaters include part of the large town of Swindon, Wiltshire (Figure 3.1).

3.3 *Land Use*

The Cole catchment is dominated by agriculture with significant urban development in the headwaters draining Swindon. Agricultural changes in the catchment have been dramatic since the 1950s. The dominant land use was originally pasture with flooding of the lowlands allowing two cuts of hay per year. The agriculture in the catchment has witnessed significant change over the past 50 years, predominantly from pasture to arable farming. Much of the floodplain shows evidence of 19^{th} century under-drainage or management for water meadows. Drainage of the floodplain soils was undertaken in the 1960s and peaked in the period 1965-1975. Downstream of Coleshill the land drainage scheme of 1976 was accompanied by large scale under-drainage and arterial drainage of the floodplain. Prior to the restoration, arable farming occupied 60 % of the floodplain riparian zone, with the main concentration downstream of Coleshill Bridge (Sear and White, 1994).

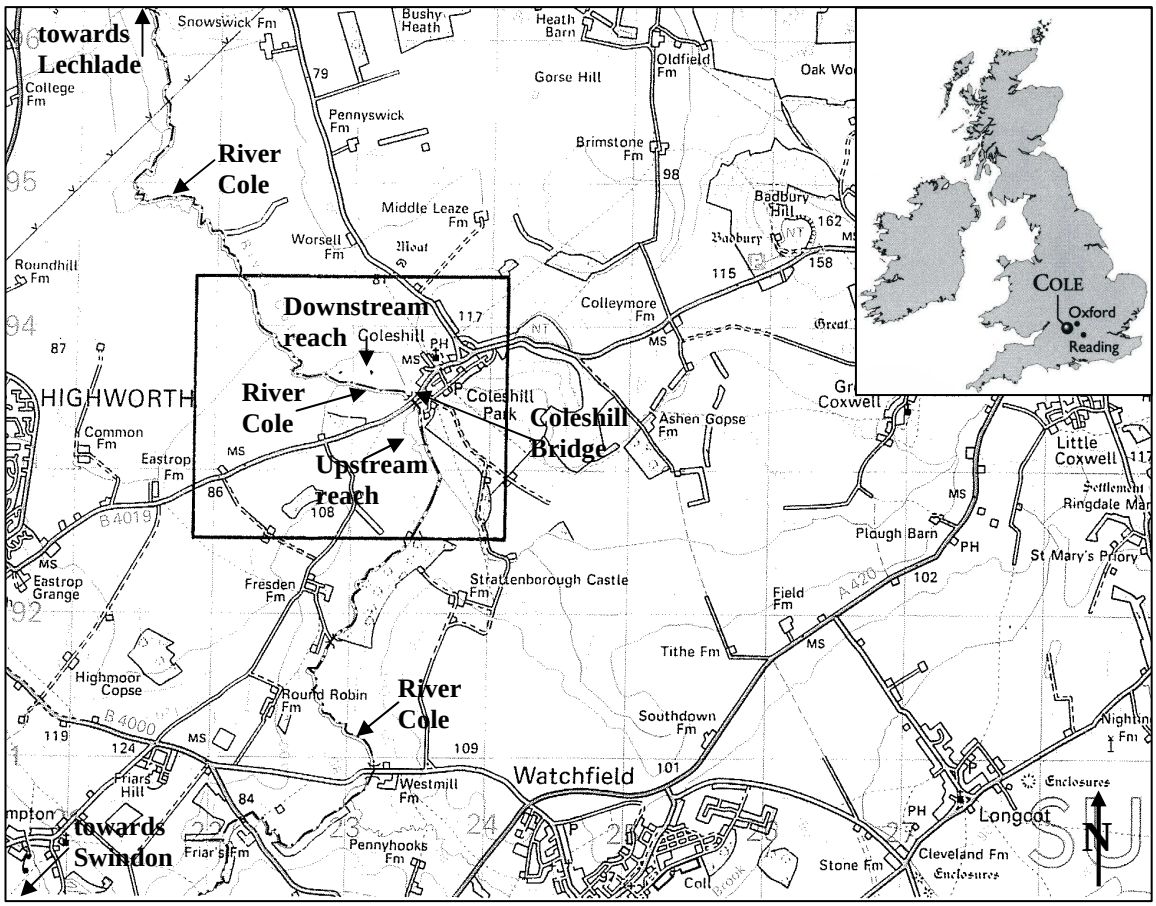

Figure 3.1: Site location

3.4 *Geology and Soils*

The valley of the River Cole is floored with alluvium. In the lower reaches of the River Cole, downstream of Coleshill Bridge, Thames gravels underlie the alluvium, and locally outcrop in the river banks. The river rises from the chalk escarpment of the Berkshire Downs before flowing across a wide expanse of Kimmeridge Clay and passing between the Corallian Rag Hills, comprising Corallian Sandstone and Limestone, to the north east of Swindon. The downstream section of the river flows over lowland clay vales comprised of Oxford Clay, before joining the River Thames at Lechlade (Sear and White, 1994).

The soils of the Cole catchment are dominated by clay based soils up onto the Downs. The main soils associations in the area are: Pelo-Stagnogley/Stagnogley (712 & 711 j/f); Brown Redzina (343h); Gleyic brown calcareous earths (512); and grey Redzinas (342a). Clay vale landscapes of this type are not particularly susceptible to erosion, due

to the low gradients associated with this landscape and the cohesiveness of the soil types (Sear and White, 1994).

3.5 *Hydrology*

The headwaters of the River Cole are in chalk, which sustains a modest baseflow throughout the year. The river is also fed by a number of springs along its course, notably at Highworth, Watchfield and Coleshill (Environmental Report River Cole Restoration, 1995). However, over 50 % of the catchment is underlain by clay which promotes a rapid response to rainfall (Kronvang *et al.,* 1998). The flashy response to rainfall events is also exacerbated by urbanisation in the upstream reaches around Swindon. The mean annual discharge of the River Cole, based on records from 1976 to 2006 at the gauging station at Inglesham (NGR: SU 208970), is 1.19 m^3s^{-1}. The Q95 (discharge exceeded at 95 % of time) is 0.14 m^3s^{-1}, while the Q10 (discharge exceeded at 10 % of time) is 2.72 m^3s^{-1}. The mean annual precipitation of the catchment is 682 mm (Source: Environment Agency of England and Wales).

Although no sewage effluent from Swindon itself enters the Cole, there are large amounts of urban runoff that have necessitated the gradual construction and continuous upgrading of 12 flood storage areas, in the urban areas of the catchment, in order to regulate flashy flows. Prior to the restoration, the 1 in 2 year flood event flooded the site mainly upstream of Coleshill Bridge, with little flooding downstream (Environmental Report River Cole Restoration, 1995). The river is a low energy system with sediment transport mainly confined to fine silts and clays.

The river has been straightened and impounded in the 17th century to enable the operation of a water mill. In the 1970s the downstream channel had been further deepened and widened to alleviate flooding in support of arable farming within a floodplain of 50 ha (Vivash *et al.,* 1998). Consequently, the Cole floodplain, which was an important store of water and fine sediments, was effectively drained in the reach downstream of Coleshill as all but the largest floods (>1:25 year recurrence interval) were contained in- bank (Sear and White, 1994).

3.6 *Water Quality*

The River Cole at Coleshill is fairly typical of many small rural rivers in lowland Britain (Environmental Report River Cole Restoration, 1995). Table 3.1 shows average concentrations for selected water quality determinants between 2005 and 2008. These indicate that in general the water quality is good, well-saturated with oxygen and usually with a low BOD and only moderate levels of ammonia. The water has a high alkalinity, with pH most of the time above neutral. Suspended sediment loads tend to be rather high, while nutrient loadings also tend to be high with nitrate nitrogen peaking near the EC drinking water threshold (10 mg N L^{-1}). Phosphate is also much higher than would be expected for an undisturbed catchment. The high nitrate and phosphate levels reflect the largely agricultural nature of the catchment, whilst the phosphate levels could also reflect sewage discharges from the small sewage treatment works (STW) at Coleshill and possibly from the larger STW at Shrivenham further upstream (Environmental Report River Cole Restoration, 1995).

Table 3.1: Values of selected water quality determinants sampled at Coleshill Bridge (NGR: SU 234935) in 2005 - 2008. * indicates data collected in 2000 - 2005 from the same location (Source: Environment Agency of England and Wales).

Determinant	**Mean**	**Range**
pH*	7.8	6.7 - 8.7
Suspended solids (mg L^{-1})	13.2	5.1 - 39.8
Biochemical Oxygen Demand (mg L^{-1})	1.7	1 - 5.3
Dissolved Oxygen (%)	88.6	61 - 117
Ammonium nitrogen (mg L^{-1})	0.06	0.03 - 0.18
Nitrate nitrogen (mg L^{-1})	5.1	1.8 - 9.7
Chloride (mg L^{-1})*	53.6	17.3 - 242
Orthophosphate (mg L^{-1})	0.28	0.1 - 0.6
Alkalinity (as $CaCO_3$) (mg L^{-1})*	153	38 - 198
Copper (dissolved) (μg L^{-1})*	4.9	0.7 - 8.8
Zinc (μg L^{-1})*	31.8	7.3 - 105

3.7 *Vegetation*

A river corridor and floodplain vegetation survey was undertaken in 1994, prior to the restoration of the site (Environmental Report River Cole Restoration, 1995). To date there has not been a follow up survey to document any changes in the vegetation composition of the floodplain following the restoration (personal communication Martin Janes).

River Corridor

As a whole the River Cole in this area is moderately rich in wetland plant species (circa 46 spp.). The ponded area upstream of the Mill supports the richest wetland reaches, including a diverse wetland herb community on the lower, cattle-poached banks. Both emergent and aquatic flora of this area include species such as: arrowhead (*Sagittaria saggittifolia*); narrow leaved water plantain (*Alisma lanceolatum*); skullcap (*Scutellaria galericulata*); tufted forget-me-not (*Myosotis laxa*); and marsh woundwort (*Stachys palustris*). The other main areas of interest are the aquatic communities, dominated by stream water-crowfoot (*Ranunculus penicillatus*) and flowering rush (*Butomus umbellatus*), both of which are associated with the shallow reaches of the River Cole (Environmental Report River Cole Restoration, 1995).

Floodplain

A Phase 1 survey of the floodplain adjacent to the Cole was also carried out in 1994 in accordance with the National Vegetation Classification (NVC) methodology (Environmental Report River Cole Restoration, 1995). Two broad habitat types emerged: arable land to the north of Coleshill Bridge and grassland to the south. The arable land in 1994 was largely down to rape. All fields on the western side of the river had broad (10 m) buffer strip areas between the arable crop and the rivers edge, supporting a variety of common ruderals.

Four NVC grassland types were recorded south of Coleshill Bridge. The grassland community of greatest species richness and conservation value was NVC type MG5-Crested Dogs-tail - Common Knapweed Meadow and Pasture Community. This type of community is characterised by red fescue (*Festuca rubra*), crested dog's tail (*Cynosurus cristatus*), bird's foot trefoil (*Lotus corniculatus*), ribwort plantain (*Plantago lanceolate*) and Yorkshire fog (*Holcus lanatus*). These pastures have usually not been

sprayed with herbicide, and they received little or no fertiliser. They were usually cut for hay and were ungrazed in summer but may have been grazed in winter (Environmental Report River Cole Restoration, 1995).

Of particular interest is the ex-SSSI Coleshill fritillary meadow north of the bridge. This is a moderately species rich site, which has been partially improved, but still retains a number of old wet meadow species including snake's head fritillary (*Fritillaria meleagris*), dropwort (*Fillipendula vulgaris*), sweet vernal grass (*Anthoxanthium odoratum*), meadow sweet (*Fillipendula ulmaria*), meadow vetchling (*Lathyrus pratensis*), ladies smock (*Cardamine pratensis*), knapweed (*Centaurea nigra*) and common vetch (*Vicia sativa*).

3.8 *River Cole Restoration project*

The 2 km reach of the River Cole, chosen also as the site of the present study, was included in an EU-*Life* Demonstration Project for damaged rivers and floodplains in 1995 along with River Brede in Denmark and River Skerne in UK (Holmes and Nielsen, 1998). The main objective for River Cole was the restoration of the river and floodplain in terms of physical features, flood storage, habitat diversity and visual appearance (Janes *et al.*, 1999).

This was achieved by both new channel creation and reshaping of existing channels over a distance of 2 km. During this process, channel width was considerably reduced from a mean of 14.9 to 9.4 m, and channel length was increased by about 8%. Bankfull capacity was reduced by raising bed levels relative to ground level by about 1m. This aimed to restore more frequent seasonal flooding to adjacent fields which would be farmed less intensively, supported by Countryside Stewardship (Janes *et al.,* 1999). Wetland vegetation was allowed to re-colonise naturally (Biggs *et al.,* 1998). Figure 3.2 illustrates the various elements of the restoration project along the restored reach.

In the upstream reach, a new meandering stream was created along what was believed to be the old course of the river and the mill leat was also kept for its heritage value. Floods are encouraged between the new course and the mill leat. In the downstream section, a new meandering channel was created along the old straightened one. The old channel was infilled in some parts and elsewhere it was turned into backwater areas.

Flooding is encouraged through the connection of the new channel with a former draining ditch surrounding the pasture meadow. In this way overbank inundation is not restricted to the riparian areas along the banks, but extends further to the higher area of the floodplain. At the end of the reach, the fritillary meadow with important conservation value was preserved and an experimental reedbed receiving runoff from agricultural land was created.

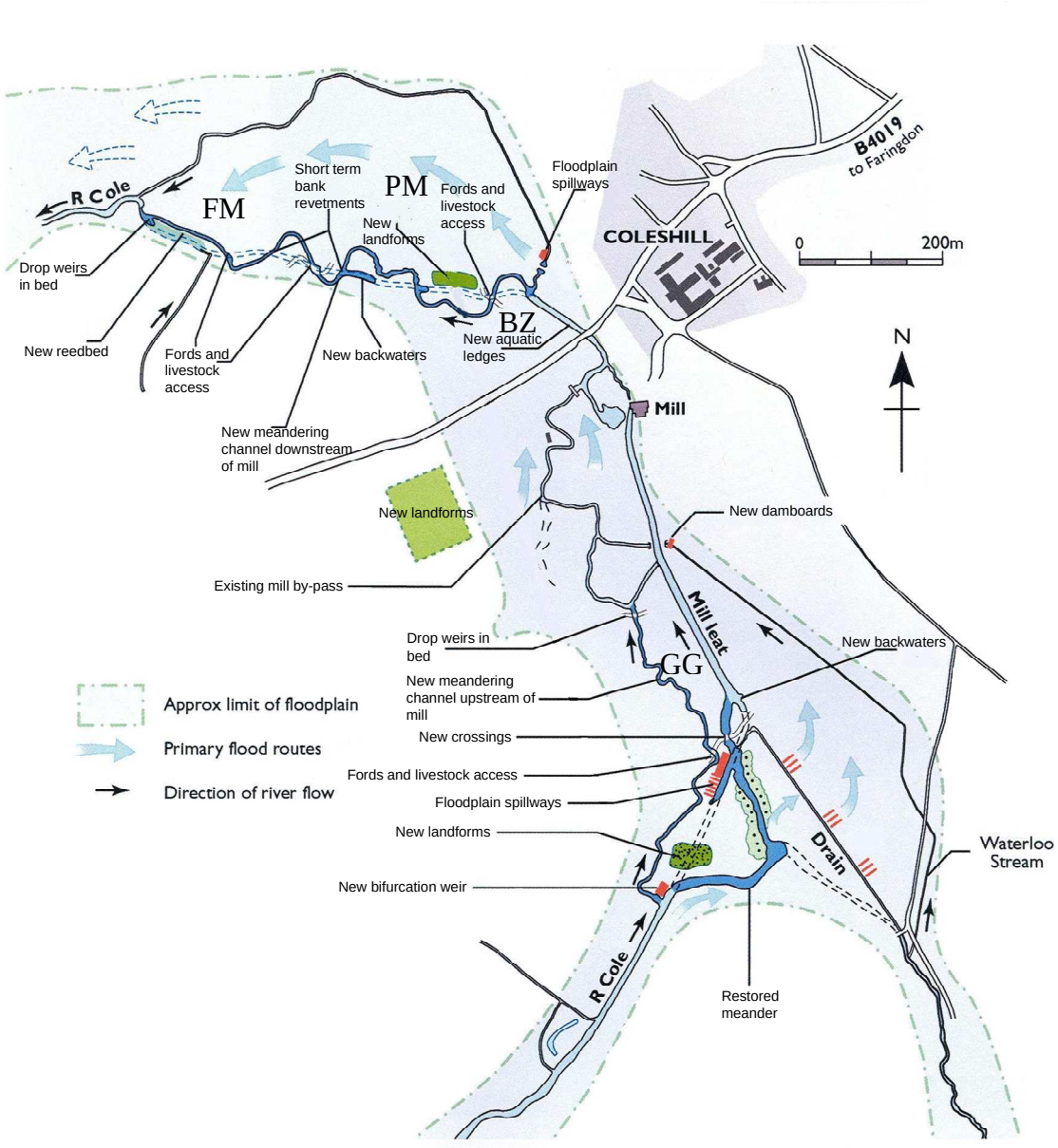

Figure 3.2: Schematic of the restoration measures implemented at the River Cole reach at Coleshill (adapted from Janes *et al.*, 1999). FM: Fritillary Meadow; PM: Pasture Meadow; BZ: Buffer Zone and GG: Grazing Grassland.

Following the implementation of the restoration plans, flood frequency and river valley inundation have increased and downstream peak water levels were reduced (personal communication Martin Janes). A variety of instream geomorphological features such as pools, berms, point bars and overbank deposits were created in the new channels. Suspended sediment loads increased during the construction phase, but soon after returned to normal levels (Kronvang *et al.,* 1998). Plant and aquatic invertebrate assemblages showed a rapid recovery of species richness in the restored sections of River Cole after channel reconstruction (Biggs *et al.,* 1998). In the case of River Cole, there was not post-restoration monitoring of the change in nutrient retention capacity of the restored floodplain, as there was the case for River Brede (Hoffmann *et al.,* 1998a).

Figure 3.3 shows the current layout of the 2 km reach of the River Cole, 14 years after the completion of the restoration project. The four land use zone areas, which are the subject of the present study, have also been delineated in Figure 3.3. With direction from upstream to downstream, the Grazing Grassland (GG) is the area between the new meandering river and the retained mill leat. The vegetation type is expected to be similar to the grassland communities identified in the 1994 survey, since the land use management has not been changed, although the effect of the increased inundation frequency on the vegetation community composition is not currently known. The dominant land use is grazing by cattle, when overbank flooding is not occurring (Figure 3.4).

The Buffer Zone (BZ) area is part of the buffer strip maintained between the arable land on the west and the new meandering section of the river downstream from Coleshill Bridge. The arable land adjacent to BZ is mainly used for winter cereals (oil seed rape and flax) but the farming practice is now less intensive, although the current rate and frequency of fertiliser and herbicide application is not known. While the vegetation composition is not expected to have changed significantly, the inundation regime has increased due to the narrowing of the river and the raising of its bed downstream of the bridge (Figure 3.5). The restoration plan predicted an increased flooding occurrence under low order events during the winter and spring months, but anticipated flooding to persist for short periods due to expected rapid drainage through the gravel underlying the alluvium. It was however noted that ‘in extreme circumstances the downstream

meadow areas could be covered with flood water for up to three weeks in winter' (Environmental Report River Cole Restoration, 1995).

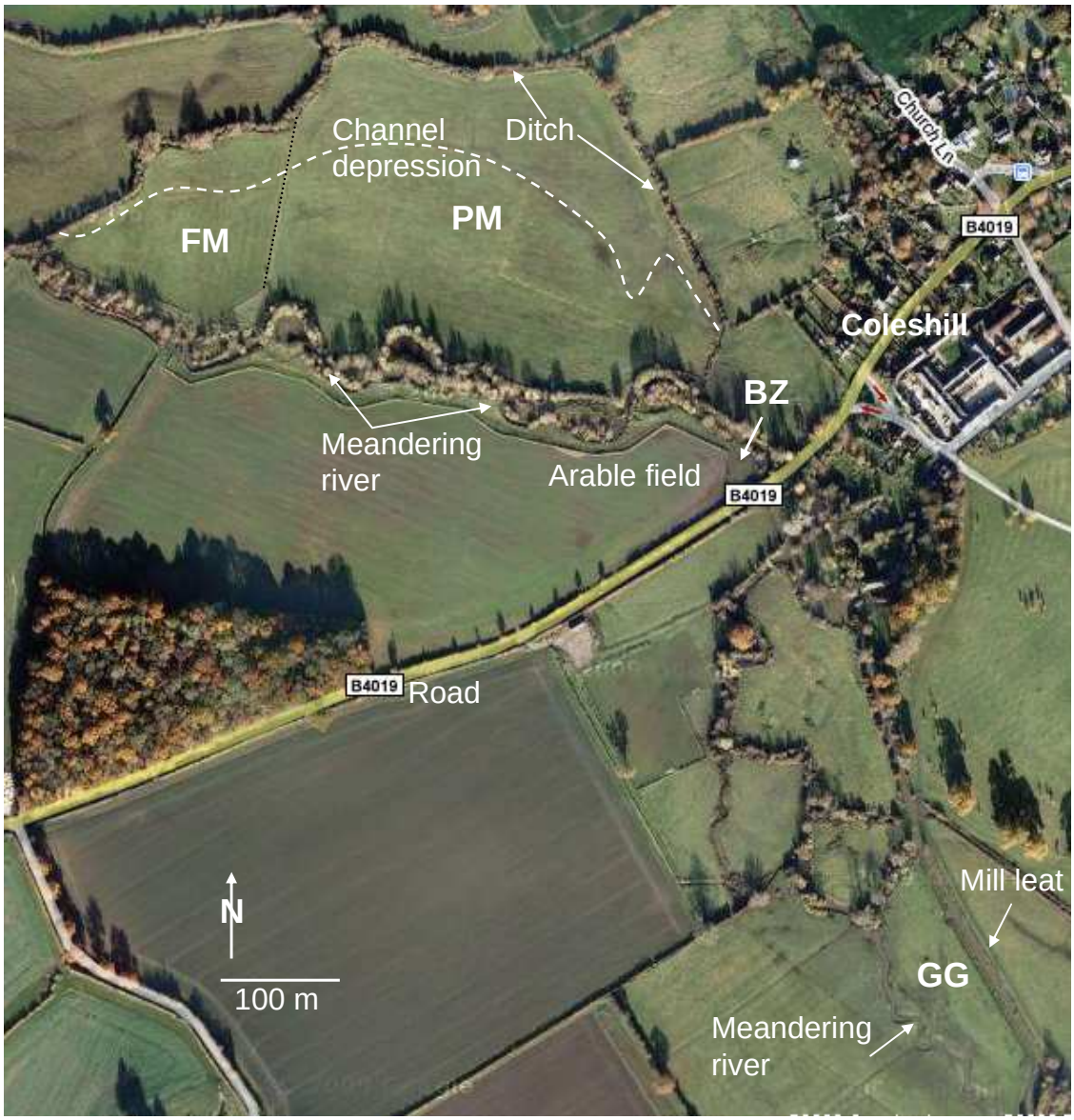

Figure 3.3: Current layout of the restored 2 km reach of the River Cole at Coleshill (Google Maps©, 2009).

The arable land to the east of the downstream section of the river was reclaimed and turned into pasture, Pasture Meadow (PM), where grazing is not allowed and hay is cut once a year. Moreover, this part of the restored reach is used for horse riding by the local equestrian clubs. Overbank flooding is encouraged by the connection of the old draining ditch, surrounding the PM, to the meandering river. In fact the overflowing of the re-connected draining ditch over the last 14 years has created a depressional

landscape feature spreading across the PM with direction from east to west. This land use zone is the most modified following the restoration, and therefore a change in the vegetation composition has probably occurred with re-colonisation of the former arable land by wet-meadow species and possibly fritillaries from the adjacent Fritillary Meadow (FM) (personal observation). The FM, north from PM, has been conserved and the abundance of fritillaries has increased (personal communication Martin Janes). Flooding is also encouraged from both the river and the draining ditch.

Figure 3.4: Flooding in the Grazing Grassland area in December 2005 (photo F. Sgouridis)

Figure 3.5: The Buffer Zone area next to the arable field in September 2006 (top) and flooded in March 2008 (bottom) (photos F. Sgouridis).

Figure 3.6: The Pasture Meadow area with a view from east to west (top) in December 2006 and flooded in March 2008 (bottom) (photos: F.Sgouridis).

3.9 *Rationale for study site selection*

The selection of the restored reach of the River Cole at Coleshill as the site for investigating the research objectives of the present study is based on the following arguments:

Objective One: Identify the main hydrological mechanisms responsible for the inundation regime in a temperate re-connected floodplain.

- It is obvious that the hydrological connectivity between the river and the floodplain has been reinstated and that the River Cole at Coleshill has an active re-connected floodplain
- Given the low relief landscape of the River Cole catchment and the heavy clay nature of the alluvium, water table fluctuations in relation to stream stage are expected to play a significant role in regulating nitrate attenuation processes
- Overbank flooding seems to be the dominant hydrological mechanism, however the contribution of hillslope processes as well as subsurface processes between interspaced permeable and impermeable alluvia can also be investigated due to the landscape position and the geology of the floodplain

Objective Two: Quantify the relative importance of potential heterotrophic denitrification and DNRA and investigate the main controlling factors influencing the two processes in a temperate agricultural re-connected floodplain.

- The intermittent saturation regime of the re-connected floodplain suggests that favourable conditions for nitrate attenuation processes are likely to develop. Moreover, the effect of the different land use management practices and the spatial distribution of nitrate attenuation can be investigated across the different land use zones of the restored reach
- It is hypothesized that due to the low relief of the River Cole re-connected floodplain, topography likely plays a minor role in creating areas of increased nitrate attenuation activity, whereas the hydrological regime is the main driver of temporal and spatial variability by controlling both the supply of nitrate and the redox potential of the soil
- There is indication for the existence of shallow groundwater table in the re-connected floodplain of the River Cole, which fluctuates between the ground

surface and 2 m depth for most of the year. Therefore its role in nitrate removal may be important during, and especially between, flood events and for this reason there is scope in investigating the nitrate attenuation potential of subsurface soils

- Being a mature re-connected floodplain, transient problems associated with the acclimation of the vegetation and microbial communities to the changing hydrological regime are not expected to be encountered.

Objective Three: Develop, validate and apply a management tool aimed at evaluating the nitrate removal capacity of candidate sites for river-floodplain restoration and/or assessing the nitrate removal capacity of restored floodplains as part of a post-project appraisal.

- The re-connected River Cole catchment is also suitable for the development and validation of a management tool for the post-project appraisal of the nitrate removal capacity of a restored floodplain
- Finally, issues of ownership, accessibility and permissions are resolved because of long established connections with the River Restoration Centre (providing advisory support to the present study) and the National Trust who are responsible for managing the area.

Chapter 4: Methods

4.1 *Introduction*

For the purpose of characterising the hydrological regime of the re-connected floodplain of the River Cole, a hydrological and meteorological monitoring program was designed and implemented according to the methodology described in section 4.2. Additionally, the water chemistry of both the surface water (river and draining ditch) and the shallow groundwater were also monitored with the aim of identifying nitrate removal patterns along SW-GW interaction flow paths, following the methodology presented in section 4.3. The potential for biological nitrate attenuation processes was investigated in soil samples from the surface and subsurface horizons of the floodplain, while a number of soil properties were also measured with the aim of identifying and quantifying the relative importance of the main controlling factors of nitrate attenuation processes. This methodology is described in section 4.4. Finally, the methodology for the development, validation and application of the floodplain restoration management tool is given in Chapter 7.

4.2 *Hydrological analysis*

4.2.1 *Meteorological dataset*

An Automatic Weather Station (AWS) (MiniMet SDL 2900, Skye, Powys, UK) was installed on site (NGR: SU 2302793645), in the Pasture Meadow (henceforth PM), on 12th February 2007 (Figure 4.2.1). Table 4.2.1 shows the various sensors connected to the AWS, their operational range and sensitivity. The sample interval for all sensors was 30 seconds and averages were stored at 30 minute intervals. The raingauge stored total rainfall at 30 minute storage intervals.

Table 4.2.1: Specifications of the AWS sensors

Sensor	Measurement	Type	Units	Range	Sensitivity
Pyranometer	Total solar radiation	SKS 1110	W m^{-2}	0 - 5000	1mV/100W/m^2
Net radiometer	Net radiation	NR Lite	W m^{-2}	-200 - 1000	10μV/W/m^2
Thermistor	Soil temperature	SKTS 200/I	^{o}C	-20 - 100	0.1^{o}C
Anemometer	Wind speed	A100R	m s^{-1}	0 - 75	0.1 m s^{-1}
Wind vane	Wind direction	W200P	Degrees	0 - 360	2^o
Raingauge	Rainfall	ARG100	mm	n/a	0.197 mm/tip
RH	Relative humidity	SKH 2070/I/RS	%	0 - 100	2%
Thermometer	Air temperature	SKH 2070/I/RS	^{o}C	-40 - 60	0.2^{o}C

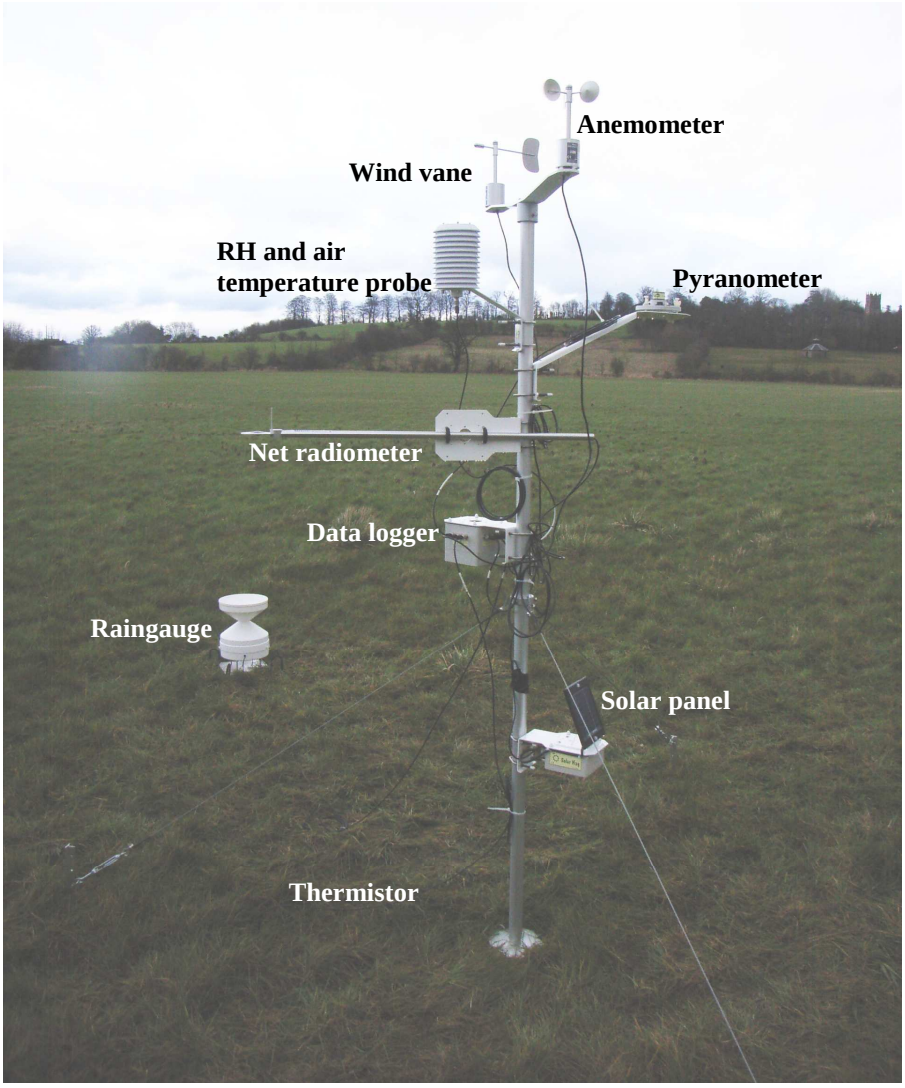

Figure 4.2.1: The AWS in the PM area of the River Cole floodplain (photo: F. Sgouridis)

The reference evapotranspiration rate (ETo; mm day^{-1}) was estimated according to the FAO Penman-Monteith method (Allen *et al.*, 1998), assuming a constant plant height of 0.12 m and a standardised height for wind speed, temperature and humidity at 2 m. The ETo formula is given in Equation 4.2.1, while Table 4.2.2 presents the definition of each parameter in Eq. 4.2.1, their units and whether they were measured or estimated.

$$ETo = \frac{0.408\Delta(Rn-G)+\gamma\frac{900}{T+273}u_2(e_s-e_a)}{\Delta+\gamma(1+0.34u_2)} \qquad (4.2.1)$$

Table 4.2.2: Parameters used for the estimation of ETo. * γ is calculated from Cp, P, ε, λ, which are used as constants. a.s.l. means above sea level.

Symbol	Definition	Units	Comment
ETo	reference evapotranspiration rate	mm day^{-1}	estimated
Rn	net radiation at the crop surface	MJ m^{-2} day^{-1}	measured
G	soil heat flux density	MJ m^{-2} day^{-1}	assumed minor
T	mean daily air temperature at 2 m	^{o}C	estimated
u_2	wind speed at 2 m height	m s^{-1}	measured
e_s	mean saturation vapour pressure	kPa	estimated
e_a	actual vapour pressure	kPa	estimated
e_s - e_a	saturation vapour pressure deficit	kPa	estimated
Δ	slope vapour pressure curve	kPa $^{o}C^{-1}$	estimated
$e^{o}(T_{max})$	saturation vapour pressure at max temp	kPa	estimated
$e^{o}(T_{min})$	saturation vapour pressure at min temp	kPa	estimated
RH_{max}	maximum relative humidity	%	measured
RH_{min}	minimum relative humidity	%	measured
γ*	psychrometric constant	kPa $^{o}C^{-1}$	0.067
Cp	specific heat at constant temp	MJ kg^{-1} $^{o}C^{-1}$	1.01E-03
P	average atmospheric pressure (77 m a.s.l.)	kPa	100.39
ε	ratio molecular weight of water vapour/dry air		0.622
λ	latent heat of vaporisation	MJ kg^{-1}	2.45

4.2.2 *River Cole stage, discharge and water chemistry*

River stage (m) and discharge (m^3s^{-1}) data were obtained as daily means and at fifteen-minute intervals from the nearest gauging station operated by the Environment Agency, at Inglesham (NGR SU 20829695; station ID 0790TH; Datum: 72.69 m above sea level), situated 5 km downstream of Coleshill Bridge and referring to a catchment area of 140 km^2, very similar to the catchment area of Coleshill (130 km^2). The gauging station consists of a compound crump weir (high central crest).

Additional water chemistry data for the River Cole were obtained from the Environment Agency's monitoring station at Coleshill Bridge (NGR: SU 234935; station ID PUTR0025) at monthly intervals. The list of the chemical determinants is presented in Table 4.2.3.

Table 4.2.3: Water chemistry determinants for River Cole

Code	Description	Units
0061	pH	
0062	Conductivity at 20°C	µS cm^{-1}
0076	Water temperature	°C
0085	BOD as O_2	mg L^{-1}
0111	Ammonia as N	mg L^{-1}
0116	Total Oxidised Nitrogen as N	mg L^{-1}
0117	Nitrate as N	mg L^{-1}
0118	Nitrite as N	mg L^{-1}
0135	Total Suspended Solids	mg L^{-1}
0162	Alkalinity pH 4.5 - as $CaCO_3$	mg L^{-1}
0172	Chloride ion as Cl	mg L^{-1}
0180	Orthophosphate as P	mg L^{-1}
0211	Potassium as K	mg L^{-1}
0237	Magnesium as Mg	mg L^{-1}
0241	Calcium as Ca	mg L^{-1}
6051	Iron as Fe	µg L^{-1}
6396	Turbidity NTU	NTU
6452	Copper as Cu	µg L^{-1}
6455	Zinc as Zn	µg L^{-1}
9901	Dissolved Oxygen as % saturation	%
9924	Dissolved Oxygen as O	mg L^{-1}

4.2.3 *Floodplain hydrological monitoring*

4.2.3.1 *Groundwater level*

An important aim of the hydrological monitoring was to measure the groundwater table elevation across the re-connected floodplain and thereby establish flow rate and direction within the subsurface, and also examine the detailed time sequence of events across the floodplain during overbank floods. Due to budget and time constraints it was not possible to monitor the hydrological regime of all four land use zones (approx. 50 ha of floodplain). Consequently, groundwater monitoring was restricted to the PM and BZ areas.

The PM (7.5 ha surface area) is the largest land use zone where the restoration project aimed at increasing the inundation frequency by connecting the river with the old draining ditch. Overbank flooding had been observed to occur at both the river to floodplain and ditch to floodplain directions. Therefore, the PM was a suitable site at

which to study the floodplain response to overbank flooding and the effect of multiple water sources on nitrate transport and inundation patterns. The BZ area (1.5 ha surface area) has the typical characteristics of a buffer strip, being situated between arable land and the river. Hence, its position is ideal for studying the attenuation of nitrate transported through groundwater flow paths from the arable land towards the river. Moreover, the gently sloping topography of BZ allows the investigation of the interplay between hillslope runoff and overbank inundation.

The PM and the BZ land use zone areas were instrumented with two transects of groundwater wells each. The locations of the wells are shown in Figure 4.2.2. Flow patterns across low-angled floodplains comprising heterogeneous sediments can be complex, and thus a single transect measurement orthogonal to the river, may not provide an adequate picture of subsurface flow paths (Burt *et al.*, 2002a). In PM, the transect perpendicular to the river (wells F1 to F7) was designed for capturing the SW-GW interactions between both the river to floodplain and ditch to floodplain directions. The transect parallel to the river (wells F9 to F14) aimed at capturing the contribution of the ditch to the overbank flooding across the floodplain. In BZ, the two perpendicular to the river transects (wells H1 to H4 and H10 to H4) aimed at intercepting the groundwater flow between the arable land and the river.

The groundwater wells were installed using a 40 mm hand auger. Each well consisted of an open hole drilled through the saturated zone to the shallowest impermeable layer, lined using a PVC pipe (I.D. 32 mm), perforated (5 mm holes at 20 mm intervals) along its entire length and sealed at the bottom to prevent ingress of sediment. The aim was to intercept the water table throughout the year and therefore the depth of the wells ranged between 1 and 2 m. The annular space between the tube and the sediment was in-filled with coarse gravel and sand while a bentonite seal was used to prevent rainwater from seeping down the hole. The top of the tube was capped and covered with a paving slab. Water table elevation was measured at every well at least monthly between October 2006 and October 2007, using a water level meter (Model 101, Solinst, Ontario, Canada). Seven wells in PM and five wells in BZ (see black circles in Figure 4.2.2) were instrumented with a pressure transducer (Levelogger Gold 3001, Solinst, Ontario, Canada) for continuous water level and temperature measurements.

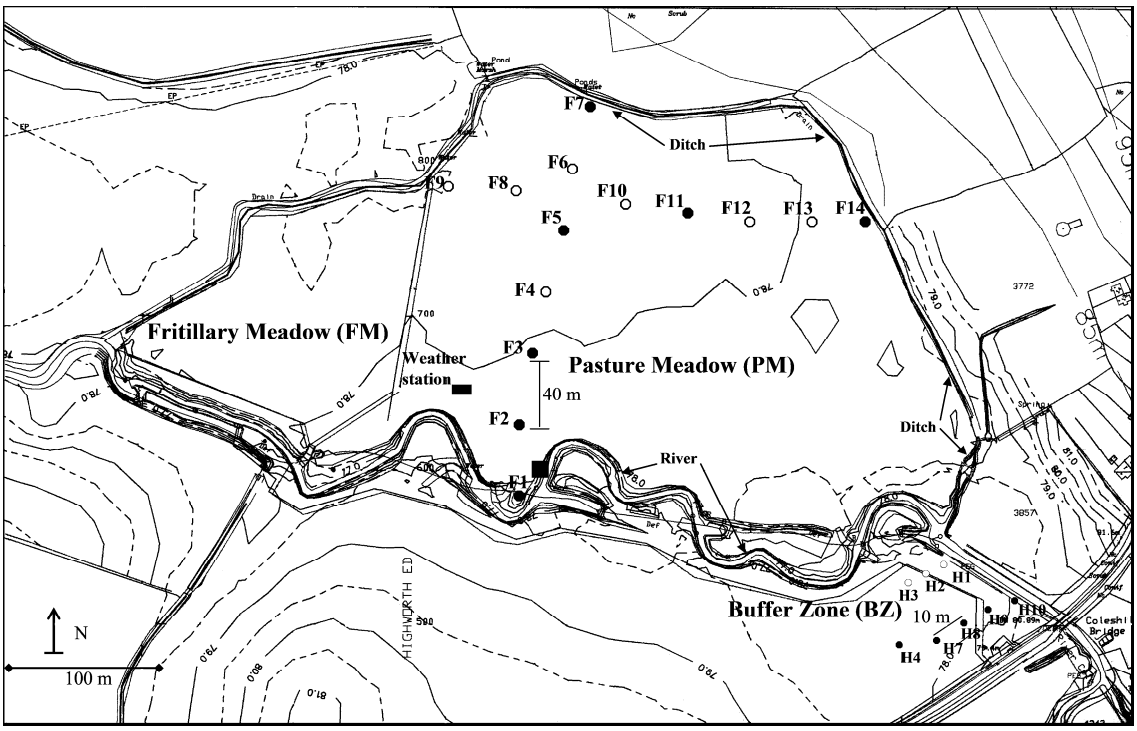

Figure 4.2.2: Location of groundwater wells in the PM and BZ sites. Dark circles indicate wells equipped with pressure transducers, while white circles indicate wells manually sampled without pressure transducers. The black square indicates the location of the Barologger™.

The Levelogger™ has internal temperature compensation, while it can be corrected for atmospheric pressure changes by using a Barologger™, which measures atmospheric instead of hydraulic pressure. The Levelogger™ has temperature sensor accuracy ± 0.05^{o}C and level sensor accuracy ± 0.3 cm at 4 m deployment depth. The logging frequency for all the Leveloggers™ and the Barologger™ was at fifteen-minute intervals between 19-10-06 and 18-12-06, and was changed to hourly intervals from then onwards. The specifications of the Leveloggers™ used in this study are shown in Table 4.2.4.

Since permission for the installation of a river stage was not granted, the wells closest to the river bank, F1 for the PM and H10 for the BZ, were used to approximate river stage at above bankfull conditions. These wells were chosen since they were located in river marginal sediments and were directly influenced by river stage fluctuations. When F1 and H10 wells are used as proxies for river stage, this is annotated in the hydrographs (see results in Chapter 5).

Table 4.2.4: Levelogger™ specifications

Well name	Sensor serial #	Longtitude (E)	Latitude (N)	Depth from ground surface to pressure plate within sensor (cm)	Well surface elevation above local datum (cm)
Pasture Meadow					
F1	1018741	423057	193589	94	0
F2	1019036	423051	193629	155	83
F3	1018742	423059	193669	144	61
F5	1019038	423077	193752	160	26
F7	1018726	423094	193832	187	17
F11	1019016	423161	193764	157	38
F14	1019010	423277	193763	183	80
Buffer Zone					
H4	1019013	423344	193491	170	57
H7	1019029	423354	193495	193	53
H8	1018478	423363	193499	103	64
H9	1018674	423372	193503	183	39
H10	1018483	423386	193509	115	45

4.2.3.2 *Floodplain surveying and floodwater volume calculation*

The surface elevation of the PM and BZ areas was surveyed using a GPS-RTK system (HiPer Pro, TOPCON, Newbury, UK) with horizontal and vertical accuracy 3 and 5 mm respectively. The PM was surveyed following a 25 x 25 m grid over a 7.5 ha surface area, while for the BZ a 5 x 5 m grid was followed over a 1.5 ha surface area. Contour plots for both areas were produced using Surfer® 8.0 (Golden Software), a grid-based contouring and three dimensional surface plotting graphics software, whereby XYZ data are interpolated on to a regular spaced grid from which a contour map is plotted. The gridding method chosen was kriging with a linear variogram. The contour plots are shown in Figures 4.2.3 and 4.2.4 for the PM and BZ respectively.

The peak floodwater volume stored on the floodplain surface during overbank events was estimated by using the Fill-Volume command in Surfer® 8.0 (Golden Software) in conjunction with the maximum water table elevation recorded above ground level for each flood event (using well F2 in the PM and the well H7 in the BZ). The linear relationships between water level and floodwater volume and flooded surface are shown in Figure 4.2.5.

Finally, the nitrate loading per flood event was estimated by multiplying the nitrate concentration of the river water on the available date closer to the event, data obtained from the Environment Agency's monitoring station at Coleshill Bridge, with the

maximum floodwater volume stored on the floodplain. This estimation assumes that all floodwater originates from river overbank flooding, without taking into account the contribution of rainwater and hillslope runoff. Nitrate removal percentages along surface and subsurface flowpaths were calculated based on concentration differences between neighbouring wells, accounting for dilution using Cl^- data, but without including the effect of flow through sediment layers of different hydraulic conductivities.

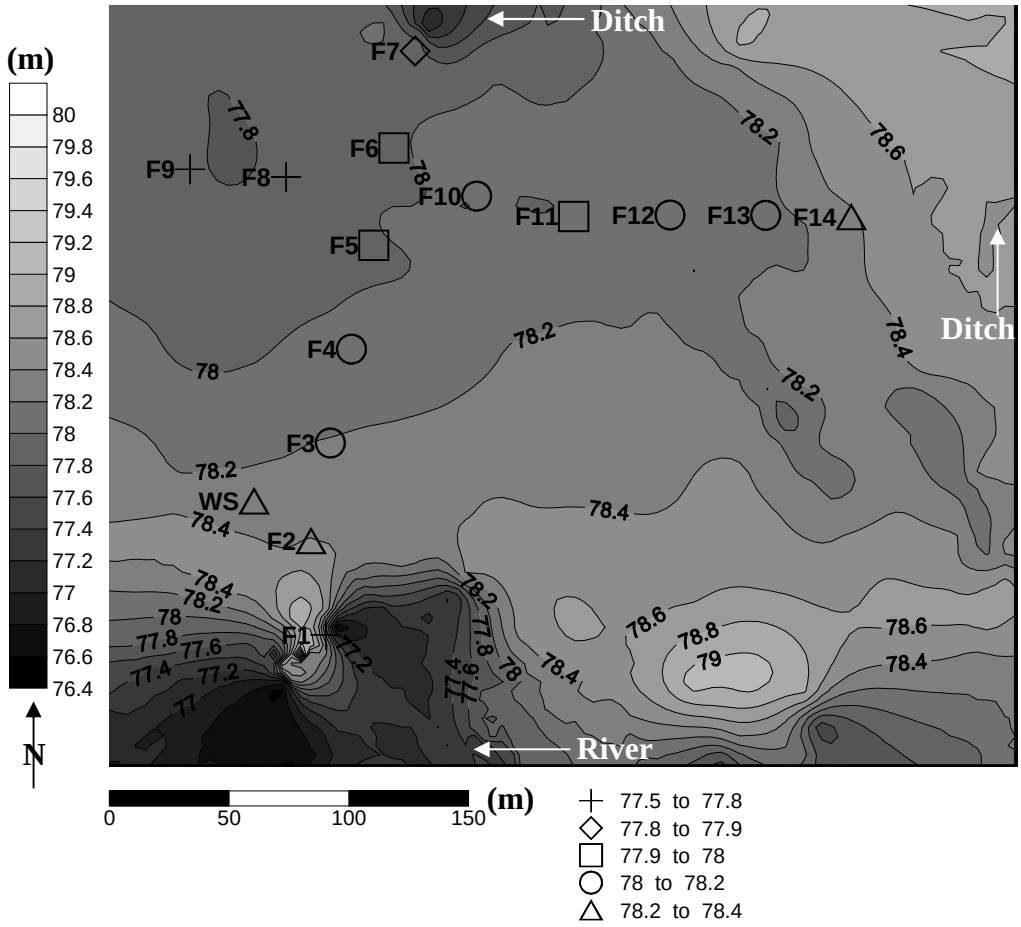

Figure 4.2.3: Contour map of the PM site. The groundwater wells have been depicted with a characteristic shape according to their elevation in (m) above sea level. The arrows indicate flow direction in the ditch and the river under baseflow conditions.

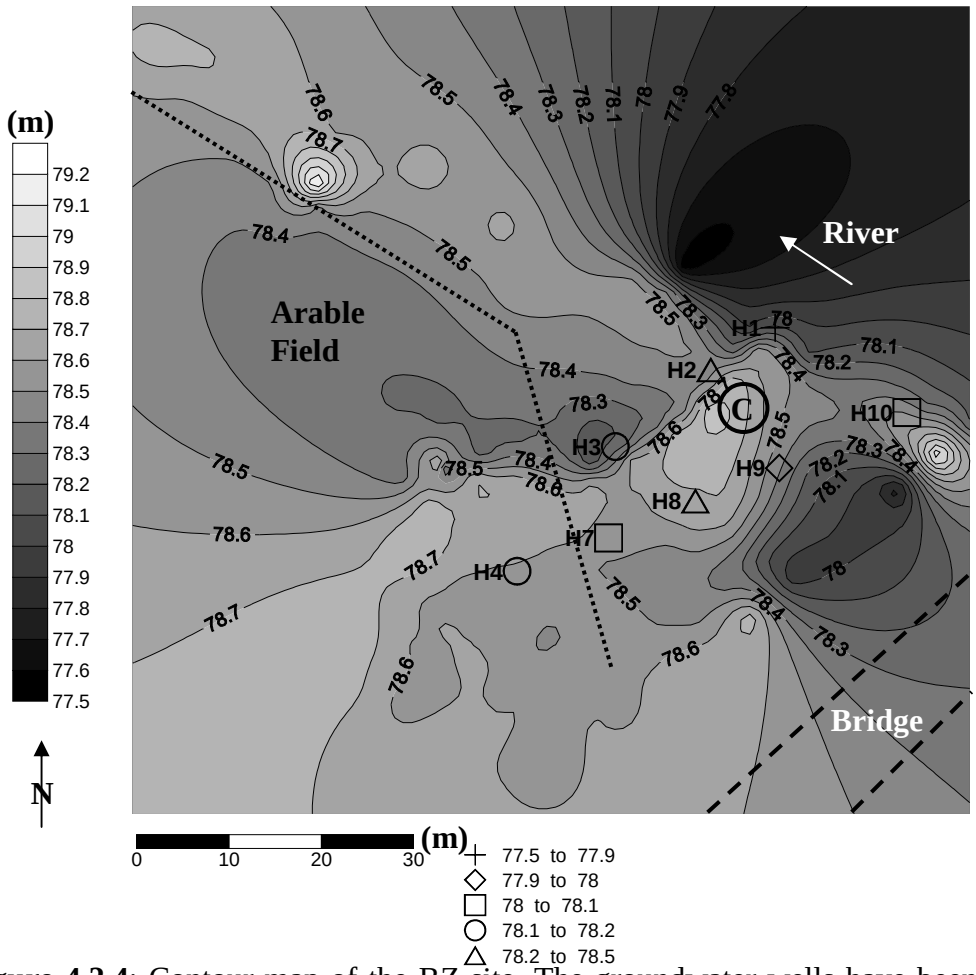

Figure 4.2.4: Contour map of the BZ site. The groundwater wells have been depicted with a characteristic shape according to their elevation in (m) above sea level. The arrow indicates flow direction in the river under baseflow conditions. The dashed line indicates the location of the road and Coleshill Bridge above the BZ. The dotted line indicates the fence of the arable field. The circled letter C indicates the location of the Campbell Logger.

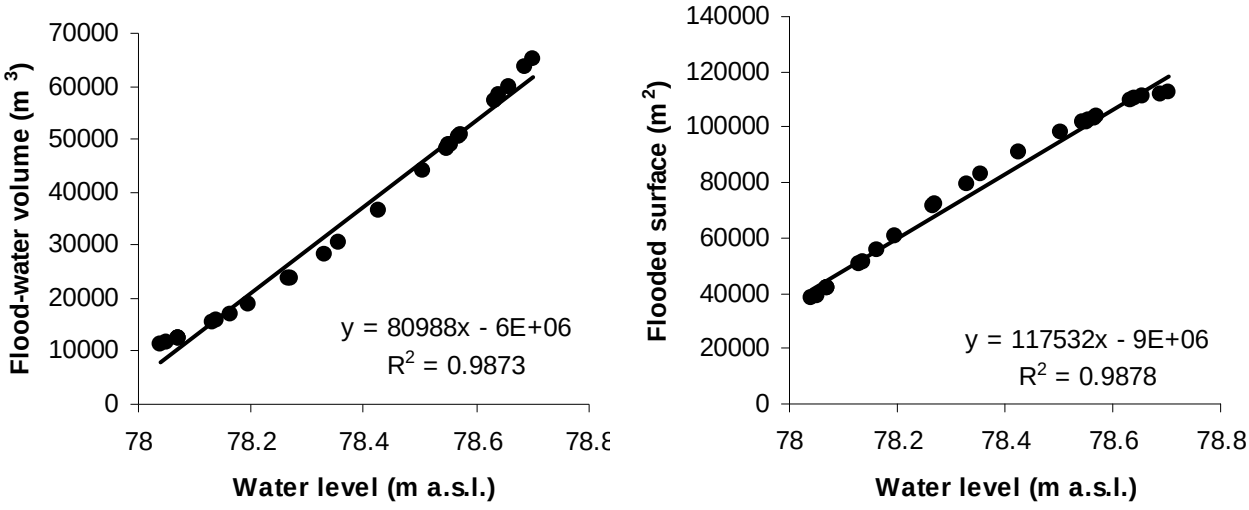

Figure 4.2.5: The linear relationships between water level above the well F2 and the floodwater volume and flooded surface in the PM area. A.s.l. stands for above sea level.

4.2.3.3 *Hydraulic conductivity*

The horizontal saturated hydraulic conductivity (K_h) was measured with piezometer slug tests according to Baird *et al.* (2004) in the A, B and C soil horizons of both the PM and BZ sites. Piezometer slug tests can provide accurate measurements of K_h as long as close attention is given to the test procedure, while destructive sampling (as in laboratory methods) is avoided (Baird *et al.,* 2004). The piezometers used in this study were made of PVC pipes (O.D., 3.3 cm; I.D. 2.9 cm) and had an intake of 21 cm length machined at the lower end of the pipe, which was sealed at its base with a wooden cone (Figure 4.2.6). Nearly 70 % of the intake was open to water flow.

The measurements were taken when the horizons to be investigated were fully saturated according to the method described by Baird *et al.* (2004). The K_h was calculated using the Hvorslev (1951) equations. The aim was to perform at least three measurements in different piezometers per horizon per site with either insertion or withdrawal of the slug. From the 18 tests that were successful, 11 (61 %) were very close (r^2= 0.99) to the required log-linear piezometer response (Hvorslev, 1951). In 28% of the tests, the deviation from log-linearity was slightly higher (r^2=0.98), while in 11% of the tests the deviation from log-linearity was significant (r^2=0.94) and these results were not used in further analyses.

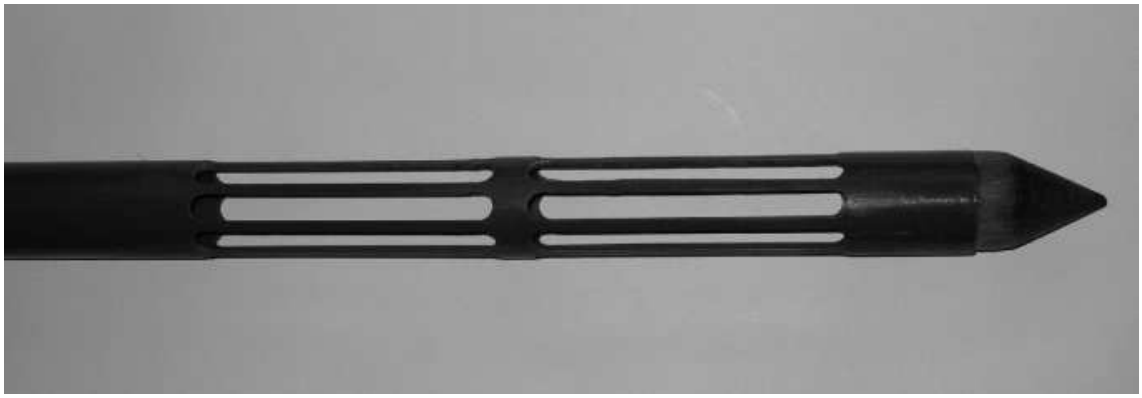

Figure 4.2.6: Detail of the piezometer intake used in the study (after Surridge *et al.*, 2005).

4.2.3.4 *Tensiometer, soil moisture and temperature data*

For the purpose of studying in detail the water table fluctuations between the different soil horizons, three tensiometers (SWT4, Delta-T Devices Ltd., Cambridge, UK), one per soil horizon, were installed in the BZ site (Lat: 193503 N Long: 423372 E) to measure soil water tension. Additionally, at the same location, three theta probes (ML2x, Delta-T Devices Ltd., Cambridge, UK) and three thermistors (Model 107, Campbell Scientific, Loughborough, UK), one per soil horizon, were installed for collecting soil moisture and temperature data to be used in modelling denitrification across the soil horizons of the BZ (for details see Chapter 7). Table 4.2.5 shows the installation depth for each of the above probes and their operational specifications.

The probes were installed in November 2007 using an appropriate diameter hand auger for each probe. A bentonite seal was used around the top of each probe to prevent seeping of rainwater along the probe. The probes were connected to two CR10X data loggers (Campbell Scientific, Loughborough, UK), one for the tensiometers and one for the theta probes and the thermistors. An hourly logging interval was chosen for all probes. The logging program of the two CR10X loggers can be found in Appendix 1.

The tensiometers were calibrated by the manufacturer (Delta-T Devices Ltd., Cambridge, UK) and the calibration values for 10.6 V_{DC} and horizontal installation are: 1000 hPa = 100 mV and offset = 0 hPa. A soil specific calibration was performed for the theta probes, using metal bulk density rings for each soil depth, following the polynomial equation conversion for very moist mineral soils (Delta-T Devices, 1999). The relationship between theta probe output (V) and square root of the soil dielectric constant ($\sqrt{\varepsilon}$) for the range 0 to 1 Volt can be described very precisely by a 3rd order polynomial:

$$\sqrt{\varepsilon} = 1.07 + 6.4V - 6.4V^2 + 4.7V^3 \qquad (4.2.2)$$

The volumetric water content (θ) is related to the $\sqrt{\varepsilon}$ through a simple linear relationship (Delta-T Devices, 1999):

$$\theta = \frac{\sqrt{\varepsilon} - a_0}{a_1} \qquad (4.2.3)$$

The coefficients a_0 and a_1 were determined experimentally from the calibration for each soil depth and their values are given in Table 4.2.6.

Table 4.2.5: Installation depths and operational specifications for the tensiometers, theta probes and thermistors used in this study. [a]Depth from the surface to the middle of the ceramic cup. [b]Linearity at 10±0.01 V_{DC} excitation, 25°C. A, B, C respective soil horizons.

	Depth from surface (cm)	Units	Range	Accuracy
Tensiometers				
A	35[a]	hPa	-1000 - 850	± 0.5%[b]
B	74[a]	hPa	-1000 - 850	± 0.5%[b]
C	115[a]	hPa	-1000 - 850	± 0.5%[b]
Theta probes				
A	20	$m^3.m^{-3}$	0 - 1	± 0.01
B	70	$m^3.m^{-3}$	0 - 1	± 0.01
C	120	$m^3.m^{-3}$	0 - 1	± 0.01
Thermistors				
A	10	°C	-35 - +50	± 0.2
B	50	°C	-35 - +50	± 0.2
C	150	°C	-35 - +50	± 0.2

Table 4.2.6: Soil moisture coefficients derived from the soil specific calibration of the theta probes for the A, B and C soil horizons of the BZ

BZ soil horizons	α_0	α_1
A	2.95	4.24
B	2.56	4.89
C	2.68	6.34

4.3 *Hydrogeochemical analysis*

4.3.1 *Water sampling*

The groundwater in the PM and BZ zones, as well as the river, ditch and rain water, were monitored at bimonthly or at least monthly intervals with the purpose of identifying chemical gradients along GW-SW interaction flow paths that would imply nitrate removal or dilution. The monitoring occurred during the period October 2006 - September 2007 and all of the groundwater wells were used as monitoring points. Since

piezometer nests at various depths in the subsurface were not used, the groundwater monitoring reflects the average groundwater conditions throughout the A, B and C soil horizons, and the focus was on tracing chemical gradients on the horizontal dimension along the well transects.

Before sampling, the wells were purged of at least one well volume using a manual inertial pump (HDPE tubing; O.D: 25 mm; max rate: 15 L min^{-1}; Waterra, Solihull, UK). Subsequently, 100 mL of 'fresh' groundwater and surface water were sampled manually using a point-source bailer (Model 429, Solinst, Ontario, Canada) and stored in Duran® glass bottles at 4^{o}C. Upon return to the laboratory, the samples were centrifuged at 3,000 rpm for 20 minutes and the supernatant was filtered through 0.45 µm Supor® hydrophilic polyethersulphone (PES) membrane filter paper and stored at 4^{o}C until analysis (maximum for 24 hours). All sample bottles and glassware had been washed in 1:10 HCl and rinsed three times in distilled water.

4.3.2 *Groundwater temperature, pH, specific conductance and dissolved oxygen concentration measurements*

The groundwater temperature, pH, specific conductance and dissolved oxygen (D.O.) concentration were measured *in situ*, after well purging, using the 100 mL sample collected for chemical analysis with portable probes. Table 4.3.1 shows the probe types used in this study and their operational specifications. The pH meter was calibrated prior to use with two calibration solutions at pH 4 and 7. The conductivity meter was calibrated once a month using a special calibration solution (HI 7031). The D.O. meter was calibrated prior to use for 0 and 100% O_2 saturation. All probes were rinsed with deionised water and wiped dry between sample readings.

Table 4.3.1: Portable water quality probes used in this study and their operational specifications. FS means full scale.

Probe	Model	Units	Range	Accuracy	Manufacturer
pH	HI8424	n/a	0 - 14	± 0.01	HANNA Instuments Ltd, Bedfordshire, UK
Conductivity	HI933000	µS cm^{-1}	0 - 1999	± 1% FS	HANNA Instuments Ltd, Bedfordshire, UK
D.O.	550A	mg L^{-1} or %	0 - 20 mg L^{-1}, 0 - 200 %	± 0.3 mg L^{-1}, ± 2%	YSI Hydrodata Ltd, Letchworth, UK
Temperature	550A	^{o}C	-5 + 45	± 0.3	YSI Hydrodata Ltd, Letchworth, UK

4.3.3 *Anion analysis*

Of the 100 mL water sample volume, 5 mL were used for anion analysis (NO_3^--N, Cl^- and $SO4^{2-}$) by ion exchange chromatography (ICS-2500, Dionex Corp., Sunnyvale, California, U.S.A.). Anions were separated on a 2 x 250 mm RFICTM IonPac® AS18 analytical column with an IonPac® AS18 guard column. The eluent used was 100 mM KOH pumped by a GP50 gradient pump at a flow rate of 0.25 mL min^{-1} in a gradient mode. Conductivity was measured by an ED50 detector and it was linear between 0 and 45 μS. The system had an AS50 autosampler for automated sample injection (25 μL injection volume) and Chromeleon® 6.5 software for system control, peak integration and data processing. A set of standards (1, 10, 20, 50 and 200 ppm) for Cl^- and $SO4^{2-}$ and (0.25, 2.5, 5, 12.5 and 50 ppm) for NO_3^--N was prepared fresh each month and the standards were injected at the beginning of the run for calibration purposes. The precision of the method for the three anions is shown in Table 4.3.2.

Table 4.3.2: Anion analysis precision data. STDEV: standard deviation; RSD: relative standard deviation

	Concentration (mg L^{-1})			
Anion (n=9)	**Standard**	**Average measured**	**STDEV**	**RSD**
Chloride	50.0	47.3	2.2	4.7
Nitrate	12.5	12.6	0.2	1.8
Sulphate	50.0	46.9	2.1	4.4

4.3.4 *Metal analysis*

Another 5 mL of the water sample was used for elemental metal analysis (Ca, Na, K, Mg, Mn, Fe, Al, and Zn) by Inductively Coupled Plasma Optical Emission Spectrometry (ICP-OES). The ICP-OES instrument used was a Vista-PRO™ (Varian, The Netherlands) spectrometer with a SPS3 autosampler. The instrument was equipped with a one-piece low flow extended high dissolved solids torch with a quartz injector tube (2.3 mm diameter), a two channel peristaltic pump, a glass cyclonic spray chamber and a concentric glass slurry nebulizer. The operating conditions were optimized using the Varian's Automax™ function designed to obtain the optimum measurement conditions for any combination of metals. These are listed in Table 4.3.3. The ICP-OES was calibrated at the beginning of each run with standards at 1, 2, 10 and 50 ppm concentrations. The calibration standards were made up from a multi-elemental standard solution. One of the calibration standards was also used as a laboratory reference after

every ten analyses to monitor drift in the analyte signal with time. The most sensitive analyte wavelengths without spectral interferences were used (Table 4.3.4). The limits of determination of the metals analysed in this study, calculated as six standard deviations of the mean of ten replicate readings of a blank sample (3σ), are shown in Table 4.3.4.

Table 4.3.3: Operating conditions of the Varian Vista-PRO^{TM} spectrometer

Operating characteristics	Units	Optimum value
Radio frequency power	W	1000
Plasma gas flow	L min^{-1}	19.5
Auxiliary gas low	L min^{-1}	1.25
Pump rate	rev. min^{-1}	15
Nebuliser gas flow	L min^{-1}	1

Table 4.3.4: Selected wavelength and determination limits for the metals analysed in this study.

Element	Wavelength (nm)	3σ (µg L^{-1})
Ca	422.673	0.01
Na	588.995	0.15
K	766.491	0.3
Mg	279.553	0.01
Mn	257.61	0.03
Fe	238.204	0.1
Al	394.401	0.2
Zn	213.857	0.2

4.3.5 *Dissolved Organic Carbon (DOC) analysis*

Finally, 30 mL of the water sample was used for DOC analysis with a HiPerTOC Carbon analyser (Thermo Electron Corp., Delft, The Netherlands). The method used was the standard high temperature combustion at 1,000^{o}C with non-purgeable organic carbon (HT_NPOC), which is recommended for groundwater and surface water samples (Thermo, 2006). Briefly, the method involves the removal of inorganic carbon (i.e carbonates and bicarbonates) from the sample by the addition of 1M HCl prior to the measurement of the DOC. All inorganic carbon is unstable at low pH and reacts to CO_2. The auto sampler then bubbles gas through the sample to homogenize and sparge off all

the purgeable compounds, i.e. CO_2 and some volatile carbon compounds. The sparged sample, containing only organic carbon, is then injected into the high temperature reactor (1,000^{o}C). The carrier gas (O_2 at 250 mL min^{-1}) leads the CO_2 to the dual NDIR detector via a condition step. The absorbed Infra Red radiation is relative to the amount of CO_2, which relates to the total organic carbon in the sample. The dual NDIR detectors measure the CO_2 simultaneously within two analytical ranges (0 - 10 and 0 - 10,000 ppm C). System control and peak integration is performed through the ThEus® software. Standards of 10, 20, 50 and 100 ppm C concentrations prepared from anhydrous potassium hydroxyl phthalate ($KHC_8H_4O_4$) were used for calibration. The precision of the HT- NPOC method was assessed by measuring 5 repeat injections and the relative standard deviation (RSD) was <5 %.

4.4 *Soil biogeochemical analysis*

4.4.1 *Soil sampling and preparation*

4.4.1.1 *Land Use Zones*

For the purpose of investigating the potential for biological nitrate attenuation across the re-connected floodplain of the River Cole, four land use zones (Objective 2B(i) in Section 2.5) (from downstream to upstream: Fritillary Meadow, Pasture Meadow, Buffer Zone and Grazing Grassland) were selected (see also section 3.8). A stratified systematic sampling approach was followed to ensure that both the spatial distribution of land use and hydrological regime effects were sampled representatively. Each land use zone was divided into three sampling transects, parallel to the river, reflecting primarily different hydrological conditions and landscape positions. Both the FM and PM areas (Figure 4.4.1) were split into the following: (i) a Riparian transect running along the meandering river and therefore receiving overbank flooding from the river, while the vegetation was characteristic of the riparian corridor. (ii) A Middle transect across the FM and PM reflected less frequent inundation conditions and the dominant land use of each area. Finally, (iii) the third transect in the FM and PM was called Channel depression and was located on a characteristic depressional feature on the north edge of the areas, created by overland flow from the ditch across the floodplain.

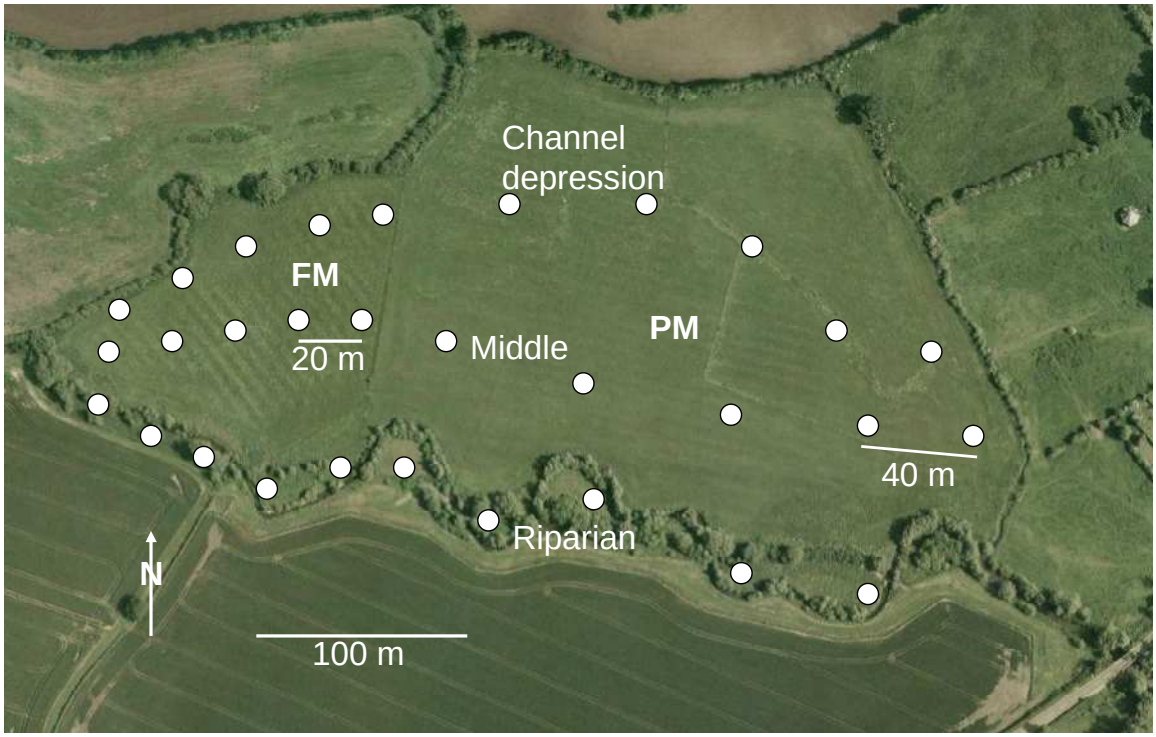

Figure 4.4.1: The sampling transects in the PM and FM areas. White circles indicate sample locations. Channel depression samples 1-5; Middle transect samples 6-10; Riparian transect samples 11-15 for both the PM and FM from east to west direction.

The same rationale was followed for delineating the sampling transects in the BZ (Figure 4.4.2). In place of the channel depression, a third ‘arable’ transect was selected inside the arable field to contrast both the hydrological and land use conditions between the buffer strip and the arable field. Finally, in the GG area (Figure 4.4.3) the hydrological regime of the ‘new’ meandering river and the ‘old’ channel were represented by the Riparian and Mill Leat transects respectively, while the land use management and the less frequent inundation conditions were reflected in the Middle transect.

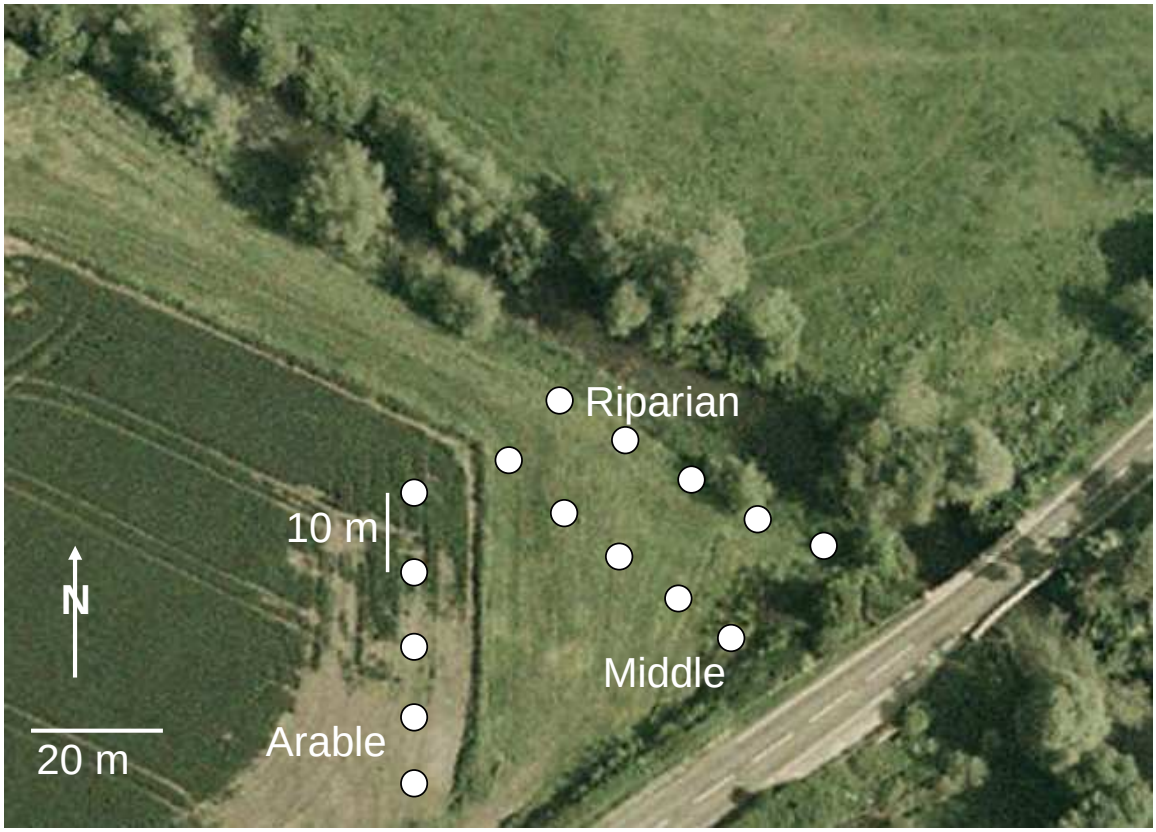

Figure 4.4.2: The sampling transects in the BZ area. White circles indicate sample locations. Riparian samples 1-5; Middle samples 6-10 from east to west direction. Arable transect samples 11-15 from south to north direction.

Five topsoil (0 - 20 cm) samples were collected equidistantly per transect, amounting to a total of 15 samples per land use area and 60 samples across all areas. Soil samples were collected in the FM in July 2006, in the GG and the BZ in June 2007 and in the PM in July 2007. Samples were collected with the aid of metal cores (38 mm I.D., 23 cm long, ELE International, Bedfordshire, UK) to minimise exposure of the soil to the atmosphere and also to make sure that all samples were collected from the same depth. A separate soil sample was collected at the same location for bulk density determination using bulk density rings (I.D: 53 mm, height: 51 mm, volume: 100 cm^3) (Type 07.53.SA, Eijkelkamp, Giesbeek, The Netherlands). Immediately after collection, the metal cores and bulk density rings were capped, sealed in plastic zip-lock bags and transported to the laboratory in refrigerated containers. The samples were stored at 4^oC overnight and extruded the next day in the laboratory with a hydraulic sample extruder (Model 23-4060, ELE International, Bedfordshire, UK) at room temperature (20^oC). After extrusion, the samples were split in two fractions, 0-10 cm and 10-20 cm. Visible

stones and roots were removed manually and the remaining sample was well homogenised by mixing before being transferred in a new plastic zip-lock bag and stored at 4^{o}C overnight. Only the 0-10 cm fraction of the soil sample was used in soil biogeochemical analyses.

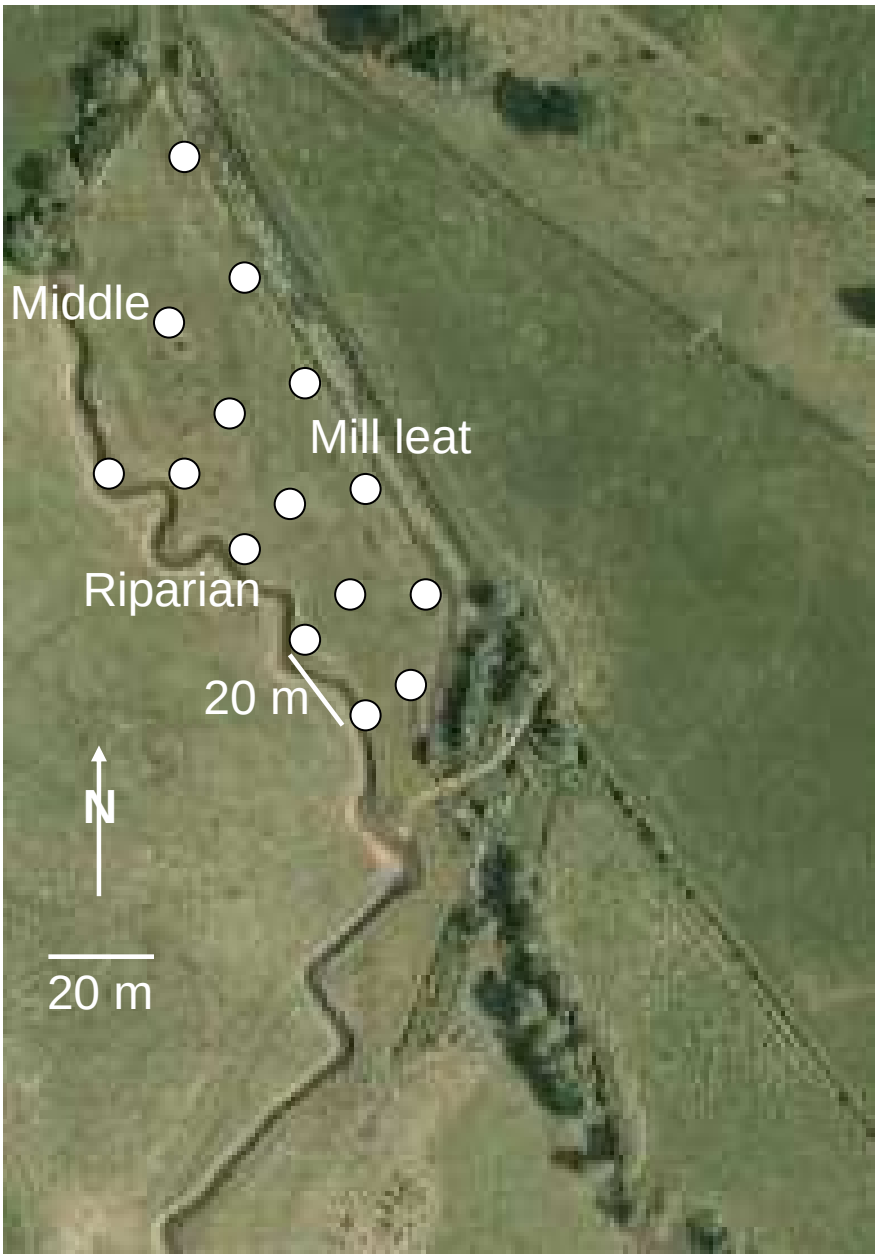

Figure 4.4.3: The sampling transects in the GG area. White circles indicate sample locations. Mill leat samples 1-5; Middle samples 6-10; Riparian samples 11-15 from south to north direction.

4.4.1.2 *Vertical variability in the Pasture Meadow and Buffer Zone subsurface*

In order to investigate the effect of vertical changes in soil stratigraphy and electron donor and acceptor availability on nitrate attenuation processes (Objective 2B(ii) in Section 2.5), soil samples were collected from the A, B and C soil horizons of the BZ and PM areas in March and July 2008 respectively. A different sampling strategy was followed for each area. In the case of the BZ, where a homogeneous subsurface soil horizon sequence was observed across the site, eight locations were randomly chosen within the 1.5 ha area. In the case of the PM, the sequence of subsurface soil horizons was represented by sampling next to the well locations along the transect F1 - F7. Soil samples were collected with a 40 mm hand auger at six depth intervals (A; 0 – 10 cm, B; 10 – 20 cm, C; 20 – 30 cm, D; 50 – 70 cm, E; 80 – 100 cm and F; 100 – 120 cm) per sampling location, covering the whole of the soil profile from the surface through the vadose zone to the water table, and amounting to a total of 48 samples per area. Bulk density rings were also collected for each depth increment, while the storage, transport and processing of the soil samples was done as per section 4.4.1.1.

4.4.1.3 *Spatial variability due to wetting - drying cycles*

In order to examine the effect of prolonged wetting and drying, under field conditions, on the spatial variability of nitrate attenuation processes (Objective 2B(iii) in Section 2.5), soil samples were collected from 0 - 10 cm depth across all the land use zones. The sampling design was based on the results from the land use zone analysis performed in the 2006 - 2007 monitoring season. Specifically, the physical soil properties and the denitrification potential of all the samples from across the land use zones (n=60) were used in a Principal Component Analysis (PCA) in order to choose 30 sample locations that represented the widest range of soil conditions and denitrification potential across all the land use zones.

The sampling of the wet conditions took place in late March 2008, after the reconnected floodplain had received 70 mm total rainfall in three weeks (3.3 mm rain d^{-1}), while the dry conditions sampling occurred in late July 2008, after the floodplain had received 11 mm total rainfall in two weeks (0.8 mm rain d^{-1}) prior to the sampling and no rain at all for 10 days before the sampling. Soil samples and bulk density rings were collected and processed as per section 4.4.1.1. Additionally, soil moisture in the top 10 cm of the soil,

right next to each sampling point, was measured *in situ* with a theta meter (Type HH1, Delta-T Devices, Ltd., Cambridge, UK; Accuracy: ± 0.016 $m^3.m^{-3}$).

4.4.1.4 *Monthly monitoring of soil nitrate content in the Buffer Zone area*

For the purpose of the denitrification modelling application (for details see Chapter 7) the soil nitrate content in the A, B, and C soil horizons of the BZ was monitored on a monthly basis. Soil sampling was performed between November 2007 and September 2008 at three depth intervals (A horizon: 0 - 10 cm; B horizon: 50 - 60 cm; C horizon: 100 - 110 cm) with the aid of a 40 mm hand auger at 5 randomly selected locations. The sampling locations were selected by random number generation (representing X and Y distances) on a 30 x 30 m surface area. The soil samples were processed as per section 4.4.1.1 and were used for soil nutrient extraction (see section 4.4.5).

4.4.2 *Soil bulk density, porosity, moisture and organic matter content, and water filled pore space (WFPS)*

The samples were extruded from the bulk density rings and analysed for soil bulk density, porosity, moisture content, organic matter content (by Loss on Ignition) and water filled pore space (WFPS) following the methods described in Rowell (1994), Heiri *et al.* (2001) and Linn and Doran (1984) respectively.

4.4.3 *Absolute particle size distribution with permeability calculations*

Following treatment of soil with hydrogen peroxide (to remove organic matter) and diaggregation using Calgon, the absolute particle size distribution was determined with optical laser diffraction (Chappell, 1998) using an LS 13320 Coulter Counter Particle Size Analyzer (Beckman Coulter Corp., Hialeah, FL, US), with precision between 0.1 and 10 μm particle size, <1 % RSD.

Soil permeability was estimated using the Carman-Kozeny equation (cited in Boudreau, 1997):

$$k = \frac{dp^2}{180} \cdot \left(\frac{P_t^3}{(1 - P_t)^2} \right) \tag{4.4.1}$$

where k is the permeability (m^2), dp is the mean diameter of soil particles and P_t the soil porosity.

This equation is one of the most commonly applied means of relating permeability to the geometric properties of soil (Hillel, 1998). However, the equation has its limitations, as permeability depends not only on porosity and particle size distribution but also on the continuity, shape and tortuosity of conducting channels (Dullien, 1979). Hence the application of this theory to terrestrial soils can be problematic due to inhomogeneous structural characteristics, such as plant roots, which may dominate permeability in places. Nevertheless, the equation allows a first approximation of the soil permeability as direct measurement was beyond the scope of this study.

4.4.4 *Soil elemental analysis for C and N*

The total organic carbon (TOC) and total nitrogen (TN) content in the soil samples was determined with elemental analysis. For determining the TOC content, all the samples were acidified prior to analysis in order to remove any carbonates (Hedges and Stern, 1983). The soil samples were homogenised using a mortar and pestle, and a sub-sample (50-100 mg) was placed in a pre-weighed scintillation vial (20 mL), dried to constant weight over night (50 ^{o}C) and then reweighed (W_o). The sample was injected with an HCl solution (2 mL, 1 M organic-free grade) as per Hedges and Stern (1983): 1.5 mL of the solution was added and left for 24 hr, after which 0.25 mL was added and the slurry re-suspended. A further 0.25 mL was added after half an hour to bring the slurry back to 1M, followed by drying (50 ^{o}C) to a constant weight. After removal from the oven the sample was left open in a fume cupboard for 24 hr to allow for hydroscopic salt equilibration. The sample was re-weighed to determine mass (W_f).

The weight percentage of either the TOC or TN in the original sample were calculated as per Hedges and Stern (1983):

$$\% \text{ TOC or TN} = \left[\left(\frac{\text{OC or TN mg}}{\text{mg sample}} \right) \text{ x} \left(\frac{W_f}{W_o} \right) \right] \text{ x } 100 \qquad (4.4.2)$$

Sub-samples of the processed soil (5-10 mg) were placed in pre-weighed containers (Tin caps, ultra clean 8x5mm, Elemental Microanalysis Ltd, Okehampton, UK) and weighed on a 6dp microbalance (Supermicro, Sartorius UK Ltd). The samples were analysed for TOC and TN using an elemental analyser (Flash EA 1112, Thermo-Finnigan, Bremen, Germany). Sample TOC and TN content were calculated from an L-

aspartic acid ($C_4H_7NO_4$) standard (C: 36.09 %; H: 5.30 %; N: 10.52 %; O: 48.08 %), using the Eager 300® software and linear regression. The precision as a coefficient of variation was better than 1 %.

4.4.5 *Soil nutrient extraction and analysis*

All soil samples (except for the FM samples in the land use zone sampling) were extracted for semi-total NO_3^-, NO_2^- and NH_4^+ analysis with 2M KCl (Rowell, 1994). Approximately 20 g of field moist soil was weighed in a 250 mL conical flask and 100 mL of 2M KCl were added. The flasks were shaken at 180 oscillations per minute on a reciprocating horizontal mechanical shaker for 1 hour. Subsequently a 50 mL sub-sample was centrifuged at 3,000 rpm for 20 minutes. The supernatant was filtered through 0.45 µm Supor® hydrophilic polyethersulphone (PES) membrane filter paper and frozen until analysis.

The analysis for NO_3^-, NO_2^- and NH_4^+ was performed on a segmented continuous flow auto analyser (SAN^{++}, SKALAR, Delft, The Netherlands) according to standard colorimetric techniques (Kirkwood, 1996). The method for each inorganic N species, instrumental range and accuracy are given in Table 4.4.1. Calibration standards were prepared fresh each week, covering the analytical range for each N species. Peak integration and calibration with linear regression was performed with the FlowAccess® software. The N content in the original soil sample was calculated according to Keeney and Nelson (1982), correcting the dilution factor for the soil moisture content of the sample.

Table 4.4.1: Method, operational range and accuracy for NO_3^-, NO_2^- and NH_4^+ determination with segmented continuous flow analysis

Inorganic N	Method	Range (mg L^{-1})	Wavelength (nm)	RSD (%)
NO_3^-	Reduction to NO_2^- by Cd-Cu reductor	0.05 - 50	540	0.98
NO_2^-	Sulfanilamide-NEDD	0.002 - 2	540	0.46
NH_4^+	modified Berthelot reaction	0.02 - 10	660	0.83

4.4.6 *Measurement of Anaerobically Mineralisable Organic Carbon (AnMOC) and methane production potential*

Several studies have measured the anaerobic mineralisation rate of organic carbon (Bijay-Singh *et al.*, 1988; Drury *et al.*, 1998; Simek *et al.*, 2000; Hill and Cardaci, 2004; Ullah and Faulkner, 2006; Dodla *et al.*, 2008) as an expression of the labile organic carbon fraction available for nitrate respiration (Gale *et al.*, 1992). In the present study, we measured the anaerobically mineralisable organic carbon (AnMOC) through the evolution of CO_2 from anaerobically incubated field moist soil without nitrate amendment. Although nitrate has been used in AnMOC measurements (Hill and Cardaci, 2004; Ullah and Faulkner, 2006) to stimulate the oxidation of organic carbon via heterotrophic denitrification, in this study it was not deemed appropriate as the soil was rich in nitrate, due to frequent replenishment by overbank flooding, and because the DNRA activity could have possibly been suppressed by lowering the C/NO_3^- ratio (Tiedje, 1988). Therefore the AnMOC measurement would not reflect the labile organic carbon available to DNRA bacteria. Moreover, the same soil incubations were used to estimate the production of methane over time via methanogenesis (Kemnitz *et al.*, 2004), which could also be suppressed by elevated nitrate content and a positive redox potential (Alewell *et al.*, 2008). Therefore the AnMOC method selected for this study represents a combined measurement of the relative availability of labile organic carbon and ambient availability of electron acceptors for anaerobic respiration and fermentation.

Field moist soil (5.5 g) was weighed into gas-tight 12.5 mL vials (Exetainer vial; Labco Ltd., High Wycombe, United Kingdom). The vials were capped airtight and purged with oxygen-free N_2 gas for 20 min to induce anaerobic conditions. After purging, the vials were stored at room temperature (22 - 25 ^oC). The headspaces of the vials were sampled every 48 h for 21 days. The incubation period for the subsurface soil samples was extended to 100 days due to the long lag phase of the methanogens (Kemnitz *et al.*, 2004). However, CO_2 production rates were calculated for the first 21 days of the incubation (i.e. the duration of linear CO_2 accumulation in the headspace). During sampling, a 100 μL sample was withdrawn from the headspace using a gas-tight syringe in an auto-sampler (Multipurpose Sampler MSP2, Gerstel, GmbH, Germany) and injected into a GC-FID, (7890A GC Agilent Technologies Ltd., Cheshire, UK) (Column 40^oC, detector 300 ^oC). CH_4 and CO_2 were separated using a stainless steel column

(length 1.8 m x diameter 12 mm) and packed with Porapak (Q 80/100), and hydrogen/air (7/93%) (Zero grade BOC) as the carrier gas (430 ml min^{-1}). CO_2 was then converted to CH_4 in a nickel catalyst set at 385 ^oC. Headspace concentrations of CH_4 and CO_2 were calculated from peak areas using an electronic integrator (ChemStation®, software). CH_4 and CO_2 were calibrated against known standards (Scientific and Technical Gases Ltd, Staffs, UK). Precision, as a coefficient of variation, was better than 2 % for CH_4 and 1 % for CO_2. CH_4 and CO_2 production rates were estimated through linear regression and expressed as μmol of CH_4 or CO_2 $kg^{-1}$of dry soil day^{-1}.

4.4.7 *Measurement of denitrification potential rate*

Groffman *et al.* (2006) have recently compiled an extensive review of methods used to measure denitrification in aquatic and terrestrial ecosystems at various scales. It is not in the scope of the present study to present another review of denitrification measurement methods, but the focus is rather on explaining the rationale for the methods selected in this study.

Sigunga (2003) attempted to clarify the concept of potential denitrification by proposing a definition: '... potential denitrification should explicitly embrace the idea of maximum attainable denitrification rate under optimal conditions within the limitations of soil's natural setting in terms of texture and C content'. In other words, Sigunga (2003) suggested that potential denitrification is measured in the laboratory, under anaerobic conditions, at 20^oC and non-limiting supply of NO_3^- but without external carbon supply, as denitrification differences mainly depend on this soil-inherent property (organic carbon). Earlier studies by Myrold and Tiedje (1985) and Yeomans *et al.* (1992) termed this measurement as denitrification capacity, which represents the active denitrifier biomass of the soil, at the time of sampling, without additional microbial growth induced by the added organic carbon. Furthermore, they showed that the added nitrate did not affect the denitrification capacity in agricultural soils with high indigenous NO_3^- (>20 mg N kg^{-1} soil).

The vast majority of studies on floodplain and riparian zone soils (e.g. Groffman *et al.*, 1992; Pinay *et al.*, 1993; Groffman and Crawford, 2003) have measured potential denitrification according to the Denitrification Enzyme Assay (DEA) as described by Smith and Tiedje (1979). The DEA involves the anaerobic incubation of soil slurries

amended with nitrate and an equal amount of a carbon source (e.g. glucose), usually in the presence of a protein synthesis inhibitor (e.g. chloramphenicol). During the first incubation stage, termed Phase I, which lasts between 1-3 h (although incubation times vary across studies depending mainly on the reactivity of the soil), the denitrification rate depends on the pre-existing denitrifying enzymes in the soil (similar to the denitrification capacity mentioned earlier). Both the denitrification capacity and the DEA (Phase I) are closely related to field denitrification rates (Smith and Tiedje, 1979; Myrold and Tiedje, 1985), but they do not reflect *in situ* rates (Groffman *et al.,* 1992). However, they are well suited for comparisons between sites and treatments (Groffman *et al.,* 2006).

In the present study we are primarily interested in the horizontal and vertical spatial variability of denitrification activity as it is affected by the hydrological regime and the land use management across the re-connected floodplain of the River Cole, while the quantification of absolute denitrification rates is of secondary importance. Therefore, for the purpose of comparing between sites and accommodating a large number of samples for representing spatial variability, the denitrification potential measurement will be used (Sigunga, 2003) instead of *in situ* denitrification measurements (see Chapter 7). Denitrification potential has been recently successfully measured in anaerobic slurries without the addition of organic carbon (Brettar *et al.,* 2002; Hill *et al.,* 2004; Ullah and Faulkner, 2006), since during short incubation times (between 1 and 6 hours) soil indigenous carbon is usually non-limiting (Tiedje *et al.,* 1982).

All the above mentioned studies that measured denitrification potential, have used acetylene (C_2H_2) to inhibit the reduction of N_2O to N_2 (Yoshinari and Knowles, 1976) and estimated denitrification rates from the linear accumulation of N_2O over time. However, a number of problems have been described in the literature (reviewed in Groffman *et al.,* 2006) related to the use of C_2H_2, of which the use of C_2H_2 as a carbon source for denitrification (Beauchamp *et al.,* 1989) is likely to affect our experiments. Alternatively, very few studies in soils (Well *et al.,* 2003, 2005) have used ^{15}N-labelled NO_3^- in slurry incubations and subsequently estimated denitrification rates by measuring the production of $^{15}N_2$. In the present study, a similar technique with ^{15}N-labelled NO_3^- (adapted from Trimmer *et al.,* 2003) will be used, thus avoiding the complications of the use of C_2H_2.

In order to estimate denitrification potential rates, a timed experiment was performed using a method adapted from Trimmer *et al.* (2003) as follows. From each sample, four sub-samples were prepared by weighing approximately 1.10 g of field moist soil into gas-tight 3 mL vials (Exetainer vial; Labco Ltd., High Wycombe, United Kingdom). The 3 mL vials were used in preference to larger volume serum bottles or gas-tight flasks because; (i) they provide better mixing of the substrate, (ii) less ^{15}N-labelled nitrate is needed, so the cost is kept low, and (iii) the headspace can be directly sampled by the autosampler of the Isotope Ratio Mass Spectrometer (IRMS), thus minimising any handling bias by transferring gas samples between vials or manually injecting the headspace into the IRMS. Finally, each soil sample was represented by one set of subsamples, as the purpose of the study was to have good spatial representativeness and therefore the replication of individual soil samples had to be sacrificed to keep an acceptable number of samples without compromising the accuracy of the experiment.

The 3 mL exetainers were transferred to an anaerobic glove box (Belle, UK) and flushed with N_2 (oxygen-free nitrogen, 30 mins) to induce anaerobic conditions. The samples were made into slurries by adding 1 ml of synthetic river water (Smart and Barco, 1985), degassed by flushing with N_2 (oxygen free) for 30 minutes, and the vials were sealed with lids containing butyl rubber septa. The samples were pre-incubated on rollers in the dark at room temperature (22 - 25^oC) for 24 hours leading to the depletion of 96.3 (± SE 0.7) % of the background $^{14}NO_3^-$ pool.

Following the pre-incubation stage, the first sub-sample from each soil sample was treated as a reference and microbial activity was inhibited at the beginning of the experiment by injecting $ZnCl_2$ (100 µL 50% w/v) through the septum with a hypodermic syringe without adding any ^{15}N-labelled nitrate. The remaining three subsamples per soil sample were enriched to 99.2 (± SE 0.2) % above the ambient level with concentrated stock of labelled $^{15}NO_3^-$ (75 µL of 2.4 mM $Na^{15}NO_3^-$ [99.3 ^{15}N atom %] Sigma-Aldrich, Poole, UK) through their septa using a gas-tight syringe (Hamilton, 1750 RN, 500 µL, VWR International). The spike solution was degassed by flushing with N_2 (oxygen free) for 15 minutes before use. The final concentration of nitrate in the slurry sample was on average 90 µM and lower than the average ambient nitrate concentration of the samples which was 500 (± se 0.05) µM. Therefore, the slurry treatment resulted in effectively replacing the ambient $^{14}NO_3^-$ pool with a $^{15}NO_3^-$ pool,

without purposely enhancing denitrifier activity by supplying nitrate above ambient concentration.

The samples were placed back on the rollers. Every two hours one sub-sample per soil sample was sacrificed and microbial activity was inhibited by injecting $ZnCl_2$ (100 μL 50% w/v) through the septa with a hypodermic syringe. The timed experiment lasted for 6 hours with T_1 = 2 h, T_2 = 4 h and T_3 = 6 h. The timed experiment in the case of the subsurface samples was adapted to account for the slower activity of the soil. The time step for the depth intervals between 20 and 70 cm was set to 3 h, while for the deeper sediments (80 - 120 cm), the time step was 24 h. At the end of the experiment, all references and time-samples were centrifuged for 5 minutes at 3,000 rpm to create a clean headspace.

Samples of the headspace (50 μL) were then injected using an autosampler (Multipurpose Sampler MSP2, Gerstel, GmbH, Germany) into an elemental analyser (Flash EA 1112, Thermo-Finnigan, Bremen, Germany) interfaced (ConFlo III Interface, Thermo-Finnigan, Bremen, Germany) with a continuous flow isotope ratio mass spectrometer (Finnigan MAT Delta^{Plus}, Thermo-Finnigan, Bremen, Germany). The reduction and oxidation columns in the elemental analyser were held at 980^{o}C to reduce trace NO and N_2O to N_2. Then N_2 and CO_2 were separated on a GC Porapak column (PoraPLOT Q). The mass spectrometer was calibrated with N_2 in air blank vials at 22^{o}C and the mass charge ratios for *m/z* 28, *m/z* 29 and *m/z* 30 ($^{28}N_2$, $^{29}N_2$, and $^{30}N_2$) was measured. Precision as a coefficient of variation was better than 1%.

Due to the pre-incubation of the samples, leading to the depletion of the $^{14}NO_3^-$ pool, and the subsequent enrichment of the sample with 99.2 % atom $^{15}NO_3^-$, the production of $^{29}N_2$ ($p^{29}N_2$) and hence the denitrification from the $^{14}NO_3^-$ and $^{15}NO_3^-$ combined (D_{29}), assuming random pairing of ^{14}N and ^{15}N, would be expected to be less than 1.5 % (Hauck, 1958). Indeed, the 24h pre-incubation of the samples was so effective that only trace amounts of $^{29}N_2$ were detected with the IRMS and therefore the use of the classic isotope pairing technique (IPT) equations according to Nielsen (1992) for estimating both D_{15} (denitrification of the $^{15}NO_3^-$ spike) (equation 4.4.3) and D_{14} (denitrification of ambient $^{14}NO_3^-$) (equation 4.4.4) was not necessary.

$$D_{15} = p^{29}N_2 + (2 \cdot p^{30}N_2) \quad (4.4.3)$$

$$D_{14} = \frac{p^{29}N_2}{2 \cdot p^{30}N_2} \cdot (2 \cdot p^{30}N_2 + p^{29}N_2) \quad (4.4.4)$$

where $p^{29}N_2$ and $p^{30}N_2$ are the production of $^{29}N_2$ and $^{30}N_2$ gas respectively. Instead, the signal from the mass spectrometer was converted into concentration of $^{30}N_2$ gas only in the headspace of the mini-exetainers and then production per unit of soil mass per unit time. Values were calculated as excess over that in the references before the addition of $^{15}NO_3^-$ according to and adapted from Thamdrup and Dalsgaard (2000):

$$\text{p mg N kg}^{-1}\text{ day}^{-1} = \left[\left(\frac{^{30}N_2}{\sum N_2}\right)_{sample} - \left(\frac{^{30}N_2}{\sum N_2}\right)_{reference}\right] \cdot \sum N_{2sample} \cdot \frac{1}{a} \cdot V \cdot 30 \cdot \frac{1}{m} \cdot 10^{-6} \cdot t^{-1} \quad (4.4.5)$$

where p mg N kg^{-1} day^{-1} was the production of $^{30}N_2$; the fraction $^{30}N_2/\Sigma N_2$ represents the signal ratio for $^{30}N_2$ to total signal ΣN_2 (total signal for *m/z* ratios 28, 29 and 30 for either *sample* or *reference*, respectively); *a* the concentration of N_2 in air; *V* the volume of the headspace (mL); 30 the molecular weight of $^{30}N_2$; *m* the dry mass of the soil sample (g) and *t* (hours) the duration of linear $p^{30}N_2$ production. An estimate for an areal rate of denitrification in the common units kg N ha^{-1} day^{-1} could then be calculated by multiplying the p mg N kg^{-1} oven dry soil day^{-1} by the mass of soil in 1 hectare at 10 cm depth, which can be calculated using the dry soil bulk density (Rowell, 1994). The dry bulk density (g dry soil cm^{-3}) can also be expressed in tonnes dry soil m^{-3}. In 1 ha at 10 cm depth there is 0.1 x 10^4 m^3 of soil. So the dry mass of soil ha^{-1} is then:

Dry bulk density (t m^{-3}) x 0.1 x 10^4= mass of soil in 1 ha at 10 cm depth (t) (4.4.6)

The denitrification rate (mg N kg^{-1} soil day^{-1}) can also be expressed as g N t^{-1} soil day^{-1}. Therefore, multiplying the latter with the product of Eq. 4.4.6 gives an areal rate of denitrification in g or kg N ha^{-1} day^{-1}. However, the areal expression adds the effect of bulk density onto the denitrification capacity of the soil increasing the complexity of the measurement. For this reason, the areal expression is not used in the statistical analysis

of the results and is calculated only for comparison purposes with the geographical literature.

4.4.8 *Measurement of DNRA potential rate*

A ^{15}N tracer method has been used in all the studies (considered in our literature review) that measured DNRA rates in a variety of ecosystems (Table 4.4.2). One of the most popular methods has been the ^{15}N isotope pool dilution technique (Kirkham and Bartholomew, 1954; Davidson *et al.,* 1991), especially among studies in tropical forest soils that aimed at estimating gross rates of N transformations. The advantage of the pool dilution technique is that gross rates of mineralisation and nitrification are estimated by supplying the ^{15}N-labelled product (i.e. $^{15}NH_4^+$ for mineralisation and $^{15}NO_3^-$ for nitrification), instead of the reactant, and subsequently the dilution of the labelled pool by each process is followed. This is particularly important in N-limited natural environments, where the supply of a labelled reactant (e.g. $^{15}NH_4^+$ for nitrification) could alter the rate (i.e. fertilisation effect) of a substrate-limiting process. Gross rates of NH_4^+ and NO_3^- consumption (e.g. denitrification and DNRA for NO_3^-) are calculated from the disappearance of the ^{15}N label by using accordingly modified calculations (for details see Silver *et al.,* 2001, 2005). Although the isotope pool dilution method is appropriate when considering a variety of gross N transformation processes, and can be further improved by coupling it to a ^{15}N tracing model to include for example the cycle of immobilisation and re-mineralisation of $^{15}NH_4^+$ (Müller *et al.,* 2004, 2007), it is better suited for environments with high transformation rates and small pool sizes, such as untilled and unfertilised soil (Davidson *et al.,* 1991). Moreover, the labelling of the pool is usually at around 10 atom % ^{15}N, which leads to low enrichment of the gaseous denitrification products ($^{15}N_2$ and $^{15}N_2O$), compared to their atmospheric concentrations, and therefore denitrification can be seriously underestimated (Templer *et al.,* 2008).

An alternative method for the measurement of DNRA is the use of ^{15}N-labelled NO_3^- as a tracer in intact core incubation experiments (Matheson *et al.,* 2002), in flow-through core experiments for sediments (An and Gardner, 2002; Scott *et al.,* 2008) or in laboratory assays for soils (Yin *et al.,* 2002; Davis *et al.,* 2008) for the direct quantification of DNRA rate through the production of $^{15}NH_4^+$. The fertilisation effect from the addition of the ^{15}N-labelled NO_3^- is not likely to be a problem in wetland

sediments and agricultural soils rich in N (Groffman *et al.*, 2006). This method allows the estimation of both the denitrification and DNRA rates in the same treatment. When C_2H_2 is used (Tiedje *et al.*, 1981), denitrification is calculated from the accumulation of N_2O. However several drawbacks have been reported regarding the use of C_2H_2 for measuring denitrification but not for DNRA (Groffman *et al.*, 2006). Alternatively, denitrification can be calculated from the production of $^{15}N_2$ and $^{15}N_2O$ (Kelso *et al.*, 1997; Yin *et al.*, 2002), provided that sensitive mass spectrometer instrumentation is available. The DNRA rate is estimated from the production of $^{15}NH_4^+$, which is subsequently diffused to ammonia and captured in acidified filters for mass spectrometric analysis (Brooks *et al.*, 1989; Herman *et al.*, 1995), or it can be oxidised to $^{15}N_2$ (Risgaard-Petersen *et al.*, 1995), which is then measured in an isotope ratio mass spectrometer (IRMS).

In the present study we are interested in measuring denitrification and DNRA rates in the same treatment using soil from a former agricultural floodplain expected to be rich in N and therefore not very sensitive to the effect of fertilisation by a ^{15}N tracer technique. Therefore, we will be using a ^{15}N-labelled NO_3^- tracer laboratory assay to measure the potential denitrification and DNRA rates by adapting the methods described by Trimmer *et al.* (2003) and Risgaard-Petersen *et al.* (1995).

The same slurry samples (references and sub-samples) prepared for the determination of denitrification potential, after the mass spectrometric analysis of their headspace for N_2, were used for investigating the DNRA potential rate by a combined microdiffusion-hypobromite oxidation method adapted from Risgaard-Petersen *et al.*, (1995) and Rysgaard and Risgaard-Petersen (1997), as follows. The 3 mL exetainers containing the denitrification potential slurries were opened and the contents were tipped in pre-weighed 12 mL exetainers (Exetainer vial; Labco Ltd., High Wycombe, United Kingdom). Subsequently, 2M KCl solution was added in the 12 mL exetainers in 4:1 ratio, the exetainers were capped and put on rollers for 30 mins. Next, the exetainers were centrifuged for 5 mins at 3,000 rpm to separate the sediment from the KCl-water solution containing the extractable NH_4^+. After passing the supernatant through a 0.45 μm PTFE syringe filter (Eurolab, VWR), 1 mL was transferred in a new 3 mL exetainer (Exetainer vial; Labco Ltd., High Wycombe, United Kingdom), and the remaining

sample was stored in a bijou at -18^{o}C for later colorimetric analysis of ammonium as per section 4.4.5.

Table 4.4.2: Summary table of methods used for the quantification of DNRA in various ecosystem types. MIMS; Membrane Inlet Mass Spectrometry, GC-MS; Gas Chromatography Mass Spectrometry, HPLC; High Performance Liquid Chromatography.

Author	Study location	DNRA method	$^{15}NH_4^+$ extraction method
Silver et al. (2001); Templer et al. (2008)	Tropical forest soil in Puerto Rico	Intact core - ^{15}N isotope pool dilution (Kirkham and Bartholomew, 1954)	Diffusion (Herman *et al.,* 1995)
Silver et al. (2005)	Tropical plantation forest soil in Costa Rica	Intact core - ^{15}N isotope pool dilution (Kirkham and Bartholomew, 1954)	Diffusion (Herman *et al.,* 1995)
Pett-Ridge and Firestone (2005); Pett-Ridge et al. (2006)	Tropical forest soil in Puerto Rico	Intact core - ^{15}N isotope pool dilution (Davidson *et al.,* 1991; Hart *et al.,* 1994a)	Diffusion (Herman *et al.,* 1995)
Huygens et al. (2007); Rütting et al. (2008)	Tropical forest soil in Chile	Laboratory assay - ^{15}N isotope pool dilution and ^{15}N tracing model (Müller *et al.,* 2004, 2007)	Conversion to N_2O (Laughlin *et al.,* 1997)
Sotta et al. (2008)	Old growth lowland forest soil in Brazil	Intact core - ^{15}N isotope pool dilution (Davidson *et al.,* 1991)	Diffusion (Corre *et al.,* 2003; Corre and Lamersdorf, 2004)
Davis et al. (2008)	Herbaceous riparian soil in Oregon, USA	^{15}N-labelled NO_3^- laboratory assay with C_2H_2 (Tiedje *et al.,* 1981)	Diffusion (Brooks *et al.,* 1989)
Wan et al. (2009)	Calcareous alluvial soil in Beijing, China	Laboratory assay - ^{15}N isotope pool dilution (Kirkham and Bartholomew, 1954)	SPINMAS technique (Stange *et al.,* 2007)
Bengtsson and Bergwall (2000)	Glacial till forest soil in Sweden	^{15}N-labelled NO_3^- laboratory assay with C_2H_2 (Tiedje *et al.,* 1981)	Derivatisation and analysis with GC-MS (Fujihara *et al.,* 1986)
Fazzolari et al. (1998)	Cultivated soil in France	^{15}N-labelled NO_3^- laboratory assay with C_2H_2 (Fazzolari *et al.,* 1990)	Fazzolari et al. (1990)
Ambus et al. (1992)	Riparian fen soil in Denmark	Intact core and laboratory assay ^{15}N isotope pool dilution (Kirkham and Bartholomew, 1954)	Diffusion (Brooks *et al.,* 1989)
Davidsson and Ståhl (2000)	Wetland sediment in Sweden	^{15}N-labelled NO_3^- in flow-through core (Nielsen, 1992; Davidsson *et al.,* 1997)	Microdiffusion BrO^- oxidation (Risgaard-Petersen *et al.,* 1995)
Yin et al. (2002)	Chinese and Australian paddy soils	^{15}N-labelled NO_3^- laboratory assay (Yin *et al.,* 2002)	Diffusion (Brooks *et al.,* 1989)
Matheson et al. (2002)	Riparian wetland in New Zealand	Intact core and ^{15}N-labelled NO_3^- laboratory assay (Matheson *et al.,* 2002)	Diffusion (Brooks *et al.,* 1989)
Matheson et al. (2003)	Riparian wetland in Durham, UK	Laboratory assay - ^{15}N isotope pool dilution (Di *et al.,* 2000)	Diffusion (Stark and Hart, 1996)
Scott et al. (2008)	Lake wetland in Texas, USA	^{15}N-labelled NO_3^- in flow-through core with MIMS (Kana *et al.,* 1994; An and Gardner, 2002)	HPLC (An and Gardner, 2002)
Kelso et al. (1997)	River sediment in Northern Ireland	^{15}N-labelled NO_3^- laboratory assay (Stevens *et al.,* 1993)	Conversion to N_2O (Laughlin *et al.,* 1997)
Tomaszek and Gruca-Rokosz (2007)	Lake sediment in Poland	^{15}N-labelled NO_3^- static core (Nielsen, 1992; Risgaard-Petersen *et al.,* 1993)	Microdiffusion BrO^- oxidation (Risgaard-Petersen *et al.,* 1995)
An and Gardner (2002)	Estuarine sediment in Texas, USA	^{15}N-labelled NO_3^- in flow-through core with MIMS (Kana *et al.,* 1994; An and Gardner, 2002)	HPLC (An and Gardner, 2002)
Rysgaard et al. (1996)	Coastal lagoon sediment in France	^{15}N-labelled NO_3^- static core (Nielsen, 1992; Risgaard-Petersen *et al.,* 1993)	Microdiffusion BrO^- oxidation (Risgaard-Petersen *et al.,* 1995)
Christensen et al. (2000)	Estuarine fjord sediment in Denmark	^{15}N-labelled NO_3^- static core (Nielsen, 1992; Risgaard-Petersen *et al.,* 1993)	Microdiffusion BrO^- oxidation (Risgaard-Petersen *et al.,* 1995)

The hypobromite iodine solution was prepared as described by Rysgaard and Risgaard-Petersen (1997). First, 60 mL of 16M KOH was added to a 100 mL flask immersed in crushed ice. The solution was allowed to cool to 5 ^{o}C and 12 mL of Br_2 was added dropwise during constant stirring over a period of 30 mins. After the addition of bromine, the hypobromite solution was left stirring for at least 1 hour before transferring it in a sealed 100 mL bottle and storing it at 5^{o}C for one week. After 1 week, the solution was filtered to remove the precipitate, and the supernatant was mixed with an equal volume of KI (0.2% w/v). The hypobromite iodine solution remains stable in the refrigerator for at least 6 months. The activity of the hypobromite was tested with a set of standards with different ^{15}N:^{14}N ratios (from 1 to 50 ^{15}N at %) and final ammonium concentration 1mM. The measured and expected values did not differ significantly (ANOVA; F= 5.98, P> 0.05, r^2=0.99) (Figure 4.4.4). The effect of the 2M KCl used for the extraction of NH_4^+ as well as the presence of $ZnCl_2$ (50% w/v) in the sample, from fixing the denitrification potential slurries, was also examined and it was negligible.

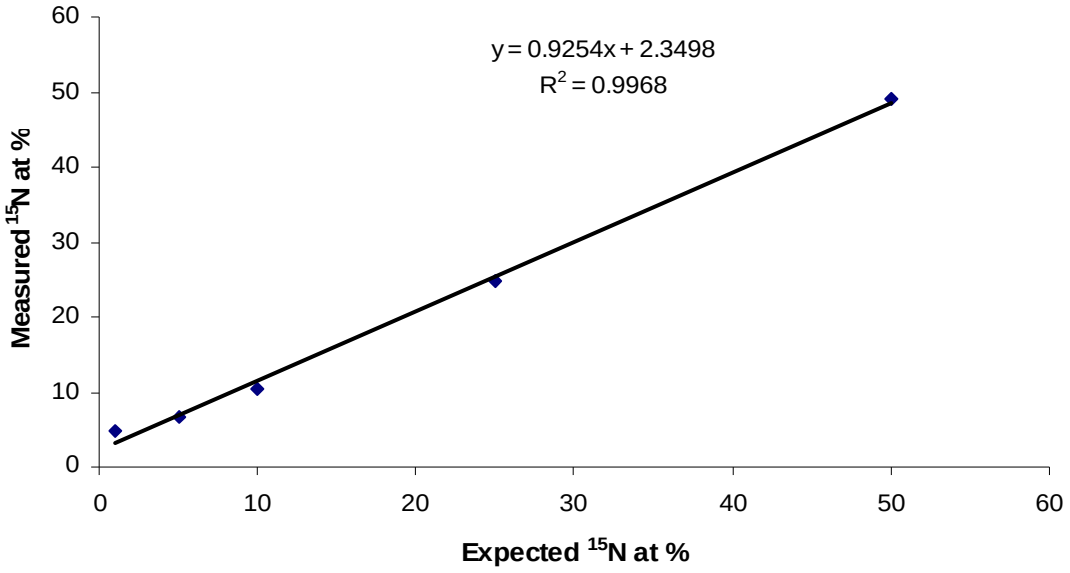

Figure 4.4.4: Measured ^{15}N at % versus expected values in 1mM NH_4^+. Coefficient of correlation (R^2) and regression line is shown in the figure.

After the ammonium extraction with 2M KCl, 1 mL of the supernatant was transferred in a 3mL exetainer, which was then sealed with a cap containing a butyl rubber septum and the sample was flushed with He (CP grade) for 10 mins. This step is important for samples having ^{15}N enrichment <5 at % (Rysgaard and Risgaard-Petersen, 1997) for

decreasing the amount of atmospheric N_2 dissolved in the sample and also for removing any dissolved ^{15}N-labelled N_2 in the sample from the denitrification potential experiment, thus increasing the sensitivity of the assay.

Then a 'reaction-needle' was prepared by flattening the tip of an injection needle and putting it in the 3 mL exetainer containing the sample as shown in Figure 4.4.5. After inserting the 'reaction-needle', 50 μL of the hypobromite iodine solution was added into the luer attachment of the needle and the exetainer was sealed again. Having the 'reaction-needle' with its tip blocked ensured that the hypobromite would not come in direct contact with the sample and the oxidation of N-compounds other than NH_4^+ would be avoided. To convert NH_4^+ to volatile NH_3, pH in the sample was increased to >12 by adding 50 μL 12M NaOH through the rubber septum with a syringe. The exetainer was then agitated gently and left for at least 24 hours at 22 ^oC in order to allow NH_3 to diffuse into the headspace, react with the hypobromite solution in the needle cup and subsequently be oxidised to N_2. The isotopic composition of N_2 in the headspace of the vials was analysed with the aid of an IRMS as per section 4.4.7.

Because the ^{15}N enrichment of the timed sub-samples was <1 at % and the $^{30}N_2$ signal was not significantly different between the samples and their respective references and air blanks, the equations (4.4.7) and (4.4.8) according to Risgaard-Petersen *et al.* (1993) were miscalculating the ^{15}N at % of the samples.

$$R = \frac{f_{29}H - f_{29}A}{f_{30}H - f_{30}A} \tag{4.4.7}$$

$$^{15}Nat\% = \frac{1 + \sqrt{1 - (R+2)\cdot(f_{29}A - R\cdot f_{30}A)}}{R+2} \cdot 100\% \tag{4.4.8}$$

where $f_{29}H$ and $f_{30}H$ are the amounts of $^{14}N^{15}N$ and $^{15}N^{15}N$ in the headspace of the sample, and $f_{29}A$ and $f_{30}A$ the amounts of $^{14}N1^5N$ and $^{15}N^{15}N$ in the headspace of an air blank.

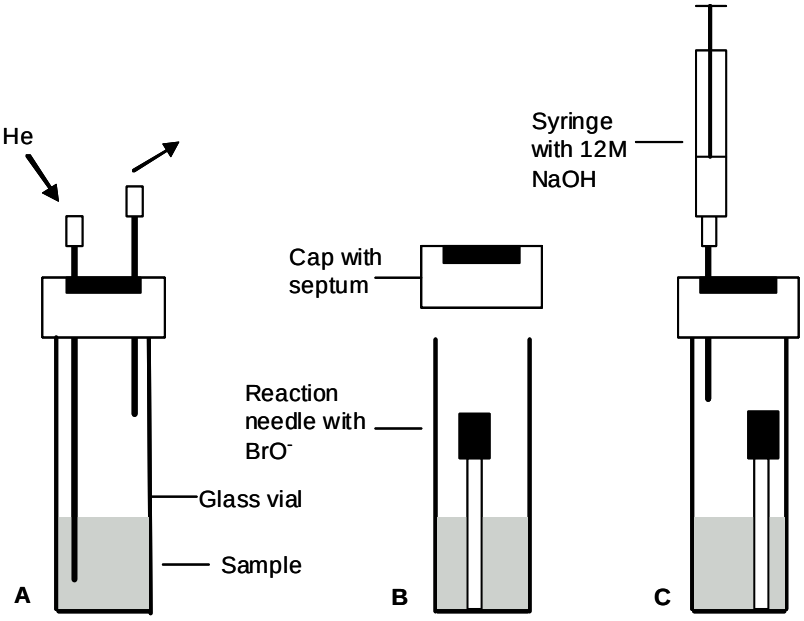

Figure 4.4.5: Procedure for preparing the microdiffusion-hypobromite oxidation assay: (A) flushing with He; (B) insertion of the 'reaction needle' with hypobromite into the glass vial; (C) addition of alkaline solution (adapted from Risgaard-Petersen *et al.*, 1995).

Alternatively, the ^{15}N at % in samples containing <10% of the ^{15}N isotope can be calculated from the signals for $^{28}N_2$ and $^{29}N_2$ as described in Platzner (1997):

$$A(^{15}N) = \frac{100}{(2 \cdot \frac{^{28}N_2}{^{29}N_2} + 1)} \qquad (4.4.9)$$

However, since the enrichment in the samples was less than 1% and approaching the natural abundance of the ^{15}N isotope (0.366 %), the effect of the background 'carrier' N_2 in the headspace of the sample had also to be taken into account. Since the headspace of the sample was exposed to the atmosphere while adding the 'reaction' needle and the hypobromite solution, atmospheric nitrogen with natural abundance in ^{15}N was mixed with the N_2 derived from the oxidation of ammonium. Therefore the ^{15}N at % of the N_2 mix in the headspace of the sample can be calculated by equation (4.4.10) adapted from Fry (2006).

$$^{15}Nat\%_{mix} = \frac{[(M_{air} \cdot ^{15}N_{air}) + (M_{sample} \cdot ^{15}N_{sample})]}{(M_{air} + M_{sample})} \qquad (4.4.10)$$

where M_{air} the amount of background N_2 in the headspace (μmol); M_{sample} the amount of N_2 deriving from the sample (μmol); ${}^{15}N_{air}$ and ${}^{15}N_{sample}$, the ^{15}N at % of the headspace background and the sample respectively.

The ^{15}N at % calculated in equation (4.4.9) by the signals for $^{28}N_2$ and $^{29}N_2$, is effectively the ^{15}N at % of the mix estimated from equation (4.4.10). Therefore, by combining equations (4.4.9) and (4.4.10) and solving for $^{15}N_{sample}$ gives equation (4.4.11) that estimates the 'true' ^{15}N enrichment of the sample:

$$ {}^{15}N_{sample}at\% = \frac{[A({}^{15}N)\cdot(M_{air}+M_{sample})]-(M_{air}\cdot{}^{15}N_{air})}{M_{sample}} \qquad (4.4.11) $$

The validity of equation (4.4.11) was tested with a set of standards with different ^{15}N:^{14}N ratios (from 0 to 0.5 ^{15}N at % above natural abundance) and final ammonium concentration 1mM. The measured and expected values did not differ significantly (ANOVA; F= 5.92, P> 0.05, r^2=0.99) (Figure 4.4.6).

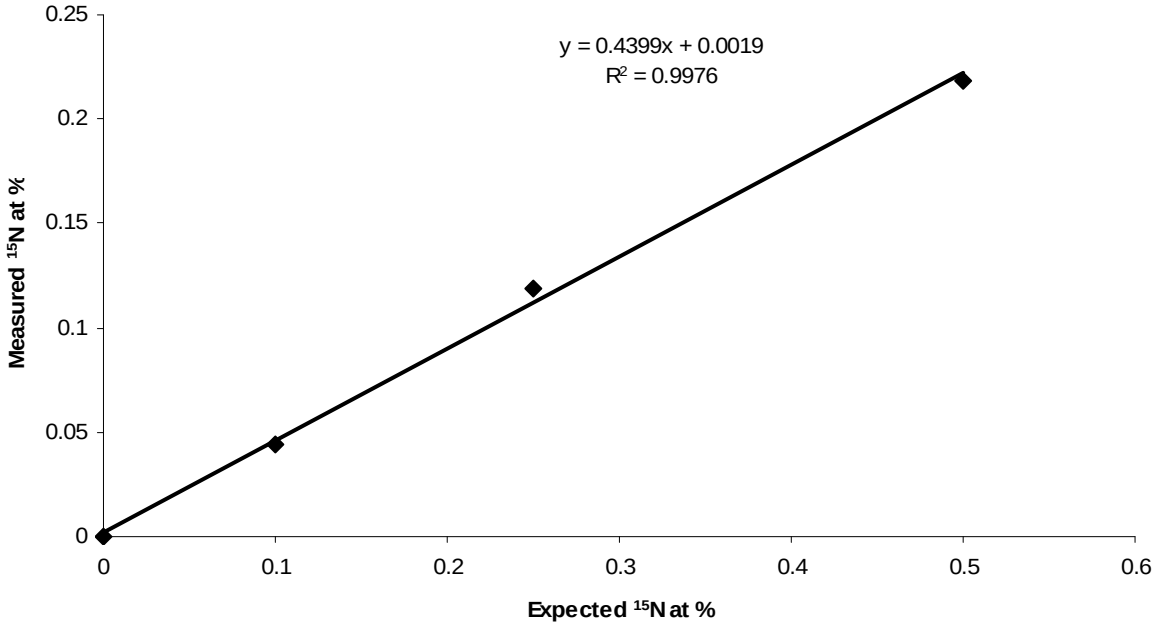

Figure 4.4.6: Measured ^{15}N at % versus expected values in 1mM NH_4^+. Coefficient of correlation (R^2) and regression line is shown in the figure.

The excess of ^{15}N at % in the sample over that in the reference was used to calculate the production of ^{15}N originating from the oxidation of NH_4^+ to N_2 per unit of dry soil mass per unit time:

$$pDNRAmgNkg^{-1}day^{-1} = \frac{(^{15}N_{sample} - {}^{15}N_{reference})}{100} \cdot [NH_4^+] \cdot df \cdot V \cdot 15 \cdot \frac{1}{m} \cdot 10^{-6} \cdot t^{-1} \quad (4.4.12)$$

where *p* DNRA mg N kg^{-1} day^{-1} was the production of ^{15}N in ammonium; ^{15}N the ^{15}N at % in the sample and the reference respectively; $[NH_4^+]$ the ammonium concentration (μM); *df* the dilution factor from the KCl extraction (volume KCl/volume of slurry); *V* the volume of the slurry (mL); 15 the atomic mass of N; *m* the dry mass of the soil sample (g) and *t* the duration of the incubation (hour). An areal rate for DNRA in kg N ha^{-1} day^{-1} was also calculated as per section 4.4.7.

4.4.9 *Measurement of nitrous oxide potential production rate*

The potential N_2O production rate during the denitrification potential slurry experiment was estimated by gas chromatography. The headspace of the slurry samples, before their extraction for DNRA analysis, was sampled (50 μL) with a gas-tight syringe in an auto-sampler (Multipurpose Sampler MSP2, Gerstel, GmbH, Germany) and injected into a GC-μECD, (7890A GC Agilent Technologies UK Limited, Cheshire) (Column 40^oC, detector 375 ^oC) equipped with a ^{63}Ni plated cell and using as carrier gas 5% Methane/Argon (60 mL min^{-1}). Headspace concentration of N_2O was calculated from peak area using an electronic integrator (ChemStation®, software). N_2O was calibrated against known standards (Scientific and Technical Gases Ltd, Staffs, UK). Precision, as a coefficient of variation, was better than 2 % for N_2O. Nitrous oxide production rate (*p* N_2O-*N mg* kg^{-1} d^{-1}) was estimated with equation 4.4.13.

$$pN_2O - Nmgkg^{-1}d^{-1} = \frac{([N_2O]_{sample} - [N_2O]_{reference}) \cdot V \cdot M \cdot 0.6521}{m \cdot 1000 \cdot t} \cdot 24 \quad (4.4.13)$$

where $[N_2O]$ the concentration of N_2O in the sample and the reference respectively (μM); *V* the volume of the headspace (mL); *M* the molecular weight of $^{15}N_2O$ (46); 0.6521 the proportion of N in N_2O; *m* the dry mass of the sample (g); *t* the incubation time (hours) and 24 the hours in one day. The $[N_2O]$ was corrected for N_2O solubility in

water by applying a Bunsen coefficient of 0.70 at 20 ^{o}C according to Weiss and Price (1980). An areal rate for N_2O production in kg N ha^{-1} day^{-1} was also calculated as per section 4.4.7. It should be noted that the above analysis was performed for the PM and BZ subsurface samples, as well as for the wet-dry conditions sampling only.

4.4.10 *Screening for potential anammox activity*

The slurry samples from the BZ subsurface sampling were used to screen for the occurrence of anammox activity throughout the soil profile, following the methodology by Trimmer *et al.* (2006). The headspace of the slurry vials, before their extraction for DNRA measurement, was sampled (10 μL) and transferred into an air-filled 12.5 mL exetainer (Exetainer vial; Labco Ltd., High Wycombe, United Kingdom). A preliminary analysis had shown that due to high ^{15}N enrichment of N_2O, the $^{45}N_2O$ and $^{46}N_2O$ were off the measuring scale of the IRMS. Therefore, a double dilution was used by transferring 10 μL of the 12.5 mL exetainer headspace to a second series of air-filled 12.5 mL exetainers (final dilution 15 x 10^3). Subsequently, the entire content of the gas-tight exetainer was swept, using a two-way needle and analytical grade He, to a trace gas preconcentrator (Cryo-Focusing; PreCon, Thermo-Finnigan), where the gases are dried and scrubbed of most of the CO_2 before being cryo-focused twice in liquid N_2 and the final separation of N_2O from CO_2 occurs on a PoraPLOT Q capillary column. The sample then passes to the CF/IRMS via an interface (ConFlo III Interface, Thermo-Finnigan) and the mass charge ratios for m/z 44, m/z 45, and m/z 46 ($^{44}N_2O$, $^{45}N_2O$, and $^{46}N_2O$) are measured. Calibration was performed with known amounts of N_2O (98 μL L^{-1}; Scientific and Technical Gases) over the range 0.41–13.25 nmol N_2O (Σ $^{44}N_2O$, $^{45}N_2O$, and $^{46}N_2O$) and was linear between 0.8 pmol and 99 pmol for $^{45}N_2O$ and $^{46}N_2O$.

As Trimmer *et al.* (2006) suggested, the r_{14}, which is the ratio between $^{14}NO_3^-$ and $^{15}NO_3^-$ in the slurry, can be estimated from the ^{15}N labelling of the N_2O produced during the incubation, i.e. $^{14}N^{15}N_2O$ ($p^{45}N_2O$) and $^{15}N^{15}N_2O$ ($p^{46}N_2O$) (equation 4.4.14). For the purposes of this technique, denitrification is assumed to be the only quantitative significant source of ^{15}N-N_2O in a $^{15}NO_3^-$ labelling experiment (Trimmer *et al.*, 2006).

$$r_{14} = \frac{p^{45}N_2O}{2 \cdot p^{46}N_2O} \qquad (4.4.14)$$

The term r_{14} can be converted to the term q, which is the proportion of ^{15}N in the total N gas pool and is directly related to r_{14}:

$$q = \frac{1}{r_{14} + 1} \tag{4.4.15}$$

The term q is calculated for both ^{15}N gas species, i.e. q' N_2 vs. q N_2O, and subjected to regression analysis. If the slope deviates significantly from 1 then the change in the predicted distribution of ^{15}N is taken as being due to anammox (Trimmer *et al.,* 2006). Because in the present study there was no spread in the $^{15}NO_3^-$ concentrations and the ambient $^{14}NO_3^-$ was consistently low (because of pre-incubation), the linear regression would generate false slopes. Instead, a paired-sample Student's t-test was used to compare the means of q' N_2 and q N_2O for each sampled depth interval.

4.5 *Statistical analysis*

All data were tested for normality and homogeneity of variance with the Kolmogorov-Smirnov test and the Levene statistic respectively. If data did not meet the requirements they were log-transformed before statistical analysis. Comparison of independent samples' variance was performed primarily with One-Way ANOVA combined with the Least Significant Difference (LSD) *post hoc* test for the assessment of inter-sample group differences. The variance of those samples that were not log-normally distributed was tested with the non-parametric Kruskal-Wallis test (for more than two groups of samples) or the Mann-Whitney U test (between two groups of samples).

Principal Component Analysis (PCA) was employed to explore which combinations of variables, 'principal components', are likely to provide the maximum discrimination between individual samples (Dytham, 2003). PCA also served in identifying and clustering together highly inter-correlated variables (Hefting *et al.,* 2003). The PCA assumes: linear relationships between all the variables, no inter-correlation of the component axes; continuity and normal distribution of the data (Dytham, 2003). Discriminant Function Analysis (DFA) was used once to test the groups of samples (i.e. the four land use zones) suggested by the PCA. The difference between PCA and DFA is that in DFA, individual samples are assigned to groups before the start of the test. Then variable weightings are calculated so that they maximise the difference between groups instead of individual samples. The power of the weightings is tested by naming

one individual sample from the dataset as ‘unknown’ and then using the variable weightings to assign it to one of the groups. The hit rate is a measure of the power of the test to discriminate real unknowns (Dytham, 2003).

The relationships among variables (e.g. soil properties), and between variables and process rates (e.g. denitrification), were tested with Pearson’s Product Moment correlation (for normally distributed data) or Spearman’s rank correlation (for non normally distributed data). Finally the prediction of the process rates’ variance by the combination of different variables was tested with multiple forward linear regression analysis. All statistical analysis was performed using SPSS® 11.5 for Windows (SPSS 2002, Chicago, Illinois, USA).

Chapter 5: Hydrology and hydrochemistry of the re-connected floodplain of the River Cole.

5.1 *The stratigraphy and the saturated hydraulic conductivity in the subsurface soil horizons of the reconnected floodplain of the River Cole*

This chapter begins with the description of the subsurface soil stratigraphy and the results for the saturated hydraulic conductivity measurements in the subsurface soil horizons of the PM and BZ sites. These results are used in the subsequent sections to explain the groundwater residence time and flow rate through the different soil horizons that in turn affect nitrate attenuation processes in the studied areas.

5.1.1 *Floodplain stratigraphy*

During the installation of the groundwater wells in the PM and BZ sites, the borehole logs were used to describe the soil stratigraphy in the cross sections along the transect F1 to F7 in PM, and H10 to H4 in BZ. The subsurface soil profile of the cross-section F1-F7 is shown in Figure 5.1.1.

The top 0 - 20/30 cm comprises the organic A soil horizon, characterised by dark brown, friable, crumbly soil. The root zone extends up to 20 cm, especially where riparian vegetation is dominant. The B soil horizon (below 20/30 cm depth) is characterised by brown clay with blocky structure. This horizon extends up to 50 cm depth near the river bank (F1) and is characterised by abundant (>50 %) ochreous and grey mottles indicating imperfect drainage (Rowell, 1994). The same horizon extends up to 85 cm between the wells F1-F4, becoming increasingly light in colour, while the abundance of ochreous and grey mottles also increases. Between the wells F4 and F7, the B horizon is more greyish below 50 cm depth and instead of ochreous mottles more abundant black anoxic zones are observed, indicating poorly drained sediments up to 1 m depth. In well F5, calcareous shell remains are observed in high abundance (> 50 %) below 80 cm depth, potentially indicating an old course of the River Cole.

The C horizon is found at 80 - 100 cm depth near the river bank (F1) and is predominantly grey clay with increasing amounts of silt. However, at 105 cm depth the C horizon abruptly changes to gritty gravel and sand. The same sand – gravel C horizon

is observed between the wells F2 and F5 below 120 cm depth. This gravel lens layer is characterised by bright brown - orange colour, very unconsolidated structure, granular texture and the presence of fines (clays and silts) between the interstices. Towards the north end of the PM area, near the ditch, no gravel lens is observed and the C horizon is predominantly grey thick clay with black and grey gley features. The C clay horizon becomes gradually more consolidated with depth at around 200 cm, and this is also found underneath the gravel lens. Although boreholes deeper than 200 cm were not excavated, and the presence of a deeper aquifer has not been documented in the literature, it could be assumed that the C clay horizon at 2 m depth is an impermeable layer confining the movement of a perched water table between the ground surface and 2 m depth. Finally, during the borehole excavation no evidence of tile or mole drainage was found.

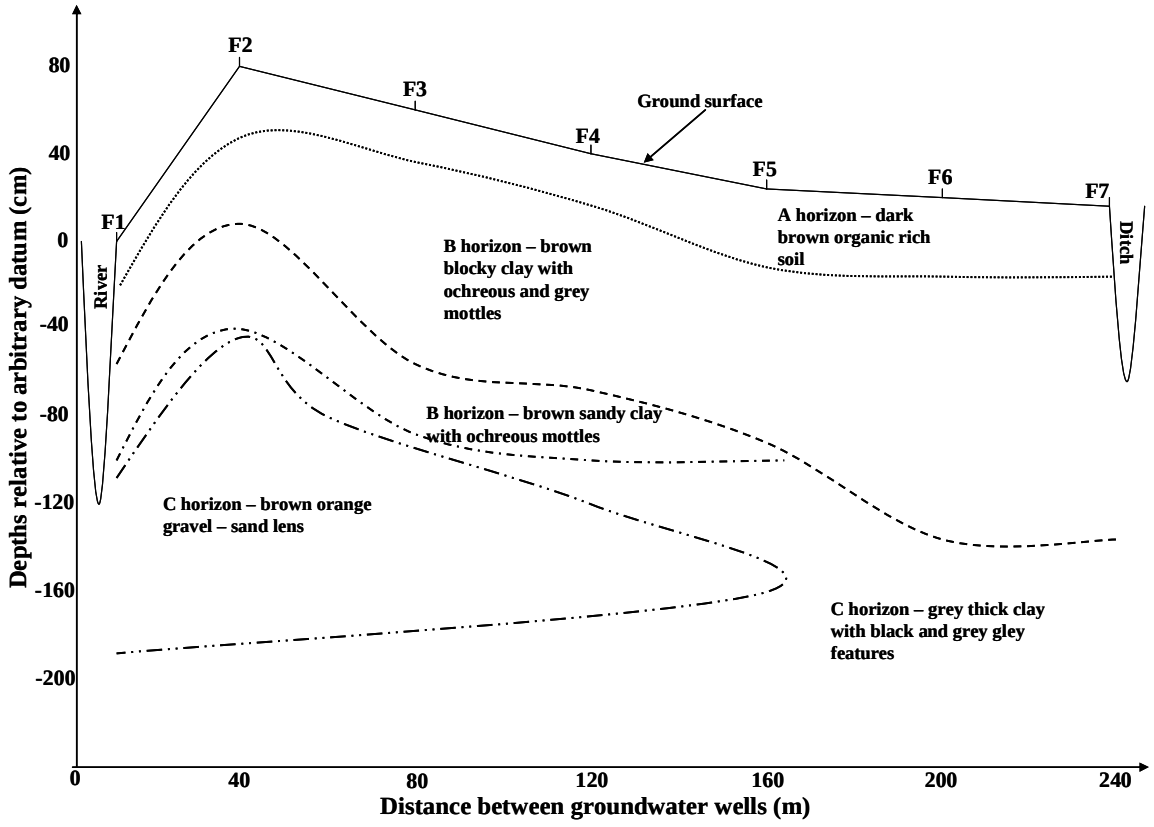

Figure 5.1.1: The soil profile in the cross-section of the perpendicular to the river transect (F1-F7) in the PM site. The arbitrary datum is the surface of the well F1.

The soil stratigraphy of the cross-section F9 to F14 is not described in detail since it is very similar to the cross section F1-F7, with the exception of the absence of a distinct gravel lens.

The subsurface soil profile of the cross-section H10 – H4, in the BZ site, is shown in Figure 5.1.2. The organic A horizon is restricted in the top 25 cm from the ground surface and is characterised by dark brown friable soil, with high root abundance of different diameters, earthworm burrows and some scattered gravel. Possibly due to the proximity of the BZ to the river, calcareous shell remains and gravel are scattered throughout the soil profile. The A horizon near the river margin, well H10, is characterised by rusty mottles due to roots along with grey silty anoxic sediments and the presence of reed root mat.

Between the wells H10 and H8, a thin layer of brown blocky clay with ochreous mottling is observed below the A horizon up to 50 cm depth. This layer is deeper in the wells H7 and H4 reaching a depth of 100 cm, whilst absent from well H8. A more sandy clay B horizon is observed between 50 and 80 cm depth in the wells H10 and H9, while this layer extends from below the A horizon to 80 cm depth in the case of well H8.

A grey thick clay C horizon extends below 100 cm depth in wells H7 and H4 and below 80 cm depth in the case of well H9. The clay C horizon is characterised by ochreous, black and grey mottles, scattered gravel and sand in places and also calcareous shell remains. This layer does not change up to the two meters depth of the borehole excavations, but becomes thicker and drier. It is therefore assumed that below 2 m depth the thick C clay horizon is an impermeable layer and the movement of a perched water table in the BZ site is restricted between the ground surface and 2 m depth. No evidence of tile or mole drainage was found in the BZ subsurface.

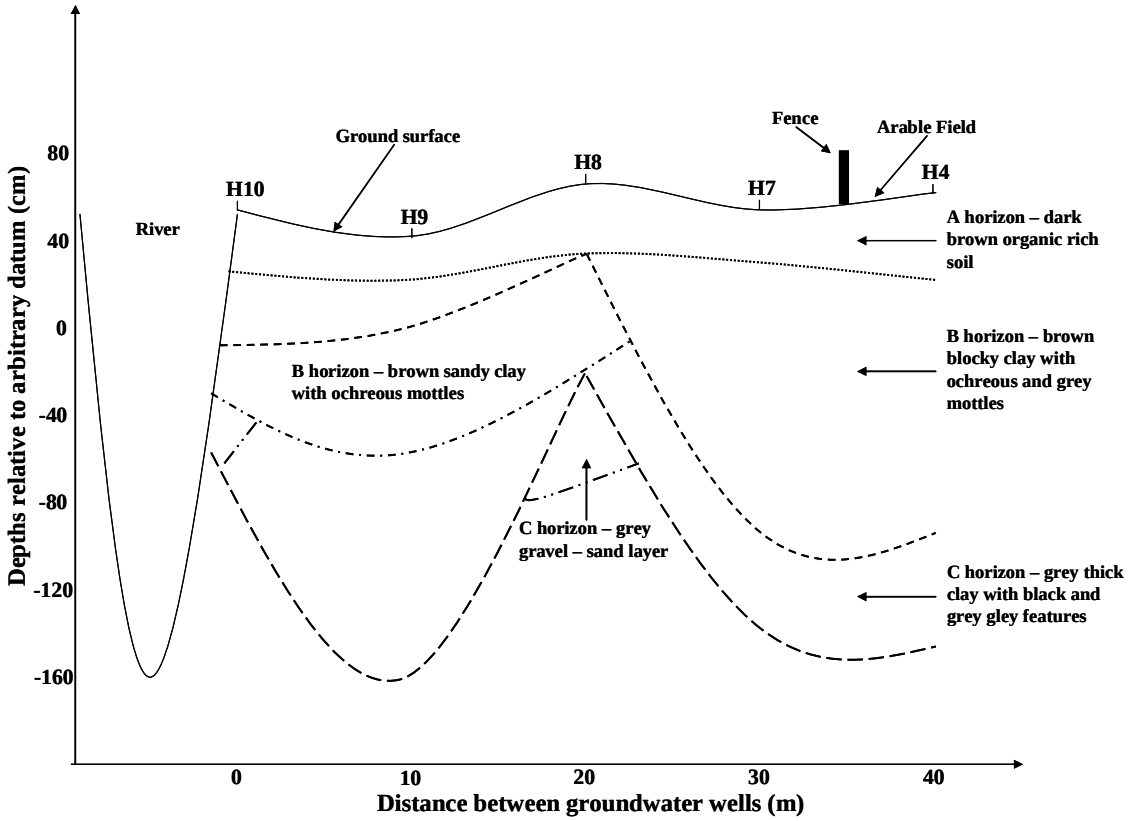

Figure 5.1.2: The soil profile in the cross-section of the perpendicular to the river transect (H10-H4) in the BZ site. The arbitrary datum is the surface of the well H1 (not shown).

5.1.2 *Saturated hydraulic conductivity*

The results from the saturated horizontal hydraulic conductivity (K_h) measurements in the A, B and C soil horizons of the PM and BZ areas are summarised in Table 5.1.1.

Table 5.1.1: The saturated horizontal hydraulic conductivity (K_h) in the soil horizons of the PM and BZ areas. Depths in brackets indicate the measurement depth. The values are minimum - maximum range and mean in brackets. N/A indicates non availability of data.

	K_h (cm d^{-1})	
Soil horizons	**Pasture Meadow (PM)**	**Buffer Zone (BZ)**
A (0 - 30 cm)	N/A	13.6 - 28.2 (20.9)
B (50 - 70 cm)	16.4 - 17.2 (16.8)	36.8 - 83.3 (55.4)
Gravel lens (122 - 140 cm)	3 - 12.3 (8.4)	N/A
C (120 - 140 cm)	0.3 - 1.2 (0.8)	9.1 - 33.9 (20.3)

The K_h of the A horizon was only measured at the BZ site at 30 cm depth. The mean was 20.9 ± SE 7.3 cm day^{-1}, which was 38 % lower than in the B horizon, opposite to our expectations. It is likely that the spatial arrangement of the soil particles and also their shape affect the K_h and moreover the presence of roots in the top 30 cm of the soil complicate further the measurement of the hydraulic conductivity.

The K_h of the B horizon, measurement between 50 and 70 cm depth, was 30 % higher in the BZ than in the PM. The mean K_h in the BZ B horizon was 55.4 ± SE 7.6 cm day^{-1}, while the mean K_h of the PM B horizon was 16.8 ± SE 0.4 cm day^{-1}. The most likely explanation for this difference between the PM and the BZ site could be the strongly alluvial nature of the BZ subsurface with a mixture of fine sediments, and therefore a low permeability value, but also scattered gravel and shell deposits that could be creating larger pore spaces where preferential flow might have been taking place.

The K_h of the gravel lens in the PM site was measured between the wells F2 and F4 at depths ranging between 122 and 140 cm from the ground surface, making sure that the intake of the measuring piezometer was exclusively in the gravel layer. The average K_h in the gravel lens was 8.4 ± SE 2.8 cm day^{-1}, being lower than the K_h of the B horizon, and indicating that the gravel lens is not hydraulically well connected to the river, and is probably constrained by surrounding clay that lowers the K_h. As for the thick clay C horizon at around 2 m depth in the PM subsurface, the mean K_h was 0.8 ± SE 0.5 cm day^{-1}, being an order of magnitude lower than the K_h of the gravel lens and confirming the assumption that the water table was restricted between the ground surface and 2 m depth, since the C clay horizon was practically impermeable.

The C horizon of the BZ site, measurement performed between the wells H9 and H2 at 120-140 cm depth, was considerably more permeable with mean K_h 20.3 ± SE 6.2 cm day^{-1}, 41 % higher than the K_h of the gravel lens. Probably, the presence of scattered gravel, apart from fine sediments, in the C horizon of the Buffer Zone could be responsible for preferential flow through larger pore spaces that were absent from the C horizon of the PM. Moreover, the unconsolidated structure of the PM gravel lens together with its high content of fine sediments probably impeded the fast recovery of hydraulic heads in the piezometers resulting in lower K_h compared to the more consolidated with sparse gravel structure of the BZ C horizon.

5.2 *The meteorological record at Coleshill, Oxfordshire (February 2007 – September 2008)*

The purpose of this section is to present an overview of the climatic conditions in the re-connected floodplain of the River Cole, in the context of the U.K. climate, focusing on the rainfall, air and soil temperature patterns during the monitoring period (February 2007 - September 2008) that influenced the hydrological regime of the floodplain. The climatic conditions are described for the two monitoring seasons; 1) from 12th February 2007 until 30th September 2007 and 2) from 1st October 2007 until 30th September 2008.

5.2.1 *Season 1 (February 2007 – September 2007)*

A monthly summary of air temperature, soil temperature at 10 cm depth in the topsoil, total rainfall and potential evapotranspiration is presented in Table 5.2.1. February 2007 was a mild month with the air temperature being 2.3°C above the 1961-1990 average, while the rainfall was also above average. The first 10 days of the month were dry, while from 10th to 12th the weather was showery, and the water table started to rise. The daily total rainfall, as well as, the daily mean soil temperature for the period 12th February till 30th September are shown in Figure 5.2.1. The PM channel depression was flooded for 10 days while the BZ was flooded for 12 days during February (Fig. 5.2.2).

Overall March 2007 was a mild and sunny month with slightly below average rainfall. The soil temperature at 10 cm depth gradually started to rise. One overbank flood event was recorded at the beginning of the month (peaking on 6th March) following 11.4 mm of rain on 4th March on already wet ground from the last event at the end of February. This event resulted in overland flow in the PM channel depression that lasted five days, while the BZ site and the riparian zone of the PM were still flooded from the previous event at the end of February (Fig. 5.2.2). For the remainder of the month, following 12th March, the water table was below the ground surface and continued to recede. The dry weather continued throughout April 2007, which was in fact a record warm month with April mean temperatures being the warmest on record since 1914, and well above average sunshine. The warm weather resulted in the topsoil temperature rising quickly, while the mean evapotranspiration rate exceeded the total daily rainfall on almost all days. The combination of high evapotranspiration and below average rainfall (fourth driest April since 1914), led to the second lowest water table recorded during the study, 130 cm below ground surface in the PM and 78 cm below ground surface in the BZ site

(lowest water table level across the sites). That dry spell lasted only for the first six days of May, which was overall a rather wet month (5th wettest May since 1979) with 130.4 mm of total rainfall. The water level in the River Cole rose to its bankfull height on the 14th, following a wet week with a total of 55.2 mm rain. Then another dry period followed until the storm of the 27th, when 39.2 mm of rain fell in 24 hours, leading to another overbank flood event, the first in the last 80 days, that led to the complete flooding of the BZ and the PM channel depression for four days, while the mean soil temperature at 10 cm depth was 14.6^{o}C.

June 2007 was warm and dry at the start, but towards the end of the month low pressure brought significant rainfall and as a consequence, it was the wettest June since 1997 and the dullest since 1998. The mean topsoil temperature was the highest recorded during the study at 17.3^{o}C. On the 25th, 27.2 mm of rain fell in 24 hours resulting in another four day overbank flood event at the River Cole reconnected floodplain. Similar conditions prevailed during most of July 2007, which was the wettest July since 1936, with the highest total rainfall of the study, 178.9 mm, while the temperature was slightly below average. The most notable event was the extremely heavy rainfall on the 20th, where 77.2 mm of rain fell in 6 hours causing a flashy response of the River Cole that overflowed onto the PM and the BZ, which then remained inundated for 11 days. August started and ended with dry and settled weather, with the majority of rainfall recorded in mid-month. Despite the mean air temperature being the highest in season one, 15.4^{o}C, August 2007 was the coldest since 1993. However, the mean evapotranspiration was the highest, 2.3 mm d^{-1}, over season one and the maximum was recorded on 23rd August with 4.8 mm d^{-1}. The fine dry weather continued during most of September and the rainfall was 64 % below the 1961-1990 average.

Overall, Season one was eventful, with extensive overbank flooding of the River Cole in the winter months, followed by an 80 day water table receding period in March and April, which was then followed by one of the wettest summers of the last 20 years, where three major overbank flood events occurred in May, June and July respectively (Figure 5.2.2).

5.2.2 *Season 2 (October 2007 – September 2008)*

October 2007 was overall a fine and settled month with rainfall being 56 % below the 1961-1990 average. The 35.3 mm of rain that fell on the 16th (Table 5.2.1 and Figure 5.2.3) led to the first overbank flood event of season two that lasted two days in both the PM and the BZ (Figure 5.2.4). November was generally more anticyclonic than a 'normal' November with rainfall being 86 % of the 1961-1990 average. However, the 30.3 mm of rain that fell between the 18th and the 22nd of the month led to a five day overbank flood event between the 20th and the 24th in the PM channel depression and the BZ (Figure 5.2.4).

The winter started with unsettled weather in December, when 52.8 mm of rain fell in the first 10 days of the month leading to yet another overbank flood event that lasted for six days in the PM channel depression and 13 days at the BZ site. This event was followed by more settled weather for about two weeks, until the 25th and the 30th when the second flood event occurred. The unsettled weather continued throughout January 2008, which was mild in terms of air temperature (mean 6.9°C), 4th warmest January since 1914, but the rainfall was the second highest recorded for season two, 107.6 mm, being the wettest January since 1995. The wet weather led to an extensive complex flood event with three peaks on 12th, 16th and 20th respectively (Figure 5.2.4). The riparian zone of the PM was flooded for 27 days, while the channel depression was flooded for 13 continuous days. Similarly, the BZ site was inundated continuously for 26 days, while the topsoil temperature ranged between 3.4 and 10°C (Figure 5.2.3). In contrast to December and January, February 2008 was a dry, sunny month, sunniest February since 1929, with rainfall being 65 % of the 1961-1990 average. Moreover, it was the coldest month in season two, mean air temperature 4.3°C, while the topsoil temperature ranged between 0.5 and 7°C.

Spring started with windy, wet weather and rainfall was well above average for March 2008, being the wettest March since 1981. Two distinct events, one on the 10th when 14.6 mm of rain fell in one day, and the other between the 15th and 16th when 41.4 mm of rain fell in two days, led to two overbank flood events. During these events, the PM channel depression was inundated for four days, while the BZ site was flooded for a week. The topsoil temperature ranged between 3.8 and 8.5°C. April was generally dry but cold, coldest April since 2001, being three degrees lower than April 2007 in both the

topsoil and the air temperature. The total rainfall, 37.8 mm, was the second lowest for season two after February. May, on the other hand, was a very warm month with average air temperature 12.9^{o}C, being the second warmest May since 1914. The average topsoil temperature of the month was 14.1^{o}C. Moreover, May had the highest total rainfall in season two, 116 mm, of which 70 mm fell between the 25th and the 28th causing another overbank flood event for 4-5 days in the PM channel depression and the BZ site.

The unsettled weather from the end of May continued in June 2008 giving another flood event following the 59.3 mm of rain that fell in 24 hours on 3rd June. This event lasted for four days, while the mean topsoil temperature was 15.2^{o}C. Similarly unsettled was the first half of July 2008. A storm on the 9th, during which 24.5 mm of rain fell in 24 hours flooded both the BZ and the PM areas for a couple of days. July was also the warmest month of season two with mean air temperature 15.8^{o}C and mean topsoil temperature 16.1^{o}C. Dry weather prevailed from the 13th till the 27th when the highest summer temperature was recorded at 27.3^{o}C. After the short dry weather break in July, August was very much unsettled with frequent showery weather and it was also exceptionally dull for this time of the year. The 23.6 mm of rain that fell on the 12th caused a brief overbank flood event that lasted for two days in the PM channel depression and the BZ site. Finally, the unsettled weather front continued until mid-September when almost 60 mm of rain that fell between the 1st and the 13th of the month led to two bankfull events on the 6th and the 13th respectively. The rest of the month was mostly dry and settled.

Overall, the second monitoring season was characterised by increasingly wet weather during the autumn and winter that peaked in January. The wet weather was responsible for 28 flood days between October and January. The unusually warm January was followed by an unusually dry and uneventful February. However, the wet and unsettled weather resumed in March with 7 more flood days, and after a relatively dry April, the wet unsettled weather continued throughout May till mid-September giving less frequent but higher magnitude flood events. Generally, monitoring season two was eventful with a total of 48 flood days recorded at the PM channel depression and 83 flood days for the BZ site, but less eventful compared to the first monitoring season, which comprised 75 flood days in the PM channel depression and 102 flood days in the

BZ. Although the number of flood events was approximately similar for both field seasons, the rainfall magnitude of the events was lower in the second season of fieldwork resulting in less frequent inundation of the floodplain.

Table 5.2.1: Monthly summary of weather at Coleshill, Oxfordshire, from 12th February 2007 to 30th September 2008. The number in brackets indicates the date of the highest daily rainfall. Number of 'flood' days in the BZ with reference to the well H10, whereas for the PM the reference well is F11 in the channel depression.

	Month							
Weather Data from Coleshill AWS	**February 07**	**March 07**	**April 07**	**May 07**	**June 07**	**July 07**	**August 07**	**September 07**
Mean air temperature (^{o}C)	7.9	6.7	10.6	11.8	14.9	15.0	15.4	13.5
Mean soil temperature at 10 cm (^{o}C)	7.4	7.6	12.5	14.6	17.3	16.6	15.0	13.3
Highest daily rainfall (mm)	10.2 (28th)	11.4 (4th)	0.8 (23rd)	39.2 (27th)	27.2 (25th)	101.1 (20th)	13.2 (15th)	6.5 (24th)
Total rainfall (mm)	43.7	41.2	3.7	130.4	93.6	178.9	33.9	23.8
Mean potential evapotranspiration (mm d^{-1})	0.4	1.1	1.9	1.8	2.2	2.2	2.3	1.5
No. 'wet' days (> 1 mm rain)	11	10	0	14	15	14	6	5
No. 'flood' days in the Buffer Zone	12	11	0	4	3	11	1	0
No. 'flood' days in the Pasture Meadow	10	8	0	4	4	11	0	0

	Month							
Weather Data from Coleshill AWS	**October 07**	**November 07**	**December 07**	**January 08**	**February 08**	**March 08**	**April 08**	**May 08**
Mean air temperature (^{o}C)	10.2	6.5	4.6	6.9	4.3	6.1	7.5	12.9
Mean soil temperature at 10 cm (^{o}C)	10.7	7.0	4.8	6.2	4.2	6.3	9.3	14.1
Highest daily rainfall (mm)	35.3 (16th)	13.4 (18th)	17.1 (25th)	26.0 (15th)	8.3 (26th)	30.5 (16th)	10.6 (29th)	29.0 (28th)
Total rainfall (mm)	75.6	50.4	79.8	107.6	24.2	84.7	37.8	116.0
Mean potential evapotranspiration (mm d^{-1})	0.5	0.2	0.1	0.2	0.4	1.0	1.4	2.0
No. 'wet' days (> 1 mm rain)	5	9	10	16	6	12	13	10
No. 'flood' days in the Buffer Zone	2	6	19	26	6	15	0	5
No. 'flood' days in the Pasture Meadow	2	5	8	13	0	7	0	4

	Month			
Weather Data from Coleshill AWS	**June 08**	**July 08**	**August 08**	**September 08**
Mean air temperature (^{o}C)	14.1	15.8	15.7	12.5
Mean soil temperature at 10 cm (^{o}C)	15.2	16.1	16.0	13.3
Highest daily rainfall (mm)	59.3 (3rd)	24.6 (9th)	23.6 (12th)	12.4 (5th)
Total rainfall (mm)	94.6	96.5	91.6	64.2
Mean potential evapotranspiration (mm d^{-1})	2.7	2.3	1.4	1.0
No. 'wet' days (> 1 mm rain)	8	10	15	11
No. 'flood' days in the Buffer Zone	4	3	3	2
No. 'flood' days in the Pasture Meadow	4	2	2	0

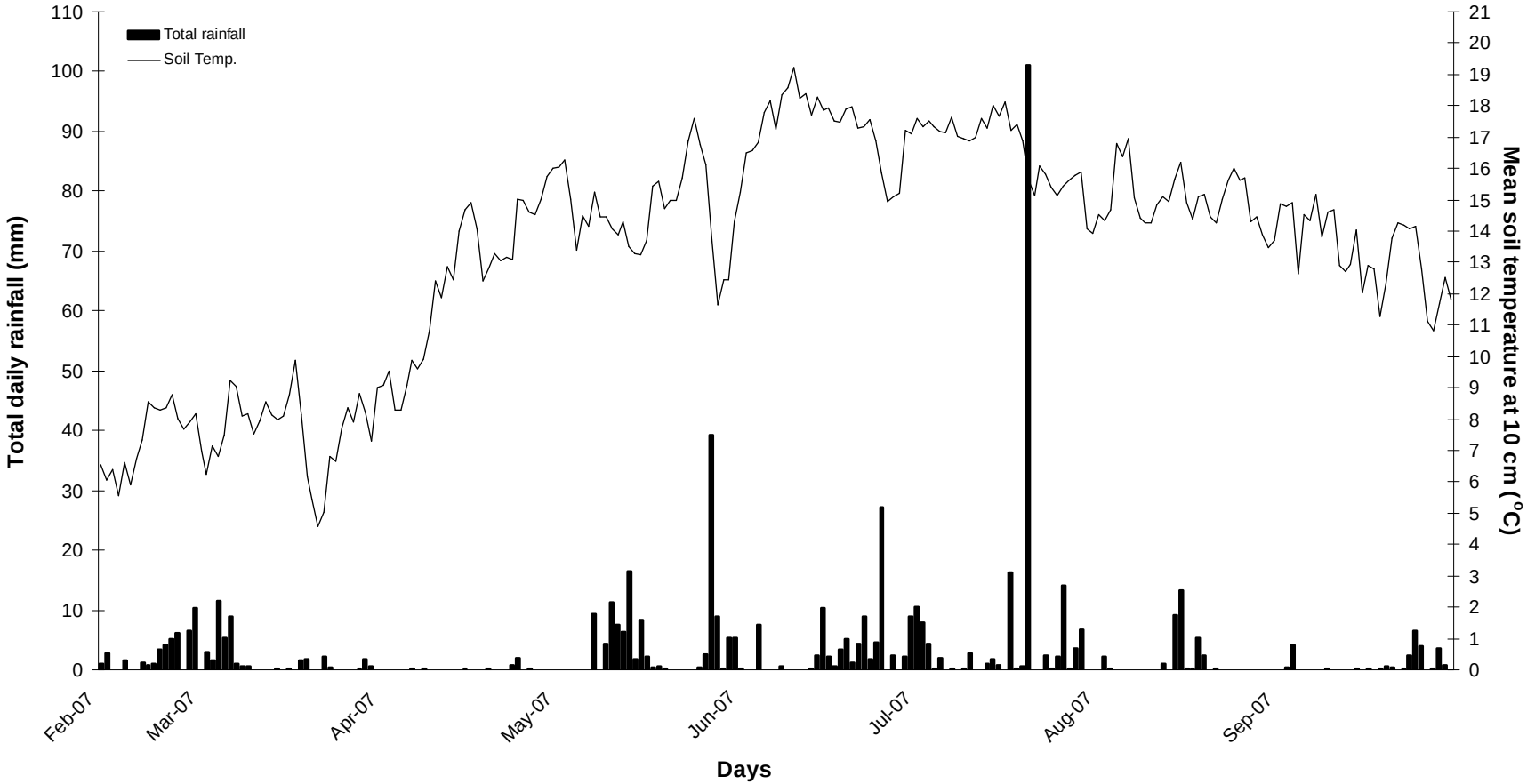

Figure 5.2.1: Total daily rainfall and mean daily soil temperature at 10 cm depth in the reconnected floodplain of the River Cole during the first monitoring season (12th February 2007 – 30th September 2007).

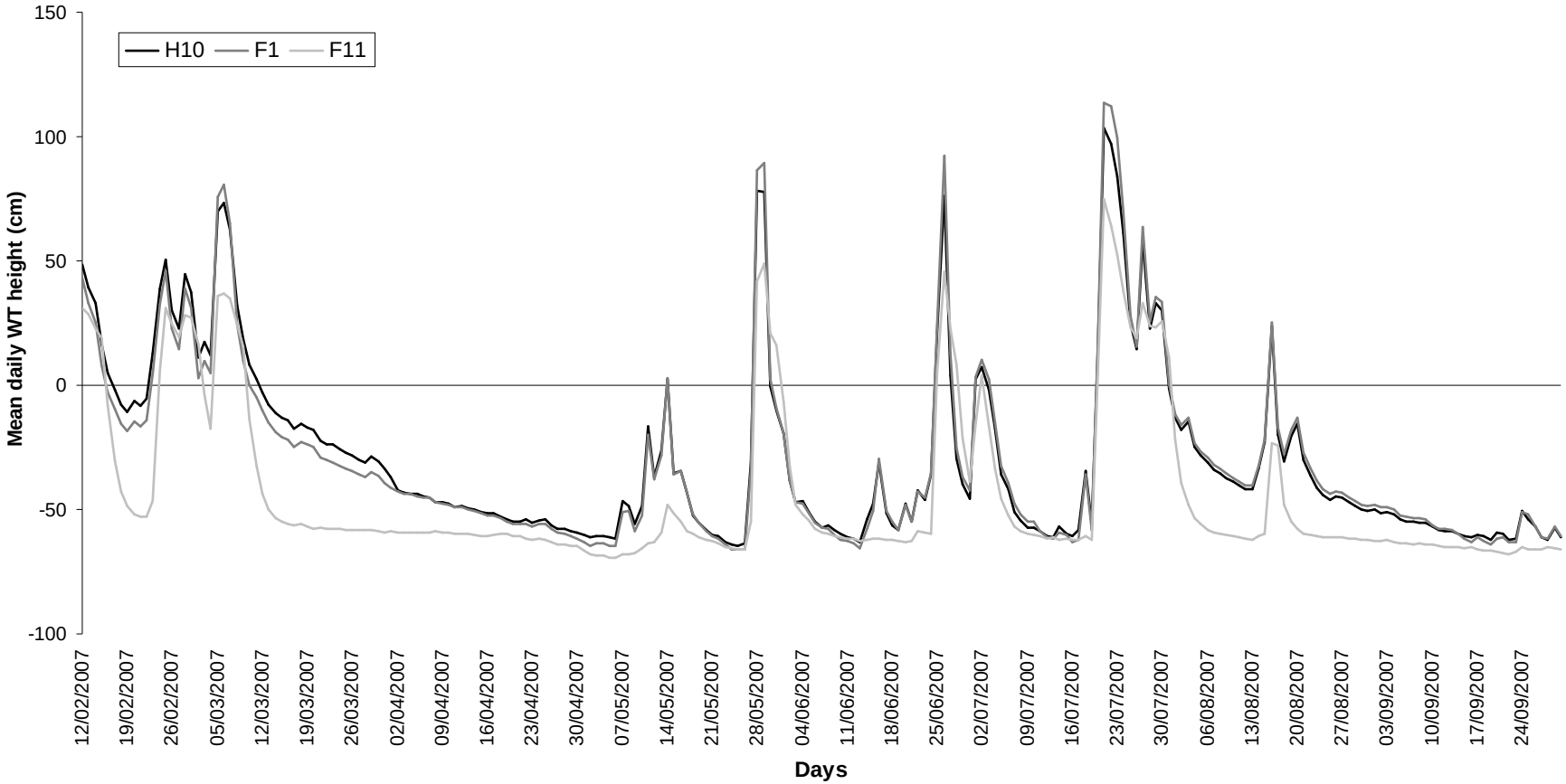

Figure 5.2.2: Mean daily actual water table (WT) height for the BZ site (well H10), the PM riparian area (F1) and the PM channel depression (F11) during the first monitoring season (12th February 2007 – 30th September 2007). The zero line indicates surface saturation.

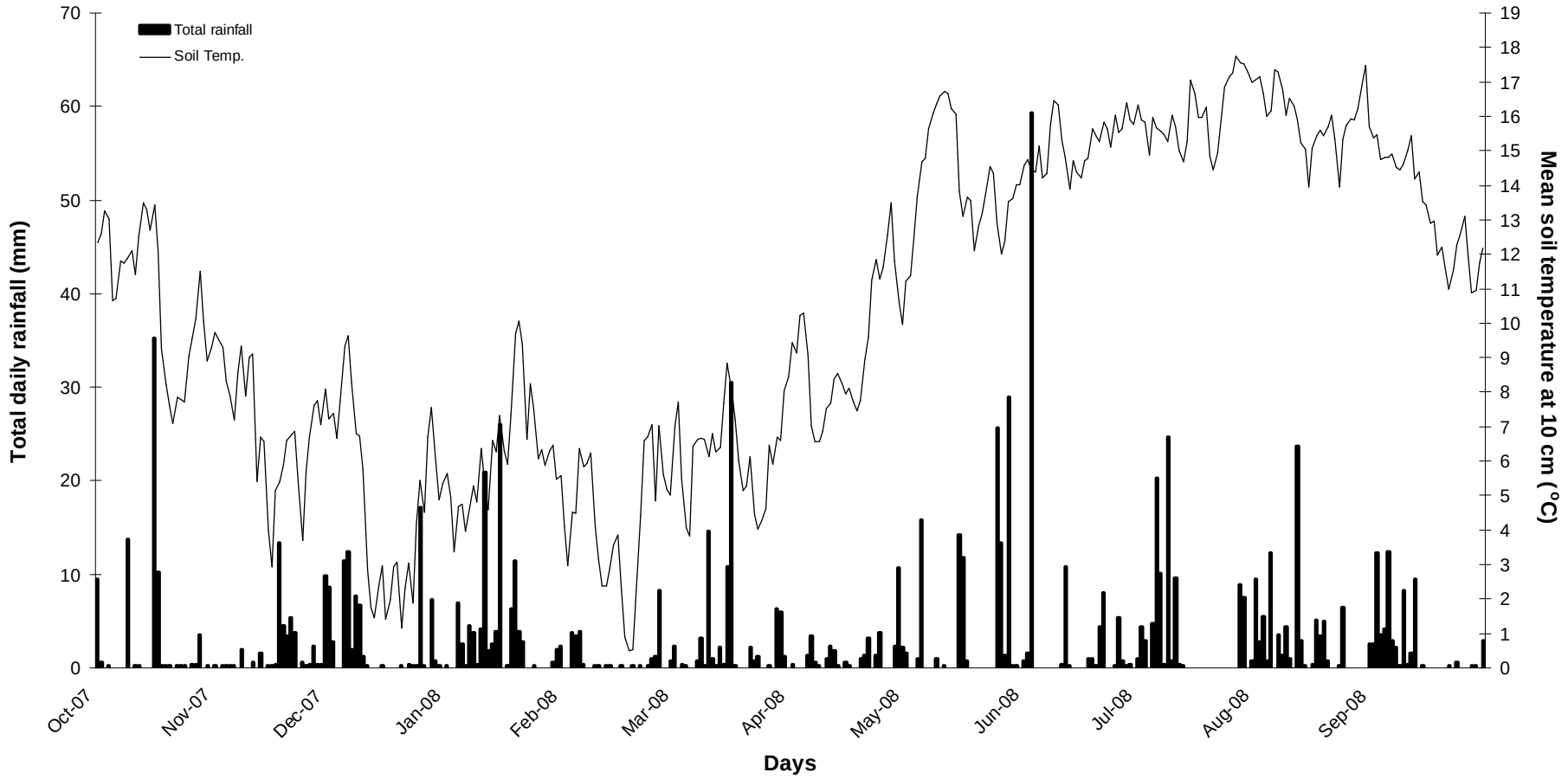

Figure 5.2.3: Total daily rainfall and mean daily soil temperature at 10 cm depth in the reconnected floodplain of the River Cole during the second monitoring season (October 2007 – September 2008).

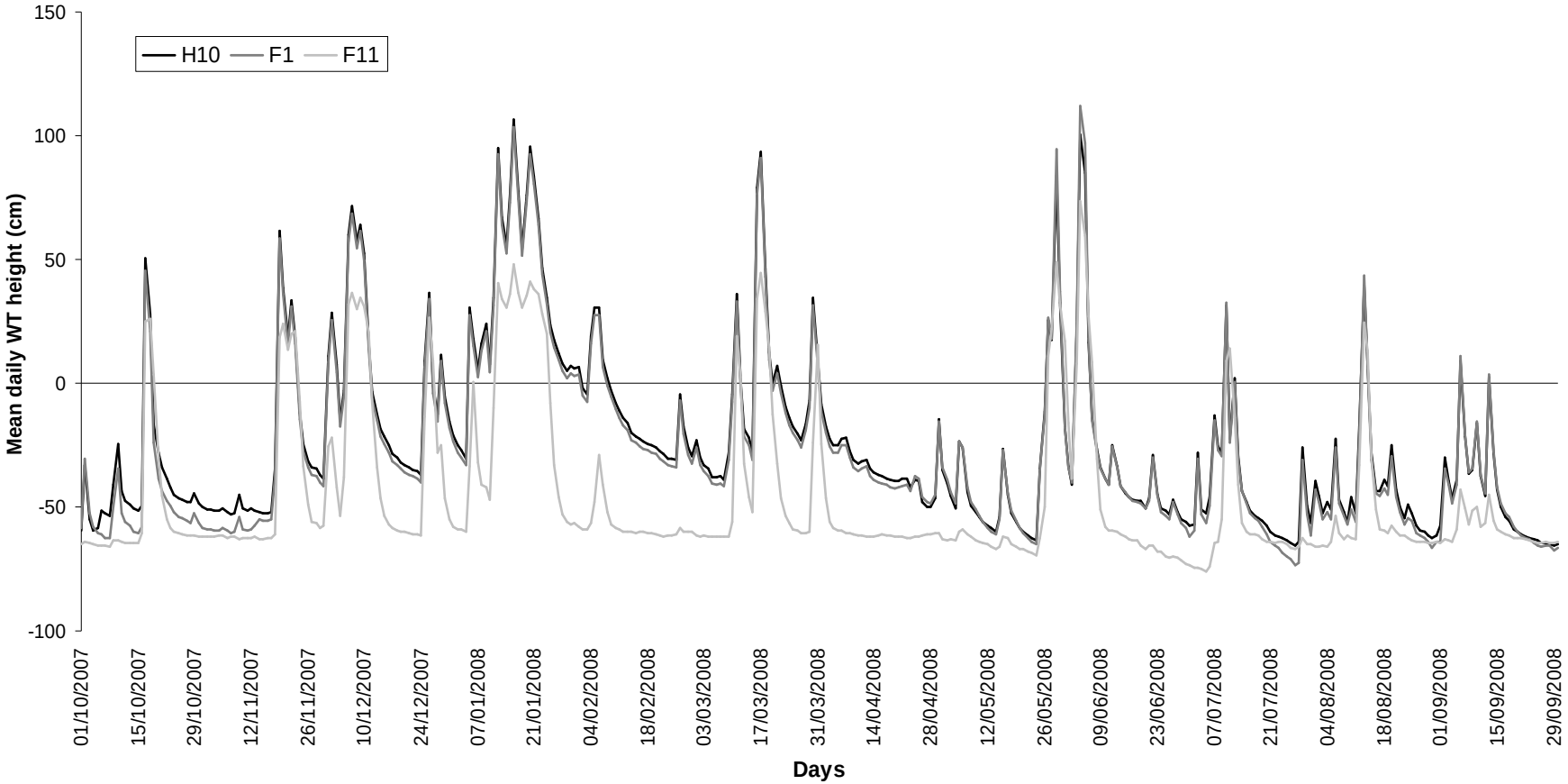

Figure 5.2.4: Mean daily actual water table (WT) height for the BZ site (well H10), the PM riparian area (F1) and the PM channel depression (F11) during the second monitoring season (October 2007 – September 2008). The zero line indicates surface saturation.

5.3 *The hydrological mechanisms of SW - GW interaction in the Pasture Meadow and Buffer Zone areas of the reconnected floodplain of the River Cole*

This section refers to the first research objective, which is to identify the main hydrological mechanisms responsible for the inundation regime in the re-connected floodplain of the River Cole and to assess the relative importance of each mechanism for: (i) the transport of nitrate; and (ii) the creation of the necessary conditions for the occurrence of nitrate attenuation via heterotrophic denitrification and DNRA.

The hydrological mechanisms are presented in order of importance in terms of their contribution to the creation and duration of saturation conditions that would favour nitrate retention processes. Moreover, each mechanism is also assessed with respect to its contribution to the transport of nitrate onto the floodplain, which is a prerequisite for the occurrence of nitrate attenuation. The mechanisms are categorised into three main types: a) overbank flooding; b) saturation excess overland flow; and c) groundwater discharge by lateral subsurface flow. One characteristic event of each type is described in detail for the PM and BZ sites respectively.

5.3.1 *Overbank flooding*

Overbank inundation of the re-connected floodplain was the dominant mechanism of soil saturation of the A/B horizon identified during the monitoring period. Tables 5.3.1 and 5.3.2 summarise the overbank flood events for the PM and BZ sites respectively. Although the same flood event frequency was observed for both monitoring years at both sites, the retention time of the flood waters on the floodplain was significantly longer during the first season compared to the second. This was probably due to higher magnitude, in terms of total rainfall, events during the first year that resulted in longer periods of inundation for both floodplain sites. More flood events were observed during the first winter period in the PM site, while the events were relatively evenly distributed between winter, spring and summer during the second year in the PM and throughout the monitoring period in the BZ, highlighting the effect of the ‘wet’ summers and ‘dry’ autumns on the hydrological regime of the floodplain. Generally, more frequent and longer flood events were observed in the BZ area due to its lower landscape position and closer connection to the river.

Table 5.3.1: Overbank flood events in the PM site during the monitoring period October 2006 - September 2008. N/A indicates non available data.

#	Date	Duration (days)	Total rainfall (mm)	Max rainfall intensity (mm h^{-1})	Soil matric potential (hPa)	Max floodwater volume ($m^3 m^{-2}$)	Nitrate loading (kg N ha^{-1})
1	18/11/06 - 20/11/06	2	N/A	N/A	N/A	0.31	13.5
2	23/11/06 - 02/12/06	9	N/A	N/A	N/A	0.35	33.3
	Autumn 06	**11**				**0.66**	**46.8**
3	02/12/06 - 09/12/06	7	N/A	N/A	N/A	0.24	17.0
4	11/12/06 - 13/12/06	2	N/A	N/A	N/A	0.09	6.4
5	30/12/06 - 05/01/07	6	N/A	N/A	N/A	0.37	27.3
6	06/01/07 - 14/01/07	8	N/A	N/A	N/A	0.41	20.8
7	17/01/07 - 23/01/07	6	N/A	N/A	N/A	0.42	28.8
8	10/02/07 - 15/02/07	5	N/A	N/A	N/A	0.16	10.6
9	24/02/07 - 02/03/07	6	38.4	3.9	N/A	0.13	8.5
	Winter 07	**40**				**1.82**	**119.4**
10	05/03/07 - 09/03/07	5	32.3	1.8	N/A	0.40	29.5
11	28/05/07 - 31/05/07	4	61.5	5.7	N/A	0.48	24.2
	Spring 07	**9**				**0.88**	**53.7**
12	25/06/07 - 28/06/07	4	34.1	7.7	N/A	0.42	14.1
13	20/07/07 - 31/07/07	11	101.1	17	N/A	0.54	21.6
	Summer 07	**15**				**0.96**	**35.7**
	Totals Season 1	**75**				**4.32**	**255.6**
14	17/10/07 - 19/10/07	3	45.5	8.3	N/A	0.20	8.4
15	19/11/07 - 21/11/07	3	21.5	3	N/A	0.20	9.1
16	22/11/07 - 23/11/07	2	8.9	3.3	8.8	0.11	5.9
	Autumn 07	**8**				**0.51**	**23.4**
17	06/12/07 - 11/12/07	6	41.6	3.3	-8.8	0.25	13.4
18	25/12/07 - 27/12/07	2	17.5	5.1	-27.7	0.13	7.6
19	11/01/08 - 24/01/08	13	83.9	8.3	5.1	0.49	28.7
	Winter 08	**21**				**0.87**	**49.7**
20	11/03/08 - 12/03/08	1	15.8	3.9	-7.1	0.10	6.2
21	16/03/08 - 19/03/08	4	41.6	4.7	-15.5	0.50	30.9
22	27/05/08 - 31/05/08	5	69.7	8.9	-338	0.41	26
	Spring 08	**10**				**1.01**	**63.1**
23	03/06/08 - 07/06/08	5	60.9	6.9	-16.5	0.53	33.7
24	10/07/08 - 11/07/08	2	78.8	6.3	-1008	0.10	3.0
25	13/08/08 - 14/08/08	2	26.8	4.7	-74.2	0.14	4.0
	Summer 08	**9**				**0.77**	**40.7**
	Totals Season 2	**48**				**3.16**	**176.9**

Table 5.3.2: Overbank flood events in the BZ site during the monitoring period October 2006 - September 2008. N/A indicates non available data.

#	Date	Duration (days)	Total rainfall (mm)	Max rainfall intensity (mm h^{-1})	Soil matric potential (hPa)	Max floodwater volume ($m^3 m^{-2}$)	Nitrate loading (kg N ha^{-1})
1	17/11/06 - 30/11/06	13	N/A	N/A	N/A	0.53	22.9
	Autumn 06	**13**				**0.53**	**22.9**
2	01/12/06 - 13/12/06	13	N/A	N/A	N/A	0.39	34.3
3	30/12/06 - 31/12/06	2	N/A	N/A	N/A	0.27	19.1
4	01/01/07 - 24/01/07	24	N/A	N/A	N/A	0.55	40.4
5	10/02/07 - 16/02/07	7	N/A	N/A	N/A	0.28	18.6
6	23/02/07 - 02/03/07	8	38.4	3.9	N/A	0.27	15.7
	Winter 07	**54**				**1.76**	**128.1**
7	03/03/07 - 11/03/07	9	29.6	1.8	N/A	0.52	40.8
8	13/05/07 - 14/05/07	1	56.9	5.7	N/A	0.12	6.1
9	27/05/07 - 31/05/07	5	61.9	5.7	N/A	0.62	31.3
	Spring 07	**15**				**1.26**	**78.2**
10	25/06/07 - 28/06/07	4	34.1	7.7	N/A	0.54	18.1
11	01/07/07 - 03/07/07	3	33.7	3.7	N/A	0.12	3.7
12	20/07/07 - 31/07/07	11	101.1	17	N/A	0.77	30.9
13	16/08/07 - 17/08/07	2	22.7	3.9	N/A	0.16	7.3
	Summer 07	**20**				**1.59**	**60**
	Totals Season 1	**102**				**5.14**	**289.2**
14	17/10/07 - 19/10/07	3	45.5	8.3	N/A	0.42	17.7
15	19/11/07 - 24/11/07	6	30.9	3.3	N/A	0.41	18.9
	Autumn 07	**9**				**0.83**	**36.6**
16	01/12/07 - 12/12/07	12	53.8	3.3	-22.6	0.50	26.7
17	25/12/07 - 27/12/07	2	17.5	5.1	-27.7	0.29	15.5
18	05/01/08 - 31/01/08	26	107.4	8.3	-20.6	0.79	46.3
19	04/02/08 - 08/02/08	5	11.4	2.2	-6.4	0.17	12.5
	Winter 08	**45**				**1.75**	**101**
20	10/03/08 - 12/03/08	3	19.1	3.9	-42.5	0.24	14.8
21	16/03/08 - 23/03/08	8	45.7	4.7	-15.9	0.80	49.4
22	30/03/08 - 31/03/08	2	13.4	2	-22.6	0.20	12.3
23	26/05/08 - 31/05/08	5	69.7	8.9	-338	0.54	34.3
	Spring 08	**18**				**1.78**	**110.8**
24	03/06/08 - 07/06/08	4	60.9	6.9	-16.5	0.68	43.2
25	09/07/08 - 12/07/08	4	78.8	6.3	-1008	0.18	5.5
26	12/08/08 - 14/08/08	3	26.8	4.7	-74.2	0.28	7.9
	Summer 08	**11**				**1.14**	**56.6**
	Totals Season 2	**83**				**5.50**	**305**

Overall, during the first monitoring year, the PM site was flooded for 75 days, while the total nitrate loading onto the floodplain was 255.6 kg N ha^{-1}. The decrease in the flood retention time observed in the second monitoring year was accompanied by a decrease in the total flood days (48) and nitrate loading (177 kg N ha^{-1}) on PM. The flood water volume correlated positively with the duration of the event (Spearman; r=0.61, P<0.01), indicating that longer flood events resulted in larger volumes of flood storage on the floodplain, while positive correlation was also found with the total rainfall volume (Spearman; r=0.60, P<0.05), showing that higher magnitude rainfall events were associated with larger flood water storage. The nitrate loading correlated positively with the duration of the flood event (Spearman; 0.68, P<0.01), showing that high nitrate loadings were associated with longer inundation periods.

The BZ area, due to its proximity to the river and the higher inundation frequency, was flooded for longer (102 days) and subsequently higher nitrate loading (289.2 kg N ha^{-1}) was observed during the first monitoring year, compared to the PM area. Although the flood retention time decreased during the second year (83 days), the total volume of stored flood water and the nitrate loading increased slightly, indicating that even lower magnitude events can cause considerable floodwater storage and nitrate loading to the BZ site. The correlation analysis indicated positive relationships between the flood water volume and the event duration (Spearman; r=0.67, P<0.01) as well as with the total rainfall (Spearman; r=0.54, P<0.05) and the rainfall intensity (Spearman; r=0.48, P<0.05). The nitrate loading correlated positively with the event duration (Spearman; r=0.73, P<0.01) and the total rainfall (Spearman; r=0.44, P<0.05).

The sequence of events and interactions between the falling precipitation, the raising river stage, the antecedent moisture conditions and subsequently the raising groundwater table across the floodplain areas are described for a characteristic overbank flood event for each area. In this way, the differences in the hydrological connectivity between the two studied areas can be demonstrated, while different sources of floodwater, and subsequently nitrate, to the floodplain are identified. Moreover, the factors that lead to surface saturation conditions are identified and evaluated in terms of their importance, while the spatial distribution of surface saturation can also indicate areas where nitrate attenuation may be more effective.

5.3.1.1 *PM area in March 2007 (05/03/07 - 09/03/07)*

The event of 5th March 2007 followed a previous overbank event in late February that peaked on the 28th of the month. Therefore, the ground was near saturation and the water table, as well as, the river stage was receding at the beginning of the event. The event was divided in three main components; A, B and C (Table 5.3.3). Hourly changes in perched water table (PWT) height in the monitoring wells of the transect F1-F7 of the PM site as well as the total hourly rainfall and river stage height for the three components of the event are shown in Figure 5.3.1.

Table 5.3.3: March 2007 rainfall and river stage data

Component	Date	Time (began)	Time (end)	Duration (mins)	Total Rain (mm)	Max. Hourly Intensity (mm/hr)	River stage response (mins)	River stage change (cm)
A	02/03/07	17:00	20:30	210	2.8	0.8	330	18.7
B	04/03/07	09:00	23:00	840	11.4	1.8	360	95.6
C	05-06/03/07	21:00	04:00	420	11	1.8	480	41

The most substantial component of the rainfall event was B, which occurred on 4th March. The response from the river stage occurred during the event, and there was a steep increase by almost 95.6 cm. The groundwater beneath the channel depression showed an almost immediate response to the falling precipitation (wells F11 and F7), possibly because of higher hydraulic conductivities in the near surface layers due to high soil moisture content. The groundwater response followed in the rest of the wells almost simultaneously with the river stage (wells F2 and F5 on Fig. 5.3.1). The maximum hydraulic gradient between the river stage and the PWT in F2 during the rising limb of event B was 0.4%. Using the maximum K_h for the B horizon of the PM (0.17 m d^{-1}) and an average porosity of 0.60, the potential seepage velocity V can be calculated from Darcy's law with equation (5.1) according to Schilling *et al.* (2006):

$$V = K_h \cdot (dh / dl) / n \qquad (5.1)$$

where dh/dl the dimensionless hydraulic gradient and n the porosity. The seepage velocity was estimated at 1.4 x 10^{-6} cm s^{-1}, and therefore could not explain the rise in PWT through Darcian flow bank seepage. However, the almost simultaneous rise of the PWT in the wells F2, F3 and F5 by the same amount as the river stage could be due to the development of a reversed groundwater ridge (Jung *et al.*, 2004) pushing as

translatory flow ‘old’ floodplain water ahead across the floodplain. The river stage (F1) - PWT height hysteresis plots for the wells F2, F5, F7 and F11 during the March ’07 event sequence are shown in Figure 5.3.2. For F2 and F5 the shape of the hysteresis curve roughly follows and includes the x = y line indicating that the PWT is influenced by the river stage change. However, during the rising limb the recharge rate of the PWT seems to be higher than the river stage, possibly as a consequence of infiltrating precipitation on top of the reversed groundwater ridge, while the recession limb indicates a slower groundwater discharge rate. The shape of the hysteresis curves, in terms of how open or closed they are approximates the temporary floodwater storage, or bank storage in the case of the river water, which is higher in the channel depression well (F5) compared to the well F2, where steeper gradients towards the river and the underlying gravel lens may be responsible for faster discharge.

The hysteresis curves for the wells F7 and F11 are very different from the x = y line indicating that the river stage has no direct influence on the PWT. In the case of F7, the PWT is rising possibly as a result of seepage from the ditch receiving hillslope runoff, while F11 rises possibly from percolating precipitation, without a concurrent increase in the river stage. When surface saturation is reached, overland flow is directed towards F5 (southward), from both F7 and F11, and no further PWT height build up is observed, while the river stage is still rising. Finally, the recession limb is very different, as the wells F7 and F11 discharge to the ditch and not the river.

The correlation coefficients between the river stage (F1) and the PWT height during the March 2007 event are shown in Table 5.3.4. All the wells were highly correlated with each other (Pearson’s $r > 0.9$, $P<0.01$), possibly as an effect of the overland flow extending across the floodplain surface (discussed later). However, stronger correlations with the river stage were found for the wells F2 and F3, indicating that the reversed groundwater ridge is more likely to extend 80 m across the floodplain subsurface perpendicular to the river. The correlation strength with the river stage diminished with the distance from the river suggesting that the influence of the ditch water becomes increasingly more important at the north and north-east side of the floodplain.

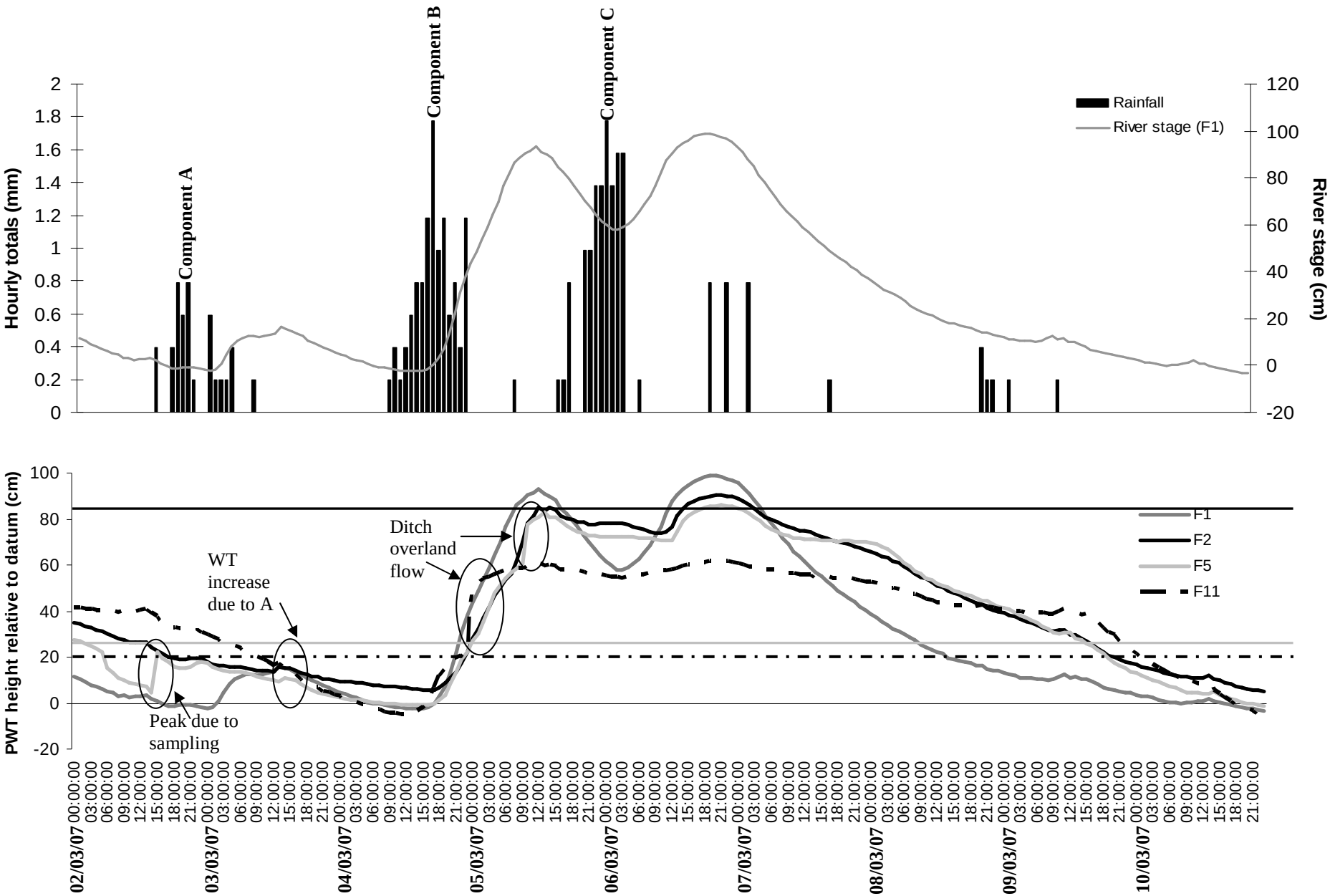

Figure 5.3.1: The hourly PWT level in the monitoring wells F2, F5 and F11 of the PM site and the hourly total rainfall and river stage (F1) for the three components of the March 2007 event. The zero line indicates the datum (F1), while the parallel to the datum lines indicate surface saturation for the wells with same colour coding.

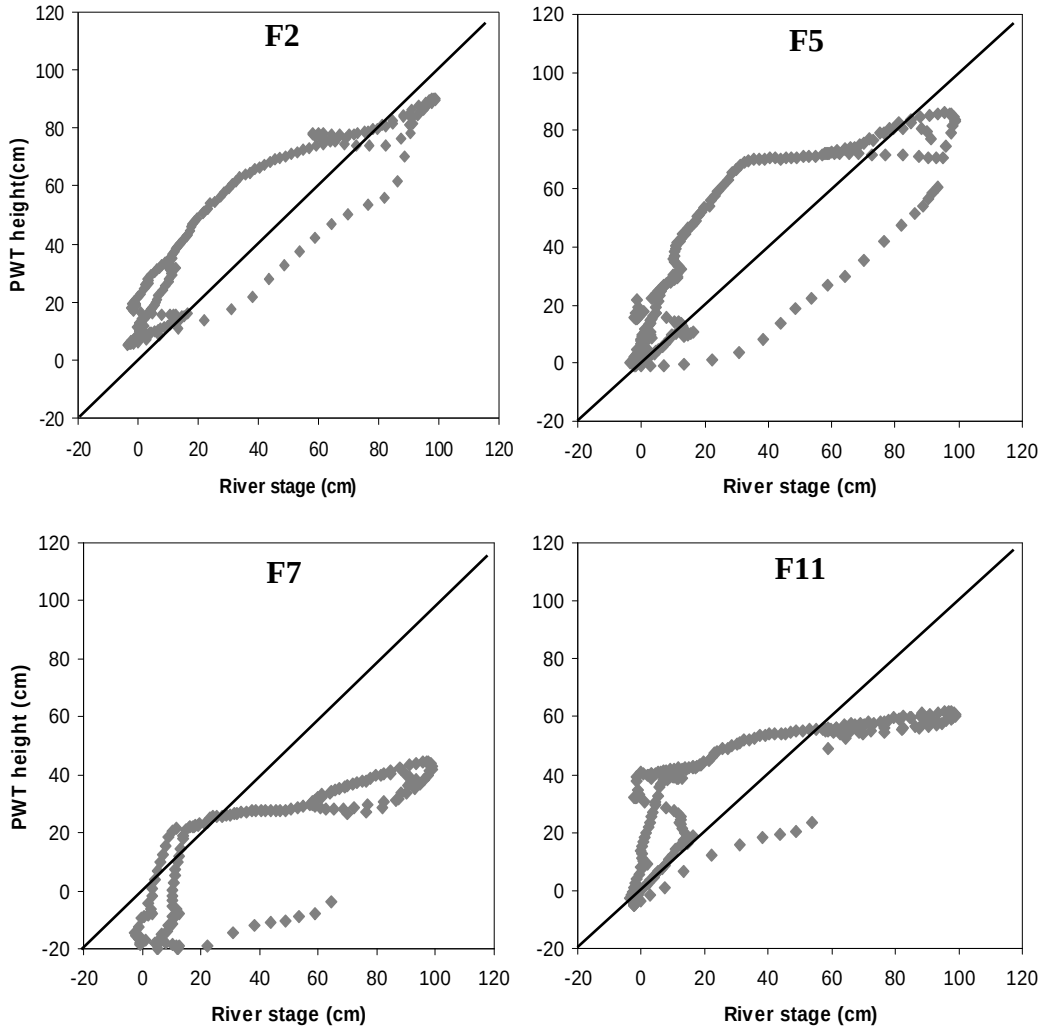

Figure 5.3.2: River stage (F1) - PWT height hysteresis plots for the wells F2, F5, F7 and F11 of the PM area during the event of March 2007. The PWT heights are relative to the datum, which is the well F1 (i.e. river stage). The diagonal lines give the relationship y = x (PWT identical to river stage).

Table 5.3.4: Correlation matrix between the river stage height (well F1) and the PWT height in the wells of the PM site during the March 2007 event. Numbers are Pearson's r significant at 0.01 probability level.

	River stage	F2	F3	F5	F7	F11
River Stage	1					
F2	**0.92**	1				
F3	**0.91**	0.99	1			
F5	**0.87**	0.98	0.98	1		
F7	**0.86**	0.97	0.98	0.96	1	
F11	**0.78**	0.91	0.93	0.91	0.93	1

Overbank flooding from the overflowing ditch to the channel depression was first observed at the end of component B. This is shown in the hydrograph of Figure 5.3.1, where at 23:00 hours on 4th March there was a sudden vertical increase in the F11 level. A similar vertical increase of the groundwater level was noted one hour later for well F7, indicating overbank flooding from the north side of the ditch. Overland water flow moved across the PM floodplain in the directions shown in Figure 5.3.3. A delay was observed between the first flood peak recorded in well F1 and the peak in the river discharge measured 4 km downstream at the Inglesham monitoring station, which was approximately 8 hours later (Figure 5.3.4), indicating that flooding in the rural catchment of the River Cole, between Coleshill and Inglesham, probably resulted in delaying and reducing the magnitude of the downstream flood peak. The flood waters slowly started to recede after the first flood peak but most of the floodplain remained inundated until component C of the event occurred.

The recession of the March 2007 flood event followed the surface gradient. The hydraulic gradient first reversed between F2 and F1 and flood waters flowed quickly towards the river. The PWT level dropped below ground surface sequentially first in F2, then in F3 and then in F7, which drained towards the north side of the ditch, while the flood waters receded last from the channel depression, first from F5, after 67 hours, and lastly from the F11, after 76 hours. Therefore the direction of the receding flood waters was exactly opposite from the overland flow direction, following generally the surface elevation gradient.

To summarise, during overbank flooding of the PM, the rise of the river stage creates a reversed groundwater ridge with direction from the river to approximately the middle of the floodplain, contributing to floodwater storage and the rise of the water table. At the same time, infiltrating precipitation and seepage from the ditch further contribute to the water table rise in the north side of the floodplain. When bankfull capacity is exceeded, the river floods the riparian area, while the east and north breaches of the ditch supply further the floodplain with river and hillslope runoff water. Therefore, two sources of floodwater and nitrate supply are identified in the PM. At the receding phase of the flood, floodwaters follow the surface gradient back to the river and ditch, while saturation conditions are maintained for longer in the riparian and channel depression zones, creating favourable conditions for nitrate attenuation.

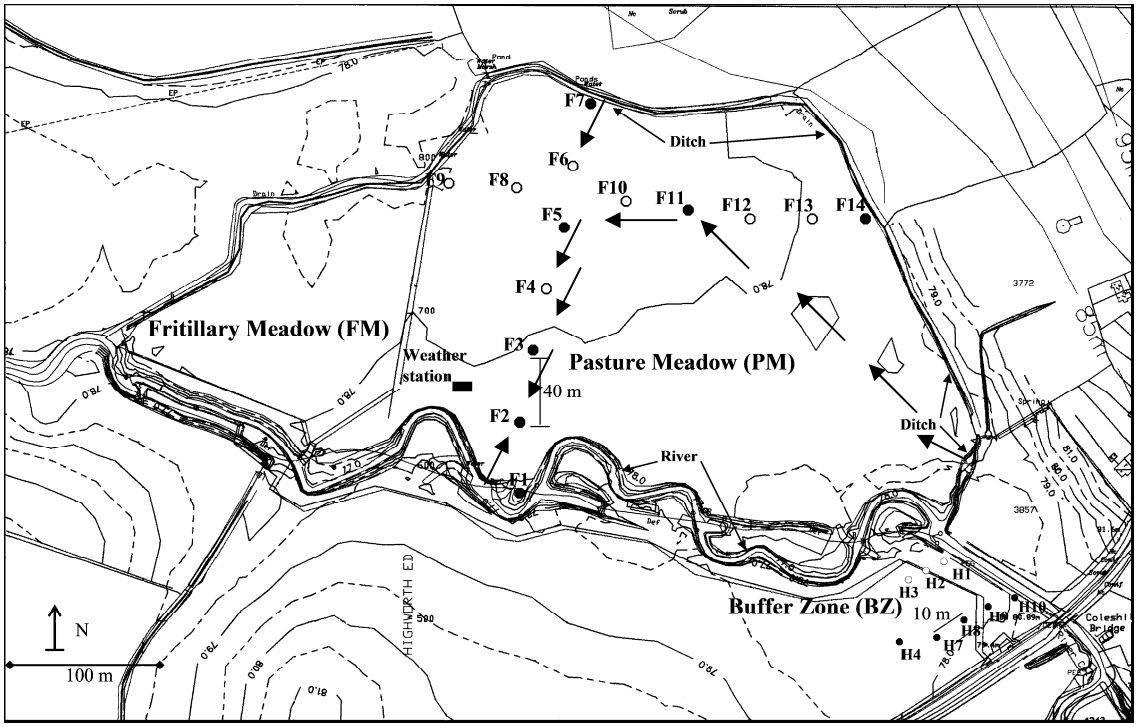

Figure 5.3.3: Overland water flow direction, indicated by large arrows, during the March 2007 event on the PM floodplain area.

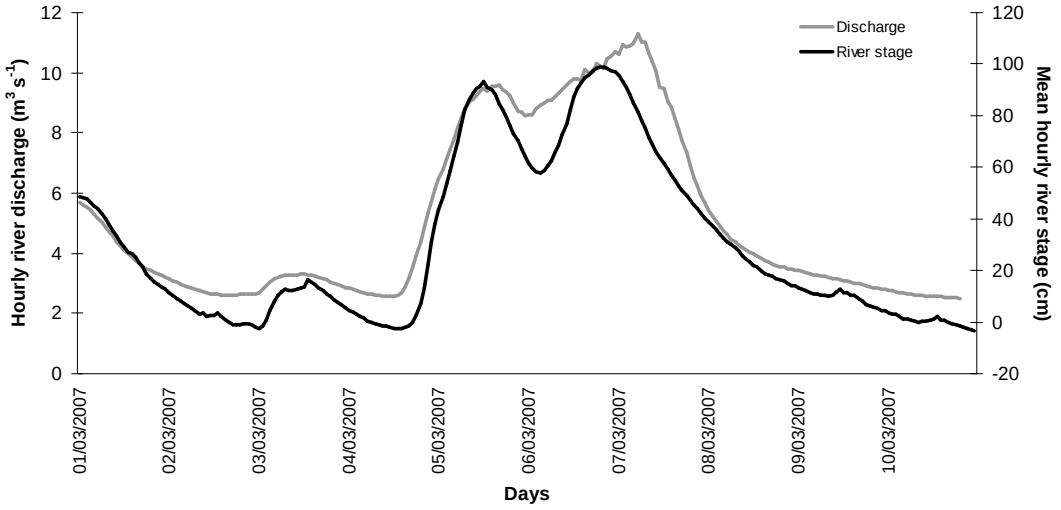

Figure 5.3.4: The hourly river discharge at Inglesham monitoring station and the mean hourly river stage (well F1 next to the river bank) in the PM site during the March 2007 event.

5.3.1.2 *BZ area in May 2007 (13/05/07 - 14/05/07)*

In order to describe the sequence of events during overbank flooding of the BZ site, a flood event with lower antecedent moisture conditions was selected. This is because the BZ site, due to its proximity to the river, its elevation and its small surface area, is rapidly flooded during a high magnitude event, especially when high antecedent soil moisture conditions are present, and therefore there is not adequate time for studying the PWT wetting up pattern during such an event.

The first week of May 2007 was characterised by dry weather continuing from April 2007, and the river stage was around -65 cm from its bankfull height (Figure 5.3.5). The first rain (> 1 mm) fell on 7th May (Component A), 46 days after the last rainfall (Table 5.3.5). The water table started to rise in all the wells of the transect H10-H4 during component A (Figure 5.3.5). The well H9 displayed a more pronounced response corresponding to the increase of the river stage, whereas the response of the other wells was more subdued, possibly due to groundwater recharge from infiltrating precipitation. As a result of component A, the hydraulic gradient between H10 and H9 changed from almost 0 at the start of the event to 4 % from H10 to H9. Using the maximum K_h for the B horizon of the BZ (0.83 m d^{-1}) and an average porosity of 0.55, the potential Darcian seepage velocity V according to equation (5.1) was 7 x 10^{-3} cm s^{-1}, three orders of magnitude higher than the seepage velocity estimated between F1 and F2 in PM. By multiplying V with the time period of the hydraulic gradient reversal (8h), the distance the stream water has potentially travelled through the B horizon from H10 to H9 was calculated at 2 m (Schilling *et al.*, 2006). Although the distance between H10 and H9 is 10 m, the theoretical calculation of Darcian seepage velocity seemed to support the possibility of seepage between the wells indicated by the hydrograph (Fig. 5.3.5), as the porosity could be higher near the stream margin and also preferential flow through macropores and animal burrows were not taken into account.

Table 5.3.5: May 2007 rainfall and river stage data

Component	Date	Time (began)	Time (end)	Duration (mins)	Total Rain (mm)	Max. Hourly Intensity (mm/hr)	River stage response (mins)	River stage change (cm)
A	07/05/07	04:30	09:30	300	9.1	2.8	330	50.4
B	10/05/07	18:30	23:30	300	7.9	1.8	360	56.3
C	13/05/07	11:00	15:30	270	15.8	5.7	270	70.2
D	15/05/07	17:00	18:30	90	4.5	3.5	90	19.1

The potential for the development of a reversed groundwater ridge at the BZ site was investigated with hysteresis plots between the PWT height in well H10 (reflecting the local river stage) and the rest of the BZ wells (Figure 5.3.6). Although the hysteresis plots for all the wells display a scatter along the y = x line, suggesting some dependence on the river stage, the picture is complicated by the multiple small peaks during the event. In all cases, when overbank inundation reaches a well, the hysteresis plot closely approximates the y = x line, thus indicating control of the PWT by the overlying water rather than a reverse groundwater ridge. Therefore the reverse groundwater ridge must be important only at the initial flood stage, before bankfull capacity is exceeded.

During the initial flood phase only the well H9 shows close correspondence with the river stage, suggesting that a reverse groundwater ridge is contributing to bank storage in H9 (i.e. 10 m inland from the stream bank). Regarding the wells in the middle and field edge of the BZ, the extent of a reversed groundwater ridge is inconclusive, but as suggested also by the rounded hydrographs, groundwater recharge by infiltrating precipitation is likely to be equally important for these wells. High correlation coefficients were found between the local river stage (H10) and the PWT height in all the wells of the BZ during the May 2007 event (Table 5.3.6). The high correlation is mostly due to the effect of overbank flooding that 'equals' the PWT across the site during the flood peak.

During component B of the May event, no seepage was observed between H10 and H9, as the hydraulic gradient was not reversed, but the water table rose quickly and the river broke its bank supplying overland flow to H9. Interestingly, well H7 displayed a similar rapid level increase. This could possibly be due to preferential flow along the well casing due to cracks on the bentonite seal because of the antecedent dry conditions. The hydrograph for H8 indicated groundwater recharge from infiltrating precipitation.

Table 5.3.6: Correlation matrix between the local river stage height (well H10) and the PWT height in the wells of the BZ site during the May 2007 event. Numbers are Pearson's r significant at 0.01 probability level.

	H10	**H9**	**H8**	**H7**	**H4**
H10	**1**				
H9	**0.97**	1			
H8	**0.91**	0.96	1		
H7	**0.93**	0.96	0.99	1	
H4	**0.93**	0.97	0.99	0.99	1

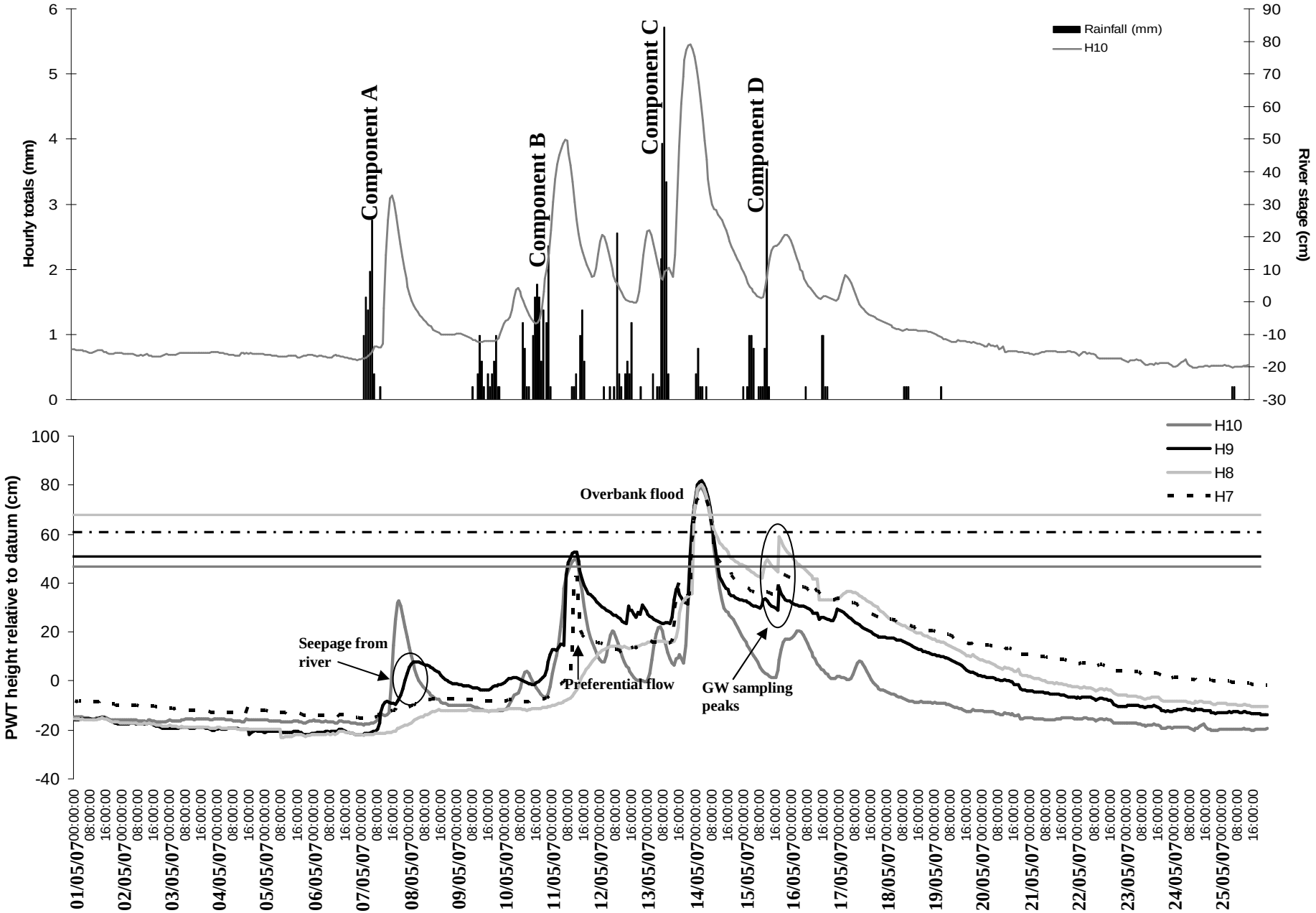

Figure 5.3.5: The hourly PWT level in the monitoring wells H10, H9, H8 and H7 of the BZ site and the total rainfall and river stage (H10) for the four components of the May 2007 event. Parallel lines on the horizontal axis indicate surface saturation for the wells with same colour coding.

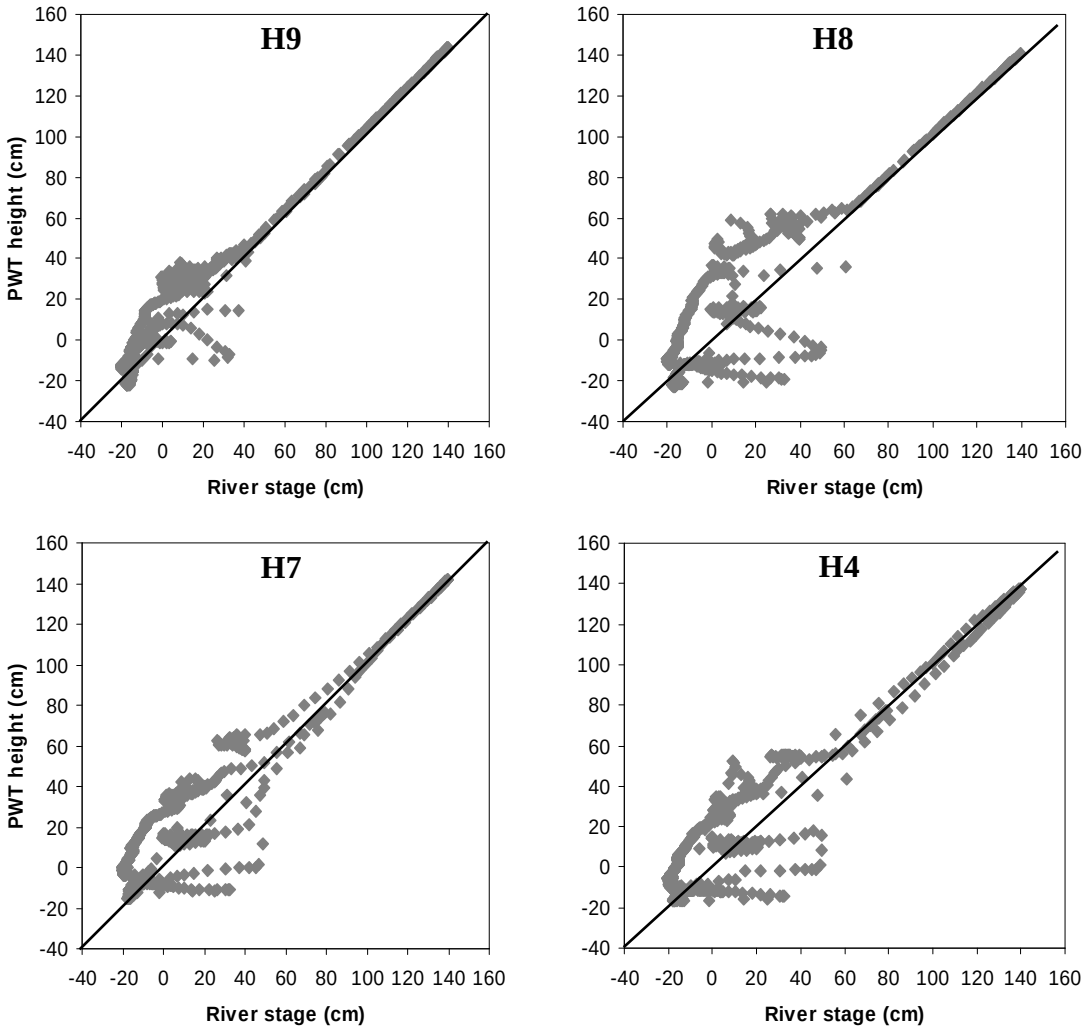

Figure 5.3.6: River stage (H10) - PWT height hysteresis plots for the wells H9, H8, H7 and H4 of the BZ area during the event of May 2007. The PWT heights are relative to the datum, which is the well F1 in PM. The diagonal lines give the relationship y = x (PWT identical to river stage).

Finally, component C of the event caused the water table to respond rapidly in all the wells due to increased infiltration rate. After the end of component C, the BZ site was completely inundated. The maximum floodwater volume stored on BZ was 0.12 m^3 m^{-2}, while the nitrate loading for this event was 6.1 kg N ha^{-1}. Therefore, a bankfull event after prolonged dry weather for the rest of the River Cole floodplain had caused an overbank flood at the BZ site, indicating the very responsive character of the site and its proneness to frequent flooding even during moderate rainfall events. The single floodwater and nitrate loading source is the river, while the reversed groundwater ridge mechanism is restricted to the near-bank margin area, as overbank inundation rapidly

spreads across the site. The drainage of the site follows the surface elevation gradient from the arable field edge (H7) towards the river (H10).

5.3.2 *Saturation excess overland flow*

In some cases, prior to an overbank flood event, saturation excess overland flow (SEOF) was observed to occur mainly in the channel depression and the middle field area of the PM and between the field edge and the river margin in the BZ. The dates on which SEOF was recorded, as well as the storm characteristics and the contribution of SEOF to the total volume of surface runoff per area are presented in Table 5.3.7. During the first season, SEOF was recorded at the beginning of the June and July 2007 storms in the BZ and only in July 2007 in the PM. Both events were characterised by high magnitude and intensity rainfall under high antecedent soil moisture conditions. The produced runoff, for the BZ, contributed only 12 % of the total floodwater volume stored on the floodplain for both events, while for the PM it was 20 % of the stored floodwater volume. Furthermore, during the second monitoring year, one SEOF case per season was recorded at the BZ site and the total runoff contribution was 6 % of the stored floodwater volume for the whole year. SEOF was only observed in the first and the last storm of the year for the PM contributing 7 % runoff volume to the yearly total floodwater volume. Therefore, it could be argued that the contribution of SEOF to the creation of surface saturation conditions, favouring nitrate attenuation processes, is minimal compared to the overbank flooding effect. Moreover, since the main source of water during SEOF generation is the falling precipitation, inherently low in nitrate concentration, the contribution of this mechanism to the nitrate loading on the floodplain is insignificant.

The possibility of infiltration excess overland flow (IEOF) was also examined, when soil matric potential data where available, especially when low antecedent soil moisture conditions where followed by summer storms. However, in all cases surface saturation had been reached when overland flow was occurring, and therefore IEOF occurrence was ruled out. The sequence of events during SEOF formation is described below for both the PM and BZ areas for the July 2007 summer storm.

Table 5.3.7: Saturation excess overland flow events in the BZ and PM sites during the monitoring period October 2006 - September 2008. N/A indicates non availability if data. [a] Soil matric potential data corrected for the maximum surface elevation of the transect H10-H4 in BZ.

#	Date	Duration (hours)	Total rainfall (mm)	Max rainfall intensity (mm h^{-1})	Soil matric potential (hPa)	Max runoff volume BZ (m^3m^{-2})	Max runoff volume PM (m^3m^{-2})
1	25/06/2007	7	30.9	7.7	N/A	0.06	0
2	20/07/2007	4	51.4	17	N/A	0.10	0.19
	Totals Season 1	**11**				**0.16**	**0.19**
3	17/10/2007	5	45.5	8.3	N/A	0.08	0.10
4	25/12/2007	5	17.5	5.1	33.8[a]	0.08	0
5	15/03/2008	9	41.6	4.7	31.1[a]	0.07	0
6	03/06/2008	8	60.9	6.9	44.2[a]	0.10	0.11
	Totals Season 2	**27**				**0.33**	**0.21**

5.3.2.1 *Summer flood in July 2007 (20/07/07 - 31/07/07)*

The beginning of July 2007 was characterised by the receding river stage and PWT. The water table was approaching the C horizon in the wells F1 and F2, while it was within the B clay horizon and closer to the ground surface for the wells F5, F11 and F7. On 20th July the main component (B) of the summer flood event occurred (Table 5.3.8 and Figure 5.3.7). This was the most extreme rainfall event in the two monitoring seasons, giving 101.5 mm of total rainfall volume in 16 hours with maximum intensity 16.9 mm h^{-1}. As a consequence of this high magnitude and intensity event the river stage increased by 174.5 cm. Within four hours from the start of component B, the water table started to rise almost simultaneously in wells F5 and F11. Twelve hours from the start, the wells F11, F7, F5 and F3 recorded surface saturation in the channel depression and the middle field of PM, while the river stage (F1) was 15 cm below its bankfull level. Although the river was already feeding the ditch (bed elevation; 54 cm below F1), there was no indication of ditch overflow as the channel depression hydrographs did not show vertical level increase, and therefore the surface saturation was attributed to saturation excess overland flow (SEOF). Four hours later, while the rainfall continued, and with 0.19 m^3 m^{-2} contributed from surface runoff, the river and ditch overflowed onto the floodplain. The maximum floodwater volume stored at the peak of the event was 0.54 m^{3}m^{-2}, while the nitrate loading was 21.6 kg N ha^{-1}.

The groundwater response of the BZ site was similar to the PM, although the hydrograph of the transect H10-H4 (Figure 5.3.8) was more homogeneous, due to the combined effects of the magnitude of the event, the smaller size of the site and its proximity to the river. The water table started to rise simultaneously across the site, from the arable field to the river bank, as a response to the precipitation from component A of the event. However, no overbank flooding or saturation excess overland flow was recorded at this stage. The water table retained some of its gain before the onset of the major component B of the event. For 14 hours the water level on the BZ site was higher than the water level at H10 (the river bank) indicating that SEOF was formed at the BZ before bankfull capacity was reached. After the lag phase of 14 hours, the water table level was almost equal across the site, which was completely under water. At the peak of the flood 0.77 m^{3}m^{-2} of floodwater was stored on BZ, although discrimination between the volume of precipitation and river water was not possible, while the nitrate load was 30.9 kg N ha^{-1}.

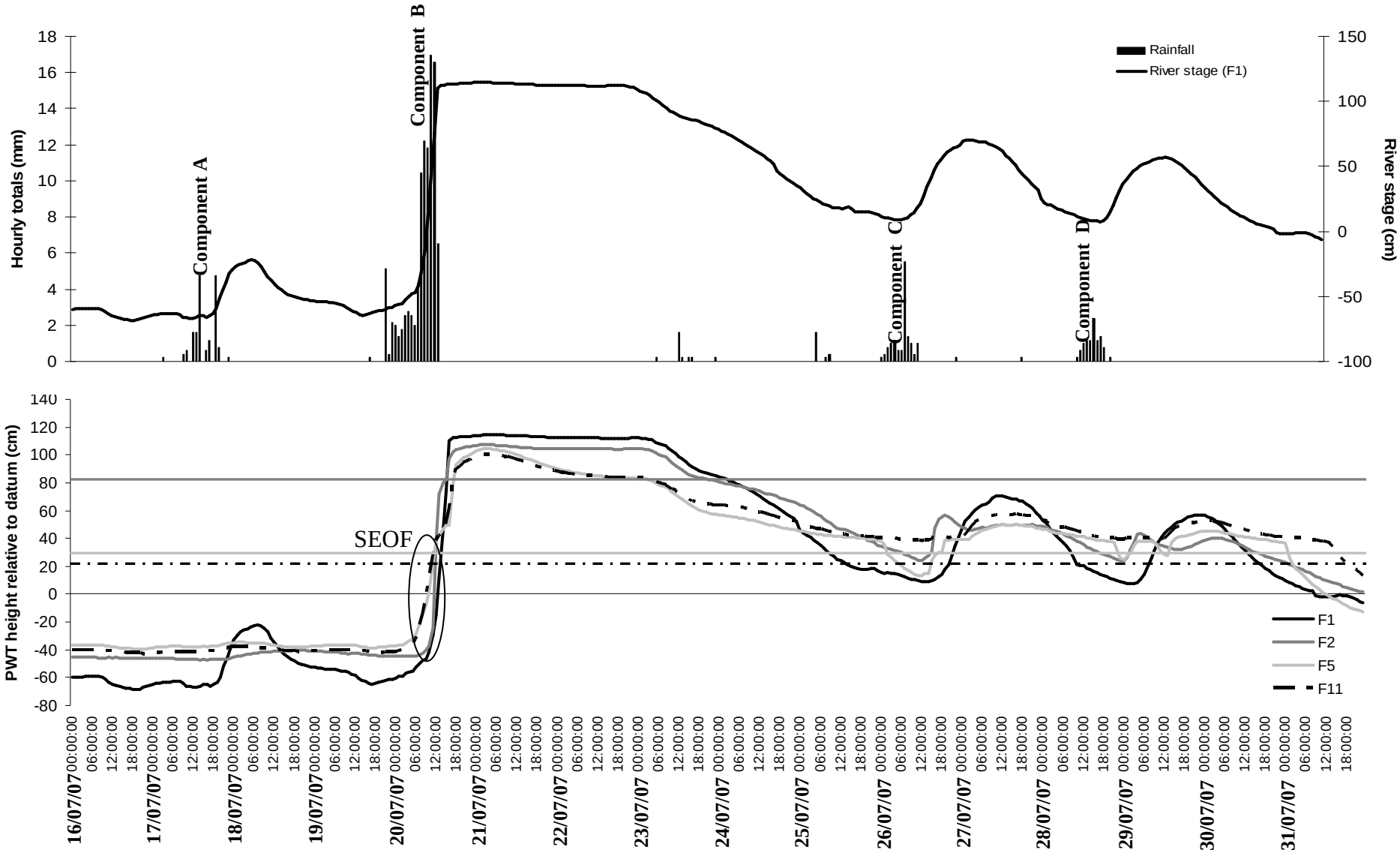

Figure 5.3.7: The hourly PWT level in the monitoring wells F2, F5 and F11 of the PM site and the hourly total rainfall and river stage (F1) for the four components of the July 2007 event. The zero line indicates the datum (F1), while the parallel to the datum lines indicate surface saturation for the wells with same colour coding.

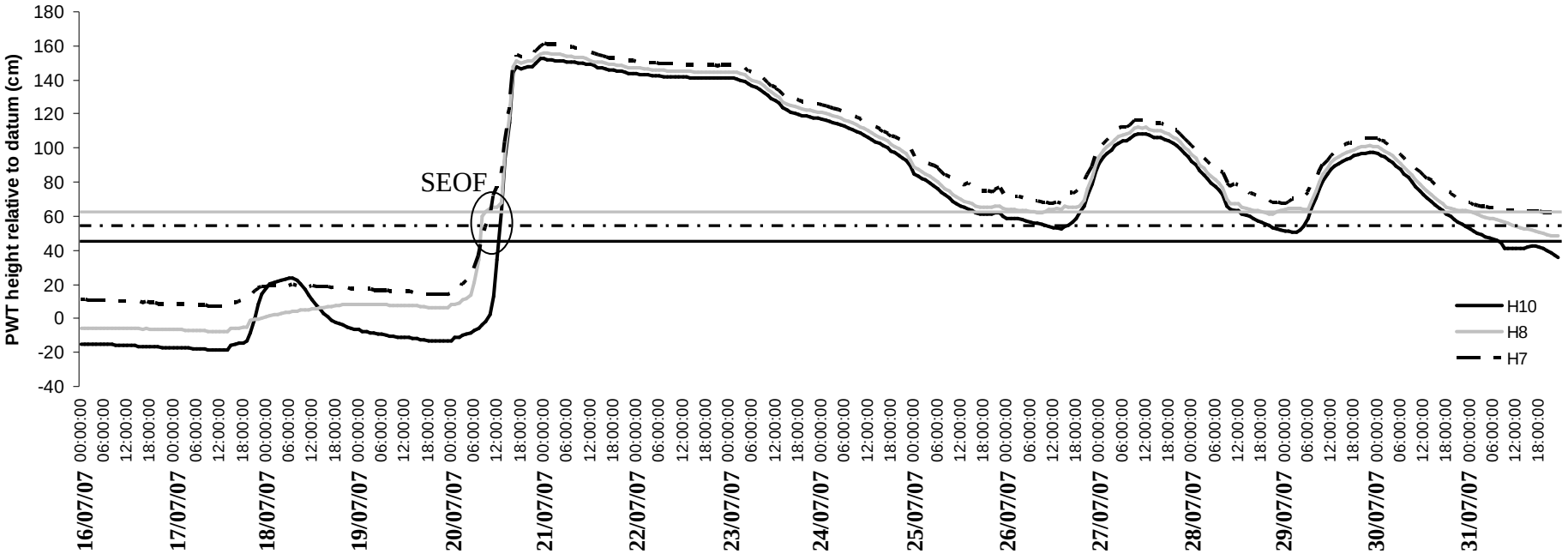

Figure 5.3.8: The hourly PWT level in the monitoring wells H10, H8 and H7 of the BZ site for the four components of the July 2007 event. Parallel lines on the horizontal axis indicate surface saturation for the wells with same colour coding.

Table 5.3.8: July 2007 rainfall and river stage data

Component	Date	Time (began)	Time (end)	Duration (mins)	Total Rain (mm)	Max. Hourly Intensity (mm/hr)	River stage response (mins)	River stage change (cm)
A	17/07/07	10:00	20:30	630	16.2	4.7	450	41.7
B	20/07/07	00:00	16:00	960	101.5	16.9	210	174.5
C	26/07/07	07:30	18:30	690	14	5.5	390	61.7
D	28-29/07/07	20:00	04:00	480	9.9	2.4	540	48.9

5.3.3 *Lateral subsurface flow - Reverse groundwater ridge*

Lateral subsurface flow and subsequent groundwater discharge to the river was observed between flood events. Tables 5.3.9 and 5.3.10 summarise those discharge periods for the PM and BZ site respectively. Regarding the PM area, the PWT was discharging in two directions, from the middle of the floodplain (well F3) towards the north side of the ditch and from F3 southwards to the river; Table 5.3.9 refers to the latter flow path. Further details about groundwater flow direction are given in the example of the spring '07 discharge period that follows.

Generally low hydraulic gradients were recorded between F3 and F1 (range 0.01 - 0.7 %) and this combined with the low K_h of the B soil horizon (0.17 m d^{-1}) resulted in low flow rates (range 0.1 - 0.9 L d^{-1} m^{-1}), according to Darcy's law for one-dimensional flow (equation 5.2):

$$Q = K_h \cdot (dh / dl) \cdot A \qquad (5.2)$$

Where Q the one dimensional groundwater flow (L d^{-1} m^{-1}), K_h the horizontal saturated hydraulic conductivity (m d^{-1}), dh/dl the dimensionless hydraulic gradient and A the cross section area estimated by the depth of the saturated B horizon and a width of 1 m.

The nitrate loading for the maximum flow rates was estimated from the groundwater nitrate-N concentration measured in F3. As it can be seen in Table 5.3.9, the N-loading to the F3-F1 groundwater flow path was low throughout the monitoring period (range 0.02 - 0.10 mg N d^{-1} m^{-1}) and given the low flow rate and hydraulic conductivity, the groundwater nitrate would be expected to be even further reduced before it reaches the river at F1 (see also section 5.4).

The groundwater in the BZ site discharged to the river following one direction from the upslope arable field (H4), or the field edge (H7), to the river margin (H10). Higher hydraulic gradients were observed between H4 and H10 in the BZ site (range 0.4 - 1.6 %) compared to the PM. Consequently, the flow rates were also significantly higher (range 1.6 - 10.3 L d^{-1} m^{-1}) considering also that the K_h of the B horizon in BZ was about 4 times higher (average 0.55 m d^{-1}) than the respective in PM.

Table 5.3.9: Lateral subsurface flow between the well F3 and the river bank (F1) in the PM site during both monitoring seasons. N/A indicates non availability of data. [a] Summer 2007 does not include Sept. 2007. [b] Autumn 2007 includes Sept. 2007

#	Date	Duration (days)	Total rainfall (mm)	Max hydraulic gradient (%)	Depth range (cm)	Max flow rate (L d^{-1} m^{-1})	Nitrate loading (mg N d^{-1} m^{-1})
1	21/10/06 - 17/11/06	28	N/A	0.7	50 - 117	0.9	0.10
	Autumn 06	**28**					
2	19/12/06 - 29/12/06	11	N/A	0.2	34.4 - 106.6	0.3	0.03
3	26/01/07 - 08/02/07	14	N/A	0.1	30.4 - 104.5	0.2	0.03
4	16/02/07 - 19/02/07	4	2.8	0.3	18.6 - 91.4	0.3	0.03
	Winter 07	**29**					
5	10/03/07 - 06/05/07	58	12.6	0.4	64.6 - 132.9	0.4	0.08
6	16/05/07 - 26/05/07	10	6.3	0.4	67.9 - 132.4	0.4	0.05
	Spring 07	**68**					
7	01/06/07 - 13/06/07	14	8.5	0.4	63.7 - 128.9	0.5	0.06
8	03/07/07 - 17/07/08	14	8.9	0.4	63.0 - 129.5	0.4	0.06
9	01/08/07 - 13/08/07	14	3.3	0.2	40.1 - 119.5	0.2	0.13
10	20/08/07 - 30/09/07	40	24	0.4	62.8 - 127.9	0.4	0.26
	Summer 07	**42[a]**					
	Totals Season 1	**207**					
11	19/10/07 - 17/11/07	30	11.4	0.4	55 - 131.2	0.5	0.06
12	24/11/07 - 30/11/07	6	4.3	0.3	41.3 - 115.4	0.3	0.03
	Autumn 07	**66[b]**					
13	12/12/07 - 24/12/07	12	1.2	0.2	39.8 - 119.1	0.2	0.03
14	08/02/08 - 25/02/08	17	3.7	0.1	33.9 - 116.9	0.2	0.03
	Winter 08	**29**					
15	01/03/08 - 08/03/08	8	6.9	0.2	41.6 - 120.6	0.3	0.05
16	22/03/08 - 27/03/08	5	2.2	0.01	25.8 - 110	0.1	0.02
17	01/04/08 - 24/05/08	54	84.1	0.4	67.6 - 130.9	0.4	0.06
	Spring 08	**67**					
18	07/06/08 - 30/06/08	23	32.9	0.3	58.7 - 128.8	0.4	0.06
19	13/07/08 - 28/07/08	15	0	0.5	72.7 - 132.2	0.5	0.07
20	15/08/08 - 31/08/08	16	23.8	0.4	63.8 - 130.5	0.5	0.07
	Summer 08	**54**					
21	14/09/08 - 30/09/08	16	4.3	0.6	66.6 - 128.5	0.6	0.09
	Totals Season 2	**202**					

Table 5.3.10: Lateral subsurface flow between the arable field (H4) and the river bank (H10) in the BZ site during both monitoring seasons. N/A indicates non availability of data. [a] Summer 2007 does not include Sept.2007. [b] Autumn 2007 includes Sept. 2007

#	Date	Duration (days)	Total rainfall (mm)	Max hydraulic gradient (%)	Depth range (cm)	Max flow rate ($L\ d^{-1}\ m^{-1}$)	Nitrate loading ($mg\ N\ d^{-1}\ m^{-1}$)
1	21/10/06 - 15/11/06	26	N/A	0.4	37.2 - 120	1.6	11.23
	Autumn 06	**26**					
2	19/12/06 - 29/12/06	11	N/A	0.6	12.3 - 120	3.6	37.52
3	28/01/07 - 08/02/07	12	N/A	0.5	13.2 - 120	2.9	14.83
	Winter 07	**23**					
4	10/03/07 - 06/05/07	58	12.6	0.7	31.5 - 120	3.4	35.19
5	16/05/07 - 26/05/07	10	6.3	1.0	32 - 120	4.9	22.67
	Spring 07	**68**					
6	01/06/07 - 13/06/07	14	8.5	1.5	12.3 - 120	8.9	41.17
7	03/07/07 - 17/07/08	14	8.9	1.5	15.1 - 120	8.8	3.84
8	01/08/07 - 13/08/07	14	3.3	1.2	1 - 120	8.2	3.67
9	20/08/07 - 30/09/07	40	24	0.8	36.6 - 120	3.6	1.61
	Summer 07	**42[a]**					
	Totals Season 1	**199**					
10	19/10/07 - 17/11/07	30	11.4	0.9	34.3 - 120	4.4	21.60
11	24/11/07 - 30/11/07	6	4.3	1.6	1.5 - 120	10.3	50.57
	Autumn 07	**66[b]**					
12	12/12/07 - 24/12/07	12	1.2	1.3	0 - 120	8.9	76.77
13	08/02/08 - 25/02/08	17	3.7	0.8	4.3 - 120	5.3	45.72
	Winter 08	**29**					
14	01/03/08 - 08/03/08	8	6.9	0.7	10.1 - 120	4.5	35.35
15	22/03/08 - 27/03/08	5	2.2	1.0	0 - 120	7.0	54.99
16	01/04/08 - 24/05/08	54	84.1	1.0	0 - 120	6.7	52.63
	Spring 08	**67**					
17	07/06/08 - 30/06/08	23	32.9	1.6	0 - 120	10.3	11.32
18	13/07/08 - 28/07/08	15	0	1.2	24.7 - 120	6.5	7.14
19	15/08/08 - 31/08/08	16	23.8	1.0	40.7 - 120	4.5	4.95
	Summer 08	**54**					
20	14/09/08 - 30/09/08	16	4.3	1.0	44.4 - 120	4.1	20.13
	Totals Season 2	**202**					

The maximum N-loading rate (range 1.6 - 76.8 mg N d^{-1} m^{-1}) was almost two orders of magnitude higher than the one observed between F3-F1, highlighting the contribution of the lateral subsurface flow from the upslope arable field to the N-loading in the subsurface of the BZ. Therefore, the arable field could potentially be a source of nitrate for the river through lateral groundwater flow, although the flow rate even at high saturation periods was not more than 10.3 L d^{-1}. Given the generally low K_h of the B horizon, it is likely that the retention time of the groundwater coming from the arable field, is long enough to allow reduction of the groundwater nitrate via denitrification before reaching the stream (see also section 5.4).

To summarise, although lateral subsurface flow between flood events is observed 55 % of the time during one year, its contribution to saturation conditions in the most biologically active A soil horizon is insignificant compared to overbank flooding. However, it contributes to the maintenance of saturated conditions in the vadoze zone (B soil horizon) of the floodplain, therefore giving the opportunity for further nitrate attenuation in the subsurface. Furthermore, in the case of the BZ, the lateral subsurface flow serves as an additional mechanism for nitrate supply to the BZ from the adjacent arable field.

5.3.3.1 *Groundwater discharge in spring 2007 (10/03/07 - 06/05/07)*

After the overbank event at the beginning of March 2007 (described earlier), the longest dry spell of the monitoring period followed, when only 12.6 mm total rainfall was recorded in 58 days. Therefore this period was selected to describe the lateral subsurface flow pattern during groundwater discharge for both the PM and BZ sites.

The PWT followed two divergent directions during the discharge period in PM, from the well F3 (second highest surface elevation) towards the river (F1) and from F3 towards the north side of the draining ditch (F7) according to the elevation of the B subsurface horizon (for the direction F3-F7), which remained saturated throughout the drainage period (Figure 5.3.9). Although the well F2 had the highest surface and B horizon elevation, in most cases drained faster than F3, which maintained the highest PWT level throughout the drainage period. This also becomes apparent from the steeper slope of the drainage hydrograph of F2 for the whole of the discharge period in spring 2007 (Figure 5.3.10). It could therefore be argued that the groundwater discharged

faster between F2 and F1 due to the steeper hydraulic gradient but also the higher hydraulic conductivity of the sandy clay layer and the gravel lens, that were thicker between F2 and F1. On the contrary, the groundwater discharged at a slower rate towards the north side of the ditch maintaining a higher water table within the B horizon for longer.

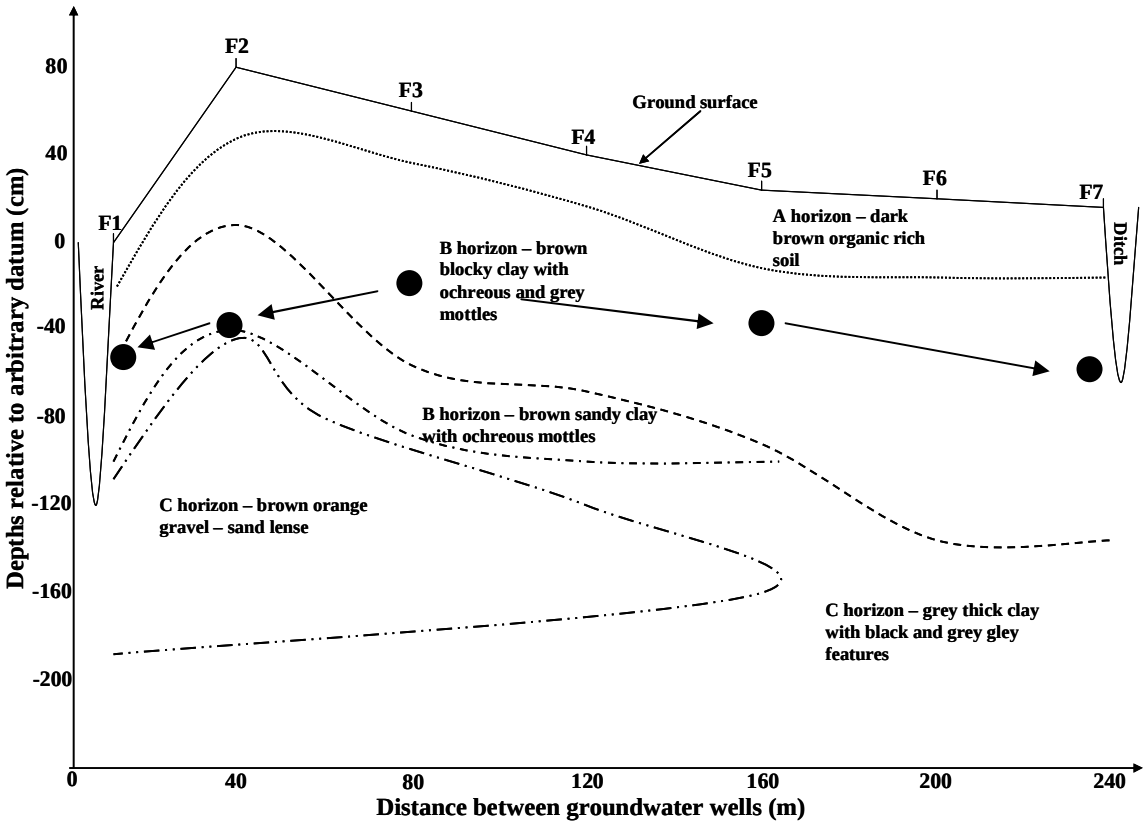

Figure 5.3.9: The PWT level (black circles) and the direction of subsurface flow at the end of April 2007 in the cross-section of the F1-F7 transect in the PM.

The groundwater velocity was estimated from Darcy's velocity equation (5.3):

$$V = K_h \cdot i \tag{5.3}$$

Where V the groundwater velocity (m d^{-1}), K_h the horizontal saturated hydraulic conductivity (m d^{-1}) and i the dimensionless hydraulic gradient. The groundwater velocity between the surface and 30 cm depth was estimated at 8 x 10^{-4} m d^{-1}. The groundwater discharge within the B horizon continued at a slower rate with groundwater velocity estimated at 4 x 10^{-4} m d^{-1}.

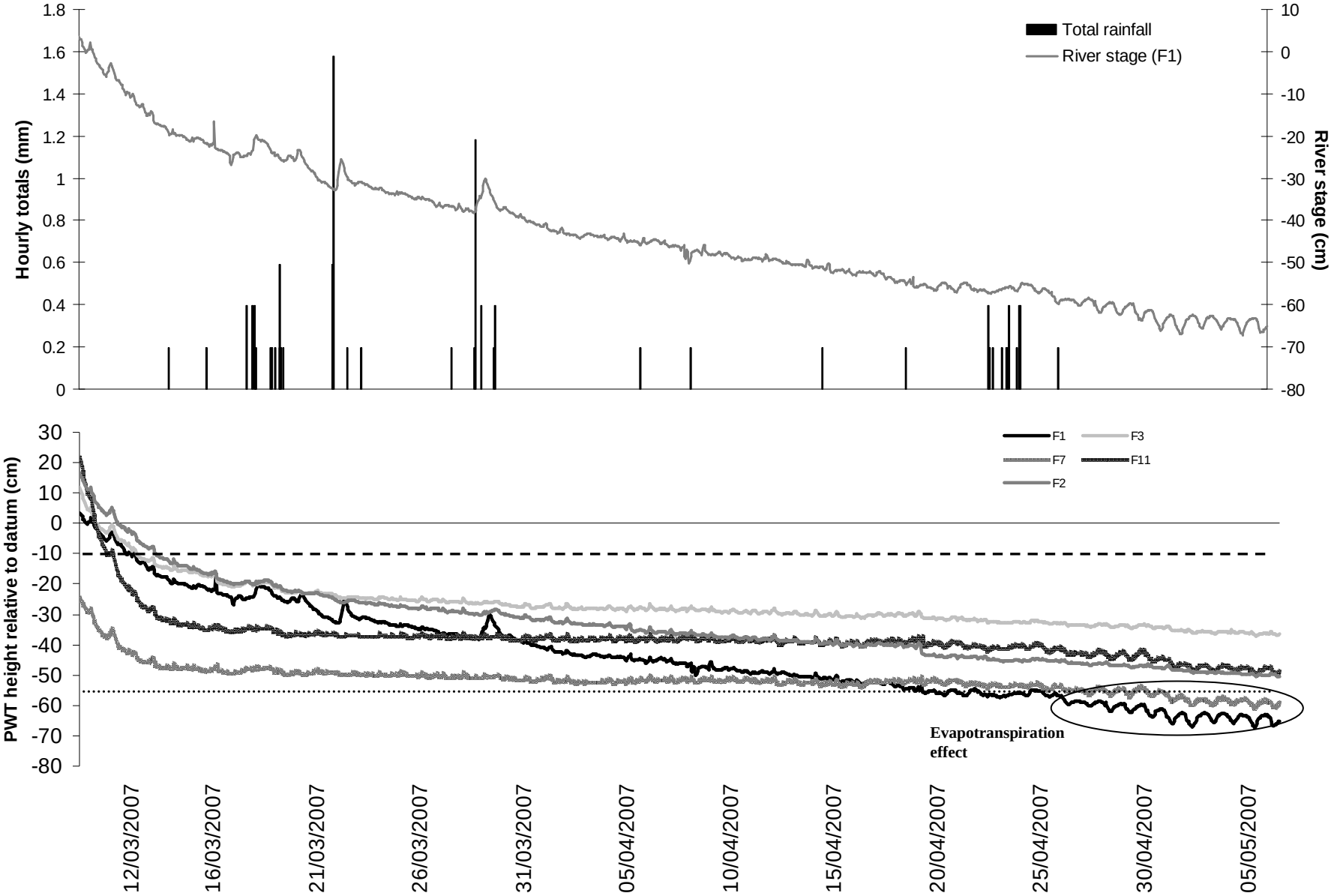

Figure 5.3.10: The hourly PWT level in the monitoring wells F1-F11 and the hourly total rainfall and river stage height of the PM site during the discharge period 10/3 - 6/5/07. The dashed line indicates the limit of the A horizon in the well F11. The dotted line indicates the river stage cut off height beyond which the river no longer flows in the ditch.

On April 18th, the river stage was 54 cm below the F1 surface (river margin) and the river stopped feeding the ditch, which was then fed exclusively by the discharging groundwater. Towards the end of April and the first six days of May 2007 (i.e. the warmest days in the drainage period) diurnal fluctuations of the PWT were recorded in the wells F7 (ditch), F11 (channel depression) and F1 (river stage). These fluctuations were attributed to the effect of increasing evapotranspiration, which during April was higher than the total daily rainfall in all but two days (Figure 5.3.11). Finally, there was no indication for the occurrence of a reversed groundwater ridge between the river and the floodplain, as the PWT level in F2 was higher than the river stage throughout the discharging period.

At the BZ site the PWT discharged to the river with direction from the arable field (H4) and/or the field edge (H7), to the river margin (H10). Although the C horizon was deeper upslope, the PWT during the lateral subsurface flow seemed to follow the elevation gradient of the B horizon (Figure 5.3.12). The groundwater discharged at the same rate across the soil horizons in the BZ as indicated by the uniform slope of the hydrographs in Fig. 5.3.13. The groundwater velocity estimated between the surface and 30 cm depth (limit of A horizon) for K_h = 0.21 m d^{-1} was 1.5 x 10^{-3} m d^{-1}.

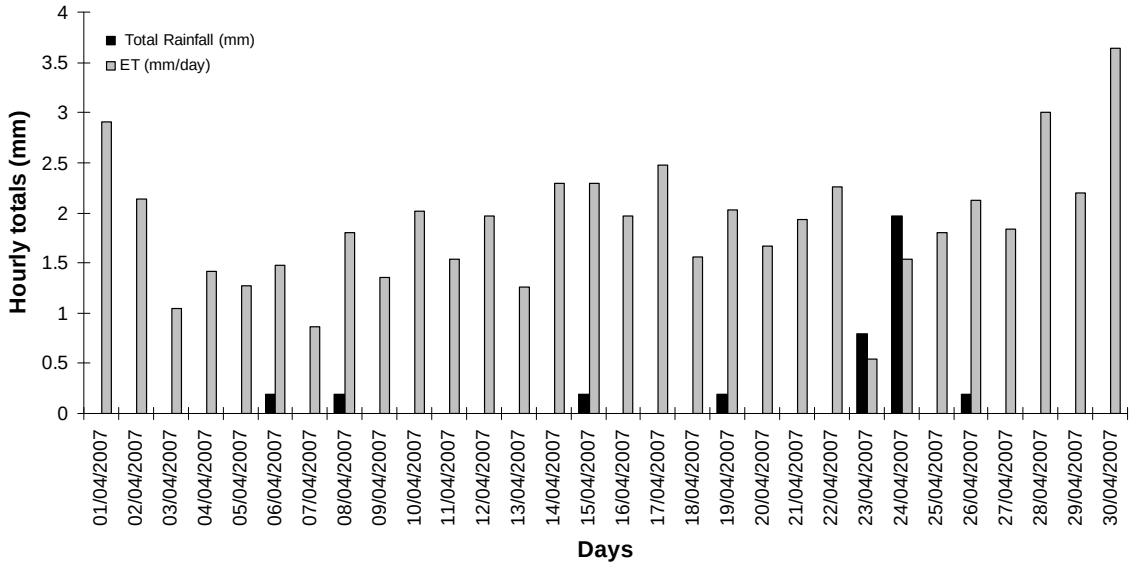

Figure 5.3.11: Daily total rainfall and mean daily evapotranspiration for April2007

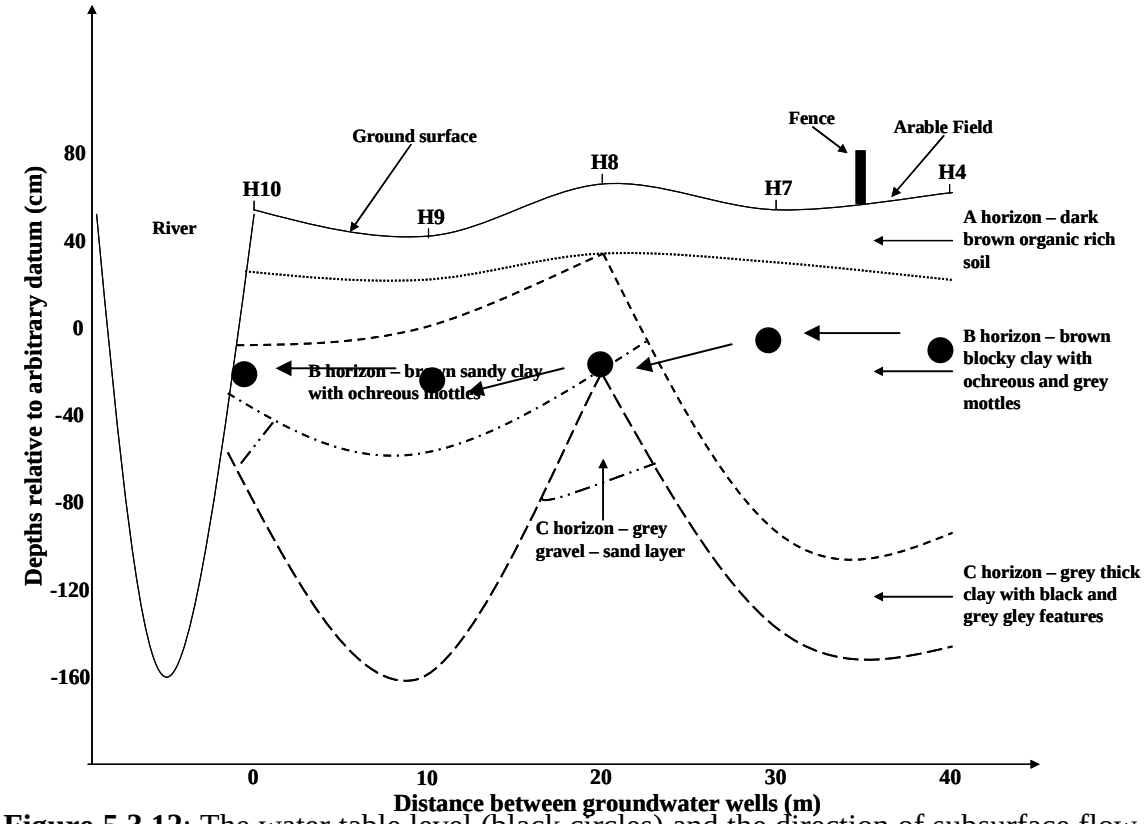

Figure 5.3.12: The water table level (black circles) and the direction of subsurface flow at the end of April 2007 in the cross-section of the H10-H4 transect in the BZ.

Despite the fact that the estimated hydraulic gradient, flow rate and groundwater velocity were all higher than the estimates for the PM (transect F3-F7), the groundwater residence time in the A horizon of the BZ was significantly longer than in the channel depression of the PM. During the rest of the discharge period, the PWT dropped between 70 and 85 cm below the ground surface in 34 days, while the estimated groundwater velocity for K_h = 0.55 m d^{-1} was 5.5 x 10^{-3} m d^{-1}.

Towards the end of April beginning of May 2007, the river stage rose higher than the PWT in the wells H9 and H8 and the conditions for the occurrence of a reversed groundwater ridge appeared. However, no such seepage from the river towards the BZ was observed within the first week of May 2007. Nevertheless, during the second dry April of the monitoring season, April 2008, the river stage exceeded the PWT height of the BZ, without the occurrence of overbank flooding, and there was indication for a reversed groundwater ridge occurring between the river margin and the well H9 (3 occasions) and the well H8 (2 occasions) (Figure 5.3.14).

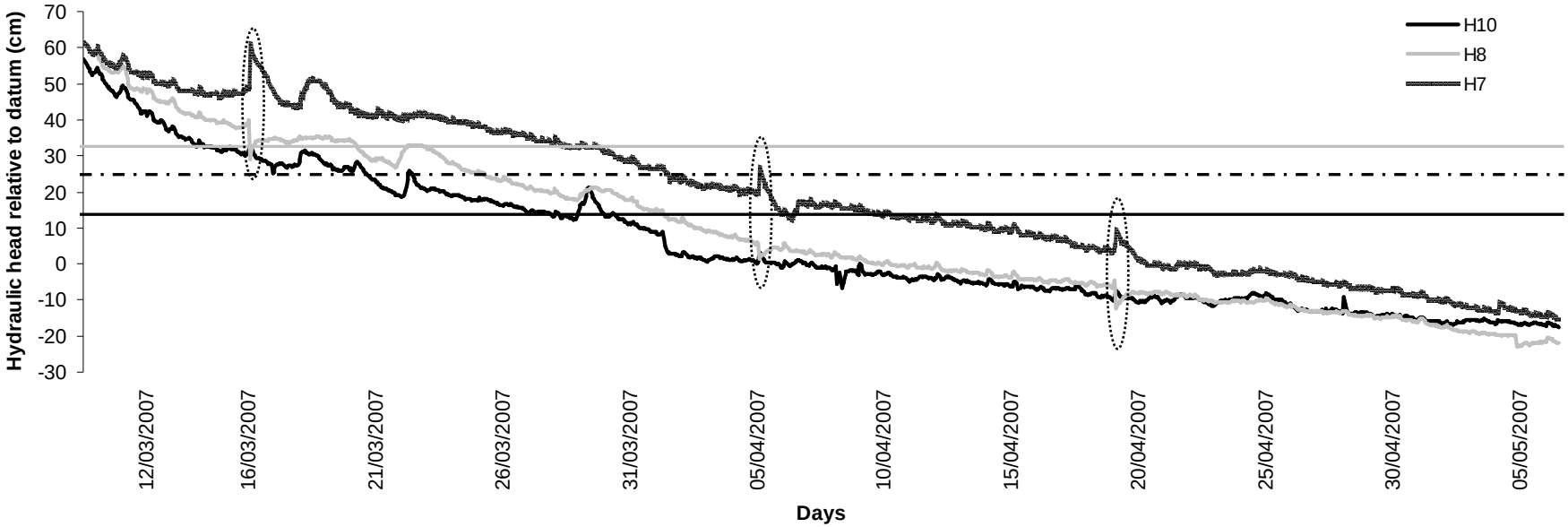

Figure 5.3.13: The hourly PWT level in the monitoring wells H7-H10 of the BZ site during the discharge period 10/3 - 6/5/07. Parallel lines indicate the limit of the A soil horizon for the respective wells with the same colour coding. Circled peaks are result of groundwater sampling.

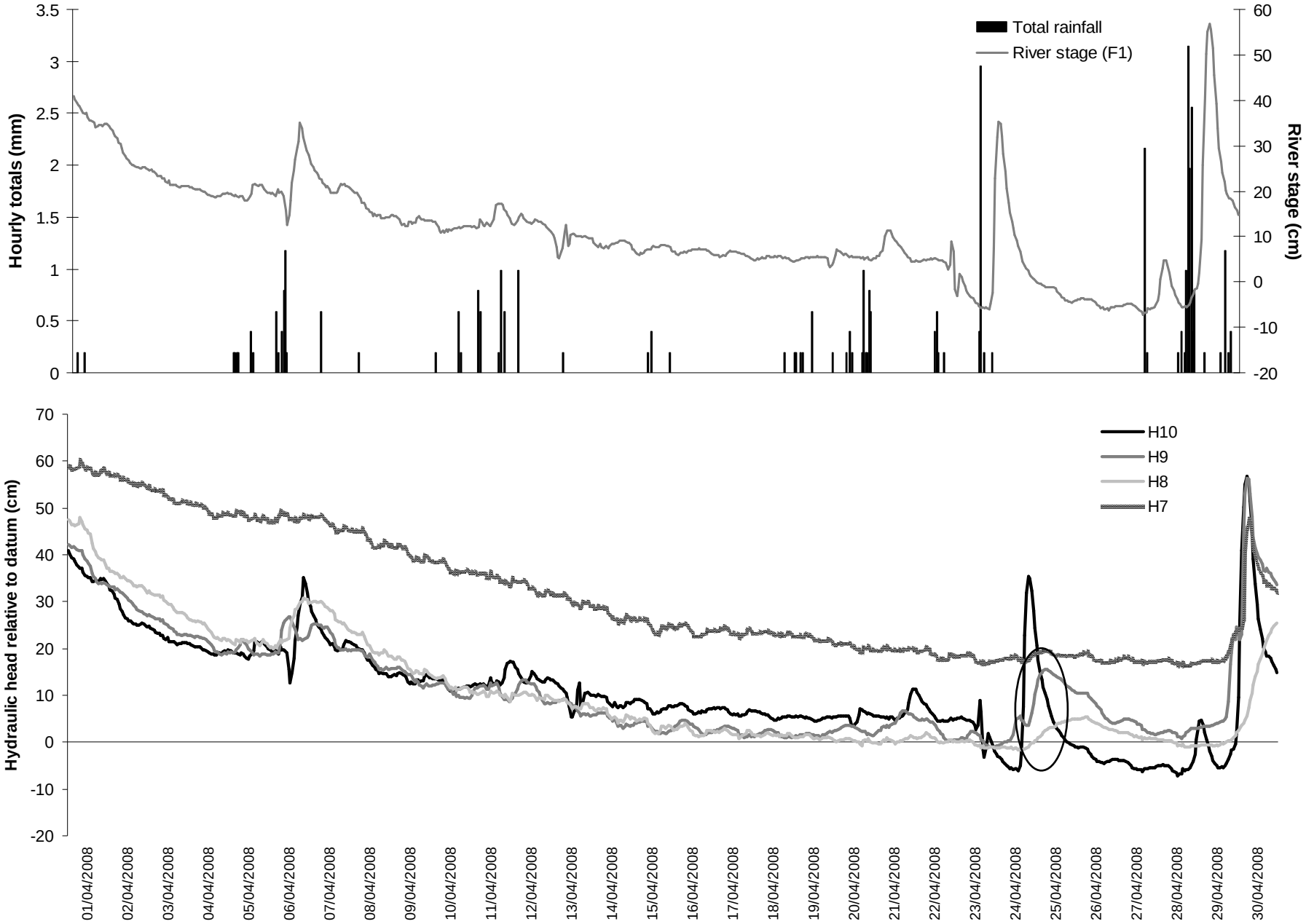

Figure 5.3.14: The hourly PWT level in the monitoring wells H7-H10 and the hourly total rainfall and river stage height of the BZ site during the discharge period April 2008. Circled hydrograph area indicates the possible occurrence of reverse groundwater ridge.

5.4 *The hydrochemistry of the surface and groundwater of the reconnected floodplain of the River Cole.*

This section aims to describe the hydrochemistry of the groundwater and adjacent surface water bodies, and identify the effect of the hydrological processes on the groundwater and surface water chemistry, mainly with respect to nitrate sources and potential fates. The specific objectives are:

- To assess how the main hydrological mechanisms identified are influencing nitrate supply and transformations in the topsoil and the subsurface of the floodplain
- To identify temporal and spatial patterns of nitrate transformation
- Inform the experimental design as to whether denitrification activity is likely to occur and where and when it is expected to occur based on hydrochemical patterns

During the first monitoring season (October 2006 – September 2007), the hydrochemistry of the surface water, the River Cole and the ditch surrounding the PM, as well as the groundwater in the PM and BZ transects were also monitored. Groundwater was sampled bimonthly during the autumn, winter and spring and monthly during the summer from the groundwater wells that were intercepting the subsurface soil horizons (A, B and C), thus providing an integrated measure of groundwater chemistry. Conductivity, pH, temperature and dissolved oxygen concentration were measured *in situ* with portable probes and the samples were also analysed for NO_3^--N, Cl^-, SO_4^{2-}, all the major cations and dissolved organic carbon (DOC) upon return to the laboratory (for method details see section 4.3). For the second monitoring season (October 2007 - September 2008), nitrate concentration data for the River Cole were obtained from the Environment Agency's monitoring station at Coleshill Bridge (Table 5.4.1). A summary of the hydrochemical data obtained during the first season is presented in Table 5.4.2. The conductivity increased from winter through the spring and the summer in both the surface water and the groundwater. The ditch water had slightly higher conductivity compared to the river water, while the BZ groundwater had consistently higher conductivity than the groundwater under the PM area.

Table 5.4.1: Concentration of NO_3^--N in the River Cole at the sampling point PUTR0025; NGR: SU2340093500. Source: Environment Agency of England and Wales (2008). N/A indicates non availability of the time of sampling.

Date	Time	NO_3^- -N (mg l^{-1})
02-Oct-07	1200	2.64
31-Oct-07	1350	4.57
27-Nov-07	1210	5.34
03-Jan-08	959	5.86
29-Jan-08	1145	7.36
25-Feb-08	1200	6.17
01-Apr-08	N/A	5.50
30-Apr-08	N/A	3.40
27-May-08	N/A	6.35
03-Jul-08	N/A	3.04
30-Jul-08	N/A	2.83
27-Aug-08	N/A	4.23
30-Sep-08	N/A	3.98

The pH was relatively constant throughout the monitoring season and was slightly alkaline in the surface water (around 8) whereas the groundwater in both areas, BZ and PM, was neutral for most of the time fluctuating moderately around 7. The groundwater temperature followed a typical seasonal cycle with lowest temperatures recorded in winter and highest in summer.

The dissolved oxygen (DO) concentration of the surface and groundwater was measured *in situ* throughout the monitoring season. However, due to the unreliability of the portable probe measurements, only the spring and summer measurements have been presented (Table 5.4.2). The DO concentration of the river water ranged between 8.7 and 15.2 mg l^{-1} and decreased in the summer compared to the spring. The DO content of the ditch water was slightly lower, ranging from 7.4 to 12.6 mg l^{-1}, and also decreased during the summer months. The groundwater had significantly lower DO concentration that was consistently below 3 mg l^{-1} and in PM ranged between 0.2 and 2.9 mg l^{-1}, while in the BZ area the range was between 0.2 and 0.9 mg l^{-1} suggesting that low redox potential prevailed throughout the saturated zone of the PWT creating the necessary conditions for the occurrence of nitrate reductive processes.

Table 5.4.2: The hydrochemical parameters in the surface and ground-water of the reconnected floodplain of the River Cole during the first monitoring season (October 2006 – September 2007). The values are means ± SE, where available. N/A indicates not available data and GW is groundwater.

	Conductivity ($\mu S\ cm^{-1}$)	pH	Temperature (^oC)	Alkalinity	D.O. ($mg\ l^{-1}$)	NO_3^--N ($mg\ l^{-1}$)	Cl^- ($mg\ l^{-1}$)	SO_4^{2-} ($mg\ l^{-1}$)	DOC ($mg\ l^{-1}$)
Autumn 2006									
River	595	7.9	N/A	- 9.8	N/A	7.1 ± 1.5	38.7 ± 4.6	62.3 ± 4.1	19 ± 4.1
Ditch	911	7.6	N/A	- 3.6	N/A	8.5 ± 0.7	40.9 ± 5.6	69.6 ± 8.8	17.6 ± 1.7
Rain	143	6.9	N/A	- 8.5	N/A	2 ± 1.5	7.3 ± 3.4	10.4 ± 7.6	2.02
PM GW	786.1 ± 33.7	7.1 ± 0.03	13.1 ± 0.3	27	N/A	1.7 ± 0.3	32.1 ± 3.2	57.8 ± 3.1	20.9 ± 0.4
BZ GW	1266.8 ± 93.2	6.9 ± 0.04	12.8 ± 0.3	4.1	N/A	4.4 ± 0.6	74 ± 8.9	87.2 ± 12.5	29.7 ± 4.9
Winter 2007									
River	551.3 ± 54.7	8.1 ± 0.1	N/A	29.9	N/A	6.5 ± 0.4	33.4 ± 8.2	46.5 ± 4.7	20.6
Ditch	498.3 ± 59.8	7.9 ± 0.3	N/A	-7.0	N/A	10.5 ± 2	44.8 ± 7.6	65.3 ± 8.1	21.5
Rain	37.3 ± 7.3	6 ± 0.7	N/A	-8.4	N/A	0.3 ± 0.1	21.2 ± 9.7	1.9 ± 0.2	14
PM GW	504.9 ± 19.5	7.2 ± 0.03	9.4 ± 0.2	29.8	N/A	2.1 ± 0.5	37.1 ± 3.2	47.5 ± 3.8	10.7 ± 1.1
BZ GW	624.3 ± 16	7.4 ± 0.1	9.4 ± 0.3	-12.0	N/A	5 ± 1.1	72.7 ± 4.8	68.9 ± 5.1	11.2 ± 1.3
Spring 2007									
River	493 ± 42.8	8.2 ± 0.1	11.7 ± 0.8	6.5	12.9 ± 1	6.2 ± 0.4	32.4 ± 0.7	48.3 ± 1.9	11 ± 0.8
Ditch	704 ± 78.1	8.2 ± 0.1	14 ± 1.3	-7.6	10.4 ± 0.6	15.9 ± 0.4	44.7 ± 0.8	68.9 ± 2.2	17.3 ± 6.3
Rain	36 ± 5.5	7.2 ± 0.2	N/A	-4.7	N/A	0.5 ± 0.1	9.2 ± 3	8.1 ± 4.6	18.7 ± 8.4
PM GW	623.1 ± 27.4	7.2 ± 0.03	10.2 ± 0.1	43.1	0.9 ± 0.2	1.4 ± 0.8	30.4 ± 2.6	49 ± 4.3	13.1 ± 0.6
BZ GW	966.2 ± 47.1	7.1 ± 0.06	10.6 ± 0.1	-14.4	0.5 ± 0.1	2.9 ± 1.3	110.5 ± 18.7	79.8 ± 11.3	19.4 ± 1.9
Summer 2007									
River	689 ± 49.8	8 ± 0.1	15.3 ± 0.5	60.4	9.7 ± 0.8	4.3 ± 0.3	31.2 ± 8	45.9 ± 8	16.5 ± 1.3
Ditch	953 ± 0.8	8.1 ± 0.02	15.8 ± 0.7	-3.1	7.7 ± 0.2	12.8 ± 0.3	41.9 ± 1.4	59.2 ± 3.1	15.4 ± 1.7
Rain	388.5 ± 156.4	7.4 ± 0.4	N/A	82.1	N/A	3.5 ± 3.3	15.9 ± 6.9	21.8 ± 12.8	25.1 ± 2.4
PM GW	761.6 ± 31.1	7.1 ± 0.03	13.9 ± 0.1	57.3	0.5 ± 0.1	0.6 ± 0.2	26.7 ± 2.2	39 ± 3.7	23 ± 2.7
BZ GW	1207.9 ± 54.1	7 ± 0.03	15 ± 0.2	27.8	0.3 ± 0.03	0.4 ± 0.1	99.7 ± 17.9	72.4 ± 15.2	27.5 ± 2.1

The concentration of NO_3^--N in the river water decreased from autumn 2006 to summer 2007, from 7.1 to 4.3 mg N l^{-1}, but the difference between seasons was not statistically significant (Kruskal-Wallis; χ^2=4.46, *df*=3, *P*>0.05). In contrast, the concentration of nitrate-N in the ditch water increased from 8.5 to 15.9 mg N l^{-1} from the autumn through spring and decreased again in summer 2007 to a mean value of 12.8 mg N l^{-1}. However, once again the difference between the seasons of the monitoring year was not statistically significant (Kruskal-Wallis; χ^2=6.9, *df*=3, *P*>0.05), but it should be noted that the concentration of nitrate remained above the drinking water limit (< 10 mg N l^{-1}) throughout the spring and summer period. Therefore, there was an indication of high nitrate inputs from the surrounding agricultural hillslope to the ditch throughout the year. During the autumn and winter (high water periods), the ditch nitrate was probably diluted with river water, while overbank flooding of the ditch could also have contributed to the reduction of nitrate via denitrification in the flooded floodplain soil. On the other hand, during the spring and summer low water periods, the mixing between the river water and the overbank flooding was more restricted resulting in nitrate accumulation in the ditch water. Similar to the river water, the nitrate-N in the groundwater of both the PM and the BZ areas decreased from a maximum in winter to a minimum in summer (Table 5.4.2), without the difference being statistically significant (Kruskal-Wallis; χ^2=5.03, *df*=3, *P*>0.05 for the PM and Kruskal-Wallis; χ^2=6.38, *df*=3, *P*>0.05 for the BZ).

Significant differences were found between the concentration of NO_3^- -N in the different water sources (i.e. the river, the ditch and the groundwater of the PM and BZ areas respectively; ANOVA; *df*=59, *F*=54.4, *P*<0.01). The ditch water displayed the highest concentration throughout the monitoring period, mean 12.2 ± 1 mg N l^{-1}, followed by the river water, mean 6.2 ± 0.4 mg N l^{-1} and the groundwater in the BZ, mean 3.3 ± 0.6 mg N l^{-1} and the PM area, mean 1.6 ± 0.3 mg N l^{-1} (Figure 5.4.1 A). The concentrations of Cl^- and SO_4^{2-} were also not significantly different between the four seasons of the monitoring period in the different water sources (Table 5.4.3). Moreover, Cl^- concentration was similar between the water sources (Figure 5.4.1 B), with only the groundwater in the BZ area displaying a significantly higher Cl^- content (ANOVA; *df*=59, *F*=6.98, *P*<0.01). The concentration of SO_4^{2-} (Figure 5.4.1 C) was similar between the river water and the groundwater in the PM, while the ditch water had

similar SO_4^{2-} concentration to the groundwater of the BZ area (ANOVA; *df*=59, *F*=12.01, *P*<0.01).

Table 5.4.3: The results of the Kruskal-Wallis test for the concentration of Cl^- and SO_4^{2-} between the four seasons of the monitoring period for the four different water sources.

	River	Ditch	PM GW	BZ GW
Cl^-				
χ^2	0.92	0.94	5.13	1.9
df	3	3	3	3
P	0.822	0.815	0.163	0.593
SO_4^{2-}				
χ^2	5.41	1.66	7.04	1.16
df	3	3	3	3
P	0.144	0.645	0.071	0.764

Principal component analysis (PCA) was used to identify the best combination of environmental variables explaining the highest proportion of the variance between the samples from the four water sources. The environmental variables used were the concentrations of NO_3^--N, Cl^- and SO_4^{2-}, while the DO and DOC were omitted as there was a considerable number of missing values (especially for DO) that would have resulted in the reduction of the sample size and unequal representation of the different seasons during the PCA. The analysis indicated two principal axes. The first axis (eigenvalue 1.558) explained 52 % of the variance between samples and correlated strongly with the SO_4^{2-} and the Cl^- (weightings; 0.89 and 0.88 respectively). The second axis (eigenvalue 1.055) explained 35 % of the variance between samples and correlated strongly with the NO_3^--N (weighting 0.98). Plotting the samples along the two principal axes produced Figure 5.4.2. The samples were clustered into four distinct groups corresponding to the four water sources. The main discrimination was along axis 2, indicating that NO_3^--N was the differentiating factor between samples. The ditch samples, higher NO_3^--N, were associated closely with the positive side of axis 2 and partially overlapped with the river water samples having the second highest NO_3^--N concentrations. Finally, the groundwater samples from both areas were more closely associated with the negative side of axis 2, having significantly lower NO_3^--N concentrations, and no overlap was observed since the higher Cl^- and SO_4^{2-} concentrations found in BZ separated the two groups along axis 1.

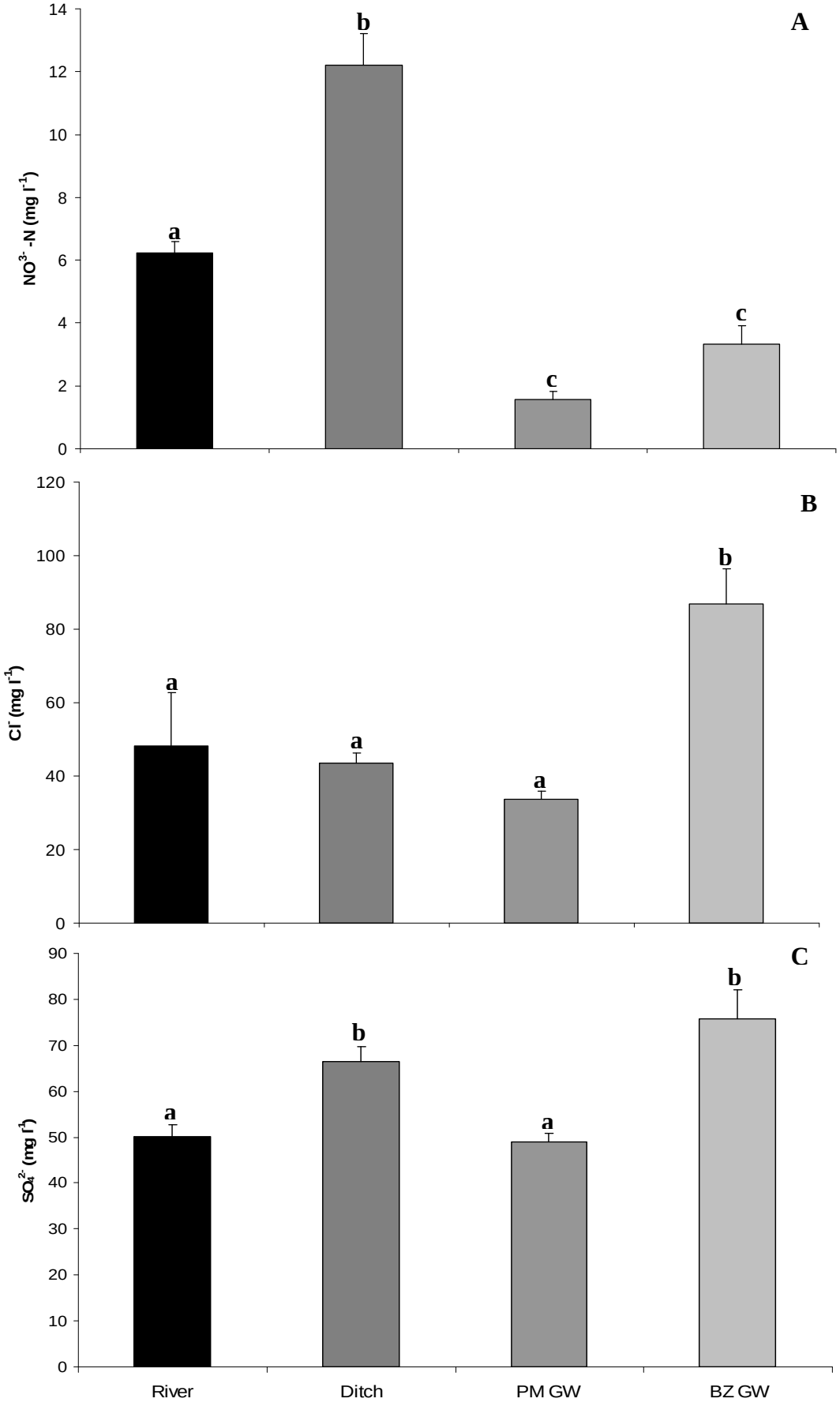

Figure 5.4.1: Mean concentration of NO_3^--N, Cl^- and SO_4^{2-} during the monitoring season (Oct. 2006 – Sept. 2007) in the river and ditch water and the groundwater of the PM and BZ floodplain areas. Different letters indicate significant differences.

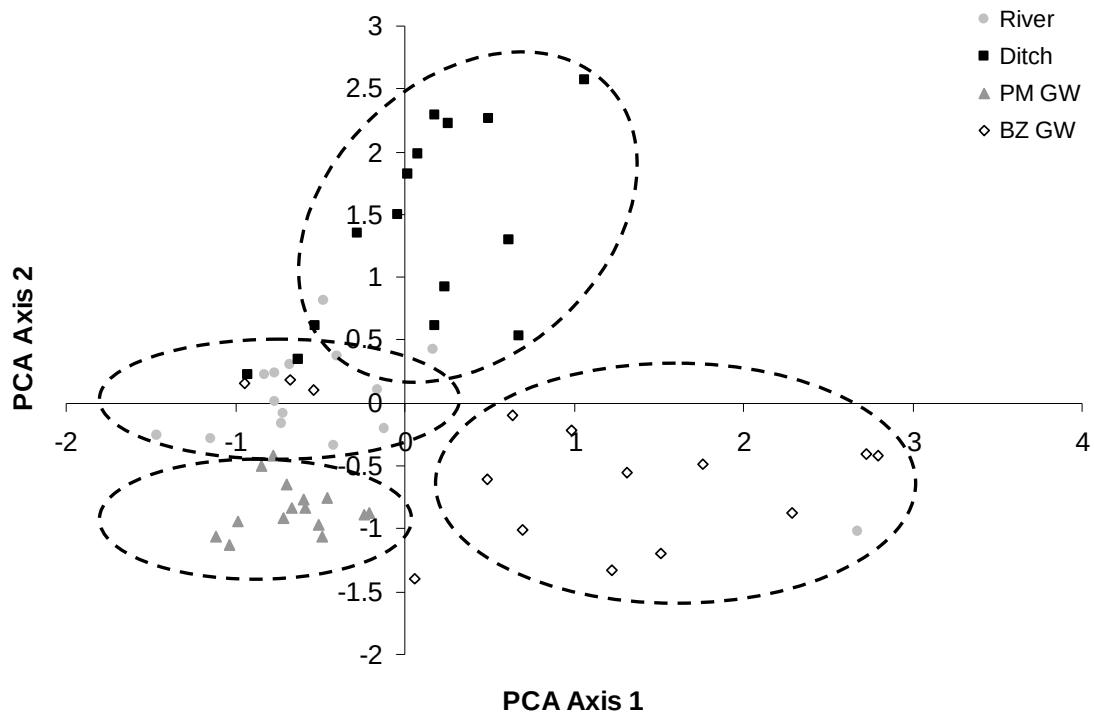

Figure 5.4.2: Plot of individual water samples from all the water sources according to their principal components in PCA.

The DOC concentration in the river water was not significantly different in autumn, winter or summer and only in spring was it significantly lower (Kruskal-Wallis; χ^2=8.14, *df*=3, *P*<0.05). Seasonal differences in the DOC concentration were also observed for the ditch water that had significantly higher DOC concentration in winter (Kruskal-Wallis; χ^2=8.1, *df*=3, *P*<0.05). Finally, no significant difference in the DOC concentration of the groundwater in both the PM and BZ areas was noted throughout the monitoring year (Kruskal-Wallis; χ^2=7.4, *df*=3, *P*>0.05 for the PM and Kruskal-Wallis; χ^2=4.3, *df*=3, *P*>0.05 for the BZ). The lowest mean DOC concentration for the monitoring year was measured for the river water, 14.7 ± 1.5 mg l^{-1}, followed by the groundwater of the PM area, 16.5 ± 1.6 mg l^{-1}, then the ditch water, 17.4 ± 3.1 mg l^{-1} and finally the groundwater of the BZ area, 22.1 ± 2 mg l^{-1}. However, these differences between the water sources were not statistically significant (ANOVA; *df*=47, *F*=2.14, *P*>0.05).

Correlation analysis between the major water anions and the DO and DOC measurements in all the samples of the monitoring year has indicated some significant relationships. The nitrate-N showed a significant but weak positive correlation with the DO (Spearman's; r=0.39, N=137, P<0.01), indicating that at higher DO concentrations higher NO_3^--N was found in the surface and groundwater samples possibly as a result of lower denitrification activity, while no relationship was found between DOC and nitrate-N. The Cl^- and SO_4^{2-} were strongly inter-correlated (Spearman's; r=0.79, N=60, P<0.01) and they both correlated positively with the DOC (Spearman's; r=0.38, N=48, P<0.01 between Cl^- and DOC, Spearman's; r=0.45, N=48, P<0.01 between SO_4^{2-} and DOC).

Correlation between the NO_3^--N concentration of the groundwater in all the wells during the monitoring year revealed some interesting relationships (Table 5.4.4). The well F1 correlated positively with the river water and the wells F5 and F6, indicating the influence of those wells by overbank flooding, while a negative correlation was found between F1, F5 and F6 with the ditch by F7, indicating mainly an opposite hydraulic gradient (i.e. discharging) towards the north side of the ditch. The well F5, apart from correlating positively with F1 and the river water, also showed strong correlation with the wells F6 and F7, indicating that nitrate is reduced along the hydraulic gradient from F5 to F7. Finally, the well F2 correlated only with the well F3 that also correlated with the well F4, suggesting that these wells located in the middle of the floodplain had nitrate-N concentrations that were closely related to each other and there was no significant effect from overbank flooding either from the river or the surrounding ditch, except during very high magnitude events.

Figure 5.4.3A summarises the subsurface spatial distribution of NO_3^--N along the transect F1-F7 in the PM. In all seasons, the water sources intercepted by the transect (i.e. the river in F1, the ditch in F7 and overland flow along the channel depression in F5) displayed higher nitrate concentration, which upon its deposition on the floodplain mainly through overbank events, infiltrated the subsurface where nitrate-N concentration was observed to be reduced. The reduction of nitrate-N was similar during autumn and winter, around 50 %, but increased considerably in spring, 97 %, and summer months, 91 %, probably as a function of prolonged inundation caused by storm events under favourable temperature conditions for denitrification and possibly

increased nitrate uptake by plants during the growth season. Figure 5.4.3 B summarises the distribution of Cl^- along the same transect. Chloride can be used as a conservative tracer to discriminate whether the reduction of nitrate-N is due to dilution or other biological or chemical processes (Schilling *et al.*, 2006). When there is lack of variability in Cl^- concentrations along a groundwater flow path, but the ratio NO_3^-:Cl^- displays similar variability as the NO_3^- concentration, then processes other than physical mixing or dilution are likely to be responsible for nitrate reduction (Schilling *et al.*, 2006). This is because Cl^- is considered biologically inactive with regards to processes occurring in water bodies (Hill *et al.*, 1998). Chloride along the transect F1-F7 seemed to increase its concentration along the main groundwater discharge pathways (F3 to F1 and F3 to F7), possibly as a result of weathering processes. Figure 5.4.3 B shows that Cl^- increased in the groundwater of F1 compared to the river water (by 38 % in autumn, 39 % in winter, 24 % in spring and 15 % in the summer). The ratio NO_3^--N:Cl^- followed the decrease pattern noted for nitrate-N indicating further that dilution plays a minor role along the groundwater discharge flowpath (Figure 5.4.3 C).

The effect of the overbank flooding of the channel depression with nitrate-rich ditch water was apparent in all the seasons apart from summer 2007 in well F5. The nitrate-rich groundwater found in F5 was reduced along the hydraulic gradient towards F4, by 80 % in autumn; 97 % in winter and 82 % in spring, while there was also some dilution occurring as shown by the reduction of Cl^- concentration along the same pathway, but at lower percentages; 27% in autumn, 20% in winter and 59% in spring. Reduction of the groundwater nitrate-N concentration was also observed along the hydraulic gradient from F5 to F6. It was slightly less than the reduction observed between F5 and F4; 76 % in autumn, 68 % in winter, 88 % in spring, but still higher than the respective reduction in Cl^-; 21 % in winter and 10 % in spring.

Table 5.4.4: Correlation matrix between the NO_3^--N concentration in the groundwater of the transect F1-F7 in the PM and the river and ditch water. Underlined correlation coefficients are products of Spearman rho correlation whereas non-underlined are products of Pearson Product-Moment correlation. ** Correlation is significant at the 0.01level and *Correlation is significant at the 0.05 level.

Variables/Correlation coefficients		River	F1	F2	F3	F4	F5	F6	F7	Ditch
River	*R or rho*	1	**0.553***	0.321	0.111	-0.221	**0.596***	0.325	0.414	-0.196
	P	.	0.032	0.243	0.694	0.428	0.019	0.237	0.125	0.483
	N	15	15	15	15	15	15	15	15	15
F1	*R or rho*		1	0.439	0.114	-0.336	**0.743****	**0.604***	0.436	**-0.589***
	P		.	0.101	0.685	0.221	0.002	0.017	0.104	0.021
	N		15	15	15	15	15	15	15	15
F2	*R or rho*			1	**0.718****	0.439	0.411	0.077	0.489	-0.361
	P			.	0.003	0.101	0.128	0.785	0.064	0.187
	N			15	15	15	15	15	15	15
F3	*R or rho*				1	**0.695****	0.211	0.450	0.461	-0.079
	P				.	0.004	0.451	0.092	0.084	0.781
	N				15	15	15	15	15	15
F4	*R or rho*					1	-0.268	0.075	-0.129	0.018
	P					.	0.334	0.791	0.648	0.950
	N					15	15	15	15	15
F5	*R or rho*						1	**0.736****	**0.729****	**-0.718****
	P						.	0.002	0.002	0.003
	N						15	15	15	15
F6	*R or rho*							1	**0.861****	**-0.700****
	P							.	0.000	0.004
	N							15	15	15
F7	*R or rho*								1	**-0.587***
	P								.	0.022
	N								15	15
Ditch	*R or rho*									1
	P									.
	N									15

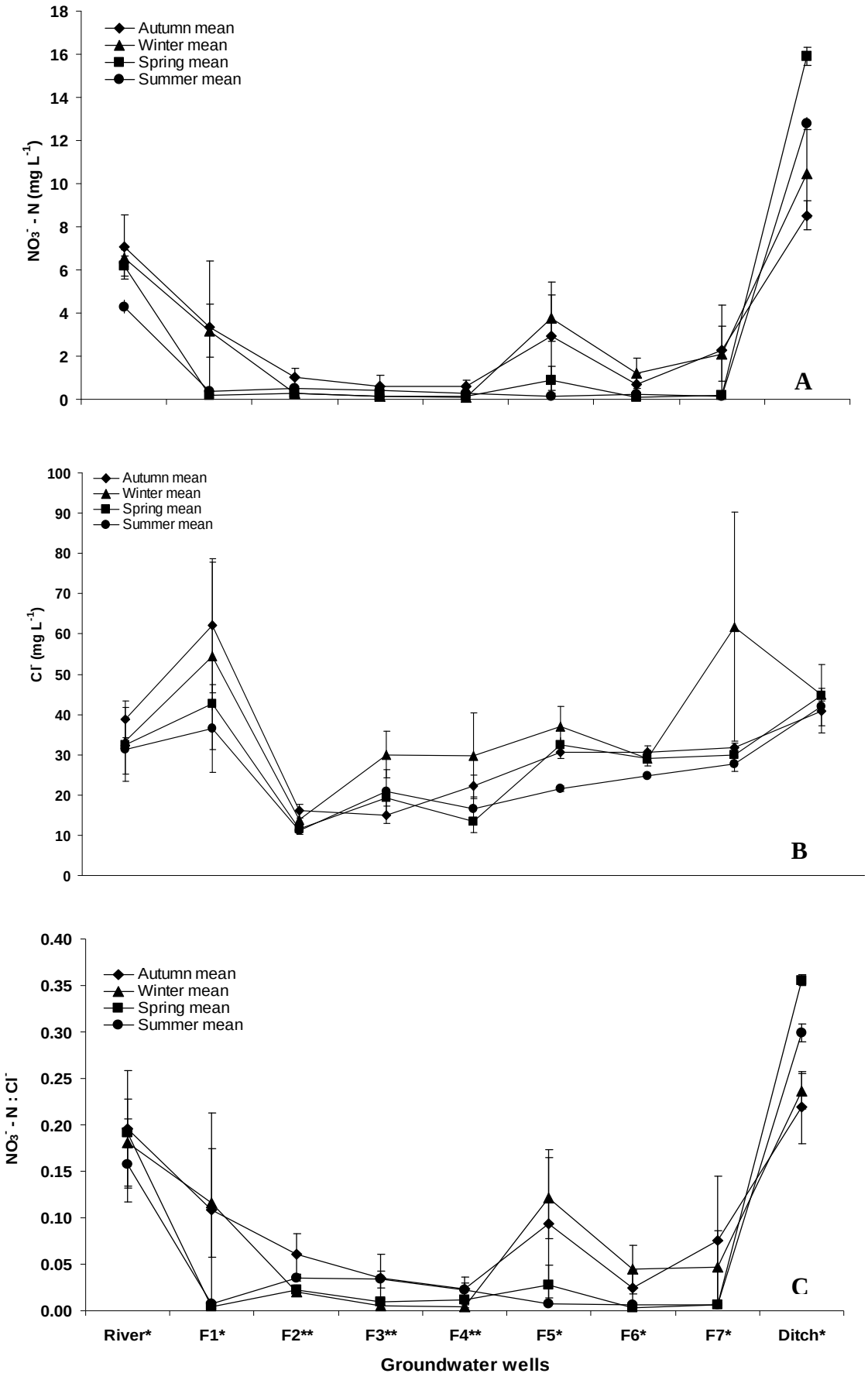

Figure 5.4.3: Mean ± SE seasonal NO_3^--N and Cl^- concentration and the ratio NO_3^--N:Cl^- in the groundwater of the PM and the surface water of the river and ditch. * and ** indicate correlations between the respective wells and water bodies.

Transect F9-F14 extended from the west to the east side of the surrounding ditch, parallel to the river, and intercepted the channel depression of the PM at well F11 (Figure 5.4.4 A) The nitrate-rich water entering the well F14 via seepage or overbank flooding from the ditch, was reduced significantly by 66 % in autumn, 36 % in winter, 29 % in spring and 83 % in summer. This highlighted the effect of the summer floods in supplying nitrate-rich water, accumulated in the ditch from hillslope runoff, onto the floodplain where reduction occured along the westward flowpath possibly via denitrification and plant uptake during the growth season. Some reduction of Cl^- due to dilution was observed along the same flowpath, but the ratio NO_3^--N:Cl^- followed largely the nitrate-N concentration change, suggesting that the important reduction of the nitrate-N in the groundwater along the hydraulic gradient is due to biological processes rather than dilution (Figures 5.4.4 B & C).

The overland input of nitrate-rich ditch water was apparent in wells F11 and F9 (Figure 5.4.4 A). The well F11 was intercepting the channel depression and received overbank flooding from the ditch in all seasons. The ditch water that entered the well F9 and moved along the hydraulic gradient towards the well F8 also showed a decrease in the nitrate concentration, while Cl^- also decreased but to a lesser extent. The well F11, within the channel depression, correlated positively with the river water ($r=0.53$, $P<0.05$), the well F1 ($r=0.76$, $P<0.01$) and the well F5 ($r=0.90$, $P<0.01$), confirming the direct influence of overbank flooding to the NO_3^--N concentration of the groundwater underneath the channel depression. Moreover, the well F14 correlated positively with the ditch water ($r=0.69$, $P<0.01$) indicating that probably seepage of ditch water through to well F14 is occurring alongside the flood events throughout the year.

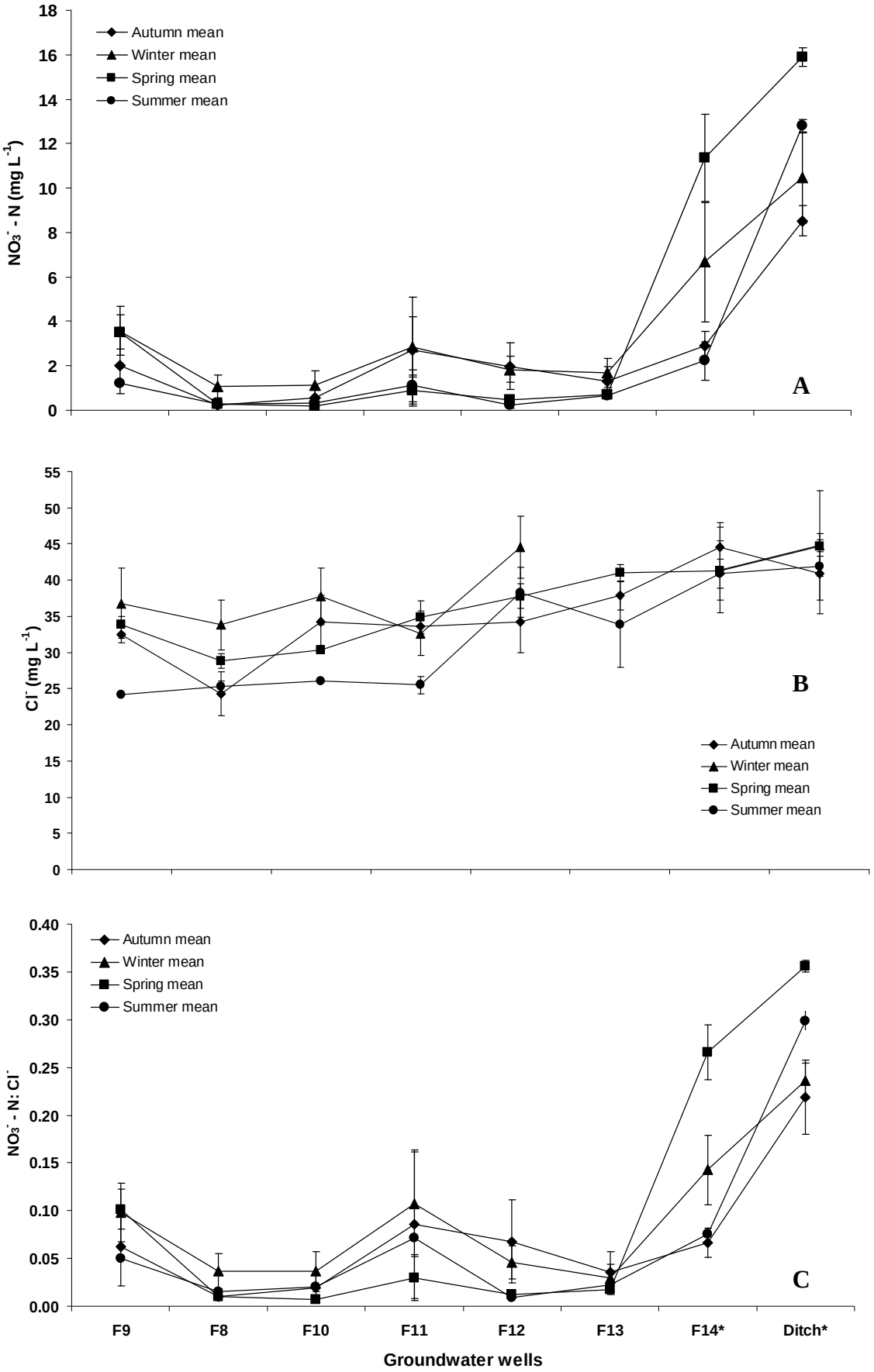

Figure 5.4.4: Mean ± SE seasonal NO_3^--N and Cl^- concentration and the ratio NO_3^--N:Cl^- in the groundwater of the PM and the surface water of the river and ditch. *indicates correlation between the well F14 and the ditch.

The distribution of NO_3^--N in the groundwater of the BZ area along the transect H4-H10 is shown in Figure 5.4.5 A. The effect of the elevated nitrate-N concentration originating from both the arable field and the river was obvious in all the seasons of the monitoring year. The highest NO_3^--N concentrations were recorded just outside the arable field (well H7) and within 10 m along the hydraulic gradient (well H8) they were reduced by 54 % in autumn, 75 % in winter, 99 % in spring, and 68 % in summer. However, considerable dilution was also observed along the same hydraulic gradient as indicated by the Cl^- concentration (Figure 5.4.5 B) that decreased by 34 % in autumn, 28 % in winter, 62 % in spring and 66 % in summer, being though less than the decrease in nitrate-N and therefore suggesting that other processes apart from dilution could be responsible for reducing the NO_3^--N leaching from the arable field to the groundwater (Figure 5.4.5 C).

The nitrate-rich river water that entered the subsurface of the buffer zone through seepage during the groundwater discharge periods, or was deposited during flood events and percolated in the subsurface, had its NO_3^--N content reduced within 20 m from the river bank by 66 % in autumn, 54 % in winter, 94 % in spring and 96 % in summer. This reduction could be entirely due to biological processes, since the concentration of Cl^- in the groundwater of the BZ was actually higher than in the river water, and therefore no dilution along the hydraulic gradient from the river to the wells H10 and H9 could be detected.

Correlation between the NO_3^--N content of the wells H4-H10 and the river water has highlighted the two main pathways of nitrate reduction in the subsurface of the buffer zone (Table 5.4.5). The wells H4 and H7 correlated strongly with each other ($r=0.76$, $P<0.01$), indicating leaching of nitrate from the topsoil of the arable field to the underlying water table. Moreover, H7 also showed some correlation with the river water ($r=0.65$, $P<0.05$) that highlighted the influence of the river water in supplying additional nitrate to that part of the BZ via overbank flooding and direct outflow of the river through the drainage tunnel under the bridge at high flow conditions. The groundwater in H8 was more strongly associated to well H9 ($r=0.67$, $P<0.01$) and to a lesser extent to well H10 ($r=0.68$, $P<0.05$). The well H9 was strongly correlated with the well H10 ($r=0.84$, $P<0.01$), which was also associated with the river water ($r=0.61$, $P<0.05$) indicating the direct connection of H10 with the river through seepage and flooding.

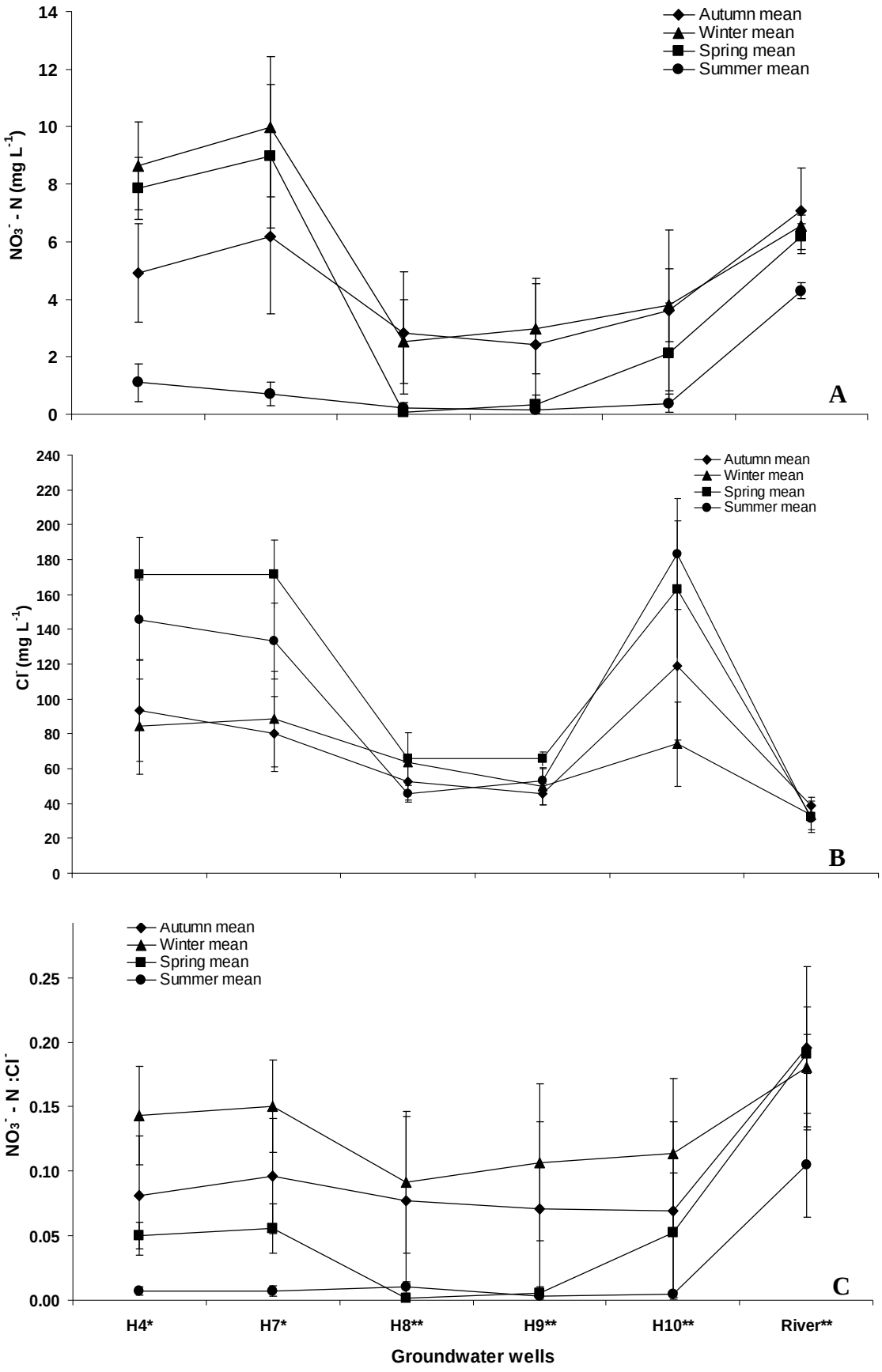

Figure 5.4.5: Mean ± SE seasonal NO_3^--N and Cl^- concentration and the ratio NO_3^--N:Cl^- in the groundwater of the BZ and the river water. * and ** indicate correlation between the respective wells and the river water.

Table 5.4.5: Correlation matrix between the NO_3^--N concentration in the groundwater of the transect H4-H10 in the BZ and the river water. Underlined correlation coefficients are products of Spearman rho correlation whereas non-underlined are products of Pearson Product-Moment correlation. ** Correlation is significant at the 0.01level and *Correlation is significant at the 0.05 level.

Variables/Correlation coefficients		River	H4	H7	H8	H9	H10
River	*R or rho*	1	0.323	**0.648***	0.354	0.368	**0.610***
	P	.	0.260	0.012	0.215	0.177	0.027
	N	15	15	15	15	15	15
H4	*R or rho*		1	**0.758****	-0.015	-0.222	0.352
	P		.	0.002	0.958	0.446	0.239
	N		15	15	15	15	15
H7	*R or rho*			1	-0.138	-0.200	0.231
	P			.	0.637	0.493	0.448
	N			15	15	15	15
H8	*R or rho*				1	**0.666****	**0.676***
	P				.	0.009	0.011
	N				15	15	15
H9	*R or rho*					1	**0.835****
	P					.	0.000
	N					15	15
H10	*R or rho*						1
	P						.
	N						15

In conclusion, the hydrochemical analysis of the groundwater in the two areas of the re-connected floodplain of the River Cole and the adjacent water bodies suggested that the main supply of nitrate to the floodplain originates from the river and ditch water. The ditch also collects hillsope runoff from the surrounding agricultural fields. The nitrate is deposited onto the floodplains mainly via overbank flooding, which has been shown to be the dominant hydrological mechanism in both areas, and subsequently infiltrates into the subsurface. However, some mixing between low nitrate groundwater and nitrate rich river and ditch water, due to seepage, was observed at the river and ditch margin groundwater wells, providing a further indication for the occurrence of groundwater ridging at the near stream and ditch zones. Finally, the arable field adjacent to the BZ had consistently higher nitrate concentration, and especially during spring and summer, it is a likely source of nitrate to the subsurface of the BZ following the main groundwater discharge flow path from upslope to the river.

Although no significant seasonal differences were observed in the nitrate concentration of surface water and groundwater during the monitoring year, nitrate reduction rates tended to be higher during the winter and summer periods in both the PM and BZ areas. This could have been an effect of higher nitrate supply due to more frequent inundation events, longer flood water residence time that would have allowed more effective denitrification, and specifically for the summer events higher soil temperature would be expected to have increased the denitrification rates, while also plant uptake could have contributed to nitrate attenuation during the growth period. Some degree of dilution along the main groundwater flow paths was also observed, but it could not account for all of the observed nitrate reduction. Therefore, biological denitrification is likely to occur in the topsoil and the subsurface of the floodplain, as was also indicated by the positive correlation between nitrate and DO. Overall the DO was consistently below 3 mg l^{-1} in the groundwater, suggesting low redox conditions that would favour subsurface denitrification. Although no significant relationship was found between nitrate and DOC, the DOC was consistently relatively high in both the groundwater and the surface water throughout the year suggesting a constant supply of organic carbon through the main hydrological flow paths. Finally, stronger nitrate reduction gradients were observed where surface water intercepted the floodplain, i.e the riparian areas, the channel depression in the PM and between the arable field and riparian zone interface in the BZ, suggesting potential areas of high denitrification activity.

5.5 *Discussion*

Conceptual model of the River Cole re-connected floodplain hydrological regime

In contrast to a 2D floodplain hydrological model proposed by Bates *et al.* (2000) and in accordance to a 3D approach adopted by Jung *et al.* (2004), the hydrological regime of the River Cole re-connected floodplain is best described by a three-dimensional approach:

- At the initial stage of a flood event, the rising river stage leads to river water bank storage which extends several meters away from the bank. Therefore mixing of SW and GW occurs first in the subsurface, while the effect of percolating precipitation and water table rise due to capillary fringe should also be taken into account.
- When bankfull capacity is exceeded, a flood pulse extends across the floodplain from two directions; perpendicular to the river towards the floodplain and parallel to the river from the ditch to the floodplain (PM case). In the BZ case, a 2D approach between the river and the field adequately describes the hydrological dynamics. The flood pulse decreases the importance of the bank seepage, and SW - GW mixing proceeds with the infiltration of the surface ponded river-ditch water into the subsurface.
- During the recession limb, GW discharges to both the river and the ditch contributing to baseflow. GW residence time is prolonged by the infiltrating surface water, the maintenance of high soil water content by the capillary fringe, and possibly by a reversed GW ridge under baseflow conditions with direction from the ditch towards the PM area and from the river towards the BZ area.

5.5.1 *Hydrological regime of the re-connected floodplain*

The hydroperiod (i.e. the frequency, duration and intensity of flood events) is a useful criterion for documenting hydrological restoration success. According to Kentula (2000), the high water table of a restored floodplain should typically be within 30 cm of the soil surface for a certain period of time (typically between 12 and 21 consecutive days) for compliance success. In the case of the River Cole re-connected floodplain, field measurements have documented relatively long periods of inundation in both the

PM and BZ areas, ranging between 1 and 26 continuous days. On an annual basis, for the monitoring year 2006-2007, the PM was flooded 21 % of the time, while the BZ was flooded for 28 % of the year. For the second 'drier' monitoring year, 2007-2008, the flooding conditions accounted for 13 % and 23 % of the year for the PM and the BZ areas respectively.

The River Cole floodplain pre-restoration (before 1995) in a 1 in 2 year flood event would result in flooding conditions in the upstream site (above the bridge and the BZ area), while both the upstream and downstream sites (including the BZ and PM areas) would be flooded in a 1 in 100 year flood event. The restoration plan predicted an increased flooding occurrence under low order events during the winter and spring months, but anticipated flooding to persist for short periods due to expected rapid drainage through the gravel underlying the alluvium. It was however noted that 'in extreme circumstances the downstream meadow areas could be covered with flood water for up to three weeks in winter (Environmental Report River Cole Restoration, 1995). The hydrological monitoring of the present study has provided evidence of restored connectivity between the river and the floodplain not only during the winter and spring months, but also during the summer storms encountered in the monitoring seasons. However, it is possible that the increased hydrological connectivity has been affected by the climatic variability observed during the monitoring period. Indeed, following two relatively dry years (2005 and 2006) the winter of 2006-2007 was warm but also notably wet across southern Britain, and after an exceptionally dry period in spring, the wettest summer since 1879 followed with three particularly significant storms in June and July (Marsh and Hannaford, 2007). The monitoring year 2007-2008, after a dry autumn that led to a significant decrease in the water table levels, was followed by a wet winter and a relatively wet summer, and therefore the duration of the observed flooding in the reconnected floodplain probably reflects the 'wet' conditions of the monitoring years.

Inadequate monitoring and post-project evaluation continues to be an important criticism of river restoration projects, and further research is needed for the assessment of the floodplain hydrological response to channel modifications (Tague *et al.,* 2008). However, assessment of the hydrological restoration success needs to account for rainfall variability when documenting changes between pre- and post- restoration

conditions. When no control study area exists, periods of nearly-average rainfall should be used for evaluating the post-restoration hydroperiod characteristics (Moorhead *et al.*, 2008). Clearly, this was not possible during the study of the re-connected floodplain of the River Cole due to the particular climatic conditions. Alternatively, a modelling approach could have been employed simulating pre- and post- restoration scenarios for flooding hydroperiod, subsurface water storage and runoff decrease, as suggested by Hammersmark *et al.* (2008). Despite the fact that the hydrological connectivity may have been overestimated due to the particular climatic conditions of the monitoring period, the flashy response of the River Cole, due to the urbanisation effect of the headwaters and the heavy clay alluvium underlying >50 % of the catchment (Environmental Report River Cole Restoration, 1995), was documented for events of variable magnitude across seasons. Moreover, the two eventful monitoring seasons allowed for a variety of hydrological mechanisms to be studied and to assess their contribution to the inundation pattern and residence times on the floodplain expected to affect the biogeochemical nitrogen transformations in the surface and subsurface soil horizons.

5.5.1.1 *The effect of topography and floodplain stratigraphy on the hydrological regime of the re-connected floodplain*

The hydrological exchange between the GW and the SW at the landscape scale is a function of: 1) the distribution and magnitudes of hydraulic conductivities associated with the alluvial-plain sediments; 2) the relation of stream stage to the adjacent groundwater level; and 3) the geometry and position of the stream channel within the alluvial plain (Woessner, 2000). The direction of the exchange processes varies with hydraulic head, whereas flow (volume/unit time) depends on sediment hydraulic conductivity (Sophocleous, 2002).

The topography of the re-connected floodplain is flat with the slope range being between 0.01 and 2 % in the PM, while the BZ is slightly undulating, range between 0.2 and 2.5 %, but still fairly flat. Therefore, the GW flow direction was governed by the lower limit of the PWT, the upper limit of the heavy impermeable clay C horizon, (McDonnell, 1990; Ward and Robinson, 2000), rather than the surface elevation which controls subsurface flow direction in headwater catchments with high angle hillslopes (Gu *et al.,* 2008; van Verseveld *et al.,* 2009). Furthermore, in riparian zones with slope

<5 %, the stream stage is the main control of water table elevation rather than any upland input (Vidon and Hill, 2004a). On the other hand, the PM site, although surrounded by arable hillslopes, at its north and north-east borders, the presence of a draining ditch at the break of slope intercepted any lateral subsurface or overland flow, thus decoupling the hillslope from the valley bottom, where hillslope runoff would have had a greater opportunity to interact with saturated soils, supporting possibly higher N-transformation rates, before reaching the stream channel (Cirmo and McDonnell, 1997).

'Switching off' of hillslope inputs was observed due to the formation of a reversed groundwater ridge (with direction from the river towards the break of slope) during modelled overbank events (Bates *et al.,* 2000) and in-bank events (Burt *et al.,* 2002b) in a floodplain of the River Severn in the UK. However, the authors assumed that the 'damming' of hillslope inputs would increase soil saturation and residence times in the floodplain and thus have a positive effect on biological nitrate removal. In our study, some bank seepage of ditch water into the floodplain was observed at the north and north-east floodplain edges, but as a result of frequent overbank inundation, hillslope runoff collected by the ditch was mixing with river water in the channel depression of the PM, thus creating a flow convergence area similar to that observed by Curie *et al.* (2009) in a tributary of the River Seine in France, and therefore giving the opportunity for biological nitrate removal of the ditch water along the channel depression.

Groundwater residence times are strongly affected by the stratigraphy of riparian zones (Cirmo and McDonnell, 1997). The PM area was characterised by the extensive clay alluvium with the cumulative clay and silt fraction being >90 % of the grain size distribution across the whole depth profile. Therefore, relatively low horizontal saturated hydraulic conductivities (K_h) were measured, which were within the range reported for similar soil textures found in eight riparian zones in southern Ontario, Canada (Vidon and Hill, 2004a). Throughout the B soil horizon (0.3 to 1 m depth) extensive soil hydromorphic features such as mottling and iron and manganese concretions were observed, suggesting anaerobic soil conditions. Similar indications were found in the riparian zone of an incised stream that maintained a shallow water table (< 1.5 m) throughout the year in Iowa, USA (Schilling and Jacobson, 2008). In the present study, a localised gravel lens was observed at depths below 1 m from the ground

surface between the middle of the floodplain with direction towards the south and the river bank. Despite the coarser texture, the gravel lens had slightly lower K_h than the silty clay B horizon, something also observed by Burt *et al.* (2002b), attributing the finding to a gravel diamict with a fine-grained matrix surrounding the well dispersed gravels that in effect lowered the hydraulic conductivity. Sandy gravel lenses with almost two orders of magnitude higher conductivities were associated with strong lateral subsurface flows in a perennial and an ephemeral stream riparian zone in a semi-arid climate (Rassam *et al.,* 2006). An impermeable heavy clay till layer at an approximate depth of 2 m acted as the limit of a perched water table that fluctuated between the surface and 1.5 m depth throughout the year. Similar impermeable clay layers with comparable very low K_h were found in a number of riparian zones studied by Vidon and Hill (2004a).

More variable hydraulic conductivities were observed in the clay loam and silty clay layers of the BZ subsurface, which were approximately five times higher than the respective conductivities measured for the PM subsurface. Additionally, no localised gravel lens was observed but instead dispersed sand and gravel patches were scattered throughout the subsurface, probably representing channel deposits preserved by the lateral migration of the river (Devito *et al.,* 2000). The fact that the K_h of the topsoil layer (0 - 30 cm) was two and a half times lower than the B horizon could be explained by the presence of scattered gravel in the subsurface that increased the K_h.

The low slope gradient in conjunction with the intermediate hydraulic conductivities in the unsaturated zone, and the effect of the stream and ditch stage but also the precipitation inputs are all conductive factors (Burt and Pinay, 2005) for frequent soil saturation in the reconnected floodplain of the River Cole. Moreover, maximum nitrate removal rates in riparian zones are traditionally associated with shallow water tables confined by an impermeable layer in depths were high carbon zones exist (Hill, 1996; Gold *et al.,* 2001). Therefore, the River Cole re-connected floodplain is a suitable location for investigating nitrate attenuation processes, as it displays the desirable hydrological properties.

5.5.1.2 *The effect of increased hydrological connectivity on the surface and sub-surface floodwater storage*

The dominant control of the PWT level in the re-connected floodplain was the river stage and subsequently the ditch stage, as a result of the establishment of increased hydrological connectivity for the downstream reach after the River Cole restoration project (Environmental Report River Cole Restoration, 1995). On average 13 overbank flood events were recorded per monitoring season, which is 10 times more than the number of overbank events observed by Burt *et al.* (2002b) in the floodplain of the much larger River Severn in the 'wetter' north-west part of Britain, reflecting both the flashy character of the River Cole, but also the specific climatic conditions of the wet winters of 2006-2007 and 2007-2008 and the exceptionally wet summer 2007 (Marsh and Hannaford, 2007). For the PM area the flooding conditions persisted on average between 4-6 days, while for the BZ the average flood water residence time was between 6-8 days, being comparable to the flooding duration observed by Andersen (2004) in a seasonally inundated wet meadow at the River Gjern catchment in Denmark. The maximum floodwater storage in the unsaturated zone of the PM (i.e. between the ground surface and the impermeable clay till layer) for an average porosity of 0.59 was 1.18 m^3m^{-2}, while for the unsaturated zone of the BZ with slightly higher porosity, 0.61, was 1.22 m^3m^{-2}. Our estimates are comparable to the cumulative floodwater storage capacity observed in the riparian zone of a semi-arid perennial and ephemeral stream, between 1.5 and 2 m^3m^{-2} (Rassam *et al.*, 2006), during a six month long wet season. However, in our case the maximum storage capacity was reached at the peak of each overbank flood event, followed by a drawdown period and a subsequent re-fill of the unsaturated zone at the next overbank event, highlighting the large floodwater storage capacity of a temperate lowland floodplain and its potential for attenuating downstream flood waves (Pinder and Sauer, 1971).

Additional floodwater volumes were stored on the floodplain surface at each overbank event contributing to the nitrate loading of the flood pulse and triggering biogeochemical nitrate removal via lowering the oxygen availability in the reactive topsoil (Olde Venterink, *et al.*, 2003; Valett *et al.*, 2005; Cabezas *et al.*, 2009; Banach *et al.*, 2009) and in parallel assisting in the recharge of the PWT (Winter, 1995). Overbank flooding from two sources, namely the river and the draining ditch in the PM area, created a 'perirheic' zone (*sensu* Mertes, 1997) combining the river water with the

hillslope runoff giving the opportunity for processing of the diffuse nitrate during ponding and recharge of the unsaturated zone. Higher magnitude and duration rainfall events were associated with larger floodwater storage volumes and subsequently increased nitrate loading, which in turn was positively related to longer residence times. In other words, long and high magnitude winter and spring storms delivered more nitrate loading onto the floodplain, which had the opportunity to be reduced during the long inundation periods (Gergel *et al.*, 2005). Specifically for the BZ, lower magnitude but high intensity events seemed to be adequate to cause complete inundation of the site, which explained the longer flooding period observed. Being adjacent to arable land and displaying a high inundation frequency, the BZ site was ideally positioned to offer a buffering function to the discharging groundwater from the arable field before entering the stream.

5.5.2 *The hydrological mechanisms of SW - GW interaction in the re-connected floodplain of the River Cole*

The relative importance of the different hydrological mechanisms with respect to their contribution in: (i) the transport of nitrate; and (ii) in the creation of saturation conditions, favouring nitrate attenuation processes, was assessed in two land use zone areas of the floodplain. The mechanisms are categorised into three main types: a) overbank flooding; b) saturation excess overland flow; and c) groundwater discharge by lateral subsurface flow.

5.5.2.1 *Overbank flooding and reversed groundwater ridge during flood events*

Overbank inundation during medium to high magnitude and intensity rainfall events has been observed for both the PM and BZ areas. With respect to the BZ area, the wetting up pattern is perpendicular to the river direction, from the stream towards the arable field, while two flood relief tunnels underneath the Coleshill Bridge supply additional longitudinal overland flows from upstream during high magnitude events.

In the case of the PM area, the overland flow pattern is more complex due to the connection of the draining ditch to the river, as long as the river stage does not drop below 54 cm from the bankfull stage height. The analysis of hourly PWT height data indicated overflowing of the ditch at three breach points, firstly at the east side of the floodplain area where the overland flow is directed towards the channel depression

flowing westwards, followed by the north breach supplying overland flow towards the south direction and finally the west breach supplying both the channel depression in the PM and FM areas. In high magnitude events, a convergence of overland flows has been observed from the north (ditch) and the south (river) towards the middle, higher surface elevation area, resulting in complete floodplain inundation. Due to the complexity of the multiple flooding sources onto the floodplain and the lack of on site discharge measurements, the relative input of ditch and river water was not quantified. However, a mixed source 'perirheic' zone (Mertes, 1997), including nitrate loading from the river and the arable hillslope runoff, was established for the PM site.

Floodwater retention time in the PM ranged between 1 and 13 days, while in 52 % of the cases it was more than 5 days. For the BZ the range was between 1 and 26 days, while in 50 % of the events, floodwaters ponded on the surface for more than 5 days. Longer residence times where observed in the riparian and channel depression areas of the PM, while the hollow areas near the well H9 and H7 in the BZ were the ones to drain last following a flood event. The total nitrate loading per monitoring year ranged between 177 and 305 kg N ha^{-1} for the PM and the BZ areas.

A hydraulic residence time of at least five days has been suggested to promote efficient nitrogen retention in treatment wetlands (Kadlec and Knight, 1996), as this period of time is assumed to be long enough to promote denitrification of inflowing nitrate and solids sedimentation. Andersen (2004) estimated that nitrate in pond water was reduced completely in two weeks for similar surface hydraulic conductivity, surface water temperature range and average river water nitrate concentration. In experimental flooding treatments of a semi-arid floodplain in New Mexico (USA) that lasted ~30 days, nitrate was reduced concurrently with DO depletion, while DOC was released from the decomposition of organic matter (Valett *et al.,* 2005). In contrast, brief overbank flooding (1-2 days) across three seasons in a floodplain in Maryland (USA) resulted in nitrate flushing from the soil to the overlying surface water as a result of ammonium nitrification (Noe and Hupp, 2007). Based on the frequency of flooding and the relatively long retention times observed, the re-connected River Cole floodplain would be expected to be a sink rather than a source of nitrate.

During an intermediate magnitude rainfall event, the stream stage responds first, in a relatively short time (between 3 and 4 hours from the start of the event), which depends on the antecedent moisture conditions of the catchment (Ward and Robinson, 2000), but also the contribution of runoff from the urbanised headwaters near the town of Swindon (Environmental Report River Cole Restoration, 1995). In the PM area, a reversed hydraulic gradient from the river towards the floodplain is observed, which at the onset of the event (i.e. before bankfull capacity is exceeded) can contribute to bank storage through seepage as it was predicted by the modelling study of Bates *et al.* (2000) and subsequently shown for the first time in a field investigation of a floodplain in River Severn (Burt *et al.,* 2002b). However, the hydraulic gradient in the PM area is low, a few centimetres compared to more than a meter observed by Burt *et al.*, (2002b) and combined with the relatively low saturated hydraulic conductivities of the silty clay layer, it is very unlikely that river water can travel through the subsurface as far as the ditch at the north side of the floodplain (240 m distance) following Darcian flow through the soil matrix. Jung *et al.* (2004), studying the same floodplain on the River Severn, suggested that the almost simultaneous increase of the water table with the rising river, at about the same rate, could only be explained by a kinematic wave similar to translatory or 'piston' flow (Anderson and Burt, 1982) that pushes 'old' floodplain water at a perpendicular direction away from the river towards the floodplain.

A similar reverse GW ridge between the river and the middle of the PM area (80 m distance) was observed at the initial stage of a high antecedent moisture condition flood event. Significant floodwater storage was observed on the pasture meadow of the floodplain. The reversed GW ridge mechanism in the BZ site was restricted between the river margin and 10 m inland, due to rapid overbank flooding, even during medium magnitude events, that exerts a stronger control on the PWT height.

Similar near stream bank storage was observed in the riparian zone of an incised stream with comparable conductivities and the 'damming' effect of upslope contributions to the water table (Schilling *et al.*, 2004, 2006). Mixing of GW and SW in the near stream zone was also observed by Curie *et al.* (2009), who suggested the extension of the hyporheic zone hydrological functioning to near stream sediments. Generally, significant reversed groundwater ridge in lowland semi-arid riparian zones during flood events (Martí *et al.,* 2000; Butturini, *et al.,* 2003; Lamontagne *et al.,* 2005; Rassam *et*

al., 2006) and in temperate low relief riparian zones throughout the year (Duval and Hill, 2006; Hill and Duval, 2009) has been associated with relatively high hydraulic conductivities of well dispersed gravel layers. Therefore, it could be argued that reverse groundwater ridging although possible in the reconnected floodplain of the River Cole, is spatially restricted due to topography and lithology to short near stream distances and temporally constrained to bankfull or the initial stages of overbank events (Bates *et al.*, 2000; Burt *et al.*, 2002b; Jung *et al.*, 2004). More conclusive results with regards to the relative importance of the GW ridging during bank storage in the River Cole floodplain could be obtained in future work by using stable isotopes ($\delta^{18}O$ and $\delta^{2}H$) to identify flow paths and residence times of 'old' floodplain GW and 'new' water from differing sources (i.e. river water and precipitation) (Wolfe *et al.*, 2007) and/or 2D modelling of GW - SW interactions between the river and the PWT (Krause and Bronstert, 2007; Peyrard *et al.*, 2008).

5.5.2.2 *Saturation and infiltration excess overland flow*

Saturation excess overland flow (SEOF) was mainly observed in summer and autumn storms under high antecedent moisture conditions and although significant surface ponding was measured, it ranged between 7 and 20 % of the floodwater volume stored on the floodplain during the event. Specifically the BZ area was more prone to SEOF, displaying one per season, probably due to the higher water tables maintained in the hollow areas. Given the low slope topography of the floodplain, SEOF did not produce any significant runoff that could have had an erosional effect or result in decoupling of the floodplain or diffuse nitrate transport to the river. Therefore, in contrast to headwater steep slope hillslope/floodplain areas where SEOF may contribute up to 80 % of the flood peak hydrograph (Wenninger *et al.*, 2004), in the lowland catchment of the flashy River Cole, SEOF is of minor importance compared to overbank flooding.

Infiltration excess overland flow (IEOF) has been mostly documented in arid and semi-arid floodplains, on impermeable surfaces or bare ground (Ribolzi *et al.*, 2000; Ward and Robinson, 2000). In temperate lowland floodplains with perennial vegetation, infiltration capacity usually exceeds rainfall intensity except for very high magnitude storms (Ward and Robinson, 2000). In the present study, although such high magnitude rainfall events were encountered, the soil moisture deficit in the topsoil was low, possibly as a result of a high capillary fringe maintained by the low PWT and the high

in clay alluvium (Gillham, 1984). Moreover, the presence of cracks in the clay as a result of a drying period probably favoured rapid macropore flow (McDonnell, 1990) that raised the water table to surface saturation before any IEOF was observed. Therefore, IEOF is not considered as a likely mechanism operating in the River Cole floodplain.

5.5.2.3 *Groundwater discharge by lateral subsurface flow and reverse groundwater ridge during baseflow conditions*

Although inevitably some of the floodwaters will return to the river as surface flow, groundwater recharge was shown to delay the recession of the PWT and subsequently contribute to river baseflow. The recession limb occurred in two divergent directions through the B soil horizon in the PM area, from F3 southwards to the river and northwards to the ditch. The highest water table was observed in the middle of the floodplain (well F3), despite the fact that the highest surface elevation was 40 m south in well F2. One likely explanation for this is that the gravel lens and the overlying sandy clay layer were thicker underneath F2, and in conjunction with the steeper hydraulic gradient towards the river, promoted faster drainage. However, the flow rate was <1 L d^{-1} m^{-1} and therefore there was no significant bypass flow through the gravel lens, as observed in gravel lenses in the River Thames catchment (Burt *et al.*, 1999). The drainage towards the opposite direction (ditch) was occurring at a lower slope and flow rate and therefore the PWT height was maintained within the limits of the B horizon (60 cm depth).

The water table dropped below the A soil horizon (30 cm depth) within two days after the flood peak, which is a relatively significant retention time for nitrate transformations in the most biologically active topsoil (Pinay *et al.*, 2000), depending also on the nitrate loading of the flood event and the temperature conditions. However, longer retention times were observed in the B soil horizon, where the heaviest clay alluvium was located. Although there is uncertainty in the theoretical flow rate estimation, it is likely that the PWT was maintained relatively constant during the discharge period through a reversed groundwater ridge under baseflow conditions in the ditch. Unfortunately, the ditch stage was not monitored, and therefore there are no data to support our assumption. There is however an indication that the assumption could be true, since when the ditch dried, the discharge rate of the north side of the floodplain increased and

diurnal fluctuations due to evapotranspiration (ET) became apparent in the hydrographs. Similar daily water table fluctuations were reported for sandy soils up to 3m depth (Krause and Bronstert, 2007), and silty loam soil under cool grass vegetation at <1m depth (Schilling, 2007) for comparable range of ET as the maximum observed in our study for April and May 2007. Therefore it could be argued that ET demand dominated the control of the PWT level when the reverse groundwater ridge ceased, while the discharge rate towards the ditch increased.

In the BZ site, the GW discharged with direction from the field edge (between the wells H7 and H4) towards the river at H10 at higher flow rates compared to the PM. However, the retention time of the GW in the A soil horizon was significantly longer than in the PM, with the hollow areas holding the PWT within 30 cm from the surface for up to 25 days, while during the whole discharge period the PWT did not drop below 1 m depth. One possible explanation for the longer residence time in the BZ could be the contribution of capillary fringe in delaying the lateral subsurface flow towards the river. The amount of capillary rise varies with soil texture and structure and it is estimated to be in the order of 1-2 m in silt loam and silt-clay soils (Gillham, 1984). Other studies in riparian and wetland areas with similar soil textures have attributed shallow water tables to capillary rise often extending to the ground surface, and also contributing to rapid water table responses to falling precipitation (Andersen, 2004; Schilling, 2007). Moreover, the fact that diurnal PWT fluctuations due to ET were not observed in the BZ could also be explained by a high capillary fringe that balanced the ET demands (Andersen, 2004). However, there is no obvious explanation as to why a similar capillary fringe does not operate in the A soil horizon of the PM, despite the high water table (at least in the channel depression and riparian areas), where also the soil texture is similar. The present study focused mainly on lateral GW-SW interactions, but it has become apparent that the vertical soil water component can also influence WT dynamics in riparian zones, which could be resolved in a future study.

During the discharge period of April 2008, there were three to four occasions when the river stage rose above the PWT level under below bankfull conditions and a reversed GW ridge was observed to extend up to 20 m inland in the BZ site. A similar ephemeral reversed GW ridge under baseflow conditions was observed in a French and a Polish riparian zone with silty-clay and loam soil textures (Burt *et al.*, 2002a) as well as in a

low gradient (<1 %) sandy-loam riparian zone in Canada (Vidon and Hill, 2004a). The mechanism behind the formation of the reversed GW ridge under baseflow conditions is similar to the kinematic wave proposed by Jung *et al.* (2004) during bankfull and overbank events.

Finally, although lateral subsurface flow between flood events is observed 55 % of the time during one year, its contribution to saturation conditions in the most biologically active A soil horizon is insignificant compared to overbank flooding. However, it contributes to the maintenance of saturated conditions in the vadose zone (B soil horizon) of the floodplain, therefore giving the opportunity for further nitrate attenuation in the subsurface. Furthermore, in the case of the BZ, the lateral subsurface flow serves as an additional mechanism for nitrate supply to the BZ from the adjacent arable field.

5.5.3 *Hydrochemical patterns along the SW - GW flow paths*

The major sources of nitrate to the floodplain GW were the ditch water, acting as a conduit for collecting hillslope runoff from the surrounding agricultural land, and the river water. The GW nitrate concentration in both sites was consistently lower than the respective concentration in SW, suggesting that following the hydrological connection during high flow events, and the possible subsurface connection during baseflow, nitrate entering the subsurface was reduced via dilution and/or biological transformation. Therefore, nitrate removal is directly controlled by SW - GW interactions (Sanchez-Perez *et al.*, 1999; Takatert *et al.*, 1999), primarily through nitrate supply and secondarily through the control of biogeochemical transformation conditions such as redox and availability of organic carbon (Burt *et al.*, 1999).

5.5.3.1 *Transformation pathways*

Generally, nitrate reduction followed the main surface and subsurface hydrological flow paths. Nitrate reduction across all seasons was observed along the bank seepage flowpaths from the river and ditch. Furthermore, the SW influence on the GW of the wells F1 (riverbank) and F5 (channel depression) through seepage and overbank flooding respectively, was highlighted by the positive correlation of their nitrate concentration. Finally, the nitrate arriving with overland flow in the channel depression

(F5) was shown to be reduced along the surface hydraulic gradient during overbank flooding (F5 to F4) and the subsurface gradient during flood recession (F5 to F6).

Regarding the parallel to the river flow direction from the ditch towards the PM floodplain, nitrate entering the subsurface via seepage was observed to be reduced along the hydraulic gradient from F14 across the floodplain. Similar response to the well F5 was shown for the well F11, intercepting the channel depression and receiving overland flow from the ditch. Finally the ditch water influence was also apparent at the west side of the site, where nitrate concentration in well F9 was reduced along the flow path towards F8.

In the BZ site, nitrate entering the subsurface through river water bank seepage and overbank deposition was reduced towards the middle of the site, while nitrate input from the arable field along the discharge flow path was reduced significantly within 20 m at the middle of the site. Significant nitrate reduction at the 'upslope'- buffer zone boundary (field edge in the BZ case) was also observed by Clément *et al.* (2003) while they attributed low to absent reduction rates at the near stream zone to inadequate nitrate supply. In contrast, Curie *et al.* (2009) observed high nitrate removal rates at near-stream wells due to mixing of SW and GW. In our case, the BZ site displayed effective nitrate removal capacity in both convergent nitrate flow directions throughout the year.

5.5.3.2 *Dilution or biological nitrate removal?*

Several riparian hydrology studies have used Cl^- as a conservative tracer in order to discriminate between nitrate dilution along subsurface flowpaths and biological removal, mainly via denitrification and plant uptake (Clément *et al.*, 2003; Hefting *et al.*, 2006a; Schilling *et al.*, 2006; Curie *et al.*, 2009). Our Cl^- data for the F1-F7 perpendicular transect showed an opposite trend from the nitrate concentration, with increasing Cl^- concentration along the main discharge flowpaths (from F2-F3 towards the river and the ditch) and therefore indicating enrichment of the GW with Cl^-, possibly as a result of weathering processes in the floodplain sediments, rather than dilution. Therefore, nitrate removal rates were estimated without accounting for dilution and ranged between 50 and 97 % throughout the year. Along the subsurface flow path parallel to the river, Cl^- concentration moderately decreased, but nitrate reduction was of a larger magnitude and therefore the ratio NO_3^--N:Cl^- followed largely the same pattern

as nitrate. However, nitrate removal estimates corrected for dilution ranged between 29 and 83 % throughout the year.

With respect to the BZ, elevated Cl^- concentrations in the arable field were observed mainly in spring and summer, possibly due to the use of chloride containing fertilisers that leached into the GW (Curie *et al.*, 2009). The dilution of Cl^- along the flow path towards the middle of the site was significant (range 28 - 66 %) and therefore the corrected nitrate removal rate was lower than in the PM ranging between 2 and 47 %. In contrast, the Cl^- concentration increased in the near stream zone compared to the river water, and therefore no dilution effect was observed. Therefore, the nitrate removal rate between the river and the middle of the site ranged between 54 and 96 % during the year.

Our average nitrate removal rates are in agreement with other studies in shallow water table, temperate agricultural riparian zones Cooper, 1990 (64 - 94 %); Haycock and Pinay, 1993 (60 - 90 %); Clément *et al.*, 2003 (76 - 99 %); Hoffmann *et al.*, 2006 (61 - 74 %); Hefting *et al.*, 2006a (63 %). The average nitrate removal rates, similarly to the nitrate concentration in SW and GW were not significantly different between seasons, indicating that denitrification is more likely to be responsible for the removal rather than plant uptake (Sabater *et al.*, 2003; Hefting *et al.*, 2006a; Hoffmann *et al.*, 2006). Nitrate can also be reduced through pyrite oxidation (Postma *et al.*, 1991), if carbon availability is limited. However, Fe was below detection limit in our GW and SW samples and therefore, heterotrophic denitrification is likely to be the dominant nitrate reduction pathway.

5.5.3.3 *Factors controlling nitrate removal*

The DO concentration in the GW was consistently lower compared to the SW, while in the PM it was always below 3 mg l^{-1}, whereas in the BZ it was <1mg l^{-1}, suggesting even lower redox conditions. Moreover, the nitrate concentration correlated positively with the DO, indicating greater nitrate removal under suboxic or anoxic conditions. Other riparian zone studies that have reported significant nitrate removal via denitrification have consistently shown DO in GW to be <2-3 mg l^{-1} (Duval and Hill, 2007, Schilling and Jacobson, 2008, Hill and Duval, 2009, Curie *et al.*, 2009).

The DOC concentration in both the SW and GW did not show any significant seasonal differences and it was comparable to the DOC concentration of buried channel sediments in an agricultural riparian zone in Canada (Devito *et al.*, 2000), but was higher than DOC concentrations reported in other riparian studies (Baker and Vervier, 2004; Hoffmann *et al.*, 2006; Schilling and Jacobson, 2008; Hill and Duval, 2009). The fact that no significant relationship was observed between nitrate and DOC likely suggests an ample supply of organic carbon from the SW to the floodplain and across the depth of the PWT to support denitrification above limiting conditions.

The pH was very stable throughout the year and it was slightly alkaline in the SW, typical for a predominantly agricultural watershed (Ward and Robinson, 2000), while it moderately fluctuated around neutrality in the GW across both sites. The stability of the pH could be partly explained by the prevalence of reduced conditions promoting denitrification and therefore de-acidification of the groundwater, compared to the acidifying effect of nitrification observed in more aerobic soils (Hefting *et al.*, 2006a). In any case, neutral pH is within the optimum range for denitrification activity (Simek and Cooper, 2002). The specific conductance (SC) was higher in the ditch water and the BZ GW compared to the river and the PM GW. Higher SC has been associated with longer residence time GW (Schilling and Jacobson, 2008), indicative of the slower drainage observed in the BZ GW and the stagnant water conditions during discharge periods in the ditch. Finally, the GW temperature was within the range of suboptimal and optimal denitrification rates (Payne, 1981).

Concluding, the hydrochemical pattern along the SW - GW interaction gradient in the re-connected River Cole floodplain suggested that nitrate supplied mainly via overland and subsurface hydrologic pathways and also via leaching from the agricultural field, can be effectively reduced along the main GW flowpaths via heterotrophic denitrification rather than chemodenitrification or plant uptake; while the high water table maintains suboxic to anoxic conditions, there is adequate supply of DOC from SW and GW sources and the pH and temperature conditions are within the optimal range for effective denitrification.

Chapter 6: Nitrate attenuation processes in the re-connected floodplain of the River Cole.

6.1 *The effect of land use on the relative importance of nitrate attenuation processes*

The aim of this section is to present the potential for nitrate attenuation in the reconnected floodplain of the River Cole, to quantify the relative importance of heterotrophic denitrification and DNRA as attenuation processes and assess the effect of land use in controlling nitrate attenuation.

6.1.1 *Soil physical properties across the land use zones*

The physical properties of the topsoil (0-10 cm) in the four land use zones: Fritillary Meadow (FM); Pasture Meadow (PM); Buffer Zone (BZ); and Grazing Grassland (GG) and in their respective sampling transects are summarised in Table 6.1.1. Although some significant differences in the absolute particle size distribution were found between the four zones (data summarised in Figure 6.1.1), the silt and clay fractions were predominant in all cases ranging between 68 and 88 % of the volume. The textural classification of the four zones according to the UK system (i.e. using 63 μm as the size limit dividing fine sand and silt according to Rowell (1994) is: Silty clay (Fritillary Meadow); Clay loam (Pasture Meadow); Silty clay loam (Buffer Zone); and Clay loam (Grazing Grassland). The predominance of the clay and silt fractions in the topsoil structure gives certain properties to the soil, such as good water holding capacity and increased surface for the binding of nutrient ions; both being conducive to potentially enhanced nitrate attenuation capacity. The higher sand content found in the PM (the middle transect classified as sandy loam) and GG samples (the mill leat transect classified as loam) is probably an indication of sand deposits from the old course of the River Cole prior to channelization. Finally, the higher silt content of the BZ and the FM reflects a frequent overbank inundation regime, found especially in the riparian areas of the two zones, that results in increased deposition of fine particulate matter on the soil surface.

Table 6.1.1: Physical properties of the topsoil in the four land use zones and their respective sampling transects (data are mean values ± 1 standard error, where data are missing are replaced by a - sign).

	Soil type	Dry Bulk Density ($g\ cm^{-3}$)		Water content (%)		Organic matter (%)		Organic carbon (%)		Total Nitrogen (%)		NO_3^--N ($mg\ kg^{-1}$)		TOC/NO_3^-	
		Mean	± 1 SE	Mean	± 1 SE	Mean	± 1 SE	Mean	± 1 SE	Mean	± 1 SE	Mean	± 1 SE	Mean	± 1 SE
Fritillary Meadow (n=15)	Silty clay	0.79	0.05	36.4	3.0	15.8	1.6	6.5	0.7	0.62	0.07	-	-	-	-
Channel depr. (n=5)	Silty clay loam	0.67	0.05	49.2	2.3	21.0	0.8	8.4	0.5	0.89	0.04	-	-	-	-
Middle (n=5)	Silty clay	0.69	0.05	35.9	1.5	18.0	1.5	7.7	0.7	0.64	0.06	-	-	-	-
Riparian (n=5)	Silty clay	1.01	0.05	24.0	2.7	8.6	1.6	3.2	0.9	0.34	0.09	-	-	-	-
Pasture Meadow (n=15)	Clay loam	0.74	0.02	51.6	2.3	13.1	0.7	5.4	0.4	0.43	0.03	9.4	1.7	1.14	0.38
Channel depr. (n=5)	Clay loam	0.68	0.04	58.2	3.6	15.9	0.7	6.6	0.7	0.52	0.03	8.0	0.8	0.70	0.12
Middle (n=5)	Sandy loam	0.76	0.03	48.9	0.3	12.8	0.6	5.6	0.5	0.43	0.03	6.6	2.6	2.23	1.03
Riparian (n=5)	Clay loam	0.78	0.03	47.7	5.1	10.6	1.2	4.0	0.5	0.33	0.02	9.6	1.5	0.47	0.10
Buffer Zone (n=15)	Silty clay loam	0.97	0.07	44.5	3.3	11.0	0.4	5.2	0.3	0.86	0.02	19.6	5.0	0.37	0.04
Riparian (n=5)	Silty clay loam	0.81	0.06	49.0	4.4	12.1	0.9	5.6	0.7	0.89	0.05	33.9	13.5	0.26	0.06
Middle (n=5)	Silty clay loam	0.93	0.12	46.2	8.5	10.9	0.6	5.1	0.6	0.88	0.04	12.9	1.4	0.40	0.04
Arable (n=5)	Silty clay loam	1.19	0.14	38.3	2.1	9.9	0.3	5.0	0.2	0.80	0.04	12.1	1.7	0.44	0.05
Grazing Grassland (n=15)	Clay loam	0.87	0.05	53.6	4.6	13.8	1.1	6.6	0.6	0.86	0.09	21.4	4.5	0.41	0.05
Mill Leat (n=5)	Loam	0.92	0.01	45.6	5.6	12.1	1.3	5.8	0.5	0.86	0.08	14.2	3.1	0.47	0.08
Middle (n=5)	Clay loam	0.66	0.09	70.6	8.4	18.5	1.8	8.7	1.2	0.91	0.26	33.7	11.9	0.44	0.14
Riparian (n=5)	Clay loam	1.04	0.03	44.6	2.8	10.8	0.6	5.2	0.4	0.82	0.09	16.3	1.5	0.33	0.04

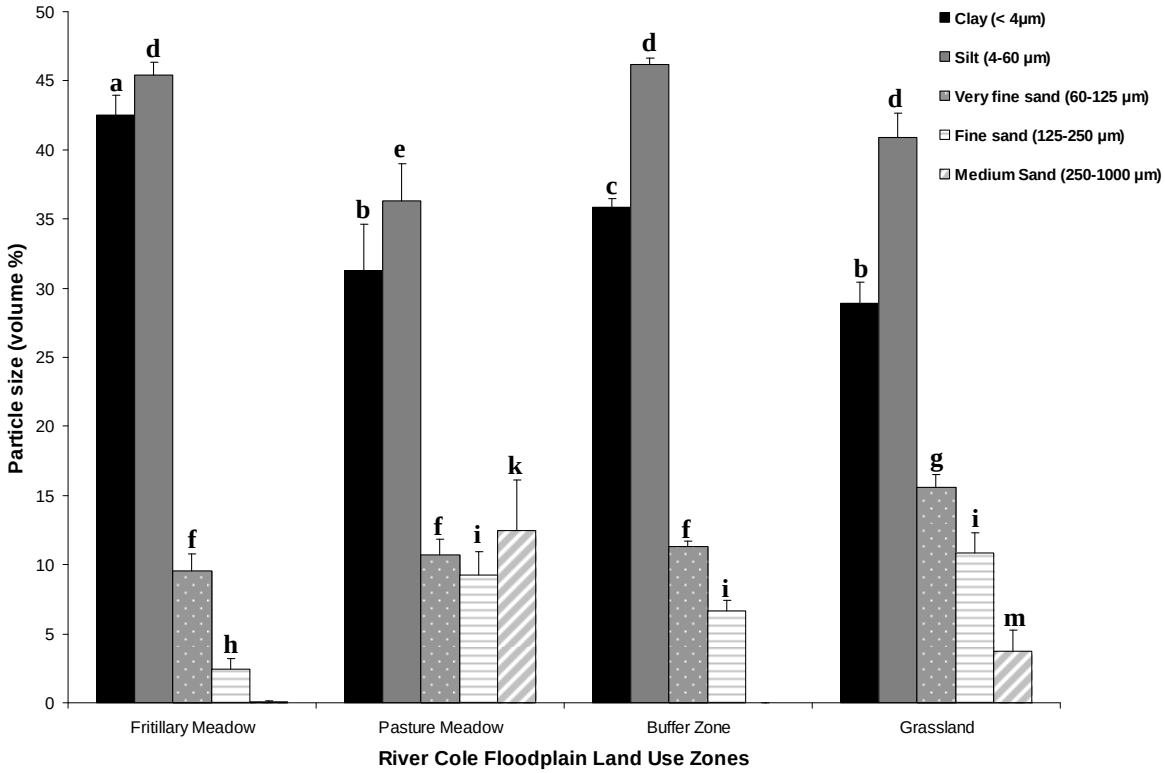

Figure 6.1.1: Absolute particle size distribution (volume %) in the four land use zones of the River Cole (mean + 1 standard error, same lower case letters indicate non significant difference between the means).

The mean dry bulk density was significantly higher (ANOVA; df=56, F= 3.93, P<0.05) in the buffer zone and the grazing grassland compared to the pasture meadow and the fritillary meadow (Figure 6.1.2 A). This is probably a result of the different land uses, with the lower bulk densities associated with the more friable, porous organic soil in the fritillary and pasture meadows, where human intervention is minimal. On the other hand, the higher bulk densities observed in the BZ and GG areas could be attributed to the compaction of the topsoil caused by the grazing animals in GG and the horse riding and angling activities at the BZ site.

Significant differences (Kruskal-Wallis; χ^2=14.5, df=3, P<0.01) were also found between the mean water content of the soil samples in the four land use zones (Figure 6.1.2 B). However, the gravimetric measurement of the water content is only an indication of the moisture conditions in the topsoil on the day of sampling, affected by the weather conditions before and on the sampling date. Since the four land use zones

were sampled at different dates, it is more appropriate to compare the moisture conditions between the sampling transects within each zone, rather than comparing the measurements between zones.

The mean organic matter content of the soil samples from the four land use zones was significantly different (Kruskal-Wallis; χ^2=8.09, *df*=3, *P*<0.05). Significantly less organic matter was found in the buffer zone compared to the FM and PM (Mann-Whitney; *U*=61, *Z*=-2.14, *P*<0.05 and *U*=57.5, *Z*=-2.82, *P*<0.05 respectively), whereas the organic matter in the FM, PM and GG samples did not differ significantly (Figure 6.1.2 C). The difference in the organic matter content could be attributed to the specific flooding regime found in BZ, where overbank inundation is more frequent than in any other zone, and could have led to increased leaching of organic matter from the soil to the river and/or increased mineralisation rates.

In contrast to the results for the organic matter content, the percentage of total organic carbon in the soil samples was not significantly different across the land use zones (Figure 6.1.3 A), ranging from 1.5 % to 12 %, which is a range characteristic of mineral agricultural soils (Rowell, 1994). The C/N ratio, total organic carbon to total nitrogen, (Figure 6.1.3 B) was significantly lower in the upstream zones (ANOVA; *df*=3, *F*=109, *P*<0.001), ranging from 3 to 7, compared to the downstream sites that ranged between 8 and 16. This is potentially due to variability in nitrogen availability between the downstream and upstream sites. It should be noted that although the BZ site is not really upstream, located just downstream of Coleshill bridge, for ease of comparison it is grouped together with the GG site as upstream, whereas the two meadows (FM and PM) are grouped as true downstream sites.

Nitrate and ammonia were significantly lower (ANOVA for NO_3^--N: *df*=2, *F*=6.68, *P*<0.01; ANOVA for NH_4^+-N: *df*=2, *F*=3.7, *P*<0.01) in the PM samples compared to the BZ and GG samples, while nitrite was lower than the other nitrogen species and not significantly different between zones (Figure 6.1.4). The results highlight an important difference between the land use zones, with the grassland and buffer zone areas being located at the foot of the surrounding hillslope and adjacent to an arable field respectively, and therefore more likely to receive increased nitrate inputs through runoff.

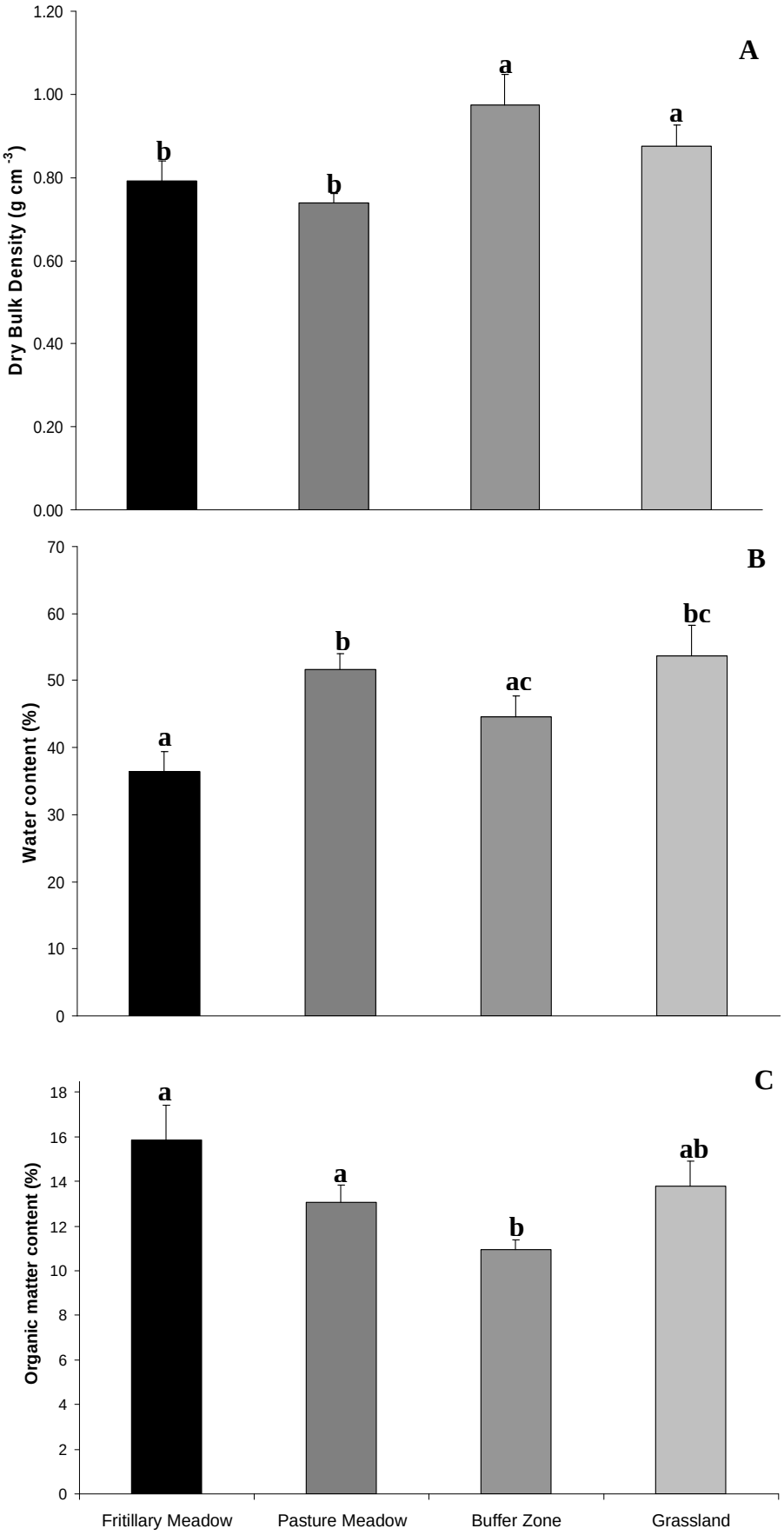

Figure 6.1.2: Mean dry bulk density, water content and organic matter content (+ 1 standard error) in the four land use zones of the River Cole (significant differences indicated with different lower case letters).

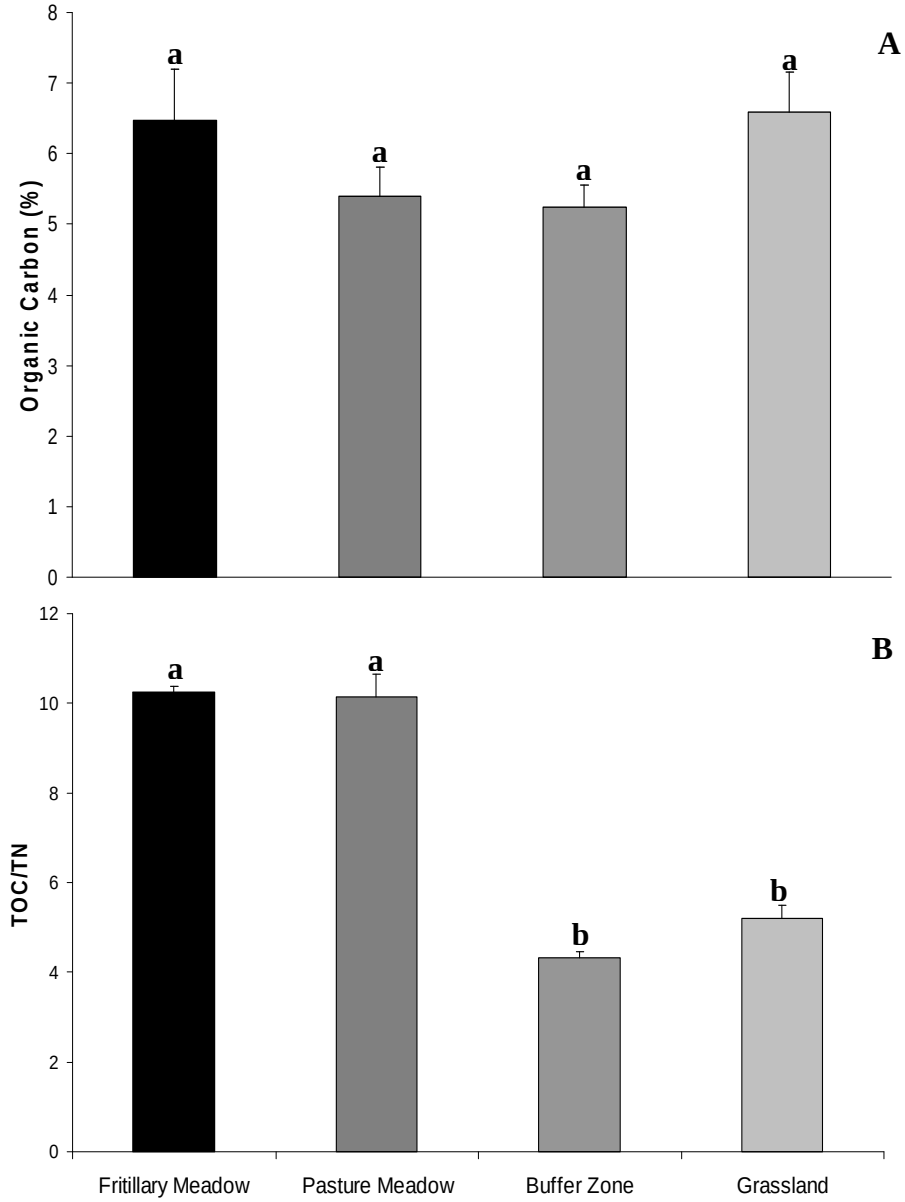

Figure 6.1.3: Mean organic carbon content and TOC/TN ratio (+ 1 standard error) in the four land use zones of the River Cole (significant differences indicated with different lower case letters)

The fact that higher concentrations for both NH_4^+-N and NO_2^--N were found in the upstream sites (Figure 6.1.4), rather than the PM zone, is an indication of possibly higher N turnover rates upstream. Build-up of ammonium could be attributed to enhanced mineralisation rates following soil disturbance, and the accumulation of nitrite, an intermediate in both the denitrification and DNRA processes, attributed to reduced conditions induced by frequent flooding.

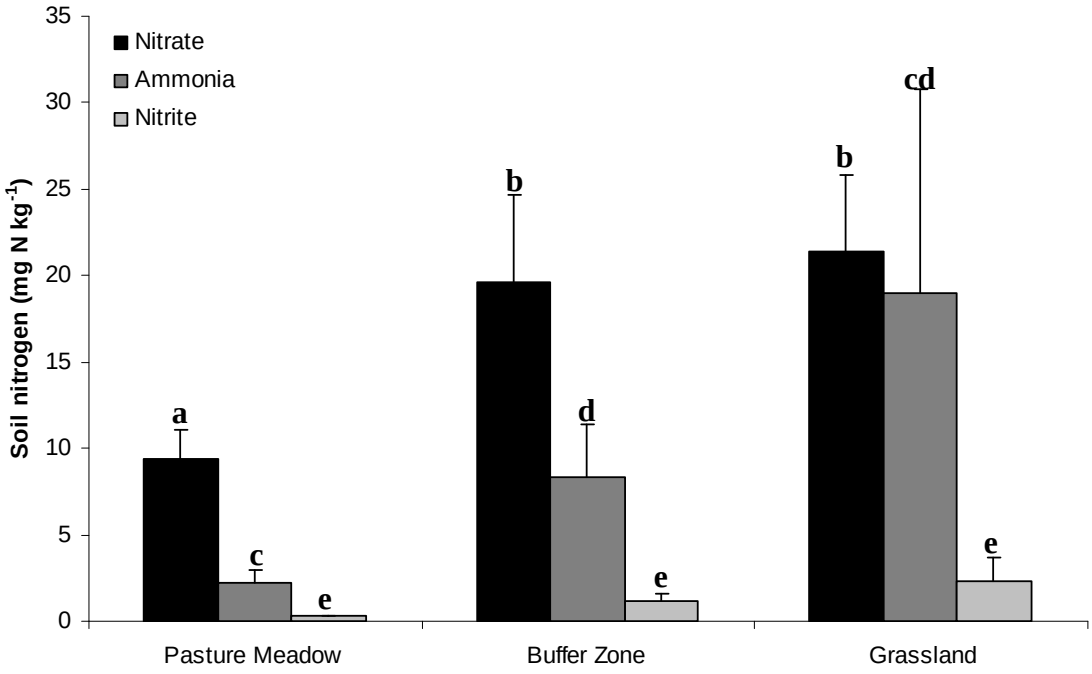

Figure 6.1.4: Mean concentrations of NO_3^--N, NH_4^+-N and NO_2^--N (+ 1 standard error) in three land use zones of the River Cole floodplain. Significant differences indicated with different lower case letters.

By combining the organic carbon and NO_3^--N data, the ratio of TOC: NO_3^--N (Silver *et al.*, 2005) can be estimated (Table 6.1.1), indicating the relative availability of organic carbon for nitrate respiration over the available nitrate. The ratio is significantly higher in the PM samples compared to the BZ and GG (Figure 6.1.5), which are not significantly different between each other (ANOVA; df=2, F=5.68, P<0.01). The results indicate that there are significant differences in the relative availability of electron donors (organic carbon) and electron acceptors (nitrate) in the four land use zones and this could potentially lead to significant differences in the relative importance of nitrate attenuation processes in these zones.

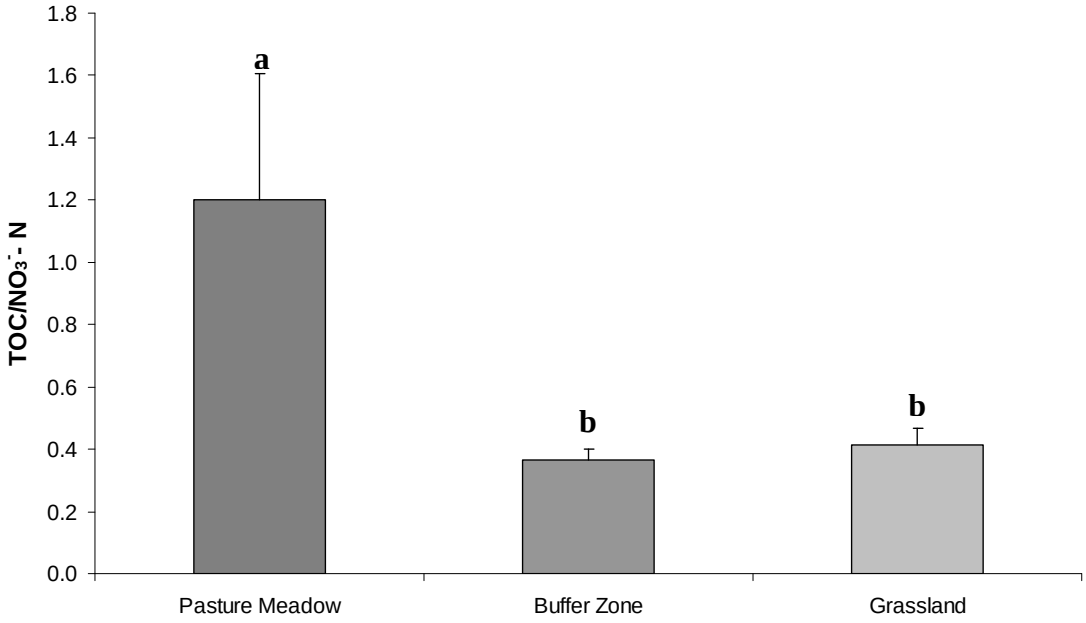

Figure 6.1.5: Mean TOC/NO_3^--N ratio (+ 1 standard error) in three land use zones of the River Cole (NO_3^--N data not available for FM, significant differences indicated with different lower case letters).

6.1.2 *AnMOC and methane production potential across the land use zones*

The Anaerobically Mineralisable Organic Carbon (AnMOC), one way of measuring the anaerobic respiration rate of the microbial biomass (Rowell, 1994), showed no significant differences across the FM, PM and BZ sites (Table 6.1.2 and Figure 6.1.6 A), and only the GG had significantly higher AnMOC (ANOVA; df=3, F=11.6, P<0.001). This was probably due to the application of animal manure on this site as a consequence of grazing and the creation of carbon 'hotspots', hence the high variability indicated by the standard error value, that could potentially affect the rates of nitrogen retention processes.

AnMOC can also be used for describing the lability of organic carbon when expressed as the amount of carbon mineralised per gram of total organic carbon (TOC) per day (Dauwe *et al.,* 2001). Similar to the anaerobic mineralisation rate results, the GG site had significantly higher (ANOVA; df=3, F=17.29, P<0.001) mean amount of labile organic carbon compared to the other three land use zones that were lower and not significantly different between them (Table 6.1.2 and Figure 6.1.6 B).

The methane production rate of field moist soil incubated under anaerobic conditions could be used as a proxy for the redox condition of the topsoil (Table 6.1.2 and Figure 6.1.6 C). The results showed no significant difference in the methane production potential of the topsoil across the four land use zones (Kruskal Wallis; χ^2=3.35, *df*=3, *P*>0.05). The amount of methane emitted during the anaerobic incubations was proportionally lower than the amount of CO_2 released from the anaerobic mineralisation of the organic carbon, and therefore it should be attributed to methanogens' respiration rather than fermentative processes that would have resulted in the production of equal amounts of methane and carbon dioxide (Middelburg *et al.*, 1996). However, the process of methanogenesis occurs at the lowest redox potential; E_h below -400 mV (Oremland, 1988), and therefore the methane production potential rates were only indicative of very reduced conditions, which were mainly found in the riparian sampling transects of each zone. Therefore, averaging the measurements per site results in smoothing these differences and creating high standard errors of the means.

Table 6.1.2: Anaerobic mineralisation rate (AnMOC), lability of organic carbon and methane production potential of the topsoil in the four land use zones and their respective sampling transects (data are mean values ± 1 standard error).

	AnMOC		**Labile org. carbon**		**Methane**	
	CO_2 (µmol kg^{-1} d^{-1})		**(µmol CO_2 g^{-1} TOC d^{-1})**		**CH_4 (µmol kg^{-1} d^{-1})**	
	Mean	**± 1 SE**	**Mean**	**± 1 SE**	**Mean**	**± 1 SE**
Fritillary Meadow (n=15)	918.6	103.5	15.2	1.4	7.6	3.7
Channel depr. (n=5)	1322.1	78.7	15.8	1.0	0.0	0.0
Middle (n=5)	979.0	56.5	12.9	1.1	1.1	1.0
Riparian (n=5)	454.8	88.2	16.8	3.9	21.6	8.3
Pasture Meadow (n=15)	767.8	56.8	15.3	1.4	1.1	0.5
Channel depr. (n=5)	738.3	130.2	11.6	2.0	0.4	0.3
Middle (n=5)	846.1	77.1	15.8	2.4	0.0	0.0
Riparian (n=5)	719.1	92.6	18.6	2.1	2.6	1.0
Buffer Zone (n=15)	970.5	131.0	17.9	1.6	1.5	0.9
Riparian (n=5)	1174.3	239.9	20.0	1.8	4.1	2.4
Middle (n=5)	1192.9	231.0	22.9	2.0	0.4	0.2
Arable (n=5)	544.5	32.6	10.8	0.6	0.0	0.0
Grazing Grassland (n=15)	2260.2	446.0	40.7	8.0	2.8	0.8
Mill Leat (n=5)	1733.1	263.4	30.0	3.8	1.6	0.4
Middle (n=5)	3929.7	1251.1	63.7	21.4	0.6	0.5
Riparian (n=5)	1451.8	106.9	28.4	2.6	5.5	1.5

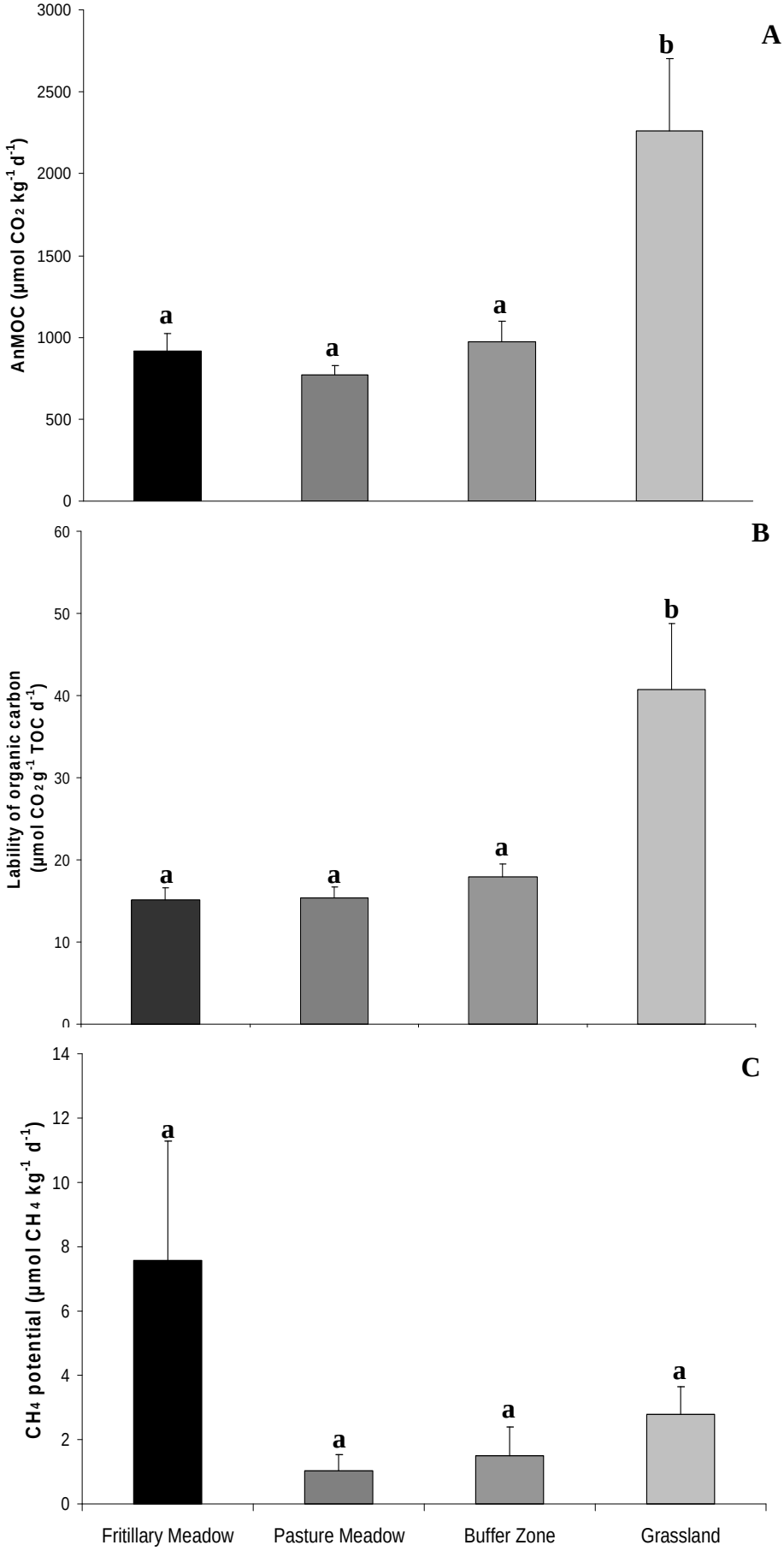

Figure 6.1.6: Mean AnMOC, lability of organic carbon and methane production potential (+ 1 standard error) in the four land use zones of the River Cole (significant differences indicated with different lower case letters).

6.1.3 *Spatial ordination of the land use zone samples*

Principal Component Analysis (PCA) was employed to explore which combinations of soil physical properties, 'principal components', are likely to provide the maximum discrimination between individual soil samples (Dytham, 2003). The properties used in the analysis were: (i) dry bulk density; (ii) organic matter content; (iii) the particle size fractions; clay, silt and very fine sand contents; (iv) AnMOC; (v) organic carbon content; (vi) total organic carbon to total nitrogen ratio (TOC/TN); and (vii) the labile organic carbon content (μmol CO_2 g^{-1} TOC d^{-1}). The water content variable was not used because there is little or no meaning in comparing measurements made on different dates and weather conditions, as mentioned earlier. Furthermore, none of the soil NO_3^- - N content measurements was used in the PCA, since there were no measurements for the FM samples and therefore all these samples would have been excluded from the derivation of principal factors. The effect of N availability is instead introduced with the TOC/TN ratio. The methane production potential variable was also not used due to the fact that it was not significantly different between land use zones and also because of the nature of the measurements that are concentrated in the riparian samples, which have high variability and a non-normal distribution.

The PCA method assumes: linear relationships between all the variables; no inter-correlation of the component axes; continuity and normal distribution of the data (Dytham, 2003). A scatter plot matrix between all the variables used in PCA indicated that all relationships were linear. As for the issue of no correlation between the component axes, this could be a potential problem since the majority of the variables used have an organic carbon component and therefore are very likely to be inter-correlated. However, since PCA is only used for exploring the distribution of data and for deriving further hypotheses regarding the environmental variables that are likely to differentiate the land use zones and possibly have an effect on nitrate attenuation processes, the assumption of inter-correlation has a minor role. Finally, the data used in the PCA were continuous and normally distributed.

The PCA generated four principal axes (Table 6.1.3). The first two are the most important with eigenvalues of 2.9 and 2.0 respectively. The first axis explained 36.6 % of the variation between samples, whereas the second axis explained 25.2 %. The variables associated more closely with the first axis were the organic matter content

(weighting 0.947), the organic carbon content (weighting 0.884) and the bulk density (weighting -0.794). The second principal axis was formed mainly by the weightings of the AnMOC (0.901) and the labile organic carbon content (0.861). The third component factor had strong association with the silt and clay contents with 0.910 and 0.870 weightings respectively.

Table 6.1.3: The principal components (axes) generated by the PCA, their respective eigenvalues, the % of variance explained by each component and the cumulative % of variance explanation.

Axes	Eigenvalues	% of Variance	Cumulative %
1	2.931	36.64	36.64
2	2.019	25.24	61.88
3	1.839	20.44	82.32
4	0.792	8.79	91.11

Plotting the position of individual samples on the first two component axes generated Figure 6.1.7. What is immediately apparent from the graph is the grouping of the individual samples into their respective land use zone groups, especially for the BZ and GG samples, whereas there is considerable overlapping between the FM and PM samples. A second interesting point is that the grouping is mainly due to the second principal axis rather than the first. Indeed, One-way ANOVA between the position of samples on axis 1 showed significant difference only between the BZ and FM samples (ANOVA; df=3, F=2.87, P<0.05), whereas One-way ANOVA between the samples' position on axis 2 showed significant differences (ANOVA; df=3, F=41.55, P<0.001) between the BZ and GG samples, and only the FM and PM samples were not significantly different.

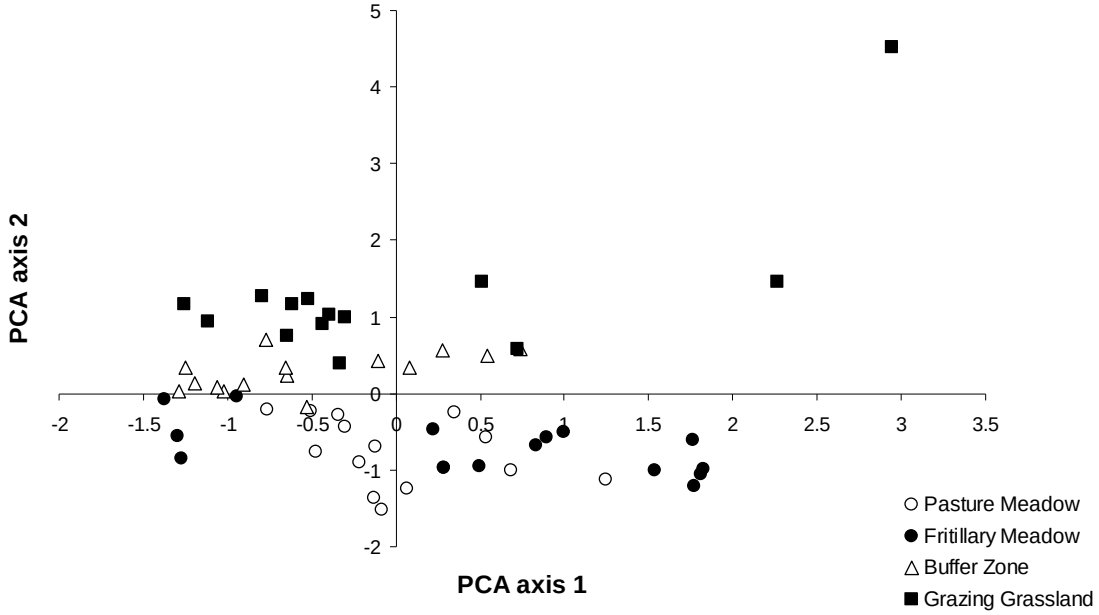

Figure 6.1.7: Plot of individual soil samples from all land use zones according to their principal components in PCA.

The overlapping of the meadow samples (FM and PM) and the separation of BZ and GG samples from the rest was even more clearly shown by using Discriminant Function Analysis (DFA) with the same environmental variables (Figure 6.1.8). The difference between PCA and DFA is that in DFA, individual samples are assigned to groups before the start of the test. Then variable weightings are calculated so that they maximise the difference between groups instead of individual samples. The power of the weightings is tested by naming one individual sample from the dataset as 'unknown' and then using the variable weightings to assign it to one of the groups. The hit rate is a measure of the power of the test to discriminate real unknowns (Dytham, 2003).

The first two axes with eigenvalues of 13.1 for the first and 1.1 for the second, explain 88.4 % and 7.3 % of the variation between the four land use zones, respectively. The variables with the highest weightings for the first axis are the AnMOC (1.383) and the total organic carbon to total nitrogen ratio (-1.058) that shows a negative correlation with the first discriminating axis. The second axis that explains only 7.3 % of the variation is strongly associated with the labile organic carbon content (2.335) and the organic carbon content (1.451). Finally, the testing of the model's weightings showed that 91.5 % of originally grouped samples were correctly assigned to groups.

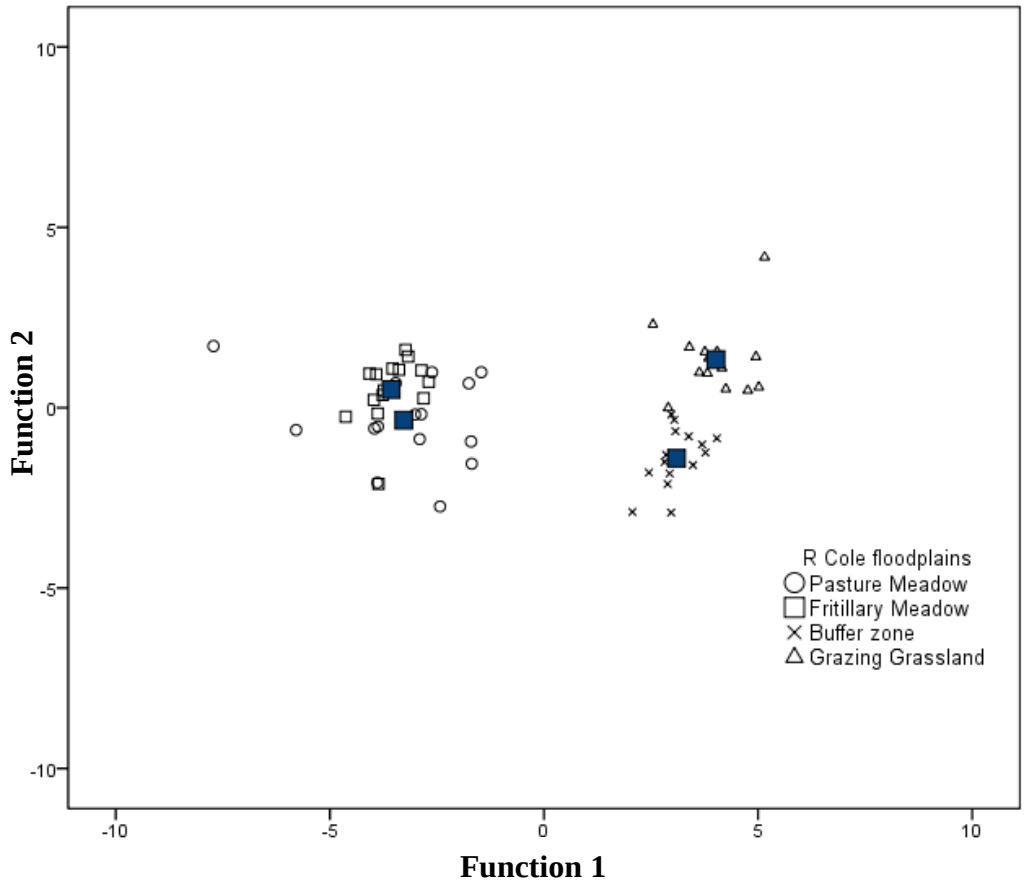

Figure 6.1.8: Plot of individual soil samples grouped in land use zones according to the discriminant functions in DFA. The large squares represent the centroid of each group.

The results from PCA indicate a gradient in individual samples, where the samples from the GG and the BZ are separated from the rest, whereas the FM and PM samples form an agglomeration of meadow samples. This is an indication of different conditions between three types of land use (pasture meadow, buffer zone and grazing grassland) found in the reconnected floodplain of the River Cole. The main reasons for this discrimination between land use zones, according to PCA, seems to be the availability of labile organic carbon and the carbon mineralisation rate as expressed from the AnMOC measurement. The groups identified from the ordination of the samples in the PCA were used in the DFA, which confirmed the grouping of samples in three distinct land use zones and indicated that apart from the labile organic carbon and the mineralisation rate (AnMOC), the organic carbon to nitrogen ratio is potentially playing a role in differentiating the land uses. It is therefore interesting to examine whether nitrate attenuation processes are correlated to a specific land use type and whether the principal factors differentiating land uses have a marked effect on the nitrogen cycling processes as well.

6.1.4 *Denitrification potential across the land use zones*

All the topsoil samples from all the land use zones showed potential for denitrification that ranged from 5.3 to 62.8 mg N kg^{-1} dry soil d^{-1}. The mean potential denitrification rates and ± 1 SE for all the land use zones and their respective sampling transects are shown in Table 6.1.4.

Table 6.1.4: Potential denitrification rates in the four land use zones and their respective sampling transects (data are mean values ± 1 standard error).

	Denitrification	
	mg N kg^{-1} soil day^{-1}	
	Mean	**± 1 SE**
Fritillary Meadow (n=15)	10.73	1.02
Channel depr. (n=5)	13.89	1.39
Middle (n=5)	8.53	1.42
Riparian (n=5)	9.76	1.76
Pasture Meadow (n=15)	14.77	1.30
Channel depr. (n=5)	16.71	3.37
Middle (n=5)	12.50	0.53
Riparian (n=5)	15.09	1.96
Buffer Zone (n=15)	15.81	1.91
Riparian (n=5)	19.26	3.43
Middle (n=5)	16.74	4.04
Arable (n=5)	11.42	1.50
Grazing Grassland (n=15)	24.06	3.98
Mill Leat (n=5)	25.73	6.38
Middle (n=5)	33.39	7.95
Riparian (n=5)	13.05	3.12

The FM samples displayed significantly lower denitrification rates (ANOVA; df=3, F=5.96, P<0.01), the PM and the BZ samples were not significantly different between each other, while the potential denitrification rate of the GG samples was significantly higher from the rest of the land use zones (Figure 6.1.9).

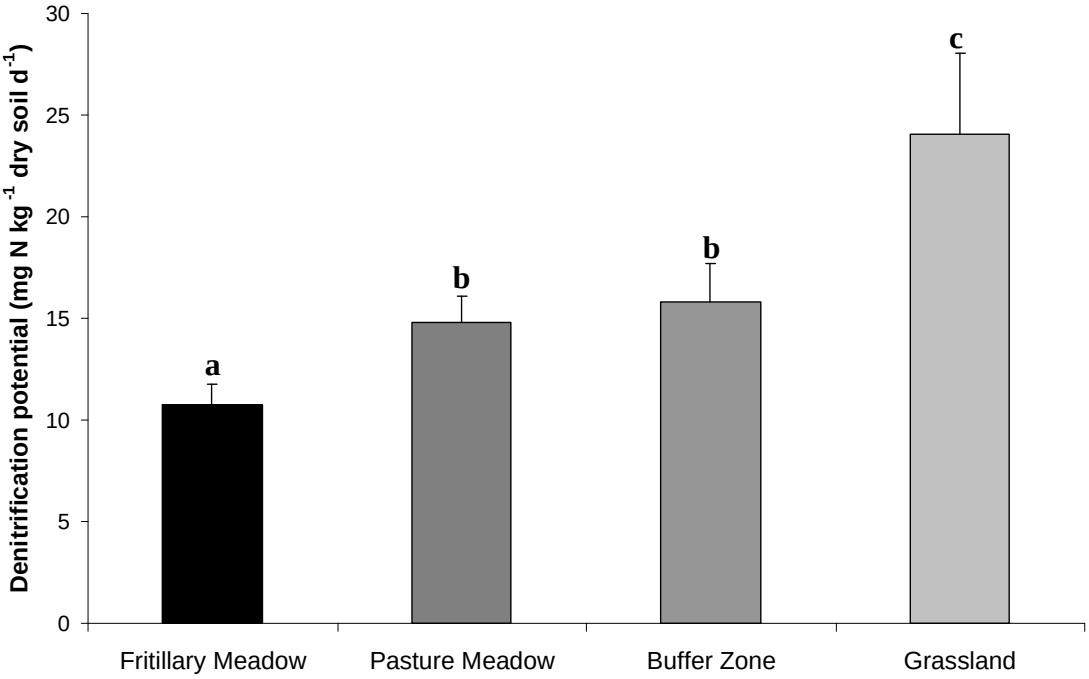

Figure 6.1.9: Mean potential denitrification rates (+ 1 standard error) in the four land use zones of the River Cole (significant differences indicated with different lower case letters).

A combination of Pearson Product-Moment (parametric) and Spearman rho (non-parametric) correlations was performed between the potential denitrification rate, the AnMOC, the lability of organic carbon, the methane production potential rate and the physical properties of the topsoil (Table 6.1.5). Significant positive correlation (Pearson; r=0.60, n=59, P<0.01) was found between the denitrification potential and the AnMOC measurement (Figure 6.1.10). The denitrification potential also correlated significantly (Pearson; r=0.52, n=58, P<0.01) with the lability of organic carbon (Figure 6.1.11).

Table 6.1.5: Correlation matrix between the potential denitrification rate, AnMOC, lability of organic carbon, methane production potential and the physical properties of the topsoil of the four land use zones of the River Cole. Underlined correlation coefficients are products of Spearman rho correlation whereas non-underlined are products of Pearson Product-Moment correlation. ** Correlation is significant at the 0.01level and *Correlation is significant at the 0.05 level.

Variables/Correlation coefficients		Denitrification potential	AnMOC	Org. carbon lability	Methane emission	Organic matter content	Organic carbon %	TOC/TN	Soil nitrate	Soil nitrite	TOC/NO_3^-
Denitrification potential	*R or rho*	1									
	P	.									
	N	60									
AnMOC	*R or rho*	**0.599****	1								
	P	0.000	.								
	N	59	59								
Org. carbon lability	*R or rho*	**0.521****	**0.712****	1							
	P	0.000	0.000	.							
	N	58	58	58							
Methane emission	*R or rho*	0.136	0.200	**0.523****	1						
	P	0.313	0.140	0.000	.						
	N	57	56	55	57						
Organic matter content	*R or rho*	0.258*	**0.468****	-0.107	-0.280*	1					
	P	0.047	0.000	0.426	0.035	.					
	N	60	59	58	57	60					
Organic carbon %	*R or rho*	0.297*	**0.528****	-0.044	-0.278*	**0.858****	1				
	P	0.021	0.000	0.742	0.036	0.000	.				
	N	60	59	58	57	60	60				
TOC/TN	*R or rho*	-0.262*	-0.231	**-0.404****	0.041	0.325*	0.110	1			
	P	0.044	0.078	0.002	0.760	0.011	0.405	.			
	N	60	59	58	57	60	60	60			
Soil nitrate	*R or rho*	**0.505****	**0.617****	**0.490****	**0.402****	**0.431****	0.343*	-0.240	1		
	P	0.000	0.000	0.001	0.008	0.003	0.021	0.113	.		
	N	45	44	43	42	45	45	45	45		
Soil nitrite	*R or rho*	**0.592****	0.052	0.243	0.248	0.283	0.263	-0.143	**0.435****	1	
	P	0.000	0.736	0.117	0.113	0.060	0.081	0.348	0.003	.	
	N	45	44	43	42	45	45	45	45	45	
TOC/NO_3^-	*R or rho*	-0.144	-0.141	**-0.417****	**-0.460****	0.055	-0.030	**0.387****	**-0.864****	-0.355*	1
	P	0.345	0.361	0.005	0.002	0.717	0.846	0.009	0.000	0.017	.
	N	45	44	43	42	45	45	45	45	45	45

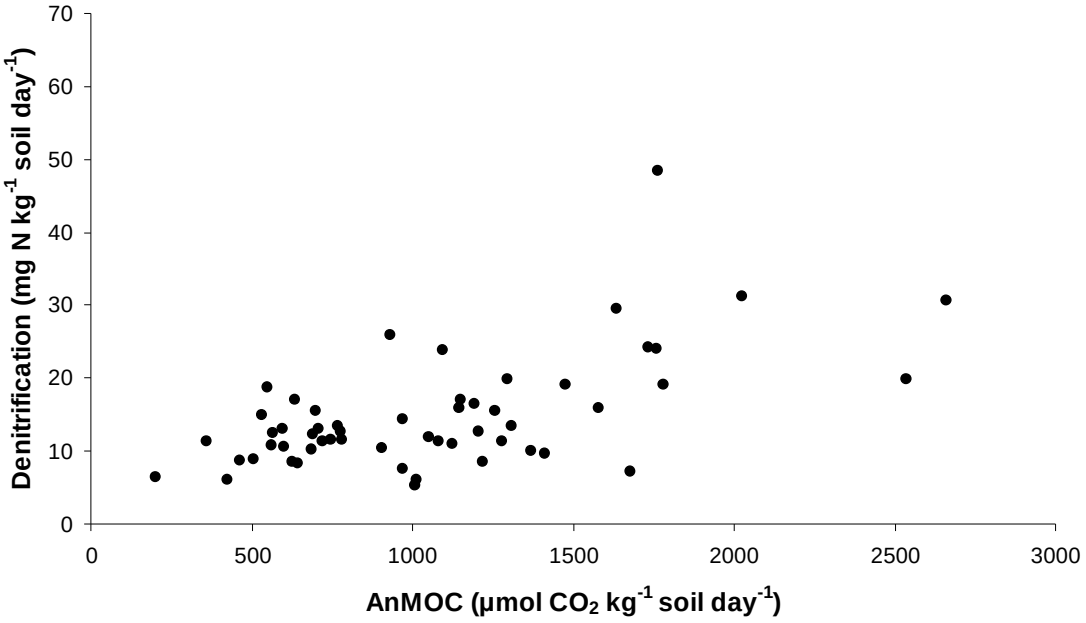

Figure 6.1.10: Scatter plot of potential denitrification rates in all land use zones against the production of CO_2 from the anaerobically mineralisable organic carbon (AnMOC) (r=0.60, n=59, P<0.01).

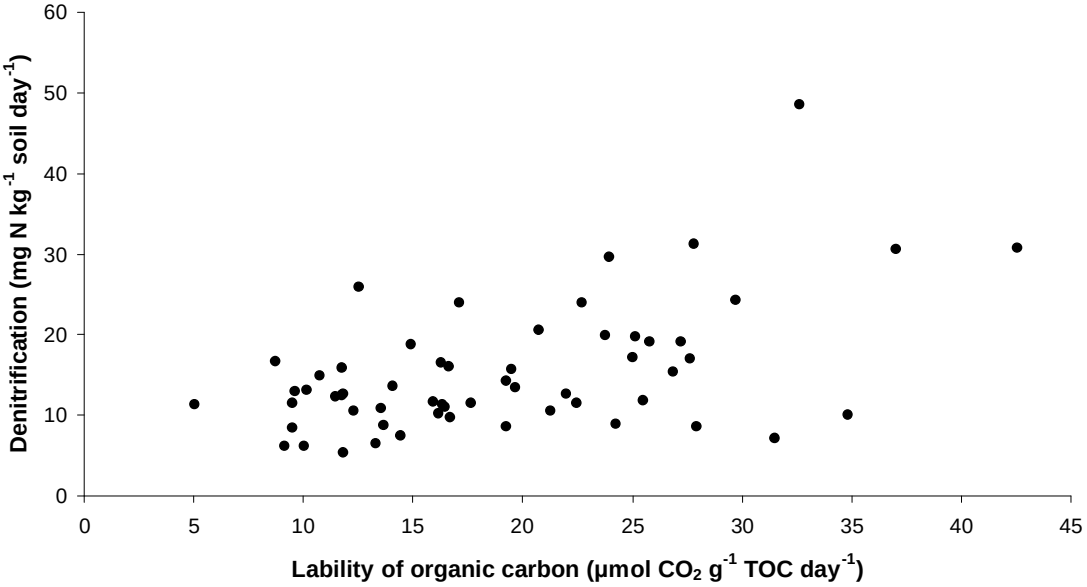

Figure 6.1.11: Scatter plot of potential denitrification rates in all land use zones against the lability of organic carbon (r=0.52, n=58, P<0.01).

Significant positive correlation was observed between denitrification rates and soil nitrate and nitrite content (Pearson; r=0.51, n=45, P<0.01 and r=0.59, n=45, P<0.01 respectively). These results possibly indicate a partial regulation of the denitrification activity in the four land use zones by the availability of nitrate in the topsoil, and also highlight nitrite as one of the products of incomplete denitrification. All of the different organic carbon measurements correlated positively with the potential denitrification rates (Table 6.1.5). However, AnMOC and the labile organic carbon expression were the more significant, indicating that they potentially give a better estimate of the fraction of organic carbon used as an electron donor by the nitrate respiring bacteria. The organic carbon measurements that correlated significantly with the denitrification activity were also highlighted by the PCA analysis of the soil samples in the four land use zones, indicating that the discriminating factors between the different land uses could possibly also have a marked effect on denitrification activity.

Multiple regression forward analysis (MRA) between the environmental variables and the denitrification activity produced similar results to the Pearson product moment correlation. Specifically, the AnMOC measurement explained 42 % of the variance in the potential denitrification rates (MRA; r^2=0.423, df=42, P<0.01), followed by the lability of organic carbon with 29 % explanatory power (MRA; r^2=0.29, df=58, P<0.01) and finally the soil nitrate content explaining 26 % of the variance in denitrification activity (MRA; r^2=0.257, df=43, P<0.01).

Therefore the available labile organic carbon seems to be mainly responsible for a gradient of denitrification activity from high rates found in the carbon rich grazing grassland, to intermediate rates found in the buffer zone and pasture meadow (the main floodplains affected by the increased hydrological connectivity following the restoration), to lower rates found in the fritillary meadow, which is the least impacted floodplain in terms of external carbon inputs and flooding frequency.

6.1.5 *Dissimilatory Nitrate Reduction to Ammonium (DNRA) potential across the land use zones*

From the 90 nmol $^{15}NO_3^-$ added per mL slurry per sample, 63.8 ± SE 1.8 % on average was recovered as $^{30}N_2$. The mean recovery was highest in the BZ samples, 71.7 ± SE 3.1 %, lowest for the FM samples (52 ± SE 2.4 %), whereas the PM and the GG samples had mean recoveries of 61.4 ± SE 1.9 % and 70.2 ± SE 4.3 % respectively. The recovery (%) was significantly different across land use zones, with only the recoveries for the GG and BZ samples not being significantly different between each other (ANOVA; df=3, F=8.67, P<0.001).

However, the mean concentration of nitrate in the samples after the 6 hour incubation was 22 μM (± SE 6), whereas from the amounts recovered as $^{30}N_2$ it would be expected to have 33 μM (± SE 2) of nitrate remaining in the sample pool. Therefore, there was a deficit of 19 μM (± SE 2) of nitrate on average in the experiment budget. Likely fates for the 'missing' nitrate could be intermediate paths of denitrification that produce NO_2^- or N_2O instead of N_2, the simultaneous occurrence of DNRA, or assimilation of nitrate into bacterial biomass. Nitrite was measured in the samples after the completion of the experiment, and its average concentration was 5 μM (± SE 0.6), thus only 26 % of the unaccounted for NO_3^-.

One possible fate for the unaccounted ^{15}N-labelled nitrate in the $^{30}N_2$ produced from denitrification could be the simultaneous occurrence of dissimilatory nitrate reduction to ammonium (DNRA). Using the same slurry samples after the completion of the timed experiment for the denitrification activity, the NH_4^+ was extracted from the sample and then subjected to a microdiffusion-oxidation assay with hypobromite to convert $^{15}NH_4^+$ to $^{29}N_2$ for subsequent quantification with a continuous flow isotope ratio mass spectrometer.

DNRA was indeed occurring simultaneously with denitrification in all the samples from all the land use zones. However, as shown in Table 6.1.6, denitrification rates were higher than DNRA rates in all cases. DNRA ranged from 0.02 to 2.64 mg N kg^{-1} dry soil d^{-1} and the mean rates across the four land use zones were not significantly different (Kruskal-Wallis Test; χ^2=4.86, df=3, P>0.05). However, the highest rate was observed

in the GG samples, followed by the FM samples then the PM and finally the BZ samples (Figure 6.1.12).

Table 6.1.6: Potential denitrification and DNRA rates in the four land use zones and their respective sampling transects (data are mean values ± 1 standard error).

	Denitrification mg N kg^{-1} soil day^{-1}		**DNRA** mg N kg^{-1} soil day^{-1}	
	Mean	**± 1 SE**	**Mean**	**± 1 SE**
Fritillary Meadow (n=15)	10.73	1.02	0.43	0.17
Channel depr. (n=5)	13.89	1.39	0.16	0.06
Middle (n=5)	8.53	1.42	0.13	0.05
Riparian (n=5)	9.76	1.76	1.01	0.43
Pasture Meadow (n=15)	14.77	1.30	0.39	0.06
Channel depr. (n=5)	16.71	3.37	0.49	0.13
Middle (n=5)	12.50	0.53	0.21	0.05
Riparian (n=5)	15.09	1.96	0.46	0.11
Buffer Zone (n=15)	15.81	1.91	0.35	0.03
Riparian (n=5)	19.26	3.43	0.38	0.06
Middle (n=5)	16.74	4.04	0.39	0.07
Arable (n=5)	11.42	1.50	0.29	0.02
Grazing Grassland (n=15)	24.06	3.98	0.49	0.07
Mill Leat (n=5)	25.73	6.38	0.61	0.14
Middle (n=5)	33.39	7.95	0.60	0.13
Riparian (n=5)	13.05	3.12	0.26	0.05

Although the four land use zones of the River Cole re-connected floodplain do not seem to differentiate in terms of their potential DNRA rates, the relative importance of denitrification versus DNRA, expressed by the ratio of mean denitrification potential/ mean DNRA potential rate, is different between the four zones (Figure 6.1.13). DNRA becomes increasingly important moving gradually from the upstream towards the downstream sites. Therefore, although the GG site displayed the highest DNRA, due to also having the highest denitrification potential rate, DNRA is 50 times less important than denitrification. In contrast, the FM site with the second highest DNRA rate but the lowest denitrification potential rate, results in denitrification being only 25 times higher than DNRA.

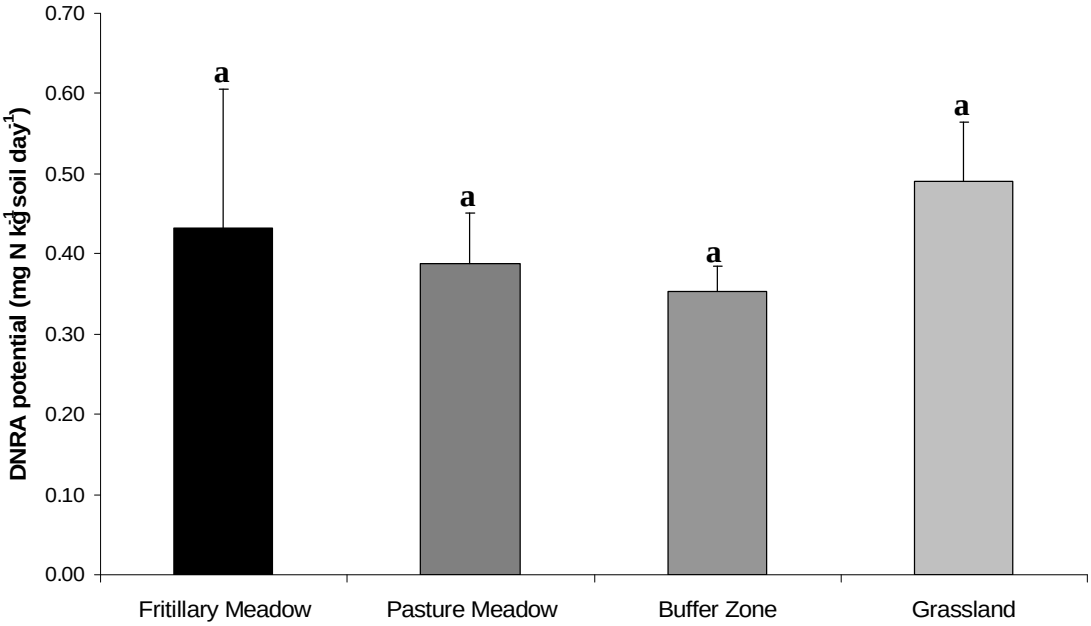

Figure 6.1.12: Mean DNRA rates (+ 1SE) in the four land use zones of the River Cole (same lower case letters indicate non significant difference of the means).

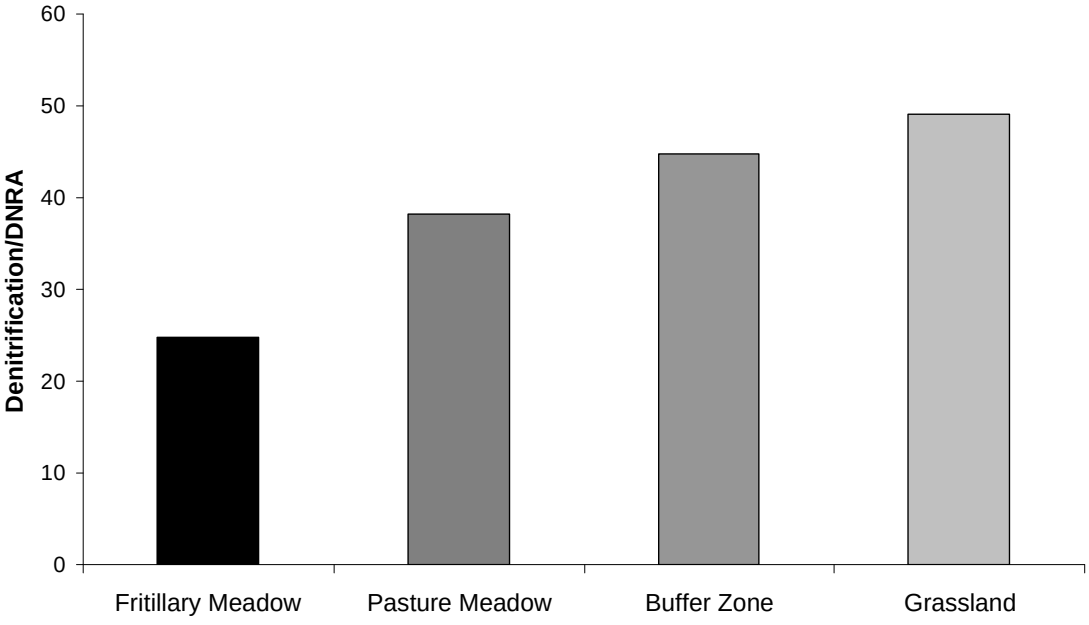

Figure 6.1.13: Relative importance of denitrification over DNRA potential rates in the four land use zones of the re-connected floodplain of the River Cole.

DNRA had no significant effect on the final ammonium concentration in the slurry samples. However, DNRA enriched the ammonium pool with ^{15}N in all the samples, although the enrichment was not greater than 1 % in any case. As a result of that, DNRA contributed on average to 2 % recovery of the initial ^{15}N-labelled nitrate as $^{29}N_2$. Therefore, the deficit in the nitrate budget of the experiment remained after the formation of nitrite and DNRA which accounted for 28 % of the introduced nitrate. The other possible fates of the ^{15}N-labelled nitrate would be the formation of ^{15}N labelled N_2O, from incomplete denitrification, which was not measured in this set of experiments, and nitrate assimilation in bacterial biomass during the course of the experiment.

A combination of Pearson Product-Moment (parametric) and Spearman rho (non-parametric) correlations was performed between the potential DNRA rate and; denitrification rate, AnMOC, lability of organic carbon, methane production potential rate and the physical properties of the topsoil (Table 6.1.7). DNRA correlated significantly (Spearman; rho=0.57, n=59, P<0.01) with the denitrification activity (Figure 6.1.14), indicating the simultaneous occurrence of the two processes. Moreover, DNRA showed significant positive correlation (Pearson; r=0.36, n=57, P<0.01) with the labile organic carbon (Figure 6.1.15) and the soil nitrate content (Spearman; rho=0.42, n=45, P<0.01). Finally, DNRA correlated significantly (Spearman; rho=0.47, n=56, P<0.01) with the methane production potential in the land use zone samples (Figure 6.1.16). If the methane production potential can be regarded as a proxy for the redox conditions in the topsoil of the land use zones, then there is an indication for increased DNRA activity in areas where reduced conditions are found more often. The correlation results suggested that DNRA was regulated by the prevalence of reduced conditions, the availability of soil nitrate and secondarily by the availability of labile organic carbon.

Multiple forward regression analysis confirmed the correlation findings. The methane production potential explained 26 % of the variance in DNRA activity (MRA; r^2=0.26, df=48, P<0.01), followed by the soil nitrate content with 15 % (MRA; r^2=0.15, df=44, P<0.01) and finally the lability of organic carbon with 13 % (MRA; r^2=0.13, df=56, P<0.01).

Table 6.1.7: Correlation matrix between the potential DNRA rate, the potential denitrification rate, AnMOC, lability of organic carbon, methane production potential and the physical properties of the topsoil of the four land use zones of the River Cole. Underlined correlation coefficients are products of Spearman rho correlation whereas non-underlined are products of Pearson Product-Moment correlation. ** Correlation is significant at the 0.01level and *Correlation is significant at the 0.05 level.

Variables/Correlation coefficients		Denitrification potential	DNRA	AnMOC	Org. carbon lability	Methane emission	Organic matter content	Organic carbon %	TOC/TN	Soil nitrate	Soil nitrite	TOC/NO_3^-
Denitrification potential	*R or rho*	1										
	P	.										
	N	60										
DNRA	*R or rho*	**0.566****	1									
	P	0.000	.									
	N	59	59									
AnMOC	*R or rho*	**0.599****	0.289*	1								
	P	0.000	0.028	.								
	N	59	58	59								
Org. carbon lability	*R or rho*	**0.521****	**0.358****	**0.712****	1							
	P	0.000	0.006	0.000	.							
	N	58	57	58	58							
Methane emission	*R or rho*	0.136	**0.468****	0.200	**0.523****	1						
	P	0.313	0.000	0.140	0.000	.						
	N	57	56	56	55	57						
Organic matter content	*R or rho*	0.258*	-0.064	**0.468****	-0.107	-0.280*	1					
	P	0.047	0.626	0.000	0.426	0.035	.					
	N	60	60	59	58	57	60					
Organic carbon %	*R or rho*	0.297*	0.003	**0.528****	-0.044	-0.278*	**0.858****	1				
	P	0.021	0.982	0.000	0.742	0.036	0.000	.				
	N	60	60	59	58	57	60	60				
TOC/TN	*R or rho*	-0.262*	-0.056	-0.231	**-0.404****	0.041	0.325*	0.110	1			
	P	0.044	0.673	0.078	0.002	0.760	0.011	0.405	.			
	N	60	59	59	58	57	60	60	60			
Soil nitrate	*R or rho*	**0.505****	**0.419****	**0.617****	**0.490****	**0.402****	**0.431****	0.343*	-0.240	1		
	P	0.000	0.004	0.000	0.001	0.008	0.003	0.021	0.113	.		
	N	45	45	44	43	42	45	45	45	45		
Soil nitrite	*R or rho*	**0.592****	0.044	0.052	0.243	0.248	0.283	0.263	-0.143	**0.435****	1	
	P	0.000	0.776	0.736	0.117	0.113	0.060	0.081	0.348	0.003	.	
	N	45	45	44	43	42	45	45	45	45	45	
TOC/NO_3^-	*R or rho*	-0.144	-0.161	-0.141	**-0.417****	**-0.460****	0.055	-0.030	**0.387****	**-0.864****	-0.355*	1
	P	0.345	0.291	0.361	0.005	0.002	0.717	0.846	0.009	0.000	0.017	.
	N	45	45	44	43	42	45	45	45	45	45	45

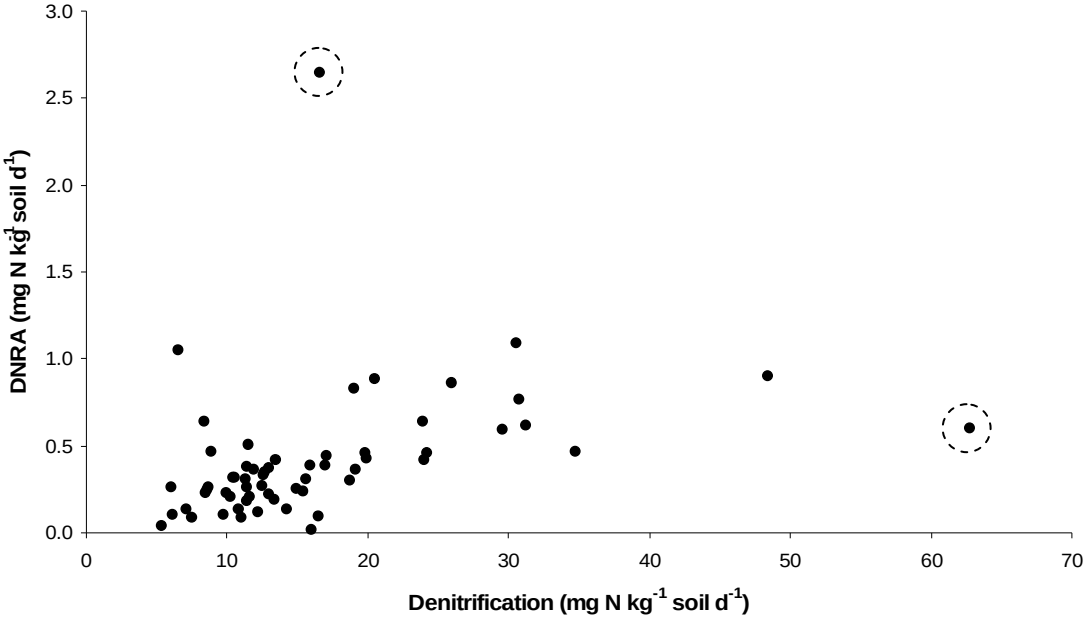

Figure 6.1.14: Scatter plot between the denitrification potential in all land use zones and the DNRA potential (*rho*=0.57, *n*=59, *P*<0.01). Samples circled with a dashed line were outliers, due to sampling next to animal manure, and were not included in the analysis.

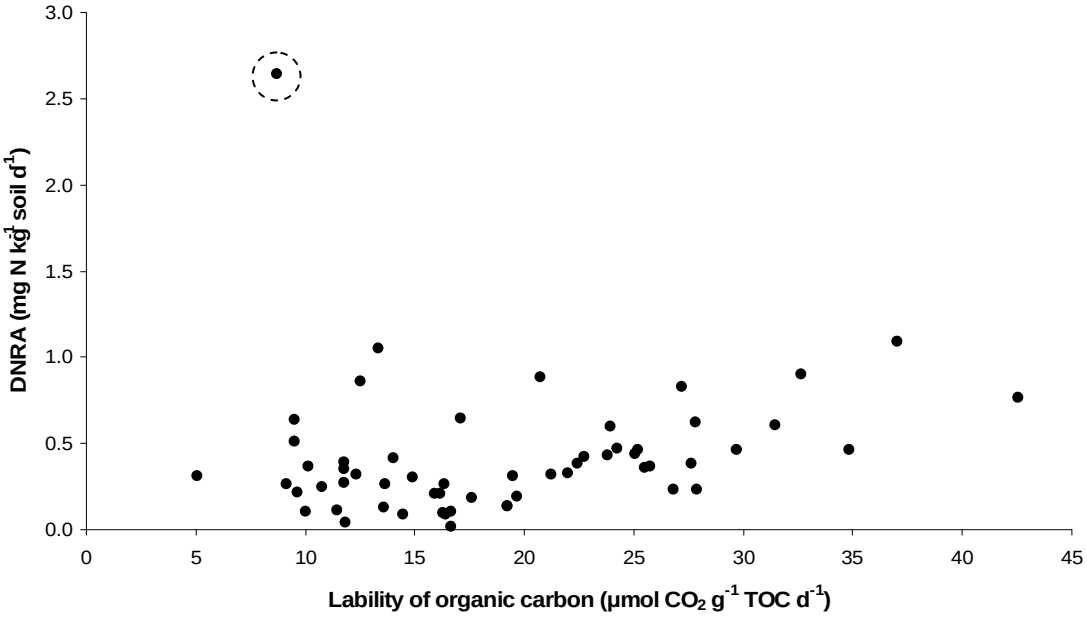

Figure 6.1.15: Scatter plot between the lability of organic carbon in all land use zones and the DNRA potential (*r*=0.36, *n*=57, *P*<0.01). The sample circled with a dashed line was an outlier, due to sampling next to animal manure, and was not included in the analysis.

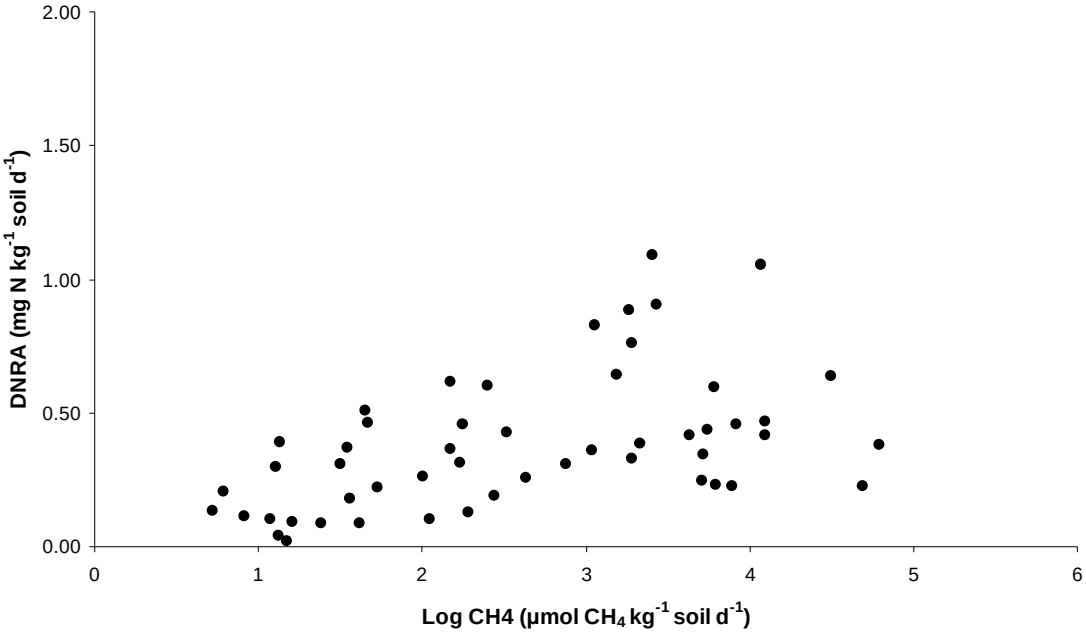

Figure 6.1.16: Scatter plot between the log-transformed methane production potential in all land use zones and the DNRA potential (*rho*=0.47, *n*=56, *P*<0.01).

Concluding, three main land use types were identified in the re-connected floodplain of the River Cole; floodplain meadow, riparian buffer strip and grazing grassland. The differentiating factor between the land uses was the availability of labile organic carbon, which decreased moving from upstream (GG and BZ areas) to the downstream meadow areas (FM and PM). The availability of labile organic carbon and the nitrate supply were the main determinants of the potential denitrification rates in the topsoil. Therefore, higher denitrification rates were observed in those land uses that combined both high availability of carbon and nitrate. DNRA, although present in all the land use zones, was on average 40 times lower than the heterotrophic denitrification rate. The land use type did not seem to affect the DNRA potential, as the latter was not primarily controlled by the availability of organic carbon, but rather by the dominance of reduced conditions and the supply of nitrate. However, the relative importance of denitrification over DNRA decreased from the upstream more 'impacted' carbon and nitrate rich areas to the 'less impacted' downstream meadows.

6.2 *The effect of the different hydrogeomorphic units within the land use zones on the nitrate attenuation processes*

This section aims to assess the effect of the different hydrogeomorphic units found within each land use zone, mainly as a result of their specific hydrologic regime, on the rate and control of nitrate attenuation via heterotrophic denitrification and DNRA. Therefore in this section, each land use zone is examined separately, while the soil physical properties and the process rates are compared between the sampling transects in each area. The riparian transects corresponded to the effect of river overbank flooding, the channel depression transects captured the effect of the ditch overbank flooding, while the middle transects reflected the less frequently flooded/drier areas of the floodplain. Additionally, an arable transect in the BZ represented the specific soil conditions of the agricultural field, while the mill leat transect in the GG contrasted the frequency of flooding between the restored River Cole and the remnant channelized part of the river.

6.2.1 *Fritillary Meadow (FM)*

The physical properties of the topsoil in the three sampling transects (Channel Depression, Middle Field and Riparian) of the Fritillary Meadow are summarised in Table 6.1.1. The Riparian samples displayed higher bulk density, lower organic matter content as well as lower organic carbon content (Table 6.2.1 and Figure 6.2.1 A,B,C). Moreover, only the clay fraction from the particle size distribution was significantly lower (Table 6.2.1) in the samples of the riparian transect, whereas there was not any significant difference between the other fractions, apart from 0.26 % of medium sand found only in the riparian samples (Figure 6.2.2).

The gravimetric measurement of the water content of the samples was significantly different (Table 6.2.1) between the three transects, forming a gradient of decreasing water content from the Channel Depression samples to the Riparian samples (Figure 6.2.1 D). There was no measurement of soil nitrate, nitrite or ammonia in the FM samples. The percent of total nitrogen (TN %) was significantly different between the transects, following a similar gradient to the water content (Figure 6.2.1 E). The ratio TOC/TN was also significantly different between the three transects (Figure 6.2.1 F). The AnMOC was significantly different between the sampling transects of FM (Table 6.1.2 and 6.2.1). Higher mean mineralisation rates were observed for the Channel

depression samples, followed by the Middle field samples and the Riparian samples (Figure 6.2.3 A). The labile fraction of organic carbon was not significantly different between transects, and the Riparian samples, although they had the lowest mineralisation rate, they displayed a higher proportion of labile organic carbon (Table 6.1.2 and Figure 6.2.3 B).

The methane production potential was significant almost exclusively in the riparian samples (Table 6.2.1). This rate was almost two orders of magnitude higher than the rates measured for the rest of the FM area, but also displayed high variability between individual samples in the Riparian transect (Table 6.1.2 and Figure 6.2.3 C).

Table 6.2.1: Comparison of the means between the three sampling transects of the FM area for selected soil properties and processes. *df*; degrees of freedom, *F*; F statistic, χ^2; χ^2 statistic *P*; probability level. Where the variable is annotated with * the non-parametric Kruskal-Wallis test has been used instead of One-Way ANOVA.

	One-Way ANOVA and Kruskal-Wallis		
Fritillary Meadow	*df*	*F or* χ^2	*P<*
Bulk density	14	14.27	0.01
Organic matter	14	28.57	0.01
Organic carbon	14	14.98	0.01
Clay fraction	14	7.21	0.01
Water content	14	31.91	0.01
Total Nitrogen*	2	10.62	0.01
TOC/TN	14	4.15	0.05
AnMOC	14	33.37	0.01
Lability of OC*	2	1.46	0.05
Methane emission	14	21.4	0.01
Denitrification	14	3.51	0.05
DNRA	14	7.11	0.01
D/DNRA*	2	8.96	0.05

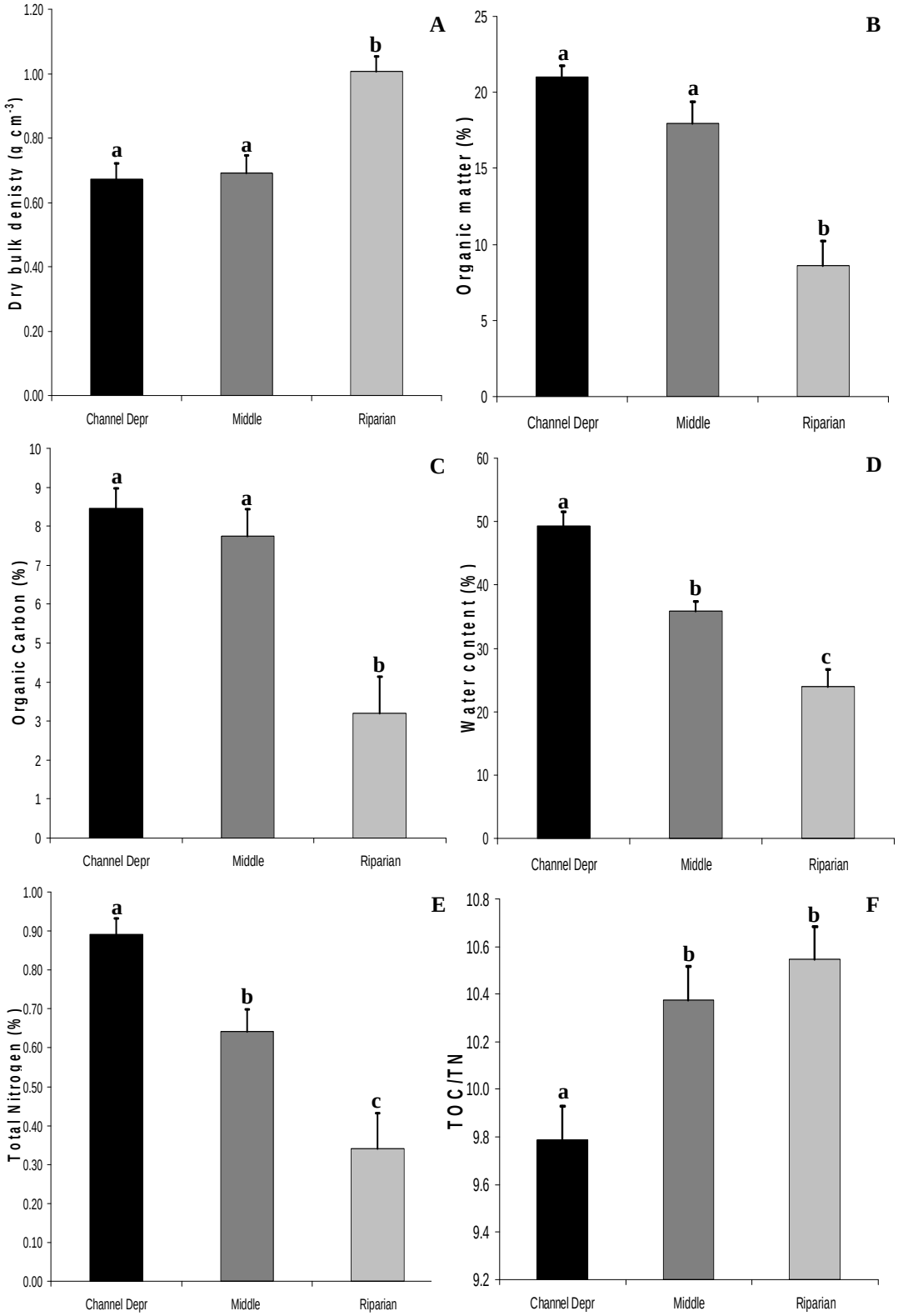

Figure 6.2.1: Soil physical properties in the sampling transects of the Fritillary Meadow. Data are means + 1 SE. Different lower case letters indicate significant difference of the means.

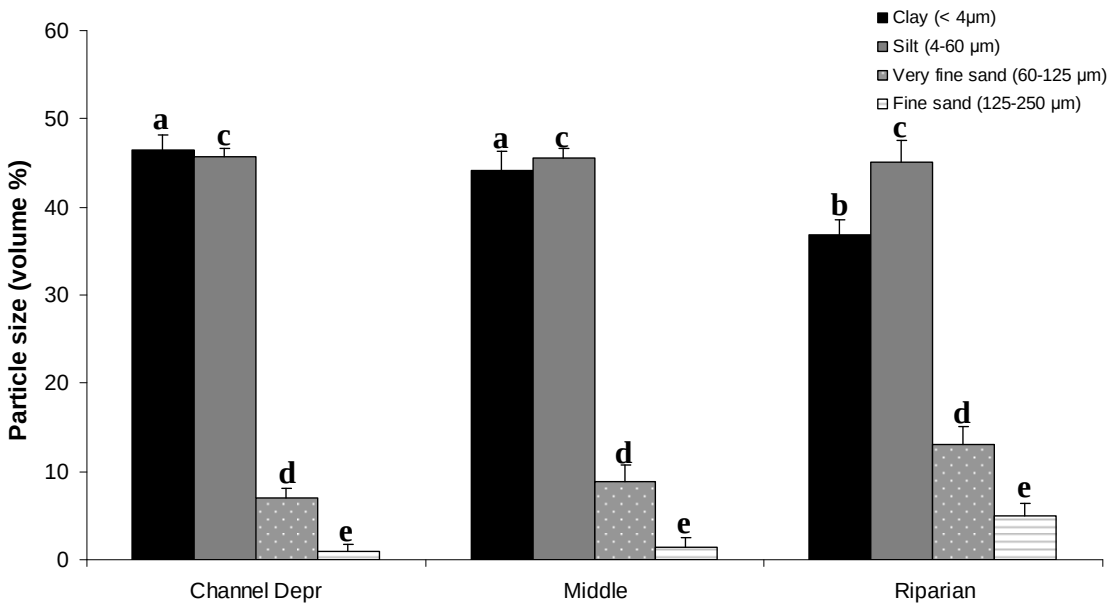

Figure 6.2.2: Absolute particle size distribution (volume %) in the three sampling transects of the Fritillary Meadow (mean and + 1 standard error, same lower case letters indicate no significant difference between the means).

PCA analysis of the FM samples, where only those environmental variables that showed some significant difference were used, resulted in a spatial ordination of the samples similar to their grouping in their respective transects (Figure 6.2.4). The first two principal axes extracted by the method explained 82.3 % of the variance between individual samples. The eigenvalues as well as the explanation percentages for the three principal axes are shown in Table 6.2.2. The first axis was more closely associated with the organic matter content (weighing 0.977), the water content (weighing 0.923) and the AnMOC (weighing 0.913), whereas the second axis was associated with the lability of organic carbon (weighing 0.917) and the methane production potential (weighing 0.442) that was mainly responsible for the observed spread of the Riparian samples shown by the standard error bars in Fig. 6.2.4. The sample clusters were separated along axis 1 due to the significant differences in water content and AnMOC potential between the three sampling transects.

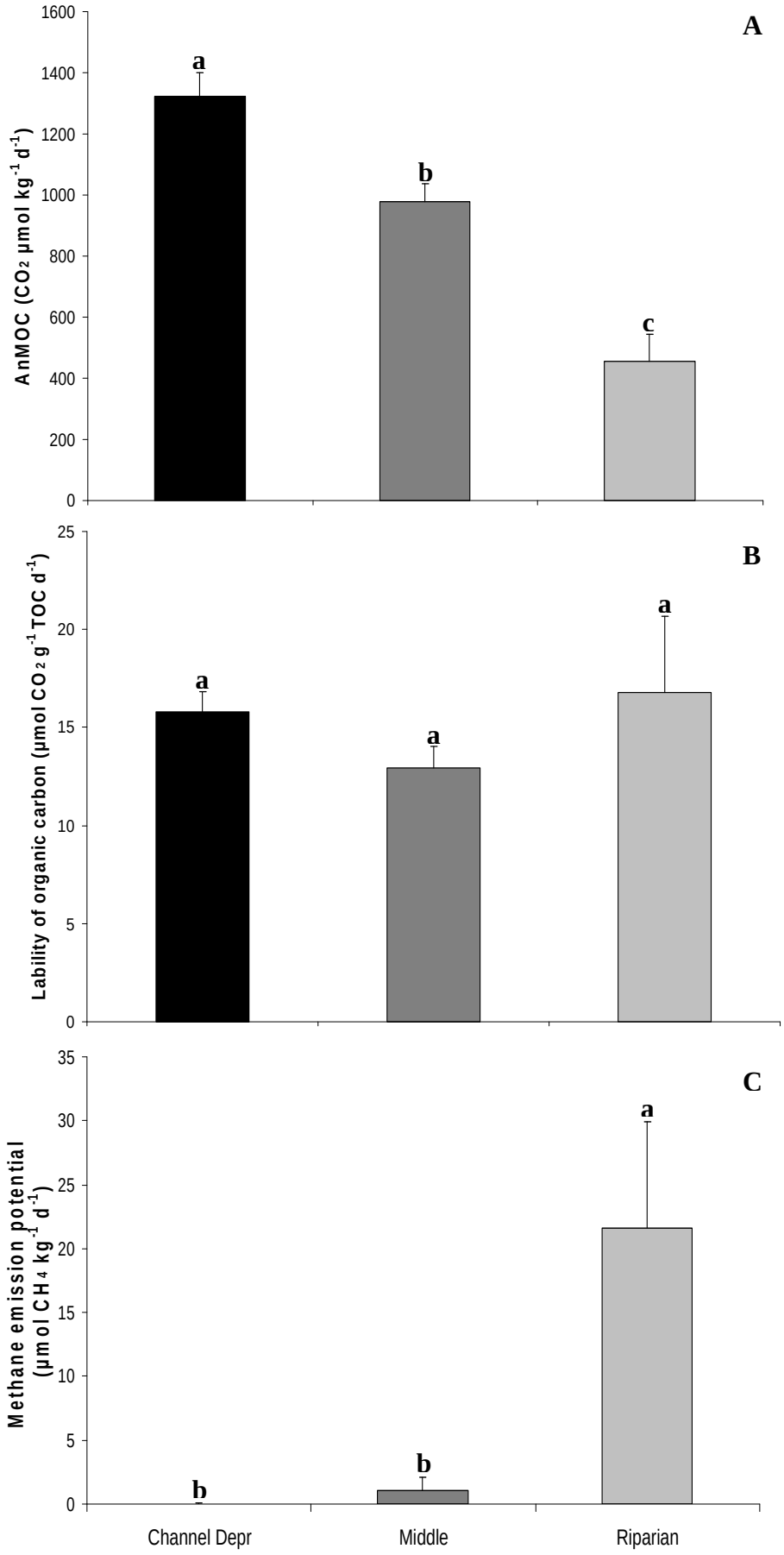

Figure 6.2.3: Mean AnMOC, lability of organic carbon and methane production potential (+ 1 standard error) in the sampling transects of the FM (significant differences indicated with different lower case letters).

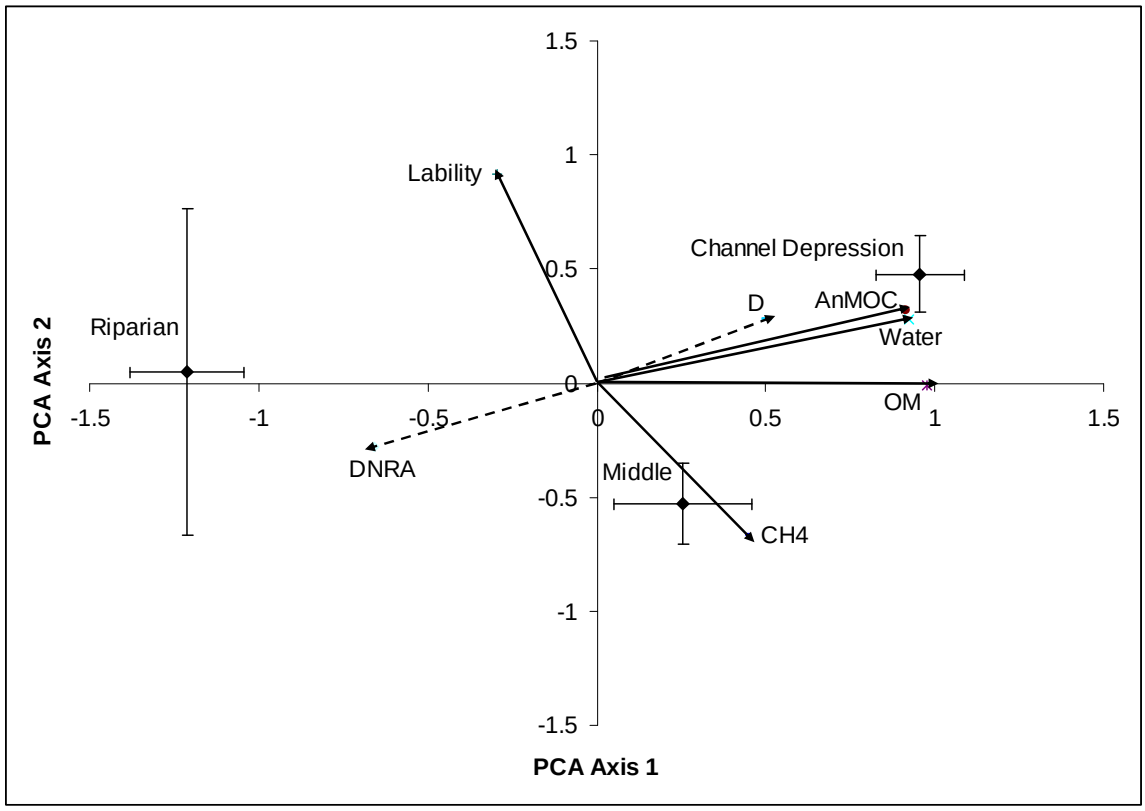

Figure 6.2.4: Correlation bi-plot from the PCA analysis with cluster centroids (average score on each component, with standard errors) for the three sampling transects in FM. Correlations of the variables with the main axes are given by solid arrows. Dashed arrows indicate the correlation of nitrate attenuation processes with the component axes. Water; water content, OM; organic matter content, CH_4; methane production, Lability; labile organic carbon, D; potential denitrification rate.

Table 6.2.2: The principal components (axes) generated by the PCA, their respective eigenvalues, the % of variance explained by each component and the cumulative % of variance explanation.

Axes	Eigenvalues	% of Variance	Cumulative %
1	4.448	63.54	63.54
2	1.312	18.74	82.28
3	0.685	9.79	92.07

A summary of the denitrification and DNRA potential rates measured in the sampling transects of the FM are presented in Table 6.1.6. Only the Middle field samples had significantly lower denitrification rate (Table 6.2.1) compared to the Channel Depression samples, which were not significantly different from the Riparian samples (Figure 6.2.5 A).

The DNRA potential rate was significantly higher (Table 6.2.1) in the Riparian samples, compared to the samples of the Channel Depression and the Middle field (Figure 6.2.5 B). The ratio Denitrification over DNRA (D/DNRA) was significantly different between the transects of FM (Table 6.2.1). Denitrification was 250 times more important in Channel depression and 87 times more important in the Middle field samples, whereas the Riparian samples had only 16 times higher potential denitrification rates than DNRA rates (Figure 6.2.5 C). Therefore, it could be assumed that the different conditions that characterise the Riparian area of the FM zone, that are potentially attributed to its specific hydrological regime, have also a marked effect on the relative importance of the two nitrate attenuation processes.

A combination of Pearson-Product Moment correlation (parametric) and Spearman *rho* correlation (non-parametric) was employed to investigate possible relationships between Denitrification, DNRA and the various environmental variables (soil physical properties, AnMOC and CH_4 production potential). The produced correlation matrix is shown in Table 6.2.3. Denitrification potential correlated poorly with the majority of the variables tested and only two correlations were significant at the 0.05 level; with the water content and the AnMOC. Furthermore, there was no significant relationship between denitrification and DNRA. One possible reason for the above result could be the fact that although the soil physical properties and the AnMOC measured in the Riparian samples were indicating conditions not so favourable for high denitrification rate, these samples displayed a denitrification rate not significantly different from the Channel depression, where more favourable conditions were observed. Therefore, the denitrification activity was more homogeneous than expected from the environmental variables variability between the sampling transects. Presumably, the relatively high lability of organic carbon measured in the Riparian samples could be partly responsible for the sustained denitrification activity.

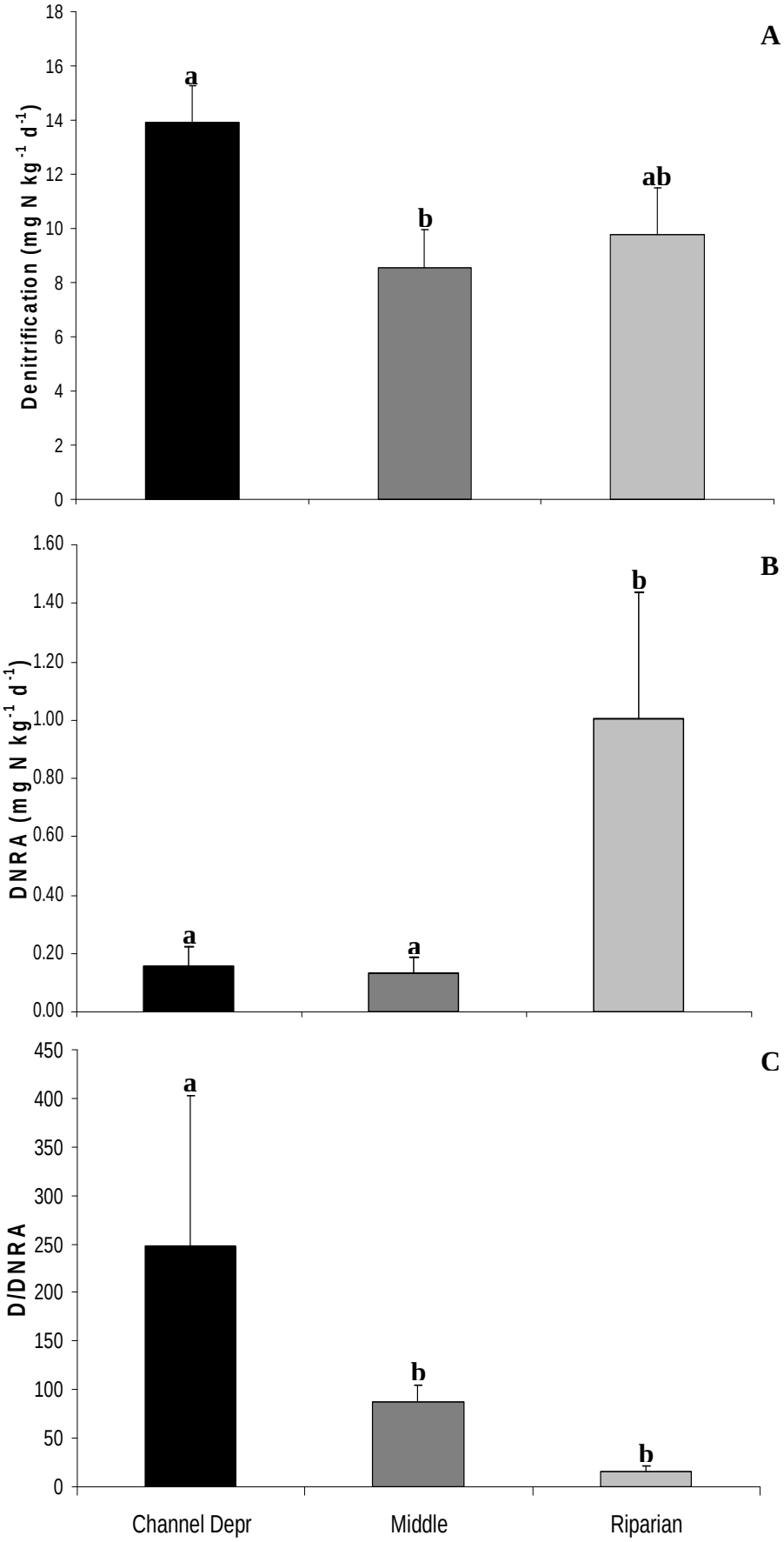

Figure 6.2.5: Mean denitrification potential, DNRA potential and D/DNRA (+ 1 standard error) in the sampling transects of the FM (significant differences indicated with different lower case letters).

On the other hand, the DNRA potential rate showed significant positive correlation with the low bulk density, the low redox conditions expressed by the CH_4 production potential and the ratio TOC/TN, while significant negative correlation was found with the AnMOC and the water content.

Multiple Regression Analysis (MRA) between the denitrification potential and the environmental variables confirmed the correlation results, with the water content explaining 37 % (MRA; r^2=0.37, *df*=13, P<0.05) of the variance in potential denitrification rates and the AnMOC (MRA; r^2=0.30, *df*=13, P<0.05) following with 30 % explanatory power as a 'causal' variable. MRA of the potential DNRA rates indicated significant negative 'causal' relationship with the AnMOC (MRA; r^2=0.64, *df*=13, P<0.01), the water content (MRA; r^2=0.46, *df*=13, P<0.01) and the organic matter content (MRA; r^2=0.44, *df*=13, P<0.05) and significant positive relationships with the bulk density (MRA; r^2=0.49, *df*=13, P<0.01) and the methane production potential (MRA; r^2=0.48, *df*=13, P<0.01).

To summarise, significant differences were found between the soil properties in the sampling transects of the FM area. Higher water content, total nitrogen and AnMOC were associated with the Channel depression creating favourable conditions for increased potential denitrification. The Riparian samples although lower in clay content and having higher bulk density, were characterised by high methane production potential as well as labile organic carbon. Therefore, although the total organic carbon was lower in the Riparian samples, the high proportion of the labile organic carbon fraction was probably adequate to sustain high potential denitrification activity. Moreover, the prevalence of reduced conditions, as shown by the methane production potential, due to frequent river overbank flooding of the Riparian transect created favourable conditions for the occurrence of DNRA. Additionally, the ratio TOC/TN, being higher in the Riparian samples, also favoured higher DNRA rates compared to the other sampling transects. Finally the decoupling of DNRA from denitrification in the FM area suggested that under relatively limited nitrogen conditions, DNRA becomes more important where reduced conditions are combined with a higher ratio of TOC/TN.

Table 6.2.3: Correlation matrix between the DNRA potential rate, the denitrification potential rate, AnMOC, lability of organic carbon, methane production potential and the physical properties of the topsoil in the sampling transects of FM. Underlined correlation coefficients are products of Spearman rho correlation whereas non-underlined are products of Pearson Product-Moment correlation. ** Correlation is significant at the 0.01 level and *Correlation is significant at the 0.05 level.

Variables/Correlation coefficients		Denitrification potential	DNRA	AnMOC	Org. carbon lability	Methane emission	Organic matter content	Organic carbon	TOC/TN	Bulk density	Water content	Total Nitrogen
Denitrification potential	*R or rho*	1										
	P	.										
	N	14										
DNRA	*R or rho*	-0.238	1									
	P	0.413	.									
	N	14	15									
AnMOC	*R or rho*	**0.549***	**-0.709****	1								
	P	0.042	0.003	.								
	N	14	15	15								
Org. carbon lability	*R or rho*	0.053	-0.328	0.049	1							
	P	0.858	0.232	0.864	.							
	N	14	15	15	15							
Methane emission	*R or rho*	-0.277	**0.642****	**-0.650****	0.225	1						
	P	0.337	0.010	0.009	0.420	.						
	N	14	15	15	15	15						
Organic matter content	*R or rho*	0.405	-0.594*	**0.892****	-0.318	**-0.814****	1					
	P	0.151	0.020	0.000	0.248	0.000	.					
	N	14	15	15	15	15	15					
Organic carbon	*R or rho*	0.342	-0.596*	**0.829****	-0.437	**-0.868****	**0.977****	1				
	P	0.232	0.019	0.000	0.103	0.000	0.000	.				
	N	14	15	15	15	15	15	15				
TOC/TN	*R or rho*	-0.522	0.560*	**-0.690****	0.001	**0.755****	**-0.719****	**-0.683****	1			
	P	0.056	0.030	0.004	0.998	0.001	0.003	0.005	.			
	N	14	15	15	15	15	15	15	15			
Bulk density	*R or rho*	-0.238	**0.761****	**-0.849****	0.302	**0.761****	**-0.916****	**-0.922****	0.589*	1		
	P	0.413	0.001	0.000	0.275	0.001	0.000	0.000	0.021	.		
	N	14	15	15	15	15	15	15	15	15		
Water content	*R or rho*	**0.610***	**-0.649****	**0.939****	-0.021	**-0.732****	**0.897****	**0.848****	**-0.717****	**-0.841****	1	
	P	0.020	0.009	0.000	0.94	0.002	0.000	0.000	0.003	0.000	.	
	N	14	15	15	15	15	15	15	15	15	15	
Total Nitrogen	*R or rho*	0.518	**-0.647****	**0.893****	-0.159	**-0.764****	**0.913****	**0.878****	**-0.686****	**-0.868****	**0.962****	1
	P	0.058	0.009	0.000	0.572	0.001	0.000	0.000	0.005	0.000	0.000	.
	N	14	15	15	15	15	15	15	15	15	15	15

6.2.2 *Pasture Meadow (PM)*

Less variability was observed between the physical soil properties in the three sampling transects (Channel Depression, Middle Field and Riparian) of the Pasture Meadow (Table 6.1.1). Specifically, there were no significant differences in the bulk density, the water content and the ratio TOC/TN, while the ratio TOC/NO_3^- was significantly lower in the Riparian samples (Table 6.2.4 and Figure 6.2.6 A,B,C,D). Moreover, the organic matter content was higher in the Channel Depression samples compared to the other two transects (Figure 6.2.6 E). Similarly, the organic carbon content was significantly lower in the Riparian samples (Figure 6.2.6 F). From the particle size fractions, significantly less clay and silt was measured in the Middle Field samples, which also had a significant amount of fine sands, despite not being statistically significant due to the high variability among the samples (Figure 6.2.7). Additionally, no significant differences were found in the soil nitrate content, soil ammonia or soil nitrite (Table 6.2.4 and Figure 6.2.8).

Table 6.2.4: Comparison of the means between the three sampling transects of the PM area for selected soil properties and processes. *df*; degrees of freedom, *F*; F statistic, χ^2; χ^2 statistic *P*; probability level. Where the variable is annotated with * the non-parametric Kruskal-Wallis test has been used instead of One-Way ANOVA.

	One-Way ANOVA and Kruskal-Wallis		
Pasture Meadow	*df*	*F or* χ^2	*P*
Bulk density	14	2.54	>0.05
Organic matter	14	9.71	<0.01
Organic carbon	14	5.45	<0.01
Clay fraction	14	7.86	<0.01
Water content*	2	3.92	>0.05
TOC/TN	13	0.48	>0.05
TOC/NO_3^{-*}	2	6.35	<0.05
Soil nitrate	13	0.68	>0.05
Soil ammonia*	2	1.04	>0.05
Soil nitrite*	2	1.82	>0.05
AnMOC	14	0.45	>0.05
Lability of OC	14	2.62	>0.05
Methane emission	11	11.91	<0.01
Denitrification*	2	0.62	>0.05
DNRA	14	2.35	>0.05
D/DNRA	14	3.13	>0.05

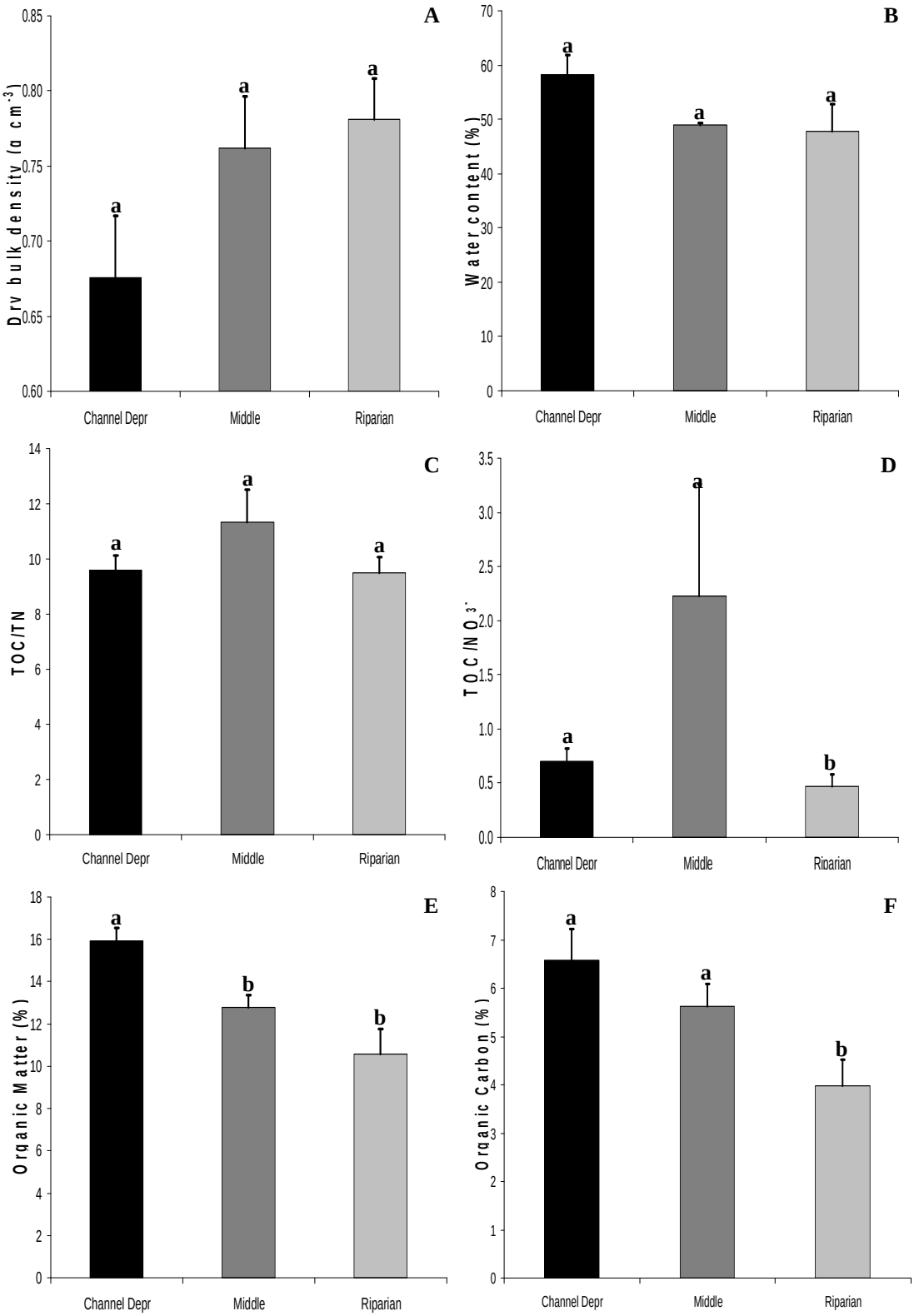

Figure 6.2.6: Soil physical properties in the sampling transects of the Pasture Meadow. Data are means + 1 SE. Different lower case letters indicate significant difference of the means.

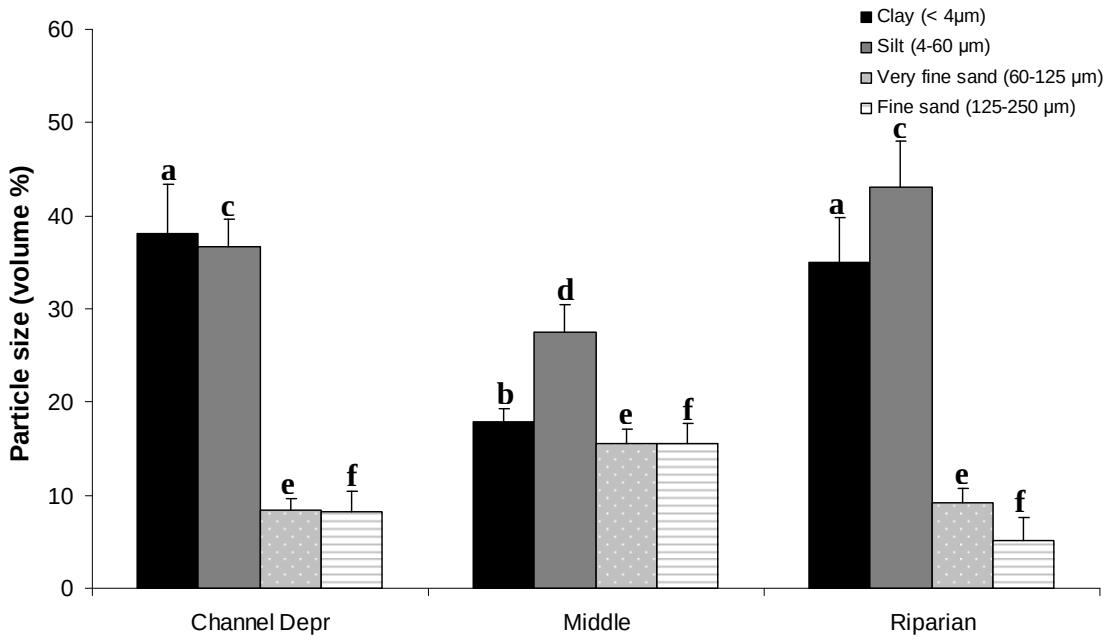

Figure 6.2.7: Absolute particle size distribution (volume %) in the three sampling transects of the Pasture Meadow (mean and + 1 standard error, same lower case letters indicate no significant difference between the means).

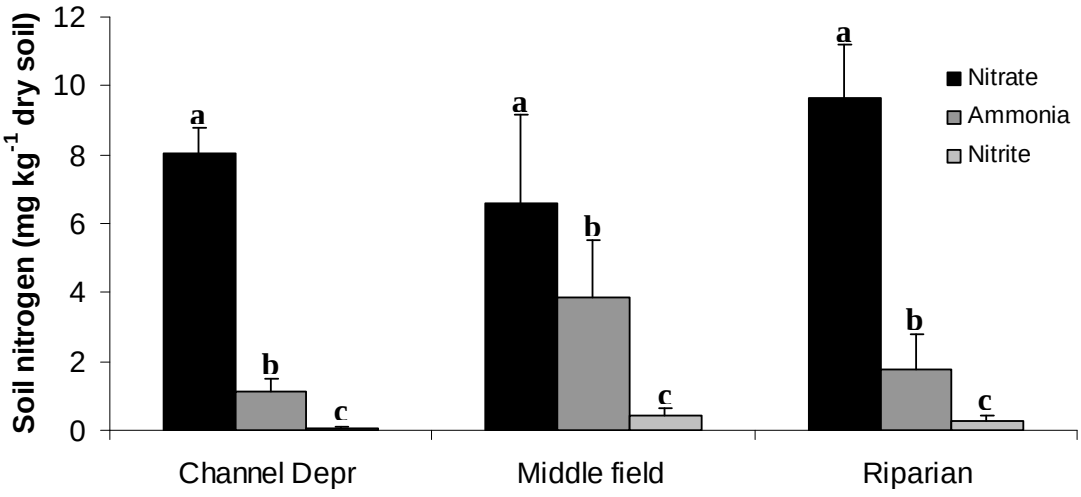

Figure 6.2.8: Mean concentrations of NO_3^--N, NH_3-N and NO_2^--N (+ 1 standard error) in the three sampling transects of the Pasture Meadow. Same lower case letters indicate no significant difference between the means.

Similar to the physical soil properties results, no significant differences were observed in the organic carbon mineralisation rate (AnMOC) between the sampling transects of the PM (Table 6.1.2, 6.2.4 and Figure 6.2.9 A). Neither the lability of organic carbon was significantly different between the PM transects, however a gradient was observed from higher lability measured in the Riparian samples, to intermediate values in the Middle field samples, and lower in the Channel depression samples (Table 6.1.2, 6.2.4 and Figure 6.2.9 B). However, the methane production potential was significantly different; with the Riparian samples displaying the highest rate, followed by the Channel depression samples and the Middle field samples (Table 6.1.2, 6.2.4 and Figure 6.2.9 C).

A PCA analysis of the environmental variables with some significant differences resulted in extracting three principal components which explained, cumulatively, 95 % of the variance between individual samples (Table 6.2.5). The first axis was associated with the water content (weighing 0.941) and the organic matter content (weighing 0.899), whereas the second axis was associated with the AnMOC (weighing 0.748) and the lability of organic carbon (weighing 0.927). A biplot of the cluster centroids (average score on each component, with standard errors) for the three sampling transects in PM is shown in Figure 6.2.10. The samples were separated along axis 2 into two groups; the first group including only the Channel Depression samples associated with lower labile OC, but higher water and organic matter content, and a second group with close association of the Middle field and Riparian samples that displayed higher labile OC but lower water and organic matter content.

Table 6.2.5: The principal components (axes) generated by the PCA, their respective eigenvalues, the % of variance explained by each component and the cumulative % of variance explanation.

Axes	Eigenvalues	% of Variance	Cumulative %
1	2.097	41.9	41.9
2	1.661	33.2	75.2
3	0.991	19.8	95.0

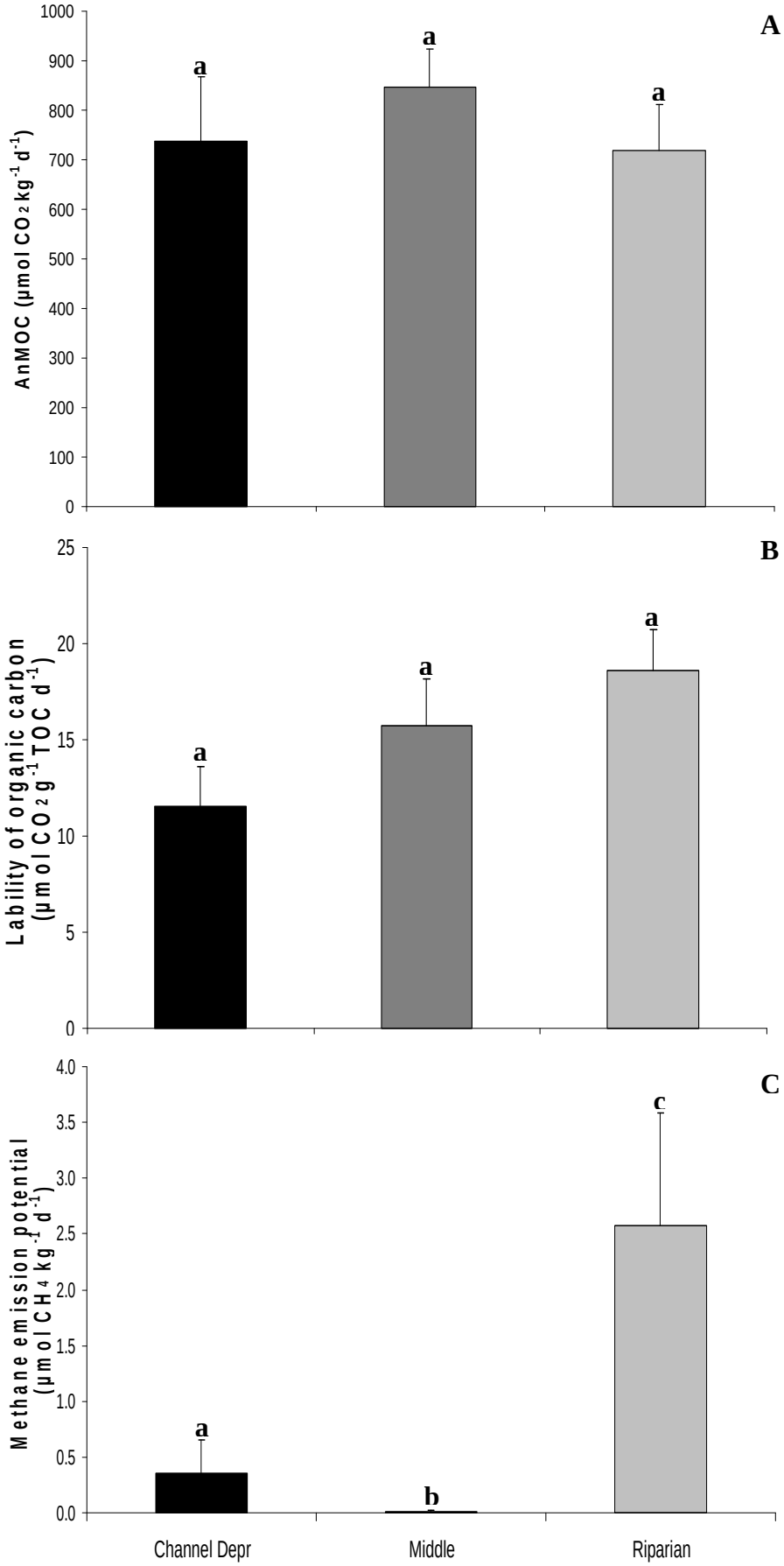

Figure 6.2.9: Mean AnMOC, lability of organic carbon and methane production potential (+ 1 standard error) in the sampling transects of the PM (significant differences indicated with different lower case letters).

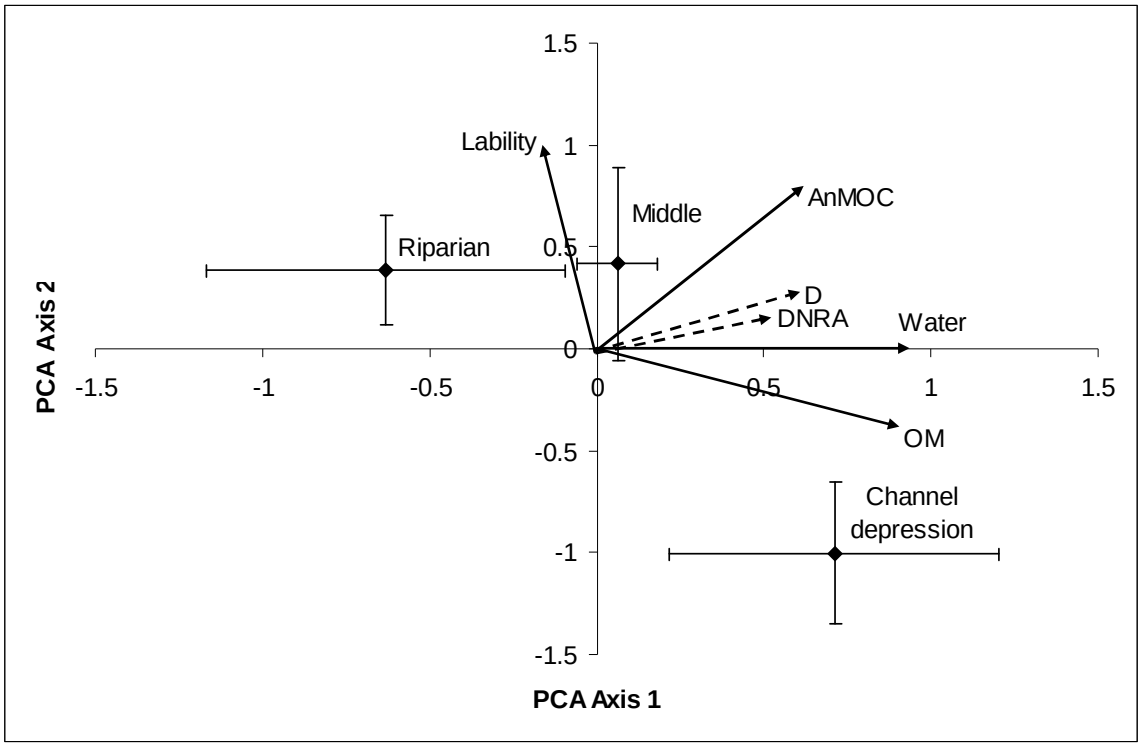

Figure 6.2.10: Correlation bi-plot from the PCA analysis with cluster centroids (average score on each component, with standard errors) for the three sampling transects in PM. Correlations of the variables with the main axes are given by solid arrows. Dashed arrows indicate the correlation of nitrate attenuation processes with the component axes. Water; water content, OM; organic matter content, Lability; labile organic carbon, D; potential denitrification rate.

Following the low variability observed between the sampling transects of the PM in terms of their soil physical properties and AnMOC and lability of organic carbon measurements, the potential denitrification was not significantly different between the transect samples (Table 6.2.4). The Channel Depression and the Riparian samples had similar denitrification rates, despite the fact that there was significant difference in their organic matter and carbon content, and the Middle field samples had slightly lower denitrification potential (Table 6.1.6 and Figure 6.2.11 A).

The potential DNRA rates were also similar between the Channel Depression and the Riparian samples, while the Middle field samples displayed a slightly lower DNRA rate (Table 6.1.6, 6.2.4 and Figure 6.2.11 B).

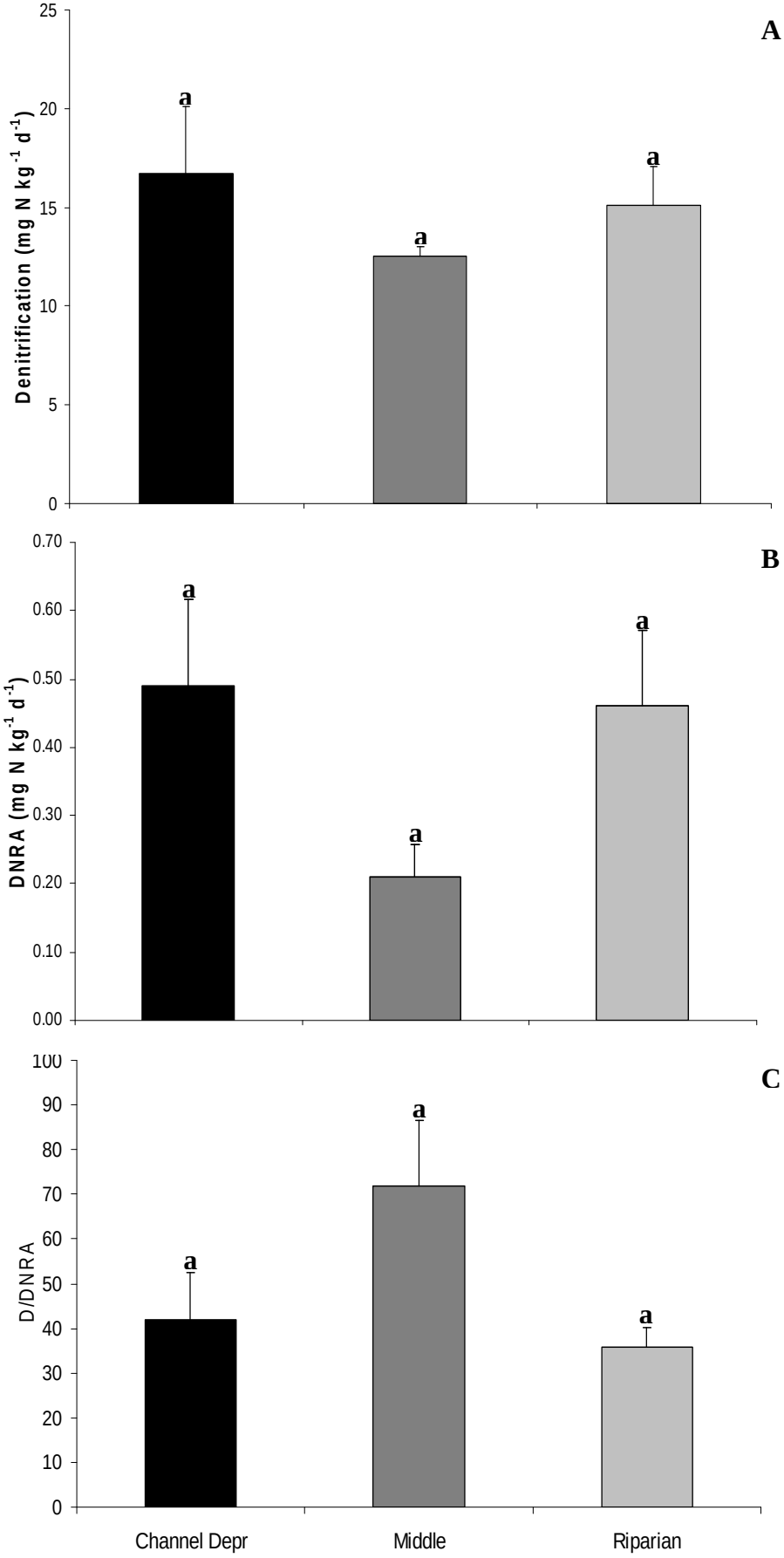

Figure 6.2.11: Mean denitrification potential, DNRA potential and D/DNRA (+ 1 standard error) in the sampling transects of the PM (significant differences indicated with different lower case letters).

Regarding the relative importance of denitrification over DNRA, the Middle field samples had on average 72 times higher denitrification than DNRA rates, followed by the Channel depression with 42 times less DNRA and finally the Riparian samples, where denitrification was 36 times higher than DNRA (Figure 6.2.11 C). Although the results indicated a shift of the relative importance in favour of DNRA towards the riparian zone of the floodplain, as shown also for the FM land use zone, the differences in the D/DNRA ratio were not statistically significant (Table 6.2.4).

Correlation analysis (Table 6.2.6) revealed a strong significant positive correlation between denitrification and DNRA, indicating the coexistence of the two processes in the sampling transects of the PM. This is also shown by the similar correlation of the two processes with the PCA axes in Fig 6.2.10. Moreover, denitrification correlated significantly with the water content and less strongly with the AnMOC. On the other hand, DNRA showed an unexpected significant negative correlation with the TOC:TN ratio and also a significant positive correlation with the water content but no significant relationship was found between DNRA and methane production potential.

Multiple Regression Analysis (MRA) resulted in the same significant relationships indicated also by the correlation analysis, with the water content explaining 51 % (MRA; r^2=0.51, df=14, P<0.01) of the variance between the PM samples and the AnMOC explaining 35 % of the variance (MRA; r^2=0.35, df=14, P<0.05). The MRA results for DNRA were also similar to the correlation results, with the ratio TOC/TN explaining 47 % (MRA; r^2=0.47, df=13, P<0.01) of the variance in DNRA rates between the PM samples, followed by the water content with 41 % explanatory power (MRA; r^2=0.41, df=14, P<0.05), and also the methane production potential explaining 35 % (MRA; r^2=0.35, df=11, P<0.05) of the variance in DNRA rates.

Table 6.2.6: Correlation matrix between the DNRA potential rate, the denitrification potential rate, AnMOC, lability of organic carbon, methane production potential and the physical properties of the topsoil in the sampling transects of PM. Underlined correlation coefficients are products of Spearman rho correlation whereas non-underlined are products of Pearson Product-Moment correlation. ** Correlation is significant at the 0.01level and *Correlation is significant at the 0.05 level.

Variables/Correlation coefficients		Denitrification potential	DNRA	AnMOC	Org. carbon lability	Methane emission	Organic matter content	Organic carbon	TOC/TN	TOC/NO_3^-	Water content	Soil nitrate
Denitrification potential	*R or rho*	1										
	P	.										
	N	15										
DNRA	*R or rho*	**0.800****	1									
	P	0.000	.									
	N	15	15									
AnMOC	*R or rho*	0.594*	0.509	1								
	P	0.020	0.053	.								
	N	15	15	15								
Org. carbon lability	*R or rho*	0.281	0.192	0.531*	1							
	P	0.310	0.493	0.042	.							
	N	15	15	15	15							
Methane emission	*R or rho*	0.217	0.264	-0.070	0.587*	1						
	P	0.457	0.361	0.811	0.027	.						
	N	14	14	14	14	14						
Organic matter content	*R or rho*	0.412	0.367	0.274	-0.454	-0.440	1					
	P	0.127	0.179	0.323	0.089	0.115	.					
	N	15	15	15	15	14	15					
Organic carbon	*R or rho*	0.204	0.259	0.243	**-0.712****	-0.468	**0.744****	1				
	P	0.466	0.352	0.383	0.003	0.092	0.001	.				
	N	15	15	15	15	14	15	15				
TOC/TN	*R or rho*	-0.280	**-0.688****	-0.200	0.058	0.014	-0.119	-0.273	1			
	P	0.333	0.007	0.493	0.843	0.963	0.684	0.345	.			
	N	14	14	14	14	13	14	14	14			
TOC/NO_3^-	*R or rho*	-0.088	-0.360	0.024	-0.574*	**-0.924****	0.411	0.556*	0.279	1		
	P	0.765	0.206	0.935	0.032	0.000	0.144	0.039	0.356	.		
	N	14	14	14	14	13	14	14	13	14		
Water content	*R or rho*	**0.714****	**0.643****	0.596*	-0.039	-0.070	**0.816****	0.556*	-0.130	-0.089	1	
	P	0.003	0.010	0.019	0.891	0.811	0.000	0.031	0.657	0.752	.	
	N	15	15	15	15	14	15	15	14	15	15	
Soil nitrate	*R or rho*	0.255	0.446	0.231	0.296	0.580*	-0.161	-0.038	-0.181	**-0.776****	0.258	1
	P	0.378	0.110	0.427	0.304	0.038	0.583	0.898	0.553	0.001	0.374	.
	N	14	14	14	14	13	14	14	13	14	14	15

Concluding, the hydrogeomorphic units represented by the three sampling transects in PM showed low variability with respect to their soil physical properties and organic carbon mineralisation rate. This could be due to the characteristic hydrologic regime in this area, with two sources of overbank flooding (see section 5.3) covering the majority of the floodplain area and resulting in fairly homogeneous conditions across the site. However, the slightly higher water, organic carbon and clay content of the Channel depression samples favoured relatively high denitrification rates, while the availability of labile organic carbon in the Riparian samples and the reduced conditions were probably responsible for increased denitrification activity. DNRA in the PM transects followed closely the denitrification conditions, while the ratio TOC/TN was associated with lower DNRA rates opposite to what was observed in the FM transects. Finally, the MRA highlighted once again the dependence of DNRA on the reduced conditions, most frequently found in the Channel Depression and the Riparian area.

6.2.3 *Buffer Zone (BZ)*

The smallest land use zone of the re-connected floodplain of the River Cole was found very homogeneous in terms of the topsoil physical properties between its sampling transects (Riparian, Middle Field and Arable). None of the measured physical properties displayed a statistically significant difference between the sampling transects (Table 6.2.7), although in most cases a gradient from the riparian towards the arable transect was observed. The bulk density was lower near the river (Riparian transect) and higher in the Arable field (Table 6.1.1 and Figure 6.2.12 A). On the contrary, the water, as well as the organic matter content followed an opposite gradient with higher values observed in the Riparian samples moving towards lower values in the Arable field (Table 6.1.1 and Figure 6.2.12 B,C). The same gradient was observed for the organic carbon content and the ratio TOC/TN (Figure 6.2.12 D,E). The ratio TOC/NO_3^- was lower in the Riparian transect and higher in the Arable field (Figure 6.2.12 F). The particle size fractions were similar across the sampling transects with the exception of silt that was significantly less in the Arable field samples (Table 6.2.7 and Figure 6.2.13).

Regarding the soil nitrate content, it was found three times higher in the Riparian samples compared to the rest of the BZ, but the variability between samples was very high and therefore the difference was not statistically significant (Table 6.2.7). As for

the soil ammonia and the soil nitrite, they both followed the common gradient with higher values near the river and lowest values in the arable field (Table 6.1.1 and Figure 6.2.14).

Table 6.2.7: Comparison of the means between the three sampling transects of the BZ area for selected soil properties and processes. *df*; degrees of freedom, *F*; F statistic, χ^2; χ^2 statistic *P*; probability level. Where the variable is annotated with * the non-parametric Kruskal-Wallis test has been used instead of One-Way ANOVA.

	One-Way ANOVA and Kruskal-Wallis		
Buffer Zone	*df*	*F or* χ^2	*P*
Bulk density	14	3.17	>0.05
Organic matter	14	3.09	>0.05
Organic carbon	14	0.34	>0.05
Silt fraction	14	4.73	<0.05
Water content	14	0.95	>0.05
TOC/TN	14	0.42	>0.05
TOC/NO_3^-	14	3.49	>0.05
Soil nitrate*	2	2.78	>0.05
Soil ammonia	14	0.67	>0.05
Soil nitrite	14	0.62	>0.05
AnMOC*	2	7.34	<0.05
Lability of OC	14	15.62	<0.01
Methane emission*	2	7.49	<0.05
Denitrification	14	1.58	>0.05
DNRA	14	0.91	>0.05
D/DNRA	14	1.22	>0.05

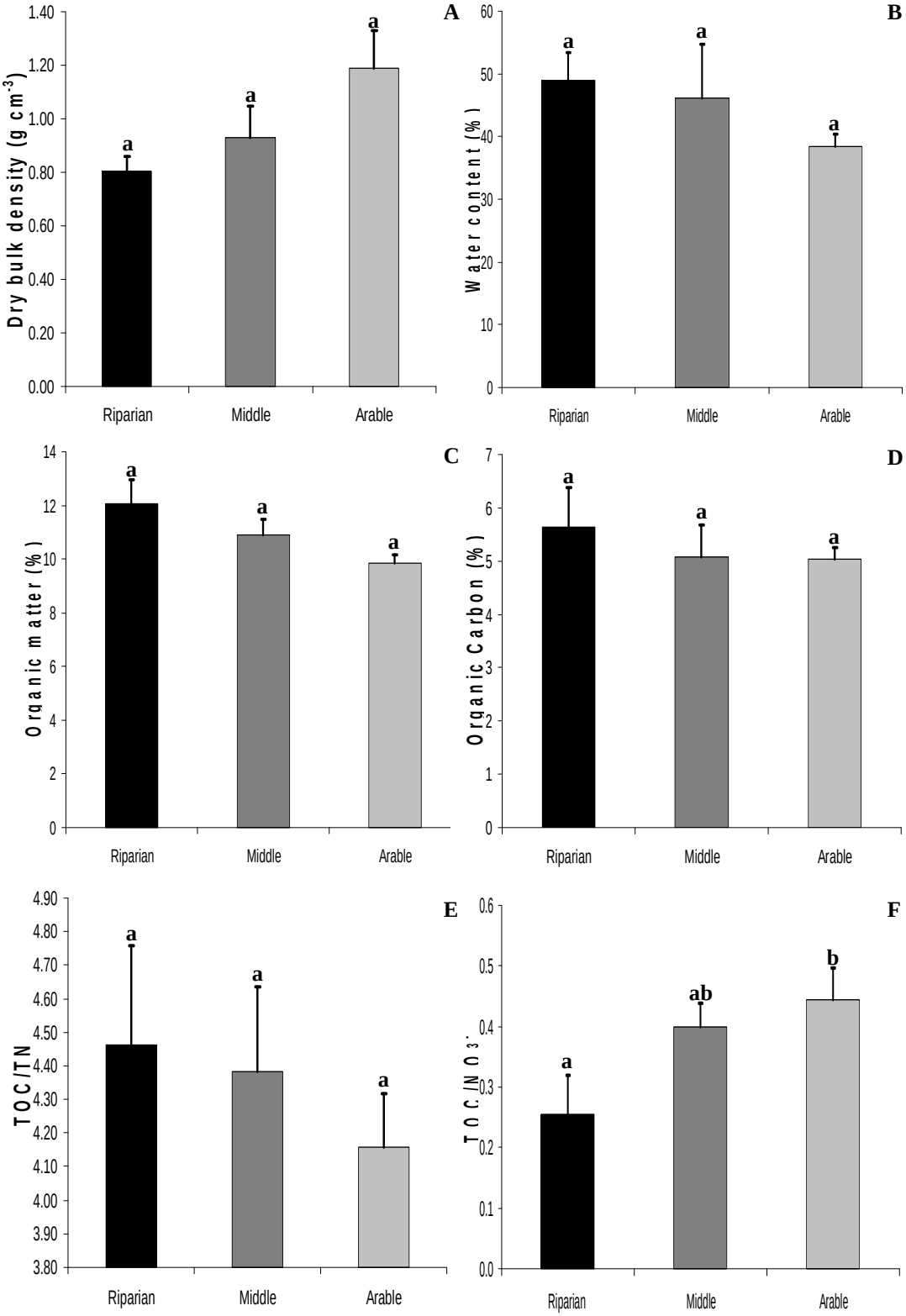

Figure 6.2.12: Soil physical properties in the sampling transects of the Buffer Zone. Data are means + 1 SE. Same lower case letters indicate no significant difference of the means.

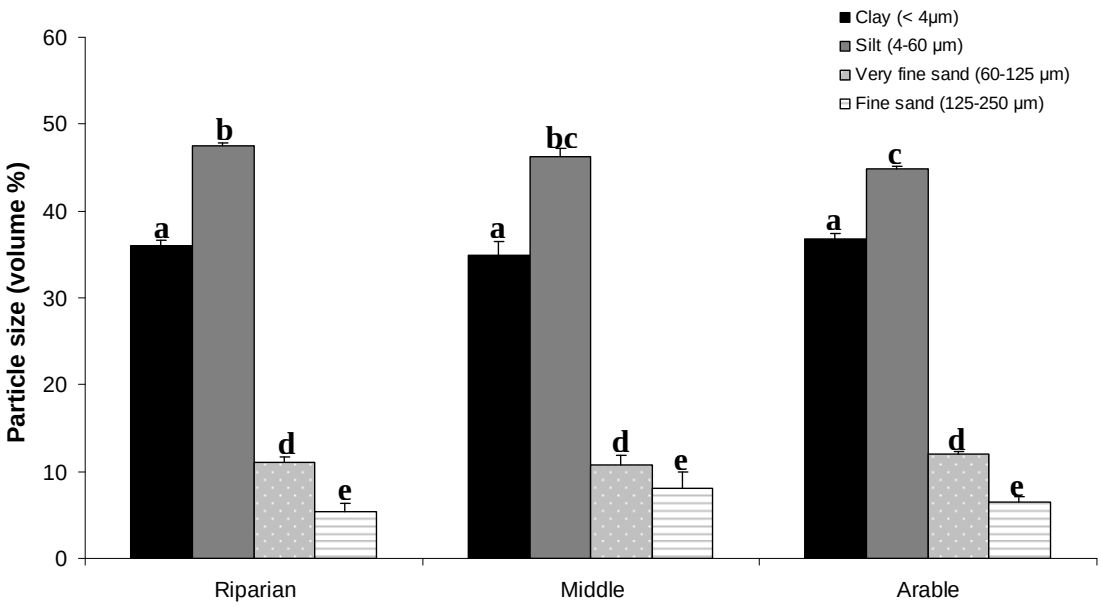

Figure 6.2.13: Absolute particle size distribution (volume %) in the three sampling transects of the Buffer Zone (mean and + 1 standard error, same lower case letters indicate no significant difference between the means).

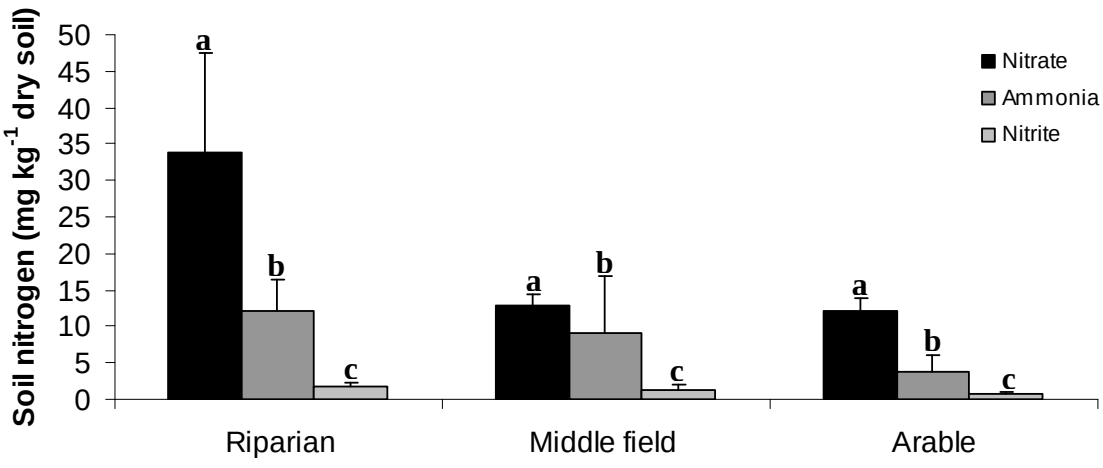

Figure 6.2.14: Mean concentrations of NO_3^--N, NH_3-N and NO_2^--N (+ 1 standard error) in the three sampling transects of the Buffer Zone. Same lower case letters indicate no significant difference between the means.

Unlike the soil physical properties, the AnMOC displayed statistically significant differences between the sampling transects of the BZ area (Table 6.2.7). Specifically, the Arable field samples had the lowest mineralisation rate, whereas the Riparian and Middle field samples were not significantly different (Table 6.1.2 and Figure 6.2.15 A). Similarly, the lability of organic carbon was significantly lower in the Arable field samples, and there was no significant difference between Riparian and Middle samples (Table 6.1.2, 6.2.7 and Figure 6.2.15 B). The same pattern was also observed for the methane production potential. The arable field samples displayed significantly lower rates, whereas the Riparian and the Middle field samples were not statistically different (Table 6.1.2, 6.2.7 and Figure 6.2.15 C).

The PCA extracted three principal component axes that combined explained 91 % of the variance between individual samples (Table 6.2.8). The correlation coefficients between the first two axes and the environmental variables are shown in Table 6.2.9. Of these axes, the first explained 58 % of the variance and was associated with the AnMOC, the organic carbon and the water content, the soil nitrate, the methane production potential and the lability of OC. The second axis explained 20 % of the variance and was associated with the clay content and the ratio TOC/NO_3^-. Plotting the scores of the first two axes for each sample resulted in the bi-plot of Figure 6.2.16. The majority of the samples formed a cluster which was positioned at the negative side of axis 1 showing weak correlation with the variables associated with this axis. The cluster included all the samples of the arable transect, which were closely related to the ratio TOC/NO_3^-, most of the middle field samples and only two of the riparian samples, those located further away from the bridge (for a detailed sampling design please see section 4.4.1.1). Interestingly, the first three riparian samples (BZ 1-3) as well as the samples BZ6 and BZ7 from Middle field were associated with the positive side of axis 1. These samples were located near the flood entry points from the river and the drainage tunnel below the road and were waterlogged for considerably longer periods (see also section 5.3). Due to the higher frequency and longer duration of suboxic conditions, these BZ locations may constitute biogeochemical activity ‘hotspots’. Therefore, the hydrologic regime of the BZ clearly affected the topsoil properties, with higher moisture content, higher AnMOC, higher NO_3^- supply and lower redox potential, hence creating favourable conditions for both denitrification and DNRA.

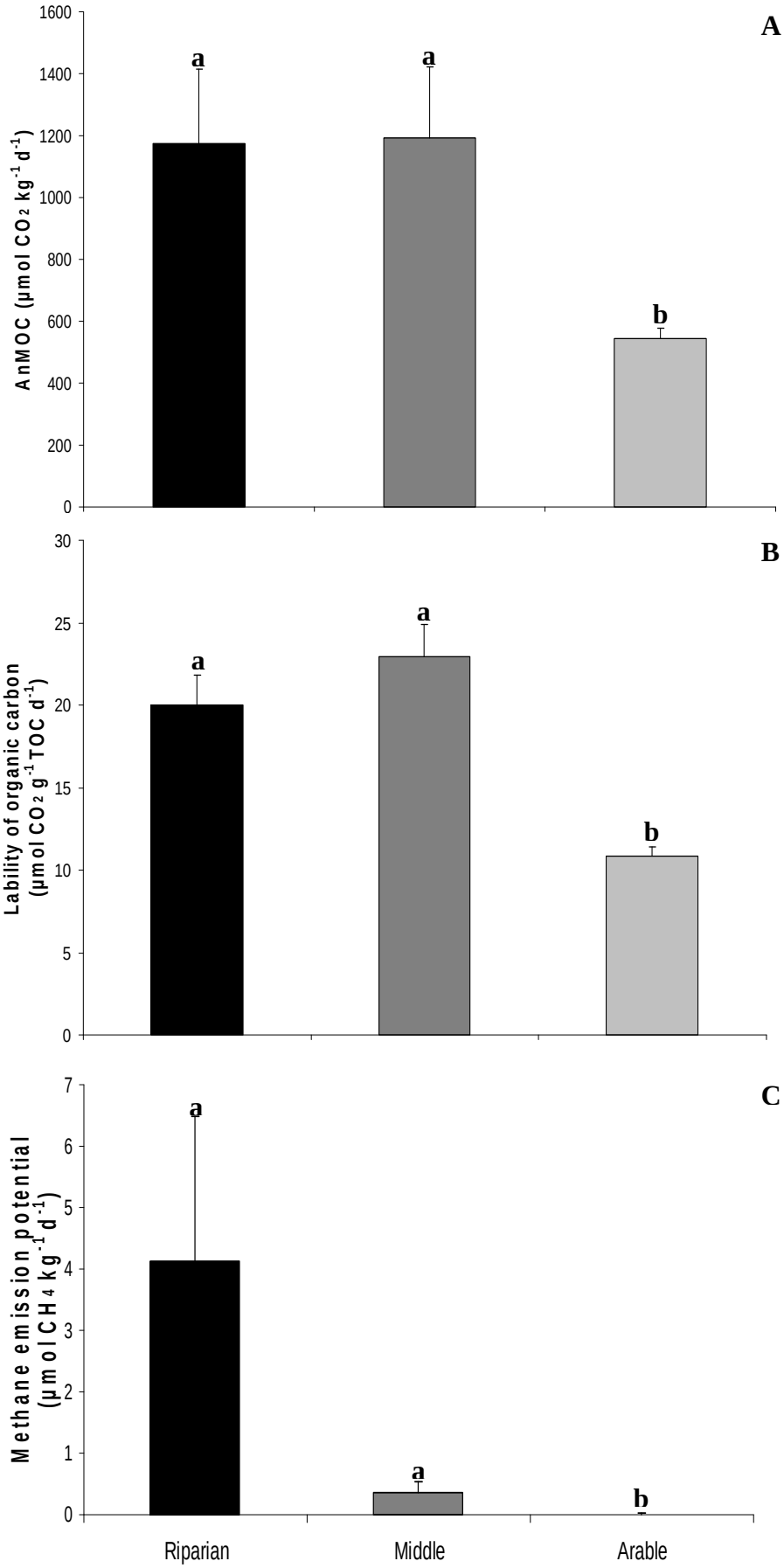

Figure 6.2.15: Mean AnMOC, lability of organic carbon and methane production potential (+ 1 standard error) in the sampling transects of the BZ (significant differences indicated with different lower case letters).

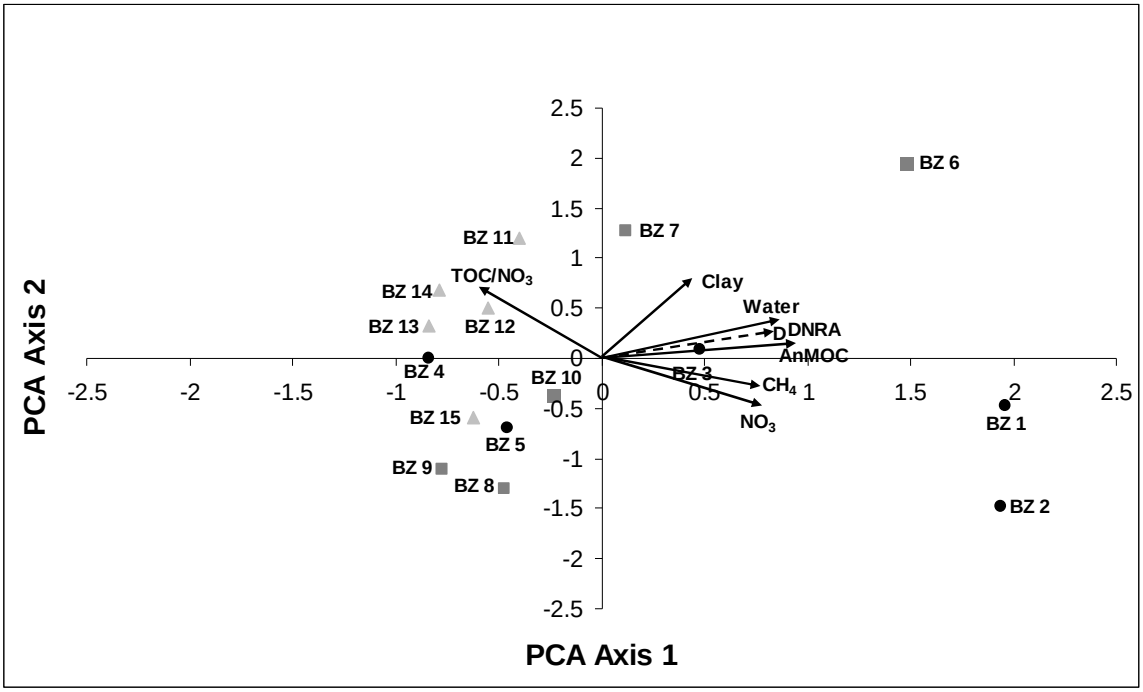

Figure 6.2.16: Correlation bi-plot from the PCA analysis in the three sampling transects in BZ. Correlations of the variables with the main axes are given by solid arrows. Dashed arrows indicate the correlation of nitrate attenuation processes with the component axes. Black circles; Riparian samples, Grey squares; Middle field samples, Light grey triangles; Arable field samples, Water; water content, CH_4; methane production potential, NO_3; soil nitrate content, D; potential denitrification rate.

Table 6.2.8: The principal components (axes) generated by the PCA, their respective eigenvalues, the % of variance explained by each component and the cumulative % of variance explanation.

Axes	Eigenvalues	% of Variance	Cumulative %
1	4.631	57.9	57.9
2	1.619	20.2	78.1
3	0.997	12.5	90.6

Table 6.2.9: Correlation coefficients of the environmental variables in PCA. ***Correlation significant at the 0.01 probability level.

Variables	Component 1	Component 2
Water content	0.859***	0.366
Clay content	0.423	0.770***
AnMOC	0.931***	0.134
Methane	0.770***	-0.303
Organic Carbon	0.897***	0.280
Soil Nitrate	0.774***	-0.446
TOC/NO_3	-0.594	0.710***
Lability of OC	0.706***	-0.022

The Buffer Zone area displayed very homogeneous soil physical properties and only the AnMOC, the lability of organic carbon and the methane production potential were significantly lower in the Arable field samples. The homogeneity was also evident in the potential denitrification rates that were not significantly different between sampling transects (Table 6.2.7). The gradient from the river towards the arable field, found in the majority of the soil properties, was also repeated for the denitrification potential; with the Riparian samples having slightly higher rates, followed by the Middle field samples and finally the Arable field samples (Table 6.1.6 and Figure 6.2.17 A).

The DNRA results were similar to the pattern for the denitrification rate; the sampling transects of the BZ were not significantly different (Table 6.2.7). The DNRA rates of the Riparian and Middle field samples were almost identical, while the Arable field samples had a slightly lower rate (Table 6.1.6 and Figure 6.2.17 B). As expected, the ratio D/DNRA was not significantly different between the sampling transects of the Buffer Zone (Table 6.2.7 and Figure 6.2.17 C).

As a result of the homogeneous conditions between sampling transects and the fact that the nitrate attenuation processes followed a similar gradient to the soil physical properties, correlation analysis indicated numerous statistically significant relationships (Table 6.2.10).

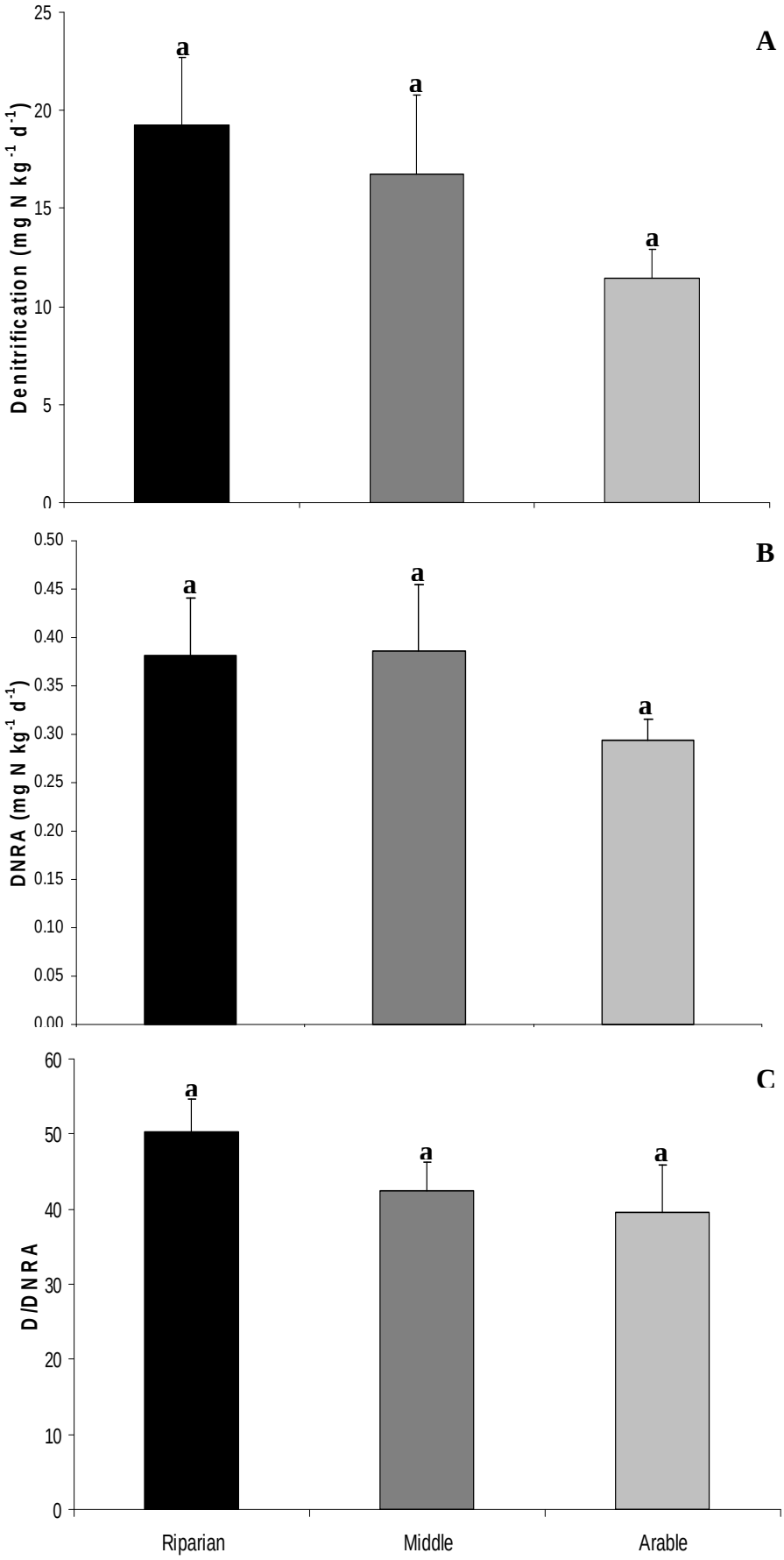

Figure 6.2.17: Mean denitrification potential, DNRA potential and D/DNRA (+ 1 standard error) in the sampling transects of the BZ (significant differences indicated with different lower case letters).

Denitrification showed a strong significant positive correlation with DNRA, with the water content, the AnMOC, the organic carbon content, the ratio TOC/TN and the soil nitrate content. Similarly, DNRA correlated strongly with the water content, the AnMOC, the organic carbon content and the methane production potential (Table 6.2.10).

MRA for the denitrification potential confirmed the results of the correlation analysis; with the water content explaining 79 % (MRA; r^2=0.79, *df*=14, *P*<0.01) of the variance observed in the denitrification potential rates, followed by the AnMOC with 70 % (MRA; r^2=0.70, *df*=14, *P*<0.01), the organic carbon content with 58 % (MRA; r^2=0.58, *df*=14, *P*<0.01) and the ratio TOC/TN with 49 % (MRA; r^2=0.49, *df*=14, *P*<0.01). MRA for the DNRA potential rates indicated the water content with 83 % (MRA; r^2=0.83, *df*=9, *P*<0.01) explanatory power, followed by the AnMOC with 69 % (MRA; r^2=0.69, *df*=9, *P*<0.01), the ratio TOC/TN with 65 % (MRA; r^2=0.65, *df*=9, *P*<0.01) and the organic carbon content with 59 % (MRA; r^2=0.59, *df*=9, *P*<0.05).

Overall the hydrogeomorphic units in the BZ area (i.e. sampling transects) were fairly homogeneous in their soil physical properties reflecting a uniform hydrologic regime dominated by overbank flooding of the river, which extends from the riparian area to the arable field. However, those locations near the river margin and the drainage tunnel beneath the road, due to their longer floodwater retention times, have been separated by the PCA as 'hotspots' of favourable conditions for denitrification and DNRA. Although not statistically significant, a decreasing gradient of favourable conditions for nitrate attenuation was observed from the riparian transect towards the arable field. Despite the AnMOC, the labile OC and the methane production potential being significantly lower in the arable field samples, the denitrification and DNRA potential was not different between the transects. The results suggest that the BZ as a whole has the potential for effective nitrate attenuation provided that the overbank flooding creates the necessary conditions of reduced oxygen availability, and increased supply of labile organic carbon and nitrate.

Table 6.2.10: Correlation matrix between the DNRA potential rate, the denitrification potential rate, AnMOC, lability of organic carbon, methane production potential and the physical properties of the topsoil in the sampling transects of BZ. Underlined correlation coefficients are products of Spearman rho correlation whereas non-underlined are products of Pearson Product-Moment correlation. ** Correlation is significant at the 0.01level and *Correlation is significant at the 0.05 level.

Variables/Correlation coefficients		Denitrification potential	DNRA	AnMOC	Org. carbon lability	Methane emission	Organic matter content	Organic carbon	TOC/TN	TOC/NO_3^-	Water content	Soil nitrate
Denitrification potential	*R or rho*	1										
	P	.										
	N	15										
DNRA	*R or rho*	**0.887****	1									
	P	0.000	.									
	N	15	15									
AnMOC	*R or rho*	**0.837****	**0.866****	1								
	P	0.020	0.000	.								
	N	15	15	15								
Org. carbon lability	*R or rho*	0.631*	**0.698****	**0.878****	1							
	P	0.012	0.004	0.000	.							
	N	15	15	15	15							
Methane emission	*R or rho*	0.498	**0.730****	**0.833****	**0.786****	1						
	P	0.059	0.002	0.000	0.001	.						
	N	15	15	15	15	15						
Organic matter content	*R or rho*	**0.652****	**0.677****	**0.824****	**0.704****	**0.909****	1					
	P	0.008	0.006	0.000	0.003	0.000	.					
	N	15	15	15	15	15	15					
Organic carbon	*R or rho*	**0.763****	**0.778****	**0.808****	0.442	0.433	**0.737****	1				
	P	0.001	0.001	0.000	0.099	0.107	0.002	.				
	N	15	15	15	15	15	15	15				
TOC/TN	*R or rho*	**0.697****	**0.722****	**0.820****	0.560*	0.396	**0.657****	**0.829****	1			
	P	0.004	0.002	0.000	0.030	0.143	0.008	0.000	.			
	N	15	15	15	15	15	15	15	15			
TOC/NO_3^-	*R or rho*	-0.219	-0.244	-0.346	-0.286	-0.506	-0.606*	-0.349	-0.447	1		
	P	0.433	0.382	0.206	0.302	0.055	0.017	0.202	0.095	.		
	N	15	15	15	15	15	15	15	15	15		
Water content	*R or rho*	**0.889****	**0.921****	**0.874****	**0.650****	**0.676****	**0.680****	**0.817****	**0.738****	-0.270	1	
	P	0.000	0.000	0.000	0.009	0.006	0.005	0.000	0.002	0.330	.	
	N	15	15	15	15	15	15	15	15	15	15	
Soil nitrate	*R or rho*	0.593*	0.610*	0.562*	0.372	0.542*	**0.696****	0.611*	0.597*	**-0.871****	0.510	1
	P	0.020	0.016	0.029	0.172	0.037	0.004	0.016	0.019	0.000	0.052	.
	N	15	15	15	15	15	15	15	15	15	15	15

6.2.4 *Grazing Grassland (GG)*

The physical properties of the topsoil in the three sampling transects of the Grazing Grassland (Mill Leat, Middle Field and Riparian) are summarised in Table 6.1.1. Opposite to the other zones of the re-connected floodplain, GG has two transects influenced by overbank flooding, the Mill Leat adjacent to the old channel, and the Riparian along the meandering river, whereas the grazing activity is concentrated in the Middle Field. The above land use and hydrological regime seem to be influencing markedly the physical properties of the topsoil.

The dry bulk density was found significantly lower (Table 6.2.11) in the Middle Field, whereas the water content and the organic matter content were significantly higher in the Middle (Figure 6.2.18 A,B,C). The organic carbon was also found significantly higher in the Middle, but the ratios TOC/TN and TOC/NO_3^- were not significantly different between transects (Table 6.2.11 and Figure 6.2.18 D,E,F).

Table 6.2.11: Comparison of the means between the three sampling transects of the GG area for selected soil properties and processes. *df*; degrees of freedom, *F*; F statistic, χ^2; χ^2 statistic *P*; probability level. Where the variable is annotated with * the non-parametric Kruskal-Wallis test has been used instead of One-Way ANOVA.

	One-Way ANOVA and Kruskal-Wallis		
Grazing Grassland	*df*	*F or* χ^2	*P*
Bulk density	14	11.67	<0.01
Organic matter	14	9.56	<0.01
Organic carbon	14	6.03	<0.05
Very fine sand	14	4.49	<0.05
Water content	14	5.90	<0.05
TOC/TN	14	3.21	>0.05
TOC/NO_3^-	14	0.61	>0.05
Soil nitrate*	2	1.82	>0.05
Soil ammonia*	2	5.29	>0.05
Soil nitrite*	2	2.66	>0.05
AnMOC*	2	4.61	>0.05
Lability of OC	12	0.06	>0.05
Methane emission*	2	10.68	<0.01
Denitrification	14	2.79	>0.05
DNRA	14	3.02	>0.05
D/DNRA	14	0.60	>0.05

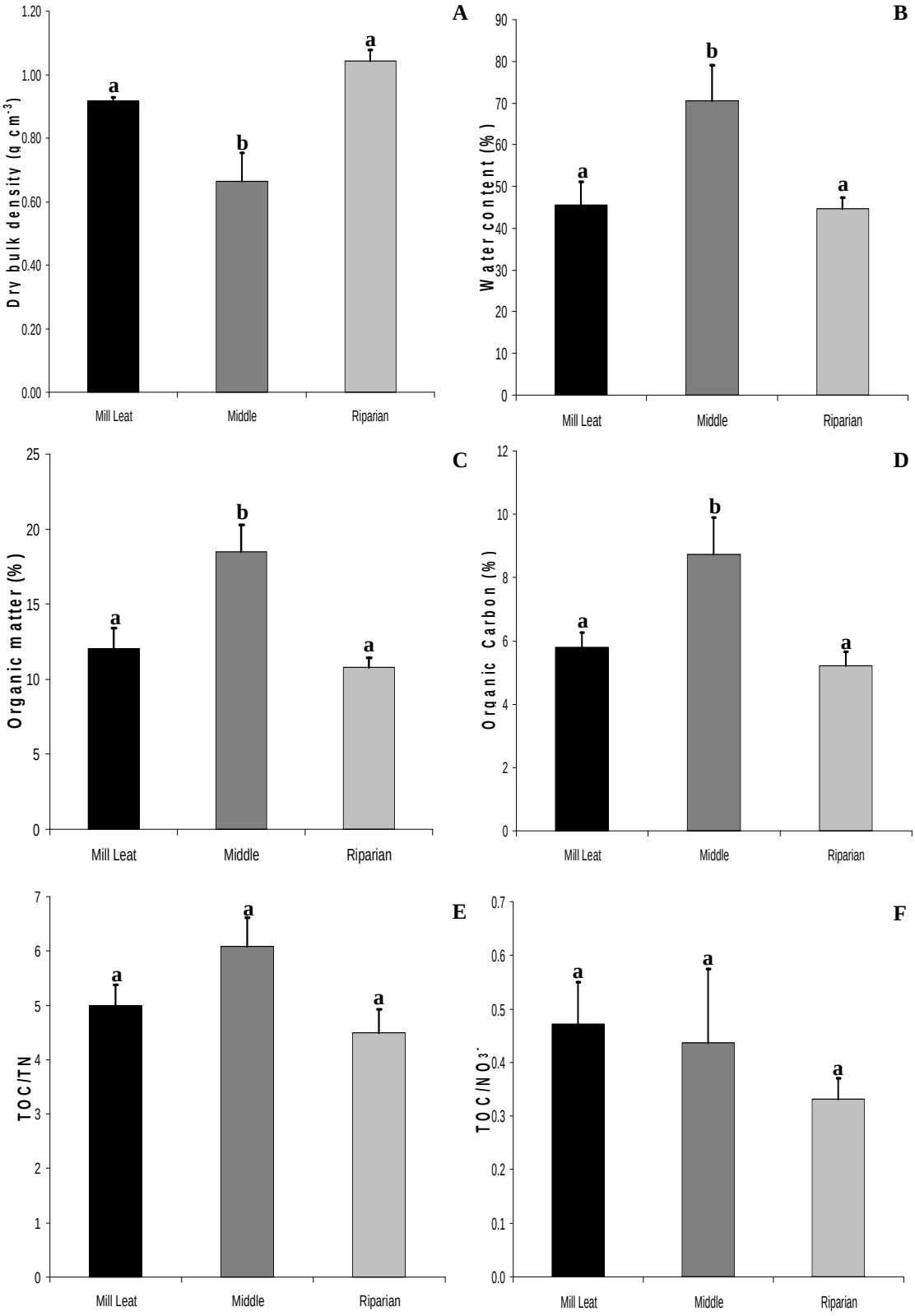

Figure 6.2.18: Soil physical properties in the sampling transects of the Grazing Grassland. Data are means + 1 SE. Same lower case letters indicate no significant difference of the means.

However, the particle size fractions were not significantly different between the transect samples, with the exception of the very fine sand fraction that was significantly higher in the Mill Leat samples compared to the Middle (Figure 6.2.19). Finally, the mean soil nitrate concentration, although double in the Middle samples, due to high inter-sample variability, it was not statistically different from the other transects. Both soil ammonia and nitrite concentrations were not found significantly different between transects (Table 6.2.11 and Figure 6.2.20).

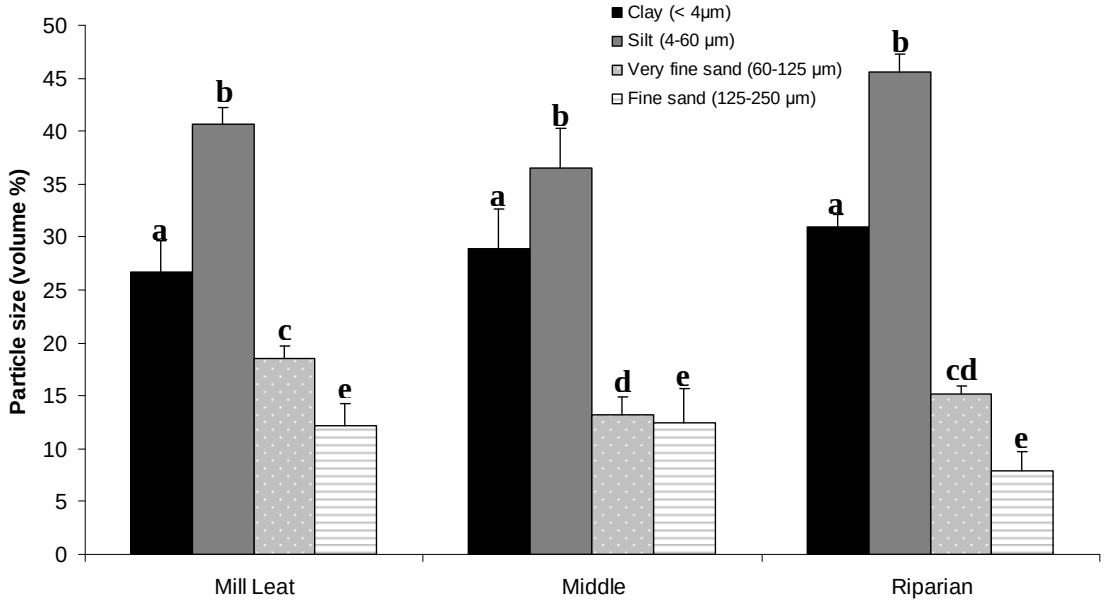

Figure 6.2.19: Absolute particle size distribution (volume %) in the three sampling transects of the Grazing Grassland (mean and + 1 standard error, same lower case letters indicate no significant difference between the means).

Although the majority of the soil physical properties showed some significant differences between the sampling transects of the GG, the AnMOC was not significantly different mainly due to the high variability observed in the Middle field samples (Table 6.1.2, 6.2.11 and Figure 6.2.21 A). Similarly, the lability of organic carbon, although it was double for the Middle field samples (Table 6.1.2 and Figure 6.2.21 B), due to the high variability it was not significantly different from the rest of the sampling transects.

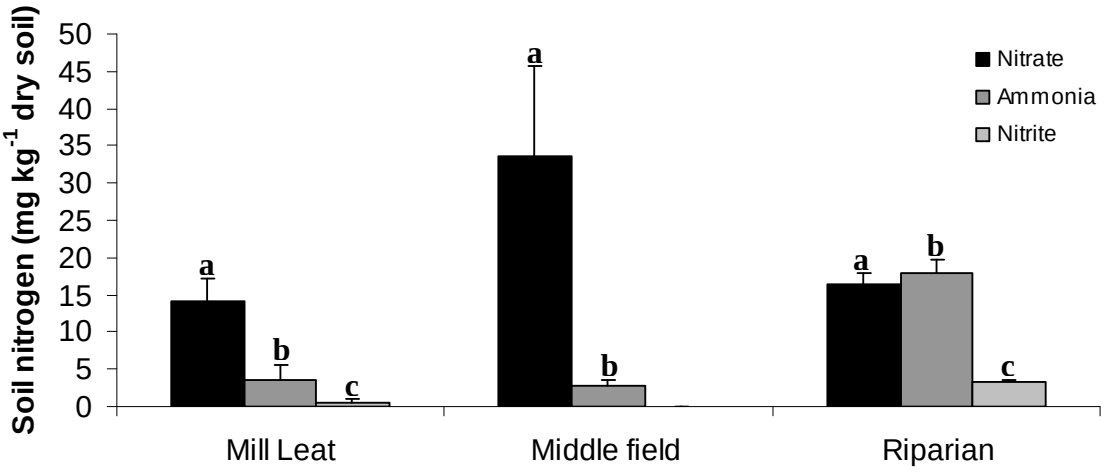

Figure 6.2.20: Mean concentrations of NO_3^--N, NH_3-N and NO_2^--N (+ 1 standard error) in the three sampling transects of the Grazing Grassland. Same lower case letters indicate no significant difference between the means.

The methane production potential was however significantly different between the sampling transects (Table 6.2.11), with the Riparian samples displaying the highest rate, followed by the Mill Leat samples and the Middle field samples (Table 6.1.2 and Figure 6.2.21 C).

The application of PCA with those variables that displayed some significant differences resulted in three principal component axes explaining 94 % of the variance between individual samples (Table 6.2.12). Axis 1 was associated with the water content, the AnMOC, the lability of OC and the soil nitrate, while the second axis was associated with the CH_4 production potential and the ratio TOC/NO_3^- (Table 6.2.13). Plotting the cluster centroids (average score per component and standard errors) for the three transects resulted in Figure 6.2.22. The Middle samples were associated with the positive axis 1, while the error bars indicated the high variability between samples. The Riparian and Mill leat samples overlapped along axis 1, while the first were closely associated with the methane potential whereas the latter were related to the ratio TOC/NO_3^-.

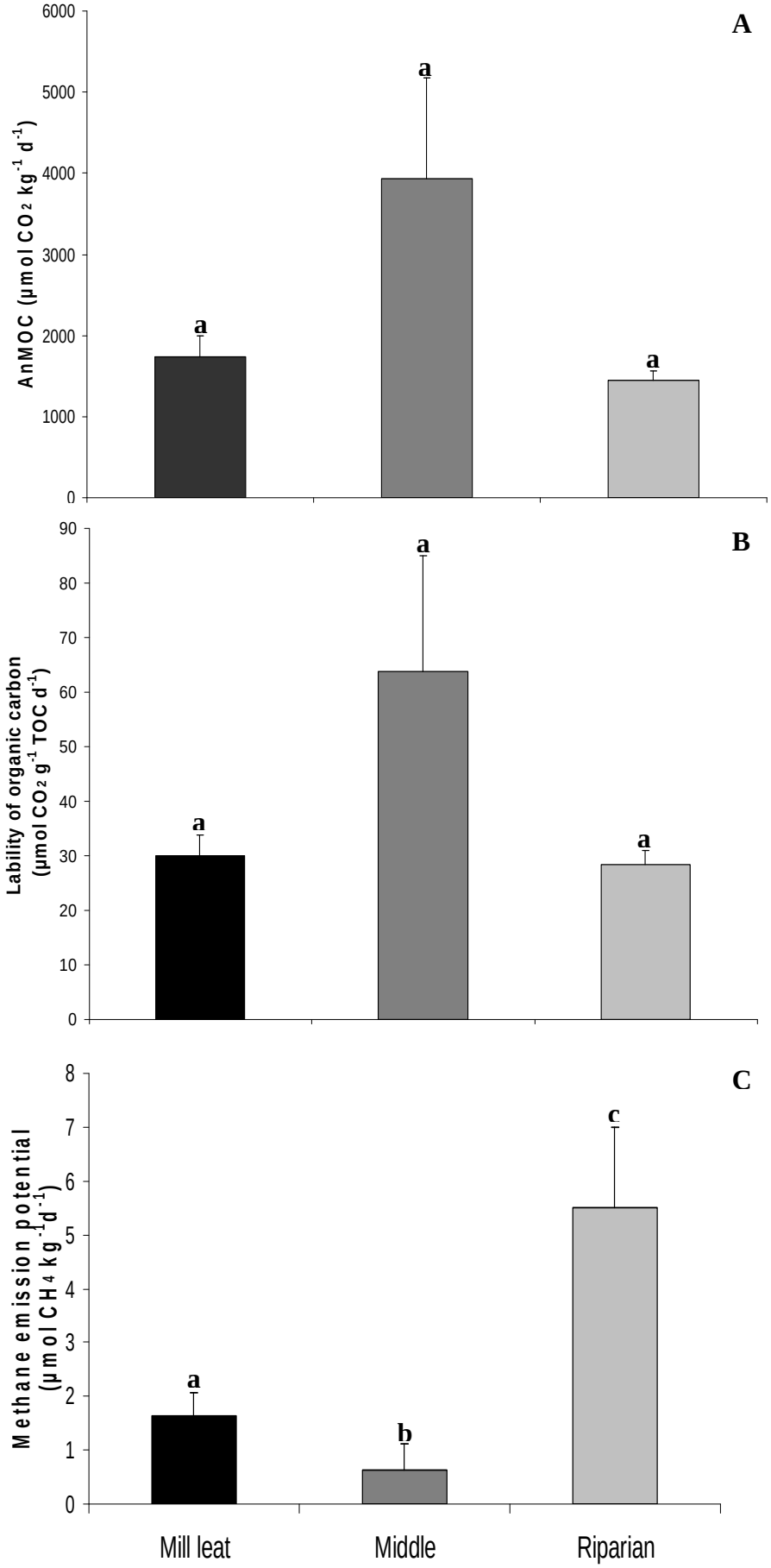

Figure 6.2.21: Mean AnMOC, lability of organic carbon and methane production potential (+ 1 standard error) in the sampling transects of the GG (significant differences indicated with different lower case letters).

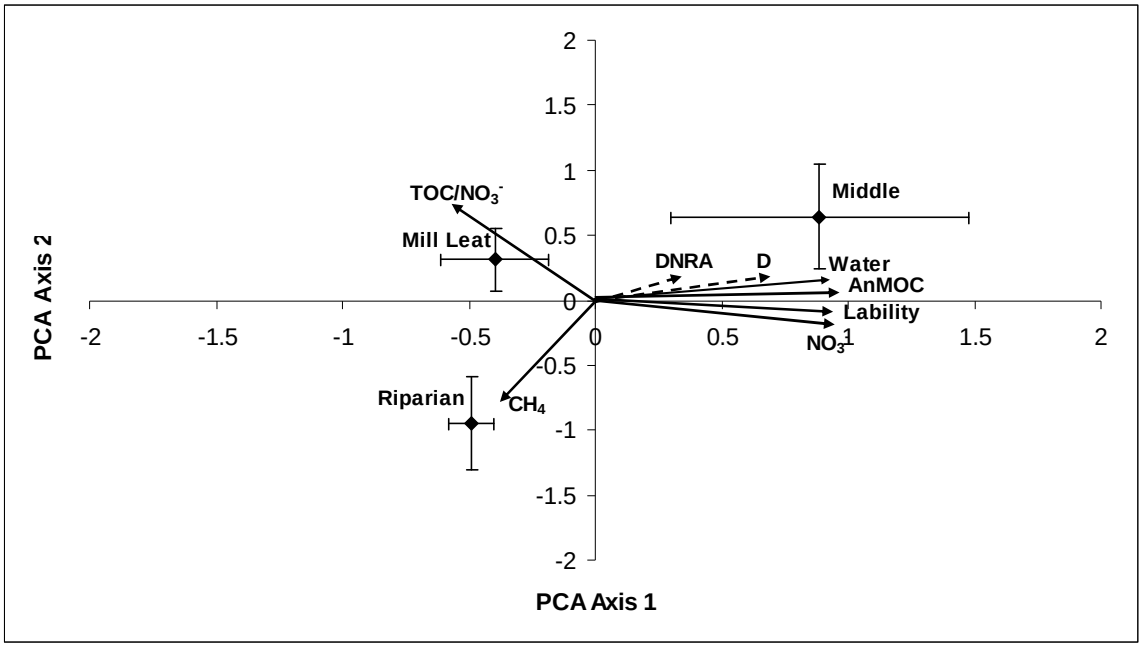

Figure 6.2.22: Correlation bi-plot from the PCA analysis with cluster centroids (average score on each component, with standard errors) for the three sampling transects in GG. Correlations of the variables with the main axes are given by solid arrows. Dashed arrows indicate the correlation of nitrate attenuation processes with the component axes. Water; water content, NO_3^-; soil nitrate content, Lability; labile organic carbon, CH_4; methane production potential, D; potential denitrification rate.

Table 6.2.12: The principal components (axes) generated by the PCA, their respective eigenvalues, the % of variance explained by each component and the cumulative % of variance explanation.

Axes	Eigenvalues	% of Variance	Cumulative %
1	4.750	67.9	67.9
2	1.338	19.1	87.0
3	0.461	6.6	93.6

Table 6.2.13: Correlation coefficients of the environmental variables in PCA. ***Correlation significant at the 0.01 probability level.

Variables	Component 1	Component 2
Water content	0.933***	0.142
Organic matter	0.865***	0.249
AnMOC	0.953***	0.050
Methane	-0.383	-0.811***
Soil Nitrate	0.929***	-0.192
TOC/NO_3	-0.574	0.739***
Lability of OC	0.940***	-0.109

The potential denitrification and DNRA rates for the sampling transects of the GG are summarised in Table 6.1.6. Despite some significant differences of the soil physical properties between the sampling transects, the denitrification rates were not significantly different (Table 6.2.11). The Middle field samples had slightly higher denitrification rate, followed by the Mill Leat samples and finally the Riparian samples (Figure 6.2.23 A). Neither the DNRA potential was significantly different between the sampling transects of the GG (Table 6.2.11). The Mill Leat and the Middle field samples had very similar DNRA rates, while the Riparian samples were lower (Figure 6.2.23 B). With regards to the relative importance of the two processes, D/DNRA ratio, there was no significant difference between the sampling transects (Table 6.2.11 and Figure 6.2.23 C).

The potential denitrification and DNRA rates showed a significant positive correlation with each other (Table 6.2.14). Moreover, both processes correlated significantly with the AnMOC, the bulk density and the water content. Finally, no significant relationship was found between DNRA and the methane production potential or the ratio TOC/TN.

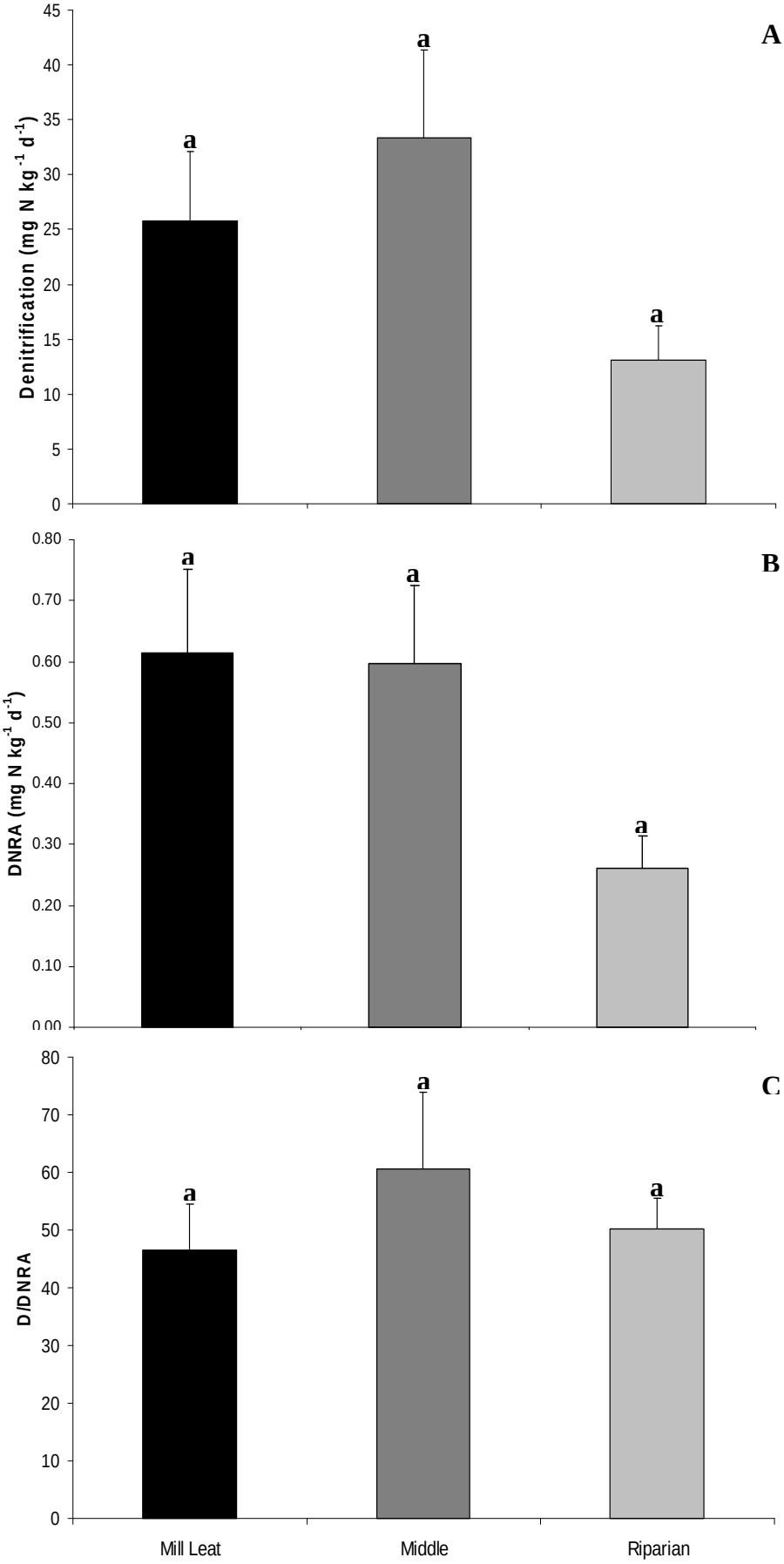

Figure 6.2.23: Mean denitrification potential, DNRA potential and D/DNRA (+ 1 standard error) in the sampling transects of the GG (significant differences indicated with different lower case letters).

Table 6.2.14: Correlation matrix between the DNRA potential rate, the denitrification potential rate, AnMOC, lability of organic carbon, methane production potential and the physical properties of the topsoil in the sampling transects of GG. Underlined correlation coefficients are products of Spearman rho correlation whereas non-underlined are products of Pearson Product-Moment correlation. ** Correlation is significant at the 0.01level and *Correlation is significant at the 0.05 level.

Variables/Correlation coefficients		Denitrification potential	DNRA	AnMOC	Org. carbon lability	Methane emission	Organic matter content	Organic carbon	TOC/TN	Bulk density	Water content	Soil nitrate
Denitrification potential	*R or rho*	1										
	P	.										
	N	15										
DNRA	*R or rho*	**0.811****	1									
	P	0.000	.									
	N	15	15									
AnMOC	*R or rho*	**0.736****	**0.692****	1								
	P	0.003	0.006	.								
	N	14	14	14								
Org. carbon lability	*R or rho*	0.493	0.544	0.561*	1							
	P	0.087	0.055	0.046	.							
	N	13	13	13	13							
Methane emission	*R or rho*	-0.396	-0.191	-0.476	0.409	1						
	P	0.181	0.532	0.118	0.212	.						
	N	13	13	12	11	13						
Organic matter content	*R or rho*	0.572*	0.521*	**0.849****	0.378	**-0.714****	1					
	P	0.026	0.047	0.000	0.202	0.006	.					
	N	15	15	14	13	13	15					
Organic carbon	*R or rho*	0.371	0.554*	0.635*	0.093	-0.665*	**0.795****	1				
	P	0.174	0.032	0.015	0.763	0.013	0.000	.				
	N	15	15	14	13	13	15	15				
TOC/TN	*R or rho*	0.313	0.502	0.613*	0.057	-0.462	**0.697****	**0.910****	1			
	P	0.256	0.057	0.020	0.854	0.112	0.004	0.000	.			
	N	15	15	14	13	13	15	15	15			
Bulk density	*R or rho*	**-0.723****	**-0.647****	**-0.907****	-0.277	**-0.740****	**-0.831****	**-0.705****	-0.637*	1		
	P	0.002	0.009	0.000	0.359	0.004	0.000	0.003	0.011	.		
	N	15	15	14	13	13	15	15	15	15		
Water content	*R or rho*	**0.739****	0.570*	**0.916****	0.531	-0.423	**0.911****	**0.686****	**0.664****	**-0.842****	1	
	P	0.002	0.026	0.000	0.062	0.150	0.000	0.005	0.007	0.000	.	
	N	15	15	14	13	13	15	15	15	15	15	
Soil nitrate	*R or rho*	0.506	0.416	**0.922****	0.622*	-0.132	**0.730****	0.532*	0.536*	**-0.799****	**0.814****	1
	P	0.054	0.123	0.000	0.023	0.668	0.002	0.041	0.040	0.000	0.000	.
	N	15	15	14	13	13	15	15	15	15	15	15

MRA between the denitrification potential and the environmental variables indicated that AnMOC can explain 61 % of the variance in denitrification (MRA; r^2=0.61, *df*=14, *P*<0.01), while the lability of organic carbon, that was not picked up by the correlation analysis, displayed 54 % explanatory power (MRA; r^2=0.54, *df*=14, *P*<0.01). Additionally, the water content explained 46 % of the variance (MRA; r^2=0.46, *df*=14, *P*<0.01), while the organic matter content 33 % (MRA; r^2=0.33, *df*=14, *P*<0.05) and the bulk density 32% (MRA; r^2=0.32, *df*=14, *P*<0.05). MRA between the DNRA potential and the environmental variables was not in good agreement with the correlation results. The highest explanatory power was shown for the organic carbon content with 30% (MRA; r^2=0.30, *df*=14, *P*<0.05), while only the organic matter content (MRA; r^2=0.27, *df*=14, *P*<0.05) and the AnMOC (MRA; r^2=0.27, *df*=14, *P*<0.05) were also significant in regression analysis and they could both explain 27 % of the variance in DNRA rates.

The specific hydrologic regime of the GG as well as the land use affected the distribution of soil moisture and organic carbon across the site. Specifically, the Middle field was associated with higher organic carbon availability, possibly as a result of the grazing activity and the animal manure, which created carbon 'hotspots', as it was also indicated by the high variability shown in the PCA. Moreover, the overbank flooding regime in both the Riparian and the Mill leat transects was responsible for lower redox conditions indicated by the methane production potential. However, neither the denitrification nor the DNRA potential were significantly different between hydrogeomorphic units, due to high variability among samples, although denitrification tended to be higher within the grazing zone. Therefore, it could be argued that the external organic carbon supply in conjunction with frequent overbank flooding from both the river and the old channel create the necessary conditions for effective nitrate attenuation across the whole extent of the GG.

6.3 *The effect of subsurface hydrology and soil properties on nitrate attenuation in two land use zones of the River Cole re-connected floodplain*

The effect of groundwater hydrology and subsurface soil properties on the nitrate attenuation processes in the vadoze zone of the reconnected floodplain of the River Cole was investigated in the Buffer Zone (BZ) and the Pasture Meadow (PM) where a detailed study of the hydrological regime was also conducted. Moreover, the potential for denitrification in the subsurface of the BZ was investigated for the purpose of the application of the NEMIS model (see Chapter 7).

6.3.1 *Soil physical properties in the subsurface of the Buffer Zone*

The soil physical properties, averaged from eight randomly sampled locations in the BZ, at six depth intervals (A; 0 – 10 cm, B; 10 – 20 cm, C; 20 – 30 cm, D; 50 – 70 cm, E; 80 – 100 cm and F; 100 – 120 cm) are summarised in Table 6.3.1. Table 6.3.2 presents the results of the parametric (One-Way ANOVA) or non-parametric (Kruskal-Wallis) statistical tests for the comparison of variable means between depth intervals. The dry bulk density was significantly different between the A, B and C depth intervals and only the D, E and F depths did not differ between them (Figure 6.3.2 A). Regarding the absolute particle size distribution, the topsoil (A depth interval) had significantly less clay and silt content, while the fine and medium sand contents were higher than in the rest of the depth intervals (Figure 6.3.1). Therefore the topsoil in the BZ was classified as sandy clay loam, as opposing to silty clay loam found in an earlier sampling for the land use analysis, whereas the subsurface was dominated by clay and silt, with appreciable amounts of fine (10 %) and medium (6 %) sands. The combination of low bulk density and high mean grain size for the topsoil leads to increased permeability k (19.3 m^2) according to Boudreau (1997). The discrepancy observed in the soil type of the BZ topsoil between the two different samplings could be due to the fact that the sampling dates were 18 months apart and during this period there were numerous high magnitude flood events that could have changed the composition of the topsoil (see Chapter 5).

Table 6.3.1: Soil physical properties in the sampled depth intervals of the buffer zone subsurface (data are mean values ± 1 SE).

	Soil type	Dry Bulk Density ($g\ cm^{-3}$)		Water content (%)		Organic matter (%)		Organic carbon (%)		TOC/TN		NO_3^--N ($mg\ kg^{-1}$)		TOC/NO_3^-	
Buffer Zone depth		**Mean**	**± 1 SE**	**Mean**	**± 1 SE**	**Mean**	**± 1 SE**	**Mean**	**± 1 SE**	**Mean**	**± 1 SE**	**Mean**	**± 1 SE**	**Mean**	**± 1 SE**
A 0-10 cm (n=8)	Sandy clay loam	0.75	0.05	51.9	4.84	11.1	0.73	4.5	0.47	10.5	0.31	15.3	2.6	0.34	0.05
B 10-20 cm (n=8)	Clay loam	1.24	0.04	38.6	2.58	8.4	0.47	2.9	0.32	10.0	0.18	7.8	2.1	0.47	0.07
C 20-30 cm (n=8)	Silty clay	1.13	0.04	36.7	2.61	6.8	0.65	1.6	0.24	11.7	0.96	6.9	1.3	0.30	0.07
D 50-70 cm (n=8)	Clay	2.20	0.06	38.8	4.04	6.2	0.44	1.3	0.18	11.0	0.92	6.0	1.1	0.26	0.07
E 80-100 cm (n=8)	Silty clay	2.20	0.06	41.0	3.87	5.1	0.33	1.4	0.12	8.4	0.95	4.8	2.1	0.56	0.16
F 100-120 cm (n=8)	Silty clay	2.15	0.11	43.3	4.57	5.0	0.58	1.3	0.28	8.1	0.77	5.4	1.7	1.10	0.71

Table 6.3.2: Comparison of the means between the depth intervals of the BZ subsurface for selected soil properties and processes. *df*; degrees of freedom, *F*; F statistic, χ^2; χ^2 statistic *P*; probability level. Where the variable is annotated with * the non-parametric Kruskal-Wallis test has been used instead of One-Way ANOVA.

	One-Way ANOVA and Kruskal-Wallis				One-Way ANOVA and Kruskal-Wallis		
Buffer Zone subsurface	*df*	*F or* χ^2	*P*	**Buffer Zone subsurface**	*df*	*F or* χ^2	*P*
Bulk density*	5	44.9	<0.01	Soil nitrate	47	4.2	<0.01
Clay fraction	47	2.6	<0.05	Soil ammonia*	5	7.7	>0.05
Silt fraction	47	6.0	<0.01	Soil nitrite*	5	15.7	<0.01
Fine sand fraction	47	8.3	<0.01	AnMOC*	5	32.9	<0.01
Medium sand fraction*	5	15.7	<0.01	Lability of OC*	5	12.0	<0.05
Water content	47	2.0	>0.05	Methane emission*	5	21.7	<0.01
Organic matter	47	17.5	<0.01	Denitrification*	5	41.0	<0.01
Organic carbon	47	19.8	<0.01	Nitrous oxide production	46	56.3	<0.01
TOC/TN	47	3.7	<0.01	DNRA	47	21.6	<0.01
TOC/NO_3^-*	5	5.1	>0.05	D/DNRA*	5	13.9	<0.05

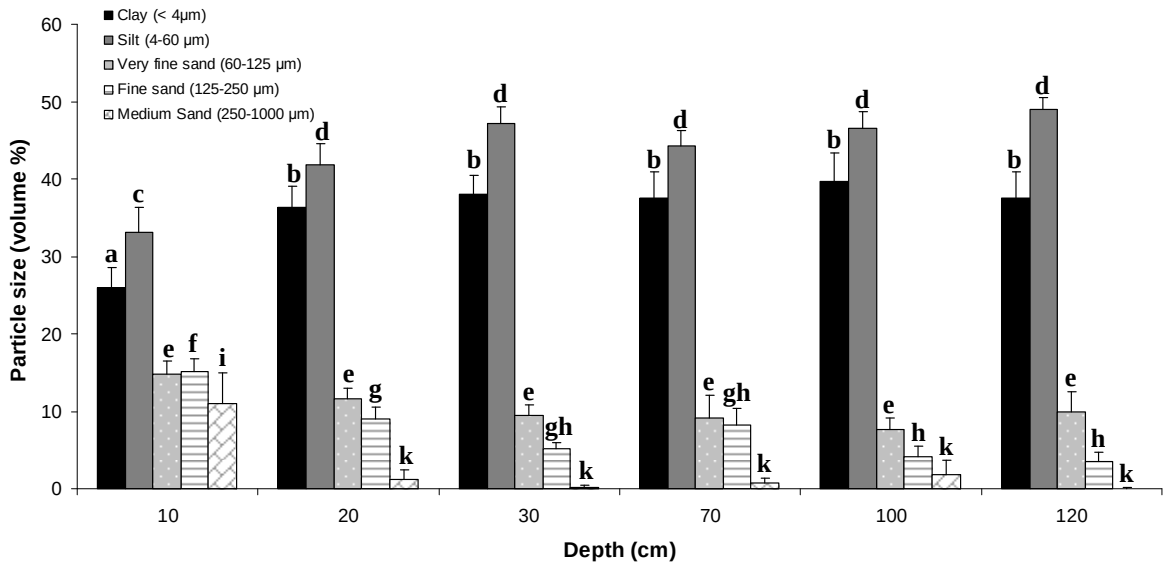

Figure 6.3.1: Absolute particle size distribution in the depth intervals of the subsurface of the BZ. Different lower case letters indicate significant differences.

Although the mean water content of the samples from the various depth intervals was not significantly different, the results showed a decreasing trend moving downwards in the soil profile from the surface, while the soil moisture increased again below 50 cm depth (Figure 6.3.2 B). The organic matter content decreased exponentially from the ground surface to 120 cm depth (Figure 6.3.2 C), whilst the organic carbon content decreased exponentially within 30 cm from the surface, with no significant difference between depths C, D, E and F (Figure 6.3.2 D). The ratio total organic carbon to total nitrogen (TOC/TN) was significantly different between the first four depth intervals (A,B,C,D) and the bottom two (E and F) (Figure 6.3.2 E). In contrast, the ratio TOC/NO_3^- was not different across the subsurface of the BZ (Figure 6.3.2 F). Significantly higher soil nitrate content was found in the topsoil of the Buffer Zone, while the other depth intervals had approximately 50 % less nitrate and were not significantly different between each other (Figure 6.3.3 A). Soil ammonia content was not significantly different between the depth intervals and the highest values were observed in the topsoil and in the saturated zone where the variability was very high driven by two hotspots in the samples 4 and 6 (Figure 6.3.3 B). Finally the nitrite content (Figure 6.3.3 C) was significantly higher in the topsoil compared to the rest of the depth intervals with the exception of depth B and the saturated zone F, indicating the possibility of nitrate reduction processes occurring in deeper horizons and especially the permanently saturated zone.

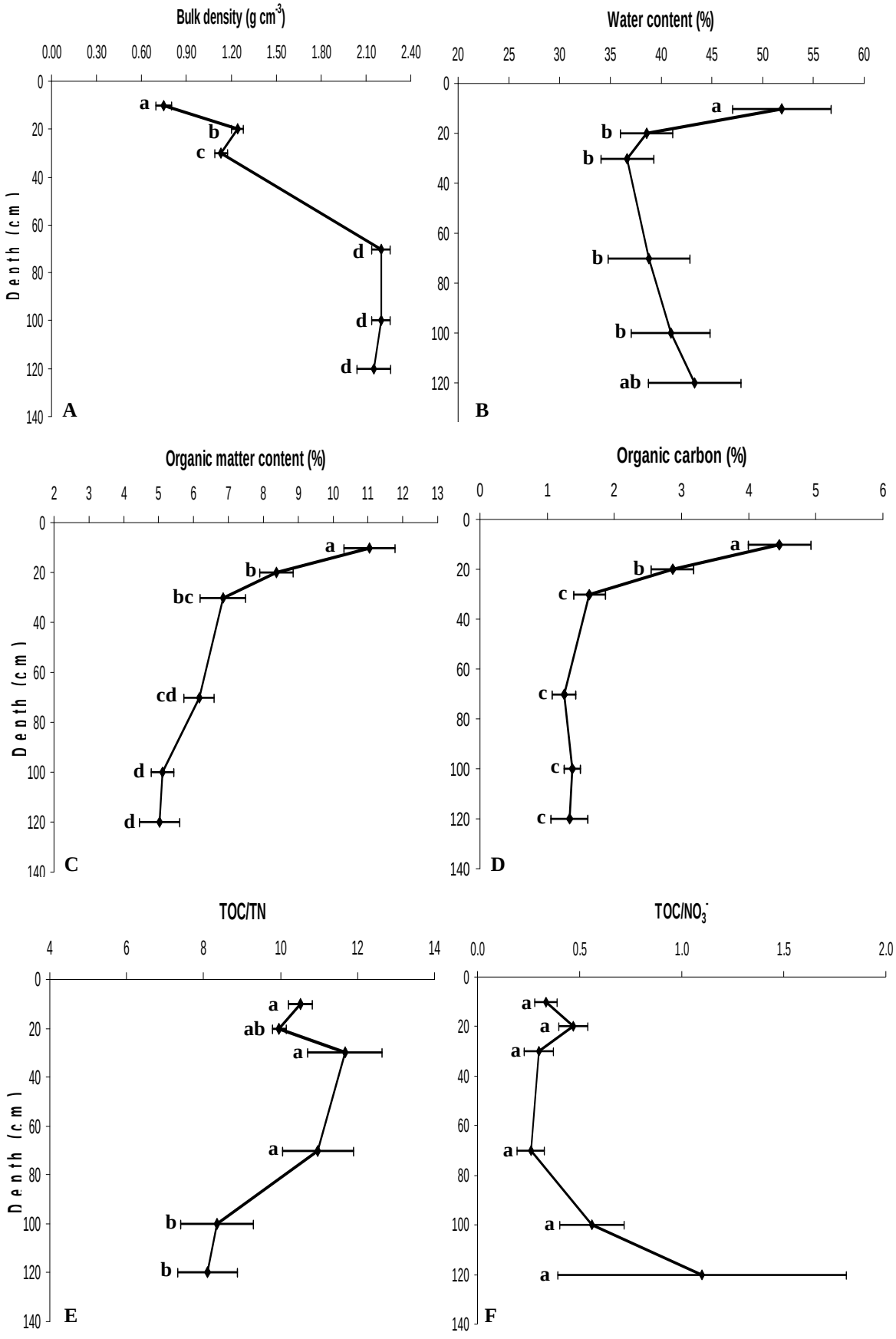

Figure 6.3.2: Dry bulk density, water content, organic matter and organic carbon contents, TOC/TN and TOC/NO_3^- ratios in the depth intervals of the BZ subsurface. Data are mean values ± 1 SE. Different lower case letters indicate significant differences

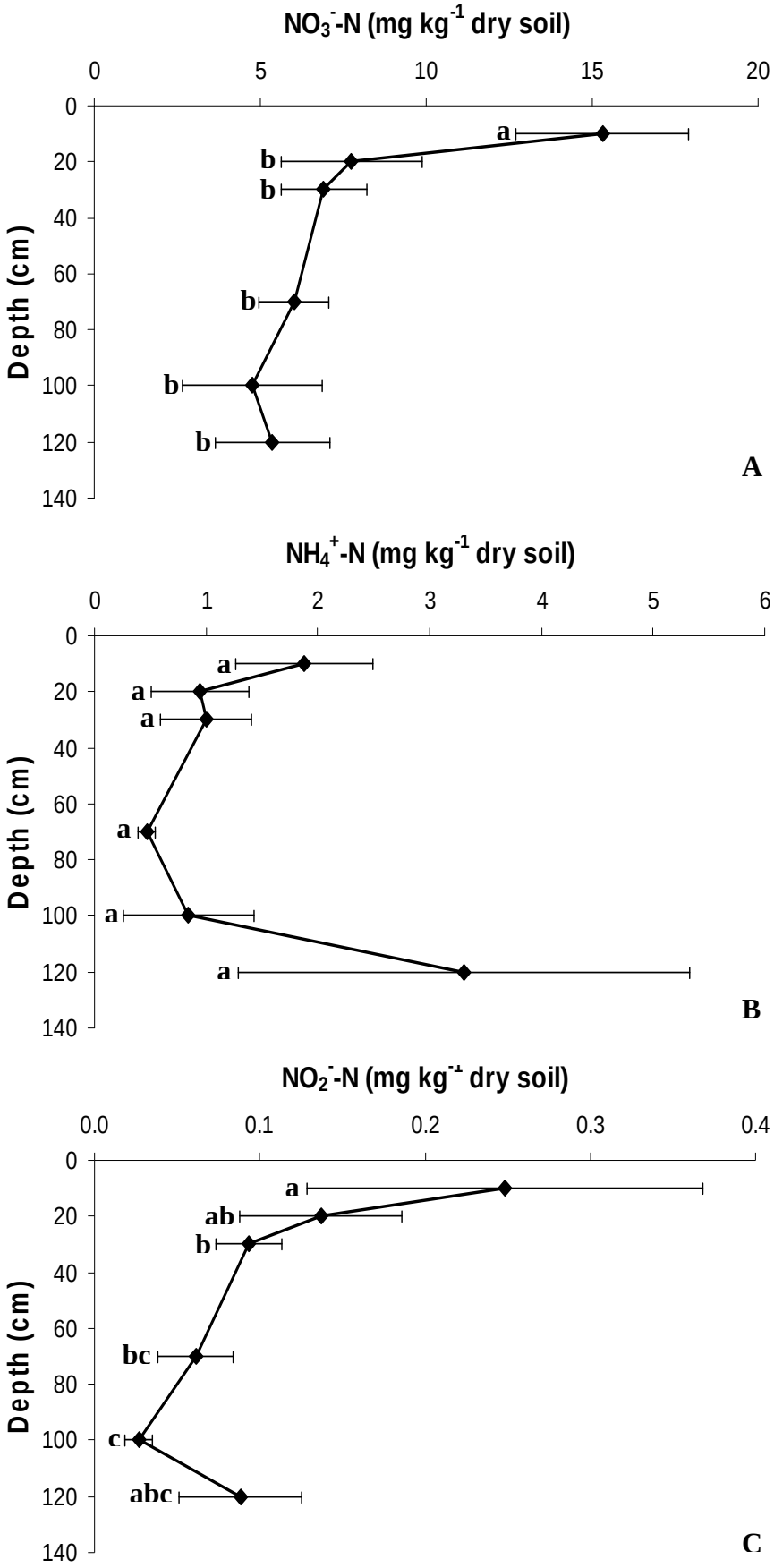

Figure 6.3.3: Soil NO_3^--N, NH_4^+-N and NO_2^--N in the depth intervals of the BZ subsurface. Data are mean values ± 1SE. Different lower case letters indicate significant differences.

6.3.2 *AnMOC and methane production potential in the subsurface of the Buffer Zone*

The anaerobic mineralisation rate of organic carbon (AnMOC) was significantly different between the depth intervals A, B and C compared to the deeper intervals D, E and F that were not different between each other (Table 6.3.2, 6.3.3 and Figure 6.3.4 A). The anaerobic mineralisation rate was reduced by 50 % within 10 cm in the topsoil (from 10 to 20 cm) and by 75 % down to 30 cm in the soil profile. Within the B soil horizon (50 – 100 cm) the AnMOC was 85 – 90 % less than the surface (top 10 cm) rate. However, the permanently saturated C soil horizon (>100 cm) retained 20 % of the mineralisation rate observed in the topsoil and that could possibly sustain a reduced rate of nitrogen retention processes.

The results for the lability of organic carbon, although they followed a similar pattern to AnMOC, only the E depth interval displayed significantly lower lability (Table 6.3.2, 6.3.3 and Figure 6.3.4 B). This was mainly due to the high variability among samples as shown by the large error bars in Figure 6.3.4 B. However, the lability of the C soil horizon, despite the variability, was comparable to the lability of the surface soil, supporting further the indication that the deepest saturated zone of the BZ area could potentially have enough electron donors to support appreciable rates of nitrogen retention processes. Methane production potential was observed predominantly in the topsoil (0 – 10 cm) samples (Table 6.3.3). Despite the high variability, the CH_4 production rate of the A samples was significantly higher than the rest of the samples (Table 6.3.2 and Figure 6.3.4 C).

Table 6.3.3: Anaerobic mineralisation rate (AnMOC), lability of organic carbon and methane production potential in the subsurface of the Buffer Zone. Data are means ± 1SE.

	AnMOC		**Labile org. carbon**		**Methane**	
	CO_2 (µmol kg^{-1} d^{-1})		**CO_2 (µmol g^{-1} TOC d^{-1})**		**CH_4 (µmol kg^{-1} d^{-1})**	
Buffer Zone depth	**Mean**	**± 1 SE**	**Mean**	**± 1 SE**	**Mean**	**± 1 SE**
A 0-10 cm (n=8)	550.2	78.5	13.0	2.0	167.3	79.0
B 10-20 cm (n=8)	273.5	26.7	9.9	1.4	2.7	2.4
C 20-30 cm (n=8)	137.1	15.2	9.3	1.5	0.012	0.01
D 50-70 cm (n=8)	85.3	12.4	8.0	1.5	0.005	0.00
E 80-100 cm (n=8)	51.4	7.7	4.1	0.9	0.004	4.07
F 100-120 cm (n=8)	109.9	25.9	10.1	2.6	0.03	0.02

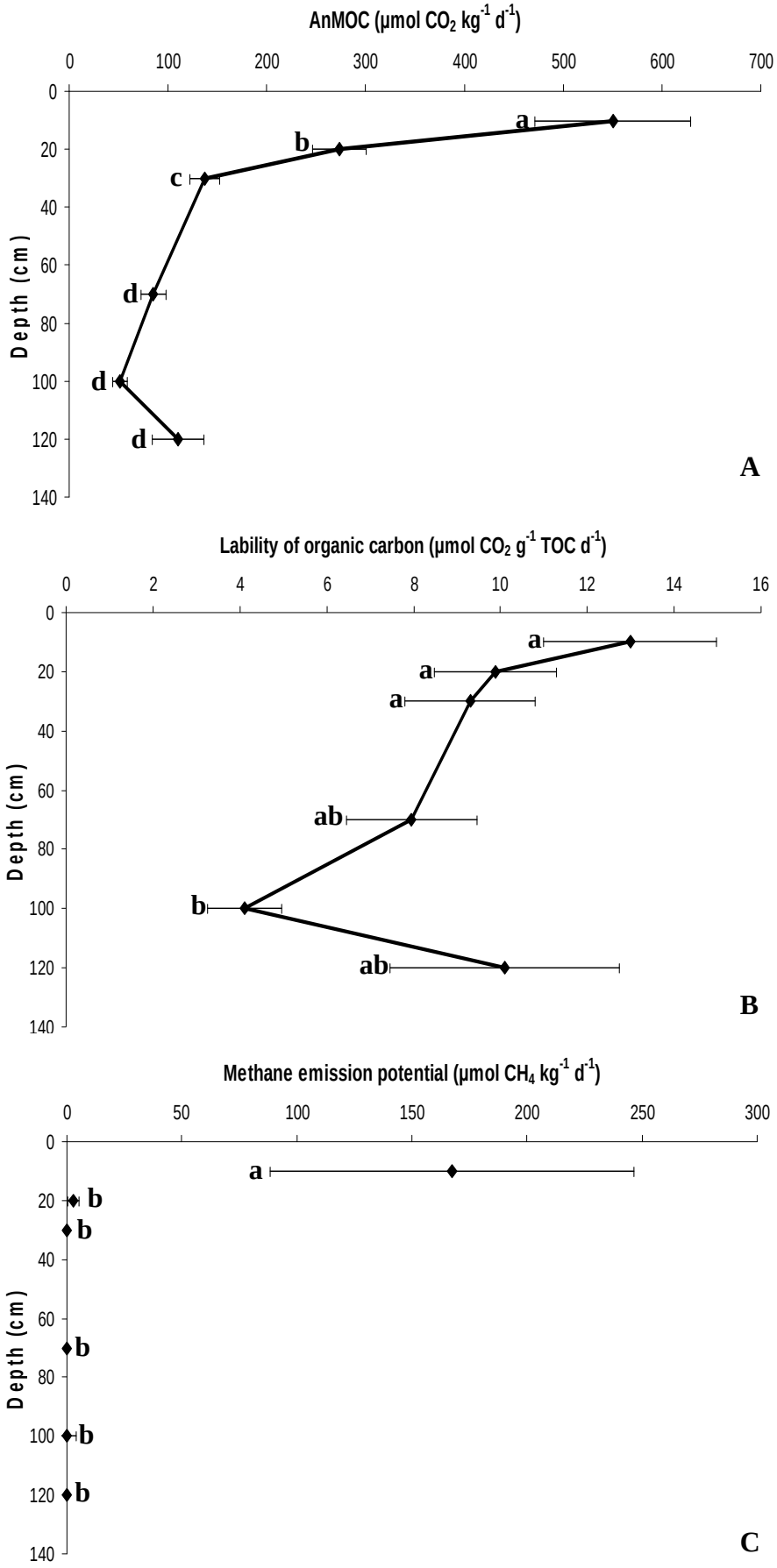

Figure 6.3.4: AnMOC, lability of organic carbon and methane production potential in the subsurface depth intervals of the BZ. Data are means ± 1 SE. Different lower case letters indicate significant differences.

Although in every depth interval some samples displayed potential for methane production, in all cases it was >90 % lower than the potential of the topsoil. The anaerobic incubation and measurement period was extended beyond the three weeks (21 days) in case there were bacterial populations, mainly in the deeper strata, that had lag phases longer than 21 days. As shown in Table 6.3.4, with the exception of one sample, the lag phase for the A samples ranged between 2 and 16 days. In the B and C depths the lag phase extended beyond 50 days in many cases (Figure 6.3.5). Fewer samples in the depth intervals below 50 cm (D, E and F) showed potential for methane production, however, the duration of the lag phase was reduced the closer to the permanently saturated C soil horizon.

Table 6.3.4: Length of lag phase (d) and mean ± 1SE methane production potential rate in the six depth intervals of the Buffer Zone subsurface.

	Lag phase range	**Lag phase days**		**CH_4 (µmol kg^{-1} d^{-1})**	
Buffer Zone depth	**Days**	**Mean**	**± 1 SE**	**Mean**	**± 1 SE**
A 0-10 cm (n=7)	2 - 50	11.4	6.7	167.3	79.0
B 10-20 cm (n=7)	2 - 85	34.9	12.3	2.7	2.4
C 20-30 cm (n=6)	13 - 85	62.3	11.8	0.012	0.01
D 50-70 cm (n=4)	13 - 85	61.8	17.0	0.005	0.00
E 80-100 cm (n=3)	1 - 53	35.7	17.3	0.004	4.07
F 100-120 cm (n=3)	2 - 23	9.7	6.7	0.03	0.02

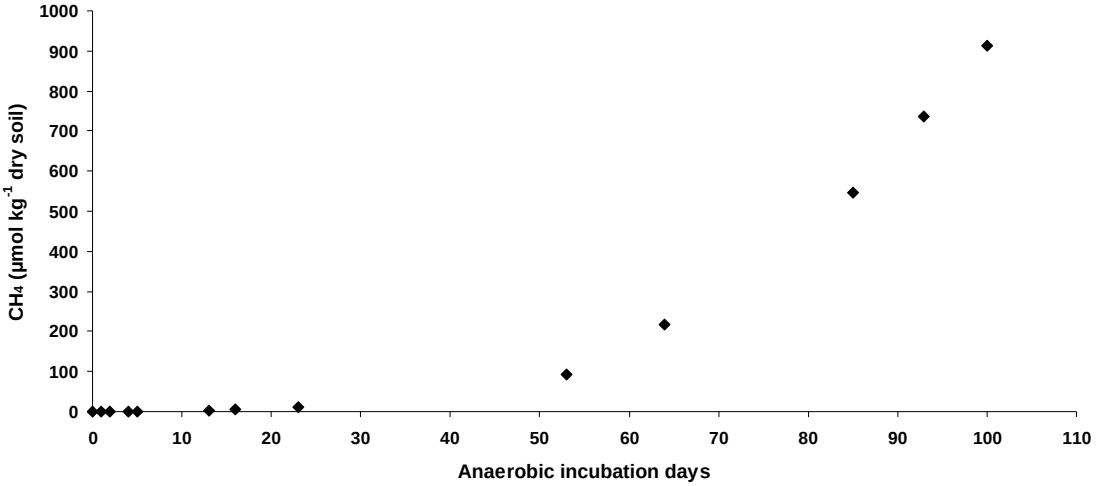

Figure 6.3.5: Methane production potential of the sample B8 following 53 days of lag phase.

6.3.3 *Spatial ordination of the Buffer Zone subsurface samples*

Principal Component Analysis (PCA) between the soil physical properties (excluding the particle size fractions) and the soil nitrate content, the AnMOC, the lability of organic carbon and the methane production potential in the six depth intervals of the BZ subsurface resulted in the extraction of three principal axes (Table 6.3.5). The correlation coefficients between the first two component axes and the environmental variables are shown in Table 6.3.6. The first axis explained 54 % of the variance between individual samples and was closely associated with the AnMOC, the organic matter content, the water content, the OC lability, the soil nitrate content and the methane production potential, while the second axis was associated only with the ratio TOC/NO_3^-.

Plotting the cluster centroids for each depth interval and projecting the significant environmental variables on the scatter plot resulted in the bi-plot of Figure 6.3.6. The topsoil samples (A) were clearly separated from the rest and were associated with the positive axis 1, suggesting that the co-occurrence of high OC mineralisation rate, high soil moisture and soil nitrate as well as low redox is more likely in the topsoil. The samples just below the topsoil (B) displayed intermediate conditions and were therefore plotted near the origin of the axes. Finally, the samples C, D, E and F formed a large cluster with significant overlapping along the negative axis 1, indicating less favourable conditions for nitrate attenuation than in the topsoil.

Table 6.3.5: The principal components (axes) generated by the PCA, their respective eigenvalues, the % of variance explained by each component and the cumulative % of inter-sample variance explanation for the BZ subsurface.

Axes	Eigenvalues	% of Variance	Cumulative %
1	3.747	53.5	53.5
2	1.208	17.3	70.8
3	0.902	12.9	83.7

Table 6.3.6: Correlation coefficients of the environmental variables in PCA. ***Correlation significant at the 0.01 probability level.

Variables	Component 1	Component 2
Water content	0.739***	0.195
Organic Matter	0.908***	-0.061
Nitrate	0.704***	-0.477
TOC/NO_3^-	-0.129	0.915***
AnMOC	0.930***	0.060
Lability of OC	0.727***	0.245
Methane	0.686***	0.192

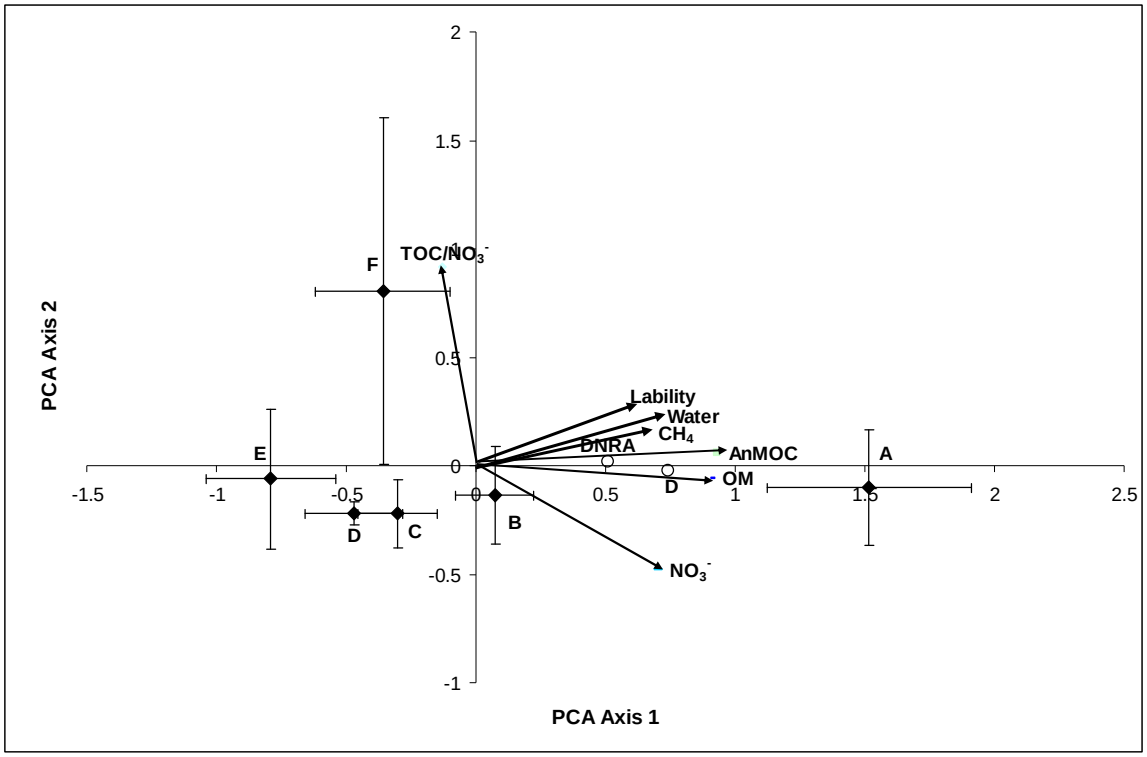

Figure 6.3.6: Correlation bi-plot from the PCA analysis with cluster centroids (average score on each component, with standard errors) for the depth intervals (ABCDEF) in BZ. Correlations of the variables with the main axes are given by solid arrows. Open circles indicate the correlation of nitrate attenuation processes with the component axes. Water; water content, OM; organic matter content, Lability; labile organic carbon, CH_4; methane production potential, NO_3^-; soil nitrate content, D; potential denitrification rate.

6.3.4 *Denitrification and DNRA potential in the subsurface of the Buffer Zone*

All the depth intervals in the subsurface of the Buffer Zone area showed potential for denitrification. The potential rate was significantly different between the A and B depths and the rest of the depth intervals (Table 6.3.2). Denitrification was not significantly different between the C and D depths and the E and F depths, following closely the subsurface zonation indicated by the PCA. The denitrification rate decreased by 56 % within 10 cm in the topsoil and by 95 % within 120 cm following an exponential decay rate (Table 6.3.7 and Figure 6.3.7 A).

The potential for nitrous oxide (N_2O) production as a product of denitrification in the subsurface of the BZ was also investigated. The B depth interval (10 – 20 cm) displayed a significantly higher N_2O production potential compared to the topsoil and the rest of the subsurface intervals (Table 6.3.2). The nitrous oxide production rate was not significantly different between the topsoil and the C and D depth intervals, whereas it was significantly lower and not different between the bottom two intervals, E and F (Table 6.3.7 and Figure 6.3.7 B). Although the B depth had 44 % lower denitrification rate than the topsoil, the incubation time for the topsoil and the B samples was the same. Therefore it could be assumed that the slower reaction rate in the B samples resulted in the accumulation of N_2O that was not further reduced to N_2 before the end of the experiment.

The ratio of the denitrification products, N_2O/N_2 followed a similar pattern to the N_2O production rate (Figure 6.3.8). The ratio increased significantly between A and B depths as a result of N_2O accumulation during the incubation, but smaller increases were also observed between the coupled depths C - D and E - F that also shared the same incubation times. Although the differences in the relative importance of the two reduction steps seemed to be an effect of the incubation time of the experiment an overall trend of decreasing importance for N_2O with depth was observed, suggesting that the production of nitrous oxide is more likely in the surface soil rather than in the subsurface.

Table 6.3.7: Denitrification, N_2O production and DNRA potential rates in the depth intervals of the BZ subsurface. Data are means ± 1SE.

	Denitrification ($mg\ N\ kg^{-1}\ soil\ d^{-1}$)		Nitrous oxide ($mg\ N\ kg^{-1}\ soil\ d^{-1}$)		DNRA ($mg\ N\ kg^{-1}\ soil\ d^{-1}$)	
Buffer Zone depth	**Mean**	**± 1 SE**	**Mean**	**± 1 SE**	**Mean**	**± 1 SE**
A 0-10 cm (n=8)	54.0	8.5	1.8	0.5	1.1	0.2
B 10-20 cm (n=8)	23.7	1.9	4.1	0.7	0.6	0.1
C 20-30 cm (n=8)	10.5	1.9	0.7	0.5	0.4	0.1
D 50-70 cm (n=8)	7.0	1.7	0.4	0.1	0.1	0.02
E 80-100 cm (n=8)	2.4	0.3	0.002	0.001	0.03	0.01
F 100-120 cm (n=8)	2.5	0.4	0.005	0.002	0.02	0.004

The Buffer Zone subsurface also showed potential for DNRA that varied with depth, but not as distinctly as the denitrification potential. The depth intervals A, B and C had significantly higher DNRA potential than the D, E and F depths (Table 6.3.2). Furthermore, the DNRA potential was not significantly different between the C and D depths and the E and F, as shown also for the denitrification potential (Figure 6.3.7 C). The DNRA rate decreased by 45 % within 20 cm in the topsoil and by 62 % within 30 cm, but the rates were not significantly different due to the high variability observed between samples (Table 6.3.7). However, DNRA significantly decreased by 89 % in the B soil horizon (50 – 100 cm) and by 92 % in the permanently saturated C soil horizon (> 100 cm).

Regarding the ratio denitrification to DNRA (D/DNRA), it was significantly lower in the A, B, C and D depths (Table 6.3.2), compared to the E and F depths, indicating that the importance of denitrification over DNRA increased significantly below the permanently saturated horizon. Denitrification was 32 to 55 times more important between the topsoil and 70 cm in the subsurface zone, while it was 97 to 113 times more important in the permanently saturated zone (Figure 6.3.9).

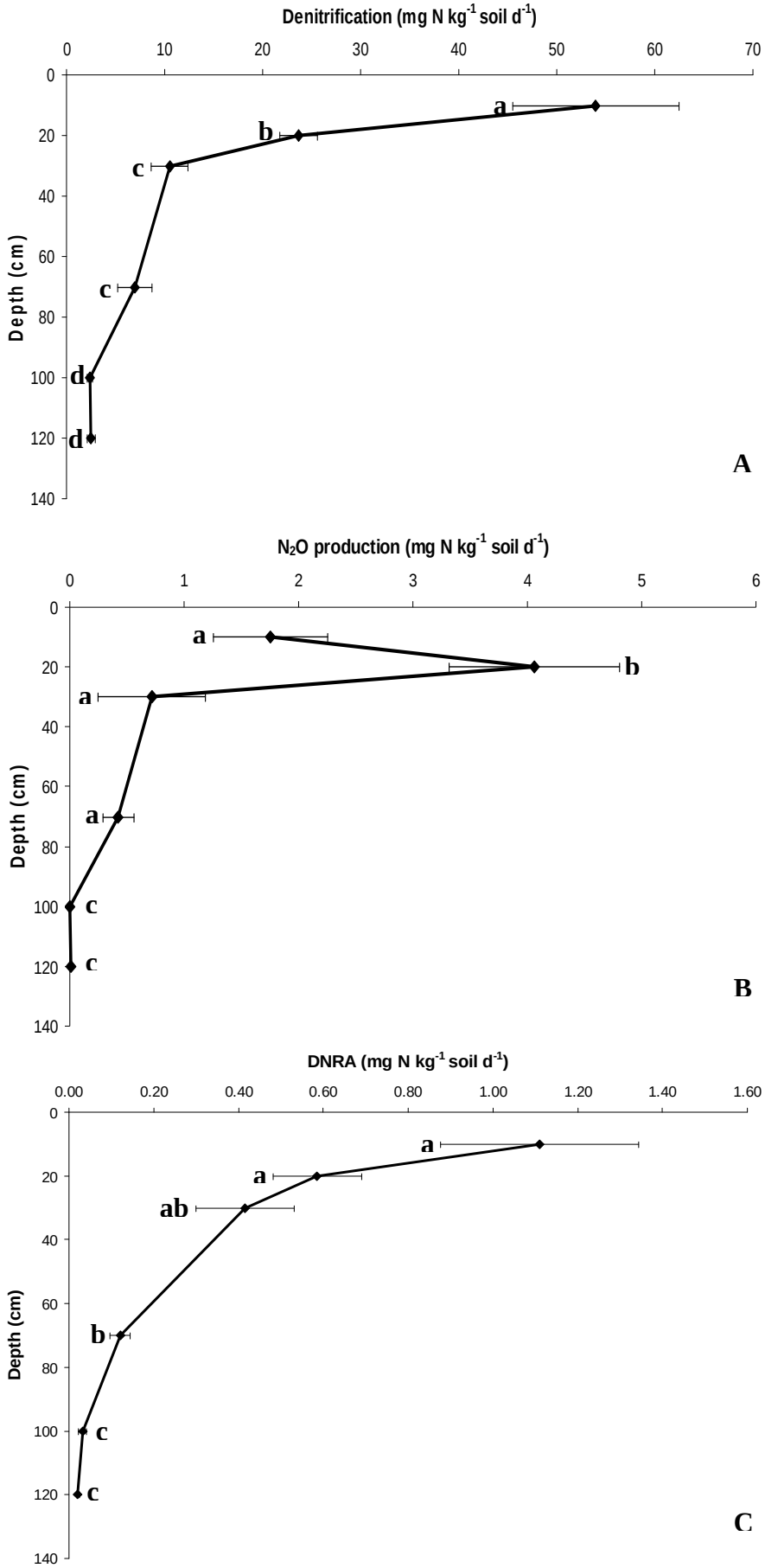

Figure 6.3.7: Denitrification, N_2O production and DNRA potential rates in the depth intervals of the BZ subsurface. Data are means ± 1SE. Different lower case letters indicate significant differences

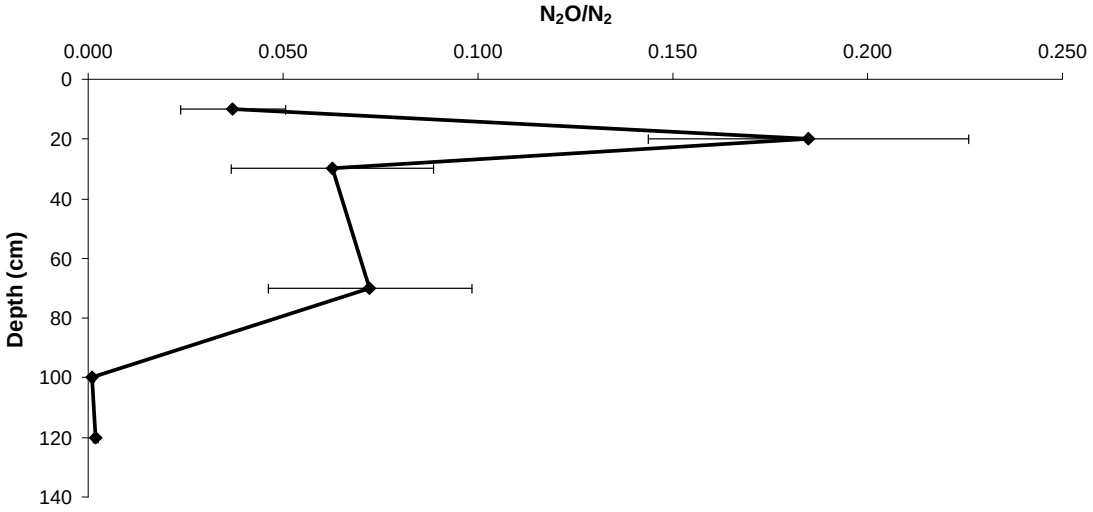

Figure 6.3.8: The ratio of N_2O/N_2 in the depth intervals of the BZ subsurface. Data are means ± 1SE.

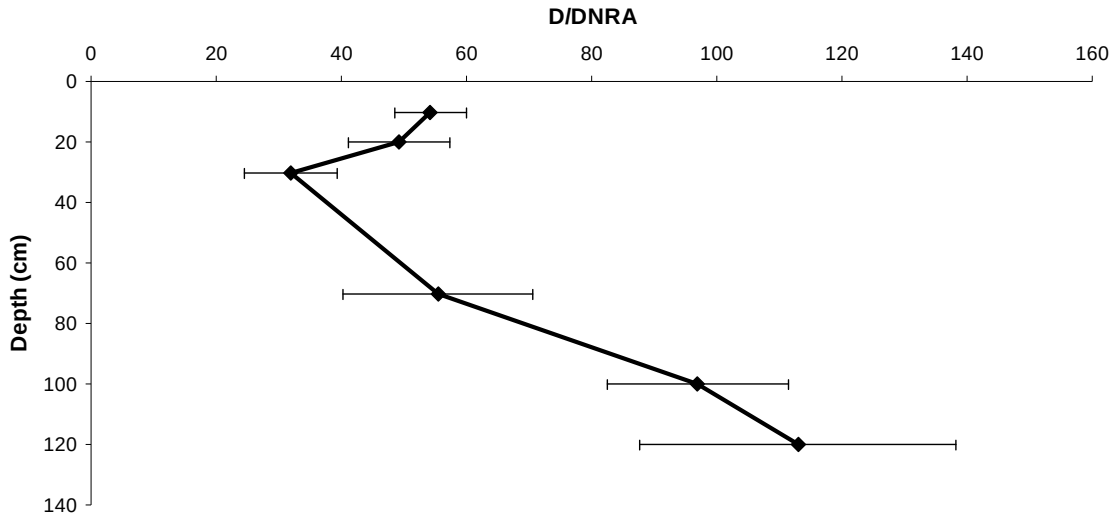

Figure 6.3.9: The ratio of D/DNRA in the depth intervals of the BZ subsurface. Data are means ± 1SE.

Measuring the NO_2^- and N_2O produced during denitrification, as well as the DNRA rate, allowed for the estimation of the NO_3^- budget of the experiment. Table 6.3.8 shows the percent contribution of the three products of denitrification, of DNRA, as well as the percentage of nitrate 'unused' during the experiment. Finally, the proportion of nitrate not accounted for in any of the above processes was assumed 'lost' by assimilation into bacterial biomass.

Regarding the topsoil samples, 77 % of the added nitrate was recovered as N_2, the end product of denitrification, while 15 % remained unused after the three hour incubation, indicating that nitrate was not limiting during the experiment. DNRA accounted for only 2 % of the added nitrate, while NO_2^- and N_2O were also present at the end of the incubation completing the budget without any indication of nitrate assimilation in bacterial biomass. In the depth intervals B, C and D, between 43 and 53 % of the spike was converted to N_2 gas via complete denitrification, whereas there was some accumulation of intermediate denitrification products, especially NO_2^- in the depths C and D, indicating probably slower reaction rates than the incubation time used (9 h). However, between 14 and 22 % of the added nitrate was not recovered and was characterised as 'lost', indicating that assimilation of nitrate into bacterial biomass could be occurring in the less reactive subsurface zones. Finally, in the deeper parts of the C soil horizon, where the incubation time was 72 h, more than 80 % of the spike was used for complete denitrification, while the intermediate products were very low. DNRA was not different from the other depths and between 4 and 5 % of the added nitrate was regarded as 'lost'.

Table 6.3.8: Nitrate budget for the BZ subsurface experiment including three products of denitrification, DNRA, unused amount of added nitrate and 'lost' amount of nitrate.

	Denitrification			**DNRA**	**Unused**	**'Lost'**	**Total**
	N_2	**NO_2^-**	**N_2O**	**NH_4^+**	**NO_3^-**		
Buffer Zone depth	**%**	**%**	**%**	**%**	**%**	**%**	**%**
A 0-10 cm (n=8)	77	1	5	2	15	0	100
B 10-20 cm (n=8)	52	1	10	1	15	20	100
C 20-30 cm (n=8)	53	9	3	3	10	22	100
D 50-70 cm (n=8)	43	17	3	3	21	14	100
E 80-100 cm (n=8)	83	1	0.12	2	9	5	100
F 100-120 cm (n=8)	81	2	0.17	1	12	4	100

Correlation analysis between denitrification, DNRA, the AnMOC mineralisation rate, the methane production potential, the lability of organic carbon and the soil physical properties of the BZ subsurface has indicated a number of significant relationships (Table 6.3.9). The denitrification and DNRA correlated positively with each other, indicating the coexistence and similar variability with depth of the two nitrate attenuation processes in the BZ subsurface (Figure 6.3.10). Moreover, the potential denitrification rate showed significant positive correlation with the AnMOC (Figure 6.3.11), the organic matter content, the methane production potential and the soil nitrate content. To a lesser degree denitrification correlated significantly with the lability of organic carbon and the water content. The DNRA potential rate showed significant positive correlation with the AnMOC, the organic matter content, the methane production potential, the ratio TOC/TN and the soil nitrate content.

Multiple Regression Analysis (MRA) highlighted the importance of the organic carbon availability in explaining the variance observed between the potential denitrification rate of the samples. The organic carbon content explained 89 % of the variance, while the AnMOC explained 88 % in a forward MRA (MRA; r^2=0.89, df=42, P<0.01 and r^2=0.88, df=42, P<0.01 respectively). Additionally, the water content of the samples (MRA; r^2=0.72, df=42, P<0.01) and the lability of organic carbon (MRA; r^2=0.43, df=42, P<0.01) explained 72 % and 43 % of the observed variance in denitrification rates, while the soil nitrate content (MRA; r^2=0.32, df=42, P<0.01) was ranked last with 32 % explanatory power, indicating that the availability of nitrate is becoming a less important controlling factor for denitrification as the depth within the subsurface zone increases.

MRA between the DNRA potential rate and those environmental variables that were significant in the correlation analysis resulted in relatively low percentages of variance explanation by the environmental variables. The highest explanatory power was observed for the ratio TOC/TN (MRA; r^2=0.25, df=42, P<0.01) with 25 %, and was followed by the organic carbon content (MRA; r^2=0.17, df=42, P<0.01) with 17 % and the AnMOC (MRA; r^2=0.16, df=42, P<0.01) with 16 %, indicating that the relative availability of organic carbon over the availability of nitrate is a more important limiting factor for DNRA, which becomes increasingly important as nitrate availability becomes limiting.

Table 6.3.9: Correlation matrix between the denitrification and DNRA potential rate, the AnMOC, the lability of organic carbon, the methane production potential and the soil physical properties in the depth intervals of the BZ subsurface. Underlined correlation coefficients are products of Spearman rho correlation whereas non-underlined are products of Pearson Product-Moment correlation. ** Correlation is significant at the 0.01level and *Correlation is significant at the 0.05 level.

Variables/Correlation coefficients		Denitrification potential	DNRA	AnMOC	Org. carbon lability	Methane emission	Organic matter content	Organic carbon	TOC/TN	TOC/NO_3^-	Water content	Soil nitrate	Bulk density
Denitrification potential	*R or rho*	1											
	P	.											
	N	48											
DNRA	*R or rho*	**0.849****	1										
	P	0.000	.										
	N	48	48										
AnMOC	*R or rho*	**0.938****	**0.666****	1									
	P	0.000	0.000	.									
	N	43	43	43									
Org. carbon lability	*R or rho*	**0.548****	**0.396****	**0.591****	1								
	P	0.000	0.009	0.000	.								
	N	43	43	43	43								
Methane emission	*R or rho*	**0.667****	**0.546****	**0.740****	**0.650****	1							
	P	0.000	0.000	0.000	0.000	.							
	N	48	48	43	43	48							
Organic matter content	*R or rho*	**0.849****	**0.649****	**0.874****	**0.564****	**0.615****	1						
	P	0.000	0.000	0.000	0.000	0.000	.						
	N	48	48	43	43	48	48						
Organic carbon	*R or rho*	**0.791****	**0.540****	**0.755****	0.035	**0.436****	**0.700****	1					
	P	0.000	0.000	0.000	0.824	0.002	0.000	.					
	N	48	48	43	43	48	48	48					
TOC/TN	*R or rho*	0.205	**0.489****	0.100	0.181	0.172	0.256	0.070	1				
	P	0.162	0.000	0.522	0.247	0.243	0.079	0.637	.				
	N	48	48	43	43	48	48	48	48				
TOC/NO_3^-	*R or rho*	-0.120	0.032	-0.062	0.006	-0.049	-0.114	-0.040	-0.142	1			
	P	0.417	0.831	0.692	0.970	0.739	0.439	0.789	0.334	.			
	N	48	48	43	43	48	48	48	48	48			
Water content	*R or rho*	**0.507****	0.068	**0.559****	**0.511****	0.219	**0.602****	0.332*	-0.101	0.153	1		
	P	0.000	0.648	0.000	0.000	0.135	0.000	0.021	0.493	0.300	.		
	N	48	48	43	43	48	48	48	48	48	48		
Soil nitrate	*R or rho*	**0.588****	**0.383****	**0.571****	0.314*	**0.465****	**0.632****	**0.517****	0.002	**-0.662****	**0.504****	1	
	P	0.000	0.007	0.000	0.041	0.001	0.000	0.000	0.988	0.000	0.000	.	
	N	48	48	43	43	48	48	48	48	48	48	48	
Bulk density	*R or rho*	**-0.763****	**-0.672****	**-0.734****	-0.370*	**-0.555****	**-0.732****	**-0.690****	-0.310*	0.147	-0.200	**-0.453****	1
	P	0.000	0.000	0.000	0.015	0.000	0.000	0.000	0.032	0.320	0.172	0.001	.
	N	48	48	43	43	48	48	48	48	48	48	48	48

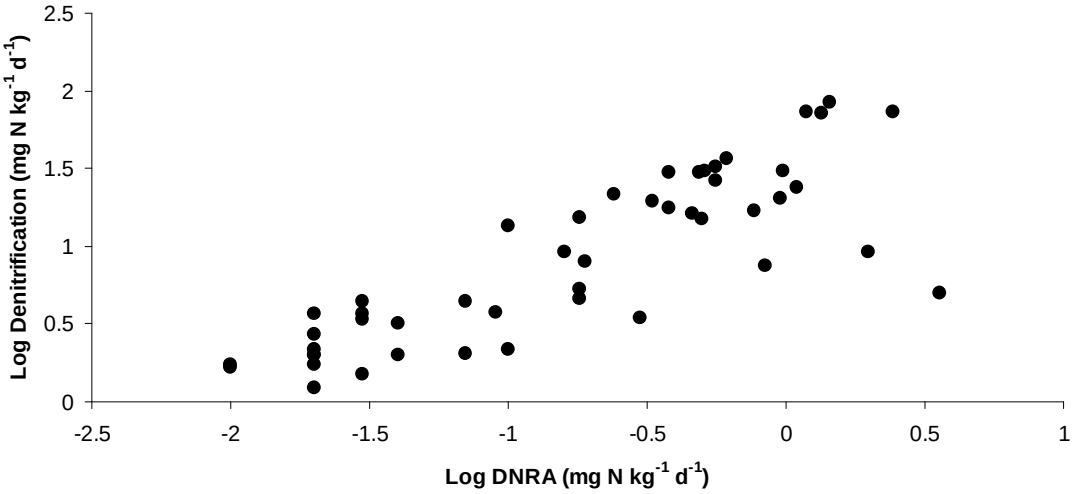

Figure 6.3.10: Scatter plot of denitrification against DNRA potential rates in the BZ subsurface (r=0.85, n=48, P<0.01).

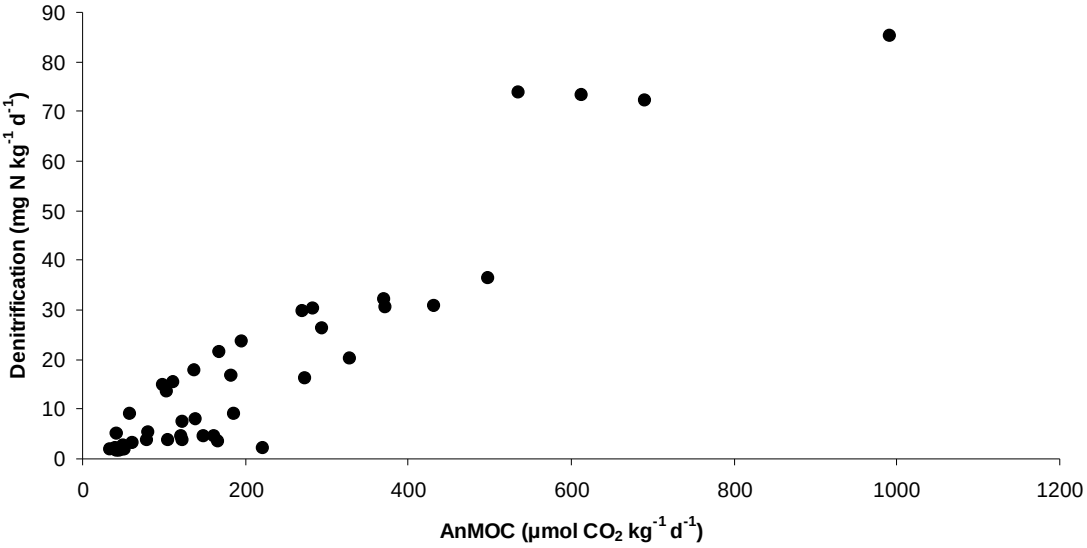

Figure 6.3.11: Scatter plot of potential denitrification rate against the AnMOC in the BZ subsurface (r=0.94, n=43, P<0.01).

6.3.5 *Anammox and chemoautotrophic denitrification in the subsurface of the Buffer Zone*

The possibility of N_2 production from the anaerobic oxidation of ammonia (Anammox) was investigated in the BZ subsurface samples as described in section 4.3.11. According to Trimmer *et al.* (2006), denitrification is assumed to be the only quantitative significant source of $^{15}N\text{-}N_2O$ in a $^{15}NO_3^-$ labelling experiment and if the ratio between $^{15}NO_3^-$ and $^{14}NO_3^-$ is constant, the produced isotopic N_2O species will be binomially distributed. Therefore, the ratio between $^{14}NO_3^-$ and $^{15}NO_3^-$ (r_{14}) as well as the proportion of ^{15}N in the total N gas pool (q) can be calculated according to Nielsen (1992). The term q was calculated for both ^{15}N gas species i.e. $q'N_2$ and qN_2O (Table 6.3.10) and since there was no adequate spread of $^{15}NO_3^-$ concentrations i.e. a range of q from 0 to 1, regression analysis, as recommended in Trimmer *et al.* (2006), could not be used. Instead a paired-sample t test was used to evaluate the differences in the distribution of ^{15}N in N_2 and N_2O. Any significant change in the predicted distribution of ^{15}N would have been attributed to the occurrence of Anammox. The two-tailed probability values (*P*) from the paired-samples t test for the depth intervals of the BZ subsurface are shown in Table 6.3.10. In all cases the probability was $P>0.05$, and therefore the distribution of ^{15}N in N_2 and N_2O was not significantly different, indicating that Anammox was not occurring in the topsoil and the subsurface sediments of the BZ. These results also showed that the only source of N_2 in the BZ subsurface experiment was denitrification and Anammox was rightly not used in the nitrate budget of the experiment described earlier.

Table 6.3.10: The proportion of ^{15}N in the N_2 (q') and the N_2O (q) produced by denitrification, and the two-tailed probability (*P*) calculated by the paired-sample t test.

	q'N_2		**qN_2O**		***P***
Buffer Zone depth	**Mean**	**± 1 SE**	**Mean**	**± 1 SE**	
A 0-10 cm (n=7)	0.97	0.002	0.98	0.013	0.804
B 10-20 cm (n=8)	0.96	0.003	0.97	0.008	0.454
C 20-30 cm (n=8)	0.97	0.003	0.97	0.006	0.691
D 50-70 cm (n=8)	0.93	0.014	0.96	0.012	0.100
E 80-100 cm (n=8)	0.94	0.019	0.91	0.040	0.553
F 100-120 cm (n=8)	0.94	0.017	0.84	0.089	0.336

The presence of 'chemolithoautotrophic' denitrifiers that could use inorganic e^- donors, such as reduced manganese (Mn^{2+}), ferrous iron (Fe^{2+}) and sulphides (Korom, 1992) instead of organic carbon, for the reduction of nitrate was investigated in the BZ subsurface samples as described in section 4.3.12. The analysis of the denitrification potential slurry extracts with the ICP-OES revealed that there were no measurable amounts of Fe in any of the topsoil or subsurface sediment samples. Therefore, the hypothesis that pyrite (FeS_2) could serve as an alternative electron donor for denitrification had to be rejected. There were, however, measurable amounts of Mn^{2+} in all the samples from the BZ subsurface and its concentration decreased with depth (Table 6.3.11). Manganese sulphide (MnS_2), like pyrite, could also serve as an e^- donor for chemoautotrophic denitrification (Korom, 1992). The oxidation of sulphur with simultaneous reduction of nitrate would result in the accumulation of sulphate in the samples following the incubation period. Paired-sample t tests between the reference and the inoculated and incubated samples showed no significant change in the concentration of sulphate (Table 6.3.11). The results for Mn^{2+} were similar, with no significant difference in concentration observed between the reference and the incubated samples. The results were inconclusive with regards to the occurrence of chemoautotrophic denitrification and since no readily identifiable patterns were observed, chemoautotrophic denitrification was assumed of negligible importance and was not included in further experiments.

Table 6.3.11: The concentration of SO_4^{2-} and Mn^{2+} and the two-tailed probability (*P*) calculated by the paired-sample t test in the references and the samples from the depth intervals of the BZ subsurface.

	Reference SO_4^{2-} (mg L^{-1})		Sample SO_4^{2-} (mg L^{-1})		*P*	Reference Mn^{2+} (mg L^{-1})		Sample Mn^{2+} (mg L^{-1})		*P*
Buffer Zone depth	**Mean**	**± 1 SE**	**Mean**	**± 1 SE**		**Mean**	**± 1 SE**	**Mean**	**± 1 SE**	
A 0-10 cm (n=6)	15.2	4.3	13.3	2.0	0.616	7.1	1.0	8.8	1.3	0.095
B 10-20 cm (n=8)	8.6	1.6	11.8	1.0	0.013	4.3	0.9	5.8	0.8	0.084
C 20-30 cm (n=8)	10.2	0.5	11.3	0.8	0.176	4.1	0.8	5.1	0.7	0.190
D 50-70 cm (n=8)	13.8	1.6	15.4	0.8	0.306	2.2	0.4	3.5	0.6	0.069
E 80-100 cm (n=8)	14.9	1.1	15.8	0.9	0.210	2.4	0.5	3.0	0.4	0.147
F 100-120 cm (n=8)	16.3	1.0	17.7	1.0	0.122	3.1	0.7	3.2	0.6	0.544

To summarise, significant differences were found in the soil properties between the ground surface and the subsurface in the BZ area. Specifically, the organic carbon availability as well as the mineralisation rate decreased exponentially with depth. Moreover, the soil nitrate content also followed an exponential decay with depth, although a small increase in both nitrate and ammonium was observed in the deeper permanently saturated zone, attributed to lateral subsurface flow with direction from the arable field towards the river. Both nitrate attenuation processes (i.e. heterotrophic denitrification and DNRA) were present in all depth intervals and they both decreased exponentially with depth following closely the decrease in organic carbon availability. The methane production potential concentrated largely in the topsoil, although, some methane was also produced in the subsurface following a long lag phase. The relative importance of nitrous oxide as a denitrification product decreased with depth as did the DNRA over the heterotrophic denitrification. The availability of labile organic carbon seemed to be the most important controlling factor of subsurface nitrate attenuation, but also the nitrate supply significantly limited the process rates with increasing depth. Finally neither Anammox nor chemoautotrophic denitrification were observed to occur in the topsoil or the subsurface of the BZ, while the nitrate budget of the laboratory incubations indicated that some proportion of the added substrate may have been assimilated in bacterial biomass during the course of the experiment.

6.3.6 *Soil physical properties in the subsurface of the Pasture Meadow*

The PM subsurface was sampled at eight locations next to the groundwater wells F1-F7, comprising the transect perpendicular to the river, in order to include all the different features of the subsurface lithology at the same depth intervals as the BZ subsurface. The soil physical properties are summarised in Table 6.3.12. Table 6.3.13 presents the results of the parametric (One-Way ANOVA) or non-parametric (Kruskal-Wallis) statistical tests for the comparison of variable means between depth intervals. The dry bulk density was significantly lower in the topsoil (A depth) and increased with depth (Figure 6.3.12 A). The particle size distribution in the PM subsurface was fairly homogeneous with the clay and silt fractions dominating in all the depth intervals (> 90 %). The clay content decreased slightly with depth, but the decrease was not statistically significant. On the contrary, the silt fraction increased with depth and the bottom two depth layers had significantly higher silt content compared to the top two layers in the PM topsoil. None of the sand fractions were significantly different between the depth intervals of the PM subsurface (Figure 6.3.13). However, the sand fractions were more abundant in the first four samples i.e. from the river towards the middle of the PM area, where a gravel lens was observed between the B soil horizon (> 70 cm depth) and the permanently saturated C soil horizon (<120 cm depth). Due to the low bulk densities, and therefore high porosity, and the dominance of the clay and silt fractions i.e. low mean grain size, the permeability k (Boudreau, 1997) was below 1 m^2 in all the samples apart from the topsoil samples next to the river (2.1 – 2.7 m^2).

The soil water content decreased with depth and the top three intervals were significantly different from the bottom three (Figure 6.3.12 B). The organic matter content decreased exponentially within 50 cm from the ground surface, while the three bottom intervals were not significantly different between each other (Figure 6.3.12 C). A similar pattern was observed for the organic carbon content which also decreased exponentially with depth (Figure 6.3.12 D). The ratio TOC/TN (Figure 6.3.12 E) was significantly different between the topsoil (first 20 cm A&B) and the depths C and DEF, which were not different between each. Finally, the ratio TOC/NO_3^- (Figure 6.3.12 F) was not significantly different between the depth intervals of the PM.

Table 6.3.12: Soil physical properties in the sampled depth intervals of the pasture meadow subsurface (data are mean values ± 1 SE).

	Soil type	Dry Bulk Density ($g\ cm^{-3}$)		Water content (%)		Organic matter (%)		Organic carbon (%)		TOC/TN		NO_3^--N ($mg\ kg^{-1}$)		TOC/NO_3^-	
Pasture Meadow depth		**Mean**	**± 1 SE**	**Mean**	**± 1 SE**	**Mean**	**± 1 SE**	**Mean**	**± 1 SE**	**Mean**	**± 1 SE**	**Mean**	**± 1 SE**	**Mean**	**± 1 SE**
A 0-10 cm (n=8)	Clay	0.69	0.03	60.1	2.64	15.3	0.93	6.0	0.82	8.5	0.36	3.3	1.3	11.7	5.5
B 10-20 cm (n=8)	Clay	1.03	0.04	54.7	3.96	12.6	1.17	4.0	0.31	7.4	0.19	3.0	0.4	1.4	0.2
C 20-30 cm (n=8)	Silty clay	0.98	0.05	48.7	5.06	9.1	1.20	2.0	0.32	5.3	0.37	1.6	0.3	1.5	0.2
D 50-70 cm (n=8)	Silty clay	1.24	0.06	42.3	4.14	5.8	0.65	1.0	0.40	3.0	0.76	0.7	0.2	1.6	0.6
E 80-100 cm (n=8)	Silty clay	1.24	0.08	39.7	4.38	5.0	0.57	0.7	0.32	2.6	0.86	0.5	0.1	1.5	0.7
F 100-120 cm (n=8)	Silty clay	1.33	0.08	37.4	3.76	4.3	0.42	0.5	0.25	2.3	0.74	0.3	0.1	5.9	5.1

Table 6.3.13: Comparison of the means between the depth intervals of the PM subsurface for selected soil properties and processes. *df*; degrees of freedom, *F*; F statistic, χ^2; χ^2 statistic *P*; probability level. Where the variable is annotated with * the non-parametric Kruskal-Wallis test has been used instead of One-Way ANOVA.

	One-Way ANOVA and Kruskal-Wallis				One-Way ANOVA and Kruskal-Wallis		
Buffer Zone subsurface	*df*	*F or* χ^2	*P*	**Buffer Zone subsurface**	*df*	*F or* χ^2	*P*
Bulk density*	5	31.3	<0.01	Soil nitrate*	5	22.0	<0.01
Clay fraction	47	1.3	>0.05	Soil ammonia*	5	20.1	<0.01
Silt fraction	47	2.5	<0.05	Soil nitrite*	5	3.3	>0.05
Fine sand fraction	47	0.5	>0.05	AnMOC*	5	39.0	<0.01
Medium sand fraction*	5	2.5	>0.05	Lability of OC*	5	4.7	>0.05
Water content	47	4.9	<0.01	Methane emission*	5	34.5	<0.01
Organic matter	47	26.5	<0.01	Denitrification*	5	42.4	<0.01
Organic carbon	47	24.3	<0.01	Nitrous oxide production*	5	32.5	<0.01
TOC/TN	47	19.1	<0.01	DNRA*	5	35.5	<0.01
TOC/NO_3^-*	5	8.2	>0.05	D/DNRA	45	1.2	>0.05

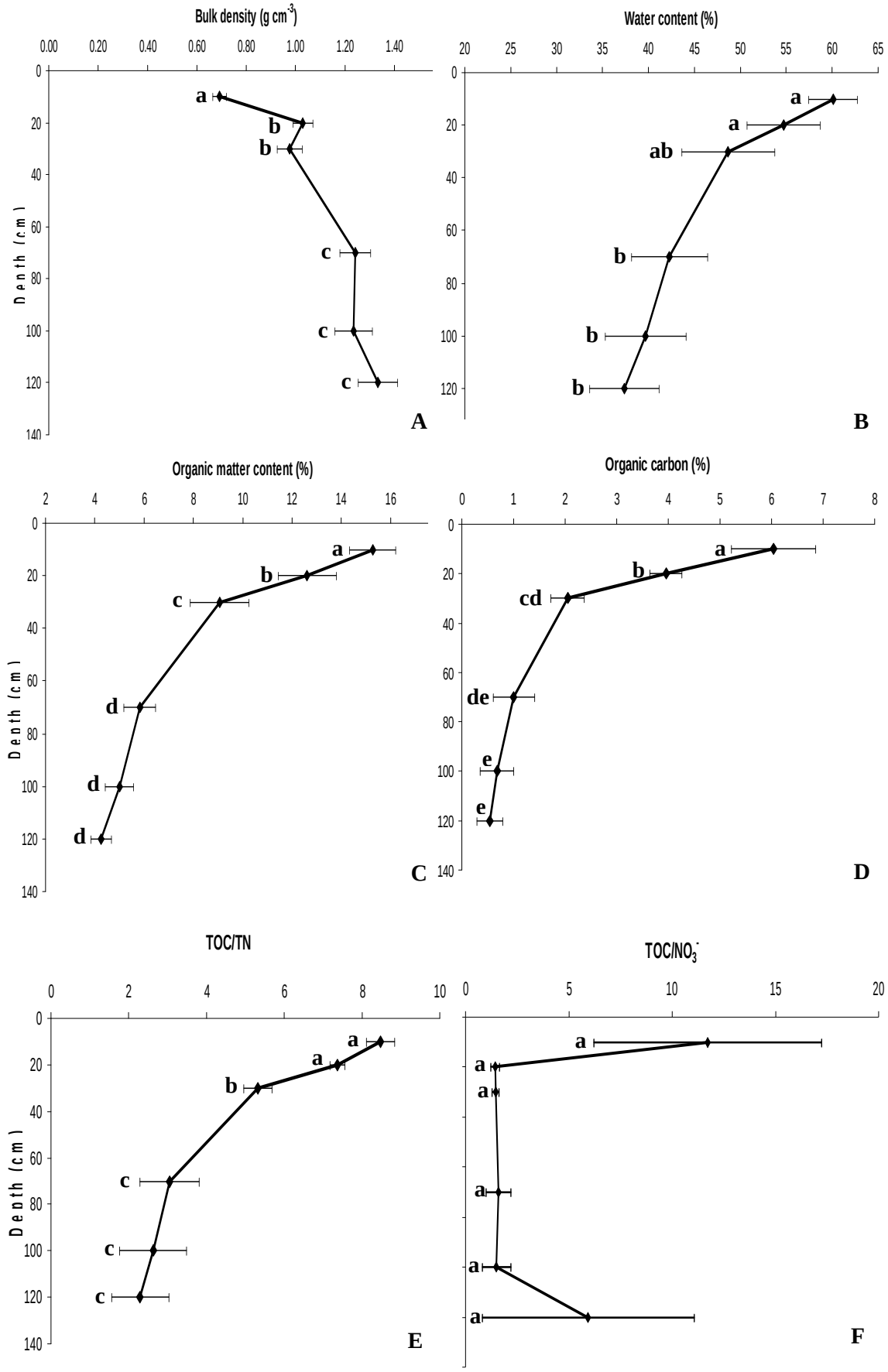

Figure 6.3.12: Dry bulk density, water content, organic matter and organic carbon contents, TOC/TN and TOC/NO_3^- ratios in the depth intervals of the PM subsurface. Data are mean values ± 1 SE. Different lower case letters indicate significant differences.

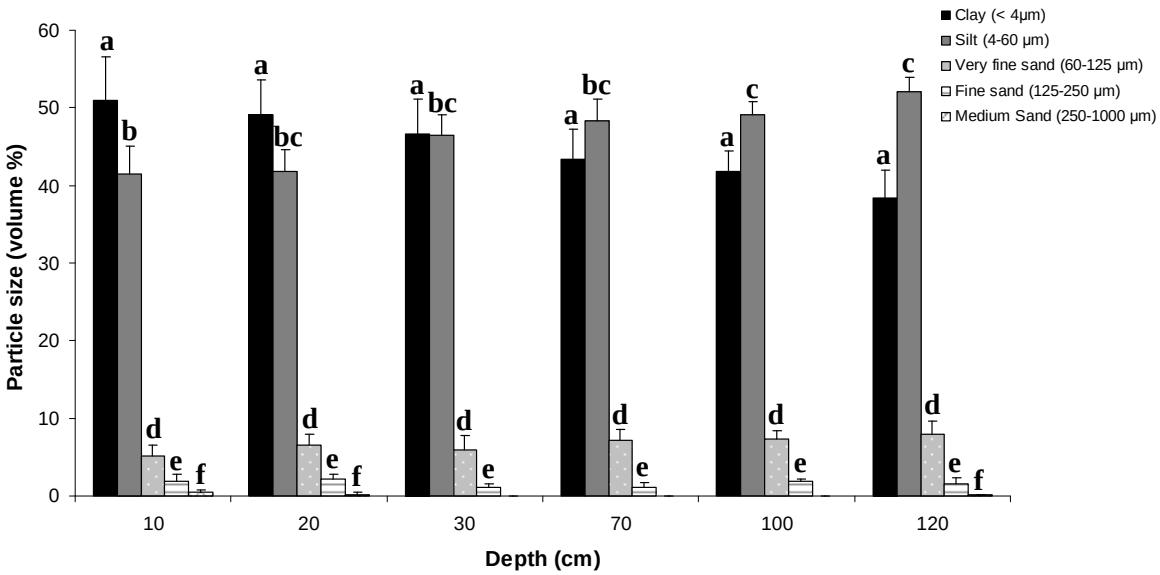

Figure 6.3.13: Absolute particle size distribution in the depth intervals of the subsurface of the PM. Different lower case letters indicate significant differences.

The soil nitrate content decreased significantly with depth below the first 20 cm of the topsoil (Figure 6.3.14 A). The first 10 cm of the topsoil (A depth), due to high variability among the samples, was not significantly different from the B and C depths, while the C depth was not significantly different from the D depth. Finally, as observed in most physical properties, the soil nitrate content between the depths D, E and F was not significantly different. The soil ammonia also decreased exponentially with depth (Figure 6.3.14 B). Finally, although the soil nitrite was not significantly different between the depth intervals of the PM subsurface, mainly due to the high variability between samples, an interesting pattern was observed with increased nitrite concentrations in the topsoil layers and the layers of the permanently saturated C soil horizon, and lower nitrite in the B soil horizon (Figure 6.3.14 C).

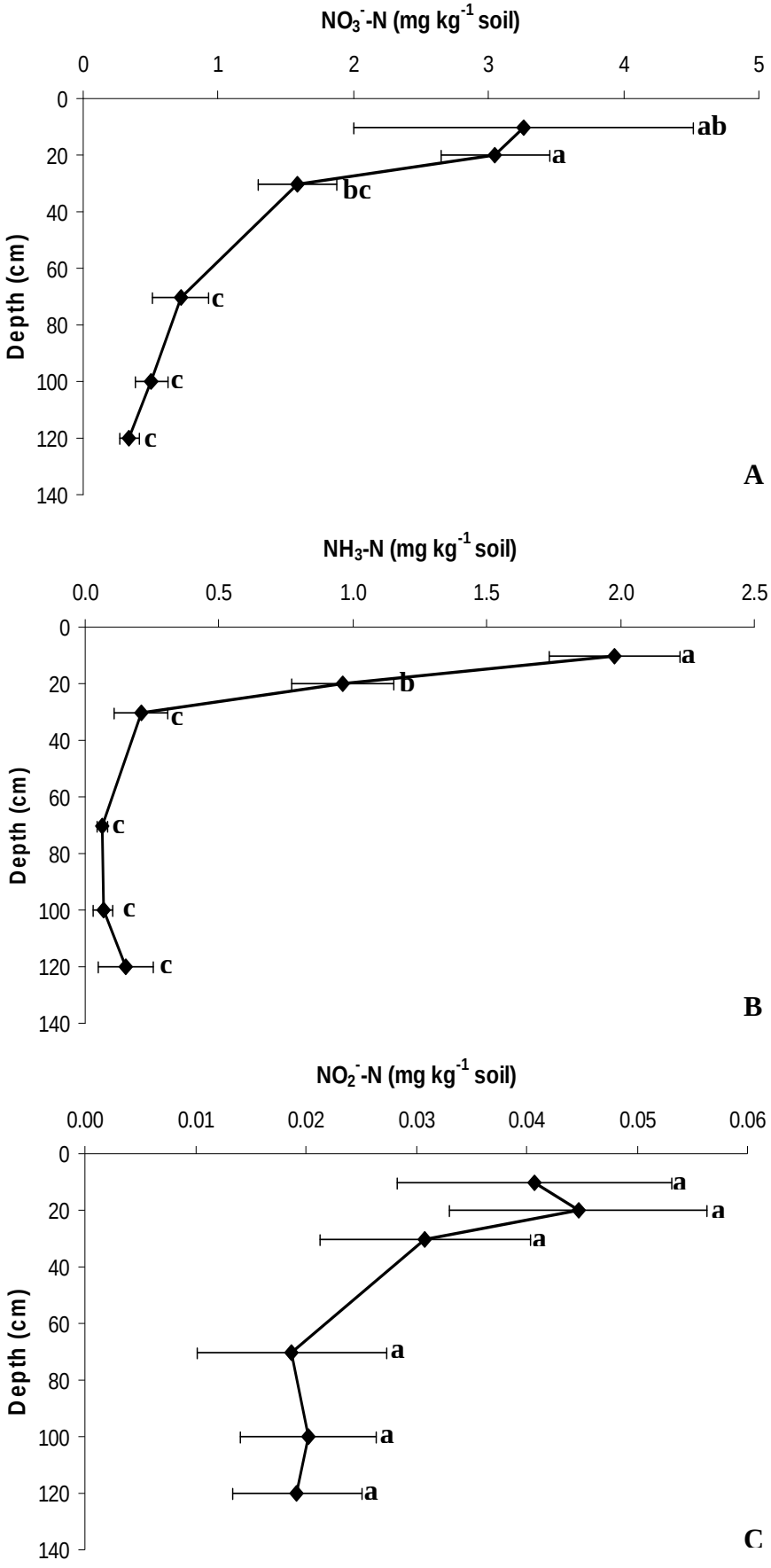

Figure 6.3.14: Soil NO_3^--N, NH_3-N and NO_2^--N in the depth intervals of the PM subsurface. Data are mean values ± 1SE. Different lower case letters indicate significant differences.

6.3.7 *AnMOC and methane production potential in the subsurface of the Pasture Meadow*

The results for the AnMOC mineralisation rate were similar to the respective results for the BZ subsurface and followed the general exponential decay pattern observed in most of the soil physical properties. The first three topsoil depth intervals (A, B and C) were significantly different while the three bottom depth intervals (D, E and F) were not different between them (Figure 6.3.15 A). The anaerobic mineralisation rate was reduced by 37 % within 10 cm in the topsoil and by 95 % in the permanently saturated C soil horizon (>100 cm) (Table 6.3.14). The lability of organic carbon did not display a decrease with depth as both the AnMOC and the organic carbon decreased at the same exponential rate with depth and therefore their ratio remained unchanged across the different depth intervals (Figure 6.3.15 B and Table 6.3.14).

Methane production potential was observed predominantly in the topsoil (0 – 10 cm), while the potential was 86 % less in the B depth interval (Figure 6.3.15 C and Table 6.3.14). The lag phase for the methanogens in the A samples ranged between 1 and 29 days, with longest lag phase length for the samples from the middle of the floodplain and shortest from the riparian and the channel depression samples. The lag phase for the B depth samples was between 15 and 60 days. The C and D samples produced measurable amounts of methane linearly for the first 12 days after which they reached a plateau. The production rates were similar regardless of the sampling location. As for the E and F depths, only one sampling location, next to the river, displayed a significant methane production potential at the depth of the permanently saturated C soil horizon.

Table 6.3.14: AnMOC, lability of organic carbon and methane production potential in the subsurface of the Pasture Meadow. Data are means ± 1SE.

	AnMOC		**Labile org. carbon**		**Methane**	
	CO_2 (µmol kg^{-1} d^{-1})		**CO_2 (µmol g^{-1} TOC d^{-1})**		**CH_4 (µmol kg^{-1} d^{-1})**	
Pasture Meadow depth	**Mean**	**± 1 SE**	**Mean**	**± 1 SE**	**Mean**	**± 1 SE**
A 0-10 cm (n=8)	764.4	34.1	13.9	1.5	158.3	57.1
B 10-20 cm (n=8)	485.1	48.2	12.7	1.3	21.8	21.1
C 20-30 cm (n=8)	272.7	56.9	14.2	2.2	0.006	0.001
D 50-70 cm (n=8)	75.2	27.4	10.5	2.3	0.001	0.001
E 80-100 cm (n=8)	68.3	17.7	10.2	2.4	0.031	0.03
F 100-120 cm (n=8)	38.1	19.3	17.1	8.8	0.03	0.02

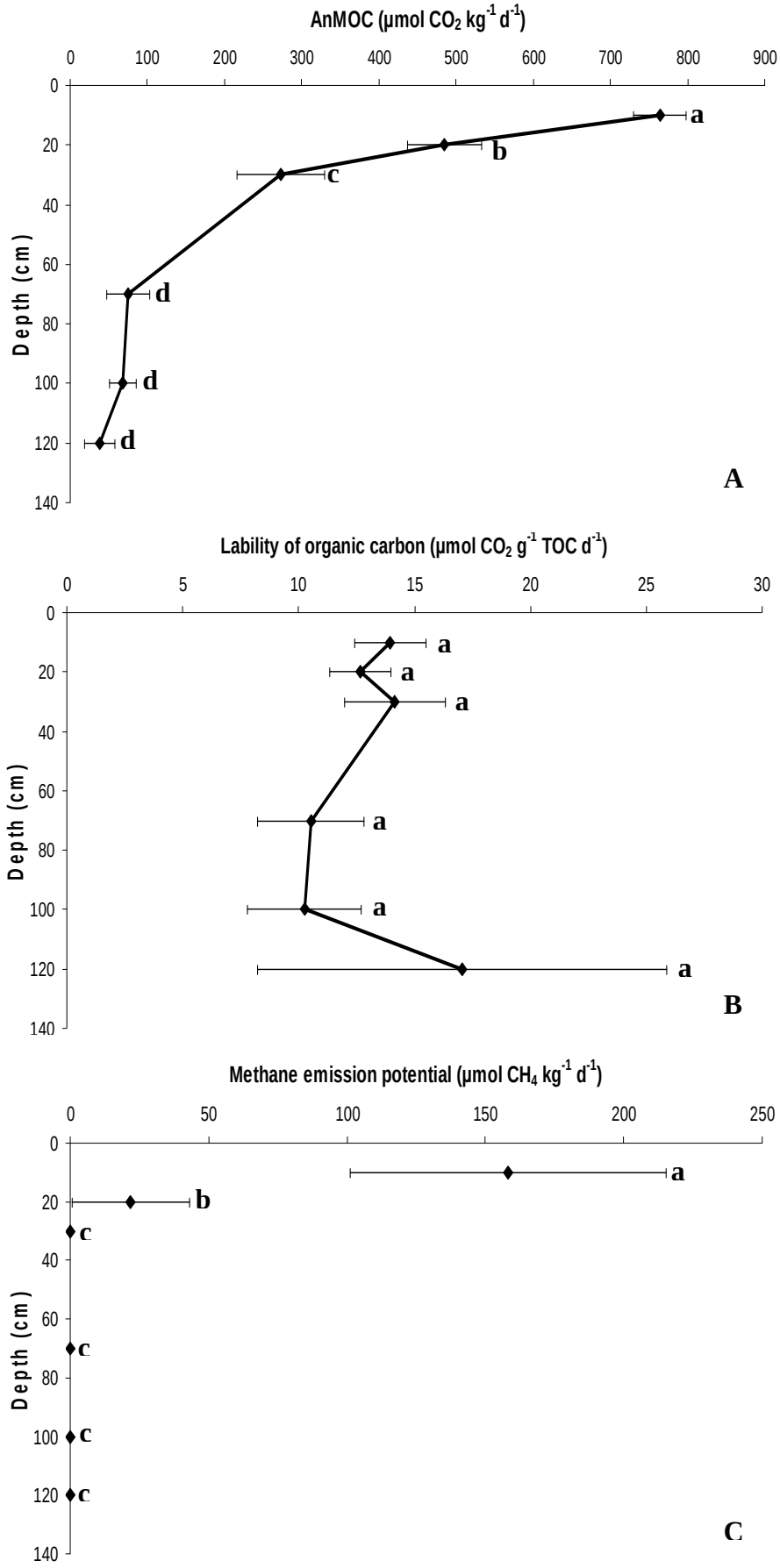

Figure 6.3.15: AnMOC, lability of organic carbon and methane production potential in the subsurface depth intervals of the PM. Data are means ± 1 SE. Different lower case letters indicate significant differences.

6.3.8 *Spatial ordination of the Pasture Meadow subsurface samples*

Principal Component Analysis (PCA) between the soil physical properties that showed some significant differences between the PM depth intervals resulted in the extraction of four principal axes that, combined, explained 95 % of the inter-sample variance (Table 6.3.15). The correlation coefficients between the first two component axes and the environmental variables are shown in Table 6.3.16. The first axis explained 58 % of the variance and was closely associated with the organic matter content, the AnMOC, the water content, the soil nitrate and the methane production potential. The second principal axis explained 21 % of the variance and was associated with the ratio of TOC/NO_3^-. It should be noted that the lability of OC was not included in the PCA since it was not significantly different between samples, while the methane was excluded as the missing values would have reduced the sample size of the PCA.

Plotting the cluster centroids of scores for the first two axes per sample depth resulted in the bi-plot of Figure 6.3.16. The topsoil samples (A depth) clearly separated from the rest and were associated with the positive side of Axis 1 (i.e. with soil conditions such as high OM availability and soil moisture, high mineralisation rates and nitrate supply and low redox potential) suggesting favourable conditions for nitrate attenuation. The B and C depth samples also formed distinct groups with decreasing association to the positive Axis 1, showing less favourable conditions for denitrification and DNRA. Finally, the depths D, E and F formed an agglomeration associated with the negative Axis 1, thus indicating a similarity of soil conditions between the B and C soil horizons in the PM that were less favourable for biogeochemical nitrate attenuation compared to the topsoil.

Table 6.3.15: The principal components (axes) generated by the PCA, their respective eigenvalues, the % of variance explained by each component and the cumulative % of inter-sample variance explanation for the PM subsurface.

Axes	Eigenvalues	% of Variance	Cumulative %
1	3.473	57.9	57.9
2	1.247	20.8	78.7
3	0.675	11.3	89.9
4	0.329	5.5	95.4

Table 6.3.16: Correlation coefficients of the environmental variables in PCA. ***Correlation significant at the 0.01 probability level.

Variables	Component 1	Component 2
Water content	0.823***	-0.141
Organic Matter	0.962***	-0.044
Soil Nitrate	0.683***	-0.585
TOC/NO_3^-	0.314	0.892***
AnMOC	0.921***	0.094
Methane Emission	0.677***	0.283

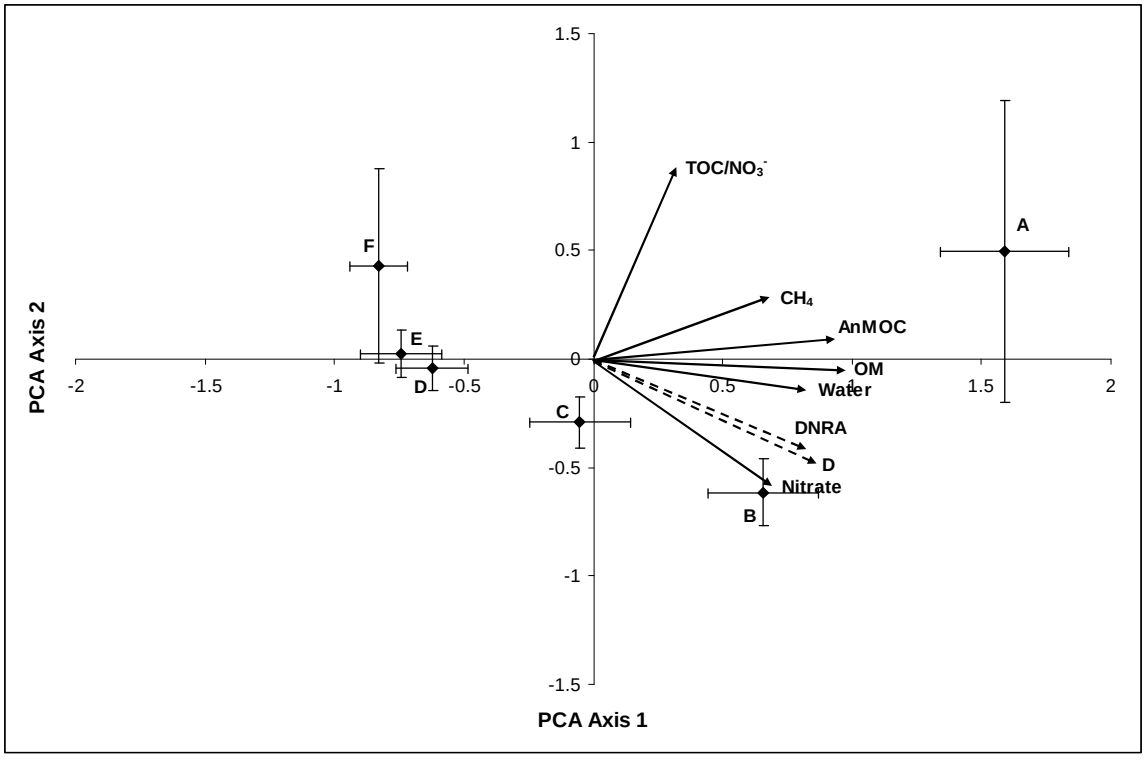

Figure 6.3.16: Correlation bi-plot from the PCA analysis with cluster centroids (average score on each component, with standard errors) for the depth intervals (ABCDEF) in PM. Correlations of the variables with the main axes are given by solid arrows. Dashed arrows indicate the correlation of nitrate attenuation processes with the component axes. Water; water content, OM; organic matter content, CH_4; methane production potential, Nitrate; soil nitrate content, D; potential denitrification rate.

6.3.9 *Denitrification and DNRA potential in the subsurface of the Pasture Meadow*

The potential denitrification rate decreased exponentially with depth in the subsurface of the PM (Table 6.3.17 and Figure 6.3.17 A). The topsoil rate decreased by 38 % within 10 cm in the B depth, while it decreased by > 95 % within 120 cm from the ground surface. The denitrification rate of the PM subsurface was generally not significantly different from the BZ subsurface, apart from the B depth that had significantly higher denitrification rate in the PM compared to the BZ (Student's t-test; df=7, $t\text{-}stat$=-3.17, P<0.05) and the F depth that displayed higher denitrification rate in the BZ than the PM (Student's t-test; df=7, $t\text{-}stat$=2.8, P<0.05).

Regarding the nitrous oxide (N_2O) production, the B depth interval displayed a significantly higher production potential compared to the topsoil and the rest of the subsurface intervals. Moreover, the two bottom layers (E and F) had significantly lower N_2O production potential (Table 6.3.17 and Figure 6.3.17 B). The ratio of N_2O/N_2 (Figure 6.3.18), indicated, as also in the case of the BZ subsurface, that the differences in the relative importance of the two denitrification reduction steps were probably an effect of the incubation time of the experiment. Adjacent depth intervals (A-B, C-D and E-F) were treated with the same incubation periods, while, as the denitrification potential results showed, had significantly different process rates. This resulted in the accumulation of N_2O as an intermediate of denitrification in the second sample set of each pair, the one that had the lowest denitrification rate.

The DNRA potential also varied with depth. The surface soil (A depth) had significantly higher DNRA potential compared to the rest of the depths, followed by the B depth, which was also significantly different from the other layers. Below the C depth DNRA decreased at a slower rate. (Table 6.3.17 and Figure 6.3.17 C). The potential DNRA rate decreased by 67 % within 10 cm in the topsoil and by 99 % within 120 cm in the subsurface. Regarding the ratio D/DNRA, it generally increased with depth (Figure 6.3.19), although the increase was not statistically significant as both denitrification and DNRA decreased exponentially with depth at similar rates, and therefore their ratio was not different across the subsurface.

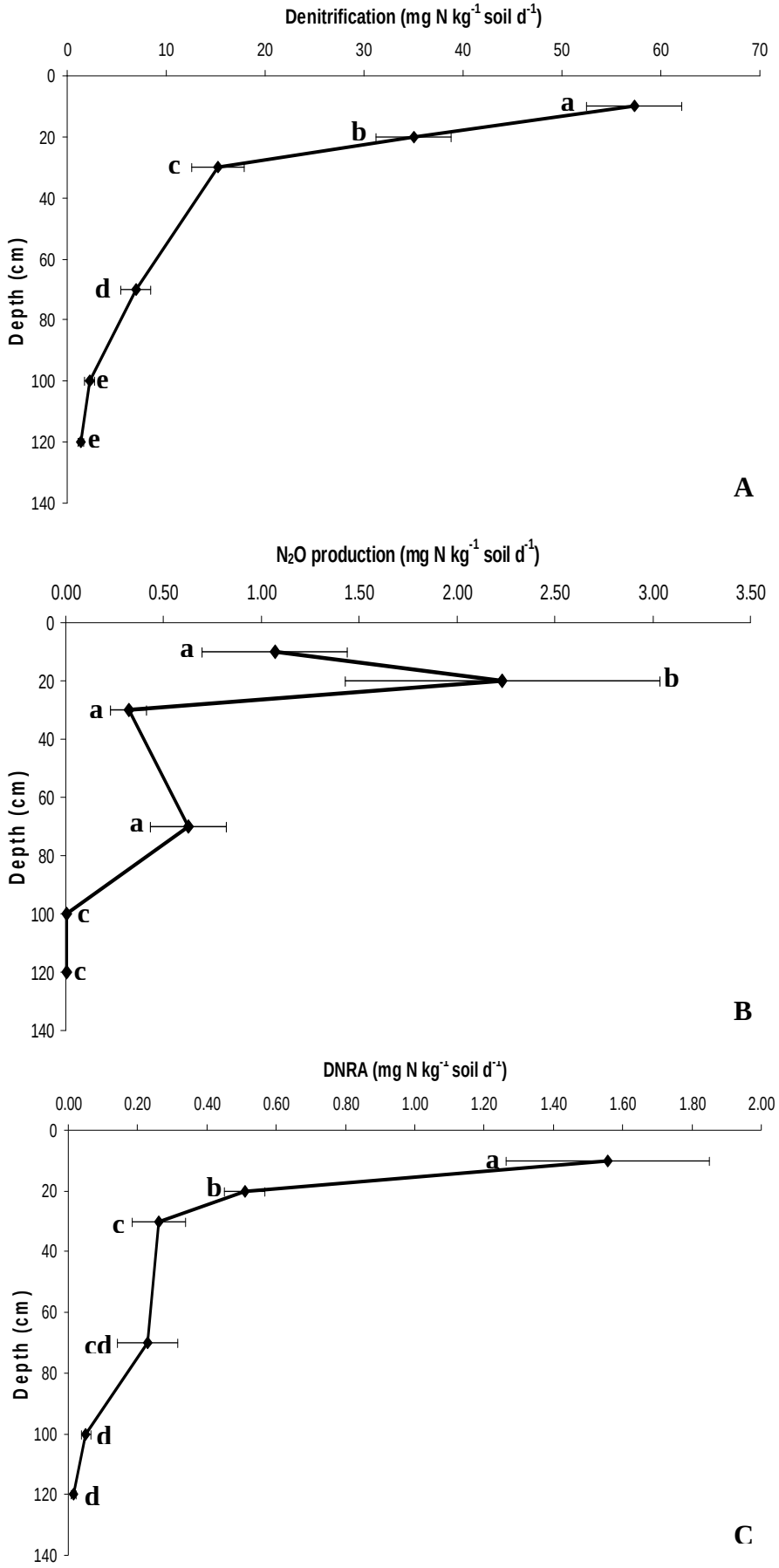

Figure 6.3.17: Denitrification, N_2O production and DNRA potential rates in the depth intervals of the PM subsurface. Data are means ± 1SE. Different lower case letters indicate significant differences.

Table 6.3.17: Denitrification, N_2O production and DNRA potential rates in the depth intervals of the PM subsurface. Data are means ± 1SE.

	Denitrification (mg N kg^{-1} soil d^{-1})		Nitrous oxide (mg N kg^{-1} soil d^{-1})		DNRA (mg N kg^{-1} soil d^{-1})	
Pasture Meadow depth	**Mean**	**± 1 SE**	**Mean**	**± 1 SE**	**Mean**	**± 1 SE**
A 0-10 cm (n=8)	57.3	4.8	1.1	0.4	1.6	0.3
B 10-20 cm (n=8)	35.0	3.8	2.2	0.8	0.5	0.1
C 20-30 cm (n=8)	15.2	2.6	0.3	0.1	0.3	0.1
D 50-70 cm (n=8)	6.9	1.5	0.6	0.2	0.2	0.09
E 80-100 cm (n=8)	2.3	0.5	0.005	0.003	0.05	0.01
F 100-120 cm (n=8)	1.3	0.3	0.005	0.003	0.02	0.008

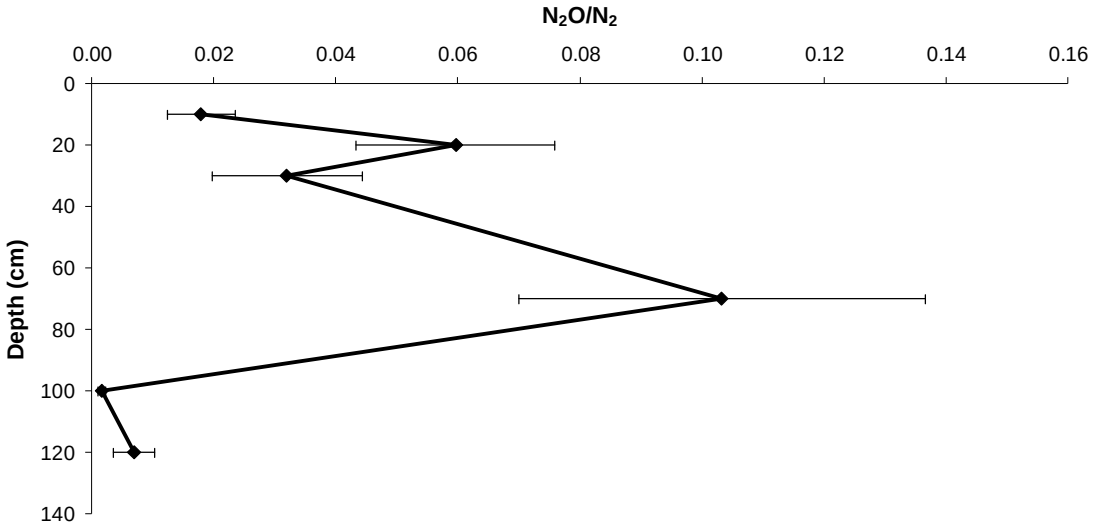

Figure 6.3.18: The ratio of N_2O/N_2 in the depth intervals of the PM subsurface. Data are means ± 1SE.

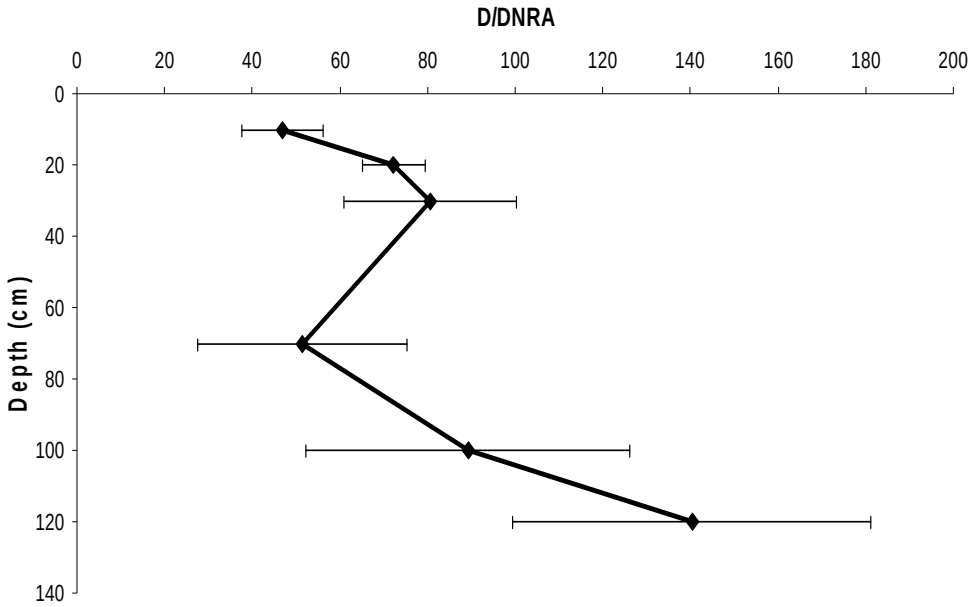

Figure 6.3.19: The ratio D/DNRA in the depth intervals of the PM subsurface. Data are means ± 1SE.

A NO_3^- budget was also estimated for the PM subsurface experiment (Table 6.3.18). Regarding the topsoil samples, 63 % of the added nitrate was recovered as N_2, the end product of denitrification, while 15 % remained unused after the three hour incubation. DNRA accounted only for 2 % of the added nitrate, while NO_2^- and N_2O were also present at the end of the incubation. However, 16 % of the originally added spike was not recovered in any of the above measurements, and it was therefore considered as 'lost', possibly assimilated in bacterial biomass. In the B depth interval, 71 % of the added nitrate was recovered as N_2, while also 6 % of the nitrate was accumulated as N_2O, possibly as a result of the short incubation time, as it was also indicated by 22 % of the added nitrate remaining in the sample vessel. Between the paired depths C & D and E & F, where each pair shared the same incubation time, more NO_2^- and N_2O accumulated in the D and F samples, while also more nitrate remained unused in the same depth intervals. DNRA accounted for 2 % of the added spike in every case, and seemed to be unaffected by the duration of sample incubation. Finally, the amount of the added nitrate, which was not recovered in any of the measured processes, and therefore was characterised as 'lost', increased with depth from 9 % in the C depth to 34 % in the F depth.

Table 6.3.18: Nitrate Budget of the PM subsurface experiment including three products of denitrification, DNRA, unused amount of added nitrate and 'lost' amount of nitrate.

	Denitrification			DNRA	Unused	'Lost'	Total
	N_2	NO_2^-	N_2O	NH_4^+	NO_3^-		
Pasture Meadow depth	**%**	**%**	**%**	**%**	**%**	**%**	**%**
A 0-10 cm (n=8)	63	1	3	2	15	16	100
B 10-20 cm (n=8)	71	1	6	1	22	0	100
C 20-30 cm (n=8)	68	0	3	2	18	9	100
D 50-70 cm (n=8)	38	10	5	2	25	20	100
E 80-100 cm (n=8)	74	1	0.14	2	0	22	100
F 100-120 cm (n=8)	47	2	0.31	2	14	34	100

Correlation analysis between the denitrification and DNRA potential, the AnMOC mineralisation rate, the methane production potential, the lability of organic carbon and the soil physical properties of the PM subsurface has indicated a number of significant relationships (Table 6.3.19). The denitrification and DNRA potential inter-correlated, indicating the coexistence and similar variability with depth of the two nitrate attenuation processes in the PM subsurface (Figure 6.3.20). Moreover, the denitrification potential rate showed significant positive correlation with the AnMOC (Figure 6.3.21), the organic carbon content, the ratio TOC/TN, the soil nitrate content, the water content, and the methane production potential. The DNRA potential rate showed significant positive correlation with the organic carbon, the AnMOC, the ratio TOC/TN, the water content, the soil nitrate content and the methane production potential.

MRA between the denitrification rate and the environmental variables produced similar results to the correlation analysis. The AnMOC explained 83 % (MRA; r^2=0.83, *df*=47, P<0.01) of the variance in the denitrification rate of the samples, followed by the organic matter content (MRA; r^2=0.75, *df*=47, P<0.01) and the organic carbon (MRA; r^2=0.68, *df*=47, P<0.01) with 75 % and 68 % explanatory power respectively, highlighting the importance of the organic carbon availability in regulating the denitrification rate in the PM vadose zone. As secondary controlling factors, the soil nitrate content (MRA; r^2=0.43, *df*=47, P<0.01) explained 43 % of the variance between samples, and the water content (MRA; r^2=0.42, *df*=47, P<0.01) 42 %.

Table 6.3.19: Correlation matrix between the denitrification and DNRA potential rate, the AnMOC, the lability of organic carbon, the methane production potential and the soil physical properties in the depth intervals of the PM subsurface. Underlined correlation coefficients are products of Spearman rho correlation whereas non-underlined are products of Pearson Product-Moment correlation. ** Correlation is significant at the 0.01level and *Correlation is significant at the 0.05 level.

Variables/Correlation coefficients		Denitrification potential	DNRA	AnMOC	Org. carbon lability	Methane emission	Organic matter content	Organic carbon	TOC/TN	TOC/NO_3^-	Water content	Soil nitrate	Bulk density
Denitrification potential	*R or rho*	1											
	P	.											
	N	48											
DNRA	*R or rho*	**0.880****	1										
	P	0.000	.										
	N	47	47										
AnMOC	*R or rho*	**0.908****	**0.826****	1									
	P	0.000	0.000	.									
	N	48	47	48									
Org. carbon lability	*R or rho*	0.158	0.084	0.348*	1								
	P	0.301	0.589	0.019	.								
	N	45	44	45	45								
Methane emission	*R or rho*	**0.532****	**0.541****	**0.617****	**0.441****	1							
	P	0.000	0.000	0.000	0.002	.							
	N	48	47	48	45	48							
Organic matter content	*R or rho*	**0.871****	**0.822****	**0.890****	0.025	**0.435****	1						
	P	0.000	0.000	0.000	0.872	0.002	.						
	N	48	47	48	45	48	48						
Organic carbon	*R or rho*	**0.875****	**0.848****	**0.862****	-0.023	**0.529****	**0.864****	1					
	P	0.000	0.000	0.000	0.883	0.000	0.000	.					
	N	48	47	48	45	48	48	48					
TOC/TN	*R or rho*	**0.838****	**0.805****	**0.831****	-0.254	**0.528****	**0.866****	**0.903****	1				
	P	0.000	0.000	0	0.092	0.000	0.000	0.000	.				
	N	48	47	48	45	48	48	48	48				
TOC/NO_3^-	*R or rho*	0.259	**0.443****	0.341*	-0.060	0.183	0.273	0.301*	**0.600****	1			
	P	0.075	0.002	0.018	0.697	0.212	0.061	0.038	0.000	.			
	N	48	47	48	45	48	48	48	48	48			
Water content	*R or rho*	**0.668****	**0.635****	**0.638****	-0.294*	0.337*	**0.857****	**0.667****	**0.696****	0.014	1		
	P	0.000	0.000	0.000	0.050	0.019	0.000	0.000	0.000	0.927	.		
	N	48	47	48	45	48	48	48	48	48	48		
Soil nitrate	*R or rho*	**0.604****	**0.568****	**0.554****	-0.082	0.259	**0.618****	**0.656****	**0.557****	-0.223	**0.503****	1	
	P	0.000	0.000	0.000	0.593	0.076	0.000	0.000	0.000	0.127	0.000	.	
	N	48	47	48	45	48	48	48	48	48	48	48	
Bulk density	*R or rho*	**-0.753****	**-0.708****	**-0.756****	0.120	**-0.478****	**-0.805****	**-0.734****	**-0.746****	-0.155	**-0.782****	**-0.496****	1
	P	0.000	0.000	0.000	0.431	0.001	0.000	0.000	0.000	0.292	0.000	0.000	.
	N	48	47	48	45	48	48	48	48	48	48	48	48

MRA between the DNRA potential rates and the environmental variables in the PM subsurface, indicated the prevalence of reduced conditions, as expressed by the methane production potential, as the most important environmental parameter that explained 67 % of the variance between DNRA potential rates (MRA; r^2=0.67, *df*=46, *P*<0.01). The AnMOC (MRA; r^2=0.57, *df*=46, *P*<0.01) and the organic carbon content (MRA; r^2=0.54, *df*=46, *P*<0.01) had 57 % and 54 % explanatory power respectively, while the ratio TOC/TN (MRA; r^2=0.40, *df*=46, *P*<0.01) explained 40 % of the DNRA variance. The results indicated that the most likely controlling factors of DNRA in the PM subsurface were the existence of reduced conditions and the relative availability of organic carbon over the availability of nitrogen.

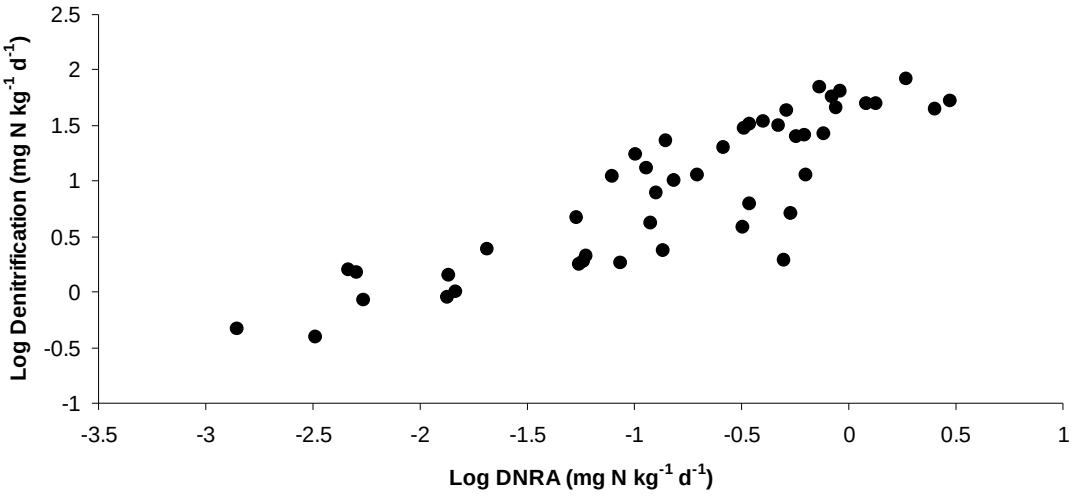

Figure 6.3.20: Scatter plot of denitrification against DNRA potential rates in the PM subsurface (*r*=0.88, *N*=47, *P*<0.01).

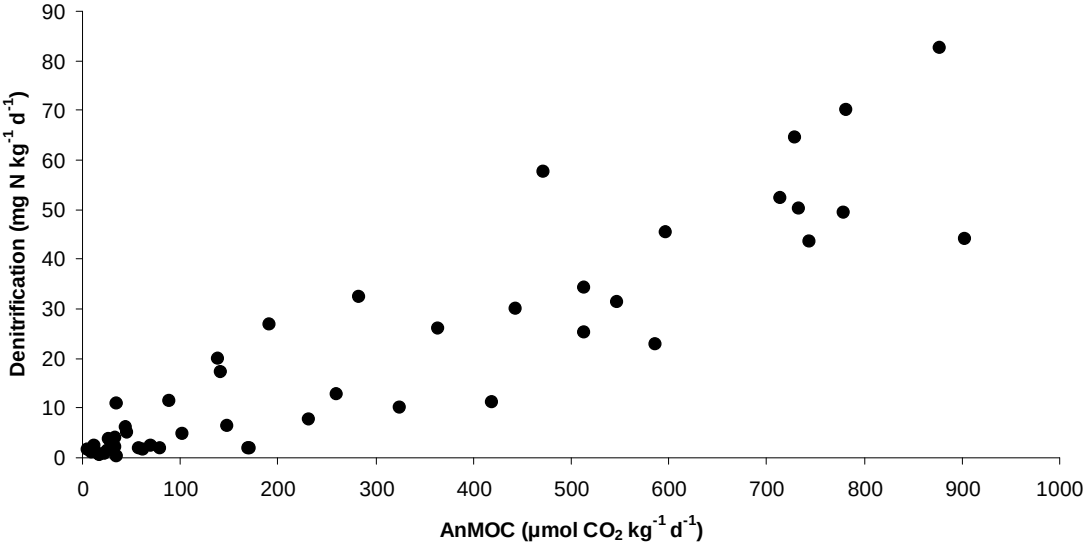

Figure 6.3.21: Scatter plot of denitrification potential rates against the AnMOC in the PM subsurface (*r*=0.91, *N*=48, *P*<0.01).

Concluding, a discrete zonation of soil properties was observed in the subsurface of the PM. Specifically, the organic carbon availability, the soil moisture and the soil nitrogen content decreased significantly within the topsoil depth intervals (i.e. every 10 cm) compared to the deeper soil horizons where less variability was observed between 50 and 120 cm depth. The same pattern was observed for the organic carbon mineralisation rate that decreased exponentially with depth up to 50 cm, while it remained unchanged at greater depths. The methane production potential concentrated in the top 20 cm of the soil with shorter lag phase length in the riparian area samples and longer lag phase in the middle of the floodplain. Both the denitrification and DNRA processes followed an exponential decay with depth up to 50 cm (i.e. within the B soil horizon), while the decrease became less significant between 50 and 120 cm depth. The primary controlling factor for denitrification was the availability of organic carbon with depth while the soil nitrate and soil moisture played a secondary role. For DNRA, the existence of reduced conditions was the most important controlling factor, followed by the availability of organic carbon. Finally the relative importance of DNRA over denitrification decreased with depth, while the importance of nitrous oxide as a denitrification product increased within the vadoze zone compared to the soil surface and then decreased again within the permanently saturated zone.

6.4 *The effect of prolonged wetting and drying on nitrate attenuation processes in the reconnected floodplain of the River Cole*

This section aims to assess the effect of prolonged wetting and drying under field conditions on the topsoil properties and subsequently the nitrate attenuation processes across the different land use zones of the re-connected floodplain of the River Cole.

6.4.1 *Soil physical properties*

The sampling of the wet conditions took place in late March '08, after the reconnected floodplain had received 70 mm total rainfall in three weeks (3.3 mm rain d^{-1}). From data available for the Buffer Zone area, the topsoil was flooded from overbank flooding for 7 days prior the sampling date. The matric potential of the topsoil in the BZ area on the day of sampling was on average -0.04 hPa, indicating near surface saturation conditions. The sampling of the dry conditions took place four months later, in late July '08, after the floodplain had received 11 mm total rainfall in two weeks (0.8 mm rain d^{-1}) prior to the sampling and no rain at all for 10 days before the sampling. The sampling day was 12 days after a summer flood peak and the matric potential of the topsoil in the BZ area on that day was on average -704.28 hPa, far from surface saturation.

The physical properties of the topsoil in all four land use zones from both the wet and the dry sampling are summarised in Table 6.4.1. Table 6.4.2 presents the results of the parametric (One-Way ANOVA) or non-parametric (Mann-Whitney) statistical tests for the comparison of variable means between wet and dry conditions across all the floodplain zones. The dry bulk density was not significantly different between wet and dry conditions (Figure 6.4.1 A). Although the wet condition samples had higher water content compared to the dry conditions, they were not statistically different (Figure 6.4.1 B). However, another measurement of the soil water content, the Water Filled Pore Space (WFPS) tends to be more accurate when soil moisture conditions are generally high (Sleutel *et al.*, 2008). The WFPS was estimated as described by Linn and Doran (1984), from the volumetric water content ($cm^3.cm^{-3}$), which was measured directly at each sampling location with a *Theta* probe (Delta-T Instruments), and the porosity of the soil, which was estimated from the dry bulk density according to Rowell (1994). The WFPS was significantly higher in the wet condition samples compared to the dry condition samples (Figure 6.4.1 C).

Regarding the absolute particle size distribution (Figure 6.4.2), the analysis was performed once after the wet conditions sampling since the particle size fractions, as shown in previous experiments, played a minor role in controlling the nitrogen retention processes in the topsoil of the reconnected floodplain of the River Cole. The Fritillary Meadow (FM) samples contained significantly higher clay from the rest of the land use zone samples that were not different between each other. Additionally, the FM samples had higher silt content from the Buffer Zone (BZ) and the Grazing Grassland (GG) samples and were not different from the Pasture Meadow (PM) samples. Similarly, the FM samples had lower very fine sand content from the BZ and GG samples, while they were not different from the PM samples. The dominance of the clay and silt fractions was observed once more in the topsoil of the reconnected floodplain of the River Cole and since this was unlikely to change during the four months between the wet and the dry conditions sampling, the analysis was not repeated after the dry conditions sampling.

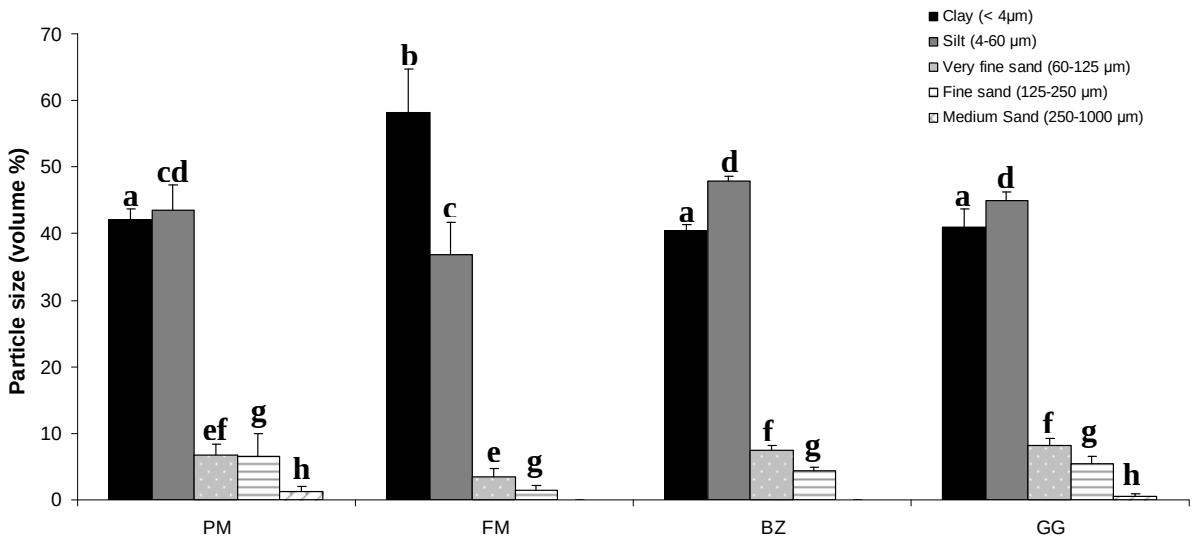

Figure 6.4.2: Absolute particle size distribution (volume %) in the topsoil of the four land use zones on the wet conditions sampling (means + 1 SE, significant differences indicated with different lower case letters).

Table 6.4.1: Physical properties of the topsoil in the four land use zones on the wet and dry conditions sampling (data are mean values ± 1 standard error, where data are missing are replaced by N/A).

	Soil type	Dry Bulk Density ($g\ cm^{-3}$)		Water content (%)		WFPS (%)		Organic matter (%)		Organic carbon (%)		TOC/NO_3^-		NO_3^--N ($mg\ kg^{-1}$)	
		Mean	**± 1 SE**	**Mean**	**± 1 SE**	**Mean**	**± 1 SE**	**Mean**	**± 1 SE**	**Mean**	**± 1 SE**	**Mean**	**± 1 SE**	**Mean**	**± 1 SE**
WET conditions (n=30)	Silty clay	0.70	0.04	57.6	4.47	67.8	2.09	12.3	1.01	4.5	0.33	0.27	0.07	34.9	6.2
Pasture Meadow (n=6)	Clay	0.77	0.06	51.4	6.25	68.8	1.79	11.0	1.52	3.2	0.62	0.22	0.05	18.3	6.4
Fritillary Meadow (n=6)	Clay	0.61	0.04	85.4	13.01	65.1	2.75	18.8	2.77	6.2	0.67	0.15	0.05	69.3	25.9
Buffer Zone (n=10)	Silty clay	0.61	0.06	43.2	2.64	62.0	2.37	8.6	0.50	3.7	0.42	0.14	0.02	30.5	4.9
Grazing Grassland (n=8)	Silty clay	0.83	0.11	59.2	7.97	76.3	5.99	12.9	1.75	5.3	0.47	0.58	0.27	35.8	15.0
DRY conditions (n=30)	N/A	0.75	0.03	47.9	4.27	51.4	2.22	13.7	1.14	4.3	0.29	1.03	0.34	11.4	2.4
Pasture Meadow (n=6)	N/A	0.84	0.03	48.7	6.16	61.3	1.94	12.6	1.91	3.3	0.46	1.49	0.88	7.0	3.0
Fritillary Meadow (n=6)	N/A	0.65	0.05	74.7	14.37	52.6	7.15	21.4	2.87	5.8	0.65	1.98	1.45	23.9	10.1
Buffer Zone (n=10)	N/A	0.82	0.06	32.8	1.58	49.1	3.95	9.5	0.49	3.8	0.33	0.54	0.07	8.2	1.4
Grazing Grassland (n=8)	N/A	0.65	0.06	45.9	5.49	45.9	2.50	14.1	1.96	4.4	0.63	0.59	0.15	9.1	1.7

Table 6.4.2: Comparison of the means between the wet and the dry conditions sampling for selected soil properties and processes. *df*; degrees of freedom, *F*; F statistic, *z*; *z* statistic *P*; probability level. Where the variable is annotated with * the non-parametric Mann-Whitney test has been used instead of One-Way ANOVA.

	One-Way ANOVA and Mann-Whitney		
WET - DRY conditions	*df*	*F or z*	*P*
Bulk density	59	0.7	>0.05
Water content*	59	-1.9	>0.05
WFPS	59	29.0	<0.01
Clay fraction	29	6.5	<0.01
Silt fraction	29	3.1	<0.05
Very fine sand fraction	29	3.1	<0.05
Organic matter*	59	-0.8	>0.05
Organic carbon	59	0.3	>0.05
TOC/NO_3^-*	56	-4.6	<0.01
Soil nitrate*	56	-3.9	<0.01
Soil ammonia*	57	-0.7	>0.05
Soil nitrite*	59	-3.2	<0.01
AnMOC*	57	-1.0	>0.05
Lability of OC	59	0.7	>0.05
Methane emission*	59	-1.4	>0.05
Denitrification	59	4.2	>0.05
Nitrous oxide production*	59	-1.1	>0.05
N_2O/N_2^*	54	-0.6	>0.05
DNRA*	59	-2.4	<0.05
D/DNRA*	59	-1.2	>0.05

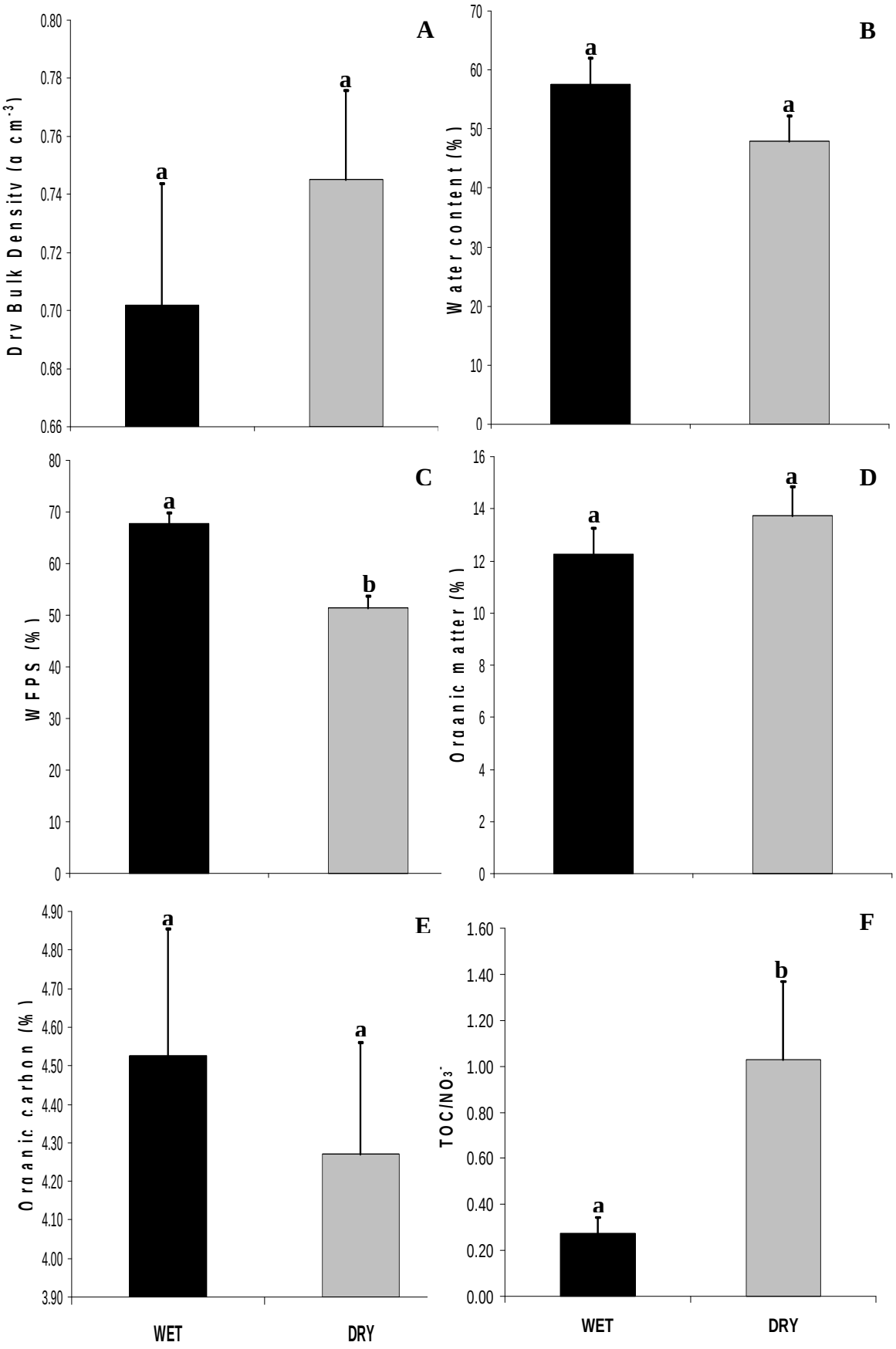

Figure 6.4.1: Mean dry bulk density, water content, WFPS, organic matter, organic carbon content and the ratio of TOC/NO_3^- (+ 1 SE) across the four land use zones on the wet and dry conditions sampling (significant differences indicated with different lower case letters).

With respect to the soil organic carbon availability between the wet and dry conditions, neither the organic matter nor the organic carbon content was significantly different between the two samplings (Figures 6.4.1 D & E respectively). However, the ratio TOC/NO_3^- (Figure 6.4.1 F) was significantly higher in the dry condition samples, compared to the wet, as a result of the different nitrate availability. The soil NO_3^--N content was three times higher in the wet condition samples, compared to the dry (Figure 6.4.3). Similarly, the soil NO_2^--N was significantly higher in the wet samples, compared to the dry samples, indicating more reduced conditions during the wet conditions sampling. Although the mean NH_3-N content of the wet samples was almost three times higher than the dry samples, due to the high variability among the wet samples the difference was not statistically significant (Table 6.4.2).

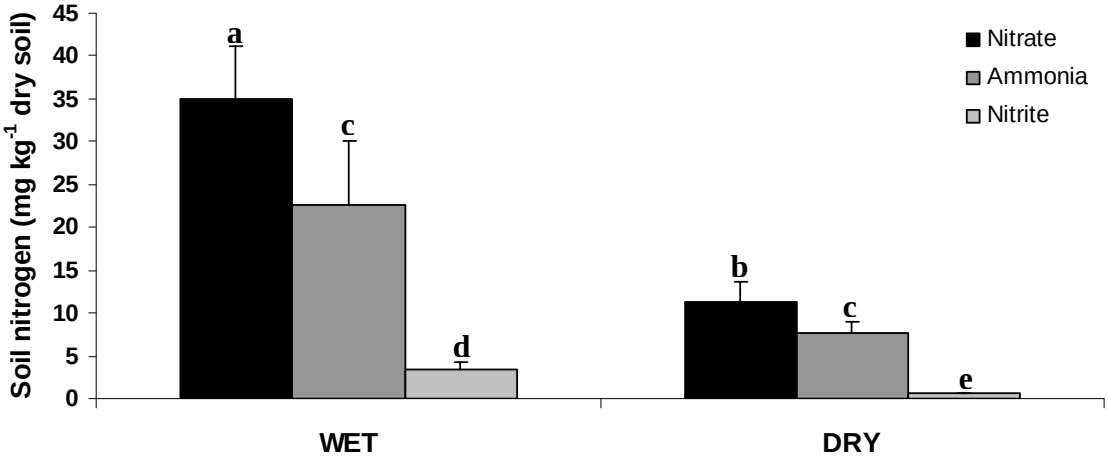

Figure 6.4.3: Mean concentrations of NO_3^--N, NO_2^--N and NH_3-N (+ 1 standard error) in the topsoil of the four land use zones on the wet and dry conditions sampling (significant differences indicated with different lower case letters).

6.4.2 *AnMOC and Methane production potential*

The Anaerobic Mineralisation rate of Organic Carbon (AnMOC) displayed the same pattern as the organic matter and the organic carbon results with no significant difference between the wet and dry condition samples (Table 6.4.3 and Figure 6.4.4 A). However, in both the wet and dry sampling, the FM samples had significantly higher AnMOC compared to the BZ and the GG, as a result of a few outliers. Similarly, the lability of organic carbon although it was 23 % less in the dry samples (Table 6.4.3 and Figure 6.4.4 B), the difference between wet and dry was not statistically significant, while no difference was found between land use zones in both samplings. Although the methane production potential (Table 6.4.3 and Figure 6.4.4 C) was slightly higher under dry conditions, the variability between samples was high under both conditions and the difference was not statistically significant, while no difference was observed between land use zones in both samplings.

Table 6.4.3: AnMOC, lability of organic carbon and methane production potential of the topsoil across the four land use zones on the wet and dry conditions samplings (data are means ± 1SE). Significant differences between land use zones for both samplings indicated with different lower case letters.

	AnMOC		**Labile org. carbon**		**Methane**	
	CO_2 (µmol kg^{-1} d^{-1})		**CO_2 (µmol g^{-1} TOC d^{-1})**		**CH_4 (µmol kg^{-1} d^{-1})**	
	Mean	**± 1 SE**	**Mean**	**± 1 SE**	**Mean**	**± 1 SE**
WET conditions (n=30)	649.3	127.4	22.9	5.9	9.8	6.8
Pasture Meadow (n=6)	587.6^{ab}	155.2	20.4^{a}	4.0	1.8^{a}	1.1
Fritillary Meadow (n=6)	1503.7^{b}	494.9	26.5^{a}	8.8	33.4^{a}	33.0
Buffer Zone (n=10)	297.8^{a}	67.2	8.5^{a}	1.8	2.0^{a}	1.3
Grazing Grassland (n=8)	593.9^{a}	176.7	11.6^{a}	3.6	7.8^{a}	7.2
DRY conditions (n=30)	704.9	102.2	17.7	2.5	14.52	9.33
Pasture Meadow (n=6)	694.2^{ab}	157.5	19.5^{a}	3.6	16.8^{a}	15.7
Fritillary Meadow (n=6)	1372.7^{b}	346.8	26.2^{a}	7.8	7.0^{a}	5.5
Buffer Zone (n=10)	388.9^{a}	53.2	10.7^{a}	1.5	27.1^{a}	26.7
Grazing Grassland (n=8)	607.2^{ab}	114.7	18.8^{a}	5.9	2.8^{a}	1.4

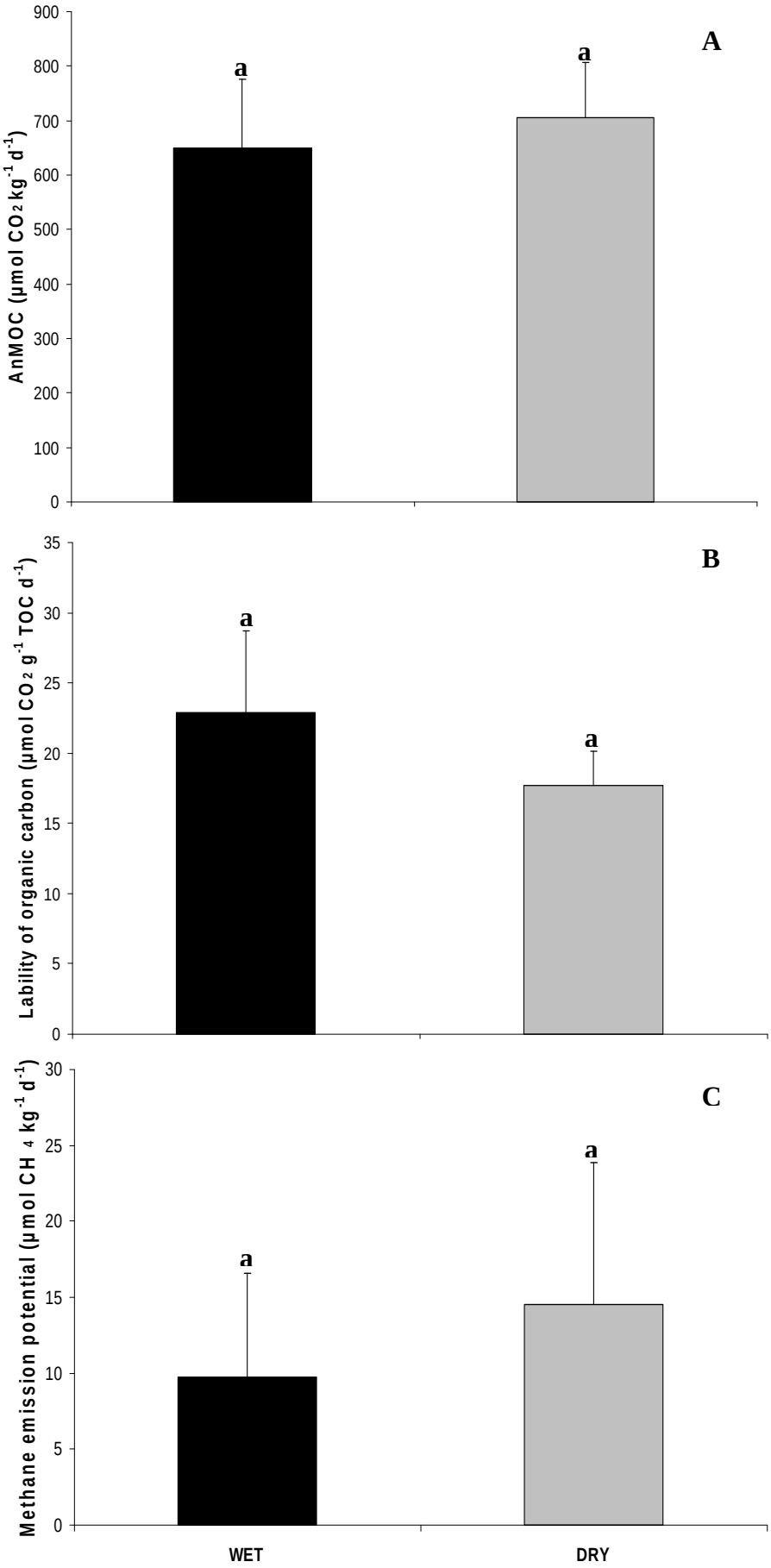

Figure 6.4.4: Mean AnMOC, lability of organic carbon and methane production potential (+ 1 SE) in the topsoil across the four land use zones on the wet and dry conditions sampling (same lower case letters indicate no significant differences).

6.4.3 *Spatial ordination of the wet and dry condition samples*

Principal Component Analysis (PCA) of the soil physical properties, the AnMOC rate and the lability of organic carbon resulted in the extraction of two principal axes with eigenvalues larger than one (Table 6.4.4). The correlation coefficients between the first two component axes and the environmental variables are shown in Table 6.4.5. The first axis explained 50 % of the variance between individual samples and was closely associated with the water content, the AnMOC, the organic matter content and the soil nitrate. The second principal axis explained 21 % of the variance between individual samples and was associated mainly with the WFPS and the ratio TOC/NO_3^-.

Plotting the cluster centroids of each land use zone for both the wet and dry samplings along the first two component axes resulted in the bi-plot of Figure 6.4.5. What becomes immediately apparent is the separation of the samples along axis 2. The wet condition samples were positioned closer to the negative side of the axis and were therefore associated with higher WFPS, while all the dry condition samples were associated with the positive side of axis 2 and the higher values for the ratio of TOC/NO_3^-. Interestingly, axis 1 separated the land use zone samples into three fairly distinct groups. The samples of the FM zone were positioned towards the positive side of the axis suggesting that higher AnMOC, water content, OM and soil nitrate were observed in this land use, while the large error bars along axis 1 highlighted the 'hotspot' nature of the FM samples. The samples of the PM and the GG had similar characteristics in both the wet and the dry samplings as indicated by the overlapping of the cluster centroids. Finally, the BZ samples were separated from the rest and were associated with the negative axis 1 (i.e. lower AnMOC, OM, water and soil nitrate), while the small error bars showed high homogeneity between samples. It should be noted that the environmental variables associated with axis 1 were not different between wet and dry conditions for each land use zone as indicated by the overlapping of the 'wet' and 'dry' cluster centroids along axis 1. This indicates further that the majority of the measured environmental variables remained unchanged between the wet and the dry conditions, while only the WFPS and the relative availability of organic carbon to soil nitrate changed significantly, something that could potentially also influence the rate of nitrate attenuation processes between wet and dry conditions.

Table 6.4.4: The principal components (axes) generated by the PCA, their respective eigenvalues, the % of variance explained by each component and the cumulative % of inter-sample variance explanation between the wet and the dry condition samples.

Axes	Eigenvalues	% of Variance	Cumulative %
1	3.472	49.6	49.6
2	1.443	20.6	70.2

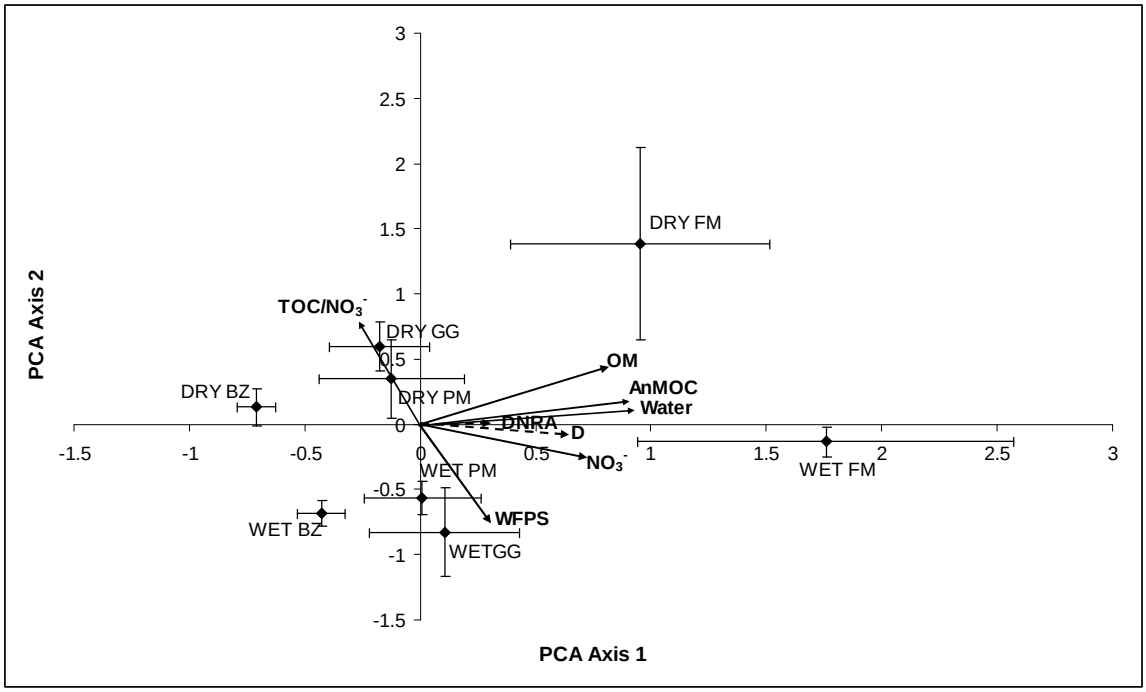

Figure 6.4.5: Correlation bi-plot from the PCA analysis with cluster centroids (average score on each component, with standard errors) for the four land use zones in wet and dry conditions sampling. Correlations of the variables with the main axes are given by solid arrows. Dashed arrows indicate the correlation of nitrate attenuation processes with the component axes. Water; water content, OM; organic matter content, WFPS; water filled pore space, NO_3^-; soil nitrate content, D; potential denitrification rate.

Table 6.4.5: Correlation coefficients of the environmental variables in PCA. ***Correlation significant at the 0.01 probability level.

Variables	Component 1	Component 2
Water content	0.916***	0.084
Organic Matter	0.805***	0.427
AnMOC	0.909***	0.163
WFPS	0.306	-0.759***
Soil Nitrate	0.703***	-0.269
TOC/NO_3^-	-0.269	0.756***
Lability of OC	0.706***	0.079

6.4.4 *Denitrification and DNRA potential*

The potential denitrification rate was not significantly different between the wet and the dry condition samples (Table 6.4.6 and Figure 6.4.6 A), although the wet samples had 37 % higher mean denitrification rate compared to the dry samples. Within the wet samples, the BZ area had significantly lower denitrification rate, while the BZ rate did not change at all under dry conditions. However, within the dry samples no significant differences were observed in the denitrification rate between the land use zones.

Similarly, the potential for N_2O production was not significantly different between wet and dry conditions (Table 6.4.6 and Figure 6.4.6 B). Moreover, only the PM samples under wet conditions had significantly higher N_2O production rate, while in the dry sampling there were no significant differences between land use zones. Regarding the ratio of N_2O/N_2 as denitrification products, there was no significant difference between wet and dry condition samples (Figure 6.4.7).

DNRA was 60 % higher in the wet samples compared to the dry samples (Table 6.4.6 and Figure 6.4.6 C), while only under dry conditions the FM samples displayed a significantly higher rate and there was no difference between land use zones under wet conditions. As for the ratio of D/DNRA, although it was 27 % higher in the dry samples compared to the wet, the difference was not statistically significant (Figure 6.4.8).

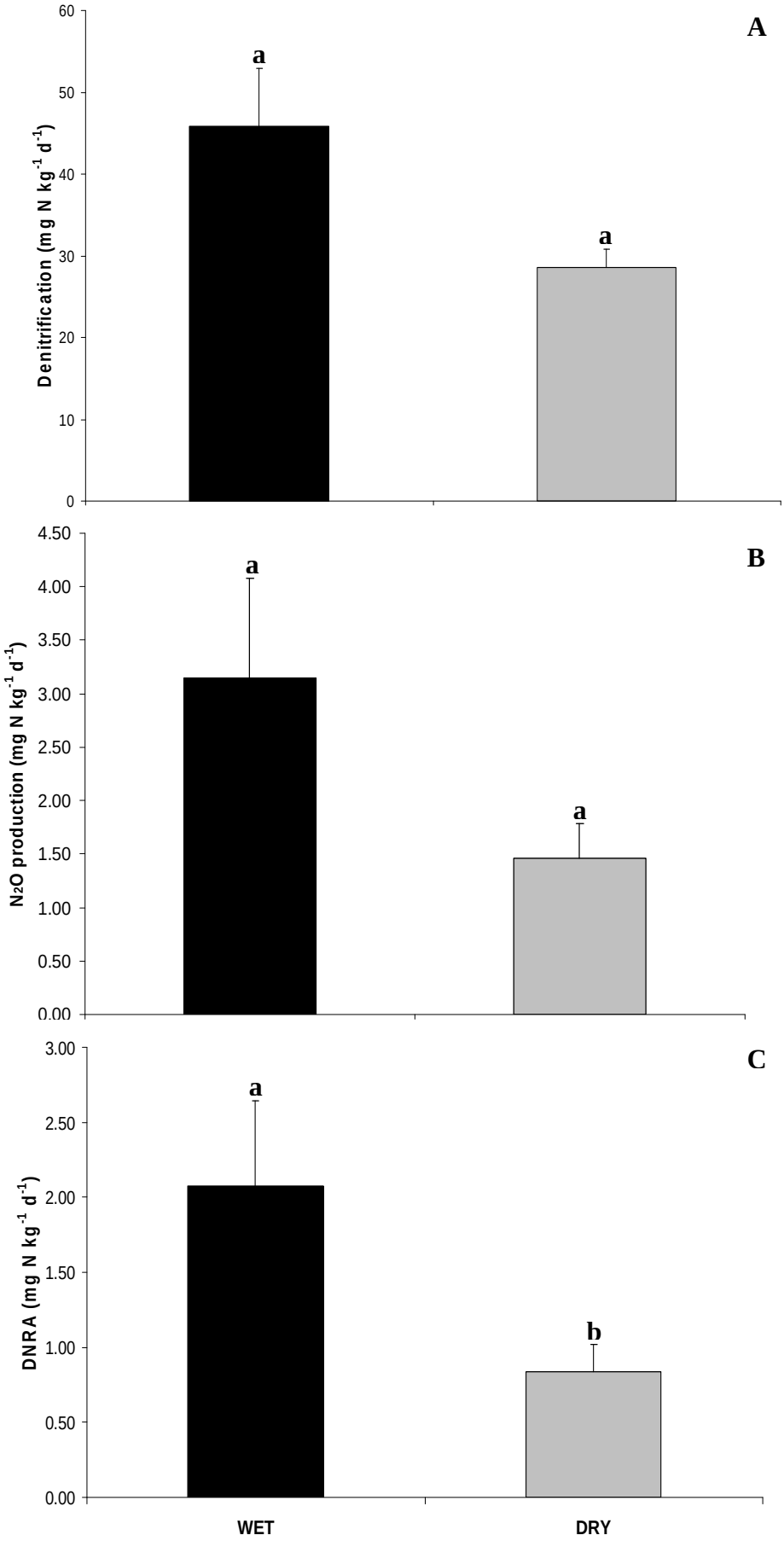

Figure 6.4.6: Denitrification, N_2O production and DNRA potential rates in the topsoil across the four land use zones on the wet and dry sampling. Data are means + 1SE. Different lower case letters indicate significant differences

Table 6.4.6: Denitrification, N_2O production and DNRA potential rates across the four land use zones on the wet and dry conditions sampling. Data are means ± 1 SE. Significant differences between land use zones indicated by different lower case letters.

	Denitrification (mg N kg^{-1} soil d^{-1})		**Nitrous oxide (mg N kg^{-1} soil d^{-1})**		**DNRA (mg N kg^{-1} soil d^{-1})**	
	Mean	**± 1 SE**	**Mean**	**± 1 SE**	**Mean**	**± 1 SE**
WET conditions (n=30)	45.8	7.1	3.2	0.9	2.1	0.6
Pasture Meadow (n=6)	55.8^{a}	9.0	8.9^{a}	2.4	1.4^{a}	0.7
Fritillary Meadow (n=6)	69.1^{a}	17.4	0.7^{b}	0.3	3.0^{a}	1.4
Buffer Zone (n=10)	23.8^{b}	6.6	2.9^{b}	1.8	0.9^{a}	0.4
Grazing Grassland (n=8)	55.6^{ab}	20.3	1.0^{b}	0.4	3.3^{a}	1.7
DRY conditions (n=30)	28.5	2.3	1.5	0.3	0.8	0.2
Pasture Meadow (n=6)	34.0^{a}	4.4	2.6^{a}	0.7	0.4^{a}	0.1
Fritillary Meadow (n=6)	43.1^{a}	8.9	1.9^{a}	1.2	1.6^{b}	0.5
Buffer Zone (n=10)	23.9^{a}	1.9	0.9^{a}	0.4	0.5^{a}	0.2
Grazing Grassland (n=8)	22.9^{a}	3.3	1.0^{a}	0.2	1.0^{ab}	0.5

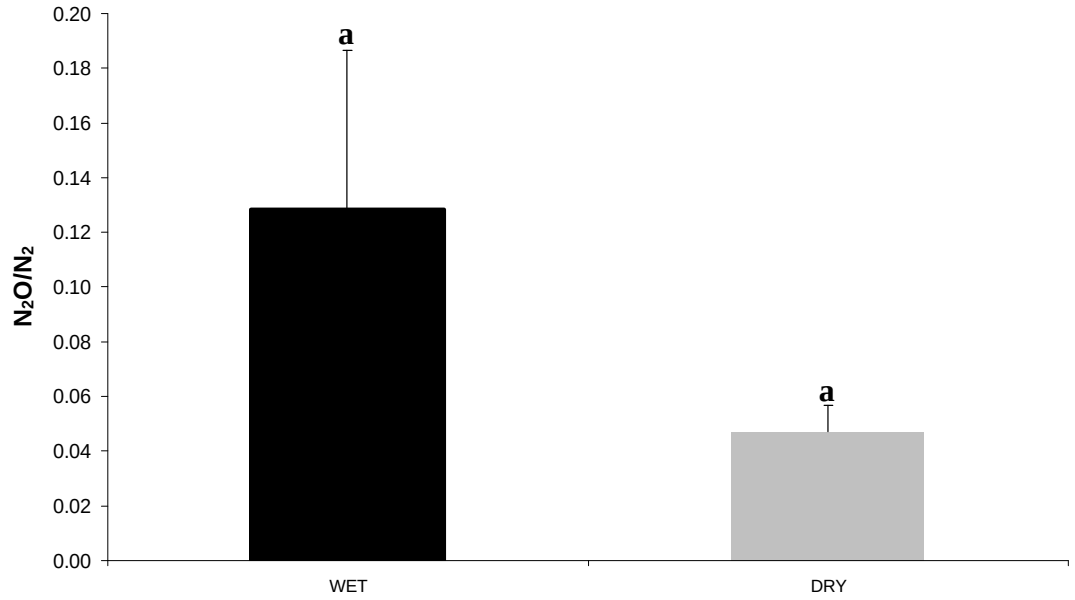

Figure 6.4.7: The ratio N_2O/N_2 in the topsoil across the four land use zones on the wet and dry sampling. Data are means + 1SE. Same lower case letters indicate no significant differences.

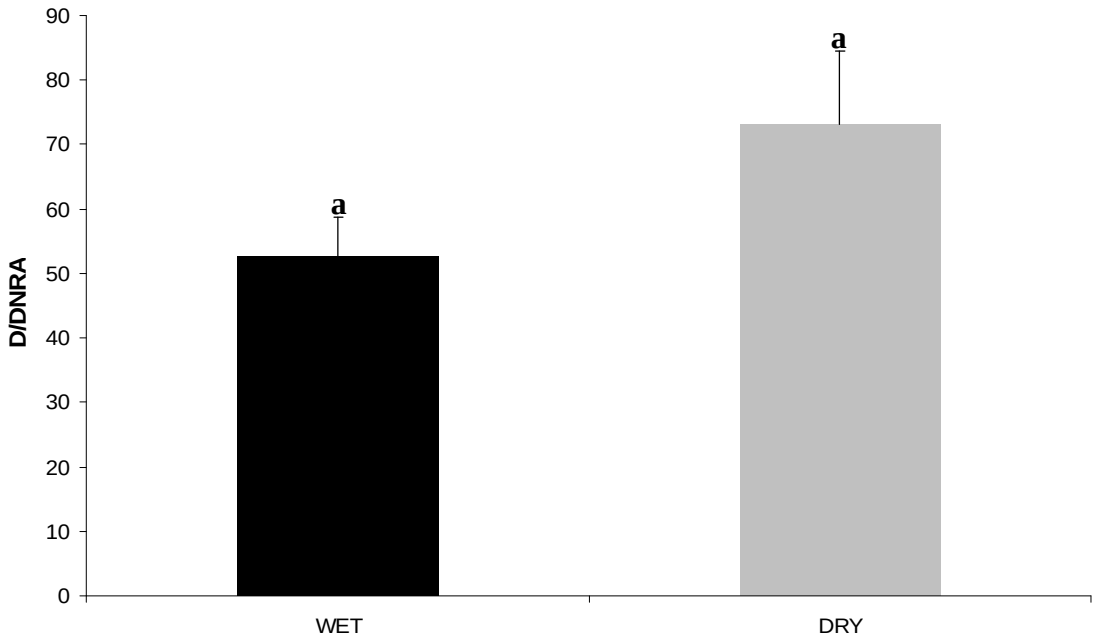

Figure 6.4.8: The ratio D/DNRA in the topsoil across the four land use zones on the wet and dry sampling. Data are means + 1SE. Same lower case letters indicate no significant differences.

Correlation analysis between the potential denitrification and DNRA rates, the AnMOC, the methane production potential, the lability of organic carbon and the soil physical properties of the samples from the wet and the dry condition samplings combined has indicated a number of significant relationships (Table 6.4.7). The denitrification and DNRA potential correlated with each other, indicating the coexistence of the two nitrate attenuation processes under both prolonged wet and dry conditions. Moreover, the potential denitrification rate showed significant positive correlation with the AnMOC, the lability of organic carbon, the water content and the WFPS. To a lesser degree denitrification correlated significantly with the organic matter content and the soil nitrate content. The DNRA potential rate showed significant positive correlation with the lability of organic carbon, the water content, the organic carbon and the organic matter content and the methane production potential.

Multiple Regression Analysis (MRA) highlighted the importance of the anaerobic mineralisation rate of the organic carbon and the WFPS as the main controlling factors regulating the potential for denitrification after prolonged wetting and drying of the

topsoil in the reconnected floodplain of the River Cole. The AnMOC and the WFPS combined explained 51 % of the variance between the denitrification potential rates (MRA; r^2=0.51, *df*=53, *P*<0.01). Moreover, the soil water content explained 33 % of the variance between denitrification rates (MRA; r^2=0.33, *df*=54, *P*<0.01), followed by the lability of organic carbon with 23 % explanatory power (MRA; r^2=0.23, *df*=54, *P*<0.01). The organic matter content explained 13 % of the variance, while the soil nitrate content only 7 % (MRA; r^2=0.13, *df*=54, *P*<0.01 and r^2=0.07, *df*=54, *P*<0.05 respectively).

MRA between the DNRA potential rate and those environmental variables that were significant in the correlation analysis resulted in relatively low percentages of variance explanation by the environmental variables. However, there was complete agreement with the correlation results in that the lability and availability of organic carbon together with the soil moisture content were the most important factors regulating DNRA rates between prolonged wetting and drying in the topsoil of the reconnected floodplain of the River Cole. The highest explanatory power was observed for the lability of organic carbon (MRA; r^2=0.31, *df*=59, *P*<0.01) with 31 %, and was followed by the water content (MRA; r^2=0.16, *df*=59, *P*<0.01) with 16 %, the organic carbon content (MRA; r^2=0.12, *df*=59, *P*<0.01) with 12 % and the organic matter content with (MRA; r^2=0.11, *df*=59, *P*<0.01) with 11 %.

Table 6.4.7: Correlation matrix between the denitrification and DNRA potential rate, the AnMOC, the lability of organic carbon, the methane production potential and the soil physical properties in the wet and dry conditions sampling. Underlined correlation coefficients are products of Spearman rho correlation whereas non-underlined are products of Pearson Product-Moment correlation. ** Correlation is significant at the 0.01level and *Correlation is significant at the 0.05 level.

Variables/Correlation coefficients		Denitrification potential	DNRA	AnMOC	Org. carbon lability	Methane emission	Organic matter content	Organic carbon	TOC/TN	TOC/NO_3^-	Water content	Soil nitrate	WFPS
Denitrification potential	*R or rho*	1											
	P	.											
	N	55											
DNRA	*R or rho*	**0.623****	1										
	P	0.000	.										
	N	55	60										
AnMOC	*R or rho*	**0.679****	0.245	1									
	P	0.000	0.063	.									
	N	55	58	58									
Org. carbon lability	*R or rho*	**0.607****	**0.554****	**0.799****	1								
	P	0.000	0.000	0.000	.								
	N	55	60	58	60								
Methane emission	*R or rho*	0.210	**0.268***	**0.312***	0.229	1							
	P	0.123	0.039	0.017	0.078	.							
	N	55	60	58	60	60							
Organic matter content	*R or rho*	**0.432****	**0.404****	**0.798****	**0.492****	0.102	1						
	P	0.001	0.001	0.000	0.000	0.436	.						
	N	55	60	58	60	60	60						
Organic carbon	*R or rho*	0.223	**0.425****	**0.494****	0.024	**0.275***	**0.671****	1					
	P	0.102	0.001	0.000	0.855	0.033	0.000	.					
	N	55	60	58	60	60	60	60					
TOC/TN	*R or rho*	0.075	0.174	**-0.291***	**-0.407****	0.009	**-0.272***	0.219	1				
	P	0.587	0.184	0.027	0.001	0.944	0.036	0.093	.				
	N	55	60	58	60	60	60	60	60				
TOC/NO_3^-	*R or rho*	-0.079	0.104	-0.051	-0.146	**0.265***	-0.022	0.123	**0.278***	1			
	P	0.570	0.442	0.705	0.277	0.046	0.87	0.362	0.036	.			
	N	54	57	57	57	57	57	57	57	57			
Water content	*R or rho*	**0.576****	**0.528****	**0.752****	**0.541****	0.016	**0.869****	**0.581****	-0.090	-0.256	1		
	P	0.000	0.000	0.000	0.000	0.906	0.000	0.000	0.493	0.055	.		
	N	55	60	58	60	60	60	60	60	57	60		
Soil nitrate	*R or rho*	**0.271***	0.202	**0.485****	0.039	-0.169	**0.445****	**0.446****	-0.044	**-0.884****	**0.593****	1	
	P	0.047	0.133	0.000	0.772	0.208	0.001	0.001	0.747	0.000	0.000	.	
	N	54	57	57	57	57	57	57	57	57	57	57	
WFPS	*R or rho*	**0.512****	0.228	0.213	**0.297***	-0.198	0.057	0.017	**0.275***	**-0.355****	**0.367****	**0.328***	1
	P	0.000	0.080	0.109	0.021	0.129	0.664	0.897	0.034	0.007	0.004	0.013	.
	N	55	60	58	60	60	60	60	60	57	60	57	60

6.5 *Discussion*

6.5.1 *The effect of different land use types on nitrate attenuation in the topsoil*

6.5.1.1 *Soil properties*

The land use zones within the restored River Cole floodplain displayed some significant differences in their topsoil properties resulting in the identification of three main land use types; the floodplain meadow, the buffer zone and the grazing grassland. With respect to the soil texture, all four land use zones had high combined silt and clay fraction (range 68 - 88 %). Silt and clay contents above 65 % have been associated with increased denitrification activity in floodplain soils (Groffman and Tiedje, 1989; Pinay *et al.,* 1995; Pinay *et al.,* 2000) due to the higher water filled porosity of fine textured soils compared to coarser ones for a given water content (Granli and Bockman, 1994) that leads to slower oxygen diffusion and faster development of anaerobic conditions (Parkin and Tiedje, 1984). Additionally, fine textured soils contain more labile C and N than coarser textured soils and often show a much greater flush of N mineralisation in response to rewetting (Sala *et al.,* 1988). Moreover, lower bulk densities were associated with the downstream floodplain meadows (FM and PM), while the BZ and GG had higher soil bulk density, probably as a result of soil compaction by grazing activity in the GG and horse riding in the BZ (McNaughton, 1984).

The soil nitrate content was also higher in the BZ and GG zones compared to the PM. Generally the soil nitrate in the land use zones of the River Cole floodplain was above the ranges reported for different agricultural land use types in the lower Mississippi valley (Ullah *et al.,* 2005; Ullah and Faulkner, 2006), in riparian wetlands in Brittany (Clément *et al.,* 2002), in a restored floodplain in Wisconsin (Orr *et al.,* 2007) and in riparian forest soils receiving prolonged nitrogen runoff in New Jersey (Ullah and Zinati, 2006), while they were comparable to chronically nitrate loaded forested riparian zones in the Netherlands (Hefting *et al.,* 2006b). Therefore it could be argued that nitrate supply is probably not limiting for nitrate attenuation processes to occur in the re-connected floodplain of the River Cole. The higher nitrate and ammonia contents observed in the GG and BZ sites could be attributed to the grazing activity in the former and to the fertilisation of the arable land in the latter. In grazing pastures, the deposition

of urine and faeces, apart from increasing the productivity of the grasses, also creates 'hot spots' of high nitrogen cycling rates (McNaughton, 1984).

The availability of organic carbon (OC) was not different among the land use zones and ranged between 2 and 12 %, which is within the range of the OC reported in other topsoil (0-10 cm) studies of similar texture (Ullah and Zinati, 2006; Sheibley *et al.*, 2006; Orr *et al.*, 2007). As a result of similar OC contents and differences in the soil nitrogen, the ratio of C/N was significantly lower in the BZ and GG areas compared to the meadows PM and FM, while the range from 3 to 16 was comparable to C/N ratios of other temperate riparian agricultural soils (Pinay *et al.*, 1995; Ullah *et al.*, 2005; Ullah and Zinati, 2006).

Several studies have measured the mineralisation rate of organic carbon under aerobic conditions (Groffman *et al.*, 1992; Hart *et al.*, 1994a; Dick *et al.*, 2000; Groffman and Crawford, 2003; Sheibley *et al.*, 2006) as a measure of microbial biomass respiration rate or under anaerobic conditions (Bijay-Singh *et al.*, 1988; Drury *et al.*, 1998; Simek *et al.*, 2000; Hill and Cardaci, 2004; Ullah and Faulkner, 2006; Dodla *et al.*, 2008) as the fraction of labile organic carbon available to the denitrifier population (Gale *et al.*, 1992). In the present study we used the anaerobically mineralisable organic carbon (AnMOC) as a measure of the relative availability of organic carbon and electron acceptors for anaerobic respiration and fermentation. We also calculated the ratio of AnMOC per gram of total organic carbon in the soil as an additional expression of the labile organic carbon fraction according to Dauwe *et al.* (2001). However, it has been shown that the mineralisation of organic carbon can be faster and more extensive when nitrate is supplied (Abell *et al.*, 2009), possibly due to enhanced flow of fermentation by-products to denitrifiers and/or increased accessibility of denitrifiers to labile organic carbon fractions. This implies that the AnMOC measurement method may have lead to an underestimation of the absolute mineralisation rate of organic carbon via nitrate reduction, although our AnMOC rates were comparable to some NO_3^--amended rates of similar organic carbon content soils, temperature conditions and duration of incubation (Hill and Cardaci, 2004; Gurwick *et al.*, 2008). Even though the absolute AnMOC rates may have been underestimated, AnMOC still has an interpretation value as a relative controlling factor of nitrate reduction processes, between different land use zones and hydrological regimes across the River Cole floodplain.

Both the AnMOC and the labile organic carbon (LOC) were higher in the GG area, while the other three land use zones were not different between each other, despite the significant differences in soil nitrate content (Fig. 6.1.4). This is a further indication that the AnMOC measurement may have not been biased by the ambient soil nitrate content during the incubation. The higher AnMOC rate in GG could be attributed to the effect of grazing and the subsequent application of animal manure that either contains more labile OC (Frank and Groffman, 1998a) and/or increases nutrient cycling and organic carbon mineralisation in the soil (McNaughton, 1984).

We used Principal Component Analysis (PCA) and Discriminant Factor Analysis (DFA) in order to identify the linear combination of environmental variables that explains the highest proportion of variance between individual samples (PCA) and between samples grouped in land use zones (DFA). In PCA, the samples were grouped into three distinct land use types, namely the grazing grassland, the buffer zone and the floodplain meadows along the second component axis formed by the AnMOC and LOC variables. The PCA also confirmed the overlap of samples from all the land use zones with respect to their organic matter and carbon content. Finally, the silt and clay fractions across the land use zones explained 20 % of the variance between samples. The grouping of samples in the PCA was also confirmed by the DFA. Therefore it could be argued that all the land use types in the re-connected floodplain receive adequate nitrate originating from a number of sources such as grazing activity (GG), leaching from arable land (BZ) and river overbank flooding (all land use zones), while there seems to be adequate organic carbon supply across all land use types. However, the differentiating factor between the land use types is the fraction of labile organic carbon in the soil that would be available for microbial nitrate respiration processes and seems to be increased by the grazing activity in the GG (Frank and Groffman, 1998a) and by the combination of horse riding (Frank and Groffman, 1998a) and frequent flooding in the BZ (Bastviken *et al.*, 2007), despite the fact that the lability of organic carbon is reduced by cultivation in the arable field (Ullah and Faulkner, 2006). Finally the two floodplain meadows (PM and FM) seem to have very similar conditions in terms of labile organic carbon and organic matter in general.

6.5.1.2 *Denitrification Potential*

The topsoil across all the land use zones showed significant potential for denitrification that ranged between 5 and 63 mg N kg^{-1} dry soil d^{-1} (mean 16.3 ± SE 2.8 mg N $kg^{-1}d^{-1}$). Comparing our potential denitrification rates to other studies in floodplain and riparian zone soils is not straight forward as in most cases the Denitrification Enzyme Activity (DEA) (Smith and Tiedje, 1979) has been used with various incubation durations and temperatures. In DEA, nitrate and organic carbon are added at non limiting concentrations and for short incubation times (Phase I; 1-3 hours) the rate reflects the cellular denitrifying enzyme activity present in the sample at the time of sampling. While DEA does not reflect *in situ* denitrification rates (Groffman *et al.*, 1992), it is well suited for comparisons between sites and treatments (Groffman *et al.*, 2006). Since indigenous carbon for short-incubation times is usually non-limiting (Tiedje *et al.*, 1982), our results could be compared with DEA studies of short duration (between 1 and 3 hours) and incubation temperatures around 20^{o}C.

Ullah and Faulkner (2006) followed a similar approach to ours in measuring denitrification potential (DP) with no added organic carbon, incubating at 22^{o}C for 6 hours, and the summer range of DP across different agricultural land use types in Mississippi was between 2.4 and 36 mg N $kg^{-1}d^{-1}$, which is close to our mean rate. A similar DP method was employed in forested and agricultural soils in the lower Mississippi Valley that displayed average potential denitrification 34 mg N $kg^{-1}d^{-1}$ and 15 mg N $kg^{-1}d^{-1}$ respectively (Ullah *et al.*, 2005) that are also within the range reported in our study. In several agricultural soils with varying degrees of fertilisation in the Czech Republic, Simek *et al.* (2000) measured DEA in the top 15 cm of the soil that ranged between 1.3 and 16 mg N $kg^{-1}d^{-1}$, being in agreement with our mean rate. Similarly, the DEA rate of the topsoil in a semi-arid riparian zone was 16.3 mg N $kg^{-1}d^{-1}$ (Harms and Grimm, 2008). Finally our potential denitrification rates compare well with the DEA rates of hydromorphic soils in Switzerland (2 - 30 mg N $kg^{-1}d^{-1}$) (Cosandey *et al.*, 2003a) and the denitrification capacity (no added carbon) of hydric soils in Germany (0.13 - 27 mg N $kg^{-1}d^{-1}$) (Well *et al.*, 2005).

The denitrification potential was significantly different between the land use zones, with the lowest rate observed in the FM area, the highest in the GG, while the BZ and the PM were not significantly different between each other. With respect to the controlling

factors of denitrification across the land use zones, both the correlation and multiple regression analysis indicated that the AnMOC (r^2=0.42) was the main predictor of denitrification, followed by the LOC (r^2=0.29) and finally the soil nitrate (r^2=0.26). Although the coefficients of determination are not very high, they indicate that the same environmental factor that discriminated the three land use types of the re-connected floodplain (i.e. the availability of labile organic carbon) is also responsible for their different potential denitrification activity. It should be noted that all the different measurements of organic carbon correlated positively with the denitrification potential, but the highest correlation coefficient was observed for the AnMOC, which represents a combined mearure of organic carbon and electron acceptor availability. This has also been found in previous studies (Bijay-Singh *et al.,* 1988; Drury *et al.,* 1998; Hill and Cardaci, 2004) that suggested the AnMOC as the most appropriate expression of the labile fraction of organic carbon available for nitrate respiration.

The fact that the soil nitrate content explained only 26 % of the variance in denitrification may be due to an overestimation of the role of AnMOC as an explanatory variable, as AnMOC represents both the organic carbon and electron acceptor availability for denitrification. The significant dependence of denitrification potential rates on organic carbon availability could have also been affected by the experimental procedure followed (i.e. the 24 hours pre-incubation of the slurries for the removal of the background $^{14}NO_3^-$), that could have decreased the availability of easily degradable organic carbon to denitrifiers. In 40 % of the samples, the amount of CO_2 produced during nitrate reduction (according to the molar stoichiometry 1 NO_3^- : 1.25 CO_2) had been reached in 24 hours anaerobic incubation, however, the slope of CO_2 production did not change after the first 24 hours, and the CO_2 production continued linearly until the end of the incubation (20 days). This suggests that the total soil organic carbon content was not in fact limiting. Upon amendment of the pre-incubated soil slurries with $^{15}NO_3^-$, denitrifiers were probably able to also utilise fermentation by-products as easily degradable electron donors, as suggested by Abell *et al.,* (2009), and hence the N_2 production during the assay (maximum 6 hours incubation) remained linear with no indication of carbon limitation during the experiment.

Numerous studies have shown a positive relationship between denitrification and the availability of organic carbon (Ambus and Lowrance, 1991; Hedin *et al.,* 1998; Hill *et*

al., 2000; Ostrom *et al.,* 2002; Brettar and Höfle, 2002; Vidon and Hill, 2004b; Hefting *et al.,* 2006b). The available labile organic carbon, apart from fuelling heterotrophic denitrification as an electron donor (Knowles, 1982), also has an indirect effect on denitrification, enhancing oxygen consumption by aerobic bacteria which leads to anaerobiosis (Tiedje, 1988). In wetlands and riparian zones receiving high NO_3^- concentration with floodwater, organic carbon might be a controlling factor for denitrification (Davidsson and Leonardson, 1996). This could be true in the case of the River Cole re-connected floodplain that has been shown to be receiving frequent overbank flooding with nitrate-rich water throughout the year, while fertiliser inputs from the surrounding arable land and the additional organic-N inputs from grazing ungulates also contribute to the N-loading of the soil.

The increased denitrification activity observed in the grazing grassland could be attributed to the presence of grazing ungulates. Higher denitrification potential in areas affected by grazing cattle has been reported in numerous studies (Frank and Groffman, 1998b; Meneer *et al.,* 2005; Patra *et al.,* 2005; Philippot *et al.,* 2009). The stimulation of denitrification by grazing associated with animal activities has been attributed to changes in hydraulic soil properties through soil compaction and in nutrient availability through the deposition of urine and faeces and limited plant N uptake after defoliation (Luo *et al.,* 1999; Meneer *et al.,* 2005). Moreover, grazing has been shown to increase the availability of labile organic carbon and decrease the ratio of C/N, both contributing to enhanced denitrification rates (Frank and Groffman, 1998a). However, the spatial distribution of soil properties due to grazing can significantly control the distribution of potential denitrification and the occurrence of biogeochemical 'hotspots' (McClain *et al.,* 2003) but does not affect the size of the denitrifier community (Philippot *et al.,* 2009).

The maintenance of natural riparian vegetation in the BZ could be partly responsible for nitrate removal via plant uptake, but also for the supply of organic matter to denitrifiers through plant litter (Hefting *et al.,* 2005). It has been shown that litter from submersed plants is more readily available to denitrifiers in wetland sediments throughout the year (Bastviken *et al.,* 2007). The fact that the BZ is more frequently flooded than any other area of the re-connected floodplain means that wetland-like waterlogged conditions develop more often and for longer and therefore could lead to the supply of LOC from

decomposing plants to the soil microbial population. However, one third of the samples of the BZ originate from the arable field, where LOC was lower due to cultivation which decreases the availability of LOC (Ullah and Faulkner, 2006). Therefore the significantly lower LOC of the BZ compared to the GG is probably the reason for the lower denitrification potential.

The PM displayed lower denitrification potential than the GG, but was not different from the BZ. Although there is no supply of LOC from grazing in the PM, it has been shown that overbank flooding from the river and the surrounding ditch is significant especially during the winter and spring, but also during summer storm events that inundate a large portion of the PM surface. Flooding in the PM, apart from enhancing the decomposition of riparian plants (Bastviken *et al.*, 2007), acts as a conduit for the transport of C and N from the surrounding hillslope that includes arable fields and horse paddocks. The amendment of restored riparian wetlands with organic matter from plant composts and animal manure was shown to stimulate microbial communities and especially denitrifiers (Sutton-Grier *et al.*, 2009). Additionally, the PM is mowed at least once every summer for hay. Mowing has been shown to increase species richness in managed grasslands by increasing the competition between plants and although root mass is reduced, the availability of C and N as well as the microbial activity is not negatively affected (Patra *et al.*, 2006; Ilmarinen *et al.*, 2009). Moreover, increased release of easily extractable carbon via rhizo-deposition processes due to mowing has been reported in mown pastures of the Mediterranean (Gavrichkova *et al.*, 2008). The availability of easily extractable carbon and the accelerated N cycling due to the short life-cycle of plants in mown grassland has been positively related to enhanced denitrification (Robson *et al.*, 2007). Therefore the combination of flooding and mowing is responsible for supplying the PM with the electron donors and nitrate so as to sustain an increased denitrification capacity. Finally, the FM zone is also subjected to the same mowing regime as the PM, but flooding is less extensive and frequent and it is mostly concentrated in the near-stream zone. However, the FM did not have significantly lower LOC, and therefore the lower denitrification potential could be possibly explained by lower nitrate supply due to restricted flooding and disconnection from the surrounding agricultural land.

Our results suggest that the re-connection of the floodplain of the River Cole, although aiming at flood attenuation and habitat creation targets (Environmental Report River Cole Restoration, 1995), also resulted in a significant potential for denitrification activity of the topsoil. This potential was evident and significant across the different land use types of the floodplain and was not restricted to areas directly adjacent to arable land (e.g. BZ) as it has been commonly shown in the literature (Clément *et al.*, 2003; Hefting *et al.*, 2003; Ullah and Zinati, 2006). This highlights the importance of the enhanced overbank flooding, following the restoration of River Cole, in supplying nitrate-rich river water on the floodplain surface and creating the necessary anaerobic conditions for the occurrence of denitrification, as it has also been shown in other cases of restored river-floodplain connectivity (Forshay and Stanley, 2005; Sheibley *et al.*, 2006; Orr *et al.*, 2007). The spatial heterogeneity in denitrification potential observed between land use types is a function of management practices that affect the availability of organic carbon (e.g. grazing and/or mowing) rather than landscape position, which has been more important in areas of more complex topographic relief than the River Cole catchment (Ullah and Faulkner, 2006; Wang *et al.*, 2009; Harms *et al.*, 2009). Therefore, the increased overbank flooding combined with the traditional grassland land-use management practices of mowing and grazing act together in creating the necessary conditions in this lowland floodplain for increased nitrate removal via denitrification on top of the other hydrological and ecological benefits of river-floodplain connectivity.

6.5.1.3 *Dissimilatory Nitrate Reduction to Ammonium (DNRA) Potential*

All the samples from all the land use zones displayed potential for DNRA that ranged between 0.02 and 2.64 mg N $kg^{-1}d^{-1}$ (mean 0.4 ± SE 0.03 mg N $kg^{-1}d^{-1}$). DNRA was on average 40 times lower than denitrification, while it accounted for 2 % of the removed nitrate during the incubation experiment, compared to 64 % removal attributed to N_2 production from heterotrophic denitrification. Although the conditions promoting DNRA and heterotrophic denitrification are similar (i.e. anoxia, available nitrate and organic substrates), DNRA is thought to be favoured in nitrate-limited environments rich in labile carbon, while denitrification would be favoured under carbon-limited conditions (Kelso *et al.*, 1997; Silver *et al.*, 2001). The reason for this is that DNRA transfers eight electrons per mole of nitrate reduced, whereas denitrification only

transfers five, and therefore DNRA is energetically more favourable in nitrate limited conditions (Tiedje *et al.,* 1982; Tiedje, 1988). Moreover, DNRA is mostly performed by obligate anaerobic fermentative bacteria, whereas denitrifiers are mostly facultative anaerobes present in the soil even under oxic conditions (Tiedje, 1988). Therefore it is not surprising that the topsoil in the reconnected floodplain of the River Cole which, as it was shown in the present study, was not controlled by nitrate availability but rather by the availability of labile organic carbon due to the different land management practices, has displayed a significantly lower DNRA potential compared to denitrification.

DNRA has been under-researched in freshwater environments (Revsbech *et al.,* 2005; Burgin and Hamilton, 2007) and especially in temperate lowland agricultural floodplains, where its role has been assumed to be minor due to the wetting-drying cycles that prevent anoxic conditions from becoming established for long periods of time (Robertson *et al.,* 1999) and the supply of nitrate from agricultural runoff and flooding (Forshay and Stanley, 2005). However, in a recent study of an herbaceous riparian zone in Oregon (Davis *et al.,* 2008), with similar soil texture and climatic conditions as ours and using anaerobic laboratory incubations, DNRA has been reported to occur in the top 15 cm of the soil ranging between 0.2 and 1.3 mg N $kg^{-1}d^{-1}$, which is within our range of values. Moreover, DNRA accounted for 3 % of *in situ* nitrate removal in the riparian zone of an ephemeral stream in Australia (Woodward *et al.,* 2009), where also denitrification was low, accounting for 3 % of nitrate removal, due to high dissolved oxygen in groundwater. Higher percentages of DNRA (between 5 and 15 % of nitrate removal), in soil slurries, were found in a riparian fen in Denmark (Ambus *et al.,* 1992), in two Chinese and Australian paddy soils (Yin *et al.,* 2002), in a riparian wetland in UK (Matheson *et al.,* 2003) and in a flow-through experiment of intact cores from a created freshwater wetland in Texas (Scott *et al.,* 2008). However, in all cases denitrification was responsible for most of nitrate removal, while DNRA was enhanced compared to our study due to lower redox under wetland conditions and higher organic matter in some of the studies.

The mean DNRA rate across the different land use zones of the River Cole floodplain (0.4 ± SE 0.03 mg N $kg^{-1}d^{-1}$) was very close to the mean DNRA rates reported in the surface soil of tropical N-limited forests investigated in soil core incubations under *in situ* conditions using the ^{15}N isotope pool dilution method (Davidson *et al.,* 1991); 0.23

mg N $kg^{-1}d^{-1}$ (Silver *et al.,* 2005); 0.45 mg N $kg^{-1}d^{-1}$ (Huygens *et al.*, 2007); 0.36 mg N $kg^{-1}d^{-1}$ (Rütting *et al.,* 2008); 0.5 mg N $kg^{-1}d^{-1}$ (Templer *et al.*, 2008). However, when our DNRA rate is compared to a laboratory assay of DNRA from a tropical forest soil (0.5 - 9 mg N $kg^{-1}d^{-1}$; Silver *et al.,* 2001) it falls within the lower range of their measurement, suggesting that the potential for DNRA of our temperate agricultural soil is lower than in a tropical N-limited forest soil. The denitrification rate in all the above tropical forest studies was significantly lower than DNRA, which highlights DNRA's role as a N-conserving mechanism in those nitrogen limited ecosystems. However, it is likely that *in situ* denitrification rates were underestimated by the isotope pool dilution technique (Templer *et al.,* 2008; Rütting *et al.,* 2008).

DNRA was not significantly affected by the land use management practices in the re-connected floodplain of the River Cole. Slightly higher DNRA was observed in the GG, followed by the FM, which showed high spatial variability, while the PM and the BZ had very similar DNRA rates, as it was also observed for the denitrification potential. The multiple regression analysis indicated that 54 % of the variance in DNRA can be explained by combining three environmental variables: the methane production potential, the availability of labile organic carbon and the availability of nitrate. Moreover, DNRA and denitrification correlated positively, which is not surprising as both processes are regulated by the same environmental conditions and reactants (Tiedje, 1988).

The production of methane occurs at the lowest redox potential in anaerobic soils (below -400 mV; Oremland, 1988) and is therefore an indicator of highly reduced conditions (Hedin *et al.,* 1998). Although DNRA bacteria can operate at the same redox range (+ 250 to + 10 mV; Mitsch and Gosselink, 2000) as denitrifiers (Myrold, 2005), they have been found to be competitively more effective, in anaerobic sediments, at redox potentials as low as -200 mV (Buresh and Patrick, 1981). Therefore, the correlation of the DNRA potential rate with the methane production potential indicates that DNRA is likely to be primarily controlled by redox fluctuations, which are in turn controlled by the hydrological/ flooding regime, in the intermittently saturated re-connected floodplain. The low but spatially variable redox conditions found in the FM (Fig. 6.1.6 C) are probably responsible for the relatively high DNRA potential in this zone. Other studies, where DNRA was a less important process compared to

denitrification, also found an increase in DNRA with low redox conditions. For example, in Ambus *et al.* (1992) pre-incubation of the soil under anaerobic conditions increased DNRA by 9 %, while DNRA in a created freshwater wetland correlated to the sediment oxygen demand (Scott *et al.,* 2008) and the clay soil with WFPS >70 % in a lowland Brazilian forest also showed higher DNRA (Sotta *et al.,* 2008). In contrast, in studies where DNRA played an important role as an N-conserving mechanism, DNRA bacteria seemed to be adapted to fluctuating redox regimes and be able to withstand unfavourable redox periods of higher O_2 concentration (Pett-Ridge and Firestone, 2005; Silver *et al.,* 2005; Pett-Ridge *et al.,* 2006). It could therefore be assumed that in the N-rich agricultural soil of the River Cole floodplain, where denitrifiers are dominant, DNRA is concentrated in more reduced environmental patches where they might have a competitive advantage against denitrifiers, while in the N-limited environments, where competition from denitrifiers is less intense, they have developed more flexible enzymatic pathways able to tolerate limited O_2 exposure in order to exploit the limited resources. A comparative study of DNRA bacterial strains from these two contrasting environments could be employed to test the above assumption.

Positive correlation between DNRA and the organic carbon has been shown in previous studies (Fazzolari *et al.,* 1998; Davidsson and Ståhl, 2000; Yin *et al.,* 2002; Sotta *et al.,* 2008; Wan *et al.,* 2009). It has been suggested that a fermentative source of carbon may be a more important controlling factor in the partitioning of nitrate between DNRA and denitrification compared to complete anaerobicity (Fazzolari *et al.,* 1998). It is possible that the increased availability of LOC in the GG due to grazing activity also stimulates DNRA by providing the substrate for fermentative respiration, although this cannot be proved in the present study as a qualitative analysis of organic carbon was not performed. Tiedje (1982) suggested that DNRA would be favoured where the ratio of C/NO_3^- is high. We have not found a significant relationship between DNRA or denitrification with the ratio of TOC/NO_3^-, while only denitrification showed a weak negative correlation with the ratio of TOC/TN (Table 6.1.7). Other studies where redox potential was an important regulating factor of DNRA have also indicated no relationship between DNRA and the ratio C/NO_3^- (Matheson *et al.,* 2002; Sotta *et al.,* 2008). Moreover, those studies where C/NO_3^- was a significant predictor of DNRA had significantly higher values of C/NO_3^- compared to our ratio of TOC/NO_3^- (Schipper *et al.,* 1994; Bengtsson and Bergwall, 2000; Silver *et al.,* 2005; Wan *et al.,* 2009) and

NO_3^- availability was limiting. Finally, the positive relationship between DNRA and soil nitrate, is probably of limited significance as nitrate supply was frequent across the floodplain and this positive correlation is likely to be skewed by the spatial co-occurrence of LOC and high nitrate due to manure application in the GG and the BZ. A positive relationship between DNRA and soil nitrate would be meaningful only where nitrate is truly limiting for both DNRA and denitrification reduction processes (Silver *et al.,* 2001).

In conclusion, our results document for the first time the occurrence of DNRA as an alternative nitrate reduction pathway in the soil of a temperate former agricultural re-connected floodplain. The reduction of nitrate via DNRA is of lower importance compared to denitrification, which has a beneficial effect on the management of diffuse-nitrate pollution in these lowland catchments. The flood pulsing creates redox fluctuating conditions across the floodplain, which in turn maintain viable DNRA bacterial populations fuelled also by the availability of labile organic carbon from the grazing and mowing management practices. However, the frequent supply of nitrate gives a competitive advantage to denitrifiers while it also increases the redox potential and lowers the ratio of C/NO_3^- in the soil (Yin *et al.,* 2002), both unfavoring DNRA. Therefore, the majority of nitrate is transformed to nitrogen gases (N_2 and possibly N_2O) and is removed rather than conserved in the system as NH_4^+ which can easily re-enter the soil cycle via plant uptake.

6.5.2 *Spatial distribution of nitrate attenuation across the hydrogeomorphic units within each land use zone*

Apart from land use management practices (Ullah and Faulkner, 2006), spatial variability of nitrate attenuation has been also attributed to differences in the hydrogeomorphic template of riparian zones (Harms and Grimm, 2008) and floodplains (Harms *et al.,* 2009). The hydrogeomorphic template consists of both temporal and spatial variation in hydrology (i.e. the hydrologic regime), and spatial variation conferred by landform (Hauer and Smith, 1998) and topography (Florinsky *et al.,* 2004). The convergence of hydrologic flowpaths carrying the necessary substrates (C and N) or the hydrologic transport of a missing reactant in a pool of substrate have been described as the main hydrological mechanisms for the occurrence of biogeochemical 'hotspots' (McClain *et al.,* 2003). It has been hypothesized that due to the low relief of

the River Cole re-connected floodplain, topography likely plays a minor role in creating areas of increased nitrate attenuation activity, whereas the hydrological regime is the main driver of variability by controlling both the supply of nitrate and the redox potential of the soil.

6.5.2.1 *Fritillary Meadow (FM)*

The overbank flooding from the ditch and the river created distinctly different conditions in the channel depression (influence from ditch) and the riparian zone (influence from river), which interestingly enough displayed similar denitrification rates but significantly different DNRA rates. The high denitrification potential of the channel depression could be explained by a combination of factors such as: high clay content (Pinay *et al.,* 2000), high moisture content (Groffman *et al.,* 1993a; Pinay *et al.,* 2007) and high AnMOC (Pinay *et al.,* 1995; Groffman and Crawford, 2003). The middle transect, receiving less frequent flooding from either the ditch or the river had a significantly lower denitrification potential due to the lower supply of the available substrates and soil moisture. The riparian samples, although they were associated with higher bulk density (i.e. lower water holding capacity), lower total nitrogen and organic carbon content and lower AnMOC, their denitrification potential was not significantly lower from the channel depression samples. At first this seems to be an unexpected result, but it could be explained by the availability of LOC in the riparian zone. Although the riparian samples were lower in both the organic carbon and the AnMOC, the proportion of LOC seems to be higher in the near stream zone (Fig. 6.2.3 B). It has been shown that the quality apart from the quantity of organic carbon can significantly affect denitrification potential in riparian wetland soils (Dodla *et al.,* 2008), where polysaccharides in the surface soil of a freshwater marsh seemed to support higher denitrification than other carbon fractions. Moreover, the natural vegetation cover and the resulting soil litter production in depressional wetlands (Ullah and Faulkner, 2006) supported higher denitrification rates than similar textured agricultural soils. Although we do not have organic carbon composition data to support this assumption, it is likely that a different source of LOC in the riparian area supports increased denitrification activity.

The DNRA potential was significantly higher in the riparian zone compared to the other two transects of the FM. This pattern could be explained by the lower redox potential

suggested by the higher methane production in this zone (Scott *et al.*, 2008; Sotta *et al.*, 2008), the lower nitrate availability (Silver *et al.*, 2001) and the higher ratio of TOC/TN (Bengtsson and Bergwall, 2000; Silver *et al.*, 2005). Surprisingly, DNRA displayed negative relationships with all the organic carbon measurements including the LOC. This finding could suggest that fermentative DNRA might not be the dominant process in the riparian zone of the FM. Chemolithoautotrophic DNRA where NO_3^- is reduced to NH_4^+ with the simultaneous oxidation of H_2S to SO_4^{2-} or S^0 has been documented in freshwater wetland sediments rich in sulphur (Burgin and Hamilton, 2008; Payne *et al.*, 2009). Although highly reduced conditions have been found in FM, the presence of S has not been determined. Therefore, although the presence of chemolithotrophic DNRA cannot be definitely rejected or accepted, it is likely that DNRA bacteria are more abundant in the riparian area of the FM, where the low redox, the low nitrate availability and the high ratio of C/NO_3^- gives them an advantage in resource competition with the denitrifiers.

In the least disturbed zone of the re-connected floodplain, where there is no pressure from grazing, horse riding or angling activities, the hydrological regime is the main controlling factor of resource availability and consequently nitrate attenuation processes. Furthermore, the conservation of natural meadow vegetation (i.e. fritillaries) together with the more hydrophilic riparian plants is likely to have increased the patchiness of soil conditions in the FM (Bruland *et al.*, 2006). Denitrification concentrated in the low-lying areas, formed by flooding, where soil moisture combines with the availability of carbon and nitrate substrates (Ullah and Faulkner, 2006; Harms and Grimm, 2008). Furthermore, DNRA has been shown to be relatively important in this most natural and more N-limited area of the River Cole floodplain (Huygens *et al.*, 2007).

6.5.2.2 *Pasture Meadow (PM)*

The widespread flooding of the PM area from the ditch and the river had as consequence fairly homogeneous soil properties across the three transects. As shown by Harms *et al.* (2008), homogenisation in soil characteristics and microbial activity occurs when the hydrologic driver (i.e. flooding) is frequent and spreads across the floodplain. Therefore, soil nitrate is supplied uniformly across the floodplain during overbank flooding, which this study has shown to occur throughout the year, while organic carbon

supply is maintained by the annual mowing regime as explained in section 6.5.1. The riparian area of the PM has also shown (as in FM) a slightly higher availability of LOC, despite the lower amounts of organic carbon measured. Consequently, the denitrification and the DNRA potentials were not statistically different across the transects, while the higher clay content in the channel depression and the riparian areas (Pinay *et al.*, 2000) may be related to the slightly higher process rates compared to the middle transect.

Denitrification in PM seems to be controlled by the availability of organic carbon and the soil moisture, as indicated by the correlation and regression analysis, while there is frequent nitrate supply. In this homogeneous land use zone with adequate nitrate supply, DNRA probably occupies the same niches as denitrification and is largely outcompeted, as indicated also by the second lowest DNRA rate in a cross-zone comparison. Finally, DNRA correlated with the soil moisture content, while its dependence on low redox conditions was also highlighted by MRA.

Interestingly, although almost all soil properties in the PM were similar or not significantly different between transects, the methane production potential was significantly higher in the riparian transect. The same pattern has been observed in all the riparian transects of the different land use zones. The riparian zone of a Scottish ombrotrophic peatland was a significant CH_4 'hotspot' contributing ~12 % of the total catchment productions whilst covering only ~0.5 % of the catchment area (Dinsmore *et al.*, 2009). Furthermore, temperate forest wetlands in Canada (Ullah *et al.*, 2008), riparian zones of the River Waal in The Netherlands (Kemnitz *et al.*, 2004) and riparian fens and floodplain soils in Germany and Switzerland respectively (Alewell *et al.*, 2008) were significant CH_4 sources. In floodplains, despite the regular change between wet anoxic and dry oxic soil conditions, soil methanogens persist during the year in abundance and diversity (Mayer and Conrad, 1990). However, methanogens were shown to be abundant in soils that were at least frequently flooded, while instantaneous methanogenic activity (i.e. no lag phase) and greatest microbial diversity was found in permanently flooded soils (Kemnitz *et al.*, 2004). The above are in agreement with our observations where despite the frequent flooding of the re-connected floodplain, significant methanogenesis was observed only in the near-stream zones during 21 days of anoxic incubation.

Therefore it could be argued that the frequent and spatially extensive flooding regime of the PM zone maintains a high denitrification capacity that can be equally effective across the whole floodplain surface in permanently removing river water and agricultural runoff nitrate, while at the same time N-conservation via DNRA is minimal and the adverse effect of CH_4 production from waterlogged soils is restricted in the near stream zones. In other words, the intermittent flooding of a re-connected floodplain can provide the benefit of nitrate removal via denitrification, without the adverse effect of increased methane productions from more permanently saturated areas in riparian zones (Itoh *et al.,* 2007) or treatment wetlands (Søvik and Kløve, 2007; Altor and Mitsch, 2006).

6.5.2.3 *Buffer Zone (BZ)*

The BZ, being the smallest in surface area and at the same time the most frequently flooded, displayed a remarkable homogeneity in the soil properties among the three transects. Although a trend of decreasing soil moisture and organic matter content with distance from the stream was observed, it was not statistically significant. However, the arable field displayed significantly lower AnMOC and LOC compared to the rest of the BZ. Cultivation has long been known to cause marked reductions in total organic C (Paul and Clark, 1989) and more serious reductions in labile or microbial C (Bowman *et al.,* 1990; Groffman *et al.,* 1993b; Boyer and Groffman, 1996; Ullah and Faulkner, 2006).

Despite this difference in the availability of LOC, neither the denitrification nor the DNRA potential was significantly different between transects. Although the arable field displayed substantially lower mean rates, due to the spatial variability observed in the riparian and middle transects (Fig. 6.2.17), the difference was not statistically significant. Other studies have found lower denitrification rates in cultivated soils (Groffman *et al.,* 1993b; Cavigelli and Robertson, 2000; Ullah and Faulkner, 2006) and at the edge of arable fields and buffer zones (Hefting *et al.,* 2003, 2006b) that were attributed to lower LOC availability and lower soil moisture.

The PCA analysis highlighted the occurrence of five biogeochemical ‘hotspots’ (sensu McClain *et al.,* 2003), three along the riparian transect nearest to the bridge and two in

the middle transect near the drainage tunnel. These 'hotspots' were associated with higher soil moisture, lower redox potential and higher availability of LOC and soil nitrate, possibly as a result of being located in surface depressions with distinctly longer residence time of floodwaters. Similar low elevation areas have been associated with increased biogeochemical activity and large pools of C and N in semi-arid riparian zones due to the longer residence time of floodwaters after the monsoon passage (Harms and Grimm, 2008). Therefore, despite the frequent flooding regime (almost 90 days per year) that extends across the BZ and within the arable field, the highest denitrification and DNRA potential rates were observed in those depressional 'hotspot' areas, that possibly extend the effectiveness of the BZ in removing nitrate beyond the time limits of the flood 'hot-moment' (McClain *et al.*, 2003). Although these 'hotspots' may benefit the BZ by increasing its denitrification capacity, care must be taken when there is the need to model denitrification at the field scale to adequately represent the contribution of those 'hotspots', both at the spatial and temporal dimension (Groffman *et al.*, 2009).

6.5.2.4 *Grazing Grassland (GG)*

The combination of the hydrologic regime and the grazing activity has shaped the spatial distribution of the soil properties between transects in the GG. The presence of grazing ungulates in the middle zone between the restored meandering river and the remnant channel had as a result higher organic matter and organic carbon soil contents, while the soil moisture also increased probably as a result of the more organic, lower bulk density soil. However, the 'hotspot' nature of the grazing influence (McClain *et al.*, 2003) was apparent by the large error bars, and therefore the high spatial variability, observed in the soil nitrate content and also the AnMOC and LOC availability that despite being on average higher in the middle transect, the difference was not statistically significant. Consequently, neither the denitrification nor the DNRA potential rates were different among transects, although the riparian zone tended to be slightly lower.

Both denitrification and DNRA seem to be controlled by the availability of LOC and the soil moisture conditions, while there is frequent nitrate supply through flooding and the animal manure application. The fact that no significant relationship was found between DNRA and the methane production potential in this zone suggests that

fermentative DNRA is the dominant process, while it is primarily regulated by the LOC availability rather than the lower redox (Fazzolari *et al.*, 1998). Despite the fact that two of the transects in this zone were affected by overbank flooding (i.e. riparian and mill leat), the riparian transect was the one that displayed the highest methane production potential, being in agreement with the observations in the other land use zones as well. This is additional evidence that the restored River Cole floods more frequently than the remnant channelized part of the river.

In contrast to the depressional 'hotspots' observed in the BZ, where the hydrology transports the C and N substrates in a low relief topography where enhanced biogeochemical activity occurs, in the GG, the reactants are supplied by the applied manure, and the 'hot-moment' of a flood is necessary to lower the redox and initiate enhanced denitrification activity. The above 'hotspot' occurrences are field scale variations of the hydrological 'hotspot' generation mechanisms reviewed in McClain *et al.* (2003).

Therefore our results suggest that within the re-connected River Cole floodplain, both micro-topography and land use act together with hydrology in creating areas of enhanced denitrification activity, thus highlighting the importance of combining river-floodplain connectivity, traditional land use practices and geomorphic diversity as an efficient measure against diffuse nitrate pollution in lowland agricultural catchments.

6.5.3 *The effect of subsurface hydrology and lithology in the vertical distribution of nitrate attenuation in the vadose zone of two land use zones*

Although overbank flooding has been identified as the dominant hydrological mechanism in the re-connected floodplain of the River Cole that supplies nitrate to the surface soil and promotes anaerobic conditions that favour nitrate attenuation via denitrification and DNRA, groundwater sub-surface flow has also been observed to occur during and in between flood events. Moreover, nitrate removal has been observed along groundwater flow paths between the floodplain and the river and ditch in the PM zone and between the arable field and the river in the BZ area. Therefore, the vertical distribution of nitrate attenuation and the relative importance of different processes were investigated in the vadose zone of these two land use zones in the context of the relative

availability of electron donors and acceptors (Vidon and Hill, 2004b) and subsurface lithology (Hill *et al.*, 2004).

6.5.3.1 *Vertical distribution of lithology and electron donors and acceptors across the vadose zone*

There were no significant differences in the lithology (as expressed by soil texture) across the vadose zone in both the BZ and the PM. Only the topsoil in the BZ was classified as sandy clay loam, containing less clay and silt compared to the BZ subsurface and the topsoil of the PM. The presence of stream margin reedbeds and depressional pools in the BZ compared to the grassland in PM, has probably caused increased deposition of coarser sediments during the winter and spring floods, as it was also found for two contrasting Dutch floodplain wetlands (Olde Venterink *et al.*, 2006).

Silt and clay fractions dominated the subsurface of the BZ, while the presence of scattered gravel was observed throughout the vadose zone, without though forming localised distinct gravel lenses (Hill *et al.*, 2004). In contrast, a localised gravel lens was observed between the middle of the PM and the river, at depths around 1 m, while gravels were also found closer to the surface near the river. The depth and lateral extent of the scattered gravel in the BZ and the gravel layer in the PM suggest that stream processes produced them (Burt *et al.*, 1999; Hill *et al.*, 2004). Reineck and Singh (1980) indicate that gravel layers are often the former bed sediments of laterally migrating stream channels and are common features of floodplain lithology. Highly conductive coarse sediments can increase groundwater flow rates and limit nitrate removal in some riparian areas (Correll *et al.*, 1997; Burt *et al.*, 1999). However, in our study the silt and clay content of the gravel layer was high and not significantly different from the upper soil layers, while the saturated hydraulic conductivity was not higher compared to the B soil horizon. Therefore the gravel lense is unlikely to act as a groundwater bypass without the opportunity for nitrate removal.

The bulk density increased with depth in both vadose zones of the BZ and the PM. The soil moisture content decreased with depth in the unsaturated zone and increased again at the top limit of the water table at depths between 0.7 and 1 m. The organic carbon and organic matter contents, as well as the AnMOC measurement followed an exponential decay with depth in both the PM and the BZ, which is consistent with the findings of

other studies in hardwood forest soils of the Upper Rhine floodplain (Brettar *et al.*, 2002; Brettar and Höfle, 2002), in agricultural and forested soil profiles of the Hudson River Valley in New York (Boyer and Groffman, 1996) and in restored urban riparian zones in Maryland (Gift *et al.*, 2008). However, due to the similar decay rate of the AnMOC and the organic carbon content, the expression of LOC (CO_2 produced per gram of organic carbon) remained largely unchanged throughout the depth profile, indicating that the labile fraction of organic carbon does not change significantly with depth, but the amount of total organic carbon is significantly reduced. Finally, there was no indication of buried organic patches (Hill *et al.*, 2000; Vidon and Hill, 2004b; Hill *et al.*, 2004) or subsurface peat layers (van Beek *et al.*, 2004) in either the subsurface of the PM or the BZ. Burt *et al.* (1999) also did not find any such deep organic rich layers in a riparian site (Cuddesdon Mill), only 50 miles away from Coleshill, underlain by similar geology.

Soil nitrate decreased significantly between 10 and 20 cm depth in the BZ and although a decreasing trend was observed throughout the unsaturated zone, due to variability among samples, the difference was not statistically significant. In contrast, in the PM, the soil nitrate followed an exponential decay with depth (Dick *et al.*, 2000; Clément *et al.*, 2002; Brettar *et al.*, 2002; van Beek *et al.*, 2004; Schilling *et al.*, 2009). This difference highlights the role of subsurface groundwater flow in the transport of nitrate from the arable field to the middle and riparian zone in the BZ. This is an additional nitrate supply mechanism, observed only in the BZ, suggesting that subsurface denitrification may be of importance in this land use zone. Ammonium and nitrite were both lower than nitrate concentration and generally decreased with depth, although in some cases the decrease was not statistically significant.

Significant methane production potential was only observed in the top 10 cm of the soil in both the PM and the BZ while the lag phase increased and the rates of CH_4 production decreased with increasing soil depth (Kemnitz *et al.*, 2004). Depending on redox potential, pH, and availability of electron acceptors, the following microbial reduction processes can occur after O_2 depletion: nitrate, manganese, iron, sulphate and finally CO_2 reduction (Zehnder and Stumm, 1988; Paul and Clark, 1989). Laboratory experiments confirm that methanogens will be out-competed by sulphate and nitrate reducers in the presence of sulphate and nitrate under controlled conditions (D'Angelo

and Reddy, 1999). However our laboratory incubations have shown that methanogens co-exist in the surface soil with nitrate reducers and can produce significant amounts of methane with lag phases as short as 1-2 days. This implies that redox sequence is not necessarily occurring in the field where several redox processes may be occurring simultaneously in anaerobic microsites (Alewell *et al.*, 2008). On the other hand, apart from redox conditions and the presence of electron acceptors, the availability of electron donors (organic carbon) has also been proposed as an additional regulating factor in anaerobic soils (Achtnich *et al.*, 1995). The lower availability of organic carbon in the unsaturated zone probably limits the abundance of methanogenic bacteria giving a competitive advantage to the nitrate reducers that can operate at much higher redox potential. The management implication of this is that there is far lower risk of increased methane productions from the subsurface of the re-connected floodplain, firstly because of the limited availability of organic carbon and secondly due to the substantially longer lag phase of the methanogens at depth that is usually beyond the duration of a flood event.

6.5.3.2 *Denitrification Potential*

The denitrification potential in both the PM and the BZ subsurface decreased exponentially with depth, while the rates were similar between the two land use zones, as it was also shown earlier in the land use analysis. Only the permanently saturated depth in the BZ had higher denitrification rate than the respective of the PM, probably as a result of higher nitrate availability through the subsurface flow from the arable field. A similar exponential decay of potential denitrification with depth has been shown in the Cuddesdon Mill floodplain near Oxford (Burt *et al.*, 1999), in three riparian wetlands in Brittany (Clément *et al.*, 2002), in a peat soil under grassland in the Netherlands (van Beek *et al.*, 2004) and in some riparian sites without buried organic patches in Ontario (Hill *et al.*, 2004). Our denitrification rate in the top 30 cm of the soil was comparable to a similar soil textured floodplain influenced by surrounding agricultural land (Burt *et al.*, 1999), while the deeper soil horizon rates were within the ranges reported in a number of studies (Clément *et al.*, 2002; Hill *et al.*, 2004; Hill and Cardaci, 2004; Well *et al.*, 2005; Gift *et al.*, 2008).

Correlation and multiple regression analyses highlighted the role of organic carbon availability in controlling the denitrification potential with depth (Drury *et al.*, 1998;

Brettar and Höfle, 2002; Hill and Cardaci, 2004; Gift *et al.,* 2008). The availability of nitrate was a secondary regulating factor (van Beek *et al.*, 2004), while the soil moisture content weakly correlated with denitrification, as the water table in the re-connected floodplain regularly fluctuates between 1 m depth and the ground surface throughout the year, maintaining a relatively high soil moisture throughout the subsurface. Finally, the soil texture did not seem to influence the denitrification potential, as it is homogeneously distributed across the subsurface and the clay and silt fraction is consistently above 65 % and thus being conducive to denitrification (Pinay *et al.,* 2000).

6.5.3.3 *DNRA Potential*

The DNRA potential also followed an exponential decay with depth in both the BZ and the PM, while the rates were similar between the two land use zones across the same depth intervals. We are aware of only one other study, in an herbaceous riparian area in Oregon (Davis *et al.,* 2008), where DNRA potential was measured below 1 m depth. Compared to their results, our DNRA rate below 1 m corresponds to their lower range (0.05 - 0.26 mg N $kg^{-1}d^{-1}$). So far DNRA has been assumed to be of minor importance as a nitrate reduction mechanism in groundwater systems (Rivett *et al.,* 2008). Bulger *et al.* (1989) observed DNRA in groundwater flowing beneath waste stabilisation ponds discharging organic-rich wastewater, while Smith *et al.* (1991) suggested that DNRA might be a minor nitrate sink in a sand-gravel aquifer contaminated with a plume of treated sewage effluent.

Our study shows for the first time that DNRA occurs within the soil profile of a riparian buffer zone that receives nitrate from arable land via subsurface groundwater flow, and in a restored former agricultural floodplain receiving river water nitrate through overbank flooding. However, DNRA is on average 40 times lower than denitrification in the topsoil, while its relative importance diminishes with increasing depth. DNRA and denitrification correlated strongly, indicating the coexistence of the two processes across the subsurface. The most important predictors of subsurface DNRA were the availability of AnMOC and the low redox potential, while the availability of nitrate exerted a less important control.

6.5.3.4 *Other nitrate fates*

The calculation of a nitrate removal budget for the anaerobic slurry incubation experiments indicated other possible fates for nitrate apart from the complete heterotrophic denitrification and DNRA. Complete denitrification (final product dinitrogen gas) accounted for 38 to 83 % of the added nitrate. Generally, highest N_2 production was observed in the top 10 cm of the soil and in the permanently saturated zone. Although this may indicate the presence of more active denitrifier populations in these depths, it is also a function of the different incubation times of the experiment. Apparently, 3 hour incubation was adequate for the expression of all the reductase enzymes (including the N_2O reductase) in the topsoil, while 72 hour incubation were needed for the saturated zone samples to produce comparable amounts of N_2, for the same amount of added nitrate and incubation temperature. This clearly shows the lower reactivity of denitrifiers in the deeper floodplain sediments (Hill *et al.*, 2004). Additionally, between 9 and 25 % of the added nitrate remained in the sample pool at the end of the experiment, showing that nitrate supply was not limiting. Finally, DNRA ranged between 1 and 3 % of the added nitrate and this was consistent across the subsurface depth layers.

The production of nitrous oxide has also been observed in all the samples from all the depth intervals in both the PM and the BZ. However, it was generally less than 5 % of the added nitrate (apart from two depth layers), which is commonly observed for incomplete denitrification in agricultural and forested soils (Davidson *et al.*, 2000). Moreover, N_2O production generally decreased with depth in the BZ (Hunt *et al.*, 2007), while a more complicated pattern was observed in the PM. It seems that the rate of denitrification activity is more stratified in the PM with more pronounced differences within small vertical distances, which led to an increased accumulation of N_2O in the deeper of the paired depths that shared the same incubation time (Figs. 6.3.8 and 6.3.18). Our N_2O production rate at the top 10 cm of the soil was comparable to slurry rates without carbon or nitrate amendment in similar riparian soils in a watershed in North Carolina (Hunt *et al.*, 2007), while they were lower compared to nitrate-only amended batch incubations of topsoil from a riparian zone in the Netherlands, identified as a nitrous oxide production hotspot (van den Heuvel *et al.*, 2009). The ratio of N_2O/N_2 (range 0.02 - 0.18) in the top 30 cm of the soil in the PM and BZ zones is within the lower range reported in the literature for other riparian areas and floodplains (Groffman

et al., 2000; Ullah *et al.,* 2005; Hefting *et al.,* 2006; Woodward *et al.,* 2009). This probably suggests that the land use zones of the River Cole floodplain are not important sources of nitrous oxide while they are effective sinks through complete denitrification. However, a slight increase of the ratio of N_2O/N_2 was observed in the unsaturated zone, which could be due to a lower soil moisture effect (Ullah *et al.,* 2005) or an artefact of our incubation time that did not allow complete expression of the N_2O reductase. Even if slightly more N_2O is produced in the unsaturated zone, there is the possibility of further reduction in the upper soil layers, although there is a complicated control of gas diffusion through the soil profile and the availability of reduced conditions and electron donors and acceptors (van den Heuvel *et al.,* 2009).

Nitrite has also been shown to accumulate at the end of the incubation experiments at proportions ranging between 1 and 17 % of the added nitrate. Elevated nitrite levels do not tend to occur during denitrification (Rivett *et al.,* 2008), while nitrite accumulation may be due to DNRA bacteria that have a different type of nitrite reductase enzyme (Knowles, 1982). It has been shown in anaerobic river sediments that NO_2^- can accumulate from DNRA when the reduction of nitrite to ammonium is inhibited by elevated nitrate concentrations (Kelso *et al.,* 1997). It is likely that this inhibitory effect occurred in our samples, from the unsaturated soil horizon, that were exposed to 'unusually' high nitrate concentrations during the incubation experiment.

On average 14 % of the added nitrate was not accounted for by any of the measured products or the remaining NO_3^- in the sample pool. This 'lost' nitrate was assumed to be assimilated into microbial biomass. Other studies have also shown similar percentages of nitrate assimilation during laboratory incubation of intact cores from the top 20 cm of a riparian fen soil (Ambus *et al.,* 1992) or a range of wetland soils from sandy loam to peat (Davidsson and Ståhl, 2000). Moreover, in an N-limited forest soil, nitrate immobilisation accounted for more than 85 % of the added nitrate and higher immobilisation was observed in the least fertilised soils (Bengtsson and Bergwall, 2000). Although nitrate assimilation by bacterial biomass is possible in soil types similar to ours, it should have been inhibited by the presence of NH_4^+ (Rice and Tiedje, 1989), which is taken up preferentially from nitrate by bacteria (Hill, 1996). The 24 hour pre-incubation of the samples increased substantially the NH_4^+ pool (Rütting *et al.,* 2008) and the relatively short incubation times of our experiment should have

minimised nitrate assimilation. Moreover, this means that assimilated $^{15}NO_3^-$ would not have had the time to be re-mineralised as $^{15}NH_4^+$ and therefore bias our DNRA results. However, not accounting for 100 % of $^{15}NO_3^-$ applied is a common challenge in tracer experiments (Templer *et al.,* 2008), but still even the assumed microbial assimilation as a temporary nitrate sink is relatively unimportant compared to the temporary nitrate removal via denitrification in the vadose zone of the River Cole floodplain.

Anaerobic ammonium oxidation (anammox), which is the chemolithotrophic process by which ammonium is combined with nitrite under anaerobic conditions to produce N_2 as a final product was not observed to occur neither in the topsoil nor in the subsurface soil horizons of the BZ and the PM areas. This process has been thoroughly described in estuarine and deep sea sediments (Trimmer and Nicholls, 2009; Nicholls and Trimmer, 2009), but its importance in freshwater environments has not yet been established (Burgin and Hamilton, 2007). Finally, the chemolithotrophic reduction of nitrate via pyrite oxidation (Schwientek *et al.,* 2008) or reduced sulphur oxidation (Burgin and Hamilton, 2008) is probably not an important process in the intermittently saturated River Cole floodplain, where iron was undetectable in surface soils and subsurface sediments; while although sulphate was present, reduced sulphur compounds were restricted only to the anoxic riparian river margins.

6.5.4 *The effect of the intermittent saturation regime on nitrate attenuation processes in the topsoil*

The effect of the intermittent saturation regime of the re-connected floodplain on the denitrification and DNRA potential was investigated with sampling of the topsoil across all the land use zones after a prolonged wet period and a subsequent sampling of the same locations after a prolonged dry spell.

6.5.4.1 *Soil properties*

The gravimetric water content was not significantly different between wet and dry conditions. However, the Water Filled Pore Space (WFPS), which is considered a better index for aeration dependent biological processes at relatively high soil moisture contents (Aulakh *et al.,* 1996; De Neve and Hofman, 2002; Sleutel *et al.,* 2008), was significantly lower following the prolonged dry period.

Neither the organic matter nor the organic carbon content was any different between the wet and the dry conditions sampling. Soil and sediment drying promotes the aerobic mineralisation of organic matter and the release of cell-bound C from sediment bacteria killed during drying (Scholz *et al.*, 2002). Therefore, upon drying, a decrease in organic matter and an increase in organic carbon should have been observed. It should be noted though that the wet and the dry samplings were four months apart, due to the very wet weather of the season 2007 - 2008 that prevented the occurrence of a prolonged dry spell, and therefore the wet sampling does not reflect the exact pre-drying conditions. Moreover, Fierer and Schimel (2002) observed significant decrease of the DOC concentration of oak and grassland soils only after multiple stresses of dry-wet cycles over two months, while the changes were greater in the less frequently wetted oak soil. This suggests that the 12 days of dry conditions may have not been long enough to stimulate an increased organic matter mineralisation, while the intermittent saturation regime of the River Cole floodplain, without overly long periods of drought, maintains increased levels of organic carbon that can fuel microbial nitrate removal all year round.

Similarly, the AnMOC and the LOC were not significantly different between wet and dry samples. Pinay *et al.* (2007b) and Fromin *et al.* (in press) have also found no effect of a rainfall perturbation in dry soils on the potential microbial respiration as expressed by the Sediment Induced Respiration (SIR) rate (Beare *et al.*, 1990). Apart from the similar availability of anaerobically mineralisable organic carbon between wet and dry samples, this result also indicates that decomposers, which are mainly responsible for the anaerobic mineralisation of organic matter, are resistant to perturbations such as dry-wet cycles (Pinay *et al.* 2007b). Finally, the methane production potential, being spatially very variable, was not different under prolonged wet or dry conditions. Boon *et al.* (1997) have shown in *in vitro* anaerobic incubations of wetland sediments that methanogenesis is decreasing with increasing sediment dessication, however, methanogenic archaea can survive long drying periods and can be subsequently revived by re-wetting with relatively short lag-phases.

Only the soil N content was significantly higher in the wet samples compared to the dry samples. Several studies have shown a flush of mineralised-N and subsequent increase in nitrate and ammonium concentrations in soils and sediments upon re-wetting by flooding, due to flushing of accumulated ammonium and enhanced nitrification

(Baldwin and Mitchell, 2000; Olde-Venterink *et al.*, 2002; Heffernan and Sponseller, 2004; McIntyre *et al.*, 2009). However, as the saturation conditions persist, the relative importance of nitrification diminishes, while losses of nitrate by denitrification increase (Baldwin and Mitchell, 2000). Although the exact sequence of events prior to our wet sampling was not determined, increased availability of inorganic N may be attributed to the above combination of processes, but also the additional supply by the river floodwater. The decrease in soil N content upon drying could be explained by an increased nitrification of ammonium coupled to enhanced denitrification at the initial stages of the dry period (Koschorreck, 2005). Moreover, the dry sampling took place in July 08, and therefore plant uptake during the growth season has probably contributed to the further reduction of soil nitrate and ammonium.

The PCA indicated that the most important discriminating factor between the wet and the dry samples was the difference in their WFPS. The samples formed three distinct clusters, with the FM samples being the most spatially variable due to the presence of organic matter and soil nitrate 'hotspots'. Considerable overlap was found between the PM and the GG samples, while the lowest spatial variability and higher homogeneity in the soil properties was observed for the BZ. Heterogeneity in the FM and more homogeneous soil conditions in the PM and the BZ were also shown in an earlier study of the same areas (see section 6.5.2). However, the presence of 'hotspots' in the GG due to grazing activity was not observed at the wet-dry sampling, highlighting that a random sampling strategy increases the probability of missing important biogeochemical 'hotspots' at the field scale (Groffman *et al.*, 2009). The same clusters were observed for both the wet and the dry conditions, while the overlap of the clusters along axis 1 suggests that flooding and drying cycles significantly affect the soil moisture conditions across the re-connected floodplain as a whole, while the spatial variability of the rest of the soil properties seems to be unaffected.

6.5.4.2 *Denitrification and DNRA potential*

Although the potential denitrification rate was 37 % higher in the wet samples, the difference was not statistically significant. As indicated by the correlation and multiple regression analysis, denitrification was mainly driven by the availability of AnMOC and the higher WFPS under wet conditions, while the effect of the elevated soil nitrate was only marginal. This is in agreement with our earlier results across the different land use

zones of the re-connected floodplain (see section 6.5.1), where also the availability of labile organic carbon seemed to be limiting denitrification, while soil nitrate was probably in excess. Under dry conditions, the control of denitrification by AnMOC was still important, while the soil moisture had a slightly more important role and no relationship was found with the soil nitrate (data not shown). This indicates further that even though nitrate was significantly lower in the dry conditions, it was still not-limiting for denitrification.

Despite the lower WFPS in the dry condition samples and in conjunction with the available organic carbon and the adequate soil nitrate, denitrification activity survived the unfavourable oxic conditions and was not significantly different compared to the wet conditions. This finding is in agreement with other studies that have found denitrifiers to be very resilient of unfavourable oxic conditions (Smith and Tiedje, 1979; Groffman and Tiedje, 1988; Olde Venterink *et al.,* 2002; Fromin *et al.,* in press). Denitrifying bacteria are predominantly facultative anaerobs (Knowles, 1982), therefore dessication-oxidation should be less toxic to them than to obligate anaerobes (Baldwin and Mitchell, 2000). The physiological cost for denitrifiers to maintain functional denitrifying enzymes under long desiccation conditions is probably compensated by their ability to rapidly use nitrate produced during drought once the sediments get flooded (Fromin *et al.*, in press).

However, the variability in denitrification activity between land use zones (Table 6.4.6) under wet conditions was lost in the dry conditions, despite the fact that most of the environmental variables did not change significantly as indicated by the PCA. This convergence of denitrifying activity following a perturbation was also observed by Pinay *et al.* (2007b), while Florinsky *et al.* (2004) found that the variability in denitrification due to topographical controls in wet soils was cancelled under drier conditions. This finding could imply a change in the community structure of denitrifiers induced by the perturbation of prolonged dry conditions. Generally, denitrifier community structure is affected on a long-term basis by the C availability, pH, and the range of moisture and temperature they experience, while nitrate can stimulate the denitrification activity but does not seem to affect its long term composition (Wallenstein *et al.,* 2006). Denitrifier community structure has been shown to be affected by the frequency of drying-rewetting cycles (Fierer *et al.,* 2003) as well as by

season and plant succession (Bremer *et al.,* 2007). The higher potential for N_2O production by denitrification under drier conditions has been attributed to changes in the structure of the denitrifier community (Fromin *et al.,* in press). However, in our study the potential for N_2O production was not significantly different between wet and dry samples and it also displayed a decreasing trend with decreasing WFPS. Moreover, changes in the denitrifier community structure have been more prominent in infrequently wetted soils than in those soils experiencing frequent wet and dry cycles (Fierer *et al.,* 2003; Fromin *et al.,* in press). Although our results with respect to the effect of the intermittent saturation regime of the re-connected floodplain on the denitrifier community structure are not conclusive, we have shown that denitrification activity is not adversely affected by brief periods of drought, and that the regular flooding of the floodplain maintains high denitrification enzyme activity that depends more on the availability of soil moisture and electron donors rather than the community composition of the denitrifiers.

The DNRA potential on the other hand, although present in the dry condition samples, was significantly affected by the dry period and was 60 % lower compared to the wet samples. The correlation and multiple regression analysis confirmed the results of the earlier study across the land use zones (see section 6.5.1) in that the most important controlling factors of DNRA were the availability of labile organic carbon, the soil moisture content and the redox potential, while no relationship was found between DNRA and the soil nitrate. We are not aware of any other studies that have investigated the effect of a wetting-drying cycle under field conditions on the DNRA potential of the topsoil. Our results suggest a higher sensitivity of the DNRA activity in a drought perturbation compared to denitrification, which could be due to the change of environmental conditions (i.e. lower WFPS, as nitrate was adequate) or a change in the bacterial community composition (Wallenstein *et al.,* 2006). DNRA bacteria are mostly obligate anaerobs (Tiedje, 1988) and therefore prolonged oxic conditions may be toxic for them; something that was shown for sulphate reducers that are also obligate anaerobs (Holland *et al.,* 1987). However, the fact that DNRA activity was observed upon re-wetting of the dry samples indicates a degree of resilience of the DNRA bacteria, while it is also possible that some bacteria survive in anaerobic microsites within the soil matrix, as it has also been shown for methanogens (Boon *et al.,* 1997).

One other possible explanation could be that some DNRA populations may be adapted to more oxic conditions (Pett-Ridge and Firestone, 2005; Silver *et al.*, 2005; Pett-Ridge *et al.*, 2006). Although DNRA under wet conditions correlated significantly with low redox conditions, under dry conditions such a relationship was not found and the single most important predictor of DNRA was the availability of labile organic carbon. It is therefore likely that a diverse DNRA population exists even in a temperate agricultural catchment with N-rich soils, where denitrifiers generally outcompete DNRA bacteria and restrict them in the lower redox, high carbon environments. However, when a perturbation like drought occurs, DNRA populations adapted to more oxic conditions can survive. These assumptions could be further explored by studying the effect of wetting-drying cycles to the community structure of DNRA bacterial populations.

In conclusion, the intermittent saturation regime of the River Cole floodplain maintains an effective denitrifying enzyme activity that is not adversely affected by short periods of drought and oxic conditions, while it significantly reduces N-conservation via DNRA that is more sensitive to oxic conditions. This balance is maintained by the frequent supply of nitrate and the availability of labile organic carbon that give a competitive advantage to denitrifiers over the DNRA bacteria. However, there is the indication that if conditions change to a more N-limited system, DNRA bacteria could evolve and be able to tolerate more oxic conditions and thus compete more successfully with denitrifiers for the limited resources.

Chapter 7: Predicting denitrification rates at the field scale for the design and appraisal of river restoration schemes

7.1 *Introduction*

Decision support tools for the assessment of the water quality function, and specifically the nitrate removal capacity, of restored floodplains and buffer zones can be broadly assigned to two types. Those that are GIS-based, or depend on geomorphological databases or field observations and scoring criteria, which usually provide a qualitative assessment of the suitability of sites for water quality improvement, and those that consist of process-based models for quantitative predictions of hydrological interactions and nitrogen transformations, are usually data intensive and their use is restricted to scientific applications. However, there is need for a rapid, cost-effective and yet reliable assessment tool to support the management decisions for river-floodplain restoration aimed at effective nitrate removal. Ideally, this tool should be based on a scientifically sound assessment of the nitrate removal capacity based on data that can be inexpensively obtained at a pre- or post- restoration stage.

In the previous chapters, the role of hydrology in nitrate transport onto the restored floodplain and in creating the necessary conditions for biological nitrate removal has been clearly shown. Moreover, in a temperate lowland agricultural setting, heterotrophic denitrification was shown to be the single most important mechanism for nitrate removal in the surface soil and the vadose zone of the floodplain. Therefore, following the hydrological reconnection of the river with its floodplain, the nitrate removal capacity of the restored floodplain could be predicted by the denitrification potential of its soil. Predictions at the pre-restoration stage would facilitate selection of sites with the highest potential for nitrate removal, and at the post-restoration stage could be used to assess the effectiveness of the restoration measures in re-instating the nitrate removal capacity of the re-connected floodplain.

7.2 *Aim and Objectives*

A major aim of this research was therefore to develop a management tool for the prediction of denitrification at the field scale to support decision making for the selection of suitable locations for river and floodplain restoration and to allow the post-

project assessment of restored floodplains targeting increased nitrate retention. For this purpose the following objectives were identified:

- Identify an appropriate model able to predict actual denitrification rates based on a simple set of measured or simulated variables;
- Build a database for validating the model simulations with actual denitrification measurements and assess the goodness of fit of the model predictions;
- Evaluate the transferability of the model to a different location from its development and assess the need for site-specific calibration or optimisation of the model parameters;
- Assess the applicability of the model to subsurface soil horizons in addition to the topsoil;
- Formulate the management tool by identifying the data requirements and the necessary steps for its application as a decision support tool.

7.3 *Simplified denitrification models*

The process-based models that have been proposed as a potential decision support tool, all include a denitrification component or a more general nitrogen biogeochemical transformation component. Numerous studies have suggested that denitrification in floodplains and riparian buffer zones is the process mainly responsible for nitrate removal, while nitrate uptake by vegetation is much less important (Haycock and Pinay, 1993; Burt *et al.*, 2002b; Clément *et al.*, 2002; Hefting *et al.*, 2004). The present study has also shown that although DNRA is occurring simultaneously with denitrification, its magnitude was, on average, 40 times less than that of denitrification. Therefore, denitrification is by far the dominant removal pathway for nitrate reaching floodplains and riparian zones from non-point agricultural sources, and therefore the prediction of the nitrate removal capacity of a re-connected floodplain could be based solely on estimating potential denitrification rates.

Different approaches exist for including denitrification in a N-cycling model: i) microbial growth models that consider the dynamics of microorganisms responsible for denitrification (e.g. DNDC; Li *et al.*, 1992a,b, 2000); ii) soil structural models that consider the diffusion of gases in and out of the soil matrix (e.g. Vinten *et al.*, 1996) and iii) simplified models where denitrification is assumed to be determined by easily

measurable parameters such as degree of saturation, soil temperature, and nitrate content of the soil. The latter is appropriate for use at the field scale, where the data can be obtained from field measurements or from simulation models (Heinen, 2006a).

In his recent review of over 50 simplified denitrification models, Heinen (2006a) provided a description of the most common formulation for denitrification found in the majority of the models. Specifically, denitrification is simulated as a function of a potential denitrification rate or is considered as a first-order decay process. Since denitrification is dependent upon environmental conditions such as oxygen scarcity, nitrate availability, temperature and pH conditions, reduction functions are estimated for the above parameters and the general mathematical function to describe actual denitrification is given by equation (7.1):

$$D_a = a f_N f_S f_T f_{pH} \tag{7.1}$$

Where D_a is the actual denitrification rate, a depends on whether the denitrification potential is used or a first-order decay coefficient, f_N is a dimensionless reduction function for nitrate soil content, f_S is a dimensionless reduction function for water content in soil, f_T is a dimensionless reduction function for soil temperature and f_{pH} is a dimensionless reduction function for soil pH.

A number of simple denitrification models deviate from Eq. (7.1) mainly by adding to or modifying the dimensionless reduction functions to account for: the effect of air temperature on the denitrification decay constant (CREAMS; Knisel, 1980 in Marchetti *et al.*, 1997); the contribution of different nitrogen transformation processes in the f_N such as N deposition, plant uptake and N immobilisation in the root zone (EXPERT-N; Priesack *et al.*, 2001); the effect of soil type on the soil water function (Lippold and Matzel, 1992 and NGAS; Parton *et al.*, 1996); a specific rainfall or irrigation regime (NLEAP and NLOS; Shaffer *et al.*, 1991, 2001a; Xu *et al.*, 1998; Bittman *et al.*, 2001) and the effect of redox potential on the maximum possible denitrification increase and the effect of organic carbon on the degree of anaerobiosis (REMM; Inamdar *et al.*, 1999ab).

Since the scope of the present study is not to present an exhaustive review of the different variations of simple denitrification models, the focus of this section will be on presenting the rationale for using the different functions in Eq. (7.1) with the aim of selecting the most suitable simple denitrification model expression that will form the basis for the development of the management tool.

The actual denitrification rate D_a can be computed at the point scale, expressed as loss of N on dry soil weight basis, loss of N on soil volume basis, or some spatial scale for a certain soil layer, where the soil layer thickness should also be indicated. The parameter a can represent a potential denitrification rate D_p (same units as D_a) or represent a first-order denitrification coefficient (constant) k_d (Heinen, 2006a). In the case where $a = D_p$, a certain point or soil layer can be characterised by a potential denitrification rate, which also provides an indirect measure of the effect of organic matter decomposition on denitrification since D_p is measured under non-limiting nitrate conditions, anaerobicity and at a default or reference temperature. Moreover, as the organic carbon availability is likely to change over time, or due to seasonal effects, the measurement of D_p should also take into account the effect of the time or season of measurement (Hénault and Germon, 2000). Finally, as the organic carbon distribution changes with depth, this should also be reflected by the D_p measurement in case several soil layers at different depths need to be considered (Heinen, 2006a).

When $a = k_d$, k_d is a first-order denitrification coefficient and the actual denitrification is still influenced by environmental conditions through the dimensionless functions f_S and f_T. However, the function f_N is no longer a dimensionless function but equals the soil nitrate content. The first-order denitrification coefficient in most cases is estimated experimentally as a function of soil type and soil nitrate content or from some expression of the soil organic carbon availability (Heinen, 2006a).

Regarding the function f_N, when D_p is used in Eq. (7.1), f_N is estimated from a Michaelis-Menten type formula as the bacterial denitrifying activity increases in a hyperbolic type curve approaching a maximum value with respect to the substrate concentration (i.e. soil nitrate concentration) (Paul and Clark, 1989). Therefore, the f_N is given by equation (7.2):

$$f_N = \frac{N}{K + N} \tag{7.2}$$

Where f_N is the dimensionless nitrate function, N the soil nitrate concentration and K, which can be determined experimentally, the half-saturation constant or the soil nitrate concentration when $f_N = 0.5$.

From Eq. (7.2), when K>>N, i.e. at low soil nitrate concentrations, nitrate becomes limiting for denitrification and the process approaches first-order kinetics and therefore k_d can be used correctly in Eq. (7.1). However, when ambient soil nitrate concentration is high, then nitrate is not limiting and a first-order decay constant should not be used, but instead a combination of D_p and f_N described by Eq. (7.2) should be used in Eq. (1) (Heinen, 2006a). Therefore, the use of the D_p in the formulation of the simple denitrification model has the advantage that it can accurately take into account low or high ambient soil nitrate contents.

Denitrification also depends on a lack of oxygen availability, but since oxygen dynamics in soil are difficult to measure (or simulate) (Rolston *et al.*, 1984; Grundmann and Rolston, 1987) the soil water content is used instead to describe anaerobic conditions. As the water content increases, the air-filled porosity of the soil decreases. However, oxygen diffusion coefficients are not related linearly to air-filled pore space, and therefore a power reduction function is usually used, as in equation (7.3):

$$f_S = \left(\frac{S - S_t}{S_m - S_t} \right)^w \tag{7.3}$$

Where f_S is the dimensionless water reduction function, S is the dimensionless degree of saturation or water-filled pore space, S_m is S above which f_S =1, S_t is a threshold value for S below which f_S = 0, and w is a curve shape parameter determining the steepness of the curve. In most cases S_m = 1, meaning that when 100% of the pore space is filled with water, denitrification will operate optimally. The threshold parameter S_t is usually determined experimentally relating it to a specific soil property and more commonly on

the value of S at field capacity, whereas w is usually $w>1$; that is (S_m - S_t) multiplied by the slope of the curve at $S = S_m$ (Heinen, 2006a).

Heinen (2006a) also gives examples of models that have used a different water reduction function based on volumetric water content (θ), groundwater level, pressure head, and the water retention characteristic (including the effect of hysteresis) or a Michaelis - Menten type function. Heinen (2006a) also acknowledges that although there is a wide range of water reduction functions (mainly due to differences in the soil gas diffusivity and soil respiration rate of the different soil types the models were based on for their development) in most cases $f_S = 0.5$ at $S > 0.7$.

All biological processes, and therefore denitrification, are regulated by temperature and they usually increase exponentially with increasing temperature until they reach a maximum where the rate levels off and if the temperature continues to increase then a rapid drop in the process rate towards inactivity is observed (Payne, 1981; Tiedje, 1988). According to Heinen (2006a), most simple denitrification models have a temperature reduction function based on the Van't Hoff law (equation 7.4) or the Arrhenius law (equation 7.5):

$$f_T = Q_{10}^{(T-T_r)/10} \tag{7.4}$$

$$f_T = \exp\left(k_A \frac{(T - T_r)}{T_r T}\right) \tag{7.5}$$

Where f_T the dimensionless temperature reduction function, T the soil temperature (in ^{o}C or ^{o}K), T_r a reference temperature where f_T =1, Q_{10} is an increase factor in f_T at an increase in T of 10 ^{o}K or ^{o}C and k_A is an exponential increase coefficient (^{o}K or ^{o}C). For each model that incorporates one of the above expressions for the f_T, the reference temperature needs to be specified and the Q_{10} needs to be computed for the range of temperatures anticipated for the purpose of the predicted denitrification rates. Furthermore, when k_A is used it can be computed from the activation energy E_A and the ideal gas constant R ($k_A = E_A / R$). In some cases, the temperature function is split in

two, around a rapture value (e.g. NEMIS; Hénault and Germon, 2000) to account for a discontinuous influence of temperature on denitrification rates (Stanford *et al.*, 1975).

The effect of pH on denitrification is reflected in the process rate, which is slower under acidic conditions compared to neutral or slightly alkaline (Simek and Cooper, 2002), but also on the relative proportion of the produced nitrogen gases (mainly N_2O and N_2), with more N_2O being produced under acidic conditions (Hefting *et al.*, 2003, 2006b). Denitrification operates optimally between pH 5 and 8, while denitrification almost ceases for pH <4 or pH> 10 (Paul and Clark, 1989). Heinen (2006a) reports that only 15% of the models considered in his review included a reduction function for pH, as in most cases if the potential denitrification or the decay coefficient is determined under the same pH conditions as occur in the soil, it is not necessary to include the effect of pH in Eq. (1).

Heinen (2006a) also computed the normalised sensitivity (elasticity) of the simplified model to its parameters according to Eq. (7.1) and performed a Monte Carlo analysis. His results indicated that $D_\alpha = D_p$ only when all reduction functions are one, but in most cases $D_\alpha < D_p$, which is an acceptable result as potential denitrification is usually several times higher than actual denitrification. When K is not large, then both K and N need to be determined accurately. The highest sensitivity was shown for the parameters S and S_t that can cause significant errors in the estimation of D_α if not determined at great accuracy. Finally, the sensitivity for T is not large and since soil temperature can easily be measured accurately, the function f_T is not expected to be a significant source of errors for the model. Currently, there is not a universally accepted model for predicting denitrification, and the existing models are usually site specific. However, if a model is required for predicting denitrification at the field scale, then care must be taken regarding the transferability of the parameters to specific soil and environmental conditions, and if a new calibration of the parameters is not possible, parameter optimisation is suggested.

7.4 *NEMIS - A simplified model for predicting denitrification at the field scale*

NEMIS (Hénault and Germon, 2000) was developed from the further calibration and adaptation of earlier models proposed by Rolston *et al.* (1984) and Johnsson *et al.* (1991), in an attempt to produce a model that is based on the general formulation of Eq.

(7.1) and would be generally applicable. The purpose of this section is to describe the conditions under which the model was developed and the specific functions of NEMIS and assess its suitability for being used as a management decision support tool.

The general form of the model is given in equation (7.6):

$$D_a = D_p f_N f_S f_T \quad (7.6)$$

Where D_a is the actual denitrification rate (in kg N ha^{-1} d^{-1}), D_p the potential denitrification rate (also in kg N ha^{-1} d^{-1}), and f_N, f_S and f_T are the soil nitrate, water content, and temperature dimensionless reduction functions respectively.

The NEMIS model uses the combination of estimated D_p and a Michaelis-Menten function for the f_N instead of a first-order decay constant, and it is therefore appropriate even for high ambient soil nitrate levels, where nitrate is not limiting and the process approaches a zero order reaction. Denitrification potential rates were estimated at the 0 - 20 cm depth in a cultivated loam soil (14 % clay, 52 % silt and 35 % sand) with pH_{water} 7.1. The acetylene block technique in undisturbed soil cores kept at 20 ^oC, saturated with water in the laboratory, and placed at nitrate content near to 200 mg N kg^{-1} soil, is recommended by the model authors for estimating D_p, and if an annual simulation of denitrification is needed then the measurement should be repeated twice, once in autumn, winter or spring and once in summer.

The Michaelis-Menten type reduction function for the effect of soil nitrate is given in equation (7.7):

$$f_N = \frac{[NO_3^-]}{22 + [NO_3^-]} \quad (7.7)$$

Where $[NO_3^-]$ is the soil nitrate content (in mg N kg^{-1} soil) and 22 is the half saturation constant K (also in mg N kg^{-1} soil). The f_N was estimated experimentally for a range of soil nitrate contents between 0 - 200 mg N kg^{-1} soil and the K was computed by fitting a Michaelis-Menten function to the experimental points (Hénault and Germon, 2000).

For the f_S function, the water filled pore space δ_{WF} (%) was calculated according to the formula by Linn and Doran (1984):

$$\delta_{WF} = 100 \bullet (\theta_v / P_t) \tag{7.8}$$

Where θ_v is the volumetric water content (%) and P_t the total soil porosity (%). The parameters in the power reduction function for the soil water content f_S (see Eq. 7.3) were computed experimentally by estimating the ratio of denitrification between untreated soil cores and wetted soil cores and plotting the ratio against the δ_{WF} and then fitting an exponential curve to the experimental points. However, the estimated parameters were very close to those reported in Grundmann and Rolston (1987) and Johnsson (1991), and therefore the NEMIS model authors decided to use the formulation included in the Grundmann and Rolston (1987) model (Equation 7.9):

$$f_S = \left[\frac{\delta_{WF} - 0.62}{0.38} \right]^{1.74} \tag{7.9}$$

With reference to Eq. 7.3, in Eq. 7.9; S_t = 0.62, S_m = 1 and w = 1.74.

With respect to the effect of temperature on the denitrification process, the NEMIS model uses two formulations for Eq. (7.4) around the rupture temperature of 11^{o}C. This is based on the work from Stanford *et al.* (1975) that proposed: i) a linear relationship between temperature and log *k*, *k* being the denitrification rate constant at temperatures $\geq$ 11^{o}C and; ii) a dramatic rupture at 11^{o}C. Therefore, two Q_{10} are calculated; one for temperatures <11^{o}C (Q_{10}=0.89) and one for temperatures $\geq$ 11^{o}C (Q_{10}=2.1). The T_r for Q_{10}=0.89 is 11^{o}C, while the T_r for Q_{10}=2.1 is 20^{o}C (equation 7.10), the temperature at which D_p is measured.

$$f_T = \exp\left[\frac{(t-11)\ln(89) - 9\ln(2.1)}{10} \right] \quad \text{t} < 11^o\text{C}$$

and

$$f_T = \exp\left[\frac{(t-20)\ln(2.1)}{10}\right] \qquad t \geq 11^oC \qquad (7.10)$$

The authors validated NEMIS with two independent databases (Ryden, 1983 and Hénault *et al.*, 1998). In Ryden (1983) D_p measurements were missing and a D_p was computed assuming that maximum soil water content corresponded to saturation and the total measured and simulated denitrification rates were equal. Comparison between the measured and simulated denitrification rates gave a coefficient of determination of 0.54. The model effectively predicted temporal patterns in denitrification rates but was not reliable for estimating actual denitrification rates since the D_p had to be assumed. In the case of the Hénault *et al.* (1998) database, that was complete, the coefficient of determination was 0.9, for a simulation using the mean value for each input variable. Sensitivity analysis of the model by a systematic change of ± 5% in the input variables and the function coefficients indicated that the determination of the δ_{WF} had the greatest impact on simulated denitrification rates due to the exponential relationship between the two. Any other variables associated with the estimation of the water filled pore space, such as the volumetric water content or the bulk density (for the indirect estimation of the % soil porosity) are therefore expected to be significant sources of error in the model and should be measured as accurately as possible. Moreover, the determination of the S_t was highlighted as the most important limitation of the model, since S_t is related to the soil texture and the soil's field capacity and it is likely that site-specific calibration or optimisation could be needed for conditions other than those described in Grundmann and Rolston (1987) and Hénault and Germon (2000). The simulations were also relatively sensitive to the temperature rupture point, while they were rather insensitive to K, which is not expected to vary greatly between soils as long as the D_p is measured according to the conditions described in Hénault and Germon (2000).

The NEMIS model was also applied to eight Dutch datasets and the Ryden (1983) dataset for comparison (Heinen, 2006b). These datasets did not aim to recalibrate the f functions of the model and included a variety of soil types, from dry and wet sand to heavy loams and peat. Since not all the available input variables were available, assumptions needed to be made and parameters were calculated indirectly or from similar datasets. All the function parameters were optimised by minimising the root

mean square error (RMSE) in D_a, and in order to compare the optimisation results between datasets the normalised root mean square error (NRMSE) was also defined according to Janssen and Heuberger (1995). The best results (smallest NRMSE) were obtained for the Ryden (1983) UK loam dataset that was already shown by Hénault and Germon (2000) to be adequately described by NEMIS. The Dutch datasets, even after parameterisation, displayed significant differences in the model parameters between similar soil types and the simulation failed to accurately predict individual actual denitrification rates. However, there was good correspondence between averaged measured and simulated denitrification rates for the sand and loam soil types, but not the peat datasets. According to Heinen (2006b), the main source of errors in the case of the Dutch datasets was probably the assumptions that had to be made and the estimation of the missing input variables (e.g. low range of measured soil N contents, D_p estimated from organic carbon decay) and also the effect of the site specific soil texture, pore geometry and pore connectivity on the f_S that was the most sensitive and prone to large errors. Therefore, NEMIS could be used in the case of sandy and loam soils to derive a reliable average denitrification rate, as long as all the necessary input variables are available and the functions are parameterised for the specific location.

NEMIS was also used to simulate N losses due to denitrification under different summer irrigation treatments in a fertilised sandy clay loam soil (around 900 mg N kg^{-1}) in Southern France (Vale *et al.*, 2007). The model parameters were not optimised and the input variables were measured *in situ* at hourly intervals, apart from the D_p, which was not determined and a value reported in Hénault *et al.* (2005) for a similar soil type was used instead. The model predictions showed good agreement with ^{15}N balance measurements for only one of the three treatments (the one with the lowest initial N content). This was probably due to the inadequate description of soil heterogeneity and oxygen diffusion variability by the unique values for total porosity and WFPS introduced in the model. Moreover, the transferability of D_p values from other studies is questionable. Finally, the model performed better at hourly time steps than at daily averages, indicating that smoothing of short term soil moisture changes may result in underestimating denitrification rates especially during summer storm events.

Coupled to the agro-hydrologic model TNT2 (Beaujouan *et al.*, 2001), NEMIS was used to simulate denitrification at the catchment scale in slightly acidic, silty, hillslope

and riparian soils in Western France (Oehler *et al.*, 2007, 2009). The D_p was measured once with the Denitrification Enzyme Activity (DEA) method (i.e. adding apart from NO_3^- also C as substrate), while the soil nitrate and water contents were measured monthly. Parameter optimisation resulted in NRMSE value of 1.24, which is relatively high but within the range also reported by Heinen (2006b). The model predicted satisfactorily daily denitrification rates (coefficient of determination 0.68). However, the discrepancy between measured and modelled denitrification rates could be due to the fact that the assumption of a constant DEA is not valid and the relationship between denitrification and soil moisture is more complex and transient than that assumed by applying the model at daily time steps (Oehler *et al.*, 2009).

From the above uses and sensitivity analyses of NEMIS, a number of advantages of the model can be drawn. The use of a measured D_p, once or twice per year for better annual representation, in conjunction with a dimensionless f_N, has the advantage that field points or a specific soil layer can be characterised by a D_p rate that also incorporates the effect of organic carbon availability on denitrification without the need of additional laborious organic carbon measurements. Additionally, the Michaelis - Menten type f_N, allows for both high and low ambient soil nitrate levels to be represented accurately. The determination of K is unlikely to be a major error source for the model, as long as the D_p is measured according to the protocol defined by the authors (Hénault and Germon, 2000). Although the model was relatively sensitive to the determination of the temperature rupture point (Hénault and Germon, 2000), additional validations of the model with different datasets have shown that this does not constitute a significant source of error, especially if optimisation is performed (Heinen, 2006b). Furthermore, if the NEMIS f_T formulation is overcomplicated, it could be replaced by the more generic Eq. 7.4, as shown in Oehler *et al.* (2009).

There is agreement between the authors of the model and its subsequent validations by other studies that the determination of the f_S parameters is the major limitation of the model. This is due to the complex nature of the relationship between soil moisture content and denitrification, which is greatly influenced by the site's soil characteristics. This fact could limit the transferability of NEMIS into conditions different from its development. Therefore, apart from ensuring that the input variables associated with the definition of f_S are measured as accurately as possible, calibration or parameter

optimisation may be needed for a site-specific application. Since a universally accepted model for simulating denitrification does not yet exist, the application of NEMIS under different conditions has shown that despite its limitations it can be a useful tool for predicting average denitrification rates at the field scale. NEMIS has therefore been selected in this study as the basis of the management decision support tool to evaluate the denitrification capacity of restored floodplains and riparian zones.

7.5 *Data requirements and site selection for the validation and application of NEMIS*

Mulligan and Wainwright (2004, and references therein) distinguish three broad categories of model validation: i) operational or whole-model validation where the model output is compared to real-world observations; ii) conceptual validation that is the evaluation of the underlying theories and assumptions of the model; and iii) validation of the data used to test the model. From the above types of validations, only the whole-model validation will be applied for assessing the suitability of NEMIS, since the conceptual background is based on established controls of the denitrification process, as described in Heinen (2006a), and the re-calibration of the model parameters is not in the scope of the present study. Moreover, validation of the data used by the model (i.e. input variables) is not possible, as one method or type of measurement is applied for each variable and no comparison could be made between different techniques for the assessment of the same variable.

The input variables for Eq. 7.6 consist of: i) a potential denitrification rate; ii) soil nitrate content; iii) volumetric water content and total soil porosity for the calculation of WFPS; and iv) soil temperature. The model authors (Hénault and Germon, 2000) have suggested a protocol for measuring potential denitrification rates based on the acetylene block technique (Yoshinary and Knowles, 1976) in static cores at 20^{o}C and nitrate content near 200 mg N kg^{-1}. The reference temperature and the added nitrate concentration were kept the same, as they affect the estimation of the K and Q_{10} parameters of the functions f_N and f_T respectively, but instead of incubations with acetylene, a ^{15}N tracer method (adapted from Trimmer *et al.*, 2003) was used for measuring potential denitrification rate in slurries (for method details see section 4.4.7). The advantages and disadvantages of the C_2H_2 inhibition technique versus ^{15}N tracer methods are discussed in detail in section 4.4.7, however in the case of estimating the

D_p for the purpose of NEMIS, no significant differences should be expected due to the method used as long as the conditions (i.e. incubation temperature, nitrate concentration and no addition of organic carbon substrate) follow the model specifications.

7.5.1 *Measurement of in situ denitrification rates*

For the purpose of whole-model validation, *in situ* denitrification measurements were needed for comparison against the model predictions. The C_2H_2 inhibition technique was used by the model authors for measuring denitrification rates on cores incubated under field water and nitrate content conditions in order to estimate *in situ* denitrification rates.

Generally, the most popular method for measuring *in situ* denitrification rates in floodplain and riparian zone surface soils (Pinay *et al.*, 2000, 2007a; Hefting *et al.*, 2003, 2006b; Forshay and Stanley, 2005; Orr *et al.*, 2007) has been (and probably still is) the static core acetylene inhibition method, as it was described by Yoshinari and Knowles (1976) and subsequently modified by Tiedje *et al.* (1989) and Groffman *et al.* (1999). Briefly, the method entails the extraction of an 'intact' soil core, typically from between 5 and 20 cm in the topsoil, and its subsequent incubation in the field or in the laboratory under 'field' conditions in a C_2H_2 atmosphere, where N_2O accumulates during an incubation period between 1 and 24 hours. While this method is simple to carry out and allows large numbers of samples to be run (Groffman *et al.*, 2006), both under aerobic or anaerobic conditions in waterlogged or simply moist soil (Yoshinari *et al.*, 1977), the use of C_2H_2 has several drawbacks (Groffman *et al.*, 2006 and references therein), of which the incomplete inhibition of N_2O reduction and the slow diffusion of C_2H_2 into fine-textured saturated soils would seriously underestimate the denitrification rates in this study.

An alternative method for the direct quantification of *in situ* denitrification is the application of ^{15}N-labelled NO_3^- and the subsequent measurement of the produced ^{15}N-labelled N_2 with the aid of an Isotope Ratio Mass Spectrometer (IRMS). Although this method has been considered one of the best for soil studies, its application has been limited due to the lengthy procedures and expensive instrumentation required (Groffman *et al.*, 2006). The most important criticism of this method is the possibility of overestimating denitrification due to the addition of ^{15}N-labelled NO_3^-, to achieve high

levels of ^{15}N enrichment, and thus the stimulation of denitrification by increasing the availability of N. It has been shown that when this method is used in agricultural soils, the fertilisation problem is less likely to appear, while where the ambient N concentrations are low or very variable, they should be determined prior to the ^{15}N tracer experiment in order to adjust dosing accordingly (Groffman *et al.,* 2006).

The ^{15}N tracer method has been successfully used to measure coupled nitrification-denitrification in sediment cores from aquatic systems (reviewed in Steingruber *et al.,* 2001) and in wetland sediment microcosm flow-through systems (Stepanauskas *et al.,* 1996; Hoffmann *et al.,* 2000), but these methods are very laborious, involve long pre-incubation times and therefore the number of samples is usually limited (Groffman *et al.,* 2006). Moreover, enclosure effects are a major problem in incubation studies, as it is essential to keep hydrodynamics and concentrations of O_2 and NO_3^- near *in situ* conditions to produce accurate estimates of *in situ* denitrification rates (Groffman *et al.,* 2006).

Enclosure effects are not a concern in aquifer and in small stream studies, where ^{15}N tracer methods have also been used with relatively little disturbance of *in situ* conditions Groffman *et al.,* 2006). The approach for groundwater involves the injection through a piezometer of an injectate solution containing the ^{15}N tracer and a conservative tracer such as Br^-, used to correct for dilution, and subsequently recover the injected plume from several piezometers along the flow path (Smith *et al.,* 1996, 2004) or use the same piezometer for dosing and sampling of the groundwater in the so-called 'push-pull' method (Istok *et al.,* 1997; Addy *et al.,* 2002; Kellogg *et al.,* 2005) and analyse the samples for dissolved ^{15}N-labelled N_2. These methods are appropriate for relatively permeable aquifers (e.g. sandy) with significant groundwater flows at depths larger than 1 m, and therefore are unlikely to be successful in the shallow groundwater table of the heavy clay alluvium of the River Cole floodplain.

For the purpose of measuring *in situ* denitrification rates in the saturated topsoil (10 cm depth) with the application of ^{15}N tracer at several locations with relatively short incubation times, a soil-probe method would be the most appropriate. Such methods have been described for saturated hydromorphic soils (Well *et al.,* 2003), for wetland sediments (Whitmire and Hamilton, 2005) and river sediments (Sanders and Trimmer,

2006). While the above methods are based on the same principle of the 'push-pull' method by Addy *et al.* (2002), they were designed for high porosity media and therefore further adaptations are needed before being applied to our silty-clay topsoil texture. The other limitation of the soil-probe method is that it is operational under saturation conditions only, but this is counteracted by the possibility of multiple measurements in several locations, thus accounting for larger spatial variability.

7.5.2 *Method description*

For the present study, a first attempt was made to use the mini-probe system developed by Sanders and Trimmer (2006) for measuring denitrification at the top 10 cm of saturated floodplain soils. However, this attempt was unsuccessful due to the fine texture of the River Cole floodplain soils that led to the immediate clogging of the mini-probe system (developed for river-bed sediments of coarser texture), thus rendering it unusable. Therefore, it was decided to follow the method principle of Sanders and Trimmer (2006) but using, instead of their mini-probe system, Rhizon samplers (Rhizon SMS, 10 cm; Eijkelkamp Agrisearch Equipment, Giesbeek, the Netherlands) for both sampling porewater nutrients and also applying ^{15}N-tracer to the saturated topsoil.

Rhizon samplers (Figure 7.5.1) are made of a hydrophilic porous polymer tube, with a typical pore diameter of 0.1 μm, extended with a PVC tube. The outer diameter of a Rhizon is 2.4 mm, and the filter section has a length of 5 or 10 cm. To support the polymer, a wire is fixed to one end of the porous polymer. The fluid sampled from the sediment flows into the tiny space between the porous tube and the supporting wire. A Rhizon has several advantages compared with other sampling devices: low mechanical disturbance of the sediment due to small diameter (2.4 mm), low dead volume (0.5 mL including the PVC tubing), minimised sorption processes on the inert polymer and no aging during long-term deployments (Seeberg-Elverfeldt *et al.,* 2005). The pore size ensures the extraction of microbial- and colloidal-free, ready-to-analyse solution (Knight *et al.,* 1998).

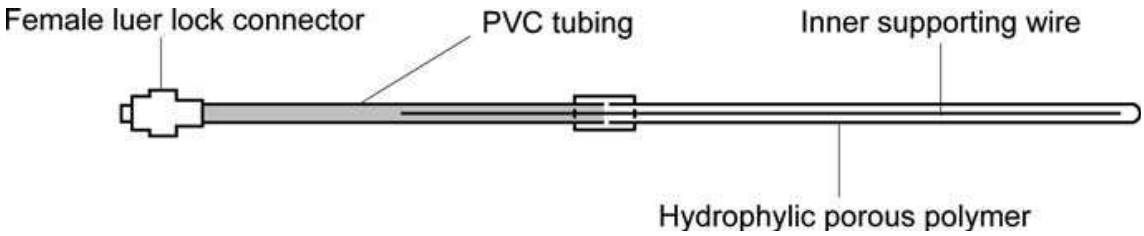

Figure 7.5.1: Schematic diagram of a Rhizon sampler (after Shotbolt, 2009).

The drainage area of a Rhizon is distributed evenly along the entire filter section. The area of influence is given by calculating the radius of a cylinder, which represents the sediment volume from which the porewater is extracted. The radius of this influenced cylindrical volume around a Rhizon is calculated according to Seeberg-Elverfeldt *et al.* (2005) by:

$$r = \sqrt{\frac{V_{sample}}{P_t \cdot \pi \cdot l}} \tag{7.11}$$

where V_{sample} is the volume of the sampled porewater (mL), P_t the porosity of the surrounding sediment or soil, and l the length of the filter section (cm). Rhizon samplers have been used for porewater sampling in sediments and soils for nitrate (Luo *et al.*, 2003), ammonium under anaerobic conditions (Song *et al.*, 2003), DOC (Sigfusson *et al.*, 2006), dissolved methane (Alberto *et al.*, 2000) and metals (Shotbolt, 2009), but not yet used for the application of ^{15}N tracer.

The sampling design for the *in situ* measurements was based on the transect set up for the BZ and PM zones described in section 4.4.1.1. Specifically, the Rhizon samplers were deployed in triplicates in three locations within each sampling transect in BZ (Figure 7.5.2), generating 27 measurements in total, in March 2008, and another 27 measurements in July 2008. Moreover, the same approach was followed in March 2008 for the riparian and channel depression transects of the PM, which shared the same hydrological and soil properties with the BZ, in order to increase the sample size for the validation of the model, generating 19 additional samples (Figure 7.5.3). Due to the chosen method, which can only be applied in saturated soil, sampling was restricted in inundated locations with a few centimetres of overlying water.

Figure 7.5.2: Location of Rhizon samples in the BZ. Each cluster represents a triplicate Rhizon deployment. GHI clusters in arable transect, DEF clusters in middle transect and ABC clusters in riparian transect.

Figure 7.5.3: Location of Rhizon samples in the PM. Each cluster represents a triplicate Rhizon deployment. KLM clusters in the channel depression transect and OPQ clusters in the riparian transect.

Before the deployment of the Rhizon sampler, a syringe (10 mL, Plastipak™, Becton Dickinson, Spain) containing degassed deionised water (10 mL, Purelab Ultra, Elga Lab Water, UK) is connected via a luer-lock adaptor (2*LL female, Eijkelkamp Agrisearch Equipment, Giesbeek, the Netherlands) to the Rhizon and the polymer filter is flushed throughout its length. The Rhizon is inserted gently in the ground (10 cm depth), simply by pushing in soft soil or using a stainless steel wire (diameter <2.4 mm) to create a narrow hole and push away any small gravel. After insertion, the syringe remains attached to the Rhizon, which is left for 30 min for the porewater nitrate concentration to stabilise (Sanders and Trimmer, 2006) and the suspended sediment in the overlying water to settle.

Following the stabilisation time, porewater is drawn from the Rhizon by pulling the syringe plunger, or if this is not possible due to high suction pressure, vacuum is applied via positioning a wooden spacer (Eijkelkamp Agrisearch Equipment, Giesbeek, the Netherlands) on the syringe plunger (Figure 7.5.4). Usually, 10 - 15 minutes of vacuum was enough for collecting 5 mL of sample. After disposing of the first 0.5 mL of the sample (dead volume of the Rhizon), approximately 2 mL of the sample is gently discharged into a crimp top (aluminium over butyl rubber with PTFE liners, Chromacol Ltd, UK) mini-vial (1,200 µl, Chromacol Ltd, UK) and allowed to overflow (to minimize atmospheric gas exchange). Bacterial activity is inhibited by adding $ZnCl_2$ (25 µL 50 % w/v) before sealing the mini-vial. The remaining sample is transferred into a glass vial for background determination of NO_3^- via ion exchange chromatography (see section 4.3.3) and DOC analysis (see section 4.3.5). The reference mini-vial represents the T0 of the *in situ* timed experiment.

As soon as the reference sample is drawn, a second syringe containing 2.5 mL of degassed 500 µM $Na^{15}NO_3^-$ (99.3 at % ^{15}N; Sigma-Aldrich, Poole, UK) is connected to the luer-lock adaptor of the Rhizon sampler and its contents are gently discharged. Following, on average, 15 minutes of incubation time, 2 mL of sample is drawn and transferred in a mini-vial, as described above, while no further samples are collected for anion analysis. If vacuum needs to be applied for collecting the sample, the duration of the vacuum application is added to the incubation time. The above step is repeated three times generating the timed samples T1, T2 and T3 of the *in situ* measurement.

After the completion of the T3 step, the Rhizon is removed and at the same location a soil sample is collected via a known volume syringe corer for porosity and particle size determination and C and N elemental analysis, while the soil moisture is measured with a theta meter (Type HH1, Delta-T Devices, Ltd., Cambridge, UK) and the soil temperature with a soil thermometer.

On return to the laboratory, all of the mini-vials were equilibrated to 22 °C and a headspace (200 µl analytical grade helium) introduced using a 2-way valve and a gas-tight micro litre syringe (Hamilton, Bonaduz, Switzerland). The mini-vials were then shaken vigorously, inverted and stored upside down overnight to allow the N_2 gas to equilibrate between the water phase and headspace. The isotopic composition of $^{15}N_2$ in the headspace of the mini-vials was analysed with a CF/IRMS as per section 4.4.7.

For the estimation of *in situ* denitrification rates, only total denitrification was considered (i.e. the coupled nitrification-denitrification was not taken into account) as suggested by Sanders and Trimmer (2006). The signal from the mass spectrometer was converted into concentrations of $^{29}N_2$ and $^{30}N_2$ in the pore water and then production per unit volume of soil per unit time. Values were calculated as excess over that in the references before the addition of $^{15}NO_3^-$ according to and adapted from Thamdrup and Dalsgaard (2000):

$$pnmolN_2 cm^{-3} h^{-1} = \left[\left(\frac{^{x}N_2}{\sum N_2} \right)_{sample} - \left(\frac{^{x}N_2}{\sum N_2} \right)_{reference} \right] \cdot \sum N_{2\,sample} \cdot \frac{1}{\alpha} \cdot V \cdot \frac{1}{Vs} \cdot \frac{Vp}{Vsd} \cdot t^{-1} \quad (7.12)$$

where p nmol N_2 cm^{-3} h^{-1} was the production of either $p^{29}N_2$ or $p^{30}N_2$; the fractions $^{x}N_2/\Sigma N_2$ represent the signal ratio for either $^{29}N_2$ or $^{30}N_2$ ($^{x}N_2$) to total signal ΣN_2 (total signal for *m/z* ratios 28, 29 and 30 for either *sample* or *reference*, respectively); α the concentration of N_2 in pure water at equilibrium with air; V the volume of the mini-vial headspace (mL); *Vs* the volume of the porewater in the mini-vial (mL); *Vp* the volume of the porewater in the soil cylinder influenced by the Rhizon (mL); *Vsd* the volume of the soil cylinder influenced by the Rhizon (cm^3) and t the duration (h) of linear $p^{29}N_2$ and $p^{30}N_2$ production. Both D_{15} (denitrification of the $^{15}NO_3^-$ spike) and D_{14} (denitrification of ambient $^{14}NO_3^-$) were calculated using the classic IPT expressions:

$$D_{15} nmolNcm^{-3}h^{-1} = p^{29}N_2 + \left(2 \cdot p^{30}N_2\right) \quad (7.13)$$

$$D_{14} nmolNcm^{-3}h^{-1} = \frac{p^{29}N_2}{2 \cdot p^{30}N_2} \cdot \left(p^{29}N_2 + 2 \cdot p^{30}N_2\right) \quad (7.14)$$

An estimate for an areal rate of denitrification in the common units kg N ha^{-1} d^{-1} was calculated by converting nmol N to kg (15 or 14 the atomic mass of N multiplied by 10^{-12}) and scaling up from cm^3 to ha (one ha at 10 cm depth equals 10^9 cm^3) and finally multiplied by the 24 hours for one day.

Figure 7.5.4: Rhizon sampler attached to a syringe via a luer-lock adaptor and vacuum application with a wooden spacer in the syringe's plunger. (photo: F. Sgouridis).

The *in situ* measurements performed in March 2008 and July 2008 were merged into one dataset that was used to validate the NEMIS predictions.

7.5.3 *Site selection and model application database*

For the purpose of assessing the suitability of NEMIS as a decision support tool for predicting the denitrification capacity of a floodplain area across a range of hydrological, temperature and nitrate loading conditions, an extended database is needed that covers the temporal variations of the above variables across at least one monitoring year. Due to the limited availability of measuring instruments but also the time and cost constraints associated with the fieldwork and subsequent laboratory analyses, the spatial variability of the NEMIS predictions was not investigated, but the study focused on assessing the temporal variability in one area of the reconnected floodplain of the River Cole. The selected sampling site for the application of NEMIS is the Buffer Zone (BZ) area for the following reasons:

- The surface and subsurface hydrology of the site has been monitored for two years and there was evidence that the hydrological conditions for the occurrence of denitrification exist.
- The topsoil in the BZ is silty clay loam, which is within the range of soil types for which the model was previously successfully applied, and therefore the calibrated model parameters should perform satisfactorily.
- The BZ site has the typical characteristics of a lowland gently sloping riparian buffer zone within a re-connected floodplain, situated between the edge of agricultural land and the river, having a maximum width of 30 m, and predominantly herbaceous vegetation adapted to frequent inundation. Therefore, it is a good representative of a restored floodplain aimed to achieve water quality targets.

The database for the annual simulation of denitrification at the BZ site was compiled for the period November 2007 - October 2008 and consisted of:

1. One D_p measurement (method adapted from section 4.4.7 with higher concentration of nitrate (3 mM) in the spike and incubation temperature 20 ^{o}C) in February 2008, representing the autumn, winter and spring potential (Hénault and Germon, 2000) and one measurement in July 2008 for the summer potential. Additionally, the D_p was also measured for the B and C soil horizons (50 and

100 cm depth respectively), with the aim of extending the application of NEMIS to subsurface soil horizons, where denitrification was also occurring.

2. A continuous record of temperature with three sensors at 10, 50 and 150 cm depth (method described in 4.2.3.5).
3. A continuous record of soil volumetric water content with three probes at 20, 70 and 120 cm depth (method described in 4.2.3.5).
4. Two measurements of soil bulk density for the A horizon (0-10 cm depth) during the sampling for the D_p in February and July 2008 and one for the B and C horizons in February 2008. The soil bulk density was used to estimate total soil porosity according to Rowell (1994) (method described in 4.4.2).
5. Monthly measurements of soil nitrate content with five replicates per horizon on each occasion (sampling strategy as per section 4.4.1.4 and analysis method as per 4.4.5). The monthly measurements were linearly interpolated for the simulation (Hénault and Germon, 2000).

7.6 *Results and Discussion*

7.6.1 *In situ denitrification rates*

The actual denitrification rates and the topsoil properties measured in March 2008 and July 2008 in the three transects (riparian, middle and arable) of the BZ and in the channel depression and riparian transects of the PM are summarised in Table 7.6.1. The mean denitrification rate of the BZ area for March 2008 was 0.57 (± SE 0.09) kg N ha^{-1} d^{-1} and no significant differences were found between the riparian and middle field transect samples (Mann-Whitney; U=35, Z=-0.49, P>0.05). The PM topsoil samples displayed similar mean denitrification rates, 0.68 ± SE 0.18 kg N ha^{-1} d^{-1}, but significantly higher rates were measured in the riparian transect samples (Mann-Whitney; U=0, Z=-3.58, P<0.01). Actual denitrification rates in July 2008 were measured only at the BZ site and they were significantly lower than the rates measured in March (Mann-Whitney; U=11, Z=-6.17, P<0.01). The mean denitrification rate for July 2008 was 0.014 ± SE 0.003 kg N ha^{-1} d^{-1}, 40 times lower than the rate measured in March, while denitrification rates decreased with increasing distance from the stream, but not significantly (Figure 7.6.1 A).

The porewater nitrate content was significantly different between the March and July samples (Mann-Whitney; U=61, Z=-5.91, P<0.01). The mean porewater nitrate content for the July BZ samples was 0.12 ± SE 0.05 mg N kg^{-1} dry soil, while no significant differences were found between transect samples (Kruskal-Wallis; χ^2=0.39, df=2, P>0.05). Higher nitrate content was measured in the porewater of the March samples, mean 2.96 ± SE 0.74 and 1.97 ± SE 0.46 mg N kg^{-1} dry soil for the BZ and PM samples respectively that were not different from each other.

Table 7.6.1: Actual denitrification rates and soil and porewater physical properties in the BZ and PM sampling transects on March 2008 and July 2008. Mean values and standard errors in parentheses. Different lower case letters indicate significant difference of the means.

	Denitrification ($kg\ N\ ha^{-1}\ d^{-1}$)	**Porewater Nitrate** ($mg\ N\ kg^{-1}$)	**Temperature** (^oC)	**Dry Bulk Density** ($g\ cm^{-3}$)	**Water content** ($cm^3.cm^{-3}$)	**Organic carbon** (%)	**TOC/TN**	**DOC** ($mg\ L^{-1}$)
BZ Mar. 08 (n=18)	0.57 (0.09)	2.96 (0.74)	7.6 (0.2)	0.68 (0.02)	0.76 (0.01)	6.1 (0.48)	11.06 (0.17)	21.67 (3.95)
Riparian (n=9)	0.54 (0.14)a	1.89 (0.73)a	8.3 (0.22)	0.65 (0.04)a	0.78 (0.02)a	5.31 (0.64)ac	10.93 (0.29)a	8.64 (1.61)ac
Middle field (n=9)	0.59 (0.12)a	4.02 (1.23)a	6.8 (0.05)	0.70 (0.03)a	0.73 (0.02)abc	6.89 (0.65)ab	11.18 (0.18)ab	34.71 (3.98)b
PM Mar. 08 (n=18)	0.68 (0.18)	1.97 (0.46)	7.4 (0.07)	0.78 (0.01)	0.75 (0.01)	5.86 (0.66)	11.98 (0.24)	10.17 (0.57)
Ch. Depression (n=9)	0.075 (0.014)b	1.20 (0.46)a	7.6 (0.07)	0.73 (0.01)a	0.73 (0.003)b	6.49 (0.9)abc	11.76 (0.29)bc	11.76 (0.56)a
Riparian (n=9)	1.28 (0.21)c	2.75 (0.72)a	7.1 (0.04)	0.81 (0.03)a	0.76 (0.02)a	5.24 (0.97)ac	12.2 (0.37)c	8.37 (0.53)c
BZ Jul. 08 (n=27)	0.014 (0.003)	0.12 (0.05)	16.4 (0.13)	0.73 (0.02)	0.7 (0.01)	6.79 (0.53)	10.07 (0.16)	37.8 (3.1)
Riparian (n=9)	0.02 (0.011)b	0.07 (0.012)b	16.6 (0.09)	0.52 (0.03)b	0.74 (0.008)ab	7.98 (0.51)b	10.58 (0.13)ad	47.73 (7.87)b
Middle field (n=9)	0.014 (0.003)b	0.08 (0.021)b	16.1 (0.2)	0.83 (0.03)a	0.69 (0.006)c	8.14 (1.12)ab	9.97 (0.32)de	36.3 (3.24)b
Arable field (n=9)	0.009 (0.003)b	0.21 (0.14)b	16.4 (0.31)	0.83 (0.04)a	0.66 (0.007)d	4.25 (0.15)c	9.65 (0.26)e	29.57 (1.86)b

The mean topsoil temperature for the March measurements was 7.6 ± SE 0.2 ^{o}C, significantly lower than the temperature during the July measurements, 16.4 ± SE 0.13 ^{o}C. The dry bulk density was not significantly different between the two seasons (Mann-Whitney; U=454, Z=-0.45, P>0.05) and ranged between 0.52 - 0.83 g cm^{-3}. Additionally, a gradient of decreasing water content with increasing distance from the stream in the BZ during the July measurements was observed (Figure 7.6.1 B). However, the water content range, with the measurements from both seasons pooled together, was 0.62 - 0.85 cm^3 H_2O cm^{-3} soil, which corresponded to a range of WFPS from 68 to 100 % that was above the threshold (62 %) that triggers denitrification in the NEMIS model.

The organic carbon content was not significantly different between measurements in the BZ and the PM areas or among transects in each area in March 2008 and ranged between 0.63 and 9.82 %. Moreover, no significant difference in the organic carbon content was observed between the two seasons (Mann-Whitney; U=416, Z=-0.98, P>0.05). The ratio TOC/TN was significantly different between the March BZ and PM samples and also the July BZ samples (Kruskal-Wallis; χ^2=25.7, df=2, P<0.01). No differences were observed between transects in March 2008, but in July, the ratio TOC/TN decreased with increasing distance from the stream towards the arable field. Finally, the DOC in the porewater was significantly higher in the BZ samples compared to the PM samples in spring (ANOVA; df=1, F=8.81, P<0.01), while the July samples had higher DOC than the March samples (Mann-Whitney; U=494, Z=-5, P<0.01). Although not significant, the DOC in the BZ summer samples ranged from higher values closer to the stream to lower values in the arable field (Figure 7.6.1 C).

The topsoil particle size distribution was investigated for the March 2008 samples (Figure 7.6.2). The PM channel depression samples had significantly higher clay content (ANOVA; df=3, F=5.48, P<0.01), while the BZ riparian samples contained more silt than the BZ middle samples that also contained significantly less silt than the PM samples (ANOVA; df=3, F=6.94, P<0.01). The sand fraction (between 60 and 2000 μm) was significantly higher in the BZ middle samples and the PM riparian samples (ANOVA; df=3, F=7.21, P<0.01). The BZ riparian samples and the PM channel depression samples were classified as silty clay, the BZ middle field samples as clay loam and the PM riparian samples as silty clay loam.

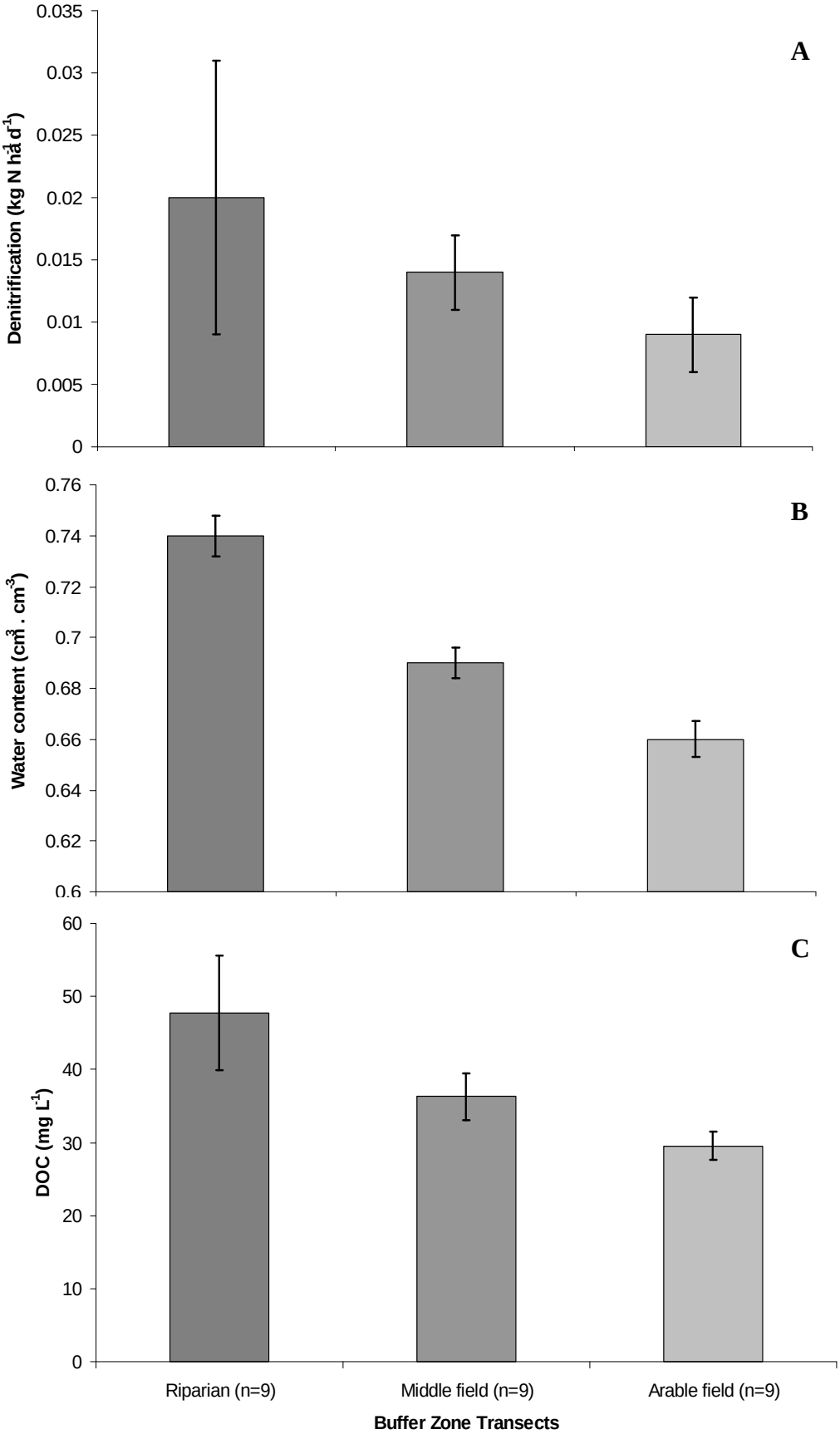

Figure 7.6.1: Mean (± SE) denitrification rate (A), volumetric water content (B) and DOC (C) in the three transects of the BZ in July 2008.

Correlation analysis between the denitrification rates (the samples from both seasons and all areas pooled) and the soil and porewater physical properties (Table 7.6.2) has indicated a significant negative correlation between denitrification and temperature (Spearman; r=-0.78, N=58, P<0.01), while denitrification correlated positively with the porewater nitrate content (Spearman; r=0.64, N=58, P<0.01) and the water content (Spearman; r=0.61, N=58, P<0.01). Forward regression analysis between the same variables and the denitrification rate indicated a stronger predictive power of the water content (MRA; r^2=0.29, F=22.42, P<0.01) followed by the temperature that explained 28% of the variance in denitrification rates (MRA; r^2=0.28, F=19.34, P<0.01) and the porewater nitrate with only 11% explanatory power (MRA; r^2=0.11, F=6.28, P<0.05).

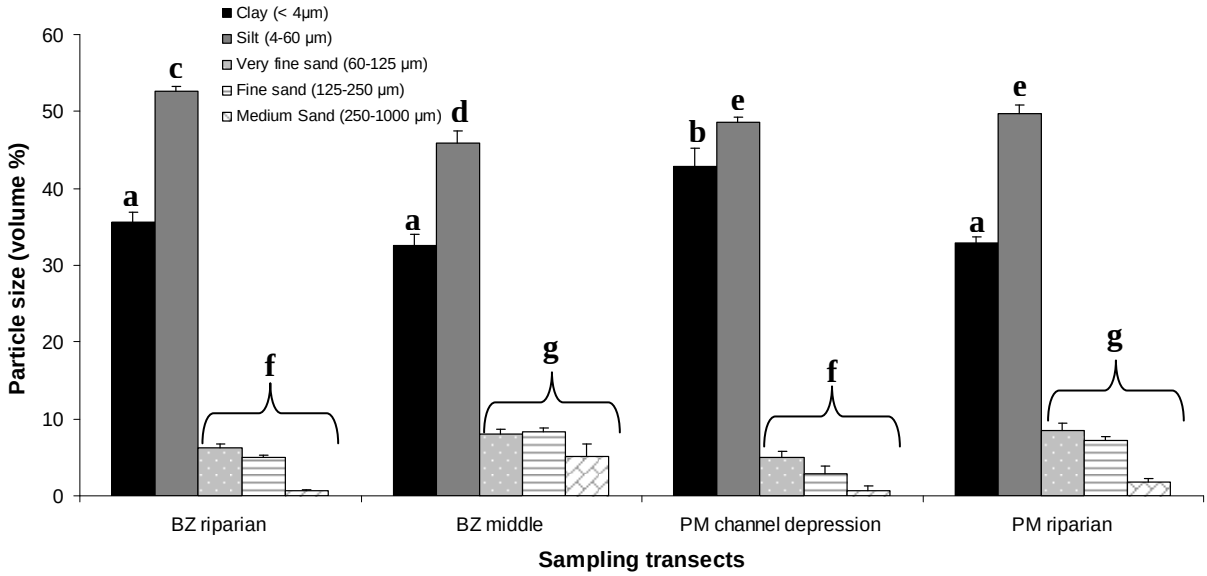

Figure 7.6.2: Particle size distribution in the topsoil of the BZ and PM sampling transects in March 2008. Different lower case letters indicate significant difference of the means. The sand fractions have been grouped into one fraction between 60 and 2000 µm for ANOVA analysis.

Table 7.6.2: Correlation matrix between actual denitrification rates and soil and porewater variables (Spearman rank-order, *Significance at the 0.05 probability level, **Significance at the 0.01 probability level).

Variables/Correlation coefficients		Denitrification	Porewater Nitrate	Temperature	Porosity	Water content	Organic carbon (%)	TOC/TN	DOC	Clay (%)	Silt (%)
Denitrification	*R*	1	**0.643****	**-0.775****	0.073	**0.608****	0.009	**0.531****	**-0.498****	-0.256	0.211
	P	.	0.000	0.000	0.585	0.000	0.942	0.000	0.000	0.131	0.216
	N	58	58	58	58	58	58	58	53	36	36
Porewater Nitrate	*R*		1	**-0.670****	0.226	**0.425****	-0.154	**0.503****	**-0.464****	0.079	-0.122
	P		.	0.000	0.075	0.000	0.229	0.000	0.000	0.648	0.477
	N		63	63	63	63	63	63	58	36	36
Temperature	*R*			1	0.010	**-0.394****	0.041	**-0.545****	**0.421****	0.324	**0.448****
	P			.	0.938	0.001	0.752	0.000	0.001	0.054	0.006
	N			63	63	63	63	63	58	36	36
Porosity	*R*				1	**0.529****	0.310*	0.193	0.111	0.054	0.139
	P				.	0.000	0.013	0.129	0.405	0.755	0.419
	N				63	63	63	63	58	36	36
Water content	*R*					1	0.107	**0.403****	**-0.360****	-0.041	**0.589****
	P					.	0.404	0.001	0.006	0.813	0.000
	N					63	63	63	58	36	36
Organic carbon (%)	*R*						1	0.199	0.278*	-0.292	-0.032
	P						.	0.118	0.035	0.084	0.854
	N						63	63	58	36	36
TOC/TN	*R*							1	**-0.475****	-0.013	-0.295
	P							.	0.000	0.941	0.081
	N							63	58	36	36
DOC	*R*								1	-0.072	-0.358*
	P								.	0.689	0.041
	N								58	33	33
Clay (%)	*R*									1	-0.063
	P									.	0.716
	N									36	36
Silt (%)	*R*										1
	P										.
	N										36

A principal component analysis (PCA) on soil and porewater variables for both seasons and all sampling transects resulted in two components with eigenvalues larger than 1, which explained 63.5 % of the total variance (Table 7.6.3). A correlation bi-plot of the PCA results on the soil and porewater variables is shown in Fig. 7.6.3. Cluster centroids (average score on each component, with standard errors) per sampling transect per season are presented in Fig. 7.6.4. As can be seen from the bi-plot, the majority of the environmental variables correlated with the first component, which explained 40% of the observed variance. The soil water content, the porewater nitrate and the ratio TOC/TN correlated with the positive axis of component 1, while the temperature and the DOC correlated with the negative axis of component 1 (Table 7.6.3). The second component explained 23 % of the observed variance and two variables, namely the total porosity and the organic carbon content correlated strongly with component 2 (Table 7.6.3). It is clear from the cluster centroids that the samples between the two seasons were separated along component 1, with the July measurements being characterised by higher temperatures, higher DOC content but lower porewater nitrate and lower volumetric water content. Moreover, the three BZ transects in July 2008 were separated along component 2 mainly due to their differences in organic carbon content. The March 2008 samples formed a more closely associated cluster with considerable overlap between the transect samples and correlated with the porewater nitrate and the soil water content that were also the most important predictors of denitrification as shown by the correlation and regression analysis.

Table 7.6.3: PCA results on the soil and porewater variables. ***Correlation significant at the 0.01 probability level.

Variable	Component 1	Component 2
Nitrate	0.673***	0.083
Temperature	-0.888***	0.187
Porosity	0.241	0.818***
Water content	0.706***	0.438
Organic carbon	-0.104	0.663***
TOC/TN	0.762***	0.028
DOC	-0.649***	0.537
Variance explained, % of total	40.2	23.3

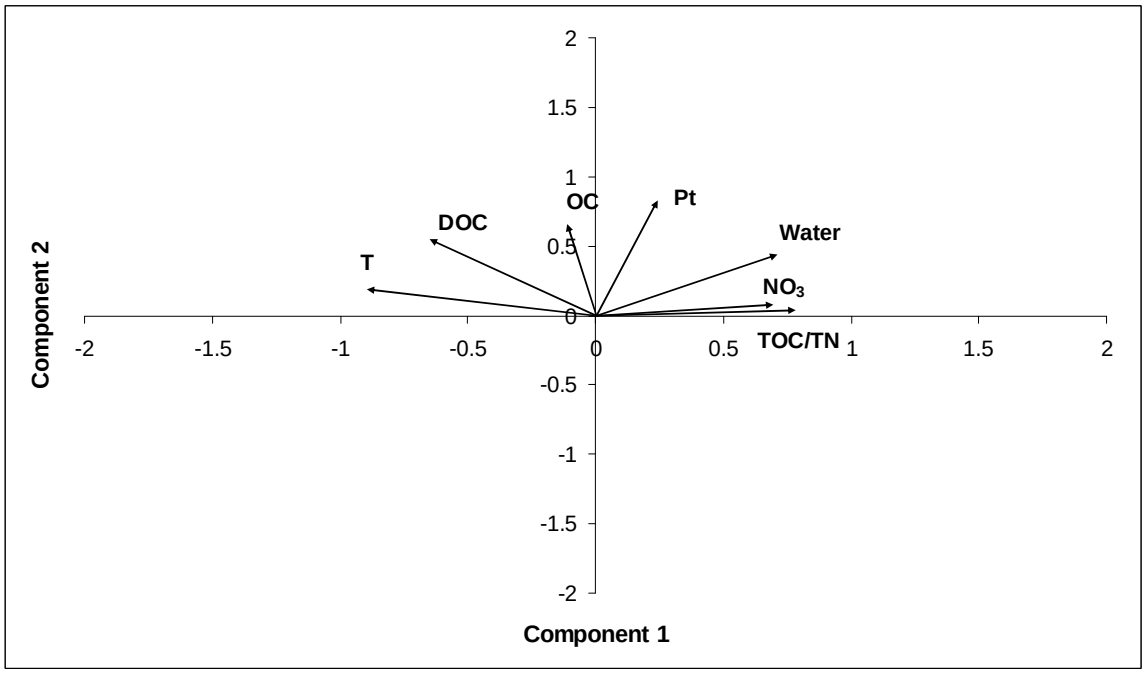

Figure 7.6.3: Correlation bi-plot from the PCA analysis on soil and porewater variables. Correlations of the variables with the main axes are given by arrows. T: Temperature; DOC: Dissolved Organic Carbon; OC: Organic Carbon; Pt: Total soil porosity; Water: Water Content; NO_3^-: Porewater nitrate.

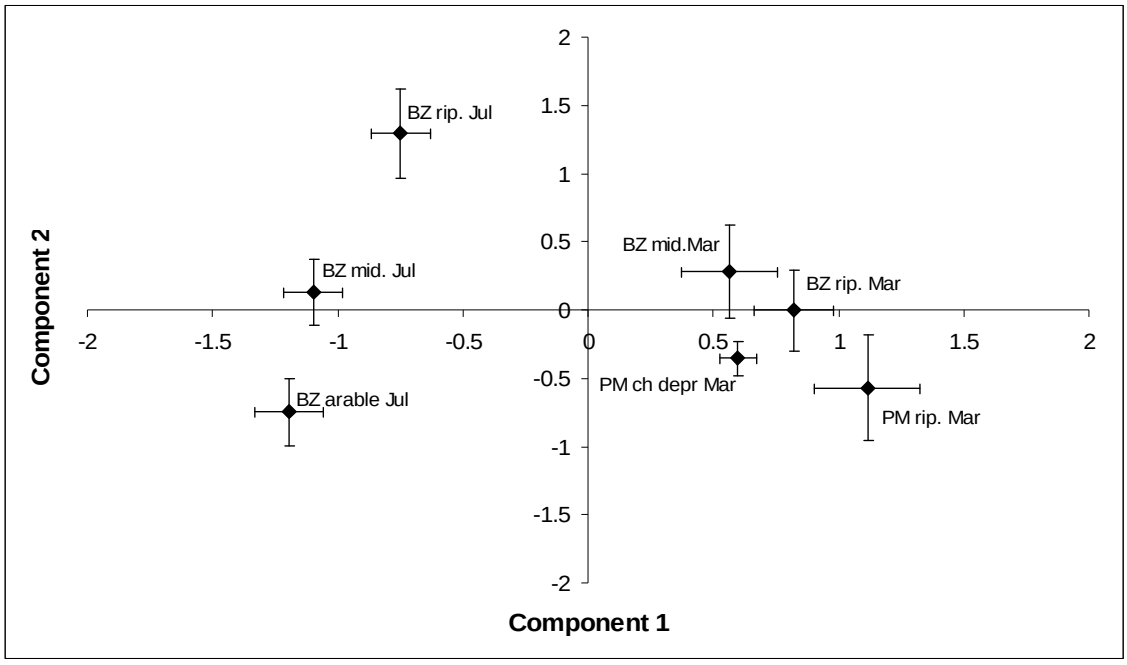

Figure 7.6.4: Correlation bi-plot from the PCA analysis with cluster centroids for the sampling transects in the BZ and PM areas for the March and July 2008 measurements.

In situ injection of $^{15}NO_3^-$ tracer and subsequent quantification of denitrification rates from dissolved ^{15}N gases (^{15}N-N_2 and ^{15}N-N_2O) has been used extensively in saturated zone studies in for example a grassed buffer strip (Mengis *et al.,* 1998), a riparian sandy aquifer (Addy *et al.*, 2002), a petroleum-contaminated sandy aquifer (Schurmann *et al.,* 2003), hydric permeable soils of riparian wetlands (Well *et al.,* 2003; Kellogg *et al.,* 2005), streambanks of restored urban riparian zones (Kaushal *et al.,* 2008) and the hyporheic zone of river islands (Clilverd *et al.,* 2008). However, these "push-pull" applications are confined to between 0.15 and 10 m below the soil surface, where denitrification usually declines with depth following the decline in groundwater DOC availability (Hill *et al.,* 2000), as it was also shown in the present study, and are therefore not suitable for comparison with surface soil denitrification rates.

The vast majority of studies that have measured actual denitrification rates in surface soil used an acetylene-based 'static core' method (Groffman *et al.,* 2006). Hefting *et al.* (2003, 2006a) have measured a mean denitrification rate of 0.8 kg N ha^{-1} d^{-1} at 10 cm depth in sandy riparian buffer zones, which is slightly higher than the mean March rate measured in the BZ and PM areas in the present study. This difference is probably due to the high nitrate-loading rates via the shallow inflowing groundwater in the Dutch buffer zones, where nitrate was not limiting denitrification. The March rates were within the range measured in silty-clay and silty-sand Swiss riparian zones in spring (Cosandey *et al.,* 2003a) and slightly higher than the annual range measured across 15 alluvial sites along the Garonne River (Pinay *et al.,* 2000). Clément *et al.* (2003) reported a narrow annual range of actual denitrification rates from silty-clay loam grassland and shrub riparian zones that corresponded to the upper bound of our measurements, but the high fertiliser application rates leading to groundwater nitrate concentrations between 10 and 20 mg N L^{-1} was responsible for shifting upwards their lower bound of the denitrification range. Finally, denitrification rates measured in alluvial soils across a European climatic range (Pinay *et al.,* 2007a) displayed a wide range between 0 and 10 kg N ha^{-1} d^{-1} that encompasses the rates measured in both seasons at the present study.

The mean denitrification rate for the BZ area in March 2008 was 1.5 % of the potential denitrification rate of the topsoil measured in spring 2008. Similarly, the mean denitrification rate for the PM was 1.6 % of the potential denitrification rate, while the low actual rate measured in BZ in July 2008 was <1 % of the corresponding potential

rate for the summer 2008. In Cosandey et al (2003a), the potential denitrification rate, measured with denitrifying enzyme activity (DEA), was 18 to 34 times higher than the actual denitrification rates in two hydromorphic riparian soils. The DEA was always significantly higher than the *in situ* rates of denitrification in the upper soil horizons (0 - 25 cm) by 2 to 25 times along different topohydrosequences in three riparian wetlands with differing vegetation cover (Clément *et al.,* 2002). Although the DEA represents the potential denitrifying activity at the time of sampling and is expected to be several times higher than the on-site measured denitrification rates (Martin *et al.,* 1999), in some situations DEA and *in situ* rates have been found to be very similar (Orr *et al.,* 2007), or at least within the same range (Schipper *et al.,* 1993; Bernal *et al.,* 2007) mainly because the *in situ* conditions were approximating the non-limiting conditions of the DEA in terms of nitrate and carbon availability, saturation conditions and temperature. In cases where DEA was measured at higher than the *in situ* temperature, the potential rates were corrected to the temperature of actual rates (Well *et al.,* 2003). The reason for the difference between the potential rates and the *in situ* rates measured in this study is that the potential was measured at 20^{o}C, ambient carbon content and non-limiting nitrate concentration to reflect the maximum potential rate, as required for the application of NEMIS, while the *in situ* measurements were performed at a temperature range (6 - 16.5^{o}C) and ambient carbon and nitrate concentrations, of which the latter were probably limiting for denitrification in the July samples.

Although the *in situ* rates were not statistically different between the BZ transects in both seasons due to high inter-transect variability, a spatial trend was observed in the summer measurements, with higher rates near the stream border (riparian transect) moving gradually to lower rates in the arable field. A similar trend was found by Ettema *et al.* (1999) and Cosandey *et al.* (2003a) and was associated with a lack of frequent anaerobiosis in the upland (arable field edge), which was responsible for lower denitrifier density despite the non-limiting supply of nitrate through high rates of ammonification and nitrification. Lower denitrification rates at the field border were also related to lower soil moisture contents (Hefting *et al.,* 2003) and specifically, denitrification rates were found to be insignificant below 70 % WFPS (Hefting *et al.,* 2006a). The water content in the arable field was significantly lower (Figure 7.6.1 B) than the middle and riparian transects, but the WFPS was not lower than 68 %, as near-saturation conditions was a prerequisite for the *in situ* technique. However, the moisture

content was probably responsible for the spatial trend as the porewater nitrate and DOC were not significantly different between transects.

The most important predictors of actual denitrification rates were the soil water content, the soil temperature, and the porewater nitrate content as indicated by the MRA and correlation analysis. Pinay *et al.* (2007a) found the same variables, with the same order, to be the main controlling factors of denitrification in riparian zones across a European climatic range. Moreover, maximum denitrification was observed for water contents between 0.6 and 0.8 (w/w), which corresponds also to the findings of the present study, although there were no measurements of denitrification with <0.6 water content. According to the PCA, all the spring denitrification rates from both sites were associated closely with higher soil moisture conditions. Higher soil moisture was also responsible for higher spring denitrification rates in created wetlands receiving flood pulses (Hernandez and Mitsch, 2007) in nitrate-stressed riparian zones in the Netherlands (Hefting *et al.,* 2003, 2006a) and in N-addition experiments in a riparian forest in Georgia (Ettema *et al.,* 1999).

Although high soil temperature is traditionally associated with higher denitrification rates (Hernandez and Mitsch, 2007, Pinay *et al.,* 2007a), in the present study the summer measurements that were performed at higher soil temperature displayed lower denitrification rates. However, Kliewer and Gilliam (1995) observed a positive correlation between the nitrous oxide evolution from C_2H_2 incubated cores with mean soil temperature at 10 cm depth, until low nitrate levels appeared to limit denitrification. Indeed, the summer measurements in the BZ were characterised by 1-2 orders of magnitude lower porewater nitrate concentrations than the March samples, and probably were limiting for denitrification despite the high temperature, the saturated conditions and the slightly higher porewater DOC. In a study of denitrification controls on organic riparian soils, Schipper *et al.* (1993) observed a significant non-linear relationship between denitrification and nitrate content and their estimated half-saturation constant was around 5 mg N kg^{-1} (or 150 μM) for nitrate contents of the same magnitude as those found in the March measurements. The fact that the July nitrate content was 2-3 orders of magnitude lower than the half saturation constant in Schipper *et al.* (1993) is an indication that denitrification was indeed limited by nitrate during the summer measurements.

In conclusion, the *in situ* denitrification measurements in the BZ and PM areas during spring and summer 2008 were within the range reported by other studies in similar soil types, nitrate loadings, and climatic range. Therefore, there is confidence that the actual measurements can be used for the validation of NEMIS predictions within a range of soil nitrate contents, a temperature range above and below the 11^{o}C threshold of the f_T function, and at water contents near saturation. Moreover, the actual denitrification rates are several times lower than the potential rate, which is acceptable in the model formulation (Heinen, 2006a). A spatial trend was observed in the summer measurements with higher denitrification rates associated with the higher soil moisture and DOC of the riparian transect, while porewater nitrate followed an opposite gradient from higher concentrations in the arable field to lower in the riparian transect. Overall, the soil water content, the soil temperature, and the porewater nitrate were the most important predictors of the observed variability in denitrification rates, with the nitrate concentration being limiting for denitrification during the summer measurements despite the high soil temperature and the saturated conditions.

7.6.2 *Model validation and parameterisation*

The validation of a model usually requires some measurement of how well the model represents actual measurements. These measurements are often known as goodness-of-fit statistics (Mulligan and Wainwright, 2004). The goodness-of-fit statistics to be used in describing the model's performance relative to the observed data should be selected prior to the validation (Engel *et al.*, 2007). In most instances, both visual comparisons of predicted and observed data, as well as goodness-of-fit statistics, should be used. Plotting predicted and observed results along with the 1:1 line can be helpful in identifying model bias. In conjunction with the plot, the coefficient of determination, r^2, which represents the proportion of variance in the observed data explained by the model results, can be calculated as in Eq. 7.15:

$$r^2 = \left(\frac{\sum_{i=1}^{n} [O_i - \overline{O}] \cdot [M_i - \overline{M}]}{\sqrt{\sum_{i=1}^{n} [O_i - \overline{O}]^2} \cdot \sqrt{\sum_{i=1}^{n} [M_i - \overline{M}]^2}} \right)^2 \quad (7.15)$$

Where M_i is a sequence of model outputs, O_i a sequence of observed values, $\overline{M}$ is the mean model output and $\overline{O}$ the mean observed value. The value of r^2 varies from 1, which means all of the variance in the data is explained by the model, to 0, where none of the variance is explained. However, this correlation-based measure may be oversensitive to extreme values (i.e. outliers) and insensitive to constant proportional deviations between model estimates and observed values (Legates and McCabe, 1999).

The Nash and Sutcliffe (1970) measure of the mean square error to the observed variance is another commonly used coefficient of simulation efficiency calculated as in Eq. 7.16:

$$NS = 1 - \frac{\sum_{i=1}^{n}(O_i - M_i)^2}{\sum_{i=1}^{n}(O_i - \overline{O})^2} \tag{7.16}$$

This criterion ranges between -∞ to 1, 1 indicating a perfect fit, while 0 indicates that the observed mean is an as good estimator as the model. If the value is negative, the mean is a better estimator. Although the NS coefficient of efficiency is a better measure than correlation-based measures, as it does not suffer from proportional effects, it is still sensitive to outliers (Legates and McCabe, 1999). As there is not only one standard or a range of values for goodness-of-fit statistical parameters that will adjudge the model performance as acceptable, statistical measures are usually project specific (Engel *et al.*, 2007). For example, in Ramanarayanan *et al.* (1997) the performance of the APEX model was judged as satisfactory if the correlation coefficient was greater than 0.5 and the NS greater than 0.4. Santhi *et al.* (2001) assumed an NS greater than 0.5 and r^2 greater than 0.6 indicated acceptable model performance when calibrating SWAT.

The Root Mean Square Error (RMSE) is a generalised measure of the standard deviation and it is often used as an indicator for the effective parameterisation of models (Heinen, 2006b; Oehler, 2009). RMSE is defined as in Eq. 7.17:

$$RMSE = \sqrt{\sum_{i=1}^{n}\frac{(M_i - O_i)^2}{n}} \tag{7.17}$$

If the model accurately describes the noise-free data, the RMSE should be approximately equal to the standard deviation of the measurement noise. However, if model-errors are significant, then due to the squared term, disproportional weight may be given to the large error (Go, 2008). A way of standardising the RMSE is by dividing it by the mean $\overline{O}$ of the observations. This results in the NRMSE and renders a kind of coefficient of variation of the discrepancies M_i - O_i around the mean $\overline{O}$ (Janssen and Heuberger, 1995). Moreover, the NRMSE is comparable between different studies.

The mean absolute error (MAE) is an absolute indicator of the agreement between model predictions and observed data. It is given by Eq. 7.18:

$$MAE = \frac{\sum_{i-1}^{n} \left| O_i - M_i \right|}{n} \tag{7.18}$$

The MAE is less sensitive to outliers than the RMSE. The MAE of zero suggests an absolute agreement between the predicted and observed data. Dividing the MAE by the observed mean $\overline{O}$, the dimensionless NMAE is obtained, which is preferred over the MAE (Janssen and Heuberger, 1995). Furthermore, the effects of outliers can be minimised by making the comparison on values above or below a specific threshold or by using log-transformed values (Mulligan and Wainwright, 2004).

All of the above goodness-of-fit statistics as well as visual representation of the predicted and observed values will be used to assess the efficiency of the model, as the more tests a model can successfully pass, the more confidence one can have in it (Mulligan and Wainwright, 2004). However, the statistic results will be interpreted cautiously with regards to the limitations of the statistic itself but also the intended accuracy and temporal and spatial resolution of the model predictions. Finally, weight will be given to those goodness-of-fit measures that have been used in the literature for the validation of NEMIS in assessing acceptable model performance levels (Engel *et al.*, 2007). The application of the model with a more extensive annual dataset will be an additional indication of how closely the model reproduces the behaviour of the system

under study and how reasonable the calibration of the model parameters has been for its use in a different setting than the one it was developed for.

The actual denitrification rates and the soil and porewater characteristics (Table 7.6.1) collected during March and July 2008 in the BZ and PM areas were used for the validation of NEMIS predictions. The characteristics of the databases used in previous studies for the validation of the model are shown in Table 7.6.4. The organic carbon content and the soil pH were within the range reported in previous model validations. The dry bulk density was lower than the loam and sandy soils used in previous studies due to the significantly higher proportion of clay (36%) in the samples. All the studies measured or estimated actual denitrification in the topsoil (0 - 40 cm) with three of them within the first 11 cm in sandy, loam and peat soils.

In the present validation, porewater nitrate concentrations were used, as the bulk soil samples collected during the *in situ* denitrification measurements were not analysed for extractable NO_3^--N. However, since the March and July 2008 samplings occurred at surface saturation conditions caused by flood events that preceded the sampling date for at least one day, the conditions were favourable for denitrification and the porewater nitrate reflected the actual soil nitrate content at the time of sampling. For the purpose of model validation, using the monthly mean soil nitrate content for March and July would result in overestimating the actual denitrification rates, as the monthly soil sampling occurred under non saturated conditions when denitrification would be less favourable while nitrification would be operating in the aerobic portions of the soil. Nevertheless, the nitrate data are not significantly different from those used by the model authors, and therefore the estimated K is expected to be acceptable in the validation. It should be noted that in applying the model for long-term denitrification prediction, soil nitrate data are preferred, rather than porewater nitrate, as explained in the following section.

All the actual denitrification measurements were taken at field saturation conditions that were very similar to those reported by previous validation attempts (except for the peat soils and the second heavy loam soil), despite the soil textural differences. The soil temperature for the present study (Table 7.6.4) is the mean temperature of all the actual measurements and is skewed towards the lower bound as more measurements were taken in March, when mean soil temperature was around 7^oC. There is no indication

whether the temperatures reported in other studies are the mean or the maximum temperature during their measurements.

The mean potential denitrification rate in this study was higher than most other soil types considered with NEMIS apart from the peat soils. However, in 7 out of the 13 studies the D_p was either estimated indirectly from the yearly organic matter decay (sand, calcareous and sedimentary loam), or was taken from other studies in similar conditions (peat soils, clay and sandy clay loam) and considering the high spatial and temporal variability of denitrification these estimates should be used cautiously (Heinen, 2006b). In the rest of the studies, the D_p was measured according to the DEA technique. Possible reasons for the high potential denitrification rate in this study are: the higher organic carbon content compared to the other similar soil types; the high percentage of silt and clay (85%) that is associated with higher denitrification rates (Pinay *et al.,* 2000); and the fact that the D_p was measured in the top 10 cm of the soil (i.e. the root zone) which is the most biologically active soil layer (Pinay *et al.,* 2007a) at 20^{o}C representing the maximum potential denitrification (Hénault and Germon, 2000). Possibly for the same reasons (except for the soil temperature) the mean actual denitrification rate in this study was higher than the mean rates reported for sandy and loamy soils, while it was closer to the rate measured in silty clay riparian soil (Oehler *et al.*, 2007).

Table 7.6.4: Characteristics and references of the databases used to validate NEMIS

Soil Type	OM (%)	pH	ρ_d (g cm^{-3})	n	H (cm)	D_p (kg N ha^{-1} d^{-1})	D_α (kg N ha^{-1} d^{-1})	N (mg N kg^{-1})	S	T ^{o}C	References
Silty clay	6.3[b]	7	0.73	58	10	33.8[c]	0.39	1.6	0.62	11.3	Present study
Dry sand[a]	6	5.4	1.34	22	20	17.4	0.04	6.5	0.52	15	Corre (1996); Dekkers (1992); Aarts (1996) in Heinen (2006b)
Wet sand[a]	3.4	5	1.43	25	20	9.8	0.17	3.4	0.62	13.9	Corre (1996); Dekkers (1992); Aarts (1996) in Heinen (2006b)
Sand[a]	3	5	1.4	22	11	5	0.05	7.6	0.66	13.9	De Klein and van Logtestijn (1994) in Heinen (2006b)
Calcareous heavy loam[a]	1.75	7.2	1.41	60	20	2.7	0.03	5.5	0.69	12.4	Corre (1995) in Heinen (2006b)
Sedimentary heavy loam[a]	2	7	1.4	24	11	3.6	0.11	7.4	0.82	11.4	De Klein and van Logtestijn (1994) in Heinen (2006b)
Peat 1[a]	45	4.8	0.46	120	20	35.1	0.41	29.8	0.80	13.7	Velthof et al. (1996); Velthof (1997) in Heinen (2006b)
Peat 2[a]	42	5	0.5	28	11	38.5	0.09	16.6	0.83	13	De Klein and van Logtestijn (1994) in Heinen (2006b)
Anaerobic sandy peat[a]	19	5.2	0.93	36	[d]	n/a	4.2[e]	69.8	1	20.3	Meijer (2000); Van Beek et al. (2004) in Heinen (2006b)
Clay loam	6	6.3	1.1	46	n/a	7.2	0.14	10.5	0.70	13.3	Ryden (1983)
Silty loam	1.1[b]	6	1.4	12	20	2.7	0.005	1.8	0.62	16	Henault et al. (1998); Henault and Germon (2000)
Sandy clay loam	7.2[b]	8.4	1.4	[f]	30	15	[f]	900	0.62	25.3	Vale et al. (2007); Henault et al. (2005); Mahmood et al. (2005)
Silty hillslope	2.3	6.1	n/a	15	40	12.7	0.10	0.94[g]	0.59	11.8[h]	Oehler et al. (2007, 2009)
Silty clay riparian	2.9	5.8	n/a	15	40	19.9	0.25	0.42[g]	0.62	11.8[h]	Oehler et al. (2007, 2009)

The characteristics are: percentage organic matter (OM), pH, dry bulk density (ρ_d), number of samples for determination of actual denitrification (n), sample height (H), potential denitrification rate (D_p), average of the measured actual denitrification (D_a; all measured using the acetylene-inhibition-technique apart from the present study), nitrate N content (N), degree of saturation (S) and soil temperature (T). When more than one reference is given, these were used to obtain additional soil characteristics.

n/a: not available; [a]These datasets are given in Heinen (2006b); [b]organic carbon (%); [c]Mean potential denitrification rate for spring and summer '08 measured in ^{15}N amended slurries; [d]disturbed soil; [e]in mg N kg^{-1} d^{-1}; [f]D_a not measured, ^{15}N mass balance used instead; [g]in g N m^{-2}; [h]mean annual air temperature.

The model simulation was run for all the measurements in March and July 2008 (n=58) using the function parameters as originally defined in NEMIS (Hénault and Germon, 2000). The mean predicted actual denitrification rate was 0.22 ± SE 0.04 kg N ha^{-1} d^{-1} and the coefficient of variation (CV) 127 %, which is within the range of CVs found in the literature for actual denitrification rates and indicates a high spatial variability (Heinen, 2006b and references therein). Heinen (2006a) suggested the estimation of the relative denitrification ($D_r=D_a/D_p$) as a simple way for gaining an insight into how reasonably the model predicts actual rates of denitrification. The relative denitrification for this database (including all 58 samples) was 0.006, which corresponds to Heinen's estimation that in 83 % of the cases $D_r<0.125$, since the model yields small values for actual denitrification when not all the soil conditions (nitrate, moisture and temperature) are favourable for denitrification. Moreover, the mean D_r of the present study is comparable to the average relative denitrification of a sand soil (0.009; De Klein and van Logtestijn, 1994), of a loam soil (0.02; Ryden, 1983), of a heavy loam soil (0.032; De Klein and van Logtestijn, 1994) and of a peat soil (0.002; De Klein and van Logtestijn, 1994).

Both the measured and the predicted denitrification datasets were not normally distributed and they were log-transformed. The log-transformation improved their distribution but also effectively removed the effects of outliers from the datasets (Mulligan and Wainwright, 2004). In Figure 7.6.5 the measured denitrification rates are plotted against the predicted values. The coefficient of determination (r^2) was 0.30, while the Pearson correlation coefficient was 0.54 both of which were significant at the 0.01 probability level. The correlation coefficient was similar to the one calculated by Hénault and Germon (2000) when they applied NEMIS to the Ryden (1983) database. However, the coefficient of determination was lower than both validations performed by the model authors. The estimated errors as well as the Nash-Sutcliffe (NS) coefficient of efficiency are shown in Table 7.6.5. Although the NRMSE was within the range reported in Heinen (2006b) and lower than the validation in Oehler *et al.* (2009), it was still high and the NS was far from the ideal situation of 1 (complete agreement between predicted and observed values). Averaging the measurements per sampling transect, thus reducing the spatial heterogeneity between point measurements to variability between geomorphic units (i.e. transects), improved the correspondence between predicted and measured rates considerably (Table 7.6.5). The coefficient of

determination (0.76) was within the range of the model authors validations, while the Pearson correlation coefficient (significant at 0.01 probability level) was higher than the correlations in Hénault and Germon (2000) and Oehler *et al.* (2009), despite the fact that the latter had also performed parameter optimisation. Finally, the NRMSE was lower than the range of NRMSE (0.50 - 1.61) achieved after parameterisation in both the Heinen (2006b) and Oehler *et al.* (2009) validations, while the NS of 0.65 indicated very good agreement between predicted and measured denitrification rates (Figure 7.6.6).

Table 7.6.5: Goodness-of-fit criteria for the model validation

	r^2	Pearson	MAE	NMAE	RMSE	NRMSE	NS
Log-transformed data (n=58)	0.30	0.54	0.61	0.56	0.80	0.75	0.28
Averaged log-transformed data (n=20)	0.76	0.87	0.45	0.37	0.52	0.43	0.65

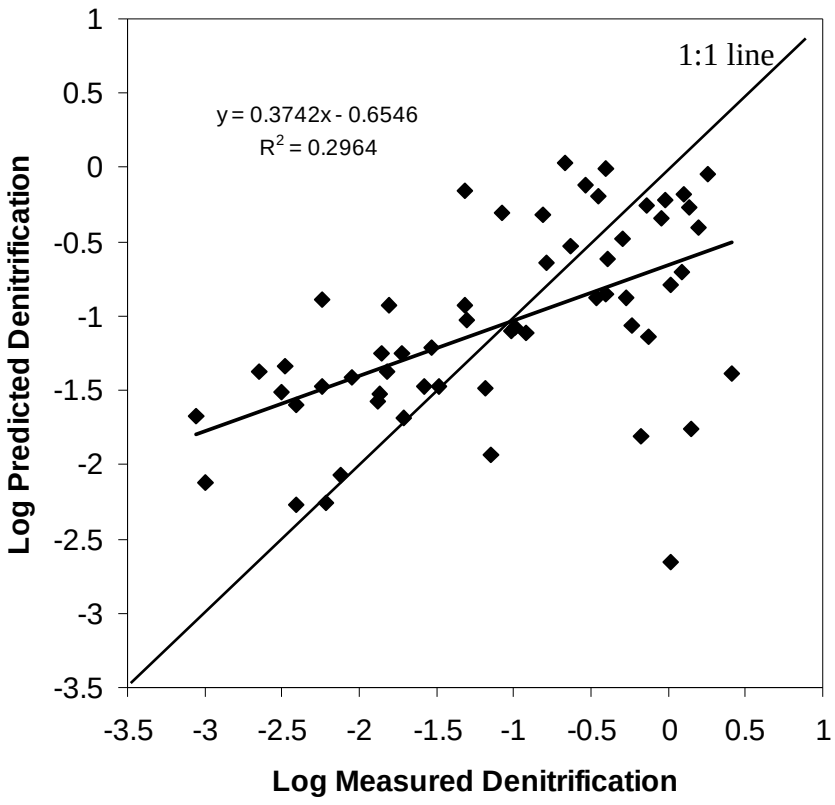

Figure 7.6.5: Performance of the model for all the available measurements (n=58). The coefficient of determination (R^2) is shown in the figure. The slope is 0.37 and the intercept -0.65, both significantly different from the 1:1 line ($p < 0.001$).

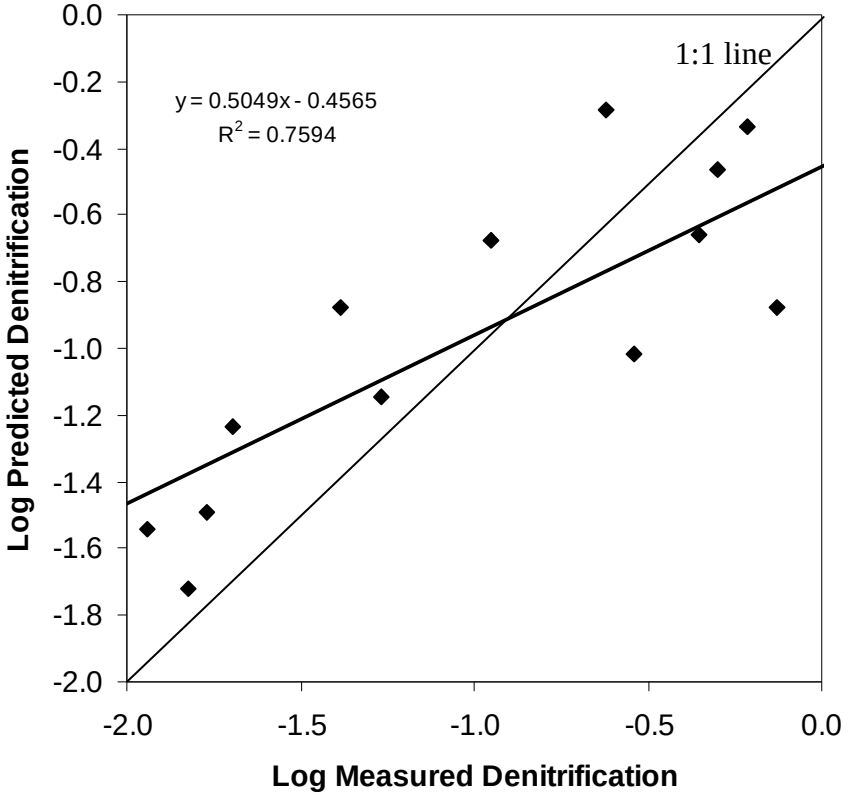

Figure 7.6.6: Performance of the model for averaged measurements per sampling transect (n=20). The coefficient of determination (R^2) is also shown in the figure. The slope is 0.50 and the intercept -0.46, both significantly different from the 1:1 line ($p < 0.001$).

The agreement between our measured actual denitrification rates and the predicted rates from the NEMIS model was satisfactory when the high spatial heterogeneity between point measurements was reduced by averaging measurements per sampling transect. This is a more meaningful spatial representation of denitrification in riparian zones found in many studies (Clément *et al.,* 2002; Hefting *et al.,* 2003 and 2006a; Hernandez and Mitsch, 2007) as it allows a variety of hydrogeomorphic controls to be studied (Pinay *et al.,* 2000) and the bias from single erroneous measurements and activity 'hotspots' is reduced (Groffman *et al.,* 2009). The goodness-of-fit criteria suggested good model performance, which in the case of the averaged measurements was better than previous validations of the model where parameter optimisation was also performed. Although the different criteria have their own limitations, obtaining satisfactory values for most of them increases our confidence that the model performed well in conditions different from its development without indicating that parameter re-calibration or optimisation is needed. Performing a sensitivity analysis was not in the

scope of the present study; however previous validation attempts have highlighted an important sensitivity of the model output to the determination of the f_S function. This was not observed in this study as due to the requirements of the *in situ* technique, only water contents near saturation were included in the validation database. Moreover, the database was built with the purpose of validating the model and therefore due care was taken to follow the specifications of the model authors during data collection and laboratory procedures. The capability of the model to reproduce adequately the annual temporal variations in denitrification rates will be tested using annual data collected for the BZ area between Nov 2007 and Oct 2008.

7.6.3 *Model application*

The nitrate content, soil moisture and soil temperature data, as well as the simulated denitrification rate for the period November 2007 (from the 24th onwards) to October 2008 (until and including the 22nd) in the three horizons (A, B and C) of the BZ area are summarised in Table 7.6.6. The results for the non-parametric Kruskal-Wallis test for the comparison of the means between seasons per soil horizon per soil variable and predicted denitrification rate are shown in Table 7.6.7. For the A horizon (10 cm depth) the soil nitrate content was higher in winter and spring whilst it was lower and similar between autumn and summer. The soil moisture content and temperature were significantly different between seasons with highest moisture in winter and lowest in summer, while the temperature pattern was exactly the opposite. The highest denitrification rate was predicted for the spring months, 0.83 ± SE 0.08, followed by winter, 0.55 ± SE 0.06, while the autumn and spring rates were lower and similar, 0.31 ± SE 0.06 kg N ha^{-1} d^{-1} respectively. The seasonal variation of denitrification has not been consistent in previous studies of floodplains and riparian zones in temperate climates. Some researchers have found higher denitrification rates in autumn and winter (Haycock and Pinay, 1993; Burt *et al.,* 1999), while others have measured highest denitrification during spring and summer (Hefting *et al.,* 2003 and 2006a) whereas there are cases where no significant seasonal variation was observed (Clément *et al.,* 2002; Sabater *et al.,* 2003).

Correlation analysis between the three soil variables and the predicted denitrification for the annual data pooled together, indicated a significant positive correlation between denitrification and soil moisture (Spearman rank; r=0.74, P<0.01).

Table 7.6.6: The soil nitrate, water content, temperature and predicted denitrification data for the period Nov 2007 to Oct 2008 for the three horizons (A, B and C) of the BZ area. Data are means with SE in parentheses. For the per season comparisons the Nov 2007 data were grouped with Sep and Oct 2008. Different lower case letters between the seasonal means per horizon per parameter indicate significant differences.

	Nitrate (mg N kg^{-1})			Water content ($cm^3.cm^{-3}$)			Temperature (^0C)			Denitrification (kg N ha^{-1} d^{-1})		
BZ Horizons	**A (10 cm)**	**B (50 cm)**	**C (100 cm)**	**A (10 cm)**	**B (50 cm)**	**C (100 cm)**	**A (10 cm)**	**B (50 cm)**	**C (100 cm)**	**A (10 cm)**	**B (50 cm)**	**C (100 cm)**
Autumn	4.92 (0.34)^a	1.82 (0.18)^a	1.09 (0.21)^a	0.422 (0.010)^a	0.462 (0.011)^a	0.439 (0.000)^a	11.9 (0.3)^a	12.8 (0.3)^a	13.2 (0.1)^b	0.31 (0.06)^a	0.08 (0.009)^a	0.04 (0.006)^a
Sep 08 (d=30)	3.54 (0.05)	1.21 (0.02)	0.49 (0.02)	0.439 (0.010)	0.520 (0.011)	0.435 (0.000)	13.7 (0.2)	14.3 (0.2)	13.9 (0.0)	0.42 (0.10)	0.13 (0.01)	0.02 (0.00)
Oct 08 (d=22)	4.59 (0.06)	1.46 (0.01)	0.51 (0.01)	0.349 (0.004)	0.363 (0.002)	0.435 (0.000)	11.2 (0.2)	12.3 (0.1)	13.1 (0.1)	0.00 (0.00)	0.00 (0.00)	0.02 (0.00)
Nov 07 (d=7)	11.85 (0.07)	5.58 (0.00)	5.45 (0.06)	0.573 (0.004)	0.525 (0.001)	0.440 (0.000)	6.9 (0.5)	8.1 (0.1)	10.6 (0.1)	0.83 (0.14)	0.11 (0.01)	0.15 (0.00)
Winter	9.23 (0.16)^b	5.02 (0.04)^b	4.84 (0.09)^b	0.585 (0.001)^b	0.528 (0.002)^b	0.440 (0.000)^b	5.4 (0.2)^b	6.8 (0.1)^b	8.6 (0.1)^a	0.55 (0.06)^b	0.07 (0.005)^a	0.06 (0.003)^b
Dec 07 (d=31)	10.04 (0.23)	5.35 (0.03)	4.85 (0.10)	0.580 (0.001)	0.510 (0.003)	0.440 (0.000)	5.2 (0.5)	7.3 (0.3)	9.6 (0.1)	0.67 (0.14)	0.08 (0.01)	0.09 (0.01)
Jan 08 (d=31)	7.61 (0.16)	4.84 (0.03)	3.99 (0.09)	0.593 (0.002)	0.534 (0.001)	0.439 (0.000)	6.3 (0.3)	7.3 (0.2)	8.3 (0.0)	0.62 (0.09)	0.09 (0.01)	0.04 (0.00)
Feb 08 (d=29)	10.10 (0.06)	4.84 (0.07)	5.73 (0.05)	0.579 (0.002)	0.542 (0.000)	0.436 (0.000)	4.7 (0.3)	5.9 (0.1)	7.8 (0.1)	0.33 (0.04)	0.05 (0.00)	0.04 (0.00)
Spring	8.05 (0.20)^c	3.83 (0.19)^c	3.47 (0.21)^c	0.516 (0.008)^c	0.471 (0.008)^a	0.439 (0.000)^a	9.5 (0.3)^c	9.3 (0.2)^c	8.8 (0.1)^a	0.83 (0.08)^c	0.06 (0.006)^a	0.04 (0.000)^a
Mar 08 (d=31)	9.09 (0.05)	6.08 (0.06)	6.00 (0.06)	0.575 (0.003)	0.536 (0.001)	0.436 (0.000)	6.4 (0.2)	7.1 (0.1)	7.8 (0.0)	0.59 (0.06)	0.09 (0.01)	0.05 (0.00)
Apr 08 (d=30)	9.36 (0.06)	3.42 (0.19)	2.88 (0.20)	0.513 (0.009)	0.472 (0.013)	0.436 (0.000)	9.0 (0.3)	8.7 (0.1)	8.4 (0.0)	0.82 (0.10)	0.06 (0.01)	0.03 (0.00)
May 08 (d=31)	5.72 (0.25)	1.99 (0.03)	1.53 (0.02)	0.460 (0.016)	0.404 (0.013)	0.435 (0.000)	13.2 (0.2)	12.1 (0.2)	10.1 (0.1)	1.09 (0.22)	0.05 (0.01)	0.04 (0.00)
Summer	5.21 (0.19)^a	2.07 (0.09)^a	1.14 (0.05)^a	0.376 (0.012)^d	0.454 (0.008)^a	0.434 (0.000)^c	15.5 (0.1)^d	15.5 (0.1)^d	12.6 (0.1)^c	0.31 (0.07)^a	0.09 (0.008)^a	0.05 (0.002)^c
Jun 08 (d=30)	3.69 (0.09)	1.39 (0.05)	0.69 (0.04)	0.405 (0.020)	0.536 (0.005)	0.434 (0.000)	14.4 (0.1)	14.2 (0.1)	11.5 (0.1)	0.34 (0.10)	0.17 (0.01)	0.03 (0.00)
Jul 08 (d=31)	7.37 (0.19)	3.14 (0.09)	1.58 (0.06)	0.347 (0.020)	0.369 (0.004)	0.434 (0.000)	15.8 (0.2)	15.8 (0.1)	12.6 (0.1)	0.36 (0.15)	0.02 (0.00)	0.06 (0.00)
Aug 08 (d=31)	4.52 (0.24)	1.67 (0.12)	1.13 (0.05)	0.375 (0.020)	0.461 (0.014)	0.434 (0.000)	16.2 (0.1)	16.5 (0.1)	13.7 (0.0)	0.24 (0.11)	0.10 (0.01)	0.05 (0.00)
Annual Total (d=334)										173.18	25.74	15.63

Table 7.6.7: Results of the Kruskal-Wallis test for the comparison of means per soil horizon per soil variable and predicted denitrification rate. The χ^2 is the test statistic, *df* the degrees of freedom between groups and *P* the probability level. Significance is reported at the 0.05 probability level.

BZ Horizons	**A (10 cm)**			**B (50 cm)**			**C (100 cm)**		
Kruskal-Wallis Test	χ^2	***df***	***P***	χ^2	***df***	***P***	χ^2	***df***	***P***
Nitrate content	158.70	3	0.000	166.1	3	0.000	202.8	3	0.000
Water content	179	3	0.000	22.2	3	0.000	271.2	3	0.000
Temperature	249.2	3	0.000	259	3	0.000	249.1	3	0.000
Denitrification	79.5	3	0.000	3.3	3	0.347	82.8	3	0.000

Multiple regression forward analysis (MRA) showed that the soil moisture alone explained 29 % of the variance in denitrification but when combined with temperature the predicting power of the two variables rises to 60 %. Combining the nitrate content together with the soil moisture and the temperature improves the variance explanation only by a further 3 %. Therefore, annually, the soil moisture and the soil temperature equally limit denitrification in the topsoil, while the soil nitrate content does not seem to be limiting in the agricultural landscape of the River Cole re-connected floodplain throughout the year.

When a similar multiple regression analysis was performed within each season, a difference in the relative importance of the three controlling factors was observed as expected. In the autumn, the soil moisture explained 67 % of the variance in denitrification rates and combined with temperature the predictive power increased to 73 %, while nitrate was not limiting. In winter, denitrification correlated strongly with the soil temperature (Spearman; r=0.99, P<0.001) which explained 72 % of the denitrification variance and when combined with the soil nitrate content they explained 77 % of the variance, while the soil moisture was not limiting. The close association between denitrification and soil temperature during the winter months can be seen in Fig. 7.6.7 A where there is close correspondence between daily mean temperature and mean denitrification peaks. Moreover, the topsoil was around its saturation level throughout the winter, therefore soil moisture was not limiting while the dry periods in September 2008 and mainly the dry October 2008 are the main reasons for soil moisture limiting denitrification during autumn (Figure 7.6.7 B). In spring, soil moisture becomes limiting again, but can account for only 22 % of the variance in denitrification, while the moisture combined with temperature have 84 % explanatory power and soil nitrate is not limiting. Therefore, the combination of fairly high soil moisture content, especially during March and May, together with the increasing soil temperature, which rises above 11^{o}C in May, and the non-limiting soil nitrate content lead to the highest mean denitrification rate. In summer, the denitrification correlated strongly with the soil moisture (Spearman; r=0.92, P<0.001), which had 60 % explanatory power and when combined with soil nitrate this raised to 66 %, while the temperature is no longer limiting. The importance of the summer floods that increase the soil moisture and lead

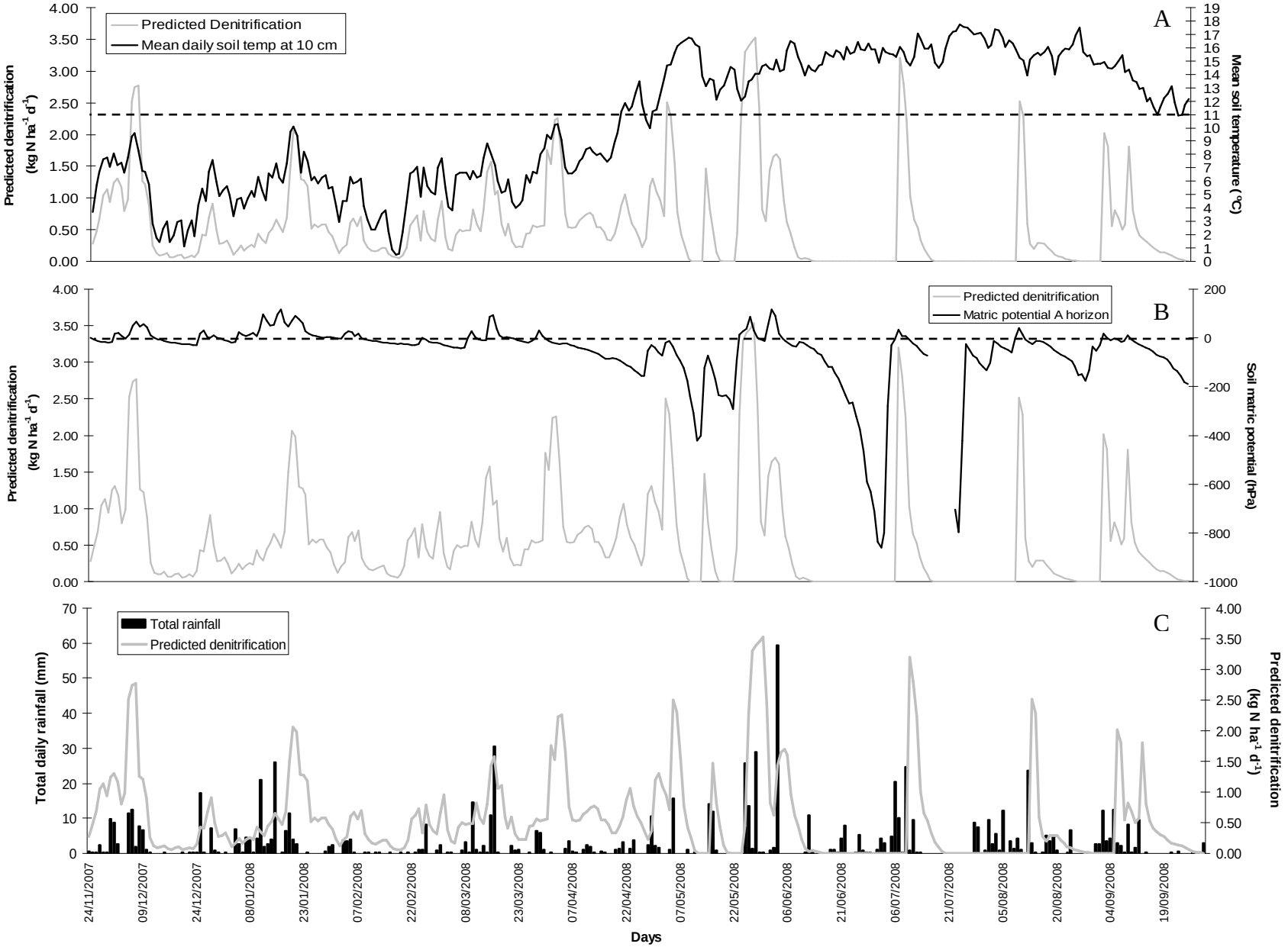

Figure 7.6.7: Predicted Denitrification against mean soil temperature (A), soil matric potential (B) and total daily rainfall (C).

to pulses of increased denitrification activity in the topsoil can be observed clearly in Figs. 7.6.7 B and C with denitrification peaks following shortly after the major summer flood events.

The soil nitrate content in the B horizon (50 cm depth) displayed a similar pattern to the one observed for the topsoil. However, the soil moisture content was less variable than in the topsoil with only the winter months having significantly higher moisture content, while the temperature fluctuated significantly between seasons with highest values in summer and lowest in winter. The predicted denitrification rate was not significantly different between seasons (Table 7.6.7) and the mean rate was 0.08 ± SE 0.01 mg N kg ha^{-1} d^{-1}, which was 75 % less than the topsoil rate in autumn and summer and 90 % less than the spring denitrification rate of the topsoil. The lower denitrification rate of the B horizon was mainly due to the D_p value used in the NEMIS formulation which was 87 % less than the denitrification potential of the surface and included the effect of decreasing carbon availability as the main limiting factor of denitrification in the vadose zone of floodplain areas (see also discussion in section 6.5.3).

Without taking into account the effect of organic carbon in further analyses, the predicted denitrification rate correlated significantly with the soil moisture content (Spearman; r=0.78, P<0.001), while in MRA analysis the soil moisture together with the temperature explained 78 % of the variance in denitrification rates, a predictive power which was higher than the respective value for the topsoil, when all the data are pooled in an annual dataset. The soil nitrate content was not limiting throughout the monitoring year. MRA for the autumn data revealed a strong dependence of denitrification on soil moisture conditions that predicted 96 % of the denitrification variance. Similarly, to the topsoil results, the winter dataset showed that the temperature is the main regulator of denitrification with 87 % explanatory power suggesting that even at 50 cm depth, where the effect of the air temperature is more subdued compared to the surface, temperature is still an important regulator of the denitrification activity (Fig. 7.6.8 A). In spring, the decreasing soil moisture combined with the increasing temperature are responsible for 91 % of the variance in denitrification rates (Fig. 7.6.8 A and B). Finally, in the summer months, the soil moisture together with the nitrate availability are the main limiting factors for denitrification and combined have 94 % explanatory power.

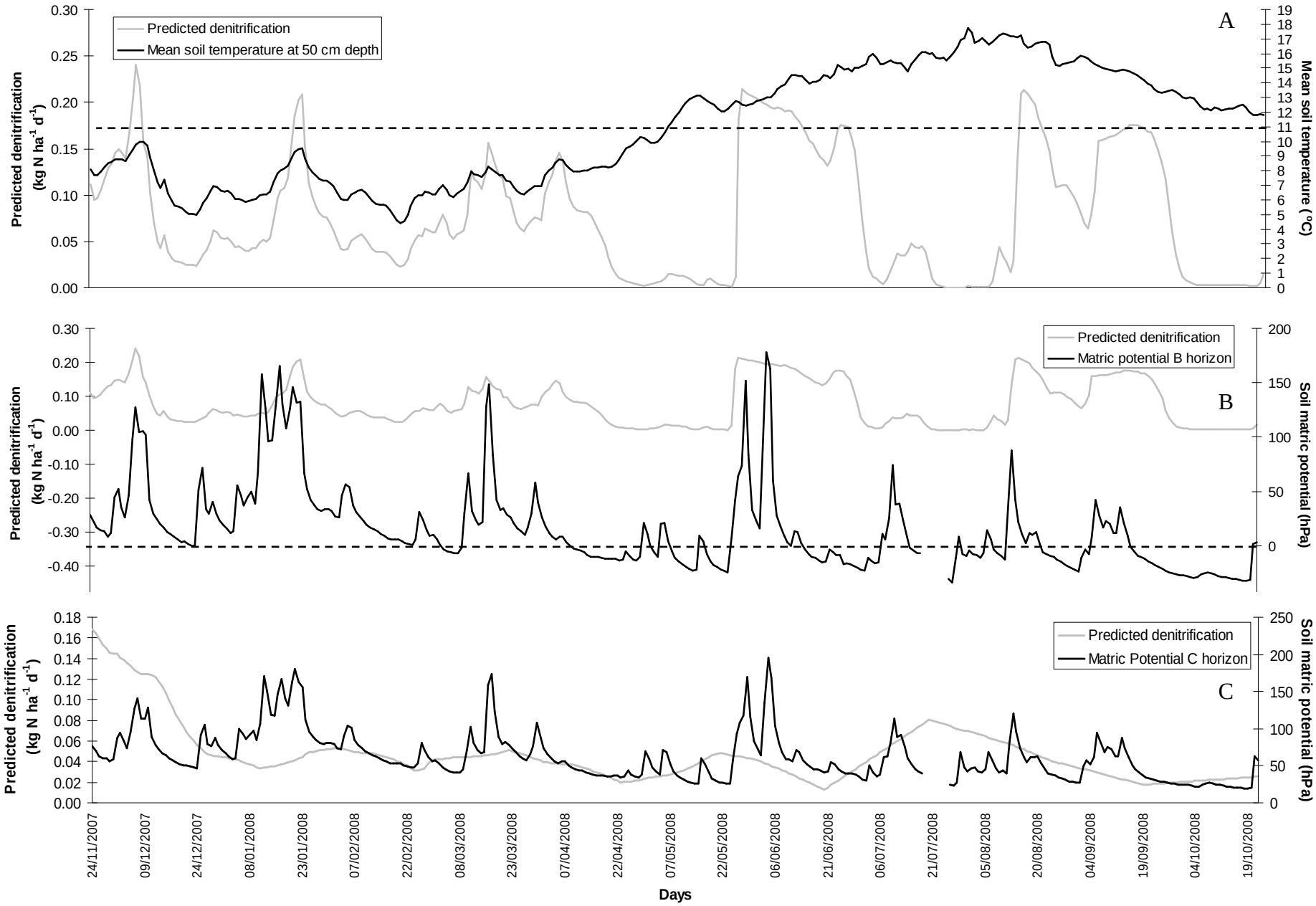

Figure 7.6.8: Predicted Denitrification against mean soil temperature (A), soil matric potential (B and C for the respective horizons).

In the saturated zone of the BZ (C horizon; 100 cm depth) seasonal variation in the nitrate content was still observed following the pattern seen for the A and B horizons. Although the C horizon was permanently saturated there was still some variation observed with higher mean moisture measured in winter and lower in the summer months. The temperature pattern between seasons was somehow different from the above soil layers, with highest temperatures observed in autumn and summer and lowest but not different between them in winter and spring. The predicted denitrification rate displayed significant differences between seasons with higher rates estimated for winter and summer and lower for autumn and spring (Table 7.6.6). The mean annual predicted denitrification rate for the C horizon was 0.05 ± SE 0.01 kg N ha^{-1} d^{-1}, which was 90 % less than the mean annual rate of the topsoil and 38 % less than the rate of the B horizon. The measured D_p used in the application of NEMIS for the C horizon was 95 % less than the denitrification potential of the surface, and therefore the lower availability of organic carbon was the main limiting factor for denitrification in the saturated zone, which is in agreement with the findings of numerous studies of denitrification in the saturated zone (see also discussion in section 6.5.3).

The annual predicted denitrification rate correlated positively (Spearman; r=0.60, P<0.01) with the nitrate content suggesting that apart from the organic carbon, nitrate availability was also limiting denitrification in the saturated zone. In MRA analysis of the annual dataset, the nitrate content explained 21 % of the variance in denitrification rates and when combined with temperature the prediction increased to 50 %, while soil moisture was not an important predictor for the annual database, as saturation conditions prevailed throughout the year (Fig. 7.6.8 C). In autumn, the sole predictor of denitrification in MRA was the nitrate content which explained 99 % of the variation, as the temperature was higher than in any other season and therefore not limiting. In the winter months temperature was the first limiting factor, predicting 88 % of the denitrification rates and combined with the nitrate content the prediction power increased to 97 %. Both in spring and summer the combination of nitrate availability and the soil temperature were the main limiting factors, with temperature being more important in spring (61 %) and nitrate (97 %) in summer.

The application of NEMIS with the annual database for the topsoil of the BZ area showed that the model accurately predicts the temporal variations of denitrification. Having included the effect of organic carbon availability in the measured denitrification potential value, the annual denitrification rate is influenced by the saturation state of the soil, the soil temperature and nitrate availability whose relative importance as controlling factors changes between the seasons of the year. The validation analysis has indicated that the model is transferable to relatively different soil type conditions from the ones used for the model development, although the temperate climatic conditions and the agricultural type of the floodplain were similar between this study and the Hénault and Germon (2000) study. Therefore, it is suggested that NEMIS can be used as a tool for predicting actual denitrification rates in temperate agricultural floodplains and riparian zones with a variety of soil types from clay and silty clay to loam and sand without the need for site specific parameter calibration or optimisation.

The annual application of the model has indicated that the soil moisture content was the primary controlling factor of denitrification followed by the soil temperature, while nitrate was not limiting in the studied agricultural landscape. Whereas the temperature of the topsoil can easily be measured accurately with one *in situ* probe, especially in grass-vegetated floodplains where there is no effect from tree shading, the representation of the spatial soil moisture variability that is influenced by the site topography and hydrological regime may require more effort. In the present study the hydrological regime of the BZ area was already known and thus it was straight forward to select a representative location for the soil moisture measurement, although for better representation of the spatial variability multiple measuring points would be suggested especially in complex topographies and/or multiple sources of surface saturation (i.e. overbank inundation, groundwater upwelling, hillslope runoff).

In the case when the soil moisture conditions are bound to change, for example in a candidate site for restoration, the use of soil moisture probes at the pre-restoration stage would not be appropriate. Therefore, when NEMIS needs to be used for predicting the nitrate attenuation capacity of a site to-be-restored, then the soil moisture conditions as they will be affected by the restoration will also need to be predicted. One way for doing this would be the coupled use of NEMIS with a hydrological model (SWIM, MIKE-SHE) for simulating the site hydrology post-restoration. However, it should be

noted that the parameterisation and validation of a hydrological model is a time and data intensive process that would considerably increase the cost and duration of the pre-restoration assessment. A more cost-effective approach would be to monitor the soil moisture conditions at a reference site, within the same catchment or in a different catchment, where the soil moisture conditions emulate those expected to be achieved with the restoration project. In this case, a similar monitoring design to the post-project appraisal of restored sites could be followed, but care should be taken to account for climatic variability and differences in nitrate-loading between the reference and the restoration candidate site. Finally, hydrological data from the literature could be used, if and when they are available, from the same or from a catchment of similar hydromorphology, but these should be applied with caution as climatic variability and land use changes may considerably change soil moisture and nitrate conditions over time.

With respect to soil nitrate data collection, due to cost and time constraints only monthly measurements were performed and these were not successful in representing the fertilisation periods of the arable land adjacent to the BZ. However, this was not a major error in the present study, as nitrate was not limiting throughout the study period. If higher resolution of denitrification activity is needed, for example during fertilisation events, then higher soil nitrate sampling frequency should be employed as recommended by the model authors.

The measurement of the potential denitrification rate is a prerequisite of the model formulation, and although other studies have used D_p measured under similar conditions or adjacent areas, it is recommended that a site specific measurement is performed as the D_p will reflect the effect of organic carbon availability on the predicted denitrification rates. In the present study, two D_p values were used, one representing the potential in autumn, winter and spring, and one in summer, but as the model authors also suggest, for the prediction of an annual denitrification rate only one D_p rate from the most active season would be adequate.

The annual simulation of denitrification in the present study indicated that spring was the most active season contributing to a total of 76.5 kg N ha^{-1} removed by denitrification, followed by winter with 49.6 and then the summer with 28.9 while the

dry autumn 2008 contributed the least with 18.3 kg N ha^{-1} respectively. However, by combining the daily topsoil denitrification rates with the nitrate loading during river overbank flood events in the BZ (see table 5.3.2 for nitrate loading in the BZ), it was observed that during the spring flood events, 25 % of the river nitrate could have been removed via denitrification in the topsoil, while during the winter floods the removal percentage increased to 39 %. This is an effect of the higher N loading in spring, possibly due to fertiliser application, despite the significantly shorter duration of floods compared to winter (Table 5.3.2). This observation highlights the importance of nitrate loading via the dominant hydrological mechanism, in the present study overbank flooding, for effective nitrate removal by the re-connected floodplain, while it suggests that spring fertilisation in the studied agricultural catchment is a current issue that can increase significantly river nitrate concentrations. Despite the lower total denitrification rate observed in summer, the combination of high temperature and soil moisture during overbank flood events, together with a moderate nitrate loading, can lead to 36 % nitrate removal via denitrification in the BZ topsoil. This finding highlights the importance of the summer storms that can trigger high denitrification activity due to the high soil temperature and therefore contribute substantially to the annual N removal budget via denitrification. It is therefore recommended that an annual simulation of denitrification is performed to capture the contribution of each season to the annual N removal budget. However, if there are budget or other constraints and only one season can be monitored then winter would give the maximum denitrification capacity in a temperate agricultural landscape such as the River Cole re-connected floodplain.

Assuming an equal mean potential denitrification rate for the PM topsoil, as it was shown in section 6.1.4 and Figure 6.1.9, to the BZ topsoil, and similar soil moisture, temperature, and nitrate content conditions during overbank flood events, the actual denitrification rate of the PM topsoil was predicted using the NEMIS model. Combining the nitrate loading data during overbank flooding in the PM (Table 5.3.1) with the actual denitrification rates during the flood days, the PM topsoil showed potential for 48 % nitrate removal in winter 2008, 35 % in spring 2008 and 45 % in summer 2008. Although more nitrate was removed via denitrification during the winter flood events, as it was also shown for the BZ area, overall the contribution of denitrification in removing river water nitrate was higher in all seasons for the PM compared to the BZ topsoil. This is probably a result of the lower nitrate loading per hectare in the PM

(Tables 5.3.1 and 5.3.2), since the denitrification capacity was chosen to be similar to the BZ, highlighting the effectiveness of a larger re-connected floodplain in nitrate removal during overbank flooding compared to a narrow buffer strip (BZ area). This result demonstrates that a re-connected floodplain, in addition to providing floodwater storage and attenuation of flood peaks, can also be more efficient as a nitrate sink during flood events compared to a narrow buffer zone adjacent to arable land.

The simulation of denitrification in the vadose and saturated zone of the BZ area has shown that the NEMIS formulation can be used for subsurface horizons, as denitrification is essentially controlled by the same factors, as long as the effect of the reduced organic carbon availability with depth is reflected in the measured D_p. The annual contribution of the BZ subsurface to the N removal via denitrification was 41.4 kg N ha^{-1}, which was 24 % of the total annual topsoil denitrification. However, monitoring or modelling the subsurface hydrology is a lot more complicated than the surface hydrology due to for example the effect of macropores, tile and mole drainage (Heppell *et al.,* 2000), and the anisotropy of hydraulic conductivities between different soil horizons (Baird *et al.,* 2004). The effect of localised buried patches of organic carbon should also be considered as denitrification 'hotspots' (Devito *et al.,* 2000; Hill *et al.,* 2000) making the application of the model a lot more complicated and costly as additional sampling and analytical effort will be required. Unless there is some strong indication that subsurface denitrification is playing an important role, then the management tool kit for predicting the denitrification capacity of floodplains and riparian zones should be restricted to the most biologically active topsoil layer.

7.6.4 *Floodplain Restoration Management Tool*

The management tool for floodplain restoration is aimed at natural resource managers and/or those statutory bodies responsible for the design and undertaking of floodplain restoration schemes. Two main applications are envisaged: first to provide a tool for the assessment of the nitrate attenuation capacity of the candidate restoration site; and second the post-project appraisal of the nitrate attenuation capacity of a restored site, via a simple prediction of the denitrification capacity. It is expected that the use of the management tool will facilitate the inclusion of water quality targets, and specifically the nitrate attenuation objective, in the design of future floodplain restoration projects. The main procedures for these two applications are outlined in the flow diagram below:

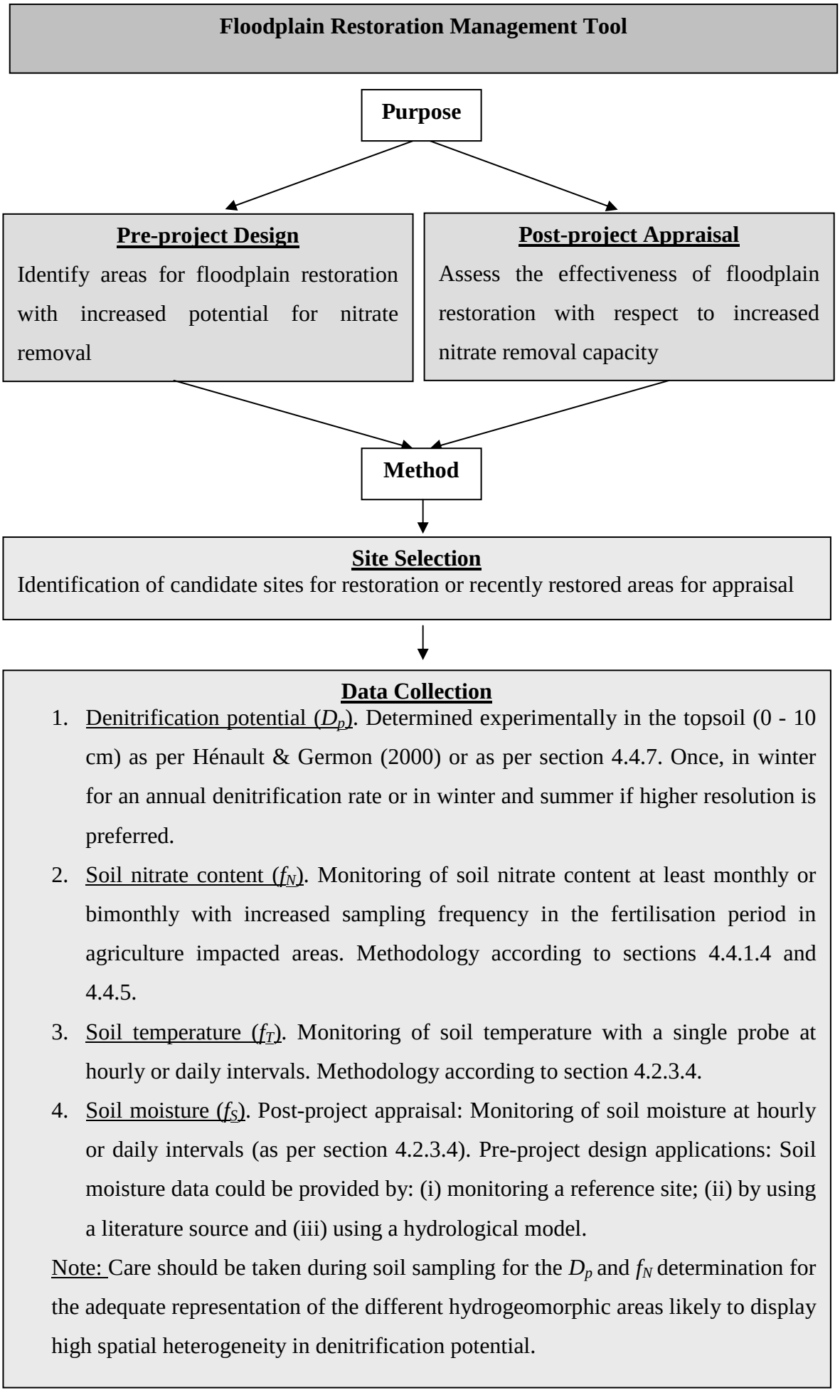
Floodplain Restoration Management Tool
Purpose
Pre-project Design
Identify areas for floodplain restoration with increased potential for nitrate removal
Post-project Appraisal
Assess the effectiveness of floodplain restoration with respect to increased nitrate removal capacity
Method
Site Selection
Identification of candidate sites for restoration or recently restored areas for appraisal
Data Collection
1. Denitrification potential (D_p). Determined experimentally in the topsoil (0 - 10 cm) as per Hénault & Germon (2000) or as per section 4.4.7. Once, in winter for an annual denitrification rate or in winter and summer if higher resolution is preferred.
2. Soil nitrate content (f_N). Monitoring of soil nitrate content at least monthly or bimonthly with increased sampling frequency in the fertilisation period in agriculture impacted areas. Methodology according to sections 4.4.1.4 and 4.4.5.
3. Soil temperature (f_T). Monitoring of soil temperature with a single probe at hourly or daily intervals. Methodology according to section 4.2.3.4.
4. Soil moisture (f_S). Post-project appraisal: Monitoring of soil moisture at hourly or daily intervals (as per section 4.2.3.4). Pre-project design applications: Soil moisture data could be provided by: (i) monitoring a reference site; (ii) by using a literature source and (iii) using a hydrological model.
Note: Care should be taken during soil sampling for the D_p and f_N determination for the adequate representation of the different hydrogeomorphic areas likely to display high spatial heterogeneity in denitrification potential.

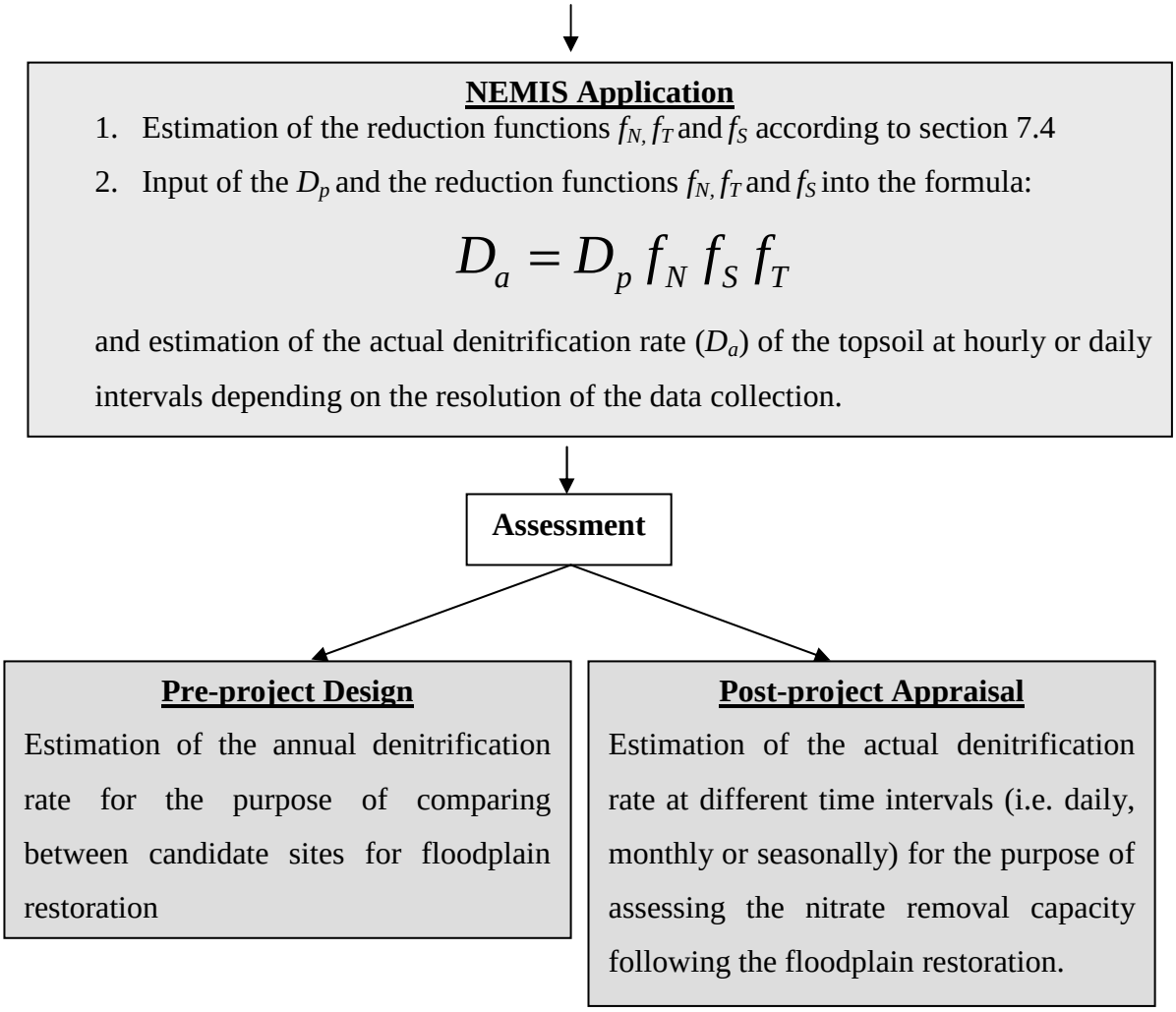

Although the tool is based on a simple prediction of denitrification at the field scale, it requires a laboratory assessment and a fieldwork monitoring effort, and it is therefore likely to be better suited to fairly large scale restoration projects, such as the River Cole restoration. Costs associated with the laboratory estimation of denitrification potential could be minimised by using a reference value from the literature. However, this is not recommended for very heterogeneous sites, as spatial variability of denitrification would be expected to be high and therefore site-specific estimation should be preferred. Additionally, the fieldwork effort for the collection of the necessary soil moisture, temperature and nitrate content data will depend on the desired resolution of the denitrification estimation. Data could possibly be obtained from the established monitoring programmes of statutory bodies, such as for example the Environment Agency, where they are available. Instead of detailed soil moisture data, the number of flooding days could be used, while soil temperature could be easily obtained from the nearest weather station. Finally, the monitoring of the soil nitrate content could be substituted by river water nitrate concentration data, where overbank flooding is the main source of nitrate on the floodplain, or fertiliser application amounts and rates could be obtained where agricultural runoff is expected to be the main nitrate source.

Chapter 8: Summary and Conclusions

8.1 *Review of the research objectives*

This chapter summarises the main findings of this study in relation to each objective before providing some concluding remarks. The results of this study have shown that re-instatement of hydrological connectivity, following the restoration of a temperate agricultural floodplain, not only increases floodwater storage but also beneficially affects nitrate attenuation in the restored floodplain via biological removal mechanisms. The objectives of this study were to:

1. Identify the main hydrological mechanisms responsible for the inundation regime in a temperate re-connected floodplain. Assess the relative importance of each hydrological mechanism for: (i) the transport of nitrate; and (ii) the creation of the necessary conditions for denitrification and DNRA in the soil (Chapter 5).

2A. Quantify the relative importance of potential heterotrophic denitrification and DNRA in the reconnected floodplain (Chapter 6).

2B. Investigate the main controlling factors influencing the two processes in a temperate agricultural re-connected floodplain. This research focused in particular on:

(iv) The role of land use management in influencing the magnitude and relative importance of heterotrophic denitrification and DNRA (sections 6.1 & 6.2).

(v) The role of vertical changes in soil stratigraphy and electron donor and acceptor availability in influencing the magnitude and relative importance of denitrification and DNRA (section 6.3).

(vi) The role of wetting-drying cycles in controlling the spatial variability of heterotrophic denitrification and DNRA (section 6.4).

3. Develop, validate and apply a management tool aimed at evaluating the nitrate removal capacity of candidate sites for river-floodplain restoration and/or assessing the nitrate removal capacity of restored floodplains as part of a post-project appraisal (Chapter 7).

8.2 *Objective One*

The inundation regime of the temperate River Cole re-connected floodplain can be best described by a 3D approach. River water bank storage, that extends several meters inland, precedes the sequence of events during a flood. When bankfull capacity is exceeded, a flood pulse extends across the floodplain from two directions; perpendicular to the river towards the floodplain, and parallel to the river from the ditch to the floodplain (PM case), or between the river and the arable field (BZ case). During the recession limb, GW discharges to both the river and the ditch contributing to baseflow. Under baseflow conditions, a perched water table is maintained through the occurrence of a reversed GW ridge and the capillary fringe effect.

The dominant hydrological mechanism responsible for the inundation regime of the re-connected floodplain is overbank flooding from the river and the surrounding ditch, leading to surface saturation conditions between 13 and 28 % of the time during one year, and thus creating the necessary conditions for the occurrence of nitrate attenuation via heterotrophic denitrification and DNRA. The low angle topography of the floodplain (maximum slope around 2 %), the heavy silt-clay alluvium (>90 % of the grain size distribution), associated with low saturated hydraulic conductivities of the floodplain sediments, and finally the flashy character of the River Cole, mainly due to its urbanised headwaters, all contribute to increased overland flows during flood events. Additionally, during high magnitude and high intensity events, SEOF in surface depressions, where the water table stays relatively close to the surface, and IEOF from artificial surfaces, further contribute to the generation of surface runoff, before bankfull capacity is reached, without contributing significantly to the nitrate loading on the floodplain. Overbank flooding is the main conduit for the transport of river water nitrate onto the floodplain, ranging between 180 and 300 kg N ha^{-1} $year^{-1}$. Moreover, overland flow from the ditch transports the nitrate from the arable hillslope runoff onto the floodplain, where nitrate can be attenuated upon its infiltration into the soil matrix.

Lateral subsurface flow is the main mechanism for groundwater discharge into the river and the ditch, while it is also responsible for maintaining baseflow under dry conditions. However, the low angle topography together with the low hydraulic conductivity, lead to slow GW flow rates (0.1 - 10 L d^{-1} m^{-1}), thus maintaining a perched water table (PWT) between 1 and 2 m depth between flood events and giving the opportunity for

further nitrate attenuation in the subsurface sediments of the floodplain. Moreover, the maintenance of the PWT is also aided by reversed groundwater ridging during baseflow conditions and possibly the capillary fringe effect. Finally, nitrate loading during lateral subsurface flow is restricted in the PM area (0.02 - 0.26 mg N d^{-1} m^{-1}), while it is more significant in the BZ area (2 - 55 mg N d^{-1} m^{-1}) due to the transport of nitrate from the arable field to the riparian zone through groundwater flow paths.

8.3 *Objective Two*

The results of the present study suggest that the re-connection of the floodplain of the River Cole, although aiming at flood attenuation and habitat creation targets, resulted also in a significant potential for denitrification activity in the topsoil (range: 5 to 63 mg N $kg^{-1}d^{-1}$). Moreover, the occurrence of DNRA (range: 0.02 to 2.64 mg N $kg^{-1}d^{-1}$) as an alternative nitrate reduction pathway was documented, for the first time, in the soil of a temperate agricultural re-connected floodplain. The reduction of nitrate via DNRA is of lesser importance compared to denitrification (on average 40 times less), which has a beneficial effect on the management of diffuse-nitrate pollution in these lowland catchments. The frequent supply of nitrate onto the floodplain, mainly via overbank flooding, gives a competitive advantage to denitrifiers while it also increases the redox potential and lowers the ratio of C/NO_3^- in the soil, neither of which conditions favour DNRA. Therefore, the majority of nitrate is transformed to nitrogen gases (N_2 and possibly N_2O) and is removed, rather than conserved in the system as NH_4^+ which can easily re-enter the soil cycle via plant uptake.

8.3.1 *The role of land use management in influencing the magnitude and relative importance of heterotrophic denitrification and DNRA*

The denitrification potential was significantly different between the land use zones of the River Cole floodplain. With respect to the controlling factors of denitrification, the Anaerobically Mineralisable Organic Carbon (AnMOC) was the main predictor of variance in denitrification, followed by the lability of organic carbon (LOC) and finally the soil nitrate content. The fact that the soil nitrate content explained only 26 % of the variance in denitrification suggests that denitrification is likely primarily controlled by the availability of labile organic carbon and secondarily by nitrate supply. However, it should be acknowledged that AnMOC, and subsequently the derivative LOC, are relative measures of the available organic carbon and available electron acceptors for

anaerobic respiration and fermentation combined and therefore they may be underestimating the anaerobic mineralisation rate by nitrate reduction. However, the importance of organic carbon in controlling denitrification rates across the land use zones of the River Cole floodplain was also highlighted by the high correlation coefficients between denitrification potential and other carbon measures, such as the organic carbon and organic matter contents. The spatial heterogeneity in denitrification potential is a function of the management practices that affect the availability of organic carbon (e.g. grazing and/or mowing) rather than landscape position.

Although a frequent supply of nitrate onto the floodplain is maintained by overbank flood events and runoff from the surrounding agricultural land (PM case), this does not necessarily create N-saturation conditions across the land use zones. Therefore, the low importance of nitrate in explaining denitrification potential variability probably means that nitrate, at the concentrations encountered in our site, has a secondary role compared to organic carbon availability in controlling denitrification. During the determination of denitrification potentials, field range concentrations of nitrate were used under the assumption that field nitrate concentration is not limiting for denitrification rates. However, studies in N-saturated soils have shown that further nitrate additions under these conditions can further increase the denitrification activity of these soils (Hanson *et al.*, 1994). This was indeed evident when the denitrification potentials at ambient nitrate concentration ('land use' samples) were compared to potentials where nitrate was at higher than ambent concentration ('dry' condition samples) between the same sampling locations in the BZ area (Box 8.1). The 'dry' denitrification potential was significantly higher than the 'land-use' one, despite the fact that the 'land-use' samples displayed higher AnMOC rate and had higher organic carbon and soil nitrate content (Box 8.1). This difference in denitrification rates could be attributed to the different nitrate concentration used in the spike (3mM $Na^{15}NO_3^-$ for the 'dry' samples instead of 2.4 mM for the 'land-use' samples) since the incubation temperature was the same (20^oC) and the samples had similar moisture content. This implies that the absolute denitrification potential rates across the River Cole floodplain may have been underestimated, however they still represent potential rates at the given nitrate concentration, rather than *in situ* rates, since they were on average two orders of magnitude higher that the actual denitrification rates measured for the NEMIS model validation. It should also be noted that since the same treatment was applied to all samples, the relative differences in

denitrification rates between land-use zones, depth intervals in the vadoze zone and between 'dry' and 'wet' condition samples are unbiased and can be interpreted with respect to the different controlling factors involved in each case.

Box 8.1: Comparison between potential denitrification rates at ambient nitrate concentration ('land-use' samples) and at higher than ambiemt nitrate concentration ('dry' samples). The bar chart shows the mean potential denitrification rate ± 1 standard error. The table presents the means ± 1 standard error for denitrification potential, AnMOC, organic carbon content, water and soil nitrate content. The *F* statistic and *P* probability value for One-Way ANOVA are also presented.

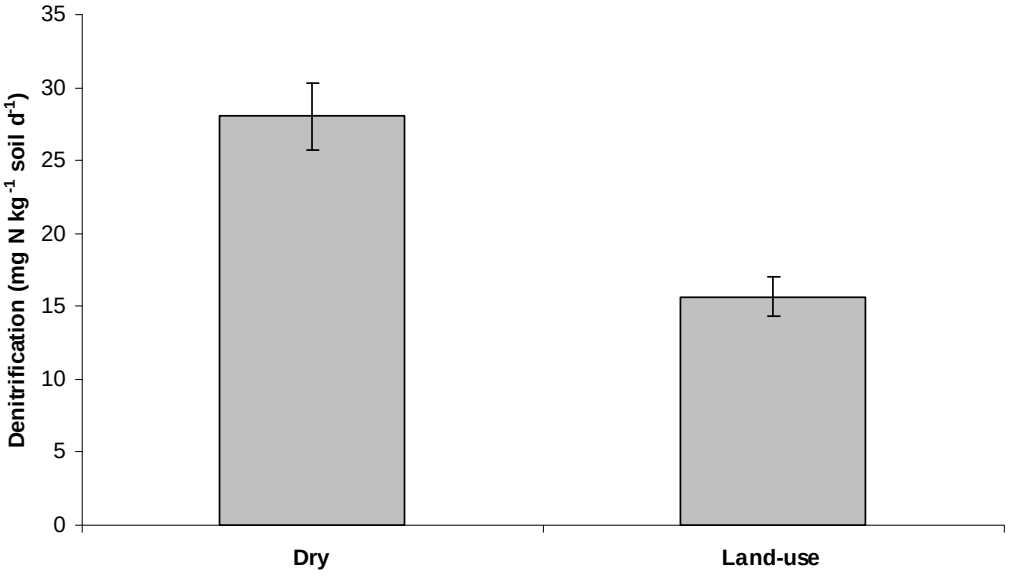

	Dry samples		Land-use samples		ANOVA	
	Mean	**± 1 SE**	**Mean**	**± 1 SE**	***F***	***P***
Denitrification (mg N kg^{-1} soil d^{-1})	28.0	2.3	15.7	1.3	27.9	0.000
AnMOC (µmol CO_2 kg^{-1} soil d^{-1})	704.9	102.2	1334.7	248.8	11.7	0.001
Organic carbon (%)	4.3	0.3	5.8	0.4	10.4	0.002
NO_3^--N (mg kg^{-1})	8.2	1.1	17.5	4.0	6.3	0.016
Water content (%)	47.9	4.3	46.0	2.7	0.0	0.990

DNRA was not significantly affected by the land use management practices. DNRA was shown to be primarily controlled by redox fluctuations, which are in turn controlled by the hydrological/flooding regime, in the intermittently saturated re-connected floodplain. It could therefore be assumed that in the N-rich agricultural soil of the River Cole floodplain, where denitrifiers are dominant, DNRA is concentrated in those environmental patches with low redox conditions, where they might have a competitive advantage against denitrifiers.

8.3.2 *The role of vertical changes in soil stratigraphy and electron donor and acceptor availability in influencing the magnitude and relative importance of denitrification and DNRA*

There were no significant differences in the soil stratigraphy (as expressed by soil texture) across the vadose zone in both the BZ and the PM areas of the River Cole floodplain. The relative availability of electron donors (organic carbon) and acceptors (nitrate) decreased exponentially with depth. Consequently, both the denitrification and DNRA potentials, which were primarily controlled by the LOC availability, decreased exponentially with depth in the vadoze zone. While this study for the first time documents the potential of subsurface floodplain sediments for DNRA, it also highlights the lower relative importance of nitrate attenuation in the subsurface soil horizons of the studied re-connected floodplain. In the subsurface horizons, GW flow is restricted by the low angle and the slow hydraulic conductivities, and the absence of buried organic carbon patches also constraints the efficiency of nitrate attenuation to the organic carbon-rich topsoil.

8.3.3 *The role of wetting-drying cycles in controlling the spatial variability of heterotrophic denitrification and DNRA*

Although the potential denitrification rate was 37 % higher in the wet samples, the difference was not significant. Despite the lower WFPS in the dry condition samples and in conjunction with the available organic carbon and the rich in nitrate soil, denitrifiers survived the unfavourable oxic conditions. However, the spatial variability in denitrification activity between land use zones under wet conditions was lost in the dry conditions. This finding could imply a change in the community structure of denitrifiers induced by the perturbation of prolonged dry conditions. Despite a possible denitrifier community structure change, denitrification activity is not adversely affected

by brief periods of drought, and the regular flooding of the floodplain maintains high denitrification enzyme activity that depends more on the availability of soil moisture and electron donors rather than the community composition of the denitrifiers.

The DNRA potential on the other hand, although present in the dry condition samples, was significantly affected by the dry period and was 60 % lower compared to the wet samples. The results suggest a higher sensitivity of the DNRA activity in a drought perturbation compared to denitrification, which could be due to the change of environmental conditions (i.e. lower WFPS) or a change in the bacterial community composition. However, the fact that DNRA activity was observed upon re-wetting of the dry samples indicates a degree of resilience of the DNRA bacteria. It is therefore likely that a diverse DNRA population exists even in a temperate agricultural catchment with N-rich soils, where denitrifiers generally outcompete DNRA bacteria and restrict them in the lower redox, high carbon environments. However, when a perturbation like drought occurs, DNRA populations adapted to more oxic conditions can survive.

8.4 *Objective Three*

The results for Research Objectives 1 and 2 (A & B) indicated that the intermittent overbank flooding, following the re-connection of the River Cole floodplain, transports river and hillslope-runoff nitrate onto the floodplain, while at the same time creates the necessary conditions (i.e. low oxygen availability, supply of organic carbon) for the occurrence of nitrate removal predominantly via microbial heterotrophic denitrification in the floodplain topsoil. Therefore, for the purpose of informing the design of a floodplain restoration project aiming at increased nitrate removal capacity, or for the post-project appraisal of a restored floodplain, the nitrate removal capacity can be assessed by predicting denitrification at the field scale with the aid of a simple model.

The simple denitrification model NEMIS (Hénault and Germon, 2000) was selected to form the basis of the management tool for floodplain restoration. The validation of the model indicated that the model performs well in conditions different from its development without the need for parameter re-calibration or optimisation. The subsequent application of the model to an annual database collected in the River Cole floodplain showed that the model reasonably predicts the denitrification capacity at the field scale at daily temporal resolution. The application of the model is not data

intensive, since it depends on one laboratory estimation of the denitrification potential of the studied area, which could also be obtained from the literature, while the annual monitoring of soil nitrate, temperature, and moisture is inexpensive and based on standard fieldwork and analytical techniques. It is therefore proposed that the management tool based on the application of the NEMIS model is used as a decision support tool for evaluating the nitrate removal capacity of candidate sites for river-floodplain restoration and/or assessing the nitrate removal capacity of restored floodplains as part of a post-project appraisal.

In conclusion, this study has demonstrated that reconnected floodplains, apart from forming temporary floodwater storage areas, can also significantly contribute to water quality improvement through for example the biological attenuation of nitrate originating from diffuse agricultural sources. Therefore, alongside the establishment of vegetated buffer zones (VBZ) restricted adjacent to agricultural land, as a measure for tackling diffuse agricultural pollution, future river-restoration projects should aim at maximising the buffering capacity of 'larger' floodplains, currently used only as flood alleviation measures. This could be done by the appropriate control of the hydrological regime, for example encouraging overbank flooding in low-angle floodplains for the transport of nitrate and the establishment of the necessary conditions for biological nitrate removal. Moreover, maintaining traditional land management practices, such as grazing and mowing for hay for example, in reclaimed floodplains can potentially have a beneficial effect on the nitrate attenuation capacity through increasing the availability of organic carbon and also temporarily removing nitrate stored in plant biomass. In terms of the processes involved in biological nitrate removal, denitrification appears as the most desirable since it results in permanent removal of nitrate, whilst the alternative pathway of DNRA would be problematic where diffuse nitrate pollution is an issue since it leads in conserving N in the system in a more bioavailable form (NH_4^+). This study however has shown that although the potential for DNRA exists in temperate N-rich agricultural soils, it is significantly lower than denitrification and does not pose a serious risk to nitrate pollution control, as long as redox conditions and nitrate supply remain favourable for denitrification. Finally, this study suggests the use of the simple denitrification model NEMIS for estimating field denitrification rates as a management tool for assisting the design process of future floodplain restoration projects targeting increased nitrate attenuation and for the post-project appraisal of restored sites.

References

Abell, J., Laverman, A. M., & Van Cappellen, P. 2009. Bioavailability of organic matter in a freshwater estuarine sediment: long-term degradation experiments with and without nitrate supply. *Biogeochemistry*, 94: 13-28.

Abramovitz, J. N. 1996. *Imperiled waters, impoverished future: the decline of freshwater ecosystems*. Washington DC, USA: Worldwatch Institute.

Achtnich, C., Bak, F., & Conrad, R. 1995. Competition for electron donors among nitrate reducers, ferric reducers, sulfate reducers, and methanogens in anoxic paddy soil. *Biology and Fertility of Soils*, 19: 65-72.

Acreman, M. C., Riddington, R., & Booker, D. J. 2003. Hydrological impacts of floodplain restoration: a case study of the River Cherwell, UK. *Hydrology and Earth System Sciences*, 7(1): 75-85.

Acreman, M. C., Fisher, J., Stratford, C. J., Mould, D. J., & Mountford, J. O. 2007. Hydrological science and wetland restoration: some case studies from Europe. *Hydrology and Earth System Sciences*, 11(1): 158-169.

Addy, K., Kellogg, D. Q., Gold, A. J., Groffman, P. M., Ferendo, G., & Sawyer, C. 2002. *In Situ* Push-Pull Method to Determine Ground Water Denitrification in Riparian Zones. *Journal of Environmental Quality*, 31(3): 1017-1024.

Alberto, M. C. R., Arah, J. R. M., Neue, H. U., Wassmann, R., Lantin, R. S., Aduna, J. B., & Bronson, K. F. 2000. A sampling technique for the determination of dissolved methane in soil solution. *Chemosphere - Global Change Science*, 2(1): 57-63.

Alewell, C., Paul, S., Lischeid, G., & Storck, F. R. 2008. Co-regulation of redox processes in freshwater wetlands as a function of organic matter availability? *Science of the Total Environment*, 404: 335-342.

Allen, R. G., Pereira, L. S., Raes, D., and Smith, M. Crop evapotranspiration: Guidelines for computing crop water requirements. 56. 1998. Rome, FAO Irrigation and Drainage Paper.

Altor, A. E. & Mitsch, W. J. 2006. Methane flux from created riparian marshes: Relationship to intermittent versus continuous inundation and emergent macrophytes. *Ecological Engineering*, 28: 224-234.

Ambus, P. & Lowrance, R. 1991. Comparison of Denitrification in Two Riparian Soils. *Soil Science Society of America Journal*, 55: 994-997.

Ambus, P., Mosier, A. R., & Christensen, S. 1992. Nitrogen turnover rates in a riparian fen determined by ^{15}N dilution. *Biology and Fertility of Soils*, 14: 230-236.

Amoros, C. & Bornette, G. 2002. Connectivity and biocomplexity in waterbodies of riverine floodplains. *Freshwater Biology*, 47: 761-776.

An, S. & Gardner, W. S. 2002. Dissimilatory nitrate reduction to ammonium (DNRA) as a nitrogen link, versus denitrification as a sink in a shallow estuary (Laguna Madre/Baffin Bay, Texas). *Marine Ecology Progress Series*, 237: 41-50.

Andersen, H. E. 2004. Hydrology and nitrogen balance of a seasonally inundated Danish floodplain wetland. *Hydrological Processes*, 18: 415-434.

Anderson, M. G. & Burt, T. P. 1982. The role of throughflow in storm runoff generation: An evaluation of a chemical mixing model. *Earth Surf.Processes Landforms*, 7: 565-574.

Anderson, M. G. & Burt, T. P. 1990. Subsurface runoff. In M. G. Anderson & T. P. Burt (Eds.), *Process studies in hillslope hydrology*: 365-400. Chichester: Wiley.

Anderson, M. G., Bates, P. D., & Walling, D. E. 1996. The general context for floodplain process research. In M. G. Anderson, D. E. Walling, & P. D. Bates (Eds.), *Floodplain Processes*: 1-13. New York: Wiley.

Arnell, N. W. 1999. The effect of climate change on hydrological regimes in Europe: a continental perspective. *Global Environmental Change - Human Policy Dimension*, 9: 5-23.

Arnold, J. G., Williams, J. R., & Maidment, D. R. 1995. A Continuous Water and Sediment Routing Model for Large Basins. *Journal of Hydrological Engineering*, 121(2): 171-183.

Aulakh, M. S., Kuldip-Singh, Bijay, S., & Doran, J. W. 1996. Kinetics of nitrification under upland and flooded soils of varying texture. *Communications in Soil Science and Plant Analysis*, 27: 2079-2089.

Baird A.J., Surridge B.W.J., & Money R.P. 2004. An assessment of the piezometer method for measuring the hydraulic conductivity of a *Cladium mariscus—Phragmites australis* root mat in a Norfolk (UK) fen. *Hydrological Processes*, 18: 275-291.

Baker, M. A. & Vernier, P. 2004. Hydrological variability, organic matter supply and denitrification in the Garonne River ecosystem. *Freshwater Biology*, 49: 181-190.

Baker, M. A. & Wiley, M. J. 2009. Multiscale control of flooding and riparian-forest composition in Lower Michigan, USA. *Ecology*, 90(1): 145-159.

Baldwin, D. S. & Mitchell, A. M. 2000. The effects of drying and re-flooding on the sediment and soil nutrient dynamics of lowland river-floodplain systems: a synthesis. *Regulated Rivers: Research & Management*, 16: 457-467.

Banach, A. M., Banach, K., Visser, E. J. W., Stepniewska, Z., Smits, A. J. M., Roelofs, J. G. M., & Lamers, L. P. M. 2009. Effects of summer flooding on floodplain biogeochemistry in Poland; implications for increased flooding frequency. *Biogeochemistry*, 92: 247-262.

Barlund, I., Kirkkala, T., Malve, O., & Kamari, J. 2007. Assessing SWAT model performance in the evaluation of management actions for the implementation of the Water Framework Directive in a Finnish catchment. *Environmental Modelling & Software*, 22: 719-724.

Bastviken, S., Eriksson, P. G., Ekstrom, A., & Tonderski, K. 2007. Seasonal denitrification potential in wetland sediments with organic matter from different plant species. *Water, Air, & Soil Pollution*, 183: 25-35.

Bates, P. D., Stewart, M. D., Desitter, A., Anderson, M. G., Renaud, J.-P., & Smith, J. A. 2000. Numerical simulation of floodplain hydrology. *Water Resources Research*, 36(9): 2517-2529.

Bear, J. 1972. Dynamics of Fluids in Porous Media. *Dover Publications*. ISBN: 0-486-65675-6.

Beare, M. H., Neely, C. L., Coleman, D. C., & Hargrove, W. L. 1990. A substrate-induced respiration (SIR) method for measurement of fungal and bacterial biomass on plant residues. *Soil Biology and Biochemistry*, 22: 585-594.

Beauchamp, E. G., Trevors, J. T., & Paul, J. W. 1989. Carbon sources for bacterial denitrification. *Adv.Soil Sci.*, 10: 113-142.

Beaujouan, V., Durand, P., & Ruiz, L. 2001. Modelling the effect of the spatial distribution of agricultural practices on nitrogen fluxes in rural catchments. *Ecological Modelling*, 137: 93-105.

Bechtold, J. S. & Naiman, R. J. 2006. Soil texture and nitrogen mineralization potential across a riparian toposequence in a semiarid savanna. *Soil Biology and Biochemistry*, 38: 1325-1333.

Bedient, P. B. & Huber, W. C. 1988. *Hydrology and floodplain analysis*. Addison-Wesley Publishing Company.

Bengtsson, G. & Bergwall, C. 2000. Fate of ^{15}N labelled nitrate and ammonium in a fertilised forest soil. *Soil Biology and Biochemistry*, 32: 545-557.

Bernal, S., Sabater, F., Butturini, A., Nin, E., & Sabater, S. 2007. Factors limiting denitrification in a Mediterranean riparian forest. *Soil Biology and Biochemistry*, 39: 2685-2688.

Betlach, M. R. & Tiedje, J. M. 1981. Kinetic explanation for accumulation of nitrite, nitric oxide, and nitrous oxide during bacterial denitrification. *Applied and Environmental Microbiology*, 42(6): 1074-1084.

Beven, K. J. 1989. Interflow. In H. J. Morel-Seytoux (Ed.), *Unsaturated flow in hydrologic modelling: theory and practice* : 191-219. Dordrecht: Kluwer.

Biggs, J., Corfield, A., Gron, P., Hansen, H. O., Walker, D., Whitfield, M., & Williams, P. 1998. Restoration of the rivers Brede, Cole and Skerne: a joint Danish and British EU-LIFE demonstration project, V-Short-term impacts on the

conservation value of aquatic macroinvertebrate and macrophyte assemblages. *Aquatic Conservation: Marine and Freshwater Ecosystems*, 8: 241-255.

Biggs, T. W., Dunne, T., & Muraoka, T. 2006. Transport of water, solutes and nutrients from a pasture hillslope, southwestern Brazilian Amazon. *Hydrological Processes*, 20: 2527-2547.

Bijay, S., Ryden, J. C., & Whitchead, D. C. 1988. Some relationships between denitrification potential and fractions of organic carbon in air-dried and field-moist soils. *Soil Biology and Biochemistry*, 20(5): 737-741.

Bissels, S., Hölzel, N., Donath, T. W., & Otte, A. 2004. Evaluation of restoration success in alluvial grasslands under contrasting flooding regimes. *Biological Conservation*, 118: 641-650.

Bittman, S., Hunt, D. E., & Shaffer, M. J. 2001. NLOS (NLEAP on STELLA) - A nitrogen cycling model with a graphical interface: implications for model developers and users. In M. J. Shaffer, L. Ma, & S. Hansen (Eds.), *Modelling Carbon and Nitrogen Dynamics for Soil Management*: 383-402. Boca Raton FL: Lewis Publishers.

Blackwell, M. S. A. and Maltby, E. Ecoflood Guidelines: How to use floodplains for flood risk reduction. EVK1-CT-2002-80017. 2005.

Boon, P. I., Mitchell, A., & Lee, K. 1997. Effects of wetting and drying on methane emissions from ephemeral floodplain wetlands in south-eastern Australia. *Hydrobiologia*, 357(1): 73-87.

Boon, P. J., Davies, B. R., & Petts, G. E. 2000. *Global perspectives on river conservation: science, policy and practice*. Chichester, UK: Wiley.

Boudreau, B. P. 1997. *Diagenetic models and their implementation*. Springer.

Bowman, R. A., Reeder, J. D., & Lober, R. W. 1990. Changes in soil properties in a central plains rangeland soil after 3, 20, and 60 years of cultivation. *Soil Science*, 150: 851-857.

Boyer, J. N. & Groffman, P. M. 1996. Bioavailability of water extractable organic carbon fractions in forest and agricultural soil profiles. *Soil Biology and Biochemistry*, 28(6): 783-790.

Bradley, C. 2002. Simulation of the annual water table dynamics of a floodplain wetland, Narborough Bog, UK. *Journal of Hydrology*, 261: 150-172.

Brady, N. C. & Weil, R. R. 2002. *The Nature and Properties of Soils*. New Jersey: Prentice Hall.

Bremer, C., Braker, G., Matthies, D., Reuter, A., Engels, C., & Conrad, R. 2007. Impact of plant functional group, plant species, and sampling time on the composition of *nir*K-Type denitrifier communities in soil. *Applied and Environmental Microbiology*, 73(21): 6876-6884.

Brettar, I. & Höfle, M. G. 2002. Close Correlation Between The Nitrate Elimination Rate By Denitrification And The Organic Matter Content In Hardwood Forest Soils Of The Upper Rhine Floodplain (France). *Wetlands*, 22(2): 214-224.

Brettar, I., Sanchez-Perez, J. M., & Trémolières, M. 2002. Nitrate elimination by denitrification in hardwood forest soils of the Upper Rhine floodplain – correlation with redox potential and organic matter. *Hydrobiologia*, 469(1): 11-21.

Bronstert, A. 2003. Floods and climate change: interactions and impacts. *Risk Anal.*, 23(3): 545-557.

Brookes, A. 1996. Floodplain restoration and rehabilitation. In M. G. Anderson, D. E. Walling, & P. Bates (Eds.), *Floodplain Processes*: 553-576. New York: Wiley.

Brooks, P. D., Stark, J. M., McInteer, B. B., & Preston, T. 1989. Diffusion method to prepare soil extracts for automated Nitrogen-15 analysis. *Soil Science Society of America Journal*, 53: 1707-1711.

Brown, A. G. 1996. Floodplain palaeoenvironments. In M. G. Anderson, D. E. Walling, & P. D. Bates (Eds.), *Floodplain Processes*: 95-138. New York: Wiley.

Bruland, G. L. & Richardson, C. J. 2004. A spatially explicit investigation of phosphorus sorption and related soil properties in two riparian wetlands. *Journal of Environmental Quality*, 33: 785-794.

Bruland, G. L., Richardson, C. J., & Whalen, S. C. 2006. Spatial Variability Of Denitrification Potential And Related Soil Properties In Created, Restored, And Paired Natural Wetlands. *Wetlands*, 26(4): 1042-1056.

Brunet, R. C. & Garcia-Gil, L. J. 1996. Sulfide-induced dissimilatory nitrate reduction to ammonia in anaerobic freshwater sediments. *FEMS Microbiology Ecology*, 21: 131-138.

Buijse, A. D., Coops, H., Staras, M., Jans, L. H., Van Geest, G. J., Grift, R. E., Ibelings, B. W., Oosterberg, W., & Roozen, F. C. J. M. 2002. Restoration strategies for river floodplains along large lowland rivers in Europe. *Freshwater Biology*, 47: 889-907.

Bulger, P. R., Kehew, A. E., & Nelson, R. A. 1989. Dissimilatory nitrate reduction in a waste-water contaminated aquifer. *Ground Water*, 27(5): 664-671.

Bullock, A. & Acreman, M. C. 2003. The role of wetlands in the hydrological cycle. *Hydrology and Earth System Sciences*, 7(3): 358-389.

Buresh, R. J. & Patrick, W. H. 1981. Nitrate reduction to ammonium and organic nitrogen in an estuarine sediment. *Soil Biology and Biochemistry*, 13(4): 279-283.

Burgin, A. J. & Hamilton, S. K. 2007. Have we overemphasized the role of denitrification in aquatic ecosystems? A review of nitrate removal pathways. *Frontiers in Ecology and The Environment*, 5(2): 89-96.

Burgin, A. J. & Hamilton, S. K. 2008. NO_3^- -Driven SO_4^{2-} production in freshwater ecosystems: Implications for N and S cycling. *Ecosystems*, 11: 908-922.

Burt, T. P. & Haycock, N. E. 1996. Linking hillslopes to floodplains. In M. G. Anderson, D. E. Walling, & P. D. Bates (Eds.), *Floodplain Processes*: 461-492. John Wiley & Sons Ltd.

Burt, T. P. 1997. The hydrological role of floodplains within the drainage basin system. In N. E. Haycock, T. P. Burt, K. W. T. Goulding, & G. Pinay (Eds.), *Buffer Zones: Their Processes and Potential in Water Protection*: 21-32. Harpenden: Quest Environmental.

Burt, T. P., Matchett, L. S., Goulding, K. W. T., Webster, C. P., & Haycock, N. E. 1999. Denitrification in riparian buffer zones: the role of floodplain hydrology. *Hydrological Processes*, 13: 1451-1463.

Burt, T. P., Pinay, G., Matheson, F. E., Haycock, N. E., Butturini, A., Clement, J. C., Danielescu, S., Dowrick, D. J., Hefting, M. M., Hillbricht-Ilkowska, A., & Maitre, V. 2002a. Water table fluctuations in the riparian zone: comparative results from a pan-European experiment. *Journal of Hydrology*, 265: 129-148.

Burt, T. P., Bates, P. D., Stewart, M. D., Claxton, A. J., Anderson, M. G., & Price, D. A. 2002b. Water table fluctuations within the floodplain of the River Severn, England. *Journal of Hydrology*, 262: 1-20.

Burt, T. P. & Pinay, G. 2005. Linking hydrology and biogeochemistry in complex landscapes. *Progress in Physical Geography*, 29(3): 297-316.

Burt, T. P. 2005. A third paradox in catchment hydrology and biogeochemistry: decoupling in the riparian zone. *Hydrological Processes*, 19: 2087-2089.

Butturini, A., Bernal, S., Nin, E., Hellin, C., Rivero, L., Sabater, S., & Sabater, F. 2003. Influences of the stream groundwater hydrology on nitrate concentration in unsaturated riparian area bounded by an intermittent Mediterranean stream. *Water Resources Research*, 39(4): 1110-1122.

Cavigelli, M. A. & Robertson, G. P. 2000. The functional significance of denitrifier community composition in a terrestrial ecosystem. *Ecology*, 81(5): 1402-1414.

Cabezas, A., Garcia, M., Gallardo, B., Gonzalez, E., Gonzalez-Sanchis, M., & Comin, F. A. 2009. The effect of anthropogenic disturbance on the hydrochemical characteristics of riparian wetlands at the Middle Ebro River (NE Spain). *Hydrobiologia*, 617: 101-116.

Cerucci, M. & Conrad, J. M. 2003. The use of binary optimization and hydrologic models to form riparian buffers. *Journal of the American Water Resources Association*, 39(5): 1167-1180.

Chappell, A. 1998. Dispersing sandy soil for the measurement of particle size distributions using optical laser diffraction. *Catena*, 31: 271-281.

Cherry, K. A., Shepherd, M., Withers, P. J. A., & Mooney, S. J. 2008. Assessing the effectiveness of actions to mitigate nutrient loss from agriculture: A review of methods. *Science of the Total Environment*, 406: 1-23.

Christensen, P. B., Rysgaard, S., Sloth, N. P., Dalsgaard, T., & Schwaerter, S. 2000. Sediment mineralization, nutrient fluxes, denitrification and dissimilatory nitrate reduction to ammonium in an estuarine fjord with sea cage trout farms. *Aquatic Microbial Ecology*, 21(1): 73-84.

Cirmo, C. P. & McDonnell, J. J. 1997. Linking the hydrologic and biogeochemical controls of nitrogen transport in near-stream zones of temperate-forested catchments: a review. *Journal of Hydrology*, 199: 88-120.

Claassen, T. H. L. 2000. Restoration of small water bodies by introducing aquatic plants. *Verh.Internat.Verein.Limnol.*, 27: 586-592.

Clarke, S. J. & Wharton, G. 2000. An investigation of marginal habitat and macrophyte community enhancement on the River Torne, UK. *Regulated Rivers: Research & Management*, 16(3): 225-244.

Clarke, S. J., Bruce-Burgess, L., & Wharton, G. 2003. Linking Form and Function: Towards an Ecohydromorphic Approach to Sustainable River Restoration. *Aquatic Conservation: Marine and Freshwater Ecosystems*, 13: 439-450.

Clément, J. C., Pinay, G., & Marmonier, P. 2002. Seasonal dynamics of denitrification along topohydrosequences in three different riparian wetlands. *Journal of Environmental Quality*, 31: 1025-1037.

Clément, J. C., Aquilina, L., Bour, O., Plaine, K., Burt, T. P., & Pinay, G. 2003. Hydrological flowpaths and nitrate removal rates within a riparian floodplain along a fourth-order stream in Brittany (France). *Hydrological Processes*, 17: 1177-1195.

Clilverd, H. M., Jones, J. B., & Kielland, K. 2008. Nitrogen retention in the hyporheic zone of a glacial river in interior Alaska. *Biogeochemistry*, 88: 31-46.

Constanza, R., d'Arge, R., de Groot, R., Farber, S., Grasso, M., Hannon, B., Limburg, K., Naeem, S., Neill, R. V., Paruelo, J., Raskin, R. G., Sutton, P., & Van der Belt, M. 1997. The value of the world's ecosystem services and natural capital. *Nature*, 387: 253-260.

Cooper, A. B. 1990. Nitrate depletion in the riparian zone and stream channel of a small headwater catchment. *Hydrobiologia*, 202: 13-26.

Corre, M. D., Beese, F. O., & Brumme, R. 2003. Soil nitrogen cycle in high nitrogen deposition forest: changes under nitrogen saturation and liming. *Ecological Applications*, 13: 287-298.

Corre, M. D. & Lamersdorf, N. P. 2004. Reversal of nitrogen saturation after long-term deposition reduction: impact on soil nitrogen cycling. *Ecology*, 85: 3090-3104.

Correll, D. L., Jordan, T. E., & Weller, D. E. 1997. Failure of agricultural riparian buffers to protect surface waters from groundwater nitrate contamination. In J. Gibert (Ed.), *Groundwater/surface water ecotones: Biological and hydrological interactions and management options*: 162-165. Cambridge: Cambridge University Press.

Correll, D. L. 2005. Principles of planning and establishment of buffer zones. *Ecological Engineering*, 24: 433-439.

Cosandey, A.-C., Maitre, V., & Guenat, C. 2003a. Temporal denitrification patterns in different horizons of two riparian soils. *European Journal of Soil Science*, 54: 25-37.

Cosandey, A. C., Guenat, C., Bouzelboudjen, M., Maitre, V., & Bovier, R. 2003b. The modelling of soil-process functional units based on three-dimensional soil horizon cartography, with an example of denitrification in a riparian zone. *Geoderma*, 112(1-2): 111-129.

Curie, F., Ducharne, A., Sebilo, M., & Bendjoudi, H. 2009. Denitrification in a hyporheic riparian zone controlled by river regulation in the Seine river basin (France). *Hydrological Processes*, 23: 655-664.

Dahl, M., Nilsson, B., Langhoff, J. H., & Refsgaard, J. C. 2007. Review of classification schemes and new multi-scale typology of groundwater–surface water interaction. *Journal of Hydrology*, 344(1-2): 1-16.

Dalsgaard, T. & Thamdrup, B. 2002. Factors controlling anaerobic ammonium oxidation with nitrite in marine sediments. *Applied and Environmental Microbiology*, 68: 3802-3808.

Dalsgaard, T., Thamdrup, B., & Canfield, D. E. 2005. Anaerobic ammonium oxidation (anammox) in the marine environment. *Res Microbiol*, 156: 457-464.

D'Angelo, E. M. & Reddy, K. R. 1999. Regulation of heterotrophic microbial potentials in wetland soils. *Soil Biology and Biochemistry*, 31: 815-830.

Daniel, C. C. I. 1981. Hydrology, geology and soils of pocosins: a comparison of natural and altered systems. In C. J. Richardson, M. L. Matthews, & S. A. Anderson (Eds.), *Pocosin Wetlands*: 69-108. Stroudsbury, PA, USA: Hutchinson Ross Publishing Company.

Dauwe, B., Middelburg, J. J., & Herman, P. M. J. 2001. Effect of oxygen on the degradability of organic matter in subtidal and intertidal sediments of the North Sea area. *Marine Ecology Progress Series*, 215: 13-22.

Davidson, E. A., Hart, S. C., Shanks, C. A., & Firestone, M. K. 1991. Measuring gross nitrogen mineralization, immobilization, and nitrification by ^{15}N isotopic pool dilution in intact soil cores. *Journal of Soil Science*, 42: 335-349.

Davidson, E. A., Hart, S. C., & Firestone, M. K. 1992. Internal cycling of nitrate in soils of a mature coniferous forest. *Ecology*, 73(1148): 1156.

Davidson, E. A., Keller, M., Erickson, H. E., Verchot, L. V., & Veldkamp, E. 2000. Testing a conceptual model of soil emissions of nitrous and nitric oxides. *Bioscience*, 50(8): 667-680.

Davidson, E. A. & Seitzinger, S. 2006. The enigma of progress in denitrification research. *Ecological Applications*, 16(6): 2057-2063.

Davidsson, E. T. & Leonardson, L. 1996. Effects of nitrate and organic carbon additions on denitrification in two artificially flooded soils. *Ecological Engineering*, 7: 139-149.

Davidsson, E. T. & Stahl, M. 2000. The influence of organic carbon on nitrogen transformations in five wetland soils. *Soil Science Society of America Journal*, 64: 1129-1136.

Davidsson, T. E., Stepanauskas, R., & Leonardson, L. 1997. Vertical patterns of nitrogen transformations during infiltration in two wetland soils. *Applied and Environmental Microbiology*, 63: 3648-3656.

Davis, J. H., Griffith, S. M., Horwath, W. R., Steiner, J. J., & Myrold, D. D. 2008. Denitrification and nitrate consumption in an herbaceous riparian area and perennial ryegrass seed cropping system. *Soil Science Society of America Journal*, 72(5): 1299-1310.

Décamps, H. 1993. River margins and environmental change. *Ecological Applications*, 3(3): 441-445.

De Klein, C. A. M. & van Longtestijn, R. S. P. 1994. Denitrification in the top soil of managed grasslands in The Netherlands in relation to soil type and fertiliser level. *Plant and Soil*, 163: 33-44.

Delta-T Devices 1999. *ThetaProbe soil moisture sensor: Type ML2x: User Manual*. Cambridge, UK: Delta-T Devices Ltd.

De Neve, S. & Hofman, G. 2002. Quantifying soil water effects on N mineralization from soil organic matter and from fresh crop residues. *Biology and Fertility of Soils*, 35: 379-386.

Department for Environment, Food and Rural Affairs DEFRA. Directing the Flow: Priorities for Future Water Policy. 2002. Department for Environment,Food and Rural Affairs (DEFRA).

Department for Environment, Food and Rural Affairs DEFRA. Making Space for Water. Developing a new Government strategy for flood and coastal erosion risk management in England. A consultation exercise. 2004. Department for Environment,Food and Rural Affairs (DEFRA).

Devito, K. J., Fitzgerald, D., Hill, A. R., & Aravena, R. 2000. Nitrate dynamics in relation to lithology and hydrologic flow path in a river riparian zone. *Journal of Environmental Quality*, 29: 1075-1084.

Di, H. J., Cameron, K. C., & McLaren, R. G. 2000. Isotopic dilution methods to determine gross transformation rates of nitrogen, phosphorus, and sulphur in soil: a review of the theory, methodologies, and limitations. *Aust.J.Soil Res.*, 38: 213-230.

Dick, R. P., Christ, R. A., Istok, J. D., & Iyamuremye, F. 2000. Nitrogen fractions and transformations of vadose zone sediments under intensive agriculture in Oregon. *Soil Science*, 165(6): 505-515.

Dingman, S. L. 1994. *Physical Hydrology*. Englewood Cliffs, NJ: Prentice Hall.

Dinsmore, K. J., Skiba, U. M., Billett, M. F., Rees, R. M., & Drewer, J. 2009. Spatial and temporal variability in CH_4 and N_2O fluxes from a Scottish ombrotrophic peatland: Implications for modelling and up-scaling. *Soil Biology and Biochemistry*, 41: 1315-1323.

Dodla, S. K., Wang, J. J., DeLaune, R. D., & Cook, R. L. 2008. Denitrification potential and its relation to organic carbon quality in three coastal wetland soils. *Science of the Total Environment*, 407: 471-480.

Drury, C. F., Oloya, T. O., McKenney, D. J., Gregorich, E. G., Tan, C. S., & vanLuyk, C. L. 1998. Long-Term Effects of Fertilization and Rotation on Denitrification and Soil Carbon. *Soil Science Society of America Journal*, 62: 1572-1579.

Ducros, C. M. J. & Joyce, C. B. 2003. Field-Based Evaluation Tool for Riparian Buffer Zones in Agricultural Catchments. *Environmental Management*, 32(2): 252-267.

Dullien, F. A. L. 1979. *Porous media*. San Diego: Academic Press.

Dunne, T. & Black, R. D. 1970. An experimental investigation of runoff prediction in permeable soils. *Water Resources Research*, 6: 478-490.

Dunne, T. & Leopold, L. B. 1978. *Water in environmental planning*. New York, USA: W.H. Freeman and Company.

Duval, T. P. & Hill, A. R. 2006. Influence of stream bank seepage during low-flow conditions on riparian zone hydrology. *Water Resources Research*, 42(10): 1397-1409.

Duval, T. P. & Hill, A. R. 2007. Influence of base flow stream bank seepage on riparian zone nitrogen biogeochemistry. *Biogeochemistry*, 85: 185-199.

Dytham, C. 2003. *Choosing and Using Statistics: A Biologist's Guide*. Blackwell Publishing.

Engel, B., Storm, D., White, M., Arnold, J., & Arabi, M. 2007. A Hydrologic/Water Quality Model Application. *Journal of the American Water Resources Association*, 43(5): 1223-1236.

Environment Agency, 2007. Environmental Facts and Figures: Nitrates in rivers and groundwater.http://www.environmentagency.gov.uk/yourenv/eff1190084/water/210440/210566/?lang=_e

Environmental report to accompany proposals for the restoration of the River Cole at Coleshill Final Report. 1995. E5516, 1-43. WS Atkins Environment.

Ettema, C. H., Lowrance, R., & Coleman, D. C. 1999. Riparian soil response to surface nitrogen input: temporal changes in denitrification, labile and microbial C and N pools, and bacterial and fungal respiration. *Soil Biology and Biochemistry*, 31: 1609-1624.

Fay, P. A., Carlisle, J. D., Knapp, A. K., Blair, J. M., & Collins, S. L. 2000. Altering rainfall timing and quantity in a mesic grassland ecosystem: Design and performance of rainfall manipulation shelters. *Ecosystems*, 3: 308-319.

Fazzolari, E., Mariotti, A., & Germon, J. C. 1990. Dissimilatory ammonia production vs. denitrification *in vitro* and in inoculated soil samples. *Can.J.Microbiol.*, 36: 786-793.

Fazzolari, E., Nicolardot, B., & Germon, J. C. 1998. Simultaneous effects of increasing levels of glucose and oxygen partial pressures on denitrification and dissimilatory nitrate reduction to ammonium in repacked soil cores. *European Journal of Soil Science*, 34(1): 47-52.

Fennessy, M. S. & Cronk, J. K. 1997. The effectiveness and restoration potential of riparian ecotones for the management of non-point source pollution, particularly nitrate. *Critical Reviews in Environmental Science and Technology*, 27(4): 285-317.

Fierer, N. & Schimel, J. P. 2002. Effects of drying-rewetting frequency on soil carbon and nitrogen transformations. *Soil Biology and Biochemistry*, 34: 777-787.

Fierer, N., Schimel, J. P., & Holden, P. A. 2003. Influence of drying-rewetting frequency on soil bacterial community structure. *Microbial Ecology*, 45: 63-71.

Florinsky, I. V., McMahon, S., & Burton, D. L. 2004. Topographic control of soil microbial activity: a case study of denitrifiers. *Geoderma*, 119: 33-53.

Forshay, K. & Stanley, E. 2005. Rapid Nitrate Loss and Denitrification in a Temperate River Floodplain. *Biogeochemistry*, 75(1): 43-64.

Fossing, H., Gallardo, V. A., Jorgensen, B. B., Huttel, M., Nielsen, L. P., Schulz, H., Canfield, D. E., Forster, S., Glud, R. N., Gundersen, J. K., Kuver, J., Ramsing, N. B., Teske, A., Thamdrup, B., & Ulloa, O. 1995. Concentration and transport of nitrate by the mat-forming sulfur bacterium *Thioploca*. *Nature*, 374: 713-715.

Frank, D. A. & Groffman, P. M. 1998a. Ungulate vs. landscape control of soil C and N processes in grasslands of Yellowstone National Park. *Ecology*, 79(7): 2229-2241.

Frank, D. A. & Groffman, P. M. 1998b. Denitrification in a semi-arid grazing ecosystem. *Oecologia*, 117: 564-569.

Frank, D. A. & Groffman, P. M. 2009. Plant rhizospheric N processes: what we don't know and why we should care. *Ecology*, 90(6): 1512-1519.

Friberg, N., Kronvang, B., Hansen, H. O., & Svendsen, L. M. 1998. Long-Term, Habitat-Specific Response of a Macroinvertebrate Community to River Restoration. *Aquatic Conservation: Marine and Freshwater Ecosystems*, 8(1): 87-99.

Fromin, N., Pinay, G., Montuelle, B., Landais, D., Ourcival, J.-M., Joffre, R., & Lensi, R. (in press). Impact of seasonal sediment desiccation and rewetting on microbial processes involved in greenhouse gas emissions. *Biogeochemistry*.

Fry, B. 2006. *Stable Isotope Ecology*. Springer.

Fujihara, S., Nakashima, T., & Kurogochi, Y. 1986. Determination of $^{15}NH_3$ by gas chromatography-mass spectrometry. Application to the measurement of putrescine oxidation by human plasma. *Journal of Chromatography*, 383: 271-280.

Gale, I. N., Marks, R. J., Darling, W. G., and West, J. M. Bacterial denitrification in aquifers: evidence from the unsaturated zone and the unconfined chalk and Sherwood sandstone aquifers. 215. 1994. National Rivers Authority.

Gale, P. M., Reddy, K. R., & Graetz, D. A. 1992. Mineralization of Sediment Organic-Matter Under Anoxic Conditions. *Journal of Environmental Quality*, 21(3): 394-400.

Galloway, J. N., Townsend, A. R., Erisman, J. W., Bekunda, M., Cai, Z., Freney, J. R., Martinelli, L. A., Seitzinger, S., & Sutton, M. A. 2008. Transformation of the Nitrogen Cycle: Recent trends, questions and potential solutions. *Science*, 320: 889-892.

Gavrichkova, O., Moscatelli, M. C., Grego, S., & Valentini, R. 2008. Soil carbon mineralization in a Mediterranean pasture: effect of grazing and mowing management practices. *Agrochimica*, 52(5): 285-296.

Gergel, S. E., Dixon, M. D., & Turner, M. G. 2002. Consequences of human altered floods: levees, floods, and floodplain forests along the Wisconsin River. *Ecological Applications*, 12: 1755-1770.

Gergel, S. E., Carpenter, S. R., & Stanley, E. H. 2005. Do dams and levees impact nitrogen cycling? Simulating the effects of flood alterations on floodplain denitrification. *Global Change Biology*, 11(8): 1352-1367.

Gift, D. M., Groffman, P. M., Kaushal, S. S., & Mayer, P. M. 2008. Denitrification potential, root biomass, and organic matter in degraded and restored urban riparian zones. *Restoration Ecology*, 1-8.

Gillham, R. W. 1984. The capillary fringe and its effect on water table response. *Journal of Hydrology*, 67: 307-324.

Go, J. 2008. PhD Thesis: Numerical Modelling of Organic Contaminant Reaction and Transport in Bed Sediments. University College London.

Gold, A. J., Groffman, P. M., Addy, K., Kellogg, D. Q., Stolt, M. H., & Rosenblatt, A. E. 2001. Landscape attributes as controls on groundwater nitrate removal capacity of riparian zones. *Journal of the American Water Resources Association*, 37(6): 1457-1464.

Granli, T. & Bockman, O. C. 1994. Nitrogen oxide from agriculture. *Norw.J.Agr.Sci.*, 128(12): 63-72.

Gregory, S. V., Swanson, F. J., McKee, W. A., & Cummins, K. W. 1991. An ecosystem perspective of riparian zones. *Bioscience*, 41: 540-551.

Groffman, P. M. & Tiedje, J. M. 1988. Denitrification hysteresis during wetting and drying cycles in soil. *Soil Science Society of America Journal*, 52: 1626-1629.

Groffman, P. M. & Tiedje, J. M. 1989. Denitrification in north temperate forest soils: Relationships between denitrification and environmental factors at the landscape scale. *Soil Biology and Biochemistry* , 21: 621-626.

Groffman, P. M., Axelrod, E. A., Lemunyon, J. L., & Sullivan, W. M. 1991. Denitrification in grass and forest vegetated filter strips. *Journal of Environmental Quality*, 20: 671-674.

Groffman, P. M., Gold, A. J., & Simmons, R. C. 1992. Nitrate dynamics in riparian forests: Microbial studies. *Journal of Environmental Quality*, 21: 666-671.

Groffman, P. M., Rice, C. W., & Tiedje, J. M. 1993a. Denitrification in a tallgrass prairie landscape. *Ecology*, 74(3): 855-862.

Groffman, P. M., Zak, D. R., Christensen, S., Mosier, A., & Tiedje, J. M. 1993b. Early spring nitrogen dynamics in a temperate forest landscape. *Ecology*, 74(5): 1579-1585.

Groffman, P. M., Holland, E. A., Myrold, D. D., Robertson, G. P., & Zou, X. 1999. Denitrification. In G. P. Robertson, D. C. Coleman, C. S. Bledsoe, & P. Sollins (Eds.), *Standard soil methods for long-term ecological research*: 272-288. New York, USA: Oxford University Press.

Groffman, P. M., Gold, A. J., & Addy, K. 2000. Nitrous oxide production in riparian zones and its importance to national emission inventories. *Chemosphere - Global Change Science*, 2: 291-299.

Groffman, P. M. & Crawford, M. K. 2003. Denitrification potential in urban riparian zones. *Journal of Environmental Quality*, 32: 1144-1149.

Groffman, P. M., Altabet, M. A., Bohlke, J. K., Butterbach-Bahl, K., David, M. B., Firestone, M. K., Giblin, A. E., Kana, T. M., Nielsen, L. P., & Voytek, M. A.

2006. Methods for measuring denitrification: Diverse approaches to a difficult problem. *Ecological Applications*, 16(6): 2091-2122.

Groffman, P. M., Butterbach-Bahl, K., Fulweiler, R. W., Gold, A. J., Morse, J. L., Stander, E. K., Tague, C., Tonitto, C., & Vidon, P. 2009. Challenges to incorporating spatially and temporally explicit phenomena (hotspots and hot moments) in denitrification models. *Biogeochemistry*, 93: 49-77.

Grundmann, G. L. & Rolston, D. E. 1987. A water function approximation to degree of anaerobiosis associated with denitrification. *Soil Science*, 144: 437-441.

Gu, C., Hornberger, G. M., Herman, J. S., & Mills, A. L. 2008. Influence of stream-groundwater interactions in the streambed sediments on NO_3^- flux to a low-relief coastal stream. *Water Resources Research*, 44(11).

Gurnell, A. M., Piégay, H., Swanson, F. J., & Gregory, S. V. 2002. Large wood and fluvial processes. *Freshwater Biology*, 47: 601-619.

Gurwick, N. P., Groffman, P. M., Yavitt, J. B., Gold, A. J., Blazejewski, G., & Stolt, M. 2008. Microbially available carbon in buried riparian soils in a glaciated landscape. *Soil Biology and Biochemistry*, 40: 85-96.

Haberstock, A. E., Nichols, H. G., DesMeules, M. P., Wright, J., Christensen, J. M., & Hudnut, D. H. 2000. Method to identify effective riparian buffer widths for atlantic salmon habitat protection. *Journal of the American Water Resources Association*, 36(6): 1271-1286.

Hammersmark, C. T., Rains, M. C., & Mount, J. F. 2008. Quantifying the hydrological effects of stream restoration in a montane meadow, Northern California, USA. *River Research And Applications*, 24: 735-753.

Hansen, H. O. 2003. Restoration of the Skjern River - Denmark's largest restoration project. *Verh.Internat.- Verein.Limnol.*, 28(4): 1810-1813.

Hanson, G. C., Groffman, P. M., & Gold, A. J. 1994. Symptoms of nitrogen saturation in a riparian wetland. *Ecological Applications*, 4(4): 750-756.

Harms, T. K. & Grimm, N. B. 2008. Hot spots and hot moments of carbon and nitrogen dynamics in a semiarid riparian zone. *Journal of Geophysical Research*, 113.

Harms, T. K., Wentz, E. A., & Grimm, N. B. 2009. Spatial heterogeneity of denitrification in semi-arid floodplains. *Ecosystems*, 12: 129-143.

Harrison, S. S. C., Pretty, J. L., Shepherd, D., Hildrew, A. G., Smith, C., & Hey, R. D. 2004. The effect of instream rehabilitation structures on macroinvertebrates in lowland rivers. *Journal of Applied Ecology*, 41(6): 1140-1154.

Hart, S. C., Nason, G. E., Myrold, D. D., & Perry, D. A. 1994a. Dynamics of gross nitrogen transformations in an old-growth forest: the carbon connection. *Ecology*, 75(4): 880-891.

Hart, S. C., Stark, J. M., Davidson, E. A., & Firestone, M. K. 1994b. *Methods of soil analysis, part 2. Microbiological and biochemical properties*. Madison, Wis.: Soil Science Society of America.

Hauck, R. D., Melsted, S. W., & Yankwich, P. E. 1958. Use of N - isotope distribution in nitrogen gas in the study of denitrification. *Soil Science*, 86: 287-291.

Hauer, F. R. & Smith, R. D. 1998. The hydrogeomorphic approach to functional assessment of riparian wetlands: Evaluating impacts and mitigation on river floodplains in the USA. *Freshwater Biology*, 40(3): 517-530.

Haycock, N. E. & Pinay, G. 1993. Groundwater nitrate dynamics in grass and poplar vegetated riparian buffer strips during the winter. *Journal of Environmental Quality*, 22: 273-278.

Haycock, N. E. & Burt, T. P. 1993. Role of floodplain sediments in reducing the nitrate concentration of subsurface runoff. A case study in the Cotswolds UK. *Hydrological Processes*, 7: 287-295.

Haycock, N. E., Pinay, G., & Walker, C. 1993. Nitrogen retention in river corridors: European perspective. *Ambio*, XXII(6): 340-346.

Hedges, J. I. & Stern, J. H. 1984. Carbon and Nitrogen Determinations of Carbonate-Containing Solids. *Limnology and Oceanography*, 29(3): 657-663.

Hedin, L. O., von Fisher, J. C., Ostrom, N. E., Kennedy, B. P., Brown, M. G., & Robertson, G. P. 1998. Thermodynamic constraints on nitrogen transformations and other biogeochemical processes at soil-stream interfaces. *Ecology*, 79(2): 684-703.

Heffernan, J. B. & Sponseller, R. A. 2004. Nutrient mobilization and processing in Sonoran desert riparian soils following artificial re-wetting. *Biogeochemistry*, 70: 117-134.

Hefting, M. M., Bobbink, R., & De Caluwe, H. 2003. Nitrous oxide emission and denitrification in chronically nitrate-loaded riparian buffer zones. *Journal of Environmental Quality*, 32: 1194-1203.

Hefting, M. M., Clement, J. C., Dowrick, D. J., Cosandey, A.-C., Bernal, S., Cimpian, C., Tatur, A., Burt, T. P., & Pinay, G. 2004. Water table elevation controls on soil nitrogen cycling in riparian wetlands along a European climatic gradient. *Biogeochemistry*, 67: 113-134.

Hefting, M. M., Clement, J. C., Bienkowski, P., Dowrick, D. J., Guenat, C., Butturini, A., Topa, S., Pinay, G., & Verhoeven, J. T. A. 2005. The role of vegetation and litter in the nitrogen dynamics of riparian buffer zones in Europe. *Ecological Engineering*, 24: 465-482.

Hefting, M. M., Beltman, B., Karssenberg, D., Rebel, K., van Riessen, M., & Spijker, M. 2006a. Water quality dynamics and hydrology in nitrate loaded riparian zones in the Netherlands. *Environmental Pollution*, 139: 143-156.

Hefting, M. M., Bobbink, R., & Janssens, M. P. 2006b. Spatial variation in denitrification and N_2O emission in relation to nitrate removal efficiency in a N-stressed riparian buffer zone. *Ecosystems*, 9: 550-563.

Heinen, M. 2006a. Simplified denitrification models: Overview and properties. *Geoderma*, 133: 444-463.

Heinen, M. 2006b. Application of a widely used denitrification model to Dutch data sets. *Geoderma*, 133(3-4): 464-473.

Heiri, O., Lotter, A. F., & Lemcke, G. 2001. Loss on ignition as a method for estimating organic and carbonate content in sediments: reproducibility and comparability of results. *Journal of Paleolimnology* , 25: 101-110.

Hénault, C., Devis, X., Lucas, J. L., & Germon, J. C. 1998. Influence of different agricultural practices (type of crop, form of N-fertilizer) on soil nitrous oxide emissions. *Biology and Fertility of Soils*, 27(3): 299-306.

Hénault, C. & Germon, J. C. 2000. NEMIS, a predictive model of denitrification on the field scale. *European Journal of Soil Science*, 51(2): 257-270.

Hénault, C., Bizouard, F., Laville, P., Gabrielle, B., Nicoullaud, B., Germon, J. C., & Cellier, P. 2005. Predicting in situ soil N_2O emission using NOE algorithm and soil database. *Global Change Biology*, 11(1): 115-127.

Heppell, C. M., Burt, T. P., & Williams, R. J. 2000. Variations in the hydrology of an underdrained clay hillslope. *Journal of Hydrology*, 227: 236-256.

Hernandez, M. E. & Mitsch, W. J. 2007. Denitrification in created riverine wetlands: Influence of hydrology and season. *Ecological Engineering*, 30: 78-88.

Herman, D. J., Brooks, P. D., Ashraf, M., Azam, F., & Mulvaney, R. L. 1995. Evaluation of methods for Nitrogen-15 analysis of inorganic nitrogen in soil extracts. II. Diffusion methods. *Communications in Soil Science and Plant Analysis*, 26(11&12): 1675-1685.

Hesse, C., Krysanova, V., Pazolt, J., & Hattermann, F. F. 2008. Eco-hydrological modelling in a highly regulated lowland catchment to find measures for improving water quality. *Ecological Modelling*, 218: 135-148.

Hewlett, J. D. and Hibbert, A. R. Factors affecting the response of small watersheds to precipitation in humid areas. Sopper, W. E. and Lull, H. W. International Symposium on Forest Hydrology. 275-290. 1967. Oxford, Pergamon Press. 10-9-1965.

Hill, A. R. 1996. Nitrate removal in stream riparian zones. *Journal of Environmental Quality*, 25: 743-755.

Hill, A. R., Labadia, C. F., & Sanmugadas, K. 1998. Hyporheic zone hydrology and nitrogen dynamics in relation to the streambed topography of a N-rich stream. *Biogeochemistry*, 42: 285-310.

Hill, A. R., Devito, K. J., Campagnolo, S., & Sanmugadas, K. 2000. Subsurface denitrification in a forest riparian zone: Interactions between hydrology and supplies of nitrate and organic carbon. *Biogeochemistry*, 51(2): 193-223.

Hill, A. R., Vidon, P. G. F., & Langat, J. 2004. Denitrification Potential in Relation to Lithology in Five Headwater Riparian Zones. *Journal of Environmental Quality*, 33(3): 911-919.

Hill, A. R. & Cardaci, M. 2004. Denitrification and Organic Carbon Availability in Riparian Wetland Soils and Subsurface Sediments. *Soil Science Society of America Journal*, 68(1): 320-325.

Hill, A. R. & Duval, T. P. 2009. Beaver dams along an agricultural stream in southern Ontario, Canada: their impact on riparian zone hydrology and nitrogen chemistry. *Hydrological Processes*, 23: 1324-1336.

Hillel, D. 1998. *Environmental soil physics*. San Diego: Academic Press.

Hoffmann, C. C., Pedersen, M. L., Kronvang, B., & Ovig, L. 1998a. Restoration of the Rivers Brede, Cole and Skerne: a joint Danish and British EU-LIFE demonstration project, IV—Implications for nitrate and iron transformation. *Aquatic Conservation: Marine and Freshwater Ecosystems*, 8: 223-240.

Hoffmann, C. C., Pedersen, M. L., & Laubel, A. L. 1998b. Headwater restoration of the river Gudenå - 2. Implications for nutrients in riparian areas. *Verh.Internat.-Verein.Limnol.*, 27: 602-609.

Hoffmann, C. C., Rysgaard, S., & Berg, P. 2000. Denitrification rates predicted by Nitrogen-15 labeled nitrate microcosm studies, in situ measurements, and modeling. *Journal of Environmental Quality*, 29(6): 2020-2028.

Hoffmann, C. C., Berg, P., Dahl, M., Larsen, S. E., Andersen, H. E., & Andersen, B. 2006. Groundwater flow and transport of nutrients through a riparian meadow - Field data and modelling. *Journal of Hydrology*, 331(1-2): 315-335.

Hoffmann, C. C. & Baattrup-Pedersen, A. 2007. Re-establishing freshwater wetlands in Denmark. *Ecological Engineering*, 30: 157-166.

Holland, K. T., Knapp, J. S., & Shoesmith, J. G. 1987. *Anaerobic Bacteria*. New York: Chapman and Hall.

Holmes, N. T. H. & Nielsen, M. B. 1998. Restoration of the rivers Brede, Cole and Skerne: a joint Danish and British EU-LIFE demonstration project, I-Setting up and delivery of the project. *Aquatic Conservation: Marine and Freshwater Ecosystems*, 8: 185-196.

Horton, R. E. 1933. The role of infiltration in the hydrological cycle. *EOS Trans.Am.Geophys.Union*, 14: 446-460.

Hunt, B. 1990. An approximation of the bank storage effect. *Water Resources Research*, 26: 2769-2775.

Hunt, P. G., Matheny, T. A., & Ro, K. S. 2007. Nitrous oxide accumulation in soils from riparian buffers of a Coastal Plain watershed- Carbon/Nitrogen ratio control. *Journal of Environmental Quality*, 36: 1368-1376.

Huygens, D., Rutting, T., Boeckx, P., Cleemput, O. V., Godoy, R., & Muller, C. 2007. Soil nitrogen conservation mechanisms in a pristine south Chilean *Nothofagus* forest ecosystem. *Soil Biology and Biochemistry*, 39: 2448-2458.

Hvorslev, M. J. 1951. *Time lag and soil permeability in groundwater observations*. Mississippi: United States Army Corps of Engineers.

Ilmarinen, K., Mikola, J., Nissinen, K., & Vestberg, M. 2009. Role of soil organisms in the maintenance of species-rich seminatural grasslands through mowing. *Restoration Ecology*, 17(1): 78-88.

Inamdar, S. P., Sheridan, J. M., Williams, R. G., Bosch, D. D., Lowrance, R., Altier, L. S., & Thomas, D. L. 1999a. Riparian Ecosystem Management Model (REMM): I. Testing of the hydrologic component for a Coastal Plain riparian system. *Trans.Am.Soc.Agric.Eng.*, 42: 1679-1689.

Inamdar, S. P., Lowrance, R., Altier, L. S., Williams, R. G., & Hubbard, R. K. 1999b. Riparian Ecosystem Management Model (REMM): II Testing of the water quality and nutrient cycling component for a Coastal Plain riparian system. *Trans.Am.Soc.Agric.Eng.*, 42: 1691-1707.

IPCC Climate Change 2007: Synthesis Report. Contribution of Working Groups I, II and III to the Fourth Assessment Report of the Intergovernmental Panel on Climate Change, IPCC, Geneva, Switzerland, 104 pp.

Istok, J. D., Humphrey, M. D., Schroth, M. H., Hyman, M. R., & O'Reilly, K. T. 1997. Single-Well, "Push-Pull" Test for In Situ Determination of Microbial Activities. *Ground Water*, 35(4): 619-631.

Itoh, M., Ohte, N., Koba, K., Katsuyama, M., Hayamizu, K., & Tani, M. 2007. Hydrologic effects on methane dynamics in riparian wetlands in a temperate forest catchment. *Journal of Geophysical Research - Biogeosciences*, 112(G1).

Iversen, T. M., Kronvang, B., Madsen, B. L., Markmann, P., & Nielsen, M. B. 1993. Re-establishment of Danish streams: restoration and maintenance measures. *Aquatic Conservation: Marine and Freshwater Ecosystems*, 3(73): 92.

Jacobs, T. C. & Gilliam, J. W. 1985. Headwater Stream Losses of Nitrogen from Two Coastal Plain Watersheds. *Journal of Environmental Quality*, 14: 467-472.

Janes, M., Holmes, N., & Haycock, N. 1999. *Manual of River Restoration Techniques*. Silsoe, UK: The River Restoration Centre.

Janssen, P. H. M. & Heuberger, P. S. C. 1995. Calibration of process-oriented models. *Ecological Modelling*, 83: 55-66.

Johnsson, H., Klemedtsson, L., Nilsson, A., & Svensson, B. H. 1991. Simulation of field scale denitrification losses from soils under grass ley and barley. *Plant and Soil,* 138: 287-302.

Jones, J. B. & Holmes, R. M. 1986. Surface-subsurface interactions in stream ecosystems. *Trends Ecol.Evol.*, 16: 239-242.

Jung, M., Burt, T. P., & Bates, P. D. 2004. Toward a conceptual model of floodplain water table response. *Water Resources Research*, 40.

Junk, W. J., Bayley, P. B., & Sparks, R. E. 1989. The flood pulse concept in river-floodplain systems. *Can.Spec.Publ.Fish Aquat.Sci.*, 106: 110-127.

Junk, W. J. & Welcomme, R. L. 1990. Floodplains. In B. C. e. al. Patten (Ed.), *Wetlands and Shallow Continental Water Bodies* : 491-524. The Hague, The Netherlands: SPB Academic Publishers.

Kadlec, R. H. & Knight, R. L. 1996. *Treatment Wetlands*. New York: CRC Press-Lewis Publishers.

Kana, T. M., Darkangelo, C., Hunt, M. D., Oldham, G. B., Bennet, G. E., & Cornwell, J. C. 1994. Membrane inlet mass spectrometer for rapid high-precision determination of N_2, O_2, and Ar in environmental water samples. *Analytical Chemistry*, 66: 4166-4170.

Kaushal, S. S., Groffman, P. M., Mayer, P. M., Striz, E., & Gold, A. J. 2008. Effects of stream restoration on denitrification in an urbanizing watershed. *Ecological Applications*, 18(3): 789-804.

Keeney, D. R. & Nelson, D. W. 1982. Nitrogen- inorganic forms. In A. L. Page (Ed.), *Methods of soil analysis, part2*: 643-698. Madison, WI: ASA and SSSA.

Kellogg, D. Q., Gold, A. J., Groffman, P. M., Addy, K., Stolt, M. H., & Blazejewski, G. 2005. In Situ Ground Water Denitrification in Stratified, Permeable Soils Underlying Riparian Wetlands. *Journal of Environmental Quality*, 34(2): 524-533.

Kelly, F. & Bracken, J. J. 1998. Fisheries enhancement of the Rye Water, a lowland river in Ireland. *Aquatic Conservation: Marine and Freshwater Ecosystems*, 1: 131-143.

Kelso, B. H., Smith, R. V., Laughlin, R. J., & Lennox, S. D. 1997. Dissimilatory nitrate reduction in anaerobic sediments leading to river nitrite accumulation. *Applied and Environmental Microbiology,* 63(12): 4679-4685.

Kemnitz, D., Chin, K.-J., Bodelier, P., & Conrad, R. 2004. Community analysis of methanogenic archaea within a riparian flooding gradient. *Environmental Microbiology*, 6(5): 449-461.

Kentula, M. E. 2000. Perspectives on setting success criteria for wetland restoration. *Ecological Engineering*, 15: 199-209.

Kim, I. J., Hutchinson, S. L., Hutchinson, J. M. S., & Young, C. B. 2007. Riparian Ecosystem Management Model: Sensitivity to soil, vegetation, and weather input parameters. *Journal of the American Water Resources Association*, 43(5): 1171-1182.

Kirkham, D. & Bartholomew, W. V. 1954. Equations for following nutrient transformations in soil, utilising tracer data. *Soil Science Society of America Proceedings*, 18: 33-34.

Kirkwood, D. S. 1996. *Nutrients: practical notes on their determination in seawater*. Copenhagen, Denmark: ICES.

Kliewer, B. A. & Gilliam, J. W. 1995. Water table management effects on denitrification and nitrous oxide evolution. *Soil Science Society of America Journal*, 59: 1694-1701.

Knight, B. P., Chaudri, A. M., McGrath, S. P., & Giller, K. E. 1998. Determination of chemical availability of cadmium and zinc in soils using inert soil moisture samplers. *Environmental Pollution*, 99(3): 293-298.

Knisel, W. G. 1980. CREAMS: a field scale model for chemicals, runoff and erosion from agricultural management systems. 26. Washington DC, USDA-ARS. USDA-SEA Conservation Research.

Knowles, R. 1982. Denitrification. *Microbiological Reviews*, 46(1): 43-70.

Korom, S. F. 1992. Natural Denitrification in the Saturated Zone: A Review. *Water Resources Research*, 28(6): 1657-1668.

Koschorreck, M. 2005. Nitrogen Turnover in Drying Sediments of an Amazon Floodplain Lake. *Microbial Ecology*, 49(4): 567-577.

Krause, S. & Bronstert, A. 2007. The impact of groundwater-surface water interactions on the water balance of a mesoscale lowland river catchment in northeastern Germany. *Hydrological Processes*, 21: 169-184.

Kronvang, B., Svendsen, L. M., Brookes, A., Fisher, K., Moller, B., Ottosen, O., Newson, M., & Sear, D. 1998. Restoration of the rivers Brede, Cole and Skerne: a joint Danish and British EU-LIFE demonstration project, III-Channel morphology, hydrodynamics and transport of sediment and nutrients. *Aquatic Conservation: Marine and Freshwater Ecosystems*, 8: 209-222.

Krysanova, V., Becker, A., & Muller-Wohlfeil, D.-I. 1998. Development and test of a spatially distributed hydrological/water quality model for mesoscale watersheds. *Ecological Modelling*, 106: 261-289.

Kuusemets, V., Mander, U., Lohmus, K., & Ivask, M. 2001. Nitrogen and phosphorus variation in shallow groundwater and assimilation in plants in complex riparian buffer zones. *Water Science and Technology*, 44: 615-622.

Lamers, L. P. M., Loeb, R., Antheunisse, A. M., Miletto, M., Lucassen, E. C. H. E. T., Boxman, A. W., Smolders, A. J. P., & Roelofs, J. G. M. 2006. Biogeochemical

constraints on the ecological rehabilitation of wetland vegetation in river floodplains. *Hydrobiologia*, 565: 165-186.

Lamontagne, S., Herczeg, A. L., Dighton, T. C., Jiwan, J. S., & Pritchard, J. L. 2005. Patterns in groundwater nitrogen concentration in the floodplain of a subtropical stream (Wollombi Brook, New South Wales). *Biogeochemistry*, 72: 169-190.

Laughlin, R. J., Stevens, R. J., & Zhuo, S. 1997. Determining nitrogen-15 in ammonium by producing nitrous oxide. *Soil Science Society of America Journal*, 61: 462-465.

Legates, D. R. & McCabe Jr, G. J. 1999. Evaluating the use of 'goodness-of-fit' measures in hydrologic and hydroclimatic model validation. *Water Resources Research*, 35: 233-241.

Lewin, J. & Hughes, D. 1980. WELSH FLOODPLAIN STUDIES II. Application of a qualitative inundation model. *Journal of Hydrology*, 46: 35-49.

Li, C., Frolking, S., & Frolking, T. A. 1992a. A model of nitrous oxide evolution from soil driven by rainfall events: I. Model structure and sensitivity. *J.Geophys.Res.*, 97: 9759-9776.

Li, C., Frolking, S., & Frolking, T. A. 1992b. A model of nitrous oxide evolution from soil driven by rainfall events: II. Model applications. *J.Geophys.Res.*, 97: 9777-9783.

Li, C., Aber, J., Stange, F., Butterbach-Bahl, K., & Papen, H. 2000. A process-oriented model of N_2O and NO emissions from forest soils: 1. Model development. *J.Geophys.Res.*, 105: 4369-4384.

Linn, D. M. & Doran, J. W. 1984. Effect of water-filled pore space on carbon dioxide and nitrous oxide production in tilled and non-tilled soils. *Soil Science Society of America Journal*, 48: 1267-1272.

Lippold, H. & Matzel, W. 1992. Denitrifizierung im Winterhalbjahr in Ackerboden - Berechnung auf der Basis experimenteller Ergebnisse und der Witterung. *Agribiol.Res.*, 45: 112-120.

Liu, Y., Yang, W., & Wang, X. 2008. Development of a SWAT extension module to simulate riparian wetland hydrologic processes at a watershed scale. *Hydrological Processes*, 22: 2901-2915.

Lowrance, R., Altier, L. S., Williams, R. G., Inamdar, S. P., Sheridan, J. M., Bosch, D. D., Hubbard, R. K., & Thomas, D. L. 2000. REMM: The Riparian Ecosystem Management Model. *Journal of Soil and Water Conservation*, 55(1): 27-34.

Luo, J., Tillman, R. W., & Ball, P. R. 1999. Grazing effect on denitrification in a soil under pasture during two contrasting seasons. *Soil Biology and Biochemistry*, 31: 903-912.

Luo, Y., Qiao, X., Song, J., Christie, P., & Wong, M. 2003. Use of a multi-layer column device for study on leachability of nitrate in sludge-amended soils. *Chemosphere*, 52(9): 1483-1488.

Lyons, J., Trimble, S. W., & Paine, L. K. 2000. Grass versus trees: managing riparian areas to benefit streams of central North America. *J.Am.Water Resour.As.*, 36: 919-930.

Maag, M., Malinovsky, M., & Nielsen, S. M. 1997. Kinetics and temperature dependence of potential denitrification in riparian soils. *Journal of Environmental Quality*,(26): 215-223.

Mahmood, T., Ali, R., Malik, K., Aslam, Z., & Ali, S. 2005. Seasonal pattern of denitrification under an irrigated wheat-maize cropping system fertilised with urea and farmyard manure in different combinations. *Biology and Fertility of Soils*, 42: 1-9.

Malanson, G. P. 1993. *Riparian Landscapes*. Cambridge: Cambridge University Press.

Mankin, K. R., Ngandu, D. M., Barden, C. J., Hutchinson, S. L., & Geyer, W. A. 2007. Grass-shrub riparian buffer removal of sediment, phosphorus, and nitrogen from simulated runoff. *Journal of the American Water Resources Association*, 43(5): 1108-1116.

Marchetti, R., Donatelli, M., & Spallacci, P. 1997. Testing denitrification functions of dynamic crop models. *Journal of Environmental Quality*, 26: 394-401.

Marriot, S. B. 1998. Channel-floodplain interactions and sediment deposition on floodplains. In R. G. Bailey, P. V. José, & B. R. Sherwood (Eds.), *United Kingdom floodplains*: 43-62. Otley, UK: Westbury Academic and Scientific Publishing.

Marsh, T. J. & Hannaford, J. 2007. *The summer 2007 floods in England and Wales - a hydrological appraisal*. Wallingford: Centre for Ecology and Hydrology.

Martí, E., Fisher, S. G., Schade, J. D., & Grimm, N. B. 2000. Flood frequency and stream-riparian linkages in arid lands. In J. A. Jones & P. J. Mulholland (Eds.), *Streams and Ground Waters*: 111-136. New York: Elsevier.

Martin, T. L., Kaushik, N. K., Trevors, J. T., & Whiteley, H. R. 1999. Review: Denitrification in temperate climate riparian zones. *Water, Air, & Soil Pollution*, 111: 171-186.

Matheson, F. E., Nguyen, M. L., Cooper, A. B., Burt, T. P., & Bull, D. C. 2002. Fate of ^{15}N-nitrate in unplanted, planted and harvested riparian wetland soil microcosms. *Ecological Engineering*, 19(4): 249-264.

Matheson, F. E., Nguyen, M. L., Cooper, A. B., & Burt, T. P. 2003. Short-term nitrogen transformation rates in riparian wetland soil determined with nitrogen-15. *Biology and Fertility of Soils*, 38(3): 129-136.

Mayer, H. P. & Conrad, R. 1990. Factors influencing the population of methanogenic bacteria and the initiation of methane production upon flooding of paddy soil. *FEMS Microbiology Ecology*, 73: 103-112.

McClain, M. E., Boyer, E. W., Dent, C. L., Gergel, S. E., Grimm, N. B., Groffman, P. M., Hart, S. C., Harvey, J. W., Johnston, C. A., Mayorga, E., McDowell, W. H., & Pinay, G. 2003. Biogeochemical hot spots and hot moments at the interface of terrestrial and aquatic ecosystems. *Ecosystems*, 6: 301-312.

McDonnell, J. J. 1990. A rationale for old water discharge through macropores in a steep, humid catchment. *Water Resources Research*, 26(11): 2821-2832.

McGlynn, B. L., McDonnell, J. J., & Brammer, D. D. 2002. A review of the evolving perceptual model of hillslope flowpaths at the Maimai catchments, New Zealand. *Journal of Hydrology*, 257: 1-26.

McIntyre, R. E. S., Adams, M. A., & Grierson, P. F. 2009. Nitrogen mineralisation potential in rewetted soils from a semi-arid stream landscape, north-west Australia. *Journal of Arid Environments*, 73: 48-54.

McKergow, L. A., Prosser, I. A., Weaver, D. M., Grayson, R. B., & Reed, A. E. 2006. Performance of grass and eucalyptus riparian buffers in a pasture catchment, Western Australia, part 1: riparian hydrology. *Hydrological Processes*, 20: 2309-2326.

McNaughton, S. J. 1984. Grazing lawns: animals in herds, plant form and coevolution. *Am.Nat.*, 124: 863-886.

Meneer, J. C., Ledgard, S., McLay, C., & Silvester, W. 2005. Animal treading stimulates denitrification in soil under pasture. *Soil Biology and Biochemistry*, 37: 1625-1629.

Mengis, M., Schif, S. L., Harris, M., English, M. C., Aravena, R., Elgood, R. J., & MacLean, A. 1999. Multiple Geochemical and Isotopic Approaches for Assessing Ground Water NO_3^- Elimination in a Riparian Zone. *Ground Water*, 37(3): 448-457.

Mertes, L. A. K. 1997. Documentation and significance of the perirheic zone on inundated floodplains. *Water Resources Research*, 33(7): 1749-1762.

Middelburg, J. J., Klaver, G., Nieuwenhuize, J., Wielemaker, W. H., Vlug, T., & Jaco F.W.A.van der Nat 1996. Organic matter mineralization in intertidal sediments along an estuarine gradient. *Marine Ecology Progress Series*, 132: 157-168.

Miller, J. R. & Russell, G. L. 1992. The impact of global warming on river runoff. *J.Geophys.Res.*, 97: 2757-2764.

Mirza, M. M. Q., Warrick, R. A., & Ericksen, N. J. 2003. The implications of climate change on floods of the Ganges, Brahmaputra and Meghna rivers in Bangladesh. *Climatic Change*, 57: 287-318.

Mitsch, W. J. & Gosselink, J. G. 2000. *Wetlands*. New York, USA: Wiley.

Molenat, J. & Gascuel-Odoux, G. 2002. Modelling flow and nitrate transport in groundwater for the prediction of water travel times and of consequences of land use evolution on water quality. *Hydrological Processes*, 16(2): 479-492.

Moorhead, K. K., Bell, D. W., & Thorn, R. N. 2008. Floodplain hydrology after restoration of a southern Appalachian mountain stream. *Wetlands*, 28(3): 632-639.

Moss, B. 2008. The Water Framework Directive: Total environment or political compromise? *Science of the Total Environment*, 400: 32-41.

Mulder, A., van de Graaf, A., Robertson, L., & Kuenen, J. 1995. Anaerobic ammonium oxidation discovered in a denitrifying Fluidized-Bed reactor. *FEMS Microbiology Ecology*, 16: 177-183.

Müller, C., Stevens, R. J., & Laughlin, R. J. 2004. A ^{15}N tracing model to analyse N transformations in old grassland soil. *Soil Biology and Biochemistry*, 36: 619-632.

Müller, C., Rütting, T., Kattge, J., Laughlin, R. J., & Stevens, R. J. 2007. Estimation of parameters in complex ^{15}N tracing models via Monte Carlo sampling. *Soil Biology and Biochemistry*, 39: 715-726.

Mulligan, M. & Wainwright, J. 2004. Modelling and Model Building. In M. Mulligan & J. Wainwright (Eds.), *Environmental Modelling: Finding Simplicity in Complexity*: 7-74. London: John Wiley & Sons, Ltd.

Myrold, D. D. & Tiedje, J. M. 1985. Establishment of denitrification capacity in soil: Effects of carbon, nitrate and moisture. *Soil Biology and Biochemistry*, 17(6): 819-822.

Myrold, D. D. 2005. Transformations of Nitrogen. In D. M. Sylvia, J. J. Fuhrmann, P. G. Hartel, & D. A. Zuberer (Eds.), *Principles and applications of soil microbiology*: 259-294. New Jersey: Prentice Hall.

Naiman, R. J. & Décamps, H. 1990. *The Ecology and Management of Aquatic-Terrestrial Ecotones*. Carnforth, UK: The Parthenon Publishing Group.

Naiman, R. J. & Décamps, H. 1997. The Ecology of Interfaces: Riparian Zones. *Annu.Rev.Ecol.Syst.*, 28: 621-658.

Naiman, R. J., Bilby, R. E., & Bisson, P. A. 2000. Riparian ecology and management in the Pacific coastal rain forest. *Bioscience*, 50: 996-1011.

Nash, J. E. & Sutcliffe, J. V. 1970. River flow forecasting through conceptual models. Part I - a discussion of principles. *Journal of Hydrology*, 27: 282-290.

Nicholls, J. C. & Trimmer, M. 2009. Widespread occurrence of the anammox reaction in estuarine sediments. *Aquatic Microbial Ecology*, 55: 105-113.

Nielsen, L. P. 1992. Denitrification in sediment determined from nitrogen isotope pairing. *FEMS Microbiology Ecology*, 86: 357-362.

Noe, G. B. & Hupp, C. R. 2007. Seasonal variation in nutrient retention during inundation of a short-hydroperiod floodplain. *River Research And Applications,* 23: 1088-1101.

Novitzki, R. P. 1979. *An introduction to Wisconsin wetlands*. Madison, WI, USA: United States Geological Survey and University of Wisconsin Geology and Natural History Survey.

Oehler, F., Bordenave, P., & Durand, P. 2007. Variations of denitrification in a farming catchment area. *Agriculture, Ecosystems and Environment*, 120: 313-324.

Oehler, F., Durand, P., Bordenave, P., Saadi, Z., & Salmon-Monviola, J. 2009. Modelling denitrification at the catchment scale. *Science of the Total Environment*, 407: 1726-1737.

Olde Venterink, H., Davidsson, T. E., Kiehl, K., & Leonardson, L. 2002. Impact of drying and re-wetting on N, P and K dynamics in a wetland soil. *Plant and Soil*, 243(1): 119-130.

Olde Venterink, H., Hummelink, E., & Van Den Hoorn, M. W. 2003. Denitrification potential of a river floodplain during flooding with nitrate-rich water: grasslands versus reedbeds. *Biogeochemistry*, 65: 233-244.

Olde Venterink, H., Vermaat, J. E., Pronk, M., Wiegman, F., Van Der Lee, G. E. M., Van Den Hoorn, M. W., Martin, W., Higler, L. W. G. B., & Verhoeven, J. T. A. 2006. Importance of sediment deposition and denitrification for nutrient retention in floodplain wetlands. *Applied Vegetation Science*, 9: 163-174.

Oremland, R. S. 1988. Biogeochemistry of methanogenic bacteria. In A. J. B. Zehnder (Ed.), *Biology of anaerobic microorganisms*: 641-706. John Wiley & Sons.

Orr, C. H., Stanley, E. H., Wilson, K. A., & Finlay, J. C. 2007. Effects of restoration and reflooding on soil denitrification in a leveed midwestern floodplain. *Ecological Applications*, 17(8): 2365-2376.

Osborne, L. L. & Kovacic, D. A. 1993. Riparian vegetated buffer strips in water-quality restoration and stream management. *Freshwater Biology*, 29: 243-258.

Ostrom, N. E., Hedin, L. O., von Fisher, J. C., & Robertson, G. P. 2002. Nitrogen transformations and NO_3^- removal at a soil-stream interface: a stable isotope approach. *Ecological Applications*, 12(4): 1027-1043.

Parkin, T. B. & Tiedje, J. M. 1984. Application of a soil core method to investigate the effect of oxygen concentration on denitrification. *Soil Biology and Biochemistry*, 16(4): 331-334.

Parkin, T. B. 1987. Soil microsites as a source of denitrification variability. *Soil Science Society of America Journal*, 51: 1194-1199.

Parkin, T. B. & Meisinger, J. J. 1989. Denitrification below the crop rooting zone as influenced by surface tillage. *Journal of Environmental Quality*, 18: 12-16.

Parton, W. J., Mosier, A. R., Ojima, D. S., Valentine, D. W., Schimel, D. S., Weier, K., & Kulmala, A. E. 1996. Generalized model for N_2 and N_2O production from nitrification and denitrification. *Global Biogeochemical Cycles*, 10: 401-412.

Patra, A. K., Clays-Josserand, A., Degrange, V., Grayston, S. J., Guillaumaud, N., & Loiseau, P. 2005. Effects of grazing on microbial functional groups involved in soil N dynamics. *Ecological Monographs*, 75: 65-80.

Patra, A. K., Abbadie, L., Clays-Josserand, A., Degrange, V., Grayston, S. J., Guillaumaud, N., Loiseau, P., Louault, P., Mahmood, S., Nazaret, S., Philippot, L., Poly, F., Prosser, J. I., & Le Roux, X. 2006. Effects of management regime and plant species on the enzyme activity and genetic structure of N-fixing, denitrifying and nitrifying bacterial communities in grassland soils. *Environmental Microbiology*, 8(6): 1005-1016.

Paul, E. A. & Clark, F. E. 1989. *Soil Microbiology and Biochemistry*. San Diego California: Academic Press, INC.

Pauwels, H., Kloppmann, W., Foucher, J.-C., Martelat, A., & Fritsche, V. 1998. Field tracer test for denitrification in a pyrite-bearing schist aquifer. *Applied Geochemistry*, 13(6): 767-778.

Payne, E. K., Burgin, A. J., & Hamilton, S. K. 2009. Sediment nitrate manipulation using porewater equilibrators reveals potential for N and S coupling in freshwaters. *Aquatic Microbial Ecology*, 54: 233-241.

Payne, W. J. 1981. *Denitrification*. John Wiley & Sons, Inc.

Peterjohn, W. T. & Correll, D. L. 1984. Nutrient dynamics in an agricultural watershed: observations on the role of a riparian forest. *Ecology*, 65: 1466-1475.

Pett-Ridge, J. & Firestone, M. K. 2005. Redox fluctuation structures microbial communities in a wet tropical soil. *Applied and Environmental Microbiology*, 71(11): 6998-7007.

Pett-Ridge, J., Silver, W. L., & Firestone, M. K. 2006. Redox fluctuations frame microbial community impacts on N-cycling rates in a humid tropical forest soil. *Biogeochemistry*, 81: 95-110.

Petts, G. E. 1996. Sustaining the ecological integrity of large floodplain rivers. In M. G. Anderson, D. E. Walling, & P. D. Bates (Eds.), *Floodplain Processes*: 535-552. New York: Wiley.

Peyrard, D., Sauvage, S., Vervier, P., Sanchez-Perez, J. M., & Quintard, M. 2008. A coupled vertically integrated model to describe lateral exchanges between surface and subsurface in large alluvial floodplains with a fully penetrating river. *Hydrological Processes*, 22: 4257-4273.

Philippot, L., Cuhel, J., Saby, N. P. A., Cheneby, D., Chronakova, A., Bru, D., Arrouays, D., Martin-Laurent, F., & Simek, M. 2009. Mapping field-scale spatial patterns of size and activity of the denitrifier community. *Environmental Microbiology*, 11(6): 1518-1526.

Pinay, G., Roques, L., & Fabre, A. 1993. Spatial and Temporal Patterns of Denitrification in a Riparian Forest. *The Journal of Applied Ecology*, 30(4): 581-591.

Pinay, G., Ruffinoni, C., & Fabre, A. 1995. Nitrogen Cycling in Two Riparian Forest Soils Under Different Geomorphic Conditions. *Biogeochemistry*, 30(1): 9-29.

Pinay, G., Ruffinoni, C., Wondzell, S., & Gazelle, F. 1998. Change in groundwater nitrate concentration in a large river floodplain: denitrification, uptake, or mixing? *Journal of North American Benthological Society*, 17(2): 179-189.

Pinay, G., Décamps, H., & Naiman, R. J. 1999. The spiralling concept and nitrogen cycling in large river floodplain soils. *Arch.Hydrobiol.*, 11(3): 281-291.

Pinay, G., Black, V. J., Tabacchi-Planty, A. M., Gumiero, B., & Decamps, H. 2000. Geomorphic control of denitrification in large river floodplain soils. *Biogeochemistry*, 50: 163-182.

Pinay, G., Clément, J. C., & Naiman, R. J. 2002. Basic principles and ecological consequences of changing water regimes on nitrogen cycling in fluvial systems. *Environmental Management*, 30(4): 481-491.

Pinay, G., Gumiero, B., Tabacchi, E., Gimenez, O., Tabacchi - Planty, A. M., Hefting, M. M., Burt, T. P., Black, V. A., Nilsson, C., Iordache, V., Bureau, F., Vought, L., Petts, G. E., & Decamps, H. 2007a. Patterns of denitrification rates in European alluvial soils under various hydrological regimes. *Freshwater Biology*, 52(2): 252-266.

Pinay, G., Barbera, P., Carreras-Palou, A., Fromin, N., Sonie, L., Couteaux, M. M., Roy, J., Philippot, L., & Lensi, R. 2007b. Impact of atmospheric CO_2 and plant life forms on soil microbial activities. *Soil Biology and Biochemistry*, 39: 33-42.

Pinder, G. E. & Sauer, S. P. 1971. Numerical simulation of flood wave modification due to bank storage effects. *Water Resources Research*, 7: 63-70.

Platzner, I. T. 1997. *Modern isotope ratio mass spectrometry*. John Wiley & Sons.

Postma, D., Boesen, C., Kristiansen, H., & Larsen, F. 1991. Nitrate reduction in an unconfined sandy aquifer: water chemistry, reduction processes, and geochemical modelling. *Water Resources Research*, 27(8): 2027-2045.

Prasad, R. & Power, J. F. 1995. Nitrification inhibitors for agriculture, health, and the environment. *Adv Agron*, 54: 233-281.

Pretty, J. L., Harrison, S. S. C., Shepherd, D. J., Smith, C., Hildrew, A. G., & Hey, R. D. 2003. River rehabilitation and fish populations: assessing the benefit of instream structures. *Journal of Applied Ecology*, 40(2): 251-265.

Priesack, E., Achatz, S., & Stenger, R. 2001. Parameterization of soil nitrogen transport models by use of laboratory and field data. In M. J. Shaffer, L. Ma, & S.

Hansen (Eds.), *Modelling Carbon and Nitrogen Dynamics for Soil Management*: 459-481. Boca Raton, Florida: Lewis Publishers.

Rabalais, N. N. 2002. Nitrogen in aquatic ecosystems. *Ambio*, 31: 102-112.

Ramanarayanan, T. S., Williams, J. R., Dugas, W. A., Hauck, L. M., and McFarland, A. M. S. 1997. Using APEX to identify alternative practices for animal waste management. 97-2209. St Joseph, Michigan, ASAE.

Rassam, D. W., Fellows, C. S., De Hayr, R., Hunter, H., & Bloesch, P. 2006. The hydrology of riparian buffer zones; two case studies in an ephemeral and a perennial stream. *Journal of Hydrology*, 325(1-4): 308-324.

Rassam, D. W. & Pagendam, D. E. 2006. A mapping tool to prioritise riparian rehabilitation in catchments. *MODFLOW and More 2006: Managing Groundwater Systems*: Colorado USA: Golden.

Rassam, D. W., Pagendam, D. E., & Hunter, H. M. 2008. Conceptualisation and application of models for groundwater-surface water interactions and nitrate attenuation potential in riparian zones. *Environmental Modelling & Software*, 23: 859-875.

Reineck, H. E. & Singh, I. B. 1980. *Depositional sedimentary environments with reference to terrigenous clastics*. New York: Springer-Verlag.

Revsbech, N. P., Jacobsen, J. P., & Nielsen, L. P. 2005. Nitrogen transformations in microenvironments of river beds and riparian zones. *Ecological Engineering*, 24(5): 447-455.

Revsbech, N., Risgaard-Petersen, N., Schramm, A., & Nielsen, L. 2006. Nitrogen transformations in stratified aquatic microbial ecosystems. *Antonie Van Leeuwenhoek*, 90(4): 361-375.

Ribolzi, O., Andrieux, P., Valles, V., Bouzigues, R., Bariac, T., & Voltz, M. 2000. Contribution of groundwater and overland flows to storm flow generation in a cultivated Mediterranean catchment. Quantification by natural chemical tracing. *Journal of Hydrology*, 233: 241-257.

Rice, C. W. & Tiedje, J. M. 1989. Regulation of nitrate assimilation by ammonium in soils and in isolated soil microorganisms. *Soil Biology and Biochemistry*, 21: 597-602.

Risgaard-Petersen, N., Rysgaard, S., & Revsbech, N. P. 1993. A sensitive assay for determination of $^{14}N/^{15}N$ isotope distribution in NO_3^-. *Journal of Microbiological Methods*, 17: 155-164.

Risgaard-Petersen, N., Rysgaard, S., & Revsbech, N. P. 1995. Combined microdiffusion-Hypobromite oxidation method for determining Nitrogen-15 isotope in ammonium. *Soil Science Society of America Journal*, 59: 1077-1080.

Rivett, M. O., Smith, J. W. N., Buss, S. R., & Morgan, P. 2007. Nitrate occurrence and attenuation in the major aquifers of England and Wales. *Q.J.Eng.Geol.Hydrogeol.*, 40(4): 335-352.

Rivett, M. O., Buss, S. R., Morgan, P., Smith, J. W. N., & Bemment, C. D. 2008. Nitrate attenuation in groundwater: A review of biogeochemical controlling processes. *Water Research*, 42: 4215-4232.

Robertson, A. I., Bunn, S. E., Boon, P. I., & Walker, K. F. 1999. Sources, sinks and transformations of organic carbon in Australian floodplain rivers. *Mar.Freshwater Res.*, 50: 813-829.

Robertson, W. D., Russell, B. M., & Cherry, J. A. 1996. Attenuation of nitrate in aquitard sediments of southern Ontario. *Journal of Hydrology*, 180(1-4): 267-281.

Robson, T. M., Lavorel, S., Clement, J. C., & Le Roux, X. 2007. Neglect of mowing and manuring leads to slower nitrogen cycling in subalpine grasslands. *Soil Biology and Biochemistry*, 39: 930-941.

Rohde, S., Hostmann, M., Peter, A., & Ewald, K. C. 2006. Room for rivers: An integrative search strategy for floodplain restoration. *Landscape and Urban Planning*, 78: 50-70.

Rolston, D. E., Rao, P. S. C., Davidson, J. M., & Jessup, R. E. 1984. Simulation of denitrification losses of nitrate fertilizer applied to uncropped, cropped, and manure-amended field plots. *Soil Science* , 137: 270-279.

Rosenblatt, A. E., Gold, A. J., Stolt, M. H., Groffman, P. M., & Kellogg, D. Q. 2001. Identifying riparian sinks for watershed nitrate using soil surveys. *Journal of Environmental Quality*, 30: 1596-1604.

Rowell, D. L. 1994. *Soil Science: Methods and Applications*. Longman Scientific & Technical.

Rütting, T., Huygens, D., Muller, C., Van Cleemput, O., Godoy, R., & Boeckx, P. 2008. Functional role of DNRA and nitrite reduction in a pristine south Chilean *Nothofagus* forest. *Biogeochemistry*, 90: 243-258.

Ryden, J. C. 1983. Denitrification loss from a grassland soil in the field receiving different rates of nitrogen as ammonium nitrate. *Journal of Soil Science*, 34: 355-365.

Rysgaard, S., Risgaard-Petersen, N., & Sloth, N. P. 1996. Nitrification, denitrification, and nitrate ammonification in sediments of two coastal lagoons in Southern France. *Hydrobiologia*, 329: 133-141.

Rysgaard, S. & Risgaard-Petersen, N. 1997. A sensitive method for determining nitrogen-15 isotope in urea. *Marine Biology*, 128(2): 191-195.

Sabater, S., Butturini, A., Clement, J. C., Burt, T. P., Dowrick, D. J., Hefting, M. M., Maitre, V., Pinay, G., Postolache, C., Rzepecki, M., & Sabater, F. 2003.

Nitrogen removal by riparian buffers along a European climatic gradient: Patterns and factors of variation. *Ecosystems*, 6: 20-30.

Sala, O. E., Parton, W. J., Joyce, L. A., & Lauenroth, W. K. 1988. Primary production of the central grassland region of the United States. *Ecology*, 69: 40-45.

Sanchez-Perez, J. M., Trémolières, M., Takatert, N., Ackerer, P., Eichhorn, A., & Maire, G. 1999. Quantification of nitrate removal by a flooded alluvial zone in the Ill floodplain (Eastern France). *Hydrobiologia*, 410(0): 185-193.

Sanders, I. A. & Trimmer, M. 2006. *In situ* application of the $^{15}NO_3^-$ isotope pairing technique to measure denitrification in sediments at the surface water-groundwater interface. *Limnology and Oceanography: Methods*, 4: 142-152.

Santhi, C., Arnold, J. G., Williams, J. R., Dugas, W. A., Srinivasan, R., & Hauck, L. M. 2001. Validation of the SWAT Model on a large river basin with point and nonpoint sources. *Journal of the American Water Resources Association*, 37: 1169-1188.

Sayama, M., Risgaard-Petersen, N., Nielsen, L. P., Fossing, H., & Christensen, P. B. 2005. Impact of bacterial NO_3^- transport on sediment biogeochemistry. *Applied and Environmental Microbiology*, 71: 7575-7577.

Schade, J. D., Fisher, S. G., Grimm, N. B., & Seddon, J. A. 2001. The influence of a riparian shrub on nitrogen cycling in a Sonoran Desert stream. *Ecology*, 82: 3363-3376.

Scheible, O. K. Manual: Nitrogen Control. EPA/625/R-93/010. 1993. United Stated Environmental Protection Agency. Risk Reduction Engineering Laboratory. Ref Type: Report

Schilling, K. E., Zhang, Y.-K., & Drobney, P. 2004. Water table fluctuations near an incised stream, Walnut Creek, Iowa. *Journal of Hydrology*, 286: 236-248.

Schilling, K. E., Zhongwei, L., & Zhang, Y.-K. 2006. Groundwater - surface water interaction in the riparian zone of an incised channel, Walnut Creek, Iowa. *Journal of Hydrology*, 327(1-2): 140-150.

Schilling, K. E. 2007. Water table fluctuations under three riparian land covers, Iowa (USA). *Hydrological Processes*, 21: 2415-2424.

Schilling, K. E. & Jacobson, P. 2008. Groundwater nutrient concentrations near an incised midwestern stream: effects of floodplain lithology and land management. *Biogeochemistry*, 87: 199-216.

Schilling, K. E., Palmer, J. A., Arthur Bettis III, E., Jacobson, P., Schultz, R. C., & Isenhart, T. M. 2009. Vertical distribution of total carbon, nitrogen and phosphorus in riparian soils of Walnut Creek, southern Iowa. *Catena*, 77: 266-273.

Schimel, J. P., Gulledge, J. M., Clein-Curley, J. S., Lindstrom, J. E., & Braddock, J. F. 1999. Moisture effects on microbial activity and community structure in

decomposing birch litter in the Alaskan taiga. *Soil Biology and Biochemistry*, 31: 831-838.

Schipper, L. A., Cooper, A. B., Harfoot, C. G., & Dyck, W. J. 1993. Regulators of denitrification in an organic riparian soil. *Soil Biology and Biochemistry*, 25(7): 925-933.

Schipper, L. A., Cooper, A. B., Harfoot, C. G., & Dyck, W. J. 1994. An inverse relationship between nitrate and ammonium in an organic riparian soil. *Soil Biology and Biochemistry*, 26(6): 799-800.

Schnabel, R. R., Cornish, L. F., Stout, W. L., & Shaffer, J. A. 1996. Denitrification in a grassed and a wooded, valley and ridge, riparian ecotone. *Journal of Environmental Quality*, 25: 1230-1235.

Scholz, O., Gawne, B., Ebner, J. M. B., & Ellis, I. 2002. The effects of drying and re-flooding on nutrient availability in ephemeral deflation basin lakes in western New South Wales, Australia. *River Research And Applications*, 18: 185-196.

Schubert, C. J., Durisch-Kaiser, E., Wehrli, B., Thamdrup, B., Lam, P., & Kuypers, M. M. M. 2006. Anaerobic ammonium oxidation in a tropical freshwater system (Lake Tanganyika). *Environmental Microbiology*, 8(10): 1857-1863.

Schurmann, A., Schroth, M. H., Saurer, M., Bernasconi, S. M., & Zeyer, J. 2003. Nitrate-consuming processes in a petroleum-contaminated aquifer quantified using push-pull tests combined with ^{15}N isotope and acetylene-inhibition methods. *Journal of Contaminant Hydrology*, 66(1-2): 59-77.

Schwientek, M., Einsiedl, F., Stichler, W., Stögbauer, A., Strauss, H., & Maloszewski, P. 2008. Evidence for denitrification regulated by pyrite oxidation in a heterogeneous porous groundwater system. *Chemical Geology*, 255: 60-67.

Scott, J. T., McCarthy, M. J., Gardner, W. S., & Doyle, R. D. 2008. Denitrification, dissimilatory nitrate reduction to ammonium, and nitrogen fixation along a nitrate concentration gradient in a created freshwater wetland. *Biogeochemistry*, 87: 99-111.

Sear, D. A. & White, R. A. 1994. *The River Restoration Project: A geomorphological survey of the River Cole, Wiltshire*. Dept. of Geography, University of Southampton.

Seeberg-Elverfeldt, J., Schlüter, M., Feseker, T., & Kölling, M. 2005. Rhizon sampling of porewaters near the sediment-water interface of aquatic systems. *Limnology and Oceanography: Methods*, 3: 361-371.

Seitzinger, S., Harrison, J. A., Bohlke, J. K., Bouwman, A. F., Lowrance, R., Peterson, B., Tobias, C., & Van Drecht, G. 2006. Denitrification across landscapes and waterscapes: A synthesis. *Ecological Applications*, 16(6): 2064-2090.

Seitzinger, S. 2008. Nitrogen Cycle: Out of reach. *Nature*, 452: 162-163.

Shaffer, M. J., Halvorson, A. D., & Pierce, F. J. 1991. Nitrate leaching and economic analysis package (NLEAP): model description and application. In R. F. Follett, D. R. Keeney, & R. M. Cruse (Eds.), *Managing Nitrogen for Groundwater Quality and Farm Profitability*: 285-322. Madison WI: ASA CSSA and SSSA.

Shaffer, M. J., Lasnik, K., Ou, X., & Flynn, R. 2001. NLEAP internet tools for estimating NO_3-N leaching and N_2O emissions. In M. J. Shaffer, L. Ma, & S. Hansen (Eds.), *Modelin Carbon and Nitrogen Dynamics for Soil Management*: 403-426. Boca Raton FL: Lewis Publishers.

Sheibley, R. W., Ahearn, D. S., & Dahlgren, R. A. 2006. Nitrate loss from a restored floodplain in the Lower Cosumnes River, California. *Hydrobiologia*, 571: 261-272.

Shotbolt, L. 2009. Pore water sampling from lake and estuary sediments using Rhizon samplers. *J.Paleolimnol.*, 10.1007/s10933-008-9301-8.

Sigfusson, B., Paton, G. I., & Gislason, S. R. 2006. The impact of sampling techniques on soil pore water carbon measurements of an Icelandic Histic Andosol. *Science of the Total Environment*, 369(1-3): 203-219.

Sigunga, D. O. 2003. Potential denitrification: Concept and conditions of its measurement. *Communications in Soil Science and Plant Analysis*, 34(17&18): 2405-2418.

Silver, W. L., Herman, D. J., & Firestone, M. K. 2001. Dissimilatory nitrate reduction to ammonium in upland tropical forest soils. *Ecology*, 82(9): 2410-2416.

Silver, W. L., Thompson, A. W., Reich, A., Ewel, J. J., & Firestone, M. K. 2005. Nitrogen cycling in tropical plantation forests: potential controls on nitrogen retention. *Ecological Applications*, 15(5): 1604-1614.

Simek, M., Cooper, J. E., Picek, T., & Santruckova, H. 2000. Denitrification in arable soils in relation to their physico-chemical properties and fertilisation practice. *Soil Biology and Biochemistry*, 32: 101-110.

Simek, M. & Cooper, J. E. 2002. The influence of soil pH on denitrification: progress towards the understanding of this interaction over the last 50 years. *European Journal of Soil Science*, 53: 345-354.

Simpkins, W. W., Wineland, T. R., Andress, R. J., Johnston, D. A., Caron, G. C., Isenhart, T. M., & Schultz, R. C. 2002. Hydrogeological constraints on riparian buffers for reduction of diffuse pollution: examples from the Bear Creek Watershed in Iowa, USA. *Water Science and Technology*, 45: 61-68.

Sklash, M. G. & Farvolden, R. N. 1979. The role of groundwater in storm runoff. *Journal of Hydrology*, 43: 45-65.

Sleutel, S., Moeskops, B., Huybrechts, W., Vandenbossche, A., Salomez, J., De Bolle, S., Buchan, D., & De Neve, S. 2008. Modelling soil moisture effects on net nitrogen mineralisation in loamy wetland soils. *Wetlands*, 28(3): 724-734.

Smart, R. M. & Barko, J. W. 1985. Laboratory culture of submersed freshwater macrophytes on natural sediments. *Aquatic Botany*, 21: 251-263.

Smith, M. S. & Tiedje, J. M. 1979. Phases of denitrification following oxygen depletion in soil. *Soil Biology and Biochemistry*, 11: 261-267.

Smith, R. L., Howes, B. L., & Duff, J. H. 1991. Denitrification in nitrate contaminated groundwater: occurrence in steep vertical geochemical gradients. *Geochimica Et Cosmochimica Acta* , 55(7): 1815-1825.

Smith, R., Garabedian, S. P., & Brooks, M. H. 1996. Comparison of Denitrification Activity Measurements in Groundwater Using Cores and Natural-Gradient Tracer Tests. *Environmental Science & Technology* , 30: 3448-3456.

Smith, R. L., Böhlke, J. K., Garabedian, S. P., Revesz, K. M., & Yoshinari, T. 2004. Assessing denitrification in groundwater using natural gradient tracer tests with ^{15}N: *in situ* measurement of a sequential multistep reaction. *Water Resources Research*, 40: W07101.

Song, J., Luo, Y. M., Zhao, Q. G., & Christie, P. 2003. Novel use of soil moisture samplers for studies on anaerobic ammonium fluxes across lake sediment-water interfaces. *Chemosphere*, 50(6): 711-715.

Sophocleous, M. 2002. Interactions between groundwater and surface water: the state of the science. *Hydrogeology Journal*, 10: 52-67.

Sotta, E. D., Corre, M. D., & Veldkamp, E. 2008. Differing N status and N retention processes of soils under old-growth lowland forest in eastern Amazonia, Caxiuana, Brazil. *Soil Biology and Biochemistry*, 40: 740-750.

Søvik, A. K. & Kløve, B. 2007. Emission of N_2O and CH_4 from a constructed wetland in southeastern Norway. *Science of the Total Environment*, 380: 28-37.

Stanford, G., Dzienia, S., & Vander Pol, R. A. 1975. Effect of temperature on denitrification rate in soils. *Soil Science Society of America Journal*, 39: 867-870.

Stange, C. F., Spott, O., Apelt, B., & Russow, R. W. B. 2007. Automated and rapid online determination of ^{15}N abundance and concentration of ammonium, nitrite, or nitrate in aqueous samples by the SPINMAS technique. *Isotopes in Environmental and Health Studies*, 43(3): 227-236.

Stark, J. M. & Hart, S. C. 1996. Diffusion technique for preparing salt solutions, Kjeldahl digests, and persulphate digests for nitrogen-15 analysis. *Soil Science Society of America Journal*, 60: 1846-1855.

Starr, R. C. & Gillham, R. W. 1993. Denitrification and organic carbon availability in two aquifers. *Ground Water*, 31: 934-947.

Steiger, J. & Gurnell, A. M. 2003. Spatial hydrogeomorphological influences on sediment and nutrient deposition in riparian zones: observations from the Garonne River, France. *Geomorphology*, 49: 1-23.

Steiger, J., Tabacchi, E., Dufour, S., Corenblit, D., & Peiry, J.-L. 2005. Hydrogeomorphic processes affecting riparian habitat within alluvial channel-floodplain river systems: A review for the temperate zone. *River Research And Applications*, 21: 719-737.

Steingruber, S. M., Friedrich, J., Gachter, R., & Wehrli, B. 2001. Measurement of Denitrification in Sediments with the ^{15}N Isotope Pairing Technique. *Applied and Environmental Microbiology*, 67(9): 3771-3778.

Stepanauskas, R., Davidsson, E. T., & Leonardson, L. 1996. Nitrogen transformations in wetland soil cores measured by ^{15}N isotope pairing and dilution at four infiltration rates. *Applied and Environmental Microbiology*, 62(7): 2345-2351.

Stevens, R. J., Laughlin, R. J., Atkins, G. J., & Prosser, S. J. 1993. Automated determination of ^{15}N-labeled dinitrogen and nitrous oxide by mass spectrometry. *Soil Science Society of America Journal*, 57: 981-988.

Stewart, M. D., Bates, P. D., Anderson, M. G., Price, D. A., & Burt, T. P. 1999. Modelling floods in hydrologically complex lowland river reaches. *Journal of Hydrology*, 223: 85-106.

Surridge B.W.J., Baird A.J., & Heathwaite A.L. 2005. Evaluating the quality of hydraulic conductivity estimates from piezometer slug tests in peat. *Hydrological Processes*, 19: 1227-1244.

Sutton-Grier, A. E., Ho, M., & Richardson, C. J. 2009. Organic amendments improve soil conditions and denitrification in a restored riparian wetland. *Wetlands*, 29(1): 343-352.

Syversen, N. 2002. Cold-climate vegetative buffer zones as filters for surface agricultural runoff. Agricultural University of Norway. PhD Thesis.

Tague, C., Valentine, S., & Kotchen, M. 2008. Effect of geomorphic channel restoration on streamflow and groundwater in a snowmelt-dominated watershed. *Water Resources Research*, 44.

Takatert, N., Sanchez-Perez, J. M., & Trémolières, M. 1999. Spatial and temporal variations of nutrient concentration in the groundwater of a floodplain: effect of hydrology, vegetation and substrate. *Hydrological Processes*, 13: 1511-1526.

Templer, P. H., Silver, W. L., Pett-Ridge, J., DeAngelis, K. M., & Firestone, M. K. 2008. Plant and microbial controls on nitrogen retention and loss in a humid tropical forest. *Ecology*, 89(11): 3030-3040.

Tesoriero, A. J., Liebscher, H., & Cox, S. E. 2000. Mechanism and rate of denitrification in an agricultural watershed: Electron and mass balance along groundwater flow paths. *Water Resources Research*, 36(6): 1545-1559.

Thamdrup, B. & Dalsgaard, T. 2000. The fate of ammonium in anoxic manganese oxide-rich marine sediment. *Geochimica Et Cosmochimica Acta*, 64(24): 4157-4164.

Thermo 2006. *HiPerTOC SA User's Guide: Version 1.0.2*. Delft, The Netherlands: Thermo Electron Corporation.

Tiedje, J. M., Sorensen, J., & Chang, Y. Y. L. 1981. Assimilatory and dissimilatory nitrate reduction: Perspective and methodology for simultaneous measurement of several nitrogen cycle processes. *Ecological Bulletin*, 33: 331-342.

Tiedje, J. M., Sexstone, A. J., Myrold, D. D., & Robinson, J. A. 1982. Denitrification: ecological niches, competition and survival. *Antonie Van Leeuwenhoek*, 48: 569-583.

Tiedje, J. M. 1988. Ecology of denitrification and dissimilatory nitrate reduction to ammonium. In A. J. B. Zehnder (Ed.), *Biology of Anaerobic Microorganisms*: 179-244. New York: Wiley.

Tiedje, J. M., Simkins, S., & Groffman, P. M. 1989. Perspectives on measurement of denitrification in the field including recommended protocols for acetylene based methods. *Plant and Soil*, 115: 261-284.

Tockner, K., Pennetzdorfer, D., Reiner, N., Schiemer, F., & Ward, J. V. 1999. Hydrological connectivity, and the exchange of organic matter and nutrients in a dynamic river-floodplain system (Danube, Austria). *Freshwater Biology*, 41(3): 521-535.

Tockner, K., Malard, F., & Ward, J. V. 2000. An extension of the flood pulse concept. *Hydrological Processes*, 14: 2861-2883.

Tockner, K. & Stanford, J. A. 2002. Riverine floodplains: present state and future trends. *Environmental Conservation*, 29(3): 308-330.

Tomaszek, J. A. & Gruca-Rokosz, R. 2007. Rates of dissimilatory nitrate reduction to ammonium in two Polish reservoirs: Impacts of temperature, organic matter content and nitrate concentration. *Environmental Technology*, 28: 771-778.

Tomer, M. D., Dosskey, M. G., Burkart, M. R., James, D. E., Helmers, M. J., & Eisenhauer, D. E. 2009. Methods to prioritise placement of riparian buffers for improved water quality. *Agroforestry Systems*, 75: 17-25.

Trepel, M. & Kluge, W. 2004. WETTRANS: a flow-path-oriented decision-support system for the assessment of water and nitrogen exchange in riparian peatlands. *Hydrological Processes*, 18: 357-371.

Trimmer, M., Nicholls, J. C., & Deflandre, B. 2003. Anaerobic Ammonium Oxidation Measured in Sediments along the Thames Estuary, United Kingdom. *Applied and Environmental Microbiology*, 69(11): 6447-6454.

Trimmer, M., Nicholls, J. C., Morley, N., Davies, C. A., & Aldridge, J. 2005. Biphasic behavior of Anammox regulated by nitrite and nitrate in an estuarine sediment. *Applied and Environmental Microbiology*, 71(4): 1923-1930.

Trimmer, M., Risgaard-Petersen, N., Nicholls, J. C., & Engstrom, P. 2006. Direct measurement of anaerobic ammonium oxidation (anammox) and denitrification in intact sediment cores. *Marine Ecology Progress Series*, 326: 37-47.

Trimmer, M. & Nicholls, J. C. 2009. Production of nitrogen gas via anammox and denitrification in intact sediment cores along a continental shelf to slope transect in the North Atlantic. *Limnology and Oceanography*, 54(2): 577-589.

Ullah, S., Breitenbeck, G. A., & Faulkner, S. P. 2005. Denitrification and N_2O emission from forested and cultivated alluvial clay soil. *Biogeochemistry*, 73: 499-513.

Ullah, S. & Faulkner, S. P. 2006. Denitrification potential of different land-use types in an agricultural watershed, lower Mississippi valley. *Ecological Engineering*, 28: 131-140.

Ullah, S. & Zinati, G. 2006. Denitrification and nitrous oxide emissions from riparian forests soils exposed to prolonged nitrogen runoff. *Biogeochemistry*, 81(3): 253-267.

Ullah, S., Frasier, R., King, L., Picotte-Anderson, N., & Moore, T. R. 2008. Potential fluxes of N_2O and CH_4 from soils of three forest types in Eastern Canada. *Soil Biology and Biochemistry*, 40: 986-994.

Vale, M., Mary, B., & Justes, E. 2007. Irrigation practices may affect denitrification more than nitrogen mineralization in warm climatic conditions. *Biology and Fertility of Soils*, 43(6): 641-651.

Valett, H. M., Baker, M. A., Morrice, J. A., Crawford, C. S., Molles, M. C. Jr., Dahm, C. N., Moyer, D. L., Thibault, J. R., & Ellis, L. M. 2005. Biogeochemical and metabolic responses to the flood pulse in a semiarid floodplain. *Ecology*, 86(1): 220-234.

van Beek, C. L., Hummelink, E. W. J., Velthof, G. L., & Oenema, O. 2004. Denitrification rates in relation to groundwater level in a peat soil under grassland. *Biology and Fertility of Soils*, 39: 329-336.

van de Graaf, A., Mulder, A., de Bruijn, P., Jetten, M., Robertson, L., & Kuenen, J. 1995. Anaerobic oxidation of ammonium is a biologically mediated process. *Applied and Environmental Microbiology*, 61: 1246-1251.

van den Heuvel, R. N., Hefting, M. M., Tan, N. C. G., Jetten, M. S. M., & Verhoeven, J. T. A. 2009. N_2O emission hotspots at different spatial scales and governing factors for small scale hotspots. *Science of the Total Environment*, 407: 2325-2332.

van der Lee, G. E. M., Venterink, H. O., & Asselman, N. E. M. 2004. Nutrient retention in floodplains of the Rhine distributaries in the Netherlands. *River Research And Applications*, 20: 315-325.

van Verseveld, W. J., McDonnell, J. J., & Lajtha, K. 2009. The role of hillslope hydrology in controlling nutrient loss. *Journal of Hydrology*, 367: 177-187.

Verchot, L. V., Franklin, E. C., & Gillham, J. W. 1997. Nitrogen cycling in piedmont vegetated filter zones. Part 1. Surface soil processes. *Journal of Environmental Quality*, 26: 327-336.

Verhoeven, J. T. A., Soons, M. B., Janssen, R., & Omtzigt, N. 2008. An Operational Landscape Unit approach for identifying key landscape connections in wetland restoration. *Journal of Applied Ecology*, 45: 1496-1503.

Vervier, P., Dobson, M., & Pinay, G. 1993. Role of interaction zones between surface and ground waters in DOC transport and processing: considerations for river restoration. *Freshwater Biology*, 29: 275-284.

Vidon, P. & Hill, A. R. 2004a. Landscape controls on the hydrology of stream riparian zones. *Journal of Hydrology*, 292: 210-228.

Vidon, P. & Hill, A. R. 2004b. Denitrification and patterns of electron donors and acceptors in eight riparian zones with contrasting hydrogeology. *Biogeochemistry*, 71(2): 259-283.

Vidon, P. & Hill, A. R. 2006. A landscape-based approach to estimate riparian hydrological and nitrate removal functions. *Journal of the American Water Resources Association*, 42(4): 1099-1112.

Vidon, P. & Dosskey, M. G. 2008. Testing a simple field method for assessing nitrate removal in riparian zones[1]. *Journal of the American Water Resources Association*, 44(2): 523-534.

Vinten, A. J. A., Castle, K., & Arah, J. R. M. 1996. Field evaluation of models of denitrification linked to nitrate leaching for aggregated soil. *European Journal of Soil Science*, 47: 305-317.

Vitousek, P. M., Mooney, H. A., Lubchenco, J., & Melillo, J. M. 1997. Human domination of earth's ecosystems. *Science*, 277: 494-499.

Vivash, R., Ottosen, O., Janes, M., & Sorensen, H. V. 1998. Restoration of the rivers Brede, Cole and Skerne: a joint Danish and British EU-LIFE demonstration project, II—The river restoration works and other related practical aspects. *Aquatic Conservation: Marine and Freshwater Ecosystems*, 8: 197-208.

Vought, L. B. M., Dahl, J., Pedersen, C. L., & LaCoursiere, J. O. 1994. Nutrient Retention in riparian ecotones. *Ambio*, 23: 342-348.

Waddington, J. M., Roulet, N., & Hill, A. R. 1993. Runoff mechanisms in a forested groundwater discharge wetland. *Journal of Hydrology*, 147(1-4): 37-60.

Wallenstein, M. D., Myrold, D. D., Firestone, M. K., & Voytek, M. A. 2006. Environmental controls on denitrifying communities and denitrification rates: insights from molecular methods. *Ecological Applications*, 16(6): 2143-2152.

Wan, Y., Ju, X., Ingwersen, J., Schwarz, U., Stange, C. F., Zhang, F., & Streck, T. 2009. Gross nitrogen transformations and related nitrous oxide emissions in an

intensively used calcareous soil. *Soil Science Society of America Journal*, 73(1): 102-112.

Wang, X., Yang, S., Mannaerts, C. M., Gao, Y., & Guo, J. 2009. Spatially explicit estimation of soil denitrification rates and land use effects in the riparian buffer zone of the large Guanting reservoir. *Geoderma*, 150: 240-252.

Ward, J. V., Tockner, K., Arscott, D. B., & Claret, C. 2002. Riverine landscape diversity. *Freshwater Biology*, 47: 517-539.

Ward, R. C. & Robinson, M. 2000. *Principles of Hydrology*. McGraw Hill Higher Education.

Weber, K. A., Picardal, F. W., & Roden, E. E. 2001. Microbially-catalyzed nitrate-dependent oxidation of biogenic solid-phase Fe(II) compounds. *Environmental Science &Amp; Technology*, 35: 1644-1650.

Weber, K. A., Urrutia, M. M., Churchill, P. F., Kukkadapu, R. K., & Roden, E. E. 2006. Anaerobic redox cycling of iron by freshwater sediment microorganisms. *Environmental Microbiology*, 8(1): 100-113.

Weiss, R. F. & Price, B. A. 1980. Nitrous oxide solubility in water and seawater. *Marine Chemistry*, 8: 347-359.

Well, R., Augustin, J., Meyer, K., & Myrold, D. D. 2003. Comparison of field and laboratory measurement of denitrification and N_2O production in the saturated zone of hydromorphic soils. *Soil Biology and Biochemistry*, 35: 783-799.

Well, R., Hoper, H., Mehranfar, O., & Meyer, K. 2005. Denitrification in the saturated zone of hydromorphic soils - laboratory measurement, regulating factors and stochastic modeling. *Soil Biology and Biochemistry*, 37: 1822-1836.

Wenninger, J., Uhlenbrook, S., Tilch, N., & Leibundgut, C. 2004. Experimental evidence of fast groundwater responses in a hillslope/floodplain area in the Black Forest Mountains, Germany. *Hydrological Processes*, 18: 3305-3322.

Wetzel, R. G. 2001. *Limnology: Lake and River Ecosystems*. California USA: Academic Press.

Wharton, G. & Gilvear, D. J. 2007. River restoration in the UK: Meeting the dual needs of the European Union Water Framework Directive and flood defence? *Intl.J.River Basin Management*, 5(2): 143-154.

Whitmire, S. L. & Hamilton, S. K. 2005. Rapid Removal of Nitrate and Sulfate in Freshwater Wetland Sediments. *Journal of Environmental Quality*, 34(6): 2062-2071.

Winter, T. C. 1995. Recent advances in understanding the interaction of groundwater and surface water. *Reviews of Geophysics* , 33: 985-994.

Woessner, W. W. 2000. Stream and fluvial plain groundwater interactions: rescaling hydrogeologic thought. *Ground Water*, 38(3): 423-429.

Wolfe, B. B., Karst-Riddoch, T. L., Hall, R. I., Edwards, T. W. D., English, M. C., Palmini, R., McGowan, S., Leavitt, P. R., & Vardy, S. R. 2007. Classification of hydrological regimes of northern floodplain basins (Peace - Athabasca Delta, Canada) from analysis of stable isotopes ($\delta^{18}O$, $\delta^{2}H$) and water chemistry. *Hydrological Processes*, 21: 151-168.

Woodward, K. B., Fellows, C. S., Conway, C. L., & Hunter, H. M. 2009. Nitrate removal, denitrification and nitrous oxide production in the riparian zone of an ephemeral stream. *Soil Biology and Biochemistry*, 41: 671-680.

World Health Organisation (WHO) 2004. *Guidelines for Drinking Water Quality*. Geneva: WHO.

WWF. *Policy and Economic analysis of floodplain restoration in Europe: Opportunities and obstacles*. -46. 2000. Report prepared by WWF European Freshwater Programme for the Wise use of Floodplains Life Environment Project.
Ref Type: Report

Xu, C., Shaffer, M. J., & Al-Kaisi, M. 1998. Simulating the impact of management practices on nitrous oxide emissions. *Soil Science Society of America Journal*, 62: 736-742.

Yeomans, J. C., Bremner, J. M., & McCarty, G. W. 1992. Denitrification capacity and denitrification potential of subsurface soils. *Communications in Soil Science and Plant Analysis*, 23(9&10): 919-927.

Yin, S. X., Chen, D., Chen, L. M., & Edis, R. 2002. Dissimilatory nitrate reduction to ammonium and responsible microorganisms in two Chinese and Australian paddy soils. *Soil Biology and Biochemistry*, 34: 1131-1137.

Yoshinari, T. & Knowles, R. 1976. Acetylene inhibition of nitrous oxide reduction by denitrifying bacteria. *Biochemical and Biophysical Research Communications*, 69(3): 705-710.

Yoshinari, T., Hynes, R., & Knowles, R. 1977. Acetylene inhibition of nitrous oxide reduction and measurement of denitrification and nitrogen fixation in soil. *Soil Biology and Biochemistry*, 9: 177-183.

Zehnder, A. J. B. & Stumm, W. 1988. Geochemistry and biogeochemistry of anaerobic habitats. In A. J. B. Zehnder (Ed.), *Biology of anaerobic microorganisms*: 469-585. New York: Wiley.

Zhu, W. X. & Ehrenfeld, J. G. 2000. Nitrogen retention and release in Atlantic white cedar wetlands. *Journal of Environmental Quality*, 29: 612-620.

Appendix 1

1.1 CR10X logger instructions for tensiometers

*Table 1 Program

01: 3600 Execution Interval (seconds)

1: Battery Voltage (P10)

1: 1 Location [Battery]

2: Do (P86)

1: 41 Set Port 1 High

3: Excitation with Delay (P22)

1:1 Excitation Channel

2: 0000 Delay W/Ex (0.01 sec units)

3: 1000 Delay After Ex (0.01 sec units)

4: 0000 mV Excitation

4: Voltage (Diff) (P2)

1:3 Replicates

2:4 250 mV Slow Range

3:1 DIFF Channel

4:2 Location [Tensiom_1]

5:10 Multiplier

6:0 Offset

5: Do (P86)

1:51 Set Port 1 Low

6: If time is (P92)

1:0000 Minutes (Seconds--) into an interval

2:60 Interval (same units as above)

3:10 Set Output Flag High (Flag 0)

7: Set Active Storage Area (P80)

1:1 Final Storage Area 1

2:100 Array ID

8: Real Time (P77)

1:1220 Year, Day, Hour/Minute (midnight=2400)

9: Sample (P70)

1:1 Reps

2:1 Location [Battery]

10: Sample (P70)

1:3 Replicates

2:2 Loc [Tensiom_1]

11: Serial Out (P96)

1:71 Storage Module

*Table 2 Program

02:0.0000 Execution Interval (seconds)

*Table 3 Subroutines

End Program

1.2 CR10X logger instructions for theta probes and thermistors

*Table 1 Program

01:3600 Execution Interval (seconds)

1: Battery Voltage (P10)

1:1 Location [Battery]

2: Do (P86)

1:41 Set Port 1 High

3: Excitation with Delay (P22)

1:1 Excitation Channel

2:0 Delay W/Ex (0.01 sec units)

3: 1000 Delay after Excitation (0.01 sec units)

4: 000 mV Excitation

4: Voltage (Diff) (P2)

1:3 Replicates

2:5 2500 mV Slow Range

3:1 DIFF Channel

4:2 Location [ThetaV]

5:0.001 Multiplier

6:0.0 Offset

5: Do (P86)

1:51 Set Port 1 Low

6: Temperature (107) (P11)

1:3 Replicates

2:7 SE Channel

3:1 Excite all replicates w/E1

4:5 Location [Temp]

5:1.0 Multiplier

6:0.0 Offset

Subroutine to convert theta probe voltage to SQRT (Dielectric) using polynomial

7: Polynomial (P55)

1:3 Replicates

2:2 X Location [ThetaV]

3:8 F(X) Location [SQRTE_1]

4:1.07 C0

5:6.40 C1

6:-6.40 C2

7:4.7 C3

8:0.0 C4

9:0.0 C5

Subroutine to convert to volumetric water content using standard calibration for mineral soil

8: Z=X+F (P34)

1:8 X Location [SQRTE_1]

2:-1.6 F

3:11 Z Location [ThetaVWC1]

9: Z=X+F (P34)

1:9 X Location [SQRTE_2]

2:-1.6 F

3:12 Z Location [ThetaVWC2]

10: Z=X+F (P34)

1:10 X Location [SQRTE_3]

2:-1.6 F

3:13 Z Location [ThetaVWC3]

11: Z=X*F (P37)

1:11 X Location [ThetaVWC1]

2:0.11904 F

3:11 Z Location [ThetaVWC1]

12: Z=X*F (P37)

1:12 X Location [ThetaVWC2]

2:0.11904 F

3:12 Z Location [ThetaVWC2]

13: Z=X*F (P37)

1:13 X Location [ThetaVWC3]

2:0.11904 F

3:13 Z Location [ThetaVWC3]

14: If time is (P92)

1:0 Minutes (Seconds--) into an interval

2:60 Interval (same units as above)

3:10 Set Output Flag High (Flag 0)

15: Set Active Storage Area (P80)

1:1 Final Storage Area 1

2:100 Array ID

16: Real Time (P77)

1:1220 Year, Day, Hour/Minute (midnight=2400)

17: Sample (P70)

1:1 Replicates

2:1 Location [Battery]

18: Sample (P70)

1:3 Replicates

2:5 Location [Temp]

19: Sample (P70)

1:3 Replicates

2:2 Location [ThetaV]

20: Sample (P70)

1:3 Replicates

2:11 Location [ThetaVCW1]

21: Serial Out (P96)

1:71 Storage Module

*Table 2 Program

02:0.0000 Execution Interval (seconds)

*Table 3 Subroutines

End Program